



Potentialités de deux espèces d’algues rouges du genre Asparagopsis : effets sur la physiologie de l’anguille européenne et sur ses pathogènes

Christelle Parchemin

► To cite this version:

Christelle Parchemin. Potentialités de deux espèces d’algues rouges du genre Asparagopsis : effets sur la physiologie de l’anguille européenne et sur ses pathogènes. Chimie organique. Université de Perpignan, 2023. Français. NNT : 2023PERP0015 . tel-04207577

HAL Id: tel-04207577

<https://theses.hal.science/tel-04207577>

Submitted on 14 Sep 2023

HAL is a multi-disciplinary open access archive for the deposit and dissemination of scientific research documents, whether they are published or not. The documents may come from teaching and research institutions in France or abroad, or from public or private research centers.

L’archive ouverte pluridisciplinaire **HAL**, est destinée au dépôt et à la diffusion de documents scientifiques de niveau recherche, publiés ou non, émanant des établissements d’enseignement et de recherche français ou étrangers, des laboratoires publics ou privés.

THÈSE

Pour obtenir le grade de Docteur

Délivré par
UNIVERSITE DE PERPIGNAN VIA DOMITIA

Préparée au sein de l'école doctorale
ED 305 Energie et Environnement
Et des unités de recherche
UAR 3278 – CRIODE – EPHE-CNRS-UPVD
et
UMR 5110 – CEFREM – UPVD-CNRS

Spécialité : **Chimie**

Présentée par
Christelle PARCHEMIN

**Potentialités de deux algues rouges du genre
Asparagopsis : effets sur la physiologie de
l'anguille européenne et sur ses pathogènes**

Soutenue le 08/06/2023

devant le jury composé de

M. Gerald CULIOLI , Professeur des Universités. <i>Université d'Avignon</i>	Rapporteur
M. Philippe POTIN , Directeur de Recherche. <i>Centre National de la Recherche Scientifique, Roscoff</i>	Rapporteur
M. Cedric BERTRAND , Professeur des Universités. <i>Université de Perpignan Via Domitia</i>	Examinateur
M. Yves DESDEVISES , Professeur des Universités. <i>Sorbonne Université, Observatoire Océanologique de Banyuls-sur-Mer</i>	Examinateur
Mme. Samira SARTER , Cadre de Recherche, HDR. <i>Institut des Sciences de l'Evolution-Montpellier</i>	Examinateuse
Mme. Nathalie TAPISSIER-BONTEMPS , Maîtresse de conférences, HDR. <i>Université de Perpignan Via Domitia</i>	Directrice de thèse
Mme. Elisabeth FALIEX , Maîtresse de conférences. <i>Université de Perpignan Via Domitia</i>	Co-encadrante
M. Pierre SASAL , Chargé de Recherche, HDR. <i>Centre National de la Recherche Scientifique, Perpignan</i>	Co-encadrant



« La science, [mon garçon], est faite d'erreurs, mais d'erreurs qu'il est bon de commettre, car elles mènent peu à peu à la vérité »

Jules Verne

Avant-Propos

Ce manuscrit est rédigé sous la forme d'une thèse sur articles. Elle débute par une introduction générale, suivie d'un état de l'art comprenant une revue de littérature publiée, des principes généraux des matériels et méthodes utilisés, et enfin de quatre chapitres. Les trois premiers portent sur les métabolites secondaires d'algues rouges envahissantes et leurs intérêts biologiques. Le quatrième est centré sur les pathogènes de l'anguille européenne et les modifications de sa physiologie en réponse à un régime alimentaire supplémenté en algues et/ou à une infestation par des pathogènes. Chaque chapitre est composé : d'un avant-propos contenant le statut de l'article, le contexte, la méthodologie générale, la contribution de chaque auteur et la disponibilité des données, de l'article et enfin d'un « ce qu'il faut retenir ? » reprenant les objectifs et les principaux résultats. Les chapitres I, III et IV sont complétés de résultats non intégrés à l'article. Le manuscrit se termine par une conclusion générale assortie de perspectives. Hormis la partie « article » de chaque chapitre, l'ensemble du manuscrit est rédigé en français. Enfin, les références et le matériel supplémentaire sont listés à la fin du manuscrit.

Remerciements

J'aimerais tout d'abord remercier la Région Occitanie, l'université de Perpignan *Via Domitia* (au travers du “Bonus Qualité Recherche” (BQR)), et l'ED305 (au travers de l'appel à projet « ApDoc ») pour l'attribution des supports financiers ayant permis la réalisation des travaux de cette thèse.

Un grand merci aux membres de mon jury, le Pr. Gerald Culoli, le Dr. Philippe Potin en tant que rapporteurs de ma thèse, le Pr. Cédric Bertrand, le Pr. Yves Desdevises et la Dr. Samira Sarter, en tant qu'examineurs pour avoir accepté d'évaluer mon travail.

J'aimerais ensuite remercier les membres de mon Comité de Suivi Individuel : la Pr. Carole Calas-Blanchard, le Pr. Yves Desdevises, la Pr. Claire Hellio et la Dr. Marie-Virginie Salvia, pour avoir accepté d'en faire partie, et pour vos conseils et encouragements.

Ensuite, et pas des moindres j'aimerais remercier ma directrice et mes encadrants de thèse, la Dr. Nathalie Tapissier-Bontemps, la Dr. Elisabeth Faliex, le Dr. Pierre Sasal. Merci pour l'opportunité que vous m'avez offert en me sélectionnant pour la réalisation de ce travail. Merci de m'avoir accompagné tout au long de cette belle aventure, merci pour votre implication qui nous a permis de passer des moments inoubliables, sous les ponts du Barcarès, lors des manips anguilles, et même pendant les réunions ! Merci à vous trois, j'admire votre vision de l'encadrement et je me rends bien compte de la chance que j'ai eu de vous avoir comme encadrants. Betty, je t'enverrai régulièrement des messages pour m'assurer que tu as toujours tes mains parce que... « je mettrais mes mains à couper qu'on aura des civelles », merci d'avoir réagi aussi vite et d'avoir trouvé une solution face à nos pêches infructueuses.

Je tiens bien sûr à remercier Annaïg Leguen et Wolfgang Ludwig, respectivement directeurs des laboratoires CRIOBE et CEFREM pour m'avoir accueillie dans leurs unités de recherche. Merci également à Christophe Gruneau directeur du laboratoire IHPE et à Arnaud Lagorce responsable de la salle de microbiologie du même laboratoire de m'y avoir facilité l'accès ainsi qu'à mes stagiaires pour la réalisation des tests d'activités antibactériennes. J'aimerais aussi remercier Jean-François Allienne pour tout le matériel et les milieux autoclavés.

A ceux sans qui je n'aurais probablement pas fait une thèse sur les macroalgues, mes professeurs et enseignants de licence et master, le Dr. Erwan Ar Gall, la Pr. Claire Hellio, la Dr. Valerie Stiger, la Dr. Solene Conan, et le Pr. Eric Deslandes. Vous m'avez transmis la

passion des algues et de leurs molécules et pour ça je ne peux que vous remercier. Un merci tout particulier à Erwan, je n'ai pas eu le temps de te le dire mais tu as fait naître en moi, avec tes cours et en étant le premier à me donner ma chance en me prenant en stage alors que je n'étais qu'en L3, la petite graine de passion pour les macroalgues. Merci pour ça, merci d'avoir continué à m'accorder du temps en thèse. Merci également à mes différents encadrants de stages : le Dr. Pierre Sauleau, Dr. Valérie Paul, Dr. Sarath Gunasekera, Dr. Blake Ushijima car chaque rencontre scientifique passée m'a menée à ce présent.

J'aimerais aussi remercier la Plateforme Bio2mar MSXM et en particulier Delphine Raviglione pour toute l'aide apportée pour la réalisation des analyses chimiques. Merci également à Camille Clerissi, pour la collaboration qui m'a permise d'étudier les communautés bactériennes associées aux algues mais aussi pour ta relecture, dans cette thèse, de la partie concernant le métabarcoding.

A la team anguille, logée au « pigeonnier », (Betty), Gaël, Elsa, Jason, Raph, merci pour votre aide, lors des manips avec le parasite, avec les stats, ou quelques fois sous les ponts du Barcarès. Merci pour votre bonne humeur, les galettes et les moments partagés !

Je n'aurais pas assez de mots pour suffisamment te remercier Gaël, mais je vais essayer quand même. Merci pour ton investissement à l'animalerie, merci pour ces longues heures passées ensemble à nettoyer les aquariums, les filtres et à nourrir les anguilles. Tu as rendu toutes ces heures bien plus que supportables avec ta bonne humeur, ta folie (que je partage !) et ton limoncello. Tout ça me manque déjà. Alors arrosoir et persil !

Un grand merci à tous les stagiaires que j'ai eu la chance d'encadrer qui ont tous montré beaucoup d'intérêt pour mon sujet de thèse et qui ont chacun apporté leur pierre à l'édifice, merci à Rachel, à Théo et à Loic.

Merci aussi à Florent, pour la conception des « réacteurs à Artémia » et pour ton aide dans la salle de microbiologie. Finalement, j'aimerai remercier de manière générale toutes les personnes qui ont contribué à la réalisation des travaux de cette thèse et que j'aurai pu oublier.

Merci au RFMF et en particulier aux copains du CA de la branche junior, pour tous les évènements organisés ensemble et ces bons moments qui m'ont permis de voir un autre aspect de la science #BonneBouffeBonneScience.

Merci aux copains du labo, les doctorants : Slimane, Hikmat, Mélina, Laurine, Christian, Mélanie, Benoit, Oumaynou, Yazid, Anouar, Claire, Zahrmina (du plus « ancien » au plus

« neuf »), pour tous les moments où on a pu s'entraider, se soutenir et rire. Un merci tout particulier à Hikmat, pour toutes ces heures à discuter, à refaire le monde de la recherche, ces longues soirées où on se battait presque pour être le dernier à partir, tu m'as beaucoup écouté, beaucoup encouragé et beaucoup aidé, sans toi cette thèse n'aurait pas été la même.

Aux copains de l'UPVDoc, on a vécu une belle aventure et même si nos routes sont amenées à se séparer je n'oublierai rien de cette belle première année de thèse passée avec vous, à galérer à organiser un congrès en pleine période de pandémie mais surtout à beaucoup rire et échanger, alors merci.

Merci à tous mes ami(e)s, qui ont montré de l'intérêt envers mon sujet de thèse, merci à ceux de toujours de Rouen, merci à ceux rencontrés à Brest et au fil de l'eau, et à ceux de Perpignan qui n'ont que davantage enrichi mon aventure en thèse. Merci à vous tous, vous êtes ma deuxième famille.

C'est maintenant le moment de remercier ma famille, mon frère, Vincent, Maman, Papa, sans vous rien de tout ce travail ne serait possible, merci de m'avoir toujours soutenu dans mes projets et d'avoir toujours tout mis en place pour me permettre de les réaliser. Merci maman pour ces belles illustrations que tu m'as faites, une thèse est par définition déjà unique, la mienne l'est encore plus grâce à toi. Une pensée aussi à tous mes grands-parents, partis trop tôt, en particulier à ma mamie Tessée, merci de m'avoir toujours demandé comment allaient mes « petites bêtes ». Tu n'auras pas pu avoir la conclusion de tout ce travail mais je sais que tu es fière de moi et c'est le plus important.

Enfin, last but not least, merci à toi, Guilhem, pour ton soutien sans faille, tes encouragements, ta patience toutes ces fois ou tu m'as écoutée me plaindre ou quand je devais aller tous les week ends m'occuper des anguilles. Merci de t'être réjoui de mes réussites et de m'avoir reboostée lors des échecs. Merci de m'avoir servi de cobaye pour mes présentations et d'avoir (presque) toujours tout compris.

Puisque je reste moi et que je ne peux pas finir sur tant d'émotions sans une note de légèreté... Merci à mes anguilles, vous m'en avez fait voir de toutes les couleurs mais cette thèse n'aurait pas existé sans vous. Pas de jalousie merci aux deux espèces d'algues *Asparagopsis armata* et *A. taxiformis* sans vous la thèse n'aurait pas existé non plus, merci pour votre odeur qui me donnait mal à la tête mais qui vous donne tout votre intérêt.

Valorisations scientifiques

Articles parus :

Etat de l'art : Parchemin, C., Tapissier-Bontemps, N., Sasal, P., and Faliex, E (2022). *Anguilla* sp. diseases diagnoses and treatments: The ideal methods at the crossroads of conservation and aquaculture purposes. *Journal of Fish Diseases* 45, 943–969. <https://doi.org/10.1111/jfd.13634>
IF : 2.58

Annexe I : Reverter, M., Rohde, S., Parchemin, C., Tapissier-Bontemps, N., and Schupp, P. J. (2020). Metabolomics and marine biotechnology: coupling metabolite profiling and organism biology for the discovery of new compounds. *Frontiers in Marine Science* 7, 1062. <https://doi.org/10.3389/fmars.2020.613471> IF : 5.247

Chapitre I : Parchemin, C., Raviglione, D., Ghosson, H., Salvia, M.V., Goossens, C., Sasal, P., Faliex, E and Tapissier-Bontemps, N., (2023). Development of a Multiblock Metabolomics Approach to Explore Metabolite Variations of two Algae of the Genus *Asparagopsis* Linked to Interspecies and Temporal Factors. *Algal Research* 72, 103138. <https://doi.org/10.1016/j.algal.2023.103138> IF : 5.276.

Chapitre III : Parchemin, C., Raviglione, D., Mejait, A., Sasal, P., Faliex, E, Clerissi, C., and Tapissier-Bontemps, N., (2023). Antibacterial Activities and Life Cycle Stages of *Asparagopsis armata*: Implications of the Metabolome and Microbiome. *Marine Drugs*, 21, 363. <https://doi.org/10.3390/md21060363> IF : 6.085

Article en préparation :

Chapitre IV : Parchemin, C., Simon, G., Jobet, E., Chaparro, C., Carpentier, M.,C., Amilhat, E., Tapissier-Bontemps, N., Sasal, P., and Faliex, E., (2023). *Asparagopsis* spp. as feed supplement for a critically endangered species? Effect on the European eel (*Anguilla anguilla*) and on its pathogens. **Soumission prevue au deuxième semestre 2023 dans Fish and Shellfish Immunology.** IF : 4.622

Communications orales :

Christelle Parchemin « Potentialités de deux algues rouges du genre *Asparagopsis* : effets sur la physiologie de l'anguille européenne et sur ses pathogènes ». Cycle de conférences de l'Université de Perpignan *Via Domitia*, 13 avril 2023, Perpignan, France.

Christelle Parchemin, Delphine Raviglione, Anouar Meijait, Camille Clerissi, Pierre Sasal, Elisabeth Faliex, Nathalie Tapissier-Bontemps. « Variations of Metabolome, Microbiota, and Antibacterial Activities in different Life Stages of *Asparagopsis armata* in relation to the Production of Halogenated Molecules». Journées 2022 du GDR MediatEC, 15 au 18 novembre 2022, Cargèse, France.

Christelle Parchemin, Delphine Raviglione, Hikmat Ghosson, Marie-Virginie Salvia, Corentine Goossens, Pierre Sasal, Elisabeth Faliex, Nathalie Tapissier-Bontemps. « Development of a Combined Metabolomics Approach to Explore Metabolite Variations of two Algae of the Genus *Asparagopsis* Linked to Interspecific and Temporal Factors». ANALYTICS, 5 au 8 septembre 2022, Nantes, France.

Christelle Parchemin, Nathalie Tapissier-Bontemps, Elisabeth Faliex, Pierre Sasal. Potentialités de deux espèces d’algues rouges du genre *Asparagopsis* : effets sur la physiologie de l’anguille européenne et de ses pathogènes », 9^e congrès des doctorants, 6 au 7 novembre 2020, Perpignan, France.

Communications orales « Flash » :

Christelle Parchemin, Delphine Raviglione, Jennifer Sola, Guillaume Iwankow, Hikmat Ghosson, Pierre Sasal, Elisabeth Faliex, Nathalie Tapissier-Bontemps. « Exploring the Interspecific, Intraspecific and Spatial Variability of two algae from the genus *Asparagopsis* Using Complementary Metabolomics Approaches ». 14e journées scientifiques du Réseau Francophone de Métabolomique et Fluxomique (RFMF), 23 au 26 novembre 2021, Aussois, France.

Communications par poster :

Christelle Parchemin, Théo Perion, Loic Maurice, Delphine Raviglione, Emilie Adouane, Pierre Sasal, Elisabeth Faliex, Raphaël Lami et Nathalie Tapissier-Bontemps. « Activité anti-quorum sensing des algues du genre *Asparagopsis* ». 11^e congrès des doctorants, 18 novembre 2022, Perpignan.

Christelle Parchemin, Delphine Raviglione, Jennifer Sola, Guillaume Iwankow, Hikmat Ghosson, Pierre Sasal, Elisabeth Faliex, Nathalie Tapissier-Bontemps. « Exploring the Interspecific, Intraspecific and Spatial Variability of two algae from the genus *Asparagopsis* Using Complementary Metabolomics Approaches ». 14e journées scientifiques du Réseau Francophone de Métabolomique et Fluxomique (RFMF), 23 au 26 novembre 2021, Aussois.

Christelle Parchemin, Rachel Caballe, Gaël Simon, Edouard Jobet, Elsa Amilhat, Nathalie Tapissier-Bontemps, Pierre Sasal, Elisabeth Faliex. « *In vitro* and *in vivo* effects of the red algae *Asparagopsis taxiformis* against eel pathogenic bacteria and a parasite ». XII International European Conference on Marine Natural Products (ECMNP), 30 aout 2021 au 01 septembre 2021, en ligne.

Christelle Parchemin, Nathalie Tapissier-Bontemps, Elisabeth Faliex, Pierre Sasal. « Potentialités de deux espèces d’algues rouges du genre *Asparagopsis* : effets sur la physiologie de l’anguille européenne et de ses pathogènes », 8^e congrès des doctorants, 8 au 9 novembre 2019, Perpignan

Autres communications

Participation à la finale régionale du concours de vulgarisation « MT180 », 22/03/2021, Montpellier.

Table des matières

Avant-Propos	5
Remerciements	7
Valorisations scientifiques	11
Table des matières	15
Liste des abréviations.....	21
Introduction générale.....	23
Etat de l'art	31
1. Revue publiée « Diagnostics et traitements des maladies d' <i>Anguilla</i> sp. : La méthode idéale à la croisée entre conservation et aquaculture ».....	33
1.1 Avant propos	33
1.2 Article	35
1.2.1 Abstract.....	35
1.2.2 Introduction	36
1.2.3 Eel pathogens, damages and symptoms	38
1.2.4 Causative agent identification	47
1.2.5 Potential treatment.....	56
1.2.6 Conclusion	68
1.3 Ce qu'il faut retenir	70
2. Les algues du genre <i>Asparagopsis</i>	71
2.1.1 Généralités	71
2.1.2 Composition chimique et activités décrites des algues du genre <i>Asparagopsis</i>	74
2.1.3 Facteurs de variation de la composition chimique et des activités biologiques	85
3. Apport des outils –omiques pour évaluer le potentiel des algues du genre <i>Asparagopsis</i>	90
Matériels et méthodes : principes généraux	95
1. L'élevage et le maintien des anguilles en conditions contrôlées	97
2. Obtention des parasites <i>A. crassus</i>	100
3. Tests <i>in vitro</i> sur les pathogènes de l'anguille européenne	100
3.1 Tests d'activité antibactérienne.....	100
3.2 Tests d'activité antiparasitaire	102

4.	Infestation expérimentale des anguillettes	103
4.1	Avec le parasite <i>A. crassus</i>	103
4.2	Avec la bactérie <i>E. anguillarum</i>	105
5.	Mise au point de l'alimentation supplémentée en algue	105
6.	Les outils analytiques	106
6.1	La métabolomique	106
6.1.1	Le workflow	106
6.1.2	Extraction.....	107
6.1.3	Acquisition des données	107
6.1.4	Pré-traitement des données	111
6.2	Le métabarcoding.....	114
6.3	La transcriptomique	115
7.	Les outils statistiques	116
7.1	Normalisation des données	116
7.2	Analyses univariées	116
7.3	Analyses multivariées	117
7.3.1	Non supervisées.....	117
7.3.2	Supervisées	118
7.4	Analyses « multiblock ».....	119
7.5	Analyses de survie	119

Chapitre I : Développement d'une approche métabolomique « multiblock » pour explorer les variations des métabolites de deux algues du genre *Asparagopsis* liées à des facteurs interspécifiques et temporels 123

1.	Avant-Propos.....	125
2.	Article.....	128
2.1	Highlights.....	128
2.2	Abstract.....	128
2.3	Graphical Abstract	129
2.4	Introduction.....	129
2.5	Materials and methods	131
2.5.1	Chemicals	131
2.5.2	Biological materials.....	132
2.5.3	Algae extracts preparation	132
2.5.4	Metabolomics analyses.....	133
2.5.5	Metabolomics data processing.....	134
2.5.6	Antibacterial assays	136

2.5.7	Statistical analyses	136
2.6	Results.....	137
2.6.1	Chemical nature of detected metabolites.....	137
2.6.2	Interspecies variability of the metabolome.....	139
2.6.3	Temporal variability of the metabolome	141
2.6.4	Influence of environmental parameters	145
2.6.5	Temporal variability of the antibacterial activity	145
2.7	Discussion	146
2.8	Conclusion	151
2.9	Acknowledgments.....	152
3.	Ce qu'il faut retenir	153
4.	Résultats non intégrés à l'article	155
Chapitre II : Activité anti-quorum sensing des algues du genre <i>Asparagopsis</i>	159
1.	Avant Propos	161
2.	Article.....	163
2.1	Abstract.....	163
2.2	Introduction.....	163
2.3	Materials and Methods.....	165
2.3.1	Materials	165
2.3.2	Algal extraction	166
2.3.3	Anti-QS effect on <i>Chromobacterium violaceum</i> CV026	166
2.3.4	Anti-QS effect on <i>Pseudomonas putida</i> F117 and <i>Escherichia coli</i> MT102167	167
2.3.5	LC-HRMS analysis of the fractions	168
2.4	Results.....	168
2.4.1	Anti-QS effect on <i>Chromobacterium violaceum</i> CV026	168
2.4.2	Anti-QS effect on <i>Pseudomonas putida</i> F117 and <i>Escherichia coli</i> MT102171	171
2.4.3	LC-HRMS analysis of the fractions	173
2.4.4	Discussion.....	175
3.	Ce qu'il faut retenir	177
Chapitre III : Activités antibactériennes et cycle de vie d'<i>Asparagopsis armata</i> : implications du métabolome et du microbiote.....	179	
1.	Avant propos	181
2.	Article.....	184
2.1	Abstract.....	184
2.2	Introduction.....	185
2.3	Materials and methods	187

2.3.1	Chemicals	187
2.3.2	Biological materials.....	187
2.3.3	Algal extraction	188
2.3.4	Metabolomics	188
2.3.5	Antibacterial activity	190
2.3.6	Bioguided fractionation and identification of a candidate molecule responsible for the antibacterial activity.....	191
2.3.7	Metabarcoding	192
2.3.8	Multivariate and statistical analyses	193
2.3.9	Multi-omics	193
2.4	Results.....	194
2.4.1	Variation of the metabolome of the three life stages	194
2.4.2	Variation in the antibacterial activity of the three life stages	197
2.4.3	Identification of candidate molecules responsible for antibacterial activity	198
2.4.4	Analysis of bacterial communities associated with <i>A. armata</i> stages	199
2.4.5	Correlation between metabolite and bacterial compositions in algal stages	202
2.5	Discussion	204
2.5.1	The three stages of the life cycle of <i>A. armata</i> harboured distinct metabolome compositions.....	204
2.5.2	Highly halogenated molecules may be responsible for some antibacterial activity	206
2.5.3	Microbiota composition differs throughout the three stages of the life cycle of <i>A. armata</i>	207
2.5.4	The overall analyses performed suggest complex interactions between the host and its microbiota	209
2.6	Conclusion	212
2.7	Acknowledgements.....	212
3.	Ce qu'il faut retenir	213
4.	Résultats non intégrés à l'article	215
Chapitre IV : <i>Asparagopsis</i> spp. comme complément alimentaire pour une espèce en danger critique d'extinction ? Effet sur l'anguille européenne (<i>Anguilla anguilla</i>) et sur ses pathogènes.....	219	
1.	Avant propos	221
2.	Article.....	224
2.1	Abstract	224
2.2	Introduction	225
2.3	Materials and methods	227
2.3.1	Rearing of eels	227

2.3.2	Collection and extraction of algae	228
2.3.3	Antiparasitic activity of algae against <i>A. crassus</i>	228
2.3.4	Antibacterial activity of algae against <i>E. anguillarum</i>	232
2.3.5	Eels growth performance.....	232
2.3.6	Transcriptomic analysis	233
2.4	Results.....	234
2.4.1	Effects of <i>Asparagopsis</i> sp. on eel pathogens	234
2.4.2	<i>In vivo</i> effects of <i>A. taxiformis</i> supplemented diet on eel growth performance 239	
2.4.3	Impact of <i>A. taxiformis</i> and/or <i>A. crassus</i> on eel transcripts	240
2.4.4	Effect of the algal feeding	241
2.4.5	Effect of the parasite.....	243
2.4.6	Combined effect of the algal feeding and the parasite	244
2.5	Discussion	244
2.5.1	<i>Asparagopsis</i> spp. extract significantly reduced <i>Anguillicola crassus</i> survival <i>in vitro</i> 245	
2.5.2	<i>A. taxiformis</i> diet supplementation impacted negatively eel growth and physiology	245
2.5.3	<i>A. taxiformis</i> supplemented diet seemed to favour infestation by <i>A. crassus</i> and did not improve <i>A. anguilla</i> survival challenged with <i>E. anguillarum</i>	248
2.6	Conclusion	250
2.7	Acknowledgements.....	251
3.	Ce qu'il faut retenir	252
4.	Résultats non intégrés à l'article	254
Conclusion générale et perspectives	259	
Références	271	
Annexes	301	
1.	Mini-Revue : Métabolomique et biotechnologies marines : coupler le profilage des métabolites et la biologie des organismes pour la découverte de nouveaux composés.....	301
1.1	Abstract	303
1.2	Introduction.....	304
1.3	Speeding up molecule identification.....	304
1.4	Linking chemical diversity and ecology	307
1.5	Host-microbe interactions	308
1.6	Multi-omics integration	309
1.7	Discussion	311
1.8	Reference	312

2.	Annexe Chapitre I	319
2.1	Supplementary methods.....	321
2.2	Supplementary figures	323
2.3	Supplementary tables	342
3.	Annexe Chapitre III.....	351
3.1	Supplementary methods.....	353
3.2	Supplementary figures	355
3.3	Supplementary tables	368
4.	Annexe Chapitre IV	379
4.1	Supplementary figures	381
4.2	Supplementart tables	383

Liste des abréviations

Aa	:	<i>A. armata</i>
ACN	:	Acétonitrile
ACP/PCA	:	Analyse en composantes principales/Principal Component Analysis
ADN/DNA	:	Acide Désoxyribonucléique/Deoxyribonucleic acid
AHL	:	Acyl-homosérine lactone
ANOVA	:	Analyse of Variance
ARN/RNA	:	Acides RiboNucléiques/Ribonucleic acid
ASV	:	Amplicon Sequence Variant
BCC/BHIA	:	Bouillon Cœur Cervelle/Brain Heart Infusion Agar
At	:	<i>A. taxiformis</i>
CER	:	Classification Error Rate
CFU	:	Colony forming unit
db-RDA	:	distance-based Redundancy Analysis
DCM	:	Dichlorométhane
		Data integration analysis for biomarker discovery
DIABLO	:	using latent variable approaches for ‘Omics studies
DMSO	:	DiMethyl SulfOxyde
DMSP	:	Dimethylsulfoniopropionate
DO/OD	:	Densité Optique/Optican Density
Ea	:	<i>Edwardsiella anguillarum</i>
GC-MS	:	Gaz Chromatographie-Mass Spectrometry
GO	:	Gene Ontology
HS-SPME	:	Head Space - Solid Phase MicroExtraction
(U)HPLC	:	(Ultra) High Performance Liquid Chromatography
LB	:	Luria Broth
LC-MS	:	Liquid Chromatography-Mass Spectrometry
Lg	:	<i>Lactococcus garvieae</i>
MB	:	Marine Broth
MeOH	:	Methanol

MH	:	Mueller Hinton
MS	:	Mass Spectrometry
MTBE	:	Méthyl tert-butyl éther
QC	:	Quality Control
QS	:	Quorum Sensing
Pa	:	<i>Pseudomonas anguilliseptica</i>
PBS	:	Phosphate Buffer Saline
PCR	:	Polymerase Chain Reaction
PLS-DA	:	Partial Least-Squares Discriminant Analysis
RMN/NMR	:	Résonance Magnétique Nucléaire/Nuclear Magnetic Resonance
RT	:	Retention Time
		Union Internationale pour la Conservation de la
IUCN/IUCN	:	Nature/ International Union for Conservation of Nature
SQDG	:	SulfoQuinovosylDiacylGlycérol
Tm	:	<i>Tenacibaculum maritimum</i>
Va	:	<i>Vibrio anguillarum</i>
VIP	:	Variable Important in Projection
W4M	:	Workflow 4 Metabolomics
Yr	:	<i>Yersina ruckeri</i>

Introduction générale



Illustration à l'aquarelle réalisée par Michèle Parchemin

Dans les écosystèmes, chaque espèce est en interaction avec son environnement et directement ou indirectement avec les autres espèces. Tout changement dans un écosystème peut être révélé par les espèces dites « sentinelles » indicatrices de l'état de santé et du fonctionnement de l'écosystème. L'anguille européenne (*Anguilla anguilla*), seul représentant du genre *Anguilla* en Europe est un exemple d'espèce sentinelle. Elle joue aussi un rôle majeur dans les écosystèmes en raison de sa position dans les réseaux trophiques. C'est un prédateur qui se nourrit, selon son stade de développement, sa taille et son habitat, de petits crustacés, vers et larves d'insectes puis de proies plus grosses comme des crevettes, des petits crabes et des petits poissons. Elle est aussi la proie de plus grands poissons et d'oiseaux. Outre son importance écologique, elle revêt une valeur économique importante, dans la mesure où tous ses stades de vie (stades civelle, jaune et argenté) sont consommés et pêchés par l'homme. Une partie de la production est issue de la pêche, à laquelle s'ajoute l'aquaculture, dont les principaux pays producteurs sont les Pays-Bas, le Danemark et l'Allemagne. En France, 770 pêcheurs professionnels pratiquent la pêche à l'anguille sur l'ensemble des façades maritimes dont environ 210 pour la façade méditerranéenne (PGA, 2018).

Cependant, depuis les années 1980, la population de l'anguille européenne a drastiquement diminuée (Feunteun, 2002). Elle est depuis 2008 classée par l'Union Internationale pour la Conservation de la Nature (IUCN) comme espèce en danger critique d'extinction (IUCN, 2022 ; Pike et al., 2020). La pêche (professionnelle, de loisir et braconnage), la fragmentation et la dégradation de ses habitats, et la pollution sont considérés comme des facteurs potentiellement responsables de l'effondrement de sa population (Arai, 2014 ; Bruslé, 1994 ; Drouineau et al., 2018 ; Elie et Rigaud, 1987 ; Knights, 2003 ; Palstra et al., 2006). De plus, l'infection par des pathogènes (virus, bactéries ou macroparasites) est également considérée comme un facteur majeur de l'effondrement de sa population en impactant les anguilles dans leur milieu naturel (et par répercussion sur la pêche) mais aussi dans les fermes piscicoles européennes en provoquant des mortalités et des pertes économiques importantes (Esteve et Alcaide, 2009 ; Haenen et al., 2009 ; Haenen, 2019 ; Kirk, 2003). En effet, les agents pathogènes peuvent causer des nécroses du tissu branchial, des hémorragies, des ulcères, des inflammations de la peau ou des organes, affecter la capacité de nage des anguilles lors de la migration de frai et impacter négativement le recrutement global (civelles) de l'anguille européenne (Haenen et al., 2009). Parmi les macroparasites affectant l'anguille européenne, *Anguillicola crassus*, un nématode hématophage, parasite de la vessie gazeuse, est considéré aujourd'hui comme l'un des acteurs du déclin de sa population. En effet, la présence de ce parasite dans la vessie gazeuse des

anguilles provoque des dommages directs à cet organe tels que inflammations et épaississement des tissus environnants (Molnár et al., 1993) pouvant conduire à une altération de ses fonctions et de la capacité de nage des anguilles (Kirk, 2003 ; Palstra et al., 2007) et mettre en péril la migration transocéanique des futurs géniteurs et même conduire à leur mort. Si des actions sont menées sur quelques-uns des facteurs potentiellement responsables de l'effondrement de la population de l'anguille européenne tels que la réglementation de la pêche, l'aménagement des barrages ou encore la surveillance des niveaux de pollution, il est très difficile d'agir sur les problématiques liées aux pathogènes. En effet, cela nécessiterait des suivis réguliers, des détections précoces et non invasives, et des traitements appropriés et respectueux de l'environnement (Parchemin et al., 2022). Le moyen de lutte le plus utilisé par les aquaculteurs, pour contrôler les maladies et prévenir les pertes de stocks, reste l'utilisation d'antibiotiques (Romero et al., 2012). Cependant, l'émergence de bactéries résistantes et la demande croissante de solutions plus « vertes » ont conduit à la recherche de traitements alternatifs.

Depuis quelques années, des méthodes de traitement alternatives ont donc été développées. Parmi celles-ci, la vaccination et le développement de préparations à base de plantes, de probiotiques ou de produits naturels ont suscité un intérêt croissant, car elles peuvent prévenir les maladies et auraient également des conséquences moins néfastes sur l'environnement (Gudding et Van Muiswinkel, 2013 ; Reverter et al., 2014, 2021). Bien que les plantes terrestres soient de loin les plus étudiées pour de telles applications (Reverter et al., 2021), l'amélioration des connaissances et de l'accessibilité des algues, leur valeur nutritionnelle (Burtin, 2003), et leur grand nombre d'activités biologiques (Cannell, 1993 ; König et Wright, 1993 ; Wang et al., 2015) ont également poussé à tester leur potentiel en tant que complément alimentaire pour l'aquaculture (Thanigaivel et al., 2016 ; Vatsos et Rebours, 2015 ; Wan et al., 2019). Des résultats prometteurs ont été obtenus et dans certains cas, l'alimentation à base d'algues s'est avérée favoriser la croissance, induire une immunostimulation et améliorer la survie des poissons exposés à des agents pathogènes (Thanigaivel et al., 2016 ; Vatsos et Rebours, 2015 ; Wan et al., 2019). Parmi les algues les plus étudiées pour de telles applications on retrouve des espèces cultivées ou envahissantes, comme *Sargassum* sp., *Ulva* sp., *Grateloupia* sp. et, dans une moindre mesure, les algues des genres *Fucus* ou *Asparagopsis*. En France, *Caulerpa taxifolia*, *Sargassum muticum*, *Undaria pinnatifida* et *Asparagopsis armata* sont quelques exemples d'espèces envahissantes. Elles sont même classées depuis 2006 dans les 100 espèces les plus envahissantes "The 100 Worst Invasives Species" en Méditerranée (Streftaris et Zenetos, 2006).

Ces algues envahissantes sont des algues non-indigènes, introduites par l'homme de manière accidentelle ou volontaire. Elles s'établissent et prospèrent ensuite, grâce à certaines de leurs caractéristiques telles qu'une valence écologique élevée, une grande fertilité, une grande capacité de dispersion et une résistance aux conditions de transport (Mooney et Drake, 2012). Ces algues peuvent nuire à la biodiversité indigène en perturbant l'écosystème existant et en induisant des stress (Ehrenfeld, 2010). La valorisation des algues envahissantes et donc leur collecte dans l'environnement peut alors constituer un moyen de limiter leur impact négatif sur les espèces indigènes et sur les écosystèmes (Pinteus et al., 2018). Ces algues représentent aussi une source importante de molécules actives exploitables. Des études ont reporté que les algues du genre *Sargassum* spp. et *Asparagopsis* spp. en particulier, sont parmi les plus prometteuses en terme de potentiel biotechnologique en raison de leur disponibilité et de leur large gamme d'activités biologiques (Félix et al., 2021 ; Pinteus et al., 2016, 2018 ; Stiger-Pouvreau et Zubia, 2020). Pour autant, cette biomasse est peu valorisée en Méditerranée française. Administrées sous forme de complément alimentaire en aquaculture, leur utilisation pourrait être une stratégie à envisager pour la préservation d'espèces aquatiques menacées par des pathogènes.

Ainsi, ce projet de thèse, financé par la Région Occitanie et mené dans deux laboratoires de recherche de l'Université de Perpignan *Via Domitia* : le Centre de Recherches Insulaires et OBservatoire de l'Environnement (CRIOBE) et le CEntre de Formation et de Recherche sur les Environnements Méditerranéens (CEFREM), **a pour objectif principal d'évaluer le potentiel de l'algue *A. armata* ainsi que de son espèce sœur *A. taxiformis*, également considérée comme envahissante, sur les pathogènes de l'anguille européenne mais aussi comme complément alimentaire en conditions d'élevage pour améliorer la résistance de l'anguille face aux infections.**

Cet objectif principal est divisé en deux sous-objectifs correspondant à différents questionnements. La valorisation d'une algue nécessite des connaissances approfondies de sa composition chimique, dont dépendent ses activités biologiques, et sur les facteurs qui la font varier. La composition chimique des algues du genre *Asparagopsis* est étudiée depuis les années 1970 ; elle est donc assez bien documentée. Plusieurs études ont fait état de différences entre les activités biologiques d'*A. armata* et d'*A. taxiformis* (Genovese et al., 2009) ainsi que de variations spatiales et temporelles de leur composition chimique et de leurs activités biologiques sur des cibles diverses (Genovese et al., 2012 ; Greff et al., 2017b ; Marino et al., 2016 ; Salvador et al., 2007). Mais peu de ces travaux ont intégré simultanément les activités biologiques et la composition chimique pour permettre l'identification de marqueurs chimiques

de variabilité. Ainsi, le premier sous-objectif de la thèse, qui fait l'objet des Chapitres I, II et III consiste à enrichir les connaissances sur la composition chimique et les activités biologiques d'*A. armata* et d'*A. taxiformis* en répondant aux questions suivantes :

- Observe-t-on des différences de composition chimique et d'activités antibactériennes (*in vitro*) notables entre les deux espèces du genre *Asparagopsis* (marqueurs chimiotaxonomiques) ? Des variations au cours de l'année sont-elles observables ? La combinaison de plusieurs outils analytiques : la LC-MS, la GC-MS et la RMN par une approche de métabolomique dite « multiblock » a été privilégiée de manière à obtenir une vision globale du métabolome des deux algues (**Chapitre I**).
- *Asparagopsis armata* peut-elle inhiber, comme *A. taxiformis*, la communication bactérienne (i.e. quorum sensing), nouvelle cible pour lutter contre les pathogènes ? Quels sont les composés à l'origine de cette activité ? Une stratégie de fractionnement bioguidé a été suivie pour orienter cette recherche (**Chapitre II**).
- Les stades du cycle de vie d'*A. armata* présentent-ils des différences en terme d'activité biologique et de composition chimique ? Ces différences sont-elles en lien avec la communauté bactérienne associée ? Pour explorer cela, une approche intégrant métabolomique et metabarcoding a été choisie (**Chapitre III**).

Répondre à ces questions permet, dans un premier temps et au regard de l'objectif principal, de savoir s'il faut prioriser une des deux espèces. Dans un second temps, cela permet d'identifier des périodes propices de collecte aux cours desquelles les molécules responsables de l'activité des algues seraient particulièrement abondantes ou d'envisager leurs collectes annuelles en cas d'activités biologiques constantes. Enfin, dans un troisième temps, cela permet de mieux définir le potentiel, en terme de valorisation, des différents stades du cycle de vie de l'algue tel que le tétrasporophyte qui est également considéré comme envahissant.

Par ailleurs, l'utilisation d'*A. taxiformis* et d'*A. armata* comme complément dans l'alimentation de différentes espèces aquacoles a conduit à une plus forte croissance des poissons traités par rapport aux témoins non complémentés, ou encore à la surexpression de certains paramètres liés à l'immunité (Castanho et al., 2017 ; Reverter et al., 2016 ; Thépot et al., 2021a, 2021b, 2022). Cependant, l'effet d'une telle alimentation supplémentée avec ces algues sur la résistance de poissons face à des pathogènes n'a pas encore été démontré. De plus, peu d'études portent sur la potentielle immunostimulation de l'anguille européenne par divers produits naturels (Parchemin et al., 2022). Enfin, aucune étude ayant pour but l'immunostimulation

d'anguilles au travers d'une alimentation complémentée n'a évalué l'effet de ce type de nourriture sur ses parasites (Parchemin et al., 2022). Ainsi, le second sous-objectif de la thèse, qui fait l'objet du Chapitre IV, consiste à évaluer l'impact d'une complémentation en algue du genre *Asparagopsis* sur la physiologie de l'anguille européenne et sur ses pathogènes en répondant aux questions suivantes :

- Quels sont les effets *in vitro* des deux espèces d'algues appartenant au genre *Asparagopsis* sur le parasite *A. crassus*, et sur les bactéries pathogènes de l'anguille européenne ? Quel est l'effet d'une complémentation en algue sur la physiologie de l'anguille européenne ? Quels sont les effets *in vivo* d'une complémentation en algue sur la bactérie *E. anguillarum* et sur le parasite *A. crassus* ? Pour répondre à ces questions, des tests *in vitro*, des tests *in vivo*, des analyses phénotypiques et transcriptomiques ont été utilisées (**Chapitre IV**).

Les principaux objectifs, l'organisation et les outils analytiques utilisés au cours de cette thèse sont présentés de manière synthétique dans la **Figure 1**.

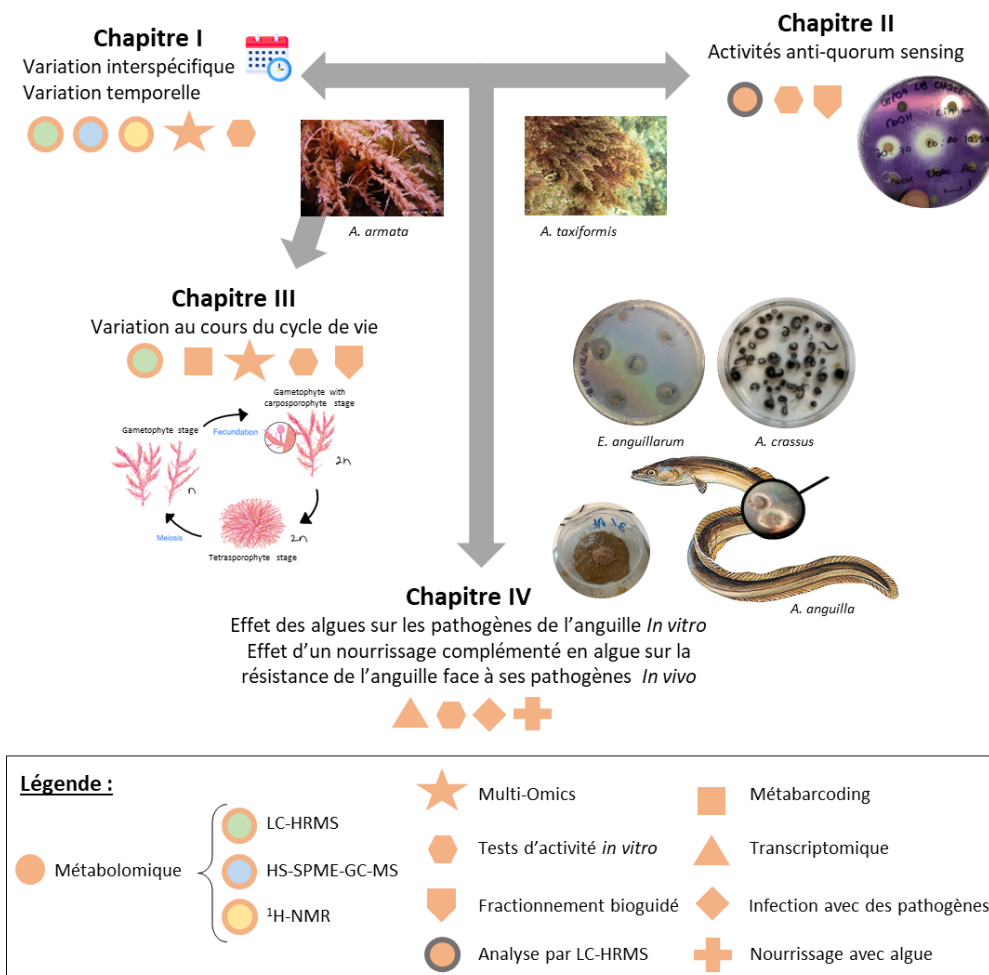


Figure 1 : Schéma général des principales thématiques et des techniques utilisées dans chaque chapitre composant la thèse.

Etat de l'art



Illustration à l'aquarelle du site de collecte à Banyuls-sur-Mer, réalisée par Michèle Parchemin.

1. Revue publiée « Diagnostics et traitements des maladies d'*Anguilla* sp. : La méthode idéale à la croisée entre conservation et aquaculture »

1.1 Avant propos

Anguilla sp. Diseases Diagnoses and Treatments: the Ideal Methods at the Cross Roads of Conservation and Aquaculture Purposes

Christelle Parchemin, Nathalie Tapissier-Bontemps, Pierre Sasal, Elisabeth Faliex

Revue de littérature publiée dans Journal of Fish Diseases le 8 mai 2022

<https://doi.org/10.1111/jfd.13634>

Publication

La revue de littérature ci-après a été publiée dans le journal « Journal of Fish Diseases » le 8 mai 2022.

Parchemin, C., Tapissier-Bontemps, N., Sasal, P., and Faliex, E (2022). *Anguilla* sp. diseases diagnoses and treatments: The ideal methods at the crossroads of conservation and aquaculture purposes. *Journal of Fish Diseases* 45, 943–969. <https://doi.org/10.1111/jfd.13634> IF : 2.58

Contexte

Comme abordé dans l'**Introduction générale**, l'anguille européenne (*Anguilla anguilla*) connaît un effondrement de sa population depuis 1970 et est considérée depuis 2008 par l'IUCN comme une espèce en danger critique d'extinction. D'autres espèces du même genre, l'anguille japonaise (*A. japonica*) et l'anguille américaine (*A. rostrata*) connaissent des effondrements de leur population et sont également considérées en danger par l'IUCN. Or ce sont les trois espèces les plus pêchées et les plus consommées par l'Homme. Les pathogènes représentent une problématique à la fois dans le milieu naturel en causant un affaiblissement de leurs populations (et par répercussion sur les pêcheries) et à la fois en anguilliculture où ils peuvent provoquer des pertes économiques importantes pour les pisciculteurs. Il existe des revues de littérature sur les parasites (Jakob et al., 2016), sur les virus (Haenen et al., 2009) ou encore sur les bactéries (Austin et al., 2012) trouvées chez l'une ou l'autre des trois espèces citées plus haut, mais pas

sur les trois. De plus, il n'existe pas de revue de littérature faisant l'état de l'art des méthodes utilisées, sur les espèces d'anguilles, pour détecter et identifier les pathogènes, et pour les traiter en prenant en compte, les aspects environnementaux, de conservation en milieu naturel et les besoins en aquaculture. C'est donc l'objet de la revue de littérature qui suit, que j'ai rédigée, et qui a été publiée dans **Journal of Fish Diseases**.

1.2 Article

***Anguilla* sp. Diseases Diagnoses and Treatments: the Ideal Methods at the Cross Roads of Conservation and Aquaculture Purposes**

Christelle Parchemin^{1,2}, Nathalie Tapissier-Bontemps¹, Pierre Sasal¹, Elisabeth Faliex²

¹ Centre de Recherches Insulaires et Observatoire de l'Environnement (CRIODE), UAR 3278 UPVD-EPHE-CNRS, Université de Perpignan - Via Domitia, 52 Av. Paul Alduy, 66860 Perpignan CEDEX, France

² CEntre de Formation et de Recherche sur les Environnements Méditerranéens (CEFREM), UMR 5110 UPVD-CNRS, Université de Perpignan - Via Domitia, 52 Av. Paul Alduy, 66860 Perpignan CEDEX, France

1.2.1 Abstract

Anguilla anguilla, *A. japonica* and *A. rostrata* are the most fished and consumed eel species. However, these species are Critically Endangered, Endangered and Endangered respectively. A combination of factors is thought to be responsible for their decline including fisheries, climate change, habitat destruction, barriers to migration, pollution and pathogens. Among them, viruses, bacteria and parasites are causing weakening of wild eels and serious economic losses for fishermen and eel farmers. Early detection of pathogens is essential to provide appropriate responses both for conservation reasons and to limit economic losses. Classic diagnosis approaches are time consuming and invasive and usual treatments e.g. antipathogenic substances are becoming obsolete because of pathogen resistance and environmental impact problems. The need for early and non-invasive diagnostic methods as well as effective and environmentally friendly treatments has increased. Vaccine development and diet supplementation have known a growing interest since their use could allow prevention of diseases. In this review, we summarize the main pathogens -viruses, bacteria and parasites- of the three northern temperate eel species, the methods used to detect these pathogens, and the different treatments used. We discussed and highlighted the need for non-invasive, rapid and efficient detection methods, as well as effective and environmentally friendly treatments for both conservation and aquaculture purposes.

Keywords: eels, illness, pathogens, detection, control

1.2.2 Introduction

Anguilla sp. are widely distributed throughout the world (Aoyama, 2009). Their life cycle starts in the ocean where they hatch as leptocephali (leaf-like small larvae of some millimeters) and migrate for several months toward their growing habitat (i.e. inland and transitional waters). After metamorphosing into glass eels (small translucent cylindrical stage of less than 10 cm), they enter inland and transitional waters, become pigmented and develop as yellow eels (growth stage). After several years of growth, they metamorphose into silver eels (future spawners) and return to the ocean to migrate to their spawning ground, reproduce and die (Cresci, 2020; van Ginneken and Maes, 2005).

Eels are of ecological importance (as food source and top predator in their freshwater and brackish habitats) and of economic importance. Huge quantities of eels, mainly *Anguilla japonica*, *Anguilla anguilla* and *Anguilla rostrata* used to be caught for direct consumption or aquaculture and this number increased up to the 70s (Dekker, 2008; FAO, 2021). While the demand for these fish is increasing, there has been a global collapse of eel populations since the end of the 70's. *A. rostrata* and *A. japonica* are now considered threatened while *A. anguilla* is critically endangered, its population being thought to have been reduced by a factor 10 (Dekker, 2008; Feunteun, 2002; IUCN, 2022; Jacoby et al., 2015). Since humans consume glass, yellow and silver stage eels, overfishing could be one factor in the population collapse of the three species; climate change, barriers to migration, pollution and pathogens (mainly viral, bacterial or parasitic infections) are also considered to be factors contributing to the decline of eel populations (Arai, 2014; Bruslé, 1994; Drouineau et al., 2018; Elie and Rigaud, 1987; Esteve and Alcaide, 2009; Haenen et al., 2009; Kirk, 2003; Knights, 2003; Palstra et al., 2006).

Efforts have been made for the recovery of eel stocks and management plans have been developed. They include fishing restriction, habitat restoration, facilitation of migration (e.g. eel ladders) and restocking programs (Bierman et al., 2012; Feunteun, 2002; Kaifu et al., 2018; Kaifu and Yokouchi, 2019; Lamson et al., 2009; Moriarty, 1990; Moriarty and Dekker, 1997; Righton and Walker, 2013). However, there is still a lack of knowledge about pathogens (e.g. prevalence of infections) as well as reliable, non-invasive detection tools and appropriate control methods.

The most cited pathogens are: viruses EVE (Egusa, 1970; Haenen et al., 2009), EVEX (Bellec et al., 2014; Haenen et al., 2012; Sano, 1976), HVA/AngHV-1 (Békési et al., 1986; Kempfer et al., 2014; Sano et al., 1990; van Beurden et al., 2010), bacteria *Edwardsiella angillarum* (Hah

et al., 1984; Joh et al., 2013), *Vibrio vulnificus* (Amaro et al., 1995; Amaro and Biosca, 1996; Dalsgaard et al., 1999; Esteve et al., 2007; Esteve and Alcaide, 2009; Haenen et al., 2014; Høi et al., 1998), *Pseudomonas anguilliseptica* (Andree et al., 2013; Ellis et al., 1983; Joh et al., 2013; Nakai and Muroga, 1982; Wakabayashi and Egusa, 1972), *V. anguillarum* (Frans et al., 2011; Hah et al., 1984; Mellergaard and Dalsgaard, 1987), and parasites *Pseudodactylogyrus anguillae* and *P. bini* (Buchmann et al., 1987) and *Anguillicola crassus* (Kirk, 2003; Køie, 1991). The latter is thought to have a significant impact on swimbladder function, especially in European and American eels (Barry et al., 2014; Kirk, 2003; Sokolowski and Dove, 2006). More generally, infections by pathogens can cause tissue damages, hemorrhages, anemia and thus general weakening and death. As a diadromous fish, migration is a critical period in the life cycle of eel and the renewal of population. Thus, infections and the resulting weakening can exacerbate the collapse of eel populations. In addition, the demand for these fish is high which implies an increased production of eels in aquaculture (FAO, 2021). In some countries such as in the Republic of Korea, eel farming is the most important freshwater aquaculture industry (Joh et al., 2011; Yi et al., 2013). Eels are fished in the juvenile stages and reared in intensive aquaculture systems. The constant renewal of juvenile eel stocks, combined with stressful farming conditions, can lead to the introduction of pathogens, development of diseases (Bruslé, 1990; Haenen et al., 2012) and important economic loss for eel farmers (Assefa and Abunna, 2018). Thus pathogens are problematic both for life cycle, renewal of the natural population and in anguiculture.

Knowledge on pathogens and outbreaks in wild and farmed eels is necessary in order to react in the right way. For example, using fish devoid of the most harmful pathogens is essential for the success of restocking programs and must only be possible via pathogen detection and the knowledge of the prevalence of infection. Early pathogen detection and effective treatments of diseases are also essential for the sustainability of eel farming. The most common methods used to detect and identify pathogens include pathogen cultures from diseased organs, serology and histology (Altinok and Kurt, 2003; Noga, 2010) but these can be time consuming and performed on already dead fish or after their sacrifice. The arrival of molecular techniques such as Polymerase Chain Reaction (PCR) amplifications, qPCR and radio techniques methods has led to the development of non-invasive methods that can detect pathogens prior to an outbreak (Altinok and Kurt, 2003). However, effectiveness is sometimes below the one of more traditional methods and their cost is often relatively high (Jousseau et al., 2021). Taken together these elements constitute a real obstacle to the use of these methods on a larger scale.

Regarding treatments, modulation of the environment and intensive use of chemicals have been employed for a long time. However, modulation of the environment, that requires a compromise between optimal conditions for growth and those that prevent the development of diseases, could result in economic loss and is not applicable in the wild. Antipathogenic substances, even though efficient for the short term, are increasingly banned because of their potential environmental impact and their ability to generate the development of resistant pathogens (Alcaide et al., 2004; Lin et al., 2016; Romero et al., 2012). There is therefore a critical need for efficient and environmentally friendly treatments for fish diseases (Lieke et al., 2020). Vaccinations and diet supplementations with plants or probiotics have received a growing interest since their use could allow the prevention of fish diseases through the stimulation of fish immunity (Gudding and Van Muiswinkel, 2013; Reverter et al., 2014).

In this review, we have focused on the three northern temperate and most fished eel species: the European eel *A. anguilla*, the American eel *A. rostrata* and the Japanese eel *A. japonica*. Focusing only on viruses, bacteria and protozoan (although a non-monophyletic group) and metazoan parasites, we have presented and summarized those that are commonly described as pathogenic for eels. We have listed the diagnosis tools used and the different treatments intended directly applied to eels. Finally, we discussed the methods, their applicability at a higher scale and we highlighted the need for more environmentally friendly and non-invasive diagnoses and treatments.

1.2.3 Eel pathogens, damages and symptoms

1.2.3.1 Viruses

Various viruses were isolates from eels and are summarized in **Table 1**. They cause major viral diseases (van Beurden et al., 2012) triggered by the Anguillid herpesvirus 1 (HVA/AngHV-1) (Békési et al., 1986; Kempfer et al., 2014; Sano et al., 1990; van Beurden et al., 2010), the Eel Virus European (EVE) (Egusa, 1970; Haenen et al., 2009) but also the two closely related rhabdovirus Eel Virus America (EVA) (Sano, 1976) and Eel Virus European X (EVEX) (Belloc et al., 2014; Haenen et al., 2012; Sano et al., 1977). Other viruses causing diseases in eels were also identified such as the Japanese eel endothelial cells-infecting virus (JEECV) that causes viral endothelial cell necrosis (VECNE) in Japanese eels and large economic losses for aquaculture (Kim et al., 2018; Mizutani et al., 2011; Okazaki et al., 2016, 2015; Okazaki-Terashima et al., 2016; Ono et al., 2003). Finally, infectious pancreatic necrosis (IPN) viruses

(Jørgensen et al., 1994), IHNV viruses (Bergmann et al., 2003; McAllister et al., 1977) were also isolated from eels. Although haemorrhagic septicaemia viruses (HSV) have also been isolated from *A. anguilla*, but no data confirmed the pathogenicity of this virus for eels (Castric et al., 1992; Jørgensen et al., 1994). In a similar way, orthomyxoviruses EV-1 and EV-2 were isolated from tumours but no clear relationship between these viruses and tumours could be demonstrated (Nagabayashi and Wolf, 1979; Neukirch, 1985; Wolf et al., 1973).

Among various direct or indirect symptoms, infected eels present haemorrhagic gills or fins and organ disorders (Shchelkunov et al., 1989; van Beurden et al., 2012; van Ginneken and Maes, 2005). For example, AnghHV1 has been reported to cause serious destructions of the gill filaments (Rijsewijk et al., 2005). The presence of viruses may also impact swimming behaviour and thus have significant effect, at least for the European eel as reviewed in Haenen et al. (2009), on eel spawning migration and thus on their overall recruitment.

Eel viruses have been detected both in wild and farmed eels (Danne et al., 2022; Haenen et al., 2010; van Beurden et al., 2012). Viruses are particularly problematic because of their ability to remain dormant, to spread through seemingly healthy populations and become virulent under certain conditions (Haenen et al., 2009). Virulence is usually associated with stress such as temperature increase (Haenen et al., 2009) or husbandry practices i.e. high stocking densities or poor water quality (Hangalapura et al., 2007; Muñoz et al., 2019). In aquaculture, reported mortalities due to viruses were, for European eels, up to 50% for EVE, around 20% for EVEX and 10% for HVA (Haenen et al., 2009). HVA infections resulted in mortality of 7% for Japanese eel (Sano et al., 1990) while experimental infection with JEECV caused 60% mortality (Ono et al., 2003). Viral infection often co-occurs or occurs with bacterial or parasitic infections (Haenen et al., 2009; Muñoz et al., 2019; van Beurden et al., 2012).

1.2.3.2 Bacteria

A significant number of bacteria has been identified as causative agents of eel diseases. Among them the most reported are: *Edwardsiella tarda*, *Aeromonas hydrophila*, *Vibrio vulnificus* and *V. anguillarum* (Amaro and Biosca, 1996; Biosca et al., 1991; Haenen et al., 2014; Hah et al., 1984; Joh et al., 2013; Tison et al., 1982). About ten other bacteria potentially pathogens and isolated from diseased eels were reported: they include *Aeromonas jandaei*, *A. aquariorum*, *A. bestiarum*, *A. caviae*, *A. salmonicida*, *A. sobria*, *A. veronii*, *Citrobacter freundii*, *Delftia acidovorans*, *E.tarda/piscida/anguillarum*, *Flavobacterium columnare*, *F. psychrophilum*, *Lactococcus garvieae*, *Mycobacterium marinum*, *Pleisomonas shigelloides*, *Pseudomonas*

anguilliseptica, *P. fluorescens*, *V. harveyi*, and *Yersina ruckeri* (**Table 2**). For most of them, their pathogenicity was confirmed by infecting healthy eels and by recording the resulting mortalities and symptoms (**Table 2**).

Some bacteria have been isolated from apparently healthy farmed eels, such as *E. tarda*, *A. hydrophila* and *V. anguillarum* (Amaro et al., 1995; Hah et al., 1984; Joh et al., 2013). These bacteria might turn into pathogenic under stress conditions such as presence of pollutants in the environment (Esteve et al., 2012; Rødsæther et al., 1977), or during warmer periods (Davis and Hayasaka, 1983; Haenen, 2019). For example, *A. hydrophila* appears to be pathogenic when the water temperature is between 17 and 22°C (Esteve et al., 1993). Similarly, at low temperature <20°C *V. vulnificus* did not induce mortality with the 50% lethal dose (LD₅₀) below 10⁸ CFU/mL, but the infection trial at 27-29°C led to high mortality rate with LD₅₀ of 8.4x10⁴ CFU/mL (Amaro et al., 1995). Bacterial infections can cause external damages to the skin, fins, mouth, eyes, tail, gills and affect internal organs: heart, liver, spleen, kidney, muscles associated with global hemorrhages and septicaemia (**Table 2**). Disease outbreaks caused by bacteria can result in important economic losses for eel farmers (Joh et al., 2013). For example, several outbreaks have been reported in Spanish eel farms resulting in the loss of 80% of elvers. The prevalence of bacterial diseases in wild eels is also of concern as it can reach significant levels. For example, 34.4% of wild eels from the Albufera lake had bacterial diseases (Esteve and Alcaide, 2009).

Among all the bacteria cited, some of them may act as primary pathogen while some others may be opportunistic acting as secondary pathogen and leading to eel co-infections (Joh et al., 2013, 2010). For example, a co-infection with *P. anguilliseptica* and *D. acidovorans* occurred in *A. anguilla* glass eels (Andree et al., 2013).

Table 1: Potential and confirmed pathogenic viruses for eels. External symptoms and Internal abbreviations: Abd: Abdomen, Cong: congestion, Dark: Darkened, Dep: Depigmentation, F: Fins, G: Gills, Hem: Hemorrhage, In: intestine, Ki: Kidney, Les: Lesion, Li: liver, Mu: muscles, Nec: Necrosis, Pet: Petechiation, Red: Reddening, Rot: Rot, S: Skin, Sp: Spleen, Swo: Swollen, Tum: Tumor, Ulc: Ulcerations. ¹Lists of symptoms and damages are not intended to be exhaustive, but include commonly encountered symptoms and damages.

Type	Viruses	<i>Anguilla</i> sp. affected	Disease name	External symptoms ¹	Internal Damages ¹	Source
Alloherpesvirus	Anguillid herpesvirus 1 (HVA/AngHV-1)	All three species	-	S/Hem,Nec ; F/Hem; G/Hem, Nec; Abd/Red	Li/Hem; Sp/Swo,Hem,Nec; Ki/Swo;	Békési 1986; Haenen 2009; Kempter 2014; Sano 1990; van Beurden 2010
Aquabirnavirus	Eel Virus European (EVE)	<i>A. anguilla</i> , <i>A. japonica</i>	Branchionephritis	S/Hem; Head/Cong; G/Swo/Cong	Glomerulonephritis	Egusa 1970; Haenen 2009
	Infectious pancreatic necrosis (IPN) viruses	<i>A. anguilla</i>	Infectious pancreatic necrosis	Overall Darkening; Abd/Swo,Hem;	Li/Dep; Sp/Dep;	Hnath 1983; Jørgensen 1994; Varvarigos 2011
Rhabdovirus	Rhabdovirus Eel Virus America (EVA)	<i>A. rostrata</i>	Rhabdoviral dermatitis	Lethargy; Anorexia; S/Les,Hem ; Head/Red;	Ki/Hem,Nec; Mu/Hem,Nec; Li/Hem,Nec;	Bellec 2014; Castric 1984; Castric and Chastel 1980; Galinier 2012; Haenen 2009, 2012; Jørgensen 1994;
	Eel Virus European X (EVEX)	<i>A. anguilla</i> , <i>A. japonica</i>		F/Cong; Abd/Cong	Pancreas/Hem,Nec	Kobayashi and Miyazaki 1996; Sano 1976; Sano 1977
Polyomavirus-like	Haemorrhagic septicaemia (VHS) viruses	<i>A. anguilla</i>	Haemorrhagic septicaemia	-	-	Castric 1992; Jørgensen 1994
	Japanese eel endothelial cells-infecting virus (JEECV)	<i>A. japonica</i>	Viral endothelial cell necrosis (VECNE)	G/Cong,Dilatation, Abnormalities; F/Red; Abd/Swo	Li/Cong; In/Cong	Kim 2018; Okazaki 2016, 2015; Okazaki-Terashima 2016; Ono 2003
Orthomyxovirus	EV-1	<i>A. anguilla</i> , <i>A. rostrata</i>	Stomatopapillomatosis	-	-	Wolf 1973
	EV-2	<i>A. anguilla</i>		-	-	Nagabayashi and Wolf, 1979; Neukirch 1985

Table 2: Potential and confirmed pathogenic bacteria for eels. External symptoms and Internal Damages abbreviations: A: Anal region, Abd: Abdomen, Cong: congestion, Dark: Darkened, Dep: Depigmentation, E: Eye, Exo: Exophthalmos, F: Fins, G: Gills, He: Heart, Hem: Hemorrhage, In: intestine, Inf: inflammation, Ki: Kidney, Les: Lesion, Li: liver, M: Mouth, Mu: muscles, Nec: Necrosis, O: Opercula, Perf: Performance, Pet: Petechiation, Red: Reddening, Rot: Rot, S: Skin, Sto: Stomach, Sp: Spleen, Swo: Swollen, T: Tail, Ulc: Ulcerations, Vaso: Vasodilatation. ¹*Edwardsiella tarda* species were recently re-affiliated to *Edwardsiella piscida* and *Edwardsiella anguillarum* species (Buján et al., 2018). ²*Aeromonas sobria* was isolated from *Anguilla anguilla* but no health status was communicated. ³*Delftia acidovorans* was isolated in a co-infection event with *Pseudomonas anguilliseptica* (Andree et al., 2013). ND: Not determined. ⁴Lists of symptoms and damages are not intended to be exhaustive, but include commonly encountered symptoms and damages.

Bacteria Species	Anguilla sp. affected	Disease	Isolated from diseased eels	Experiment to support pathogenocity against eels	LD50 (intraperitoneal injection)	External symptoms ⁴	Internal Damages ⁴	Source
<i>Aeromonas aquariorum</i>	<i>A. japonica</i>	-	Yes	ND	-	ND	ND	Yi 2013
<i>Aeromonas bestiarum</i>	<i>A. anguilla</i>	-	Yes	Yes	3.3×10^6 – 2.3×10^7 cfu.fish ⁻¹	F/Red, T/Nec		Esteve and Alcaide 2009
<i>Aeromonas caviae</i>	<i>A. japonica</i>	-	Yes	ND	-	ND	ND	Yi 2013
<i>Aeromonas hydrophila</i>	All three species	Red fin disease	Yes	Yes	10^5 to $10^{7.5}$ cfu.fish ⁻¹ , $10^{6.2}$ to $10^{7.4}$ cfu.fish ⁻¹ , $3.3 \times 10^{6-2.3} \times 10^7$ cfu.fish	S/Pet, S/Ulc	Global Hem, Septicemia	Davis and Hayasaka, 1983; Esteve, 1995; Esteve, 1993; Esteve and Alcaide, 2009; Hah, 1984; Hossain and Kawai, 2011b; Joh, 2013; Rickards and Gregg, 1978; Zhang, 2010
<i>Aeromonas jandaei</i>	<i>A. anguilla</i> , <i>A. japonica</i>	-	Yes	Yes	$10^{5.4}$ to $10^{7.5}$ cfu.fish ⁻¹ , 3.3×10^6 to 2.3×10^7 cfu.fish ⁻¹ , $10^{6.6}$ cfu.fish ⁻¹	T/Ulc	ND	Esteve 1993, Esteve 1993; Esteve and Alcaide 2009; Hossain and Kawai 2011b
<i>Aeromonas salmonicida</i>	<i>A. rostrata</i>	Furunculosis	Yes	Yes	-	skin lesion with softened and haemorrhagic dermis centres	ND	Davis and Hayasaka 1983; Hayasaka and Sullivan 1981
<i>Aeromonas sobria</i>	<i>A. anguilla</i>	-	? ²	Yes	2×10^7 cfu.fish ⁻¹ , $>10^{7.9}$ cfu.fish ⁻¹	ND	ND	Esteve 1993; Guan 2011; Hossain and Kawai 2011b
<i>Aeromonas veronii</i>	<i>A. japonica</i>		Yes	Yes	2.15×10^7 cfu.mL ⁻¹	ND	ND	Joh 2013; Songlin 2012
<i>Citrobacter freundii</i>	<i>A. japonica</i>	Tail rot disease	Yes	Yes	5.62×10^5 cfu.mL ⁻¹	T/Rot, F/Rot	ND	Cao 2016; Joh 2013

<i>Delftia acidovorans</i> ³	<i>A. anguilla</i>	-	Yes	ND	-			Andree 2013
<i>Edwardsiella tarda/piscida/anguillarum</i> ¹	All three species	Edwardsiellosis	Yes	Yes	4.55×10^4 cfu.g ⁻¹ , between $10^{4.85}$ to $10^{6.83}$ cfu.fish ⁻¹ , 1.5×10^4 to 7.4×10^5 cfu.fish ⁻¹	S/Dep,Sw,Les; G/Dep,Ulc; E/Sw; mucus oversecretion,posterior part of the body paralysis	Li/Hem, Sp/Ulc, St/Ulc, Septicemia	Alcaide 2006; Chang and Liu 2002; Chen 2011; Esteve and Alcaide 2009; Guo 2013; Hah 1984; Joh 2013; Joh 2011; Miyazaki and Egusa 1976a, 1976b, 1976c; Mohanty and Sahoo 2007; Nakai 1985; Wakabayashi and Egusa 1973
<i>Flavobacterium columnare</i>	<i>A. anguilla</i>	Columnaris	Yes	Yes	ND	G/nec,sw, hyperplastic gill epithelium, partial or total fusion of secondary gill lamellae	He/Perf,	Alvarado 1989; Egusa 1989; Foscarini 1989
<i>Flavobacterium psychrophilum</i>	<i>A. anguilla</i>	Bacterial Cold Water	Yes	ND	ND	F/Hem; Mu/hem; A/Blister;	In/Inf	Lehmann 1991; Soares 2019
<i>Lactococcus garvieae</i>	<i>A. japonica</i>	Lactococciosis	Yes	ND	-	E/Exo, O/Pet, F/Cong	In,Li,Sp,Ki/Con g,Hem	Kusuda 1991; Vendrell 2006
<i>Mycobacterium marinum</i>	<i>A. anguilla</i>	Mycobacteriosis						
<i>Pleisomonas shigelloides</i>	<i>A. japonica</i>	-	Yes	Yes	$> 10^{8.5}$ cfu.fish ⁻¹	ND	ND	Esteve 1993; Joh 2013
<i>Pseudomonas anguilliseptica</i>	<i>A. japonica, A. anguilla</i>	Red spot disease/Sekiten-byo	Yes	Yes	ND	M/Pet,Hem; O/Pet,Hem; F/Red; G/Cong,Vaso	Li/Pet,Cong, Licapsule/Nec, Ki/Cong,Vaso	Andree 2013; Ellis 1983; Haenen and Davidse 2001; Joh 2013; Michel 1992; Nakai and Muroga 1982; Wakabayashi and Egusa, 1972; Wiklund and Bylund, 1990
<i>Pseudomonas fluorescens</i>	All three species	-	Yes	Yes	$10^{7.3}$ cfu.fish ⁻¹	S/Pet, S/Ulc	-	Davis and Hayasaka 1983; Esteve 1993; Hossain and Kawai 2011b
<i>Vibrio anguillarum</i>	<i>A. anguilla</i>	Vibriosis	Yes	Yes	$10^{7.3}$ cfu.fish ⁻¹	S/Ulc, S/Pet	Sp/Sw,Cong ; Global Hem, Septicemia	Esteve 1993; Frans 2011; Hah 1984; Mellergaard and Dalsgaard 1987
<i>Vibrio harveyi</i>	<i>A. rostrata</i>	Vibriosis	Yes	Yes	1.67×10^3 cfu.g ⁻¹	S/Ulc, S/Pet	Li/Nec, Ki/Swo, Hem	Wan et al., 2021

<i>Vibrio vulnificus</i>	All three species	Vibriosis	Yes	Yes	$<3.6 \times 10^3$ cfu.fish $^{-1}$, 2.6×10^1 to 1.4×10^4 cfu.fish $^{-1}$, $<9.4 \times 10^3$ to 2.3×10^5 cfu.fish $^{-1}$	M/Red, F/Red, A/Ulc	Global Hem, Mu/Nec, Septicemia	Amaro 1995; Amaro and Biosca 1996; Dalsgaard 1999; Esteve 2007; Esteve and Alcaide 2009; Høi 1998
<i>Yersina ruckeri</i>	<i>A. japonica</i>	Enteric redmouth disease	Yes	Yes	ND	S/Dep; Abd/Red; G/Ret	Li/Red, Ki/Dark	Joh 2013, Joh 2010

1.2.3.3 Protozoan and Metazoan Parasites

Various parasites can affect eels; these are protozoan or metazoan parasites. Parasites can be ecto- or endo-parasite, they can be found on the gills, the skin and fins, in the blood and on/in almost all organs (e.g. kidney, liver, intestine, stomach...) (Jakob et al., 2016; Nagasawa and Katahira, 2017). 161 species of parasites have been isolated from specimens of *A. anguilla* in European and north African countries and are reviewed in Jakob et al. (2016). This checklist summarizes data on parasites acquired up to 2007. In the meantime, other parasite species have been isolated from European eels, including *Henneguya psorospermica*, *Cystidicola farionis*, unidentified species of *Dactylogyrus* (Dzido et al., 2020) but also *Bucephalus anguillae* (Giari et al., 2020). 50 species from Ciliophora, Microspora, Myxozoa, Trematoda, Monogenea, Cestoda, Nematoda, Acanthocephala, Hirudinida, Bivalvia, and Copepoda taxa have also been reported as parasites for *A. japonica* and *A. anguilla* in Japan and are reviewed in Nagasawa and Katahira (2017). Finally, about 63 parasites (Monogenea, Trematoda, Cestoda, Nematoda and Acanthocephala) have been reported in *A. rostrata* (Hanek and Threlfall, 1970; Hoffman, 2019; Kennedy, 2007). Among all reported species some are eel-specific parasites such as *Bothriocephalus claviceps*, *Proteocephalus microcephalus*, *A. crassus*, *P. anguillae*, or *P. bini* (Jakob et al., 2016). Although the diversity and number of parasites found in eels is huge, only a small proportion of species have been identified as true pathogens. The other species cause mainly little damage, either locally by attaching to tissues or more globally by diverting nutrients from the host to themselves, as intestinal acanthocephalans can do (Gérard et al., 2013; Kennedy, 2007). However, those little damages can become dangerous under stressful conditions especially to the gills (Kennedy, 2007; Køie, 1988). Of the parasites found in eels, the gill parasites *Pseudodactylogyrus* spp. (Buchmann et al., 1987) and the swim bladder parasite *A. crassus* (Kirk, 2003) often represent the highest prevalence (Sures et al., 1999). They are also the main confirmed harmful pathogens, although with different intensities depending on the eel species (Sokolowski and Dove, 2006) but also on factors such as temperature, salinity, eels foraging and ontogeny, or intermediate host density (Barry et al., 2017; Giari et al., 2021; Jakob et al., 2009; Li et al., 2015).

Pseudodactylogyrus bini and *P. anguillae* are two species of *Pseudodactylogyrus* occurring in eels (Buchmann et al., 1987). They were first described on *A. japonica* (Kikuchi, 1929), and have been reported in *A. anguilla* in different European countries (Buchmann et al., 1987; Mellergaard and Dalsgaard, 1987; Molnár et al., 1993) and a few years later in the American eel (Cone et al., 1993; Hayward et al., 2001). The parasites attach themselves to the gills with

hooks called "hamuli" that can cause damage to the gill tissue. When high in number and/or under stressful conditions (lack of oxygen), damage to the gills can impair the eel's gas exchange and have a sublethal effect leading to mortality (Buchmann et al., 1987; Køie, 1991).

Anguillicola crassus is a nematode, originally found on Japanese eel, which was introduced into Europe in the 1980s through the eel trade (Koops and Hartmann, 1989). This parasite was also reported in the 90s in American eels from North American Atlantic coast rivers and estuaries (Barse and Secor, 1999; Fries et al., 1996). Differences in eel species susceptibility to *A. crassus* were reported. The European and American eel are apparently more susceptible to the parasite than the original host species, the Japanese eel (Egusa, 1979). Indeed, it has been shown that the survival rate of the parasite larvae was lower in the Japanese eel compared to the European eel (60% of Japanese eels had live worms compared to 100% for European eels) (Knopf and Mahnke, 2004; Knopf, 2006). Regarding the effects of the presence of parasites on the swim bladder, no clear damage was found in Japanese eel (Nagasaki et al., 1994) whereas it causes direct damage such as inflammations, reduction of elasticity and thickening of the swim bladder wall in American and European eels (Barry et al., 2014; Dezfuli et al., 2021; Kirk, 2003; Molnár et al., 1993; Pelster, 2015; Sokolowski and Dove, 2006). These damages could lead to altered swimbladder functions and swimming ability (Newbold et al., 2015; Palstra et al., 2007; Pelster, 2015; Sjöberg et al., 2009; Sprengel and Lüchtenberg, 1991). Sprengel and Lüchtenberg (1991), showed a 19% reduction in the swimming speed of infected European eels and Newbold et al. (2015) observed a delay in downstream passage of eels with high abundance of *A. crassus*. In Hungary, an important mortality episode was attributed to *A. crassus*, eels being found to be heavily parasitized with 30-50 parasites in the swim bladders (Molnár et al., 1991). The presence of the parasite may also make eels more susceptible to secondary bacterial infection (van Banning and Haenen, 1990).

1.2.3.4 Are external symptoms sufficient to identify a causative agent?

As explained above, pathogens can cause several types of external symptoms (**Figure 1**). For example, clinical symptoms have been recorded in 122 *A. anguilla* from the Albufera Lake such as haemorrhagic fins (55%), ulcers on the opercula and anal regions (29%), reddened mouth (25%), necrosis of the tail (23%), petechiae on the belly (11%), over secretion of skin mucus (4%), and discoloured skin spots (3%). Microbial isolation was performed and multiple bacteria were identified including *V. vulnificus*, *E. tarda*, *A. hydrophila*, *A. bestiarum* or *A. jandae*. When eels were intraperitoneally infected with the bacteria and the external symptoms were recorded, bacterial infections seemingly caused the same type of clinical symptoms:

haemorrhagic fins, ulcers on opercula and anal regions, reddened mouth, oversecretion of skin mucus, discoloured skin spots (Esteve and Alcaide, 2009). Thus, the observation of external symptoms may be the first step in identifying the presence of a pathogen or the development of a disease but is not specific enough to identify the causative agent. Moreover, infections are not always accompanied by external symptoms (Hudson et al., 1981; Stewart et al., 1983) particularly in the early stages of infections, when pathogens are present at low levels. Finally, external symptoms such as haemorrhagic fins could be the result of a fight or an aggression between eels or with another species. Therefore, research and identification of a possible pathogen is essential in order to implement appropriate treatments.

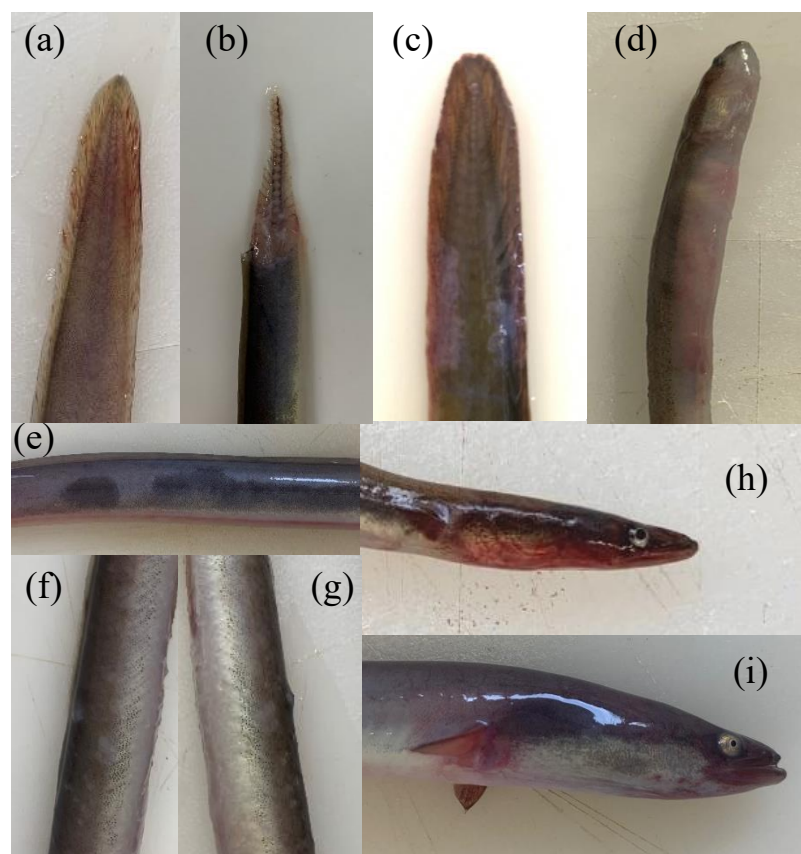


Figure 1: Illustration of common symptoms of diseases: haemorrhagic fins (a, i), necrosis of the tail (b), discolored skin spots (c, e), mucus oversecretion (f, g), haemorrhagic and reddened head and mouth (h), petechiae on the body, redness and swelling of the peritoneal cavity part (d). All photos belong to the author.

1.2.4 Causative agent identification

Detecting and identifying the pathogens responsible for a disease is an essential step in providing appropriate solutions to control outbreaks or limit the spread of pathogens. In parallel, knowledge on prevalence of pathogens in wild eel populations is essential to adapt management plans. Several methods exist to detect pathogens including pathogen cultures followed by

morphological and biochemical identifications, serology, molecular techniques such as PCR amplification (Adams and Thompson, 2011) but also radio or biomarkers detections. A summary of the methods used and applied to eels is presented in **Table 3**.

Table 3: Methods used to identify the main reported eel pathogens.

Pathogen	Detection method	Matrice	Source
Anguillid herpesvirus 1 HVA/Ang HV-1	Cell culture on specific cell-line RTG2, FHM, and EK-1 followed by electron microscopy identification and eventual seroneutralization	pooled organs	Rijsewijk, 2005; Van Ginneken, 2004; van Nieuwstadt, 2001
	ELISA test	blood	van Nieuwstadt, 2001
	PCR	pooled organs, gill fragments	Kemper, 2014; Rijsewijk, 2005
	Real-time PCR	organ suspension and infected cell cultures	van Beurden, 2016
Viruses	PCR, nested PCR	pooled organs	Nguyen, 2017
	Cell culture on specific cell-line RTG2, FHM, and EK-1; EPC, BF-2 followed by electron microscopy identification	pooled organs	Caruso, 2014; Van Ginneken, 2004
	ELISA test	infected cell cultures/whole fish/viscera/fish without heads, tails and musculature	Dixon and Hill, 1984
	Real time RT-PCR	infected cell cultures and pooled organs	van Beurden, 2011
Eel Virus European X EVEX	Duplex real time RT-PCR	pooled organs	McConville, 2018
	Cell culture on specific cell-line RTG2, FHM and EK-1 followed by electron microscopy identification	pooled organs	Van Ginneken, 2004
	Duplex real time RT-PCR	infected cell cultures/ pooled organ	McConville, 2018
	Cell culture cellobiose-colistin-polymyxin B plates	mucus, gills, and intestinal contents	Høi, 1998
<i>Vibrio vulnificus</i>	Antibody detection	blood	Le, 2018
	PCR	whole eel, liver and kidney tissues	Coleman, 1996
	Cell culture TSA supplemented with sodium chloride	organs/damaged tissues	Austin, 2017
Bacteria	Indirect ELISA	blood	Iida, 1991
	PCR	pooled organs	Lee, 2013
	Cell culture TSA, BHIA and TCBS, horse blood or nutrient agar containing 0.5 % (w/v) sodium chloride	blood/liver/spleen/kidney/damaged tissues	Andree, 2013; Haenen and Davidse 2001; Wakabayashi and Egusa 1972
Parasites	Microscopic examination	dissected swimbladder	Sures, 1999
	Competitive ELISA	blood	Inui, 1999
	Indirect ELISA	blood	
	Radio detection	swim bladder	Beregi, 1998
	Ultrasound	swim bladder	Frisch, 2016
<i>Pseudomonas anguilliseptica</i>	PCR	faeces	De Noia, 2022; Jousseaume, 2021
	Microscopic examination	gill filaments, entire gill arches	Larrat, 2012; Monni and Cognetti-Varriale, 2002

1.2.4.1 Classic isolation

The classical identification approach consists of combining isolation, culture (specially for viruses and bacteria) and/or identification of pathogens by microscopic/histological, chemical or molecular methods. For example, the *Herpesvirus anguillae* (HVA) was isolated through organ grinding, centrifugation, and culturing on eel kidney (EK-1) cells. Electron microscopy was used to confirm the type of virus (rhabdovirus in this case) and specific identification was achieved by seroneutralization (van Nieuwstadt et al., 2001). Similarly, after inoculation of organ samples from eels (single organ or pool of various crushed organs) on specific cell lines: RTG2 - Rainbow Trout Gonad cells, FHM – Fat Head Minnow cells, and EK-1, observation of cytopathic effect and microscopy, EVEX, HVA and EVE were detected, isolated and identified (van Ginneken et al., 2004).

In a similar way, pathogenic bacteria can be isolated from lesions or crushed organs using antibiotic-enriched media or specific agar plates (e.g. TCBS plates for *Vibrio* sp., Sheep Blood Agar, Cytophaga Agar or Shieh Medium for *Flavobacterium* spp.) (Alcaide et al., 2004). Then, the morphology, phenotype and biochemistry of the isolates can be compared with those of reference bacteria (Caruso et al., 2014; Haenen and Davidse, 2001). Usually, to be identify as the causative agent for an occurring outbreak, the bacterium must fit the Koch's postulates: the microorganism is found in diseased organisms, is grown in pure culture, induces the disease when inoculated into healthy organisms and must be reisolated from these newly diseased organisms. For example, in an outbreak in an eel farm in Japan, the observed clinical symptoms, apparently those of the red spot disease, were attributed to *P. anguilliseptica*. The causative bacterium was isolated from the blood, liver or kidneys of diseased eels on blood-enriched media, the morphology described and physiological and biochemical tests were performed for its identification. The morphological characteristics led to the classification of the bacterium in the genus *Pseudomonas*, and due to some specific differences with other *Pseudomonas* sp., the bacterium was apparently attributed to *P. anguilliseptica*. Finally, the isolate obtained was used to experimentally infect healthy eels. The infected eel developed the same symptoms as those of the farmed eels. However, the bacterium was not reisolated from the newly infected organisms (Wakabayashi and Egusa, 1972). Thus, even if application of the Koch's postulates is quite robust in identifying pathogens, recent studies have highlighted the need to adapt Koch's postulates to include the whole bacterial communities and their interactions as they can influence diseases (Byrd and Segre, 2016). In addition, some bacterial species responsible for new diseases might not be cultured under laboratory conditions (Austin, 2017). In addition to,

or instead of, morphological and biochemical tests, and, to increase the robustness of bacterial identification at a species level, 16S rDNA sequencing can be performed.

The isolation and identification of parasites is a very long, fastidious and delicate process: the whole body of the fish being observed under stereomicroscope, opened following standard protocols, then parasitic species isolated for direct morpho-anatomical observations under a microscope or after histological staining (Sures et al., 1999). Thus, the identification of parasites is based on the observer's knowledge, ability to distinguish morphologically similar parasites, skills in taxonomy and available literature. Nevertheless, in the case of targeted studies on known eel parasites such as *Pseudodactylogyrus* spp. and *A. crassus*, their presence can be detected more easily by targeting the examination to specific organs: the gills for the former and the swim bladder for the latter. In the case of *Pseudodactylogyrus* spp. the classical approach consists of microscopic observations of the gill filaments and the parasites themselves (morpho-anatomical recognition on the sclerotized parts involved in their fixation) (Monni and Cognetti-Varriale, 2002). Gill biopsies can also be performed but the prevalence of parasites using this technique was lower (20%) than the prevalence found by complete microscopic observation of the entire gill arches (70%) (Larrat et al., 2012). For *A. crassus*, its morphological identification is quite easy, the only tricky point being the identification of L3 and L4 larval stages, very difficult to distinguish, and which is often done only according to their size (Blanc et al., 1992; Sures et al., 1999).

Thus, classical methods are easy to set up and relatively cheap but the identification of pathogens is long and may require very special qualifications as for parasite identifications. These methods have the disadvantage of, most of the time, having to sacrifice organisms. In a context of conservation of eels and optimization of eel farming as well as routine detection of pathogens, these processes appear less and less feasible. Thus, there is a need for rapid and non-invasive identification methods to quickly apply treatment after detection of pathogens and to select the appropriate treatment depending on the pathogen.

1.2.4.2 Antibodies detection

Pathogens can also be detected by the presence of specific antibodies or antigens, mainly using enzyme-linked immunosorbent assay (ELISA) tests. The advantages are that these tests are relatively non-invasive since they can be performed on blood samples from eel's caudal vein and do not need a pathogen isolation to be performed. This type of detection method has been employed for detection of various types of eel pathogens. ELISA tests have been used to detect

the presence of HVA antibodies in eel sera (van Nieuwstadt et al., 2001). They have also been used to detect Anti-*A. hydrophila* antibodies in *A. anguilla* after experimental infection. Blood samples were collected at 1,4, 7, 14 and 28 days post-infection and the optical density of serum was read to infer the presence and amount of antibodies. Serum OD values were significantly higher since the first day post-infection, which confirmed the possibility of detecting *A. hydrophila* infection by ELISA tests (Guo et al., 2013). Finally, ELISA tests have been performed to detect the presence of *A. crassus* in eels (Höglund and Pilström, 1994; Inui et al., 1999; Knopf et al., 2000). However, these tests based on *A. crassus* wall antigens performed on blood samples from European eels showed a positive predictive value but low specificity and predictive negative value (Knopf et al., 2000). Various types of ELISA tests exist, such as the competitive ELISA developed to detect antibodies to *A. crassus* in *A. japonica*. The positive detection rate and the false positive rate were compared with those of a conventional indirect ELISA method. They were 95% and 5% for the competitive ELISA and 80% and 20% for the indirect ELISA (Inui et al., 1999).

Thus, the above studies showed that ELISA tests are relatively successful and could be applied on some types of pathogens that can be viruses, bacteria or parasites. The identification and detection of a pathogen by antibodies and antigens detection have the advantages of being relatively non-invasive, easy to set up and results can be obtained rapidly. However, when using these methods, specific features must be taken into account such as specificity or the risk of false positives, especially in the case of parasites sero-diagnosis where antibodies may cross-react (Knopf et al., 2000). In addition, a positive test based on antibodies detection against a specific pathogen may result from a previous infection and may not reveal a current infection. For example, HVA antibodies have been detected before an experiment, and did not increase after a recrudescence of the virus (van Nieuwstadt et al., 2001). Knopf et al. (2000) also pointed out that ELISA tests may not be applicable for *A. crassus* diagnostic purposes since in wild populations with high parasite prevalence, the currently non-infected (negative) eels could not be detected, probably because of previous contact with these parasites and of antibodies persistence in these individuals. For aquaculture purposes, the test remains very specific but needs an *a priori* idea of the type of pathogens responsible for the disease. In conclusion, ELISA tests are more applicable for management and eel immune responses studies (if the aim is to detect and follow the presence of a single pathogen), but may only be applicable in certain conditions, such as experimental studies or field survey where low prevalence of the pathogen allow the detection of the negative eels.

1.2.4.3 PCR amplification

Invasive methods

Most of the methods mentioned above have been described as laborious and time consuming. Also, in addition to the detection issues previously listed, infections may not be detected if the amount of pathogen present in the sample is below the test's sensitivity threshold (Adams and Thompson, 2011). The development of molecular techniques using Polymerase Chain Reaction (PCR) amplification of DNA can provide other possibilities of pathogen identification (Ador et al., 2021). PCR methods allow rapid identification of genetic material from pathogens with results available within a day or less (Coleman et al., 1996). Routinely deployed, PCR could allow early detection of pathogens, and appropriate actions could be quickly set up before outbreaks. Detection of various types of eel pathogens such as viruses, bacteria or parasites can be performed using PCR amplification. For example, a sensitive PCR was developed to detect HVA in eel tissue (Rijsewijk et al., 2005). In the same perspective, a two-step real time reverse transcriptase PCR assay has also been developed to detect EVEX virus (van Beurden et al., 2011). Similarly, PCR amplification has been developed to detect *V. vulnificus* in *A. anguilla* pre-infected with the bacterium (Coleman et al., 1996). Although PCR currently allows detection of a single pathogen per reaction, the development of Multiplex-PCR assays with the development of multiplex kits including specific primers directed against more than one pathogen could allow detection of multiple pathogens in a single reaction (Adams and Thompson, 2011). To date, multiple pathogens have not yet been detected using these techniques on eels, but they have already been used to identify different types of parasites in a single reaction on goldfish (Jaruboonyakorn et al., 2022), different species of bacteria (*V. parahaemolyticus*, *Salmonella* spp. and *Escherichia coli*) on fish products (Triwibowo et al., 2020).

It should be noted, however, that genetic material of pathogens may persist over time, preventing any evidence of ongoing infection or infectious agents (Hiney, 2001). Classical isolations could improve PCR detections but have the disadvantage of adding steps to the detection processes. PCR applicability in the wild or in ponds is still low since it requires specific and costly machines. In addition, a first DNA extraction step is required which is time consuming, requires equipment and can be costly if kits are used. However, the democratization of these techniques could make them more accessible with regard to their cost. Finally, PCR amplification is mainly performed on pooled organs (**Table 2**) which makes this method invasive.

Non-invasive methods

Non-invasive methods for the detection of DNA from *A. crassus* in eel faeces have also been developed (De Noia et al., 2022; Joussemae et al., 2021). De Noia et al. (2022) used a pair of parasite-specific DNA primers (designed from the most conserved regions within the ten cytochrome oxidase subunit 1 (COI) available gene sequences) for PCR amplification while Joussemae et al. (2021) designed three new pairs of primers to amplify three *A. crassus* specific microsatellite markers to optimize specificity. In both cases the robustness of the method was determined by comparing results with microscopic examinations of the swim bladder to check for the presence of the parasite. Time for DNA extraction and PCR amplification was relatively quick. The method could also be performed in the wild since it was highlighted that the whole machinery necessary for performing the test was small and could be used with a battery (De Noia et al., 2022).

1.2.4.4 Other non-invasive methods

Various other less invasive approaches have been developed. A radio diagnostic based method has been used to detect inflammation on the swim bladder caused by *A. crassus* (Beregi et al., 1998). However, this method needs costly equipment and the success of the method is dependent on the quality of the image. Ultrasound has also been used as a detection tool for *A. crassus* but, although able to detect moderately infected animals, the technique was not sensitive enough for the diagnosis of low-infected eels. Finally, this technique could not be applied on severely infected animals (Frisch et al., 2016). Although non-invasive, these methods do not make it possible to give more precise information on the parasite such as its developmental stage or the presence of eggs. The color of the anal region of eels was also used as a diagnostic tool for *A. crassus* infection, with greater redness of the anal region of eels being significantly correlated with *A. crassus* infection. Thus, the use of anal redness as a rapid indicator of the infection by the parasite has been proposed with caution as anal redness can have multiple other causes and validation of the indicator is therefore required (Crean et al., 2003).

Finally, the detection of diseases-specific biomarkers using metabolomics could be a non-invasive alternative method since metabolomics analyses can be performed on blood, mucus or faeces samples with minimal impact on the animal. In addition, it is an inexpensive, quick and easy method to identify the presence of pathogens (Low et al., 2017). Metabolomics relies on the study of small molecules in an organism. Thus, any change in metabolite levels can be

statistically detected between groups (Johnson et al., 2016). To our knowledge, this method has not yet been evaluated on eels, but metabolomics using GC-MS has already been used in survival vs death crucian carps (*Carassius auratus*) challenged with 5×10^6 CFU/mL *E. tarda*. 67 metabolites including amino acids, carbon sources, lipids and nucleotides were found to be differentially detected in the different fish groups (Guo et al., 2014). Similarly, ¹H-NMR metabolomics was used to study the responses of metabolite expression in Atlantic salmon *Salmo salar* exposed to *A. salmonicida*. Lipids and choline-residues were metabolites that most contributed to the observed differences in the metabolite profiles of survivors, control and dead fish (Solanky et al., 2005). These molecules could be used as biomarkers for disease detections, however the specificity of the method is poor and does not allow a precise identification of pathogens.

The different methods listed above present a combination of advantages and disadvantages, none of them being applicable to all situations. The use of one method over another is often dependent on factors such as ease of implementation, speed of action, cost, invasiveness but also the purpose of the identification. For example, budgets allocated to projects to identify sites with the lowest prevalence of parasites for conservation purposes are different from those allocated for the identification of pathogens in aquaculture outbreaks. The following table summarizes the main factors in choosing a method over another (**Table 4**).

Table 4: Comparison of the different methods used to identify pathogens responsible for a disease. ¹ Whether methods can be applied on Bacteria, Viruses or Parasites. ² Scale based on whether a non-specialist could easily use the method. ³ Scale based on the estimated cost of consumables and heavy equipment ⁴High for results obtained in few hours, Medium for more than 12 hours. ⁵ High for identification to species level, low for detection of disease state only. ^{6,7}Differences lie in the spatial scale in which to implement the method which is higher in the natural environment. ⁸ High: the use of the method results in the sacrifice of the animal, Low: low animal impact.

Method	Pathogens ¹	Easy to implement ²	Cost ³	Rapidity ⁴	Specificity of identification ⁵	Application in natural environment ⁶	Application in aquaculture ⁷	Invasiveness ⁸
<i>Classic isolation (from organs)</i>	Bacteria, Viruses	Relatively High	Relatively low	Medium	Relatively high	Limited	Medium	High
<i>Classic isolation (from wounds)</i>	Bacteria, Viruses	Relatively High	Relatively low	Medium	Relatively high	Limited	Medium	Medium
<i>Classic isolation (parasites)</i>	Parasites	Relatively high	Low	Relatively High	High	Limited	Medium	High
<i>Antibodies (blood from caudal vein)</i>	All	Medium	Relatively High	Medium	Relatively High	Limited	Limited	Relatively low
<i>PCR amplification (from organs)</i>	All	Medium	High	High	High	Limited	Limited	High
<i>PCR amplification (from faeces)</i>	<i>A. crassus</i>	Medium	High	High	High	Medium	Limited	Relatively Low
<i>Radio detection/Ultrasounds through eel</i>	<i>A. crassus</i>	Medium	High	High	Low	Medium	Medium	Low
<i>Detection of diseases-specific biomarkers</i>	All	Medium	Medium	Medium	Low	Medium	Medium	Low

1.2.5 Potential treatment

1.2.5.1 Modulation of abiotic parameters in anguilliculture

Due to the interaction between pathogen virulence and abiotic factors (temperature, salinity...), the spread of the disease in aquaculture can often be controlled by a simple modification of these factors. For example, an increase or a decrease in temperature or salinity might turn off the pathogenicity of some pathogens. This practice has been successfully applied to control outbreaks in eel farms (Mellergaard and Dalsgaard, 1987).

The virulence of various eel viruses was described as temperature dependent (van Beurden et al., 2012). Consequently, the modulation of the rearing temperature might avoid intense mortalities. For example, the optimal temperature for virus development were established for EVE (15 °C and 23 °C), for EVEX (10 °C and 15 °C), and for HVA (20 °C and 26 °C) (Haenen et al., 2009; Shchelkunov et al., 1989). Viruses can survive outside of these temperature ranges at a dormant state, but illness does not develop in the host (Haenen et al. 2009). To illustrate the impact of water temperature, mortality of fry rainbow trout infected with EVA virus was found to decrease with the decrease of the rearing temperature (26 % at 20 °C, 0 % at 15 °C and 2 % at 10 °C) (Nishimura et al., 1981). The same observations were made for fry rainbow trout infected with EVEX (Nishimura et al., 1981). Conversely when Japanese eels were infected with a rhabdovirus (EVA/EVEX-like AM92 strain), Kobayashi et al. (1999), reported a maximum rate of moribund individuals and/or exhibiting cutaneous lesions for a rearing temperature of 15 °C this rate decreased to zero at 25 °C. From these previous studies, it appears that the temperature-dependent susceptibility of fish to a given virus may differ according to the fish species. For example, at low temperature, eels could be more susceptible to EVEX virus than trouts. In case of bacterial infection, mortality due to a disease outbreak apparently caused by *P. anguilliseptica* was controlled by increasing water temperature in a Danish eel farm (Ellis et al., 1983; Mellergaard and Dalsgaard, 1987; Muroga et al., 1973). Similarly, in a Scottish eel farm, an epizootic of *P. anguilliseptica* was eradicated, when raising the water temperature to 26-27°C (Stewart et al., 1983).

Regarding the impact of salinity on the pathogenicity of bacteria and therefore their control, it has been shown that vibriosis caused by *V. anguillarum* does not occur in freshwater (Mellergaard and Dalsgaard, 1987). On the contrary, the pathogenicity of *A. hydrophila* could be inactivated by an increase of salinity (Mellergaard and Dalsgaard, 1987). In general, low salinity has been associated with lower prevalence of *A. crassus* in eels (Giari et al., 2021; Li

et al., 2015). This was verified in particular through a compilation of *A. crassus* prevalence data from 28 sampling sites in Europe (Giari et al., 2021). Lower salinity was also reported to impact hatching, survival and infectivity of *A. crassus* larvae (Kennedy and Fitch, 1990; Kirk et al., 2000). For example, larval infectivity lasted 8 days in 100 % sea water versus 80 days in freshwater. Similarly, salinity had a negative impact on hatching and survival of the larvae (Kirk et al., 2000). Finally, no *Pseudodactylogyrus* sp. has been reported in *A. anguilla* sampled in a marine environment with salinity between 32 and 35 (Jakob et al., 2009). As for *A. crassus*, a modulation of salinity could allow the control of *Pseudodactylogyrus* sp. infections.

These studies highlight the importance of global knowledge on pathogens and conditions of their development as well as the complexity in choosing the rearing conditions to optimize the growth of the fish while avoiding pathogens development. Modulating rearing conditions is a quick, easy and inexpensive way to control pathogens virulence and may be sufficient, in the short term, to stop mortalities. However, for long term efficiency, conditions may need to be maintained which may lead to additional costs in aquaculture and may provide ideal conditions for other pathogens. Finally, this practice is absolutely not applicable in the wild for conservation purposes.

1.2.5.2 Antipathogenic substances administration

Another possibility to treat or prevent diseases is by chemical administration. These may include antivirals, antibiotics and anthelmintic molecules. They can be administered through food or bath treatments and usually lead to good results. Some of them also have a broad range of activity and may act on different pathogens. However, a growing number of studies have highlighted the emergence of antimicrobial resistance (Defoirdt et al., 2011; Romero et al., 2012; Santos and Ramos, 2018). The susceptibility of *A. salmonicida* and *A. hydrophila* strains isolated from American eels to 18 different antibiotics has been assessed. While most antibiotics were effective against the isolates, the susceptibility of *A. hydrophila* to nitrofurazone isolated monthly varied greatly over time which could be a barrier to the use of this antibiotic in aquaculture (Davis and Hayasaka, 1983). In two eel Spanish farms, the first with high and the second displaying lower densities of fish, the potential resistance of some fish pathogenic bacteria to oxolinic acid (OXA), oxytetracycline (OTC), sulfamethoxazole-trimethoprim (SXT) and nitrofurantoin (NIT) was assessed. A significant number of the isolated bacteria were resistant to the antibiotics tested especially against SXT in the farm with high density of fish (Alcaide et al., 2004). This latest study highlights the limits of the use of antibiotics in eel farming in a context of high demand for eels and therefore an increase in eel production.

The efficiency of nematicidal drugs on eel platyhelminths is rather limited as they present several disadvantages. For example, drugs (such as metrifonate, fenbendazole, mebendazole, and ivermectin), used both in food and water baths to control *A. crassus*, may have solubility problems which constitute a limiting factor for treatment efficiency. No clear results (elimination of the parasites) were found although damaged worms were detected (Taraschewski et al., 1988). Potassium permanganate, sodium chloride, ammonia, formaldehyde and trichlorfon have been used against *Pseudodactylogyrus* sp. as reviewed in Buchmann et al. (1987). In most cases, the intensity of the infection was reduced, but some molecules had an impact on eels: ammonia induced mortality at a certain concentration and sodium chloride induced mucus sloughing. In European eels, for example, a treatment with 0.5 and 1 mg/mL mebendazole used against *Pseudodactylogyrus* sp. infection eliminated all adults and postlarvae after 4 days but also induced an oversecretion of mucus as a side effect (Mellergaard, 1990). Finally, in some cases, specimens of *Pseudodactylogyrus* sp. from European eels have shown resistance to mebendazole and flubendazole treatments while the use of praziquantel, another anthelmintic drug, has significantly reduced the prevalence and abundance of this parasite in eels (Buchmann, 2011).

These studies highlight the fact that chemical, although easy to use, efficient and with a broad range of action can induce pathogen resistances to drugs not only for bacteria but also for parasites as well as negative impacts on the fish (Buchmann et al., 1987). In addition to drug resistances and negative impacts on fish, the use of chemicals can lead to the release of products whose potential persistence might induce negative impact in the environment (Gothwal and Shashidhar, 2015; Preerna et al., 2020; Weston, 1996). Moreover, some studies have shown that, regarding parasite infections, although effective in the first few days, stopping treatment led to a resumption of the parasitosis (increase in parasites number) (Geets et al., 1992; Mellergaard, 1990). In summary, there is a strong need for new treatments: that are effective in the long term (or very effective in the short term and capable of reducing the presence of pathogens to zero), do not induce pathogen resistance phenomena, do not alter negatively the physiology of fish and have no impact on the environment.

1.2.5.3 Vaccination

Vaccination can prevent the development of diseases. Vaccines against several species of bacteria and parasites, including *V. vulnificus*, *E. tarda*, *A. hydrophila*, *A. sobria* and *A. crassus* (**Table 5**) have been developed. Most of them consist of formalin-killed cells or outer membrane protein (Omp) of the pathogens (**Table 5**). For example, a vaccine was developed

against *V. vulnificus* in Spain (Collado et al., 2000). After testing different types of vaccine, a final formulation consisting of a toxoid-enriched bacterin from *V. vulnificus*, inactivated with formalin and heated, was selected for its efficiency. This vaccine, called Vulnivaccine, was used in a Spanish eel farm (Fouz et al., 2001). Vaccination consisted in the immersion of glass eels in water containing the vaccine at three different times after the arrival of the glass eels. The immune response and protection induced by vaccination was studied by the presence of antibodies and by challenging glass eels with the pathogen. The relative percentage of survival ranged from 62 % to 86 % demonstrating the protective effect of the vaccination. Vulnivaccine was then administrated by oral and anal intubation, intraperitoneal injection and prolonged immersion (Esteve-Gassent et al., 2004a). Oral and anal intubation showed the best efficacy in protecting eels against vibriosis, with a cumulative mortality under 10 %. Since efficacy is limited to six months, the possibility of reimmunization has also been studied and an oral vaccine that could be administered to any stage of eel's life has been developed (Esteve-Gassent et al., 2004b). Other outer membrane proteins (Omp)-based vaccines have been developed, the most used being OmpU, OmpA and OmpII from *V. vulnificus*, *E. anguillarum* and *A. hydrophila* respectively (**Table 5**). After vaccination and challenge with a given pathogen, eels vaccinated with Omp generally had significantly higher relative survival than those vaccinated with control solution (Guo et al., 2019, 2020; He et al., 2020; Le et al., 2018; LiHua et al., 2019).

Vaccination has also been used to prevent infection and development of *A. crassus* in *A. japonica* and *A. anguilla*. *A. crassus* infective larvae (L3) were attenuated by irradiation with ^{135}Cs and then orally administered to several groups of eels. After challenging immunized and control eels with L3 larvae, results showed that the number of *A. crassus* adults was significantly reduced in immunized *A. japonica* compared to the control. However, the treatment did not appear to be effective for *A. anguilla*. (Knopf and Lucius, 2008). While most vaccines are developed to protect against a single pathogen, promising bivalent (Guan et al., 2011; Guo et al., 2019) and trivalent (Zhao et al., 2020) vaccines are also being developed and could protect against different pathogens.

Vaccination appears to be a good alternative to the use of chemicals, and it may prevent diseases before their apparition. However, in most studies vaccines are intraperitoneally-injected, which is difficult to implement on a larger scale and even more in natural conditions. Vaccination by immersion has shown good results and would be suitable for eel farms. The development and democratization of vaccines on a larger scale could make them even more accessible. Although

vaccination has already been tested against many bacterial infections and one eel parasite, to our knowledge no vaccine has yet been developed against eel viruses. Thus, complementary studies are necessary for this purpose but also to study the long term efficiency of the protection against pathogens. The inclusion of vaccinated eels in restocking programs could be considered in the future.

Table 5: Summary of the different vaccines developed and used to protect eels against bacteria and parasites. List of abbreviations: Omp: Outer membrane protein; FKC: Formalin-killed cells. IP: Intraperitoneal injection; I: Immersion; OA: Oral Administration; AA: Anal administration. CM: Cumulative mortality (%); RPS: Relative percentage survival (%); SR: Survival rate (%); RIPR: Relative Immune Protection Rate. Vv: *Vibrio vulnificus*; Va: *Vibrio anguillarum*; Ea: *Edwardsiella tarda/anguillarum*; Ah: *Aeromonas hydrophila*, As: *Aeromonas sobria*.

Vaccination against	Anguilla sp.	Type of vaccine	Method of vaccination	Efficiency (Measured Parameter)	Efficiency	Source
<i>Monovalent vaccine</i>						
<i>Ah</i>	<i>A. anguilla</i>	Omp (46kD maltoporin) of <i>Ah</i>	IP	CM	Ah B10: 45% (Control), 20% (FKC), 10% (Omp); Ah B11: 95% (Control), 50% (FKC), 35% (Omp); Ah B15: 35% (Control), 0% (FKC), 0% (Omp); Ah B19: 22% (Control), 0% (FKC), 0% (Omp); Ah B20: 100% (Control), 32% (FKC), 10% (Omp);	Feng, 2017
<i>Ah</i>	<i>A. anguilla</i>	OmpF and rOmpK of <i>Ah</i>	IP	RIPR	35.5% (OmpF); 70% (OmpK)	Zhang, 2019
<i>Ea</i>	<i>A.japonica</i>	Eel or rabbit hyperimmune anti <i>Ea</i> sera	I	SR	<25% (Control), 30 to 50% (Anti <i>Ea</i> sera)	Kusuda, 1991
<i>Ea</i>	<i>A.japonica</i>	FKC or sonicated products (SP) of <i>Ea</i>	OA	RPS	<10% (Control), 75% (FKC), 25% (sonicated products)	Salati, 1991
<i>Ea</i>	<i>A.japonica</i>	Egg yolk IgY anti <i>Ea</i>	OA		Absence of <i>Ea</i> in the intestine	Gutierrez, 1993
<i>Ea</i>	<i>A.japonica</i>	FKC or lipopolysaccharide (LPS) of <i>Ea</i>	IM	CM	Trial 1: 100% (Control), 87.5% (FKC); Trial 2: 80% (Control), 60% (FKC); Trial 1: 90% (Control), 57% (LPS); Trial 2: 80% (Control), 40% (LPS)	Gutierrez and Miyazaki, 1994
<i>Ea</i>	<i>A.japonica</i>	Formalin, pressure and electric current inactivated bacterin of <i>Ea</i>	IP	SR	0% (Control), 70% (Formalin), 85% (Pressure), 38% (Electric current)	Hossain and Kawai, 2009
<i>Ea</i>	<i>A.japonica</i>	Formalin, formalin with heat, heat, potassium chloride, tannic acid, citric acid, pressure and electric current killed cells of <i>Ea</i>	IP	CM	>70% (Control), 25% (Formalin), 45% (Formalin with heat), 65% (Heat), ND (potassium chloride), ND (tannic acid), 65% (citric acid), <10% (pressure), 60% (electric current killed cells)	Hossain, 2011a

<i>Ea</i>	<i>A.japonica</i>	Formalin, formalin with heat, citric acid, pressure and electric current inactivated cells of <i>Ea</i>	IP	CM	70% (Control), 10% (Pressure), 30% (Formalin), 50% (Formalin heat), >60% (Electric current and citric acid)	Hossain, 2012
<i>Ea</i>	<i>A. anguilla</i>	<i>Ea</i> ghosts	IP, I, OA	RPS	<i>Ea</i> ghosts: 75% (IP), 52.5% (IM), 37.5% (OA); Formalin killed cells: 55% (IP), 40% (IM), 32.5% (OA)	Li, 2014
<i>Ea</i>	<i>A.japonica</i>	FKC of <i>Ea</i>	I, OA	RPS	67.4% (Control), 64% (Immersion 5mg/mL), 25.2% (Immersion 10 mg/mL), 58.5% (Oral 10mg/g), 65.1% (Immersion (5 mg/mL) + Oral (10 mg/g)), 32.2% (Immersion (10 mg/mL) + Oral (10 mg/g))	Jung, 2015
<i>Ea</i>	<i>A.japonica</i>	OmpA of <i>Ea</i>	IP	CM	90% (Control), <20% (Omp)	LiHua, 2019
<i>Ea</i>	<i>A.japonica</i>	FKC of <i>Ea</i> starch hydrogel-based oral (SHO)	OA	SR	<50% (Control), 75% (SHO1), >80% (SHO4 and 8)	Jun, 2020
<i>Ea</i>	<i>A.japonica</i>	OmpA of <i>Ea</i>	IP	CM	90% (Control), <20% (Omp)	He, 2021
<i>Vv</i>	<i>A. anguilla</i>	Formalin (with or without heating (H) inactivated whole cells bacterin with (WCB) or without toxoids (TWCB); + opaque (o) or translucent cells (t) attenuated live vaccines (LCV) and purified lipopolysaccharides (LPSV) = WCBFo, WCBFt, WCBHo, WCBHt, TWCBHo, TWCBHt	IP and I	RPS	ND (Control), 79.6% (WCBFo), 54.9% (WCBFt), 74.6% (WCBHo), 25.5 (WCBHt), 92.7% (TWCBHo), 49.2% (TWCBHt), ND (LCV), 2.72% (LPSV)	Collado, 2000
<i>Vv</i>	<i>A. anguilla</i>	Vulnivaccine (FKC and extracellular products = toxoid-enriched bacterin)	I	% bacterial survival in surface mucus	300% (Control), 75% (Vaccinated eels)	Fouz, 2001
<i>Vv</i>	<i>A. anguilla</i>	Vulnivaccine (FKC and extracellular products = toxoid-enriched bacterin) Frozen (FV) or lyophilised (LV)	I	RPS	65% (FV), 75% (LV)	Esteve-Gassent, 2004a
<i>Vv</i>	<i>A. anguilla</i>	Omp-ISCOMs of <i>Vv</i>	IP	RIPR	100% (200µg/ml), 87.5% (100µg/ml), 75% (50µg/ml), 50% (25µg/ml)	Xu, 2012
<i>Vv</i>	<i>A.japonica</i>	OmpU of <i>Vv</i> or FKC of <i>Vv</i>	IP	RPS	0% (Control), 80% (Omp), 60% (FKC)	Le, 2018
<i>A. crassus</i>	<i>A. anguilla, A. japonica</i>	Infective larvae (L3) attenuated with 135Cs irradiation	OA	-	<i>A japonica</i> : number of parasites significantly decreased. <i>A anguilla</i> : no decrease	Knopf and Lucius, 2008

<i>Bivalent vaccine</i>						
<i>Ah, As</i>	<i>A. anguilla</i>	OmpG of <i>Ah</i>	IP	SR	<i>As B10</i> : 40% (Control), 85% (Omp); <i>Ah B27</i> : 30% (Control), 60% (Omp); <i>Ah B33</i> : 15% (Control), 75% (Omp)	Guan, 2011
<i>Ea, Ah</i>	<i>A. rostrata</i>	Omp with porin II of <i>Ah</i> and OmpS2 of <i>Ea</i> or bivalent FKC of <i>Ah</i> and <i>Ea</i>	IP	RPS	<i>Ah</i> : 0% (Control), 50% (FKC), 50% (Omp); <i>Ea</i> : 0% (Control), 50% (FKC), 37.5% (rOmp)	Guo, 2013
<i>Vv, Ah</i>	<i>A. rostrata</i>	Omp with OmpU of <i>Vv</i> and porinII of <i>Ah</i> or bivalent FKC of <i>Vv</i> and <i>Ea</i>	IP	CM	<i>Vv</i> : 100% (Control), 60% (FKC), 50% (Omp); <i>Ah</i> : 100% (Control), 37.5% (FKC), 50% (Omp)	Guo, 2015
<i>Ea, Vv</i>	<i>A. japonica</i>	Omp with Omp A of <i>Ea</i> and Omp U of <i>Vv</i> or bivalent FKC of <i>Ea</i> and <i>Vv</i>	IP	SR	<i>Ea</i> : 50% (Control), 100 % (Omp); <i>Vv</i> : 40% (Control), 83% (Omp)	Guo, 2019
<i>Vv</i>	<i>A. anguilla</i>	Vulnivaccine (FKC and extracellular products = toxoid-enriched bacterin)	IP, I, OA, AA	CM	<i>Vv</i> serovar E: >60% (Control), 35% (I), 10% (IP), 0% (OA), <10% (AA); <i>Vv</i> serovar A: 60% (Control), 37% (I), 0% (IP), <10% (OA), 0% (AA)	Esteve-Gassent, 2004b
<i>Ea, Vv, Ah</i>	<i>A. anguilla</i>	Omp with OmpA of <i>Ea</i> and OmpII <i>Ah</i>	IP	CM	<i>Ah</i> : 60% (Control), 50% (Freund's incomplete adjuvant), 10% (Omp); <i>Ea</i> : 90% (Control), 80% (Freund's incomplete adjuvant), 40% (Omp); <i>Vv</i> : 90% (Control), 80% (Freund's incomplete adjuvant), 50% (Omp);	Guo, 2020
<i>Trivalent vaccine</i>						
<i>Ea, Vv, Ah</i>	<i>A. japonica</i>	Omp with OmpU of <i>Vv</i> , OmpA of <i>Ea</i> , OmpII of <i>Ah</i> or trivalent FKC of <i>Vv</i> , <i>Ea</i> and <i>Ah</i>	IP	CM	<i>Ah</i> : 60% (Control), 50% (Freund's incomplete adjuvant), 20% (Omp); <i>Vv</i> : 90% (Control), 80% (Freund's incomplete adjuvant), 50% (Omp); <i>Ea</i> : 90% (Control), 80% (Freund's incomplete adjuvant), 70% (Omp);	He, 2020
<i>Ea, Vv, Ah</i>	<i>A. japonica</i>	Omp with OmpU of <i>Vv</i> , OmpA of <i>Ea</i> , OmpII of <i>Ah</i> or trivalent FKC of <i>Vv</i> , <i>Ea</i> and <i>Ah</i>	IP	CM	<i>Vv</i> : B88 100% (Control), 90% (FKC), 80% (Omp); <i>Ea</i> : B79 >90% (Control), 80% (FKC), 50% (Omp); <i>Ah</i> : B11 90% (Control), 80% (FKC), 50% (Omp)	Zhao, 2020

1.2.5.4 Diet supplementation

Alongside vaccination and in response to the issues surrounding the use of antibiotics, plant, probiotic and other natural product derivative supplementations to enhance fish immunity and their disease resistance have shown promising results in the past leading today to their growing interest. Hundreds of studies have reported that their use in diet positively impacts fish physiology, immunity and disease resistance (Reverter et al., 2014, 2021; Thanigaivel et al., 2016; Vallejos-Vidal et al., 2016). By colonizing the gut, probiotics may increase host resistance to pathogens (Gatesoupe, 1999). On the other hand, plants and algae, are known for their high nutritional value (proteins, B12 vitamins...) and for exhibiting several activities (antioxidant, antibacterial, antiviral...) which can protect but also optimize fish growth (Thanigaivel et al., 2016; Wan et al., 2019). Several attempts to add probiotics and/or plants to eel feed followed by pathogen challenges have also been made. These include probiotic bacteria (Chang and Liu, 2002; Lee et al., 2013, 2017), association of a bacterium and mannooligosaccharides (S. Lee et al., 2018), alternative protein sources (Garcia-Gallego et al., 1998), and various other natural product derivatives (Bae et al., 2008, 2012; Choi et al., 2008; Huang et al., 2020; S. Lee et al., 2018) (**Table 6**).

Most of the experiments were conducted with *A. japonica*, few ones with *A. anguilla* and to our knowledge none with *A. rostrata*. They showed an increase in growth performance, e.g. Japanese eels whose diet was supplemented with 10^7 or 10^8 CFU/mL *B. subtilis* had significantly greater weight gain compared to the control group (106 and 107 % vs 101 % respectively) (Lee et al., 2017). An increase in disease resistance has also been highlighted in some studies. For example, the survival rate of *A. japonica*, challenged with *E. tarda* and fed with a supplemented diet comprising quartz porphyry and stimulants BAISM, ranged from 40 to 60 % nine days post-infection compared to 0 % in control fish (Bae et al., 2008). **Table 6** summarizes the protocols and results of the studies in which eel diets were supplemented and challenged with pathogens to study their disease resistance.

Thus, food supplemented with probiotics or other compounds or stimulants have shown good results in strengthening eels' immune system and their disease resistance against several known eel pathogens: *V. anguillarum*, *E. tarda*, *A. hydrophila* and *P. fluorescens*. Long term studies are needed to find out whether resistance to disease decreases over time and therefore whether the supplemented diet should be applied continuously. In terms of applicability in the wild, if the increase in disease resistance is permanent, the use of supplemented feed could be a good alternative to boost the immunity and resistance of eels that are part of restocking programs. To

be suitable, the diet should be constituted of available and stable resources such as cultivable or invasive plants or algae. Furthermore, there is a necessity of data regarding disease resistance against viral and parasitic infections because to date, the first feed supplementation trials applied to eels have only focused on resistance to bacterial diseases.

Finally, as for pathogen identification, the selection of a treatment over another depends on factors such as its cost, ease of implementation, speed of action, short and long term efficiencies, but also its potential impact on the environment. The following table/figure summarizes the main factors discussed above in choosing a treatment over another (**Table 7**).

Table 6: Summary of methods and results obtained for diet supplementation to enhance eel disease resistance. Abbreviations: IP: Intraperitoneal injection, OA: Oral administration ND: Not determined.

Diet supplemented with	Anguilla sp.	Weight (g)	Administration Dose	Duration (weeks)	Challenge pathogens	Pathogen administration	Dose for bacterial infection (CFU.mL ⁻¹)	Mortality recorded for (days)	Efficiency against disease (significant survival rates)	Reisolation from infected fish	Source
Probiotics											
<i>Enterococcus faecium</i> SF68 or <i>Bacillus toyoi</i>	<i>A. anguilla</i>	30	Food 1x10 ⁻² g/mL sprayed over 1000 g	2	<i>Edwardsiella tarda</i>	OA	1% v/bw 7x10 ⁸	14	Yes with <i>E. faecium</i> No with <i>B. toyoi</i>	ND	Chang and Liu, 2002
<i>Lactobacillus pentosus</i> PL11	<i>A. japonica</i>	25.62 ± 2.54	Food 10 ⁸ cfu.g ⁻¹	4	<i>Edwardsiella tarda</i>	IP	0.1 mL of 3.5 × 10 ⁸	7	No	Yes	Lee, 2013
<i>Bacillus subtilis</i> WB60 (BS) and <i>Lactobacillus plantarum</i> KCTC3928 (LP)	<i>A. japonica</i>	8.29 ± 0.06	Food BS or LP at 10 ⁶ CFU/g diet at 10 ⁷ CFU/g diet at 10 ⁸ CFU/g diet Food Combinaison of BS at: 0.0 × 10 ⁷ CFU/g diet, or 0.5 × 10 ⁷ CFU/g diet, or 1.0 × 10 ⁷ CFU/g diet, and M at: 0 or 5 g/kg diet	8	<i>Vibrio anguillarum</i>	IP	0.1 mL of 5 × 10 ⁷	10	Yes	Yes	Lee, 2017
<i>Bacillus subtilis</i> WB60 (BS) and mannaoligosaccharide (M)	<i>A. japonica</i>	9.00 ± 0.11		8	<i>Vibrio anguillarum</i>	IP	0.1 mL of 5 × 10 ⁷	10	After 10 days survival range 40-60% vs <25% control	ND	Lee, 2018
Natural product derivatives											
korean mistletoe extract	<i>A. japonica</i>	200	Food 0.1, 0.5, 1%	2	<i>Aeromonas hydrophila</i>	IP	0.1 mL of 3x10 ⁶	14	11 days PI: 26,6% (control), 33,3, 66,6 80 (0.1, 0.5, 1%).	ND	Choi, 2008
quartz porphyry (QP) and feed stimulants BAISM (BS)	<i>A. japonica</i>	15 ± 0.3	Food 0.7% QP+0,0,3,0,5,0,75,1 % BS	8	<i>Edwardsiella tarda</i>	IP	0.1 mL of 1x10 ⁶	15	Yes after 4 days PI for all	ND	Bae, 2008
propolis	<i>A. japonica</i>	7.7 ± 0.22	Food 0.25, 0.5, 1, 2, 4%	12	<i>Edwardsiella tarda</i>	IP	0.1 mL of 3x10 ⁶	10	Significant differences in the first 3 days PI	ND	Bae, 2012

yellow loess	<i>A. japonica</i>	11.5 ± 0.4	Food, 5, 10, 20 g/kg	20	<i>Edwardsiella tarda</i>	IP	0.1 mL of 2x10 ⁷	14	Relative per cent survival higher in diet supplemented groups (ctrl: 0%, 21 to 38% for diets)	Yes	Lee, 2018
--------------	--------------------	------------	-------------------------	----	---------------------------	----	-----------------------------	----	---	-----	-----------

Table 7: Comparison of the main potential treatments to control or improve disease resistance in fish. ¹ Scale based on whether a non-specialist could easily use the method. Scale based on the estimated cost of consumables and heavy equipment. ³ High for complete disappearance of disease symptoms or mortality few days after administration, Medium in case of treatment more preventive than curative. ⁴ Low when use leads to unsustainable additional cost or development of other pathogens or resistant organisms, "?" for data that are still preliminary or not available. ⁵ Medium: can be applied under specific conditions (release of vaccinated or diet supplemented eels in the natural environment). ⁶ Limited: due to cost and ease of implementation.

Method	Easy to implement ¹	Cost ²	Short term Efficiency ³	Long term Efficiency ⁴	Application in natural environment ⁵	Application in aquaculture ⁶	Main risk	Tested against		
								Viruses	Bacteria	Parasites
Modulation of abiotic parameters	High	Low	Relatively High	Low	No	Medium	Trade/off growth/ elimination pathogen	Yes	Yes	Yes
Antipathogenic substances	High	Medium	High	Low	No	Medium	Resistance and environmental impact Weak response	Yes	Yes	Yes
Vaccination	Medium	High	Medium	?	Medium	Limited	Inefficiency on all fishes	No	Yes	Yes
Diet supplementation	Medium	High	Medium	?	Medium	Limited	Inefficiency against all pathogens Weak response	No	Yes	No

1.2.6 Conclusion

While the consumption and demand for eel continue to increase, *A. japonica*, *A. anguilla* and *A. rostrata* still experience very low stocks. Some organisms, including viruses, bacteria and parasites, can be pathogenic to eels which can lead to economic losses for eel farmers and could even be a significant factor in overall populations weakening of eels.

The early detection of pathogens and their identification is therefore an essential step in the fight against diseases. Effective methods of early detection of disease could also lead to effective and relevant management plans based on knowledge of diseases (appearance, prevalence, environmental factors...) and their potential preventions. Particular attention should be paid to the management of stocks, both in the context of aquaculture and the restocking of natural populations, in order to avoid the exchange of pathogens and their introduction into new environments as in the case of *A. crassus*.

Most detection methods are invasive and results are usually obtained in more than one day. Regarding parasite detections, non-invasive methods such as radio/ultrasonic detection or detection from eel faeces have been developed, but they may not be as effective as conventional methods. Finally, the development of portable devices and multiplex kits including specific primers directed against more than one pathogen could allow detection of multiple pathogens in a single reaction and, applied on non-invasive matrices appears as the most promising pathogen detection method applicable in both wild environment and anguilliculture.

It should also be noted that many potential pathogens have been isolated from apparently healthy eels showing no signs of disease (EVE, EVA, EVEX, *E. tarda*, *A. hydrophila*, *V. anguillarum*...) emphasizing that an eel can carry pathogens without ever developing disease. Also, as methods become more sensitive, they could detect past infections, intact/fragmented or non-viable pathogen fragments. Thus the reaction to a positive result should always be accompanied by a consideration of the risk involved (risk of symptom development, risk of spread, risk of economic loss) and thus an appropriate response.

Following pathogen identification, a rapid, effective and adapted action is often necessary. In anguilliculture, modulation of abiotic parameters and antivirals, antibiotics and/or antiparasitic drugs have long time been used and are still used. However, their use is and will be reduced due to supplementary cost, drug resistance for pathogens and molecules persistence in the environment. Thus, other types of treatments that can allow the prevention of diseases are being developed. Vaccination for example shows promise especially since development of bi and tri-

valent vaccines could provide one-step protection against multiple pathogens species at once. However, to date, few vaccines have been developed against eel parasites or viruses. Efforts should therefore be focused on this as well as on strengthening the data on long-term protection and the need for reimmunization or not. Finally, the incorporation of probiotics and plants in eel food is now known to enhance their immune system and make them more resistant to multiple pathogens such as *E. tarda*, *V. anguillarum* or *A. hydrophila*. However, more data on the resistance of these eels challenged with other types of bacteria, viruses and parasites, on whether or not continued supplementation is necessary to maintain protection as well as long-term follow-ups on the protection provided by supplementation are needed to conclude on the potential of supplemented diets as a replacement for chemical use. These methods however, seem difficult to apply in the natural environment unless diet supplemented or vaccinated eels are included in restocking programmes.

To conclude, in this review, we have summarized i) the main pathogens, viruses, bacteria and parasites, of the three northern temperate eel species *A. anguilla*, *A. japonica* and *A. rostrata*, ii) the methods used to detect diseases and pathogens and, iii) the different treatments used. Finally, we have highlighted the need for non-invasive, rapid and efficient detection methods as well as effective and environmentally friendly treatments, as an essential prerequisite to be taken into account in management plans, particularly when considering endangered species, or during any action intended to preserve biodiversity.

1.3 Ce qu'il faut retenir

Cette revue de littérature avait pour objectif un état de l'art sur les différents pathogènes déjà isolés et provoquant des maladies chez l'anguille européenne, l'anguille japonaise et l'anguille américaine, et sur les différents moyens de détection et de traitements utilisés ou en cours de développement.

J'ai souligné le besoin de détecter et d'identifier de façon précoce les agents pathogènes comme étape essentielle dans la lutte contre les maladies en anguiculture, mais aussi d'apporter des connaissances permettant une gestion plus efficace et pertinente des populations naturelles. Les méthodes de détection initiales sont souvent invasives et lentes, ce qui a mené au développement de nouvelles méthodes non léthales comme l'utilisation d'ultrasons ou la recherche d'ADN dans les fèces, mais ces méthodes ne se révèlent pas aussi efficaces que celles qui sont invasives. Il faut également porter une attention particulière au fait que, les méthodes devenant de plus en plus sensibles, elles pourraient conduire à détecter des infections passées, des fragments d'agents pathogènes intacts/fragmentés ou non viables.

Concernant les méthodes de traitement en anguiculture, l'utilisation d'antiviraux, d'antibiotiques et/ou d'antiparasitaires paraît aujourd'hui de moins en moins envisageable tant pour des problématiques liées à l'apparition de pathogènes résistants que de pollutions environnementales. Une alternative est la modulation des paramètres abiotiques, mais cette méthode peut entraîner des surcoûts significatifs et si elle peut empêcher le développement de certains pathogènes, elle peut en favoriser d'autres. Ainsi, la vaccination et l'immunostimulation par l'alimentation s'imposent comme les méthodes les plus prometteuses, grâce à leurs aspects préventifs et plus respectueux de l'environnement, mais elles nécessitent encore des recherches et du développement pour évaluer leurs effets à long terme avant de pouvoir être déployées.

Finalement, cette revue permet d'introduire et d'expliciter le choix des deux pathogènes utilisés dans la thèse (le parasite *Anguillicola crassus* et la bactérie *Edwardsiella anguillarum*) ainsi que l'objectif principal de la thèse à savoir l'incorporation d'algues dans l'alimentation d'anguilles européennes comme traitement préventif et/ou curatif pour lutter contre les pathogènes qui affectent cette espèce.

2. Les algues du genre *Asparagopsis*

2.1.1 Généralités

Le genre *Asparagopsis* appartient au Phylum des Rhodophyta (algues rouges), à la classe des Florideophyceae et à la famille des Bonnemaisoniaceae. Plusieurs espèces ont été décrites pour ce genre mais seules *Asparagopsis armata* Harvey, 1855 et *A. taxiformis* (Delile) Trevis, 1845 sont communément acceptées par la communauté scientifique (Dixon, 1964). Elles ont un cycle de vie hétéromorphe trigénétique haplodiplophasique (succession de trois générations/stades de formes différentes dont l'une est haploïde (le gamétophyte) et les deux autres diploïdes (le carposporophyte microscopique « parasite » du gamétophyte femelle et le tétrasporophyte) (Feldmann, 1939) (**Figure 2**). Le stade gamétophyte est la morphologie communément décrite pour les deux espèces tandis que le stade tétrasporophyte a longtemps été considéré comme une autre espèce (Feldmann et Feldmann, 1942) et a été nommé "*Falkenbergia rufolanosa* (Harvey) Schmitz, 1897" et "*Falkenbergia hillebrandii* (Bornet) Falkenberg, 1901" pour *A. armata* et *A. taxiformis* respectivement. Ces algues peuvent aussi se propager par multiplication végétative.

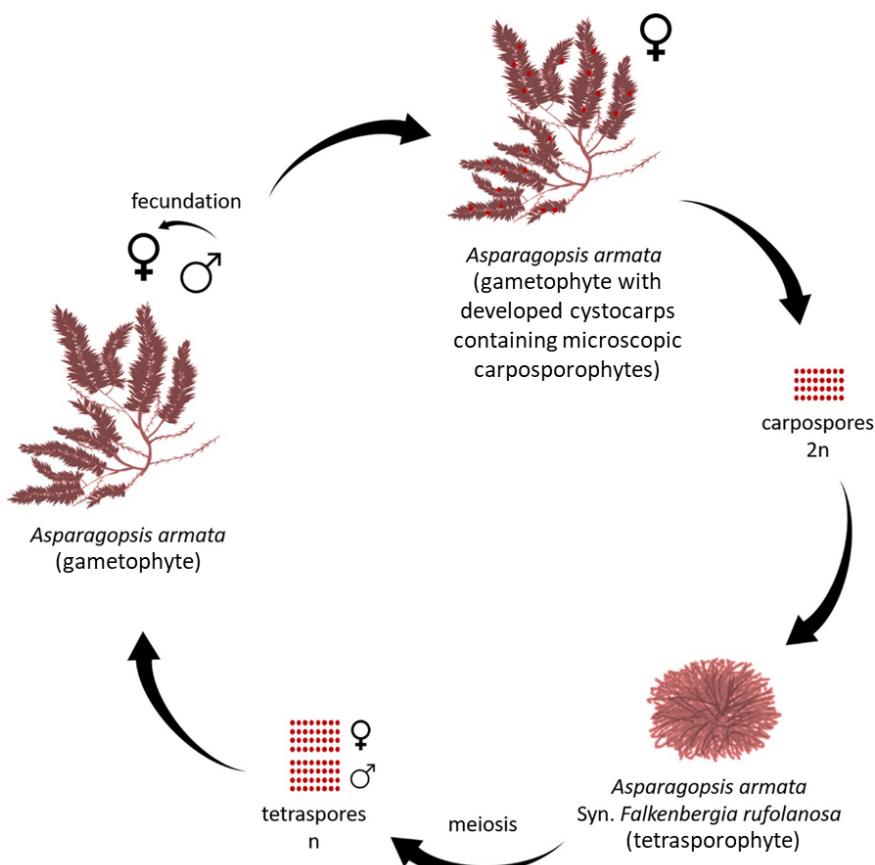


Figure 2 : Cycle de vie d'*A. armata* adapté de Félix et al. (2021).

Pour les deux espèces, le gamétophyte mesure jusqu'à 30 cm de hauteur, est d'aspect plumeux et sa couleur peut aller de jaune à rouge foncé. Le thalle est composé de plusieurs axes principaux dressés et reliés par des stolons rampants. Les axes principaux sont ramifiés avec des rameaux secondaires (Andreakis et al., 2004). Contrairement à *A. taxiformis*, *A. armata* possède des stolons supplémentaires en forme de « harpon » (**Figure 3**). Cette distinction est le principal critère de différentiation morphologique des deux espèces dans leur stade gamétophyte (Andreakis et al., 2004). Le tétrasporophyte est quant à lui plus petit et composé de filaments très fins formant de petites boules duveteuses assimilables à des « pompons » (**Figure 3**). Les stades tétrasporophytes des deux espèces ne sont pas distinguables morphologiquement, bien que par des observations microscopiques certains caractères comme la longueur et la largeur des cellules apicales et axiales paraissent les différencier (Zanolla et al., 2014).



Figure 3 : Tétrasporophytes et gamétophytes d'*A. armata* avec présence de stolons en forme de « harpons » dont quelques-uns sont indiqués par les flèches blanches. Crédits photo : C. Parchemin.

Les deux espèces sont cosmopolites mais présentent une aire de répartition différente. Majoritairement distribuée dans les eaux tempérées, *A. armata* a été décrite pour la première fois dans l'ouest de l'Australie (Harvey, 1855) mais pourrait être originaire de Nouvelle-Zélande. *Asparagopsis taxiformis* est plutôt retrouvée dans les zones tropicales à tempérées « chaudes ». Dans les zones tempérées « chaudes » les deux espèces peuvent vivre en sympatrie, c'est le cas dans certains endroits de Méditerranée comme dans le sud de l'Espagne, du Portugal, ou encore de l'Italie.

La première observation d'*A. armata* en mer Méditerranée a été faite en Algérie en 1923 (Feldmann et Feldmann, 1942). Depuis lors, cette espèce est devenue abondante sur toutes les côtes françaises. Sur les côtes méditerranéennes, l'algue a tendance à former de larges tapis ou

« amats » (**Figure 4**). Dès 2002, elle est considérée comme une espèce envahissante (Boudouresque et Verlaque, 2002) et depuis 2006, selon un rapport établi par Streftaris et Zenetos (2006), elle est classée dans les 100 espèces "Worst Invasives" en Méditerranée. Contrairement à *A. armata*, *A. taxiformis* est peu présente sur les côtes françaises métropolitaines, bien qu'elle fasse l'objet d'observations récurrentes de Marseille jusqu'à Menton en passant par la Corse (Greff et al., 2017b). En revanche, elle est très présente sur les côtes des départements d'outre-mer : en Polynésie Française, en Nouvelle Calédonie, à Mayotte ou encore à La Réunion.



Figure 4 : Tapis d'*A. armata* à Banyuls-sur-mer (Nord-Ouest Méditerranée) lors d'un échantillonnage. Crédits photo : P. Sasal.

Ces deux espèces sont considérées comme cryptique et sont composées de plusieurs populations non distinguables par leur morphologie mais avec des différences génétiques significatives. Les données les plus récentes font état, pour *A. armata*, de deux lignées principales comportant chacunes deux « sous-ensembles » (L1A, L1B, L2A et L2B) (Preuss et al., 2022) et pour *A. taxiformis*, de 6 lignées (L1 à L6) (Andreakis et al., 2016). La population d'*A. armata* envahissante et présente en Europe correspond à L1A. Les populations méditerranéennes d'*A. taxiformis* correspondent majoritairement à L2 qui, avec les lignées L1, L3 et L4 ont des distributions assez larges tandis que les lignées L5 et L6 ont des distributions plus restreintes, globalement autour de l'Australie et de la Nouvelle Zélande avec quelques individus dans le Pacifique notamment en Polynésie française (Andreakis et al., 2016 ; Dijoux et al., 2014).

La culture des deux espèces est déjà réalisée ou en cours de développement. En France, seule l'espèce *A. armata* est cultivée. C'est l'entreprise Algues et Mer (Île d'Ouessant, Bretagne) qui réalise sa culture depuis la fin des années 1990 pour la production d'un extrait antibactérien et antifongique pour la cosmétique (Moigne, 1998). Le tétrasporophyte peut être cultivé en

condition « indoor » car il ne nécessite pas de surface d’encrage (**Figure 5A, B**), contrairement au gamétophyte qui a besoin d’un support pour s’attacher. La culture du gamétophyte d'*A. armata* est généralement réalisée par multiplication végétative. Ainsi, les gamétophytes collectés dans le milieu naturel (océan) sont fragmentés puis accrochés grâce à leurs stolons en forme de harpon sur des filières, avant d’être immergés dans l’océan pour y effectuer leur croissance (Wright et al., 2022 ; Zanolla et al., 2022a). En revanche, cette technique est plus difficilement applicable pour le gamétophyte d'*A. taxiformis* qui ne dispose pas des mêmes structures pour s’attacher. L’une des possibilités pour sa culture est la réalisation de la totalité de son cycle à partir du tétrasporophyte à savoir : la fixation naturelle des tétraspores sur une filière elle-même entourée autour d’une corde, et la croissance des gamétophytes jusqu’à un stade suffisant pour supporter le déploiement dans l’océan (Batista, 2020 ; Zanolla et al., 2022a) (**Figure 5C**).

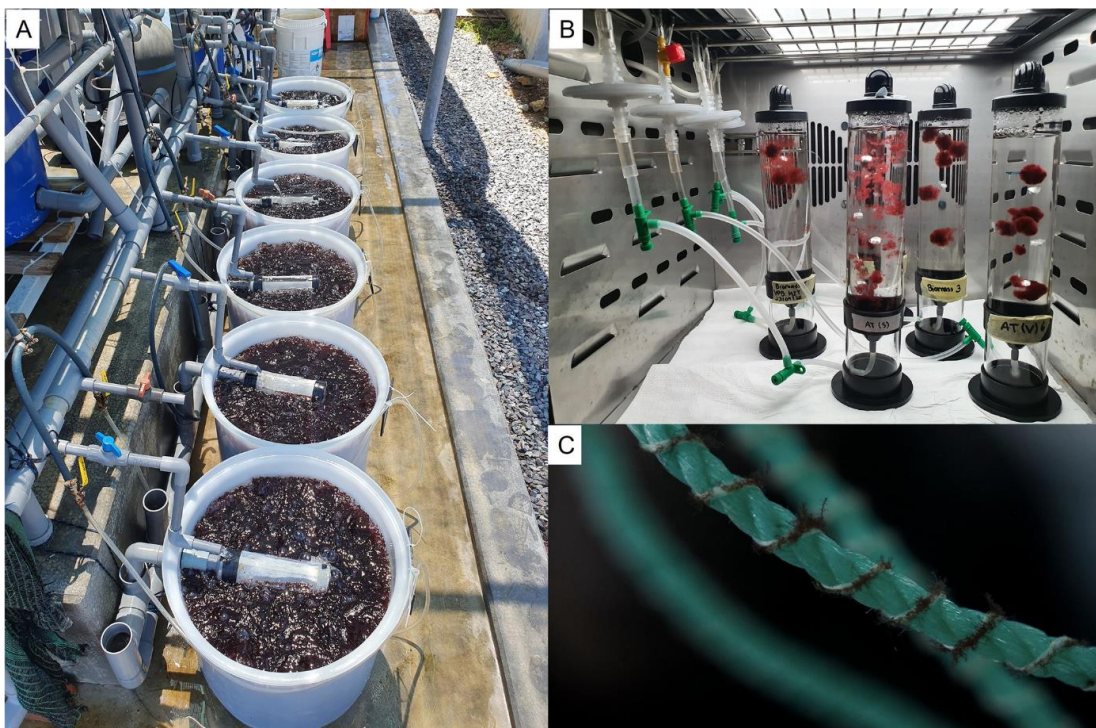


Figure 5 : Cultures de tétrasporophytes d'*A. taxiformis* dans un système en plein air au Vietnam (A) (Crédits : L. Mata dans Zanolla et al., 2022a). Cultures de tétrasporophytes d'*Asparagopsis* sp. pour servir de stock pour la production de tétraspores, dans un incubateur (B) (Crédits : L. Mata dans Zanolla et al., 2022a). Semis de gamétophytes d'*A. taxiformis* attachés à une filière et enroulés autour d'une corde, prêts à être déployés dans l'océan pour être cultivés au Vietnam (C) (Credits : P. Brix dans Zanolla et al., 2022a).

2.1.2 Composition chimique et activités décrites des algues du genre *Asparagopsis*

Les algues sont, pour la plupart, composées à 90% d'eau. Leur composition peut ensuite se diviser en métabolites primaires, dont la production est nécessaire pour la croissance et la

reproduction, et en métabolites secondaires (ou spécialisés) qui regroupent les molécules produites en réaction à des stress abiotiques (liés à l'environnement tels que des périodes d'émersion, d'ensoleillement intense...) ou biotiques (communication, défenses contre les prédateurs ou contre le biofouling...) (Demain et Fang, 2000).

La composition chimique du stade gamétophyte du genre *Asparagopsis* est assez bien documentée, contrairement à celle du stade trétrasporophyte. Les études relatives à la composition chimique du gamétophyte ont débuté dans les années 60-70 avec la description de molécules halogénées produites par ces algues (abordées en 2.1.2.2). La composition chimique du stade gamétophyte d'*A. armata* a d'ailleurs récemment fait l'objet de deux revues de littérature (Félix et al., 2021 ; Ponte et al., 2022). Les teneurs et la composition en métabolites énoncés ci-dessous concernent, sauf mention contraire, les stades gamétophytes.

2.1.2.1 Métabolites primaires

Chez *A. armata* et *A. taxiformis*, le taux de protéines reporté est compris entre 5 et 18 % de la masse sèche. Les principaux acides aminés sont l'acide glutamique (1,82 et 1,91 % de la masse de matière sèche pour *A. armata* et *A. taxiformis* respectivement) et l'acide aspartique (1,49 % de la masse de matière sèche pour les deux espèces), les autres acides aminés représentant moins de 1 % de la masse de matière sèche (Pellegrini, 1969).

La teneur en lipides des macroalgues est généralement assez faible (1-4 % de la masse de matière sèche en moyenne). Chez *A. armata* et *A. taxiformis* elle est de 2,5 et 4,7 % de la masse de matière sèche respectivement (El-Baroty et al., 2007 ; Zemke-White et Clements, 1999). Les acides gras majoritaires sont l'acide palmitique et l'acide myristique chez *A. armata* (Pereira et al., 2012 ; Pinto et al., 2022) alors que chez *A. taxiformis* les acides gras identifiés comme majoritaires sont l'acide linoléique et l'acide palmitique (El-Baroty et al., 2007). On peut aussi trouver des sulfolipides et des phospholipides. Les deux espèces contiennent également des stérols. Majoritairement du cholestérol mais aussi du desmostérol et du 22-déhydro-cholestérol chez *A. armata* (Combaut et al., 1979 ; El Hattab et al., 2006 ; Lopes et al., 2011) et du cholestérol et du stigmastérol chez *A. taxiformis* (El-Baroty et al., 2007).

Concernant la composition pigmentaire, *A. armata* et *A. taxiformis* possèdent des phycobiliprotéines dont la teneur de 0,3316 % de la masse de matière sèche pour *A. taxiformis*, dépasse celle des chlorophylles (0,06 % de la masse de matière sèche) (El-Baroty et al., 2007). Parmi les phycobiliprotéines, les plus abondantes dans le tetrasporophyte d'*A. armata* (Zanolla et al., 2022a) sont la phycoérythrine, la phycocyanine et l'allophycocyanine avec des teneurs

de $11,46 \pm 0,35$ mg/g de matière sèche pour la phycoérythrine, $72,13 \pm 1,74$ mg/g de matière sèche pour la phycocyanine et, dans le gamétophyte d'*A. taxiformis*, 0,145 % de la masse de matière sèche pour la phycoérythrine et 0,185 % g de la masse de matière sèche pour l'allophycocyanine (El-Baroty et al., 2007).

Enfin, les glucides peuvent être séparés en deux groupes : les mono et disaccharides, et les polysaccharides. Les mono et disaccharides sont pour la plupart des glucides de réserve comme le floridoside et l'iso-floridoside. Les polysaccharides sont dits de structure ou pariétaux puisqu'ils composent la paroi des végétaux et des algues en particulier. Les polysaccharides d'*A. armata* ont été caractérisés comme étant des carragénanes (type xi- et pi- ainsi que gamma- et psi- sulfatés) et des agars (Haslin et al. 2000 ; Garon-Lardiére, 2004).

2.1.2.2 Métabolites secondaires

Les métabolites secondaires retrouvés chez *A. armata* et *A. taxiformis* sont principalement des métabolites halogénés. Des mycosporines-like-amino-acids (principalement la palythine, la shinorine et l'astérine-330) (Figueroa et al., 2008 ; Lalegerie et al., 2019 ; Zanolla et al., 2022b), des flavonoïdes, des composés phénoliques ou encore des terpénoïdes (El-Baroty et al., 2007) ont également été reportés dans ces deux algues.

Les métabolites halogénés dans les algues du genre *Asparagopsis* ont commencé à être étudiés dans les années 1970 principalement par chromatographie gazeuse couplée à la spectrométrie de masse (GC-MS) (Burreson et al., 1975, 1976 ; McConnell et Fenical, 1977 ; Woolard et al., 1976, 1979a). Ce n'est que très récemment que la chromatographie liquide couplée à la spectrométrie de masse à haute résolution a été utilisée, ce qui a permis de décrire de nouvelles molécules halogénées (Pinto et al., 2022 ; Thapa et al., 2020). Les différentes études ont révélé la présence d'une grande quantité de composés volatils halogénés : des haloformes (Burreson et al., 1975), des alcanes halogénés à chaîne courte, des cétones (Burreson et al., 1976), des alcools (Woolard et al., 1976), des acides carboxyliques (Woolard et al., 1979) ou encore des acides acryliques (Kladi et al., 2004) halogénés.

Parmi toutes ces molécules, le bromoforme (CHBr_3) est décrit comme le dérivé halogéné le plus abondant. Il a d'abord été décrit comme le principal constituant de l'huile essentielle d'*A. taxiformis* (Burreson et al., 1975). Sa quantification a montré que cette molécule pouvait représenter jusqu'à 5% de la masse sèche de l'algue (Paul et al., 2006). Dans une étude récente, Romanazzi et al. (2021) ont mesuré des teneurs en bromoforme de 20 mg/g et de 10 mg/g en masse sèche dans des extraits d'*A. taxiformis* et d'*A. armata* respectivement. L'acide

dibromoacétique est également significativement majoritaire, représentant jusqu'à 3% de la masse sèche d'*A. armata* (Paul et al., 2006a).

Jusqu'à l'utilisation plus récente de la LC-MS et notamment en haute résolution, la majorité des dérivés halogénés décrits étaient des molécules possédant une chaîne carbonée courte (C1-C4) et un nombre d'halogènes inférieur à 4. **Ce dernier élément est d'ailleurs utilisé, dans la suite du manuscrit, comme critères de distinction entre les molécules dites faiblement halogénées (=low halogenated molecules) et les molécules hautement/fortement halogénées (=high halogenated molecules).** Avant le début de cette thèse, seules deux études faisaient références à des molécules hautement halogénées extraites d'*A. taxiformis* (Greff et al., 2014 ; Sugano et al., 1990). Ainsi, ont été isolées, en 1990, par un fractionnement bioguidé, des enolacétates de formules brutes C₅HBr₇O₂ et C₅Br₈O₂ (Sugano et al., 1990) et en 2014, par un fractionnement chimioguidé en UHPLC-DAD-ELSD, deux cyclopenténones, la mahorone et la 5-bromomahorone (Greff et al., 2014). Très récemment, grâce à la LC-MS, un ion intense sur les chromatogrammes d'extraits d'*A. taxiformis* (tétrasporophyte) avec un *m/z* de 572.49 ± 0.05 Da (*m/z* du pic le plus intense de l'amas isotopique), a été proposé comme étant une 1,1,1,5,5,5-hexabromo-2,4-dione de formule brute C₅H₂Br₆O₂, sur la base de spectres de fragmentation MSⁿ (Thapa et al., 2020). Dans le même travail, d'autres 2,4-dione halogénées ont également été caractérisées : C₅H₂Br₅ClO₂, C₅H₃Br₅O₂ et C₅H₃Br₄ClO₂ (Thapa et al., 2020). Par ailleurs, la structure d'une molécule présente dans un extrait d'*A. armata* et possédant 4 atomes de brome, a été proposée comme étant celle du méthyl 2,3-dibromo-5-(2,5-dibromo-3,4-dihydroxyphénoxy)-4-hydroxybenzoate (Pinto et al., 2022). Ces deux études mettent en avant que l'utilisation d'une autre méthode analytique a pu conduire à la découverte de nouvelles molécules plus riches en halogènes que celles décrites auparavant et pourrait donc permettre de revisiter la diversité chimique d'une espèce largement étudiée.

Au moins deux rôles écologiques différents expliquant la production de molécules halogénées et leur effet bénéfique pour l'algue ont été décrits. D'une part, les molécules halogénées agiraient comme répulsif et permettraient d'éviter le broutage par les herbivores (Paul et al., 2006b ; Vergés et al., 2008). Cela a été montré pour l'espèce *A. armata* vis-à-vis de différents herbivores : l'amphipode *Hyale nigra*, les juvéniles du mollusque *Haliotis rubra* (Paul et al., 2006b) et l'aplysie *Aplysia parvula* (Vergés et al., 2008). En effet, dans ce dernier article, les auteurs ont observé qu'*A. parvula* consommait préférentiellement le gamétophyte mâle dont la teneur en bromoforme était plus faible que celle du gamétophyte femelle et ne consommait pas

les cystocarpes du gamétophyte femelle dont la teneur en bromoforme était élevée (Vergés et al., 2008).

D'autre part, les molécules halogénées auraient également un rôle dans la régulation des communautés bactériennes épiphytes de l'algue (Kladi et al., 2004 ; Paul et al., 2006a ; Paul et Pohnert, 2011). En effet, il a été observé une augmentation de la densité bactérienne épiphyte sur des individus d'*A. armata* dont le brome était absent du milieu de culture par rapport à celle d'individus dans des conditions de culture avec brome (Paul et al., 2006a). Les molécules halogénées pourraient donc avoir un rôle dans le contrôle du broutage ainsi que dans la médiation des communautés bactériennes épiphytes. Cependant, le rôle des molécules fortement halogénées reste encore à découvrir. Il a été proposé qu'elles pourraient servir de précurseurs de molécules halogénées plus petites (Thapa et al., 2020).

Les composés halogénés sont stockés dans des cellules spécialisées, dont la présence a été décrite chez différentes espèces d'algues rouges : *Delisea pulchra*, *Bonnemaisonia hamifera* et *A. armata* (Paul et Pohnert, 2011). Dans le genre *Asparagopsis*, ils seraient ainsi stockés dans des vésicules à l'intérieur des cellules péricentrales (**Figure 6**). En effet, plusieurs études ont établi un lien entre la présence de brome dans le milieu de culture de l'algue et l'apparition de ces vésicules (Marshall et al., 2003 ; Paul et al., 2006a). Leur nombre est directement corrélé à la concentration de brome dans l'environnement. A contrario, l'absence de brome dans l'environnement de culture résulte en l'absence de formation de ces vésicules (Marshall et al., 2003 ; Paul et al., 2006a). Il a également été mis en évidence l'existence de structures tubulaires reliant les vésicules à la surface de l'algue et pouvant constituer une voie d'émission des molécules halogénées en surface (**Figure 6**) (Paul et al., 2006a).

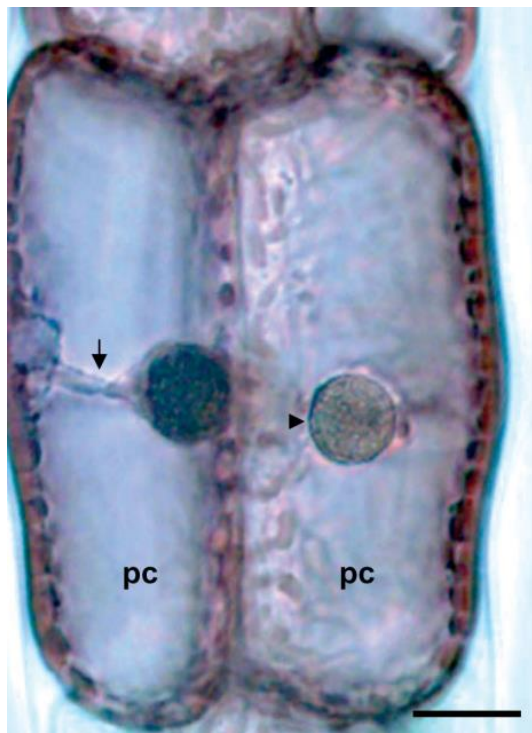


Figure 6 : Image au microscope optique de deux cellules péricentrales (pc) du tétrasporophyte d'*A. armata* avec des vésicules (indiquée à droite par la pointe de flèche) et une structure reliant la vésicule à la paroi cellulaire externe (indiquée par la flèche à gauche) (Source : Paul et al., 2006). Echelle : barre = 10 µm.

Une voie possible de biosynthèse du bromoforme chez *Asparagopsis* spp. a été proposée récemment (Thapa et al., 2020 ; Zhu et al., 2021). Lors de ce travail les auteurs ont détecté, chez *A. taxiformis* (tétrasporophyte), des gènes codant pour des haloperoxydases dépendantes du vanadium qui sont des enzymes qui catalysent les réactions d'halogénéation, déjà décrites chez les algues (Almeida et al., 2001 ; Fournier et Leblanc, 2014 ; Paul et Pohnert, 2011), et ont établi que des dérivés hydrocarbonés provenant de la voie de biosynthèse d'acides gras pouvaient servir de substrat à ces enzymes (Thapa et al. 2020). Ils ont donc pu proposer une voie de biosynthèse possible pour le bromoforme. Le génome d'*A. armata* n'ayant pas été séquencé à ce jour, cette voie de biosynthèse reste donc à confirmer pour cette espèce.

2.1.2.3 Activités biologiques

De nombreuses activités ont été décrites pour les algues du genre *Asparagopsis* et sont résumées dans des revues de littérature (Félix et al., 2021 ; Pinteus et al., 2018 ; Zanolla et al., 2022a). Parmi ces activités, sont citées les activités antioxydantes (Pinteus et al., 2016 ; Zubia et al., 2009), antitumorales (Pinteus et al., 2018 ; Zubia et al., 2009), antifongiques (Pinteus et al., 2015), anti-quorum sensing (Jha et al., 2013), antibactériennes (Bansemir et al., 2006 ; Manilal et al., 2009 ; Salvador et al., 2007), antiparasitaires (Genovese et al., 2009 ; Hutson et al., 2012; Vitale et al., 2015), mais aussi plus récemment, anti-méthanogènes pour les ruminants (Glasson

et al., 2022 ; Machado et al., 2014 ; Roque et al., 2019, 2021) et immunostimulantes pour les poissons (Reverter et al., 2016 ; Thépot et al., 2021a, 2021b, 2022) et les crevettes (Manilal et al., 2013) provoquant un regain d'intérêt pour ces algues. Pour cette partie, je me limiterai à résumer les travaux concernant les activités directement concernées par les objectifs de cette thèse : antibactériennes et anti-quorum sensing, antiparasitaires, et les études ayant eu pour objectif d'évaluer le potentiel des deux espèces du genre *Asparagopsis* comme complément alimentaire pour l'aquaculture.

2.1.2.3.1 Activité antibactérienne et anti-quorum sensing

Les activités antibactériennes *in vitro* d'extraits d'*A. armata* et d'*A. taxiformis* ont été évaluées vis-à-vis de pathogènes de poissons (Bansemir et al., 2006 ; Genovese et al., 2012 ; Marino et al., 2016) et de crevettes, ou de pathogènes humains (Manilal et al., 2009a, 2009b ; Salvador et al., 2007). Plusieurs études ont rapporté que, parmi plusieurs espèces de macroalgues, *A. armata* (gamétophyte et tétrasporophyte) était la seule à présenter une forte activité antibactérienne contre tous les pathogènes testés (Bansemir et al., 2006 ; Salvador et al., 2007). De même, Manilal et al. (2009a) ont montré qu'*A. taxiformis* était la seule algue active contre toutes les bactéries testées.

En plus des activités antibactériennes, une étude a rapporté une activité anti-quorum sensing d'extrait d'*A. taxiformis* (Jha et al., 2013). Le quorum sensing (QS) est un mode de communication bactérien basé sur la densité cellulaire et la concentration en molécules inductrices (« auto-inductrices ») (le plus souvent des *N*-acyl homosérines lactones = AHLs) qui déclenchent l'expression de certains gènes liés à divers mécanismes tels que la formation de biofilm ou la virulence (Kalia, 2013 ; Miller and Bassler, 2001). Son inhibition est une nouvelle cible pour le contrôle des pathogènes car elle pourrait limiter les phénomènes de résistances aux molécules actives (Taylor et al., 2014). Chez *A. taxiformis*, la molécule proposée et potentiellement responsable de l'activité, identifiée sur la base de la variation de l'intensité de son signal en spectrométrie de masse par rapport à l'activité des différentes fractions obtenues, est le 2-dodecanoyloxyethanesulfonate (Jha et al., 2013). Cependant, la molécule n'a pas été isolée et son activité n'a donc pas été confirmée. Ce type d'activité n'a à ce jour fait l'objet d'aucune étude chez l'espèce *A. armata*.

2.1.2.3.2 Activité antiparasitaire

Des activités antiparasitaires ont également été rapportées pour *A. taxiformis* et *A. armata*. Genovese et al. (2009) ont étudié l'effet des extraits obtenus à l'aide de plusieurs solvants, à

partir des deux algues, contre *Leishmania donovani* (protiste) causant la leishmaniose. Ils ont découvert que les extraits bruts obtenus par extraction avec différents solvants (hexane, dichlorométhane, éthanol) présentaient une activité *in vitro* contre ce parasite avec par exemple, pour l'extrait au dichlorométhane, des IC₅₀ minimales de 16 µg/mL et de plus de 40 µg/mL pour *A. taxiformis* et *A. armata* respectivement. Hutson et al. (2012) ont étudié l'effet *in vitro* d'extraits d'*A. taxiformis* sur *Neobedenia* sp., un ectoparasite de poisson. L'exposition des œufs du parasite aux extraits a conduit à une inhibition du développement des embryons, un retard sur le temps de la première et de la dernière éclosion, et une inhibition significative du succès d'éclosion des œufs (3 % de succès d'éclosion) (Hutson et al., 2012).

2.1.2.3.3 Potentiel pour l'aquaculture

D'autres études ont été menées *in vivo* pour étudier la toxicité des deux espèces du genre *Asparagopsis* mais aussi pour explorer leur potentiel comme complément alimentaire immunostimulant avec des applications possibles en aquaculture. Ces études ainsi que leurs résultats principaux sont résumés dans le **Tableau 1**.

La plupart de ces études ont été menées avec *A. taxiformis*. Par exemple, après l'exploration de l'effet antibactérien d'*A. taxiformis* *in vitro* contre les pathogènes des poissons, Marino et al. (2016) ont étudié les paramètres de cytotoxicité et de réponse au stress oxydatif sur le bar et la daurade nourris avec de la poudre ou des extraits d'*A. taxiformis*. Ces auteurs ont montré que la viabilité des hépatocytes entre le régime témoin et les régimes supplémentés (en poudre ou en extrait) n'était pas différente. De plus, aucune mortalité ni symptôme pathologique sur les poissons nourris avec la poudre ou les extraits d'algue n'ont été observés, ce qui a conduit les auteurs à conclure que l'algue ne serait pas toxique pour les espèces de poissons étudiées (Marino et al., 2016). L'effet immunostimulant d'une alimentation complémentée avec *A. taxiformis* a également été testé à travers l'étude de l'expression de deux gènes liés à l'immunité chez l'espèce de poisson *Platax orbicularis* (Reverter et al., 2016). Les gènes codant pour le lysozyme g (Lys G) et le facteur de croissance transformant bêta 1 (TGF-β1) étaient significativement sur-exprimés dans le rein et la rate des poissons nourris pendant deux et trois semaines avec une nourriture supplémentée en *A. taxiformis* par rapport aux poissons contrôles. Les auteurs ont également observé un gain de poids de 13,8 % et de 23,8 % chez les poissons nourris avec l'algue pendant deux et trois semaines respectivement par rapport aux poissons contrôles, ce qui souligne l'effet positif d'*A. taxiformis* sur *P. orbicularis*. Enfin, plusieurs études récentes ont montré qu'un ajout d'*A. taxiformis*, en poudre ou sous forme d'extrait dans

l'alimentation des poissons *Siganus fuscescens* et *Salmo salar* avait des effets positifs sur leur croissance et sur leur système immunitaire inné (Thépot et al., 2021a, 2021b, 2022).

Une seule étude a rapporté les effets d'une incorporation d'*A. armata* dans l'alimentation de larves de daurade royale (Castanho et al., 2017). Les proies des daurades royales ont été préalablement immergées dans une solution contenant 0,5 % d'un extrait commercial d'*A. armata* (Ysaline 100, YSA). Une diminution du nombre de Vibrionaceae dans l'intestin des daurades et un impact positif sur la croissance (+15 %) ont été mis en évidence. En revanche, pendant les deux premières semaines de supplémentation, les auteurs ont observé une mortalité plus importante des poissons nourris avec l'extrait d'*A. armata* (Castanho et al., 2017).

Si de manière générale, l'incorporation d'*A. armata* ou d'*A. taxiformis* paraît avoir des impacts bénéfiques sur la croissance et sur certains paramètres immunitaires de plusieurs espèces de poissons, aucune étude n'a, à ce jour, décrit l'effet de ce type d'alimentation sur leurs pathogènes. Pour autant, deux études encourageantes ont été réalisées sur la crevette *Penaeus monodon* (Manilal et al., 2012, 2013). La première a permis de montrer qu'une supplémentation en *Asparagopsis* sp. a permis de réduire de 80% le pourcentage de crevettes infectées et leur mortalité après infection par plusieurs espèces de *Vibrio* (Manilal et al., 2012). Une étude ultérieure, réalisée par les mêmes auteurs a permis d'expliquer les mécanismes liés à ces réductions, puisque des crevettes nourries pendant un mois avec une alimentation supplémentée en *A. taxiformis* ont montré, par rapport à celles nourries avec l'alimentation non-supplémentée, des activités phénoloxydases, phagocytaires des hémocytes et bactéricide de l'hémolymphé plus élevées. Ces observations ont permis de souligner l'effet positif d'*A. taxiformis* sur le système immunitaire de *P. monodon*.

Tableau 1 : Résumé des principales études utilisant *A. taxiformis* ou *A. armata* comme complément alimentaire pour des poissons et crevettes.

Espèce ¹	Algues	Méthode	Principaux résultats	Source
<i>Penaeus monodon</i>	Asparagopsis sp. Extrait brut (méthanol)	Incorporation dans l'alimentation -Expérience 1 (285, 575, 850 and 1150 mg.kg ⁻¹) (3 semaines) -Expérience 2 (850 mg.kg ⁻¹) (4 semaines)	Augmentation significative du taux de survie des crevettes exposées à différentes espèces de <i>Vibrio</i> sp. (jusqu'à + 80 %)	Manilal et al., 2012
<i>Penaeus monodon</i>	<i>A. taxiformis</i> Extrait brut (méthanol)	Incorporation dans l'alimentation (850 mg.kg ⁻¹) (4 semaines)	Effet positif sur le système immunitaire (taux d'hémocytes, phagocytose, activité phenoloxydase)	Manilal et al., 2013
<i>Dicentrarchus labrax</i>	<i>A. taxiformis</i>	Incorporation dans l'alimentation (1 g algue lyophilisée/10 g nourriture ou 0,1 g extrait/1 g nourriture)	Diminution pour <i>S. aurata</i> du nombre de globules rouges, du taux d'hémoglobine et de l'hématocrite (%)	Marino et al., 2016
<i>Sparus aurata</i>	Lyophilisé ou extrait brut (éthanol)	(2 mois pour l'algue lyophilisé) (2 semaines pour l'extrait brut)	Effet négatif sur le système immunitaire Pas d'impact sur la croissance	
<i>Platax orbicularis</i>	<i>A. taxiformis</i> Lyophilisé	Incorporation dans l'alimentation -3 % (2 semaines) -3 % et 1,5 % (3 semaines)	Impact positif sur la croissance (jusqu'à +24 %) Augmentation de l'expression de gènes liés à l'immunité (Lys G et TGF-β1)	Reverter et al., 2016

Tableau 1 : (Suite)

<i>Sparus aurata</i>			Diminution du nombre de Vibrionaceae dans l'intestin	
	<i>A. armata</i>	Immersion des proies dans un bain à 0,5 % d'extrait pendant 30 min	Impact positif sur la croissance	Castanho et al., 2017
	Extrait commercial (Ysaline 100, YSA)	Puis poissons nourris avec les proies	Mortalité plus importante les 2 premières semaines de supplémentation	
<i>Siganus fuscescens</i>				
	<i>A. taxiformis</i>	Incorporation dans l'alimentation (3 %) (2 semaines)	Augmentation de l'activité haemolytique (x4)	Thépot et al., 2021a
	Lyophilisé			
<i>Siganus fuscescens</i>				
	<i>A. taxiformis</i>	Incorporation dans l'alimentation -Expérience 1 (1.5 %, 3 % et 6 %) (4 semaines) (lyophilisé, extrait, biomasse résiduelle)	Impact positif sur la croissance (jusqu'à +40 %)	
	Lyophilisé, extrait (méthanol), biomasse résiduelle de l'extraction	-Expérience 2 (3 %) (3 mois) (lyophilisé et extrait)	Diminution de l'abondance de <i>Tenacibaculum</i> sp. dans l'intestin	Thépot et al., 2021b
			Augmentation de la réponse immunitaire innée	
<i>Salmo salar</i>				
	<i>A. taxiformis</i>	Incorporation dans l'alimentation (3 % lyophilisé) et (0,6 % et 1,2 % extrait) (4 semaines)	Impact positif sur la croissance (+33 %)	
	Lyophilisé et extrait (méthanol)		Augmentation de la réponse immunitaire innée	Thépot et al., 2022

¹Les images sont déposées sous licence Creative Commons Attribution-Share Alike Generic et sont libres de partage et d'utilisation à condition de citer les auteurs : *Penaeus monodon* : I /CC-BY-SA, *Dicentrarchus labrax* : Citron / CC-BY-SA, *Sparus aurata* : Roberto Pillon/ CC-BY-SA *Platax orbicularis* : Derek Keats/CC-BY-SA *Siganus fuscescens* : John Turnbull/CC-BY-SA *Salmo salar* : Hans-Petter Fjeld/CC-BY-SA

2.1.3 Facteurs de variation de la composition chimique et des activités biologiques

2.1.3.1 L'espèce et la lignée génétique

La grande majorité des études sur la composition chimique ou les activités biologiques des deux espèces d'*Asparagopsis* a été menée sur l'une ou l'autre des deux espèces mais rarement sur les deux simultanément. Ceci crée des déséquilibres sur la qualité et la quantité des connaissances relatives aux deux espèces au sein du genre *Asparagopsis* rendant difficile toute comparaison interspécifique. De plus, des différences dans les protocoles utilisés ou dans les unités d'expression des résultats obtenus rendent encore plus difficiles ces comparaisons. Quelques travaux reportent cependant des différences entre les deux espèces. Par exemple, Genovese et al. (2009) ont décrit des différences d'activités biologiques entre les deux espèces contre le parasite *Leishmania* sp., avec des IC₅₀ et IC₉₀ plus faibles pour les extraits d'*A. taxiformis* que pour ceux d'*A. armata*. McConnell et Fenical (1977) ont rapporté des différences de composition chimique entre les deux espèces. Ils ont par exemple détecté la présence d'acétones chlorées dans les extraits d'*A. armata* mais pas dans ceux d'*A. taxiformis*. Cependant, la provenance des échantillons des deux espèces était différente, le golfe de Californie pour *A. taxiformis* et l'Espagne pour *A. armata*. Dans ce cas, les différences de composition chimique pourraient donc être liées, soit à l'espèce soit à l'influence géographique. L'un des freins à l'étude conjointe des deux espèces est d'ailleurs lié à la possibilité de collecter des échantillons au même endroit afin d'éviter une potentielle influence de l'environnement. Plus récemment, l'utilisation d'une approche métabolomique a permis de détecter, en LC-MS, des différences significatives entre les profils métaboliques d'échantillons d'*A. taxiformis* et d'*A. armata* collectés dans le même site (La Herradura, Espagne). En revanche, aucun marqueur chimio-taxonomique n'a été caractérisé (Greff et al., 2017b).

La composition chimique et les activités biologiques associées peuvent également varier entre lignées d'une même espèce. La composition chimique de 3 lignées d'*A. taxiformis* (L1, L2, L4), toutes collectées au sud d'Hawaii, a été étudiée (Clark et al., 2018). Les analyses métabolomiques (GC-MS) et génétiques ont montré que la lignée 4 se différenciait chimiquement et génétiquement des deux autres lignées, et que ces différences prédominaient par rapport à celles potentiellement liées à la date ou au site de collecte. Parmi les métabolites caractéristiques de la lignée 4, le methyl bromoiodoacétate, le methyl tribromoacétate, le tetrabromure de carbone et la dibromoacétone ont été identifiés (Clark et al., 2018).

2.1.3.2 Le cycle de vie

La littérature comporte peu d'études prenant en compte l'ensemble des stades de vie de l'algue. La distinction entre le gamétophyte mâle et le gamétophyte femelle n'est pas forcément réalisée. Pourtant il a déjà été montré que les gamétophytes mâles avaient une teneur en nutriment (azote total) plus importante que les gamétophytes femelles, ces derniers ayant tendance à avoir une teneur plus importante en bromoforme (quantifié par GC-MS) que les gamétophytes mâles (Vergés et al., 2008). Plus précisément, parmi les organes du gamétophyte femelle, la teneur la plus importante en bromoforme a été trouvée au niveau des parois des cystocarpes (Vergés et al., 2008). Dans la littérature, l'étude des carposporophytes est peu fréquente puisqu'elle nécessite de prélever les cystocarpes sur le gamétophyte femelle et d'en extraire les carposporophytes par microdissection (Haslin et al., 2000). Une autre étude a rapporté des différences de composition chimique entre les stades gamétophyte, carposporophyte et térasporophyte. Ainsi, la composition en polysaccharides du carposporophyte, avec 16 % d'acide uronique (contre ~3 % pour les deux autres stades) et un niveau de sulfatation trois fois plus faible, s'est révélée différente de celle des deux autres stades (Haslin et al., 2000).

Les molécules halogénées produites par les gamétophytes d'*A. armata* et d'*A. taxiformis* sont largement plus documentées que celles des térasporophytes (Greff, 2016 ; Kladi et al., 2004). Quelques études datant des années 70, ont reporté des différences de composition chimique entre le térasporophyte et le gamétophyte. Par exemple, des extraits des deux stades d'*A. armata* collectés à Banyuls-Sur-Mer, étudiés en GC-MS, ont montré une composition en molécules halogénées différente ; la tétrabromo-1,1,3,3-propanone-2 étant le composé majoritaire du térasporophyte, la tribromo-1,1,3-propanone-2 celui du gamétophyte (Bruneau et al., 1978). D'autres composés, détectés chez l'un des stades du cycle d'*A. armata*, sont absents chez l'autre. C'est notamment le cas de la dichloro-1,1-bromo-3 propan-2-one, absente de l'extrait du stade gamétophyte d'une part, et des acides acryliques, acrylates de méthyle et d'éthyle bromés et iodés, absents du stade térasporophyte d'autre part (Bruneau et al., 1978). Une deuxième étude, réalisée sur des échantillons provenant également de Banyuls-sur-Mer, a mis en évidence que la teneur en stérols du térasporophyte d'*A. armata* était plus élevée que celle du gamétophyte (sans distinction des femelles et des mâles) (Combaut et al., 1979). Enfin plus récemment, Paul et al. (2006a) ont montré que le térasporophyte d'*A. armata* avait une teneur en acide dibromoacétique et en acide bromochloroacétique (GC-MS), plus importante que le gamétophyte (Paul et al., 2006a). Depuis ces études, la composition chimique du térasporophyte conjointement à celle du gamétophyte a été assez peu ré-explorée et à ma

connaissance, jamais en LC-MS. Une meilleure description de sa composition chimique conjointement à celle du gamétophyte pourrait permettre de valoriser ce stade du cycle de l'algue. Par exemple, une étude très récente a permis la détection de 2,4-dione halogénées dans le tétrasporophyte d'*A. taxiformis*, qui à ce jour n'ont pas été détectées dans le gamétophyte (Thapa et al., 2020).

Peu d'études portant sur les activités antibactériennes ou antiparasitaires de l'ensemble des stades du cycle de vie des algues du genre *Asparagopsis* ont été réalisées. Deux études sur les activités antibactériennes de plusieurs espèces d'algues, incluant des échantillons de gamétophytes et tétrasporophytes d'*A. armata*, ont montré une forte activité antibactérienne des extraits de ces deux stades contre différentes espèces bactériennes (Bansemir et al., 2006 ; Salvador et al., 2007). Ces deux études ont également montré que l'activité mesurée pour les extraits du gamétophyte étaient supérieure à celle des extraits du térasporophyte (Bansemir et al., 2006 ; Salvador et al., 2007). Ces études n'incluaient pas de données sur la composition chimique. Ainsi, le lien entre métabolome et activités biologiques des extraits manque dans la littérature.

2.1.3.3 La géographie

Outre la variabilité rapportée dans la composition chimique des différents stades d'une même espèce d'algue, comme montré pour les stades gamétophyte et térasporophyte d'*A. armata*, la composition chimique des algues est également décrite comme variable en fonction de la localisation géographique en lien avec des spécificités locales de paramètres abiotiques (exposition aux vagues, température...) ou biotiques (pression des herbivores, compétition pour l'espace...) (Stengel et al., 2011).

Les variations spatiales décrites dans la littérature peuvent concerner des lignées différentes ou des lignées identiques géographiquement éloignées. Une étude métabolomique d'envergure a été menée sur 289 échantillons collectés sur des sites géographiquement éloignés les uns des autres (Réunion, Nouvelle Calédonie, Marseille, Polynésie Française) et comportant vraisemblablement des lignées L2, L3, L4 et L5 d'*A. taxiformis* (Greff et al., 2017b). L'étude menée a permis de montrer une différence entre les profils chimiques des échantillons d'*A. taxiformis* collectés en eaux tempérées et en eaux plus chaudes. Huit potentiels marqueurs ont été sélectionnés, mais si leurs formules brutes ont été déterminées, les identifications n'ont pas encore pu être confirmées (Greff et al., 2017b). Des différences de composition en molécules halogénées d'échantillons d'*A. taxiformis*, collectés au nord et au sud du Golfe de Californie,

avaient déjà été reportées dans les années 70 (McConnell et Fenical, 1977). De même en Australie, les teneurs en bromoforme et acide dibromoacétique d'échantillons d'*A. taxiformis* collectés dans des eaux tropicales étaient supérieures à celles des échantillons collectés dans des eaux plus tempérées (Mata et al., 2017).

La variabilité spatiale de l'activité antibactérienne du genre *Asparagopsis* a également été rapportée. Par exemple, des extraits d'*A. armata* (gamétophyte) issus de collectes réalisées sur la côte méditerranéenne ont montré une activité antibactérienne plus élevée que celle des extraits d'échantillons collectés sur la côte atlantique (Salvador et al. 2007). Les mêmes observations ont été faites pour l'activité antibactérienne du stade tétrasporophyte d'*A. armata* (Salvador et al., 2007). Pour *A. taxiformis*, il a été montré que globalement les échantillons collectés dans des eaux tempérées présentaient une activité toxique plus élevée contre *Allivibrio fischeri* que celle des échantillons collectés dans des eaux plus chaudes (Greff et al., 2017b).

Les auteurs de ces études, ont rapproché les variations observées à de possibles différences dans les conditions environnementales des sites d'échantillonnage. Par exemple, Greff et al. (2017b) ont émis les hypothèses de pression de prédation par les herbivores plus importantes dans les régions tropicales que dans les régions tempérées où les conditions environnementales sont plus variables pour expliquer les variabilités de composition chimique et d'activités observées. Ces études montrent bien que la localisation et surtout les conditions environnementales spécifiques locales ont un impact significatif sur la composition chimique des algues et sur les activités biologiques des extraits des algues.

2.1.3.4 Le temps

Il existe peu d'études sur les variations temporelles de la composition chimique des deux espèces du genre *Asparagopsis*. Greff et al. (2017b) ont rapporté une variabilité temporelle de la composition chimique d'échantillons du stade gamétophyte d'*A. taxiformis* collectés à différents mois de l'année à la Réunion ainsi que dans le Sud de la France (Greff et al., 2017b). De plus, cette variabilité temporelle observée était plus importante pour les échantillons de La Réunion que ceux du Sud de la France et semblait correspondre à un patron saisonnier. Toutefois, aucun marqueur chimique de cette saisonnalité n'a pu être identifié. De manière similaire, ces mêmes échantillons collectés à la Réunion présentaient une variabilité temporelle de leur activité toxique contre *Allivibrio fischeri* qui semble correlée négativement à la température de surface de l'eau de mer (Greff et al., 2017b). A ma connaissance il s'agit de la

seule étude sur la temporalité de la composition chimique et des activités biologiques d'échantillons collectés *in situ*.

Il existe en revanche un plus grand nombre d'études portant sur la temporalité de l'activité antibactérienne d'extraits des deux algues collectées à différents moments. Genovese et al. (2012) ont étudié l'effet antibactérien d'extraits d'*A. taxiformis* collectés au niveau du détroit de Messine en mars, mai, juillet et septembre sur des bactéries pathogènes de poissons. Ces auteurs ont montré que les extraits des mois de mars et mai présentaient une activité antibactérienne, mais pas ceux des mois de juillet et septembre. De plus, l'activité antibactérienne des extraits d'algues du mois de mai était significativement supérieure à celle des extraits du mois de mars. Des résultats comparables ont été mis en évidence par Marino et al. (2016) sur des extraits d'*A. taxiformis* échantillonnés également au niveau du détroit de Messine dans la mesure où les extraits issus des collectes de juin et juillet ne montraient aucune activité antibactérienne contre des bactéries pathogènes de poissons, alors que ceux d'avril et mai présentaient cette activité (Marino et al., 2016). Les auteurs ont émis l'hypothèse que le maximum d'activité observé pourrait correspondre à la période de croissance maximale de l'algue. Une variation temporelle de l'activité antibactérienne des extraits d'*A. armata* a également été rapportée ; les échantillons collectés en hiver montrant une activité antibactérienne plus élevée que ceux collectés au printemps (Salvador et al., 2007). En plus de la variation de la croissance de l'algue, les auteurs des différentes études citées ont émis les hypothèses de variations de l'irradiance, de la disponibilité en nutriment comme facteurs potentiellement responsables des variations temporelles de l'activité antibactérienne.

3. Apport des outils –omiques pour évaluer le potentiel des algues du genre *Asparagopsis*

Les sciences dites –omiques telles que la génomique, la transcriptomique, la protéomique, ou la métabolomique ont pour but la caractérisation et la quantification relative de l'ensemble des gènes (ADN), des transcripts (ARN), des protéines et des métabolites d'une cellule, d'une structure ou d'un organisme (Vailati-Riboni et al., 2017) (**Figure 7**). Ces différents niveaux moléculaires sont liés et interdépendants et forment la cascade omique dont le dernier niveau est le phénotype qui désigne les caractères observables (**Figure 7**). Sous l'effet de perturbation, chaque niveau va subir des modifications se répercutant aux niveaux inférieurs. Les techniques –omiques permettent alors une compréhension des structures, des fonctions et des dynamiques des processus biologiques impactés par la perturbation. La génomique, la transcriptomique et la protéomique permettent d'étudier les premiers niveaux des processus biologiques d'un organisme (**Figure 7**).

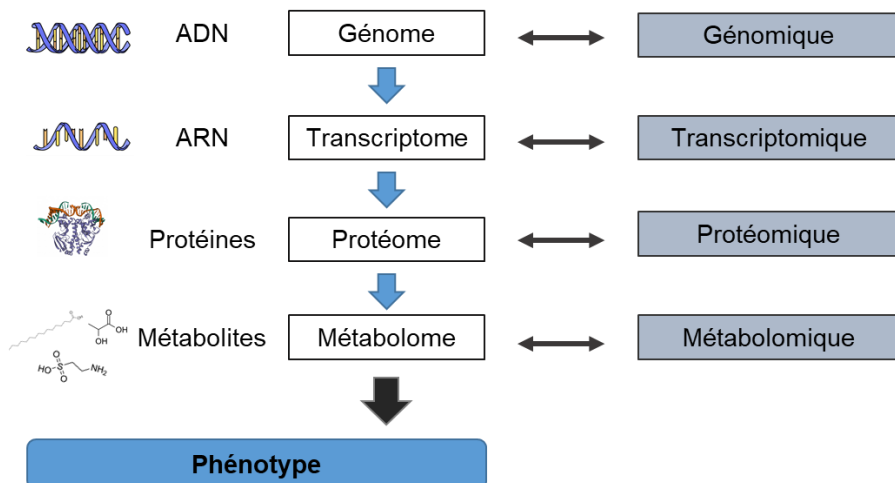


Figure 7 : Schématisation de la cascade « omique »

La métabolomique quant à elle, permet d'analyser l'ensemble des métabolites, constituant le métabolome, qui représente le dernier niveau des processus biologiques, le plus proche du phénotype. Cette approche permet notamment, par rapport aux approches classiques comme le fractionnement bioguidé, d'accélérer l'identification et la déréPLICATION des molécules actives ou encore de faciliter l'étude de la diversité chimique en lien avec l'écologie (Reverter et al., 2020). Ainsi, la métabolomique permet d'étudier l'impact de différents facteurs, inter ou intra-spécifiques, biotiques ou abiotiques sur la composition métabolique d'un organisme en incluant

un plus grand nombre de métabolites (Reverter et al., 2020). Par ailleurs, les analyses métabolomiques permettent non seulement d'étudier les métabolites produits par un organisme mais incluent aussi ceux produits par tous les organismes (micro- ou macro-) présents dans l'échantillon de manière fortuite ou non lors de l'analyse. Il est alors important d'en tenir compte lors de toute interprétation. Or, il est aujourd'hui largement reconnu que les organismes, notamment les communautés bactériennes, associés à chaque individu ont un rôle essentiel dans le maintien des fonctions et de la santé de cet individu. Ainsi, de plus en plus d'études s'intéressent à ces communautés, ce qui est rendu possible grâce aux méthodes « métagénomiques ». La métagénomique et la métatranscriptomique consistent à étudier l'ensemble des ADN et ARN contenus dans un échantillon. Couplées à des techniques comme la métabolomique (approche multi-omique), la métagénomique et la métatranscriptomique ouvrent de nouvelles perspectives pour une meilleure compréhension des interactions entre hôte et microorganismes, et notamment vis-à-vis du rôle potentiel de ces microorganismes pour la production de molécules actives (Reverter et al., 2020) mais aussi sur les dynamiques des interactions hôtes-microorganismes en lien avec différents facteurs (Paix et al., 2019, 2020, 2021a, 2021b).

Les apports de la métabolomique, pour la découverte de nouvelles molécules, pour l'étude de la diversité chimique en lien avec l'écologie ou des interactions hôtes-microorganismes ou encore couplée à d'autre techniques omiques pour l'étude des voies métaboliques sont abordés dans une mini revue de littérature, dont je suis co-auteure, publiée dans **Frontiers in Marine Science** le 10 Décembre 2020 <https://doi.org/10.3389/fmars.2020.613471>. Cette mini-revue a été rédigée au cours de l'année 2020, lors des différents confinements de la crise COVID et figure en annexe de ce manuscrit (**Annexe 1**).

Dans la suite, je présente plus spécifiquement l'apport de ces outils dans la connaissance des modèles biologiques de cette thèse. Le génome et le protéome du tétrasporophyte d'*A. taxiformis* ont été caractérisés et ont permis de décrire des différences d'expression de gènes entre des échantillons de térasporophyte cultivés et sauvages (Zhao et al., 2022, prépublication). Ainsi, des gènes liés à des mécanismes de stress et de défense et à la production de molécules halogénées étaient sur-exprimés chez le térasporophyte « sauvage » (Zhao et al., 2022, prépublication). Dans une autre étude, l'utilisation de la protéomique a permis la comparaison du protéome du térasporophyte d'*A. taxiformis* à ceux des stades gamétophytiques

mâle et femelle (Patwary et al., 2023). Seules 87 protéines étaient communes à tous les stades de vie (sur 741) et donc un grand nombre spécifique à chaque stade.

Concernant *A. anguilla*, son génome a été séquencé en 2005 (Minegishi et al., 2005). Depuis, la génomique a été utilisée pour comprendre la différenciation génétique entre *A. anguilla* et *A. rostrata*, dont les aires de distribution sont différentes mais dont les lieux de reproduction sont chevauchants (Nikolic et al., 2020). La transcriptomique a permis d'étudier des interactions hôtes-pathogènes, avec, lors d'une infection, l'identification des gènes sur-exprimés dans la bactérie *E. anguillarum* et dans l'hôte *A. anguilla* (Xiao et al., 2022). La transcriptomique a aussi été utilisée pour évaluer l'impact du parasite *A. crassus*, 3 jours après une infestation expérimentale, sur l'expression de gènes du foie et du rein de spécimens d'aquaculture d'anguilles européennes (Bracamonte et al., 2019). Enfin, l'impact de polluant sur l'anguille européenne a été caractérisé par une approche transcriptomique (Perrier et al., 2020).

La métagénomique, notamment via le métabarcoding qui consiste à séquencer un fragment d'ADN particulier, en général hautement conservé, a été appliquée d'une part à l'étude de l'impact de « l'invasion » par *A. armata* sur la diversité et la richesse des communautés benthiques (Wangensteen et al., 2018) et d'autre part à l'étude des communautés bactériennes associées aux algues du genre *Asparagopsis* dans des contextes de variation des conditions environnementales (*A. taxiformis* et *A. armata*) (Aires et al., 2016) ou d'interaction avec le corail *Astrocoites calycularis* (*A. taxiformis*) (Greff et al., 2017a).

La métabolomique a permis d'étudier l'influence de facteurs spatiaux et temporels sur le métabolome d'*A. taxiformis* (Greff et al., 2017b). L'utilisation de la métabolomique, par GC-MS, a également permis d'identifier des différences de composition chimique entre les lignées 4, 1 et 2 d'*A. taxiformis* (Clark et al., 2018). Encore plus récemment, une étude métabolomique par LC-MS, réalisée sur des extraits d'*A. taxiformis* a permis la description de nouvelles molécules dont la structure correspondrait à des 2,4-diones polyhalogénées (Thapa et al., 2020). Sur l'anguille européenne, la métabolomique a, par exemple, été utilisée pour caractériser l'impact de polluant sur son métabolisme (Alvarez-Mora et al., 2023).

Outre leurs utilisations pour l'étude de l'hôte et des communautés associées, les approches multi-omiques, qui associent souvent la génomique/transcriptomique avec la protéomique/métabolomique permettent d'avoir une vision complète, « intégrative », des processus biologiques et des mécanismes moléculaires au sein d'un organisme (Reverter et al., 2020). Par exemple, appliqués à l'étude des algues du genre *Asparagopsis*, l'utilisation de la

génomique et de la transcriptomique couplée à la métabolomique, a permis de décrire une voie de biosynthèse du bromoforme par *A. taxiformis* (Thapa et al., 2020).

Les techniques –omiques n'ont été utilisées que récemment sur les modèles biologiques de cette thèse. Elles s'imposent comme des outils de choix pour évaluer le potentiel des algues du genre *Asparagopsis* pour l'aquaculture et répondre aux objectifs de la thèse. Elles pourront permettent l'étude de la composition chimique des deux algues en lien avec différents facteurs de variation (métabolomique) et avec les communautés associées (métagénomique) en utilisant des outils analytiques peu utilisés sur ces algues, tels que la LC-MS, la RMN et le métabarcoding. En outre, elles pourront aussi faciliter l'étude de l'effet de ces algues sur la physiologie de l'anguille en fournissant une vision globale et sans *a priori* des variations au sein de l'organisme (transcriptomique).

Matériels et méthodes : principes généraux

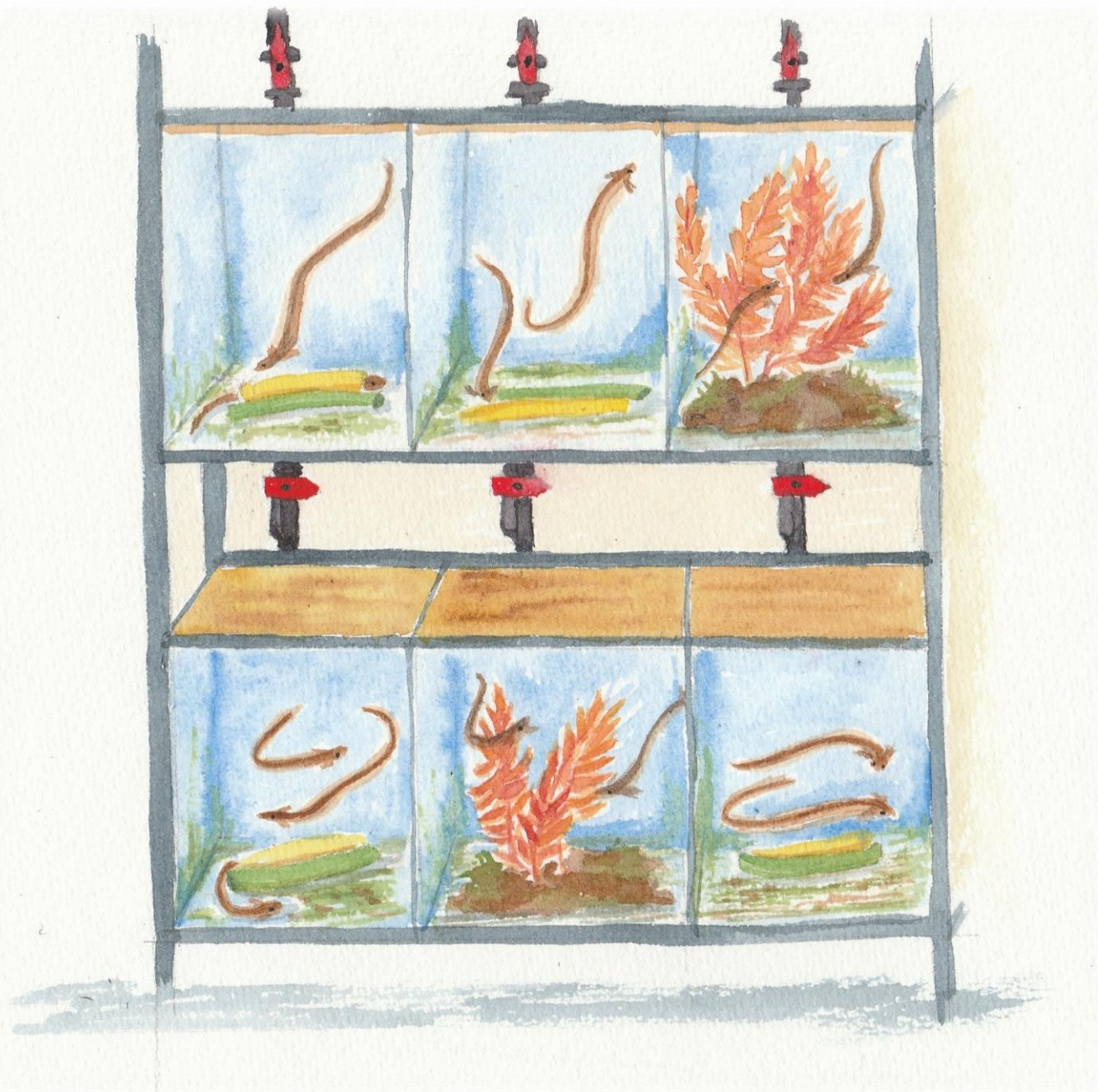


Illustration à l'aquarelle réalisée par Michèle Parchemin

L'objectif de cette partie est de présenter les modèles biologiques ainsi que les principes généraux des méthodes utilisées afin de faciliter la compréhension de chaque chapitre, le détail (quantité, volume, temps...) étant indiqué dans chaque chapitre. Les analyses par métabarcoding et transcriptomique ne sont décrites que de manière très générale par rapport à la métabolomique car pour cette thèse, elles ont été réalisées dans le cadre de collaborations au cours desquelles j'ai participé au traitement des données.

1. L'élevage et le maintien des anguilles en conditions contrôlées

La réalisation des expériences présentées dans le **Chapitre IV** de cette thèse a nécessité l'obtention et l'élevage d'anguilles. Ces anguilles ont été obtenues au stade civelle (**Figure 8**) lorsqu'elles arrivent de la mer, de manière à minimiser au maximum le risque d'infestation par le nématode parasite (*Anguillicola crassus*) qui sera étudié dans cette thèse. Une autorisation de prélèvement et de transport de civelles nous a été octroyée par le préfet de la région Provences-Alpes-Côtes-d'Azur (décision n° 93 du 17 février 2020). Les civelles ont été capturées au niveau d'une passe à anguilles située au grau de la Fourcade (Saintes-Maries-de-la-Mer) par l'Association Migrateurs Rhône-Méditerranée. Ainsi, 1 kg de civelles représentant environ 5000 individus (masse estimée par civelle de 0,2 g) a été ramené au sein de la structure expérimentale de l'Université de Perpignan *Via Domitia* (UPVD). Les civelles y ont été élevées pendant un peu plus d'1 an afin qu'elles atteignent une taille suffisante pour permettre leur infestation par le parasite *A. crassus* en condition contrôlée.



Figure 8 : Civelles. Crédits : C. Parchemin

Les civelles ont d'abord été stockées dans des bacs de 400 L (**Figure 9A, B**) pour permettre leur adaptation progressive aux conditions d'élevage (i.e. température et salinité). La température de la structure expérimentale a été maintenue à 25 °C pour obtenir une température d'eau dans les aquariums d'environ 19 °C, et la photopériode calée sur la lumière naturelle extérieure. Elles ont ensuite été réparties dans des aquariums de 25 et 50 L, dont l'eau a été maintenue à 15 g/L (sel commercial, Instant Ocean – Aquarium systems Salt) en vue de leur élevage proprement dit (**Figure 9C**). Les aquariums, indépendants les uns des autres du point de vue de la circulation d'eau (circuit fermé) étaient munis chacun d'un filtre biologique et leur eau renouvelée pour un tiers chaque semaine pendant toute la durée de l'élevage et des expérimentations.



Figure 9 : Bacs de 400 L (A), civelles dans le fond d'un bac de 400 L (B) et aquariums de 50L (C). Crédits : C. Parchemin

Les civelles ont d'abord été nourries (**Figure 10A**) avec des nauplii d'artémias obtenues à partir de l'éclosion d'œufs (Ocean Nutrition ; Société Groupe Antinéa, St Jean de Védas, France) (**Figure 10B**).

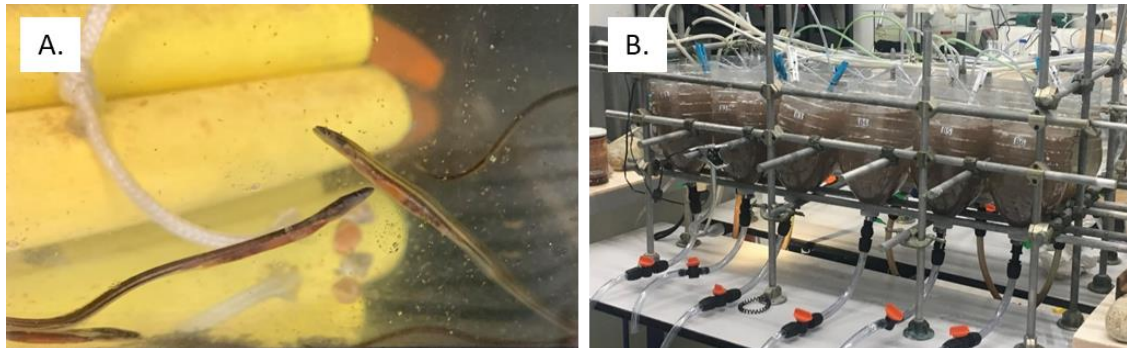


Figure 10 : Civelles se nourrissant des nauplii (A) et élevage de nauplii d'artémia (B). Crédits : C. Parchemin

Après l'apparition d'une pigmentation, les civelles maintenant considérées comme des anguillettes ont été nourries d'une « pâte » constituée d'un mélange de granulés d'aquaculture broyés (INICIO plus M ; Société BioMar, Nersac, France) et de vers de vase rouges congelés (Ocean Nutrition ; Société Groupe Antinéa, St Jean de Védas, France) pour leur appétence avérée et faciliter la prise d'une nourriture artificielle (**Figure 11**).



Figure 11 : Anguillettes se nourrissant de la pâte composée de vers de vase rouges et de granulés d'aquaculture broyés. Crédits : C. Parchemin

Afin d'éviter les phénomènes de compétition, les anguillettes ont été régulièrement triées et réparties par taille dans les différents aquariums (**Figure 12A**). Après environ 1 an et demi d'élevage, et malgré les tris réguliers effectués, une grande disparité de taille subsistait, les plus petites anguilles mesurant 11 cm pour moins de 2 g, et les plus grandes jusqu'à 34 cm pour 61 g (**Figure 12B**).



Figure 12 : Anguillettes destinées à être triées selon leur taille (A), et photo de la plus grosse des anguilles obtenues après 18 mois d'élevage (~34 cm, 61 g) (B). Crédits : C. Parchemin.

2. Obtention des parasites *A. crassus*

L'ensemble des expériences sur/avec le parasite *A. crassus* (*in vitro* ou *in vivo*) a été réalisé à partir de spécimens présents dans les vessies gazeuses d'anguilles sauvages (**Figure 13A**) pêchées et récupérées auprès des pêcheurs de la lagune de Canet. Ainsi, des parasites adultes (**Figure 13B**) et des œufs issus de femelles gravides du parasite (**Figure 13C**), ont été collectés pour réaliser les tests *in vitro*, et les infestations expérimentales des anguillettes maintenues en élevage, respectivement.

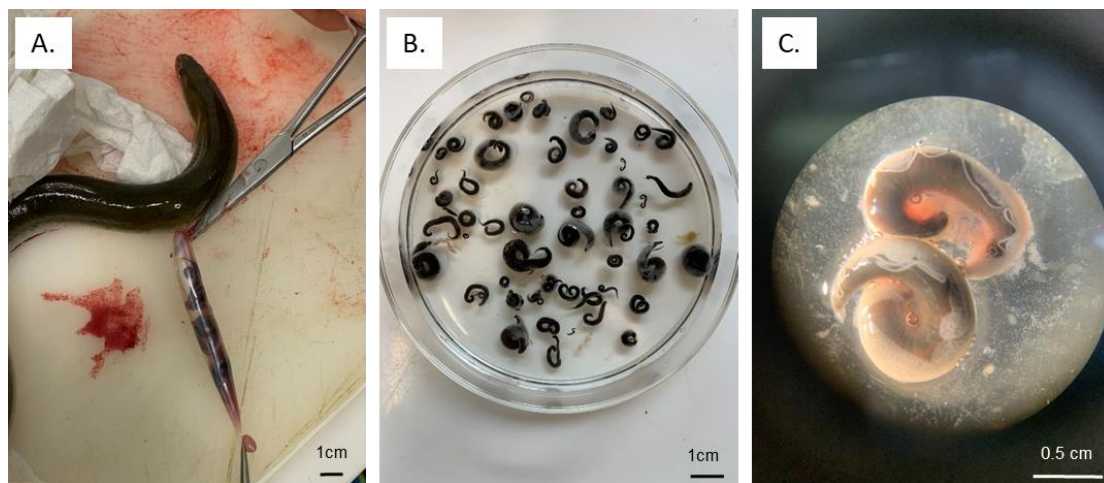


Figure 13 : Vessie gazeuse d'une anguille sauvage contenant des spécimens d'*A. crassus* (A), parasites adultes (B) et femelles gravides observées à la loupe binoculaire (grossissement x40) (C). Crédits : C. Parchemin

3. Tests *in vitro* sur les pathogènes de l'anguille européenne

3.1 Tests d'activité antibactérienne

Les souches utilisées pour les tests d'activité antibactérienne sont toutes des espèces ayant été décrites au moins une fois comme pathogènes pour l'anguille européenne (**Voir - Etat de l'art**

– **1. Revue**) : *Edwardsiella anguillarum* (DSMZ-27202, « Ea »), *Lactococcus garvieae* (CIP102507T, « Lg »), *Pseudomonas anguilliseptica* (CIP106711T, « Pa »), *Tenacibaculum maritimum* (CIP103528T, « Tm »), *Vibrio anguillarum* (CIP 63.36T, « Va »), *V. harveyi* (CIP103192T, « Vh ») et *Yersina ruckeri* (CIP82.80T, « Yr »). Ce sont toutes des bactéries Gram- sauf Lg qui est Gram+.

Les tests d’activité antibactérienne ont été réalisés soit en boîtes de pétri avec la méthode de diffusion des disques soit en microplaques 96 puits. Le test en boîtes de pétri est plus représentatif des processus naturels d’adhésion et de développement des bactéries en biofilm, tandis que ceux en microplaques sont réalisés sur des bactéries en solution, donc non adhérees. Il est cependant plus facile et moins onéreux de réaliser des screenings à grande échelle en microplaques que sur boîtes de pétri. Dans les deux cas, les bactéries ont été remises en culture sur boîtes de pétri afin de ne prélever qu’une seule colonie pour mise en culture et croissance en milieu liquide (**Tableau 2**).

Tableau 2 : Détail des conditions de culture utilisées pour les différentes souches bactériennes

Souche	Milieu de culture	Temperature d’incubation (°C)	Temps d’incubation (h)	Sensibilité à l’antibiotique
<i>Edwardsiella anguillarum</i> (DSMZ-27202)	Luria Broth	26	24	Kanamycine
<i>Lactococcus garvieae</i> (CIP102507T)	Bouillon coeur cervelle	37	24	Erythromycine
<i>Pseudomonas anguilliseptica</i> (CIP106711T)	Marine Broth	26	48	Ampicilline
<i>Tenacibaculum maritimum</i> (CIP103528T)	Marine Broth	26	24	Ampicilline
<i>Vibrio anguillarum</i> (CIP 63.36T)	Marine Broth	26	24	Kanamycine
<i>Vibrio harveyi</i> (CIP103192T)	Marine Broth	26	24	Kanamycine
<i>Yersina ruckeri</i> (CIP82.80T)	Marine Broth	26	24	Amoxicilline

Après une nuit d’incubation à 26 °C (ou 37 °C pour Lg), le niveau de croissance a été contrôlé avec la mesure de la densité optique (DO) du milieu. Si nécessaire, la culture a été diluée, afin d’atteindre une DO à 620 nm de 0,1 correspondant à une concentration bactérienne de la culture de 10^8 UFC.ml⁻¹. Pour les tests en boîtes de pétri, ces dernières ont été ensemencées selon la méthode dite par « inondation ». Les extraits (10 mg/mL) ou fractions (5 mg/mL) d’algues à tester ont été déposés (10 µL) sur des disques de papier stériles de 6 mm qui, après séchage, ont ensuite été placés sur les boîtes de pétri préalablement ensemencées. Par diffusion, les potentielles molécules antibactériennes conduiront à l’apparition d’une zone d’inhibition de la

croissance bactérienne autour du disque. Après 24 h de culture (ou 48h pour Pa), l'activité antibactérienne a été déterminée grâce à la mesure du diamètre de cette zone d'inhibition (**Figure 14A**). Pour les tests en microplaques 96 puits, la culture bactérienne (180 µL) a été déposée dans les puits auxquels 20 µL de fractions d'algues (2,5 mg/mL), solubilisés dans une solution contenant 25 % de diméthylsulfoxyde (DMSO) et 75 % d'eau stérile (pour une concentration finale non toxique de DMSO dans le puit de 2,5 %), ont été ajoutés. Après 24h de culture (ou 48h pour Pa), l'activité antibactérienne a été déterminée grâce à la mesure de la densité optique à 620 nm et par comparaison avec celle d'un puit d'une culture contrôle sans extrait (**Figure 14B**).

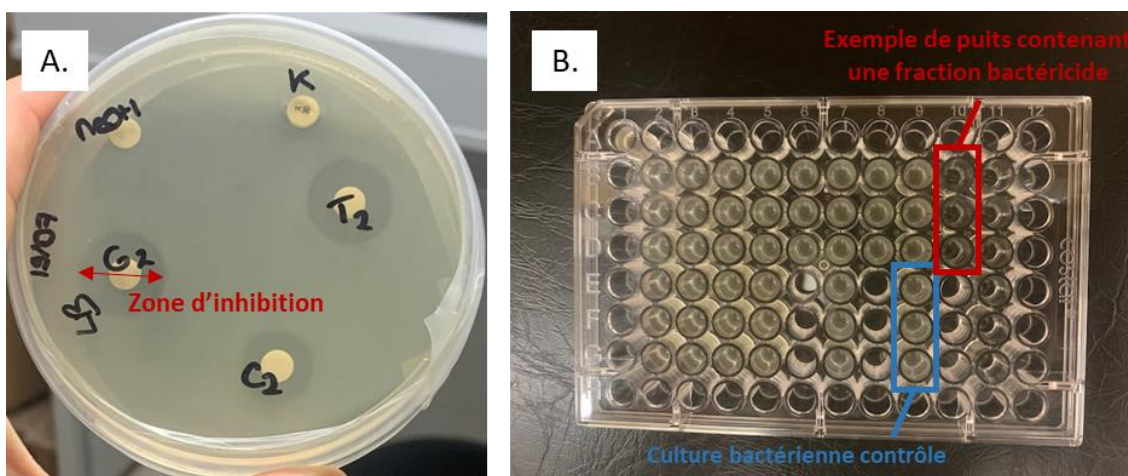


Figure 14 : Illustration de résultats de tests d'activités antibactériennes sur boîte de pétri (A) et en microplaques 96 puits (B). Sur (A) la zone d'inhibition de croissance bactérienne induite par l'extrait sur le disque est indiquée par la double flèche rouge. Sur (B) les puits encadrés en rouge contiennent un extrait bactéricide et la densité optique de ces puits est inférieure à celle des puits contrôles en bleu. Crédits : C. Parchemin

3.2 Tests d'activité antiparasitaire

Les tests *in vitro* relatifs à l'effet des extraits issus des deux algues sur le parasite *A. crassus* ont consisté à mettre des parasites en contact avec les extraits d'algues, et à observer leur mouvement et leur mortalité toutes les 20 minutes pendant 2 heures en comparaison avec un contrôle. Les parasites ont donc été immergés dans 20 mL d'une eau saline reconstituée à 8 g/L NaCl à laquelle ont été ajoutés 2 mL d'extrait (10, 5, et 0,5 mg/mL dans une solution contenant 75 % Eau et 25 % DMSO) (**Figure 15**). Les contrôles ont consisté à mettre des parasites dans 20 mL d'eau saline reconstituée (8 g/L NaCl) et des parasites dans 18 mL d'eau saline reconstituée (8 g/L NaCl) à laquelle ont été ajoutés 2 mL de solvant (solution contenant 75 % Eau et 25 % DMSO). Après deux observations sans mouvement malgré une légère agitation de la boîte de pétri (afin de provoquer un mouvement lorsque les parasites sont immobiles), les parasites ont été considérés morts.

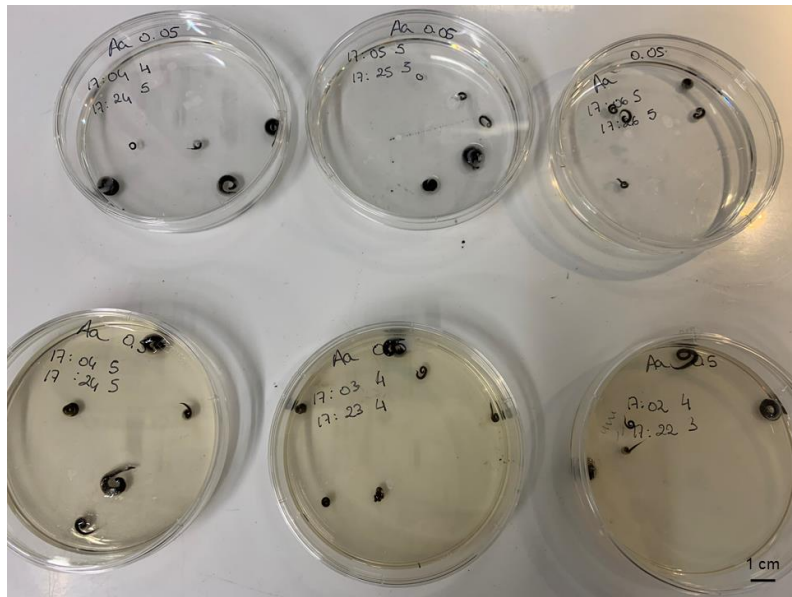


Figure 15 : Illustration des tests d'activité antiparasitaire sur les adultes d'*A. crassus*.

4. Infestation expérimentale des anguillettes

4.1 Avec le parasite *A. crassus*

L'infestation expérimentale contrôlée des anguilles avec le parasite *A. crassus* est basée sur la réalisation du cycle du parasite adaptée de De Charleroy et al. (1990). Les œufs du parasite récupérés de femelles gravides ont été incubés à 25° C jusqu'à éclosion (environ 3 jours après le début de l'incubation) pour l'obtention de larves de 2^{ème} stade (larves L2). En parallèle, 15 copépodes (hôte intermédiaire du parasite), pêchés à Villeneuve-de-La-Raho (**Figure 16A**), ont été mis en contact, dans une boîte de pétri, avec 150 à 200 larves L2 du parasite pendant 24h (**Figure 16B**). Ce nombre de larves et ce temps de contact permet d'optimiser la réussite d'infestation des copépodes tout en évitant des niveaux d'infestations trop élevés, ce qui pourrait mettre en péril leur survie. L'opération a été répétée environ 150 fois (150 boîtes de pétri) de manière à obtenir un nombre de larves L3 suffisant pour assurer la totalité des infestations nécessaires pour l'expérimentation. Après 24h de mise en contact, le contenu des boîtes est filtré pour ne garder que les copépodes et éviter leur surinfestation. Ceux-ci ont été ensuite maintenus à 25 °C pendant environ deux semaines pour permettre le développement des larves L2 en larves L3 (**Figure 16C, D**). Après deux semaines, les copépodes ont été doucement broyés à l'aide d'un Potter pour permettre la récupération des larves L3. Celles-ci ont alors été observées sous microscope (agrandissement x400), pour vérifier leur stade de développement par la présence d'une « dent » proximale, structure qui permet aux larves L3 de traverser le tube digestif de l'anguille pour gagner la paroi de la vessie gazeuse (Blanc et al.,

1992) (**Figure 16E**). Enfin, chaque anguille a été infestée par un lot de 20 larves L3 dans une solution saline à 8 g/L. Ce nombre de larves a été défini afin de reproduire un taux d'infestation moyen représentatif de celui rencontré en milieu lagunaire. Un volume maximal de 0,2 mL de solution saline a été utilisé afin de ne pas surcharger l'estomac de l'anguille et d'éviter tout rejet. L'infestation expérimentale proprement dite a été réalisée en introduisant les larves dans l'estomac de l'anguille par intubation à l'aide d'une seringue munie d'un cathéter souple (dont le bout est émoussé pour limiter tout dommage à la paroi du tube digestif de l'anguille) (**Figure 16F**). Les anguilles contrôles non infestées ont été intubées avec 0,2 mL de solution saline seule.

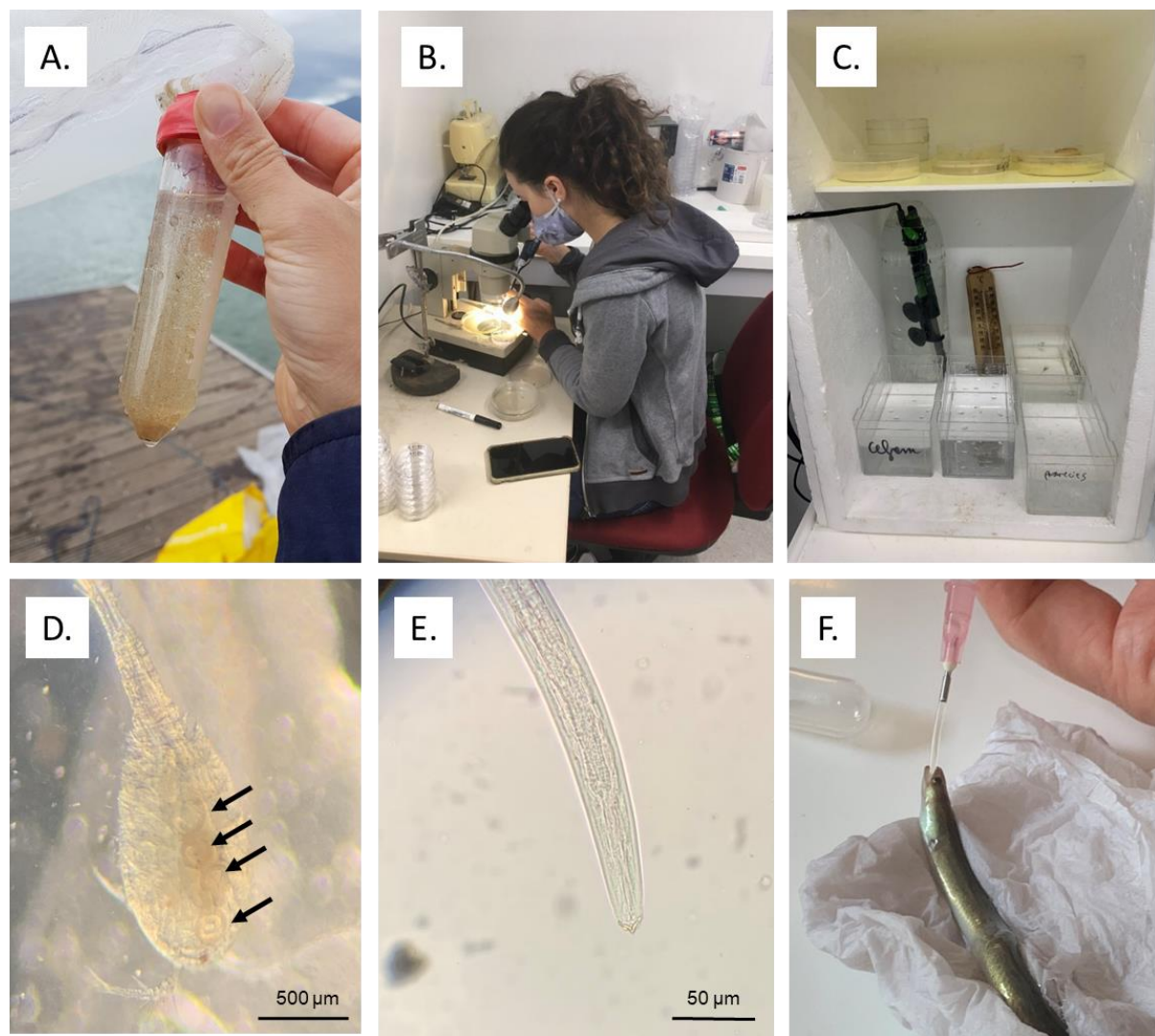


Figure 16 : Illustrations des différents points clés dans la réalisation du cycle du parasite *A. crassus* et l'infestation des anguilles. Collecteur rempli de copépodes après une séance de pêche au filet à plancton à main (A). Mise en contact des larves L2 après éclosion des œufs avec des copépodes (B). Maintien des copépodes à 25 °C pour permettre le développement des larves du parasite (C). Copépode présentant au moins 4 larves L3 désignées par les flèches, loupe binoculaire (agrandissement x40) (D). Larves L3 présentant la « dent » qui leur permet de traverser l'intestin de l'anguille pour atteindre la vessie gazeuse, microscope optique (agrandissement x400) (E). Infestation par intubation d'une anguille avec des larves L3 du parasite (F). Crédits : C. Parchemin

4.2 Avec la bactérie *E. anguillarum*

La méthode utilisée pour l'infection expérimentale contrôlée des anguilles avec la bactérie *E. anguillarum* a été adaptée à partir de celles utilisées dans plusieurs études rapportant l'effet d'alimentations supplémentées en divers produits naturels sur la survie d'anguilles japonaises (Bae et al., 2008, 2012 ; Lee et al., 2018). Ainsi, une culture liquide d'*E. anguillarum* a été réalisée et diluée pour atteindre une concentration de 1×10^8 CFU.mL $^{-1}$ ($DO_{620nm} = 0,1$). La culture diluée a ensuite été centrifugée, le surnageant éliminé et le culot resuspendu dans un même volume d'une solution de PBS (pour culture cellulaire, pH 7,4). Finalement, 0,1 mL de cette solution a été injecté directement dans la cavité péritonéale des anguilles. Un suivi de la mortalité a ensuite été réalisé pendant 7 jours. La concentration de la culture bactérienne a été choisie après réalisation de tests d'infection d'anguilles à des concentrations de 1×10^8 CFU.mL $^{-1}$, 1×10^7 CFU.mL $^{-1}$, et 1×10^6 CFU.mL $^{-1}$ au cours desquels seule la concentration de 1×10^8 CFU.mL $^{-1}$ a induit une mortalité.

5. Mise au point de l'alimentation supplémentée en algue

La mise au point de l'alimentation supplémentée en algue a nécessité plusieurs étapes. Il a d'abord été indispensable d'effectuer un choix entre *A. armata* et *A. taxiformis*. Ce choix a été réalisé à partir d'une expérience d'appétence et de la mesure de la croissance des anguilles à l'issue de cette expérimentation. Au cours de celle-ci, 26 anguilles ont été réparties dans 5 aquariums et ont été nourries pendant 3 semaines avec l'une des cinq alimentations suivantes : 0 % d'algue, 3 % et 10 % de poudre d'*A. armata*, 3 % et 10 % de poudre d'*A. taxiformis*. Les 3 % de supplémentation correspondent à ceux utilisés dans la littérature et ayant abouti à des effets bénéfiques pour les poissons (Reverter et al., 2016 ; Thépot et al., 2022) et les 10 %, à une supplémentation suffisamment éloignée de la précédente pour observer d'éventuelles différences. L'alimentation a été formulée à partir de la nourriture qui était donnée quotidiennement aux anguilles à laquelle a été ajoutée la quantité de poudre d'algue permettant d'atteindre les pourcentages cités. Des comportements de refus d'alimentation ont été observés pour les anguilles nourries avec les deux alimentations supplémentées à 10 %, tant pour *A. taxiformis* que pour *A. armata*, et dans une moindre mesure, pour les anguilles nourries avec l'alimentation supplémentée à 3 % d'*A. armata*. Ces refus se sont traduits par une perte de poids significative pour ces anguilles. Seules les anguilles nourries avec l'alimentation supplémentée à 3 % d'*A. taxiformis* ont montré un gain de poids non différent de celui des anguilles contrôles. Ces résultats ainsi que ceux des résultats des tests *in vitro* relatifs à l'effet des extraits des deux

espèces d’algues sur la survie du parasite *A. crassus* (présentés dans le **Chapitre IV**) ont permis de cibler l’espèce *A. taxiformis* et un pourcentage de supplémentation de 3 %.

6. Les outils analytiques

6.1 La métabolomique

6.1.1 Le workflow

L’approche métabolomique comprend la réalisation d’un ensemble d’étapes appelé couramment le « workflow » (**Figure 17**). Ces étapes vont du questionnement initial jusqu’à l’interprétation biologique des résultats. Entre ces étapes se succèdent : la conception et la réalisation du design expérimental, la collecte et la préparation des échantillons, leur extraction, l’acquisition des données relative à leur composition chimique (qui peut être réalisée via différents appareils analytiques), le pré-traitement des données « brutes » via des outils informatiques et statistiques, qui permettent la détection de variables correspondant à des molécules, et la création d’une matrice contenant les échantillons, n variables et l’aire détectée de chaque variable. Après le traitement des données brutes, des analyses statistiques réalisées sur les matrices permettent de comparer les différents groupes et échantillons d’un point de vue de leur composition chimique et d’identifier des variables (molécules) discriminantes (avec des abondances significativement différentes). Ces variables sont ensuite caractérisées en utilisant les informations issues de la ou des analyse(s) (spectre de masse, spectre de fragmentation...), en comparant avec des bases de données ou avec des standards commerciaux. Il existe plusieurs niveaux d’identification, allant du calcul de la formule brute la plus probable à la comparaison avec un standard commercial. L’étape ultime du workflow en métabolomique est l’interprétation biologique (**Figure 17**).

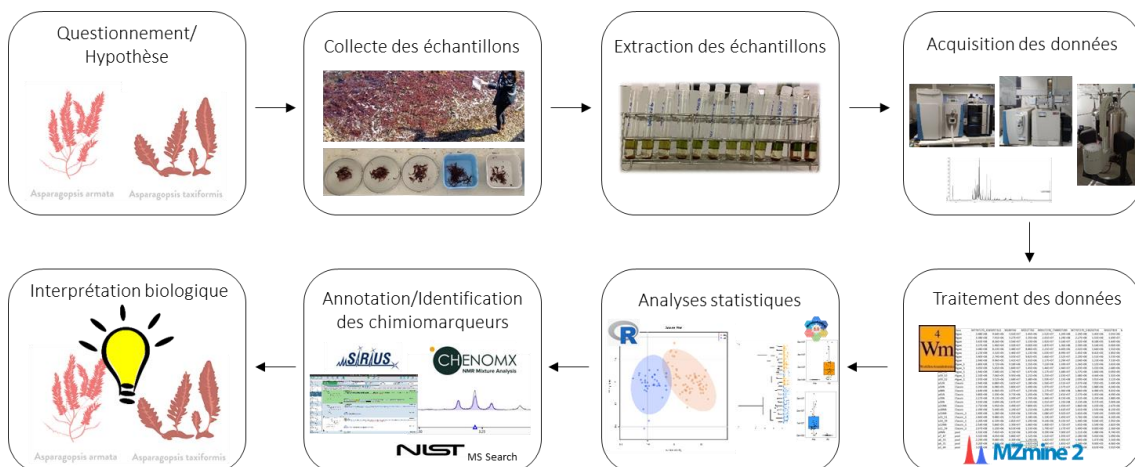


Figure 17 : Schéma général des principales étapes (= workflow) pour la réalisation d’une étude métabolomique

6.1.2 Extraction

L'extraction principalement utilisée dans cette thèse pour la réalisation des analyses métabolomiques est une extraction biphasique adaptée de Matyash et al. (2008). Cette extraction solide-liquide a été réalisée grâce à l'ajout d'abord d'un mélange de Méthanol (MeOH) et de Méthyl tert-butyl éther (MTBE) (2 : 6) puis d'eau (2x MeOH). L'extrait a été homogénéisé puis placé dans un bain à ultra-sons. L'émulsion formée se sépare alors en 2 phases après centrifugation. La phase supérieure contient les molécules apolaires comme les pigments et les lipides tandis que la phase inférieure contient les molécules polaires comme les acides aminés et les sucres (**Figure 18**). Ce type d'extraction permet ensuite, en fonction des questionnements, de cibler des types de molécules selon leur polarité et de choisir le ou les outil(s) d'analyse adapté(s). Dans le cadre d'études sur les organismes marins, cette extraction permet aussi de dessaler en grande partie la phase apolaire qui peut alors être analysée via des appareils comme la LC-MS ou la GC-MS.



Figure 18 : Illustration des deux phases obtenues après centrifugation *via* l'extraction biphasique des algues

6.1.3 Acquisition des données

L'acquisition des données relative à la composition chimique des échantillons présentée dans cette thèse a été réalisée à l'aide de trois méthodes d'analyses : la LC-HRMS, la HS-SPME-GC-MS et la RMN ¹H. Chacune des techniques explicitées ci-dessous présente des avantages et des inconvénients. La RMN possède les avantages d'être non destructive, quantitative et plus reproductible que les deux autres méthodes (Zhang et al., 2012). La spectrométrie de masse présente une meilleure sensibilité que la RMN, contribue à la détection de métabolites même à

de très faibles concentrations et, couplée à de la chromatographie, permet de séparer des molécules. La GC-MS est préférentiellement utilisée pour l'étude de composés volatiles, la RMN plutôt pour l'étude des molécules polaires tandis que la LC-HRMS permet l'étude d'une plus large gamme de molécules.

6.1.3.1 La LC-MS

La LC-MS ou « liquid chromatographie-mass spectrometry » est une méthode d'analyse qui permet de séparer les molécules d'un échantillon par chromatographie liquide puis d'identifier les masses moléculaires des molécules séparées grâce à la spectrométrie de masse. La séparation des molécules est réalisée à l'aide d'une colonne de chromatographie et d'une phase mobile liquide. La phase mobile consiste en un solvant ou mélange de solvant dont les proportions vont changer au cours de l'analyse permettant d'éluer les molécules en fonction de leur affinité soit pour le solvant soit pour la colonne. Pour les travaux présentés dans cette thèse, la colonne choisie est une colonne de type Luna Omega Polar C18 (Phenomenex), stable avec un éluant totalement aqueux, et qui permet de retenir et séparer les molécules polaires tout en gardant une bonne séparation des composés apolaires. La phase mobile initiale est donc composée d'une proportion plus importante de solvant polaire et est modifiée au cours du temps de la séparation pour évoluer vers une proportion plus importante en solvant apolaire. L'appareillage utilisé est une chaîne de chromatographie liquide à ultra haute performance « UHPLC » (Ultra High Performance Liquide Chromatography) « Vanquish » de ThermoScientific (MA, USA) équipée d'un spectromètre de masse « Q ExactiveTM Plus » (spectromètre de masse hybride quadripôle-OrbitrapTM) avec une source d'ionisation à electronébulisation (electrospray). L'UHPLC rend possible l'utilisation de colonnes de séparation de petit diamètre composées de particules également de petite taille (<2 µm) permettant une meilleure séparation des molécules ainsi qu'une meilleure résolution, et grâce à l'utilisation d'une pression plus élevée, de raccourcir les temps d'analyses. Brièvement, après séparation dans la colonne UHPLC, les molécules arrivent en solution dans l'électronébuliseur. Un champ électrique est appliqué et transforme les molécules en solution en mini gouttelettes chargées électriquement. La taille des gouttelettes va diminuer avec l'évaporation du solvant jusqu'à une taille critique permettant l'ionisation et la libération des ions sous forme gazeuse. L'ionisation peut être réalisée en mode positif et/ou négatif, les ions sont le plus fréquemment formés par protonation ou déprotonation aboutissant à des adduits $[M+H]^+$ et/ou $[M-H]^-$. Les ions sont ensuite envoyés dans l'Orbitrap dans lequel ils sont piégés dans un mouvement orbital où la fréquence de rotation est fonction du rapport m/z (masse sur charge). Finalement, le

détecteur génère un spectre de masse en convertissant le courant des ions piégés en spectre de fréquence via la transformée de Fourier. En sortie d'analyse, à chaque échantillon est associé un chromatogramme qui est la somme de tous les ions détectés ainsi qu'un spectre de masse en tout point du chromatogramme (**Figure 19**).

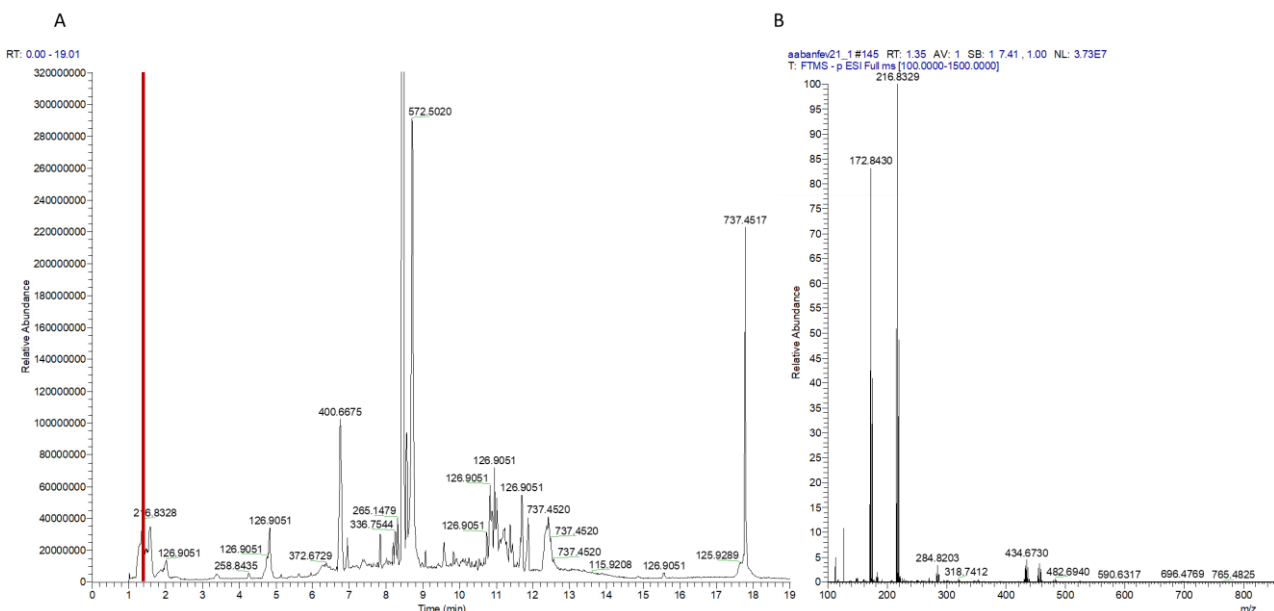


Figure 19 : Exemple de chromatogramme (A) et du spectre de masse (100-800 m/z) du composé élué au temps de rétention 1,35 minutes (B) représenté par la droite rouge sur le chromatogramme.

6.1.3.2 La GC-MS

La GC-MS (« gaz chromatography-mass spectrometry ») et la LC-MS reposent sur le même principe général mais la phase mobile en GC-MS est un gaz. Pour la réalisation des travaux de cette thèse, la GC-MS utilisée est couplée à une méthode d'extraction appelée « Microextraction en phase solide » (« Solid Phase MicroExtraction/SPME ») de « l'espace de tête » (HeadSpace/HS), introduite par Janusz Pawliszyn en 1989 (Pawliszyn, 1997), qui donne l'abréviation de la méthode d'analyse dans son ensemble : HS-SPME-GC-MS ou « Head Space-Solid Phase MicroExtraction-Gaz Chromatography-Mass Spectrometry ». Le principe de cette extraction repose sur l'augmentation de la température de l'échantillon dans un flacon permettant l'extraction des composés les plus volatiles qui se trouvent alors dans l'espace de tête (**Figure 20**) (Pawliszyn, 2012). L'insertion d'une fibre permet alors aux molécules de s'adsorber puis de se désorber une fois introduite dans la GC-MS. Enfin, les molécules seront séparées grâce à une colonne de chromatographie, et les masses moléculaires détectées grâce au spectromètre de masse (**Figure 20**).

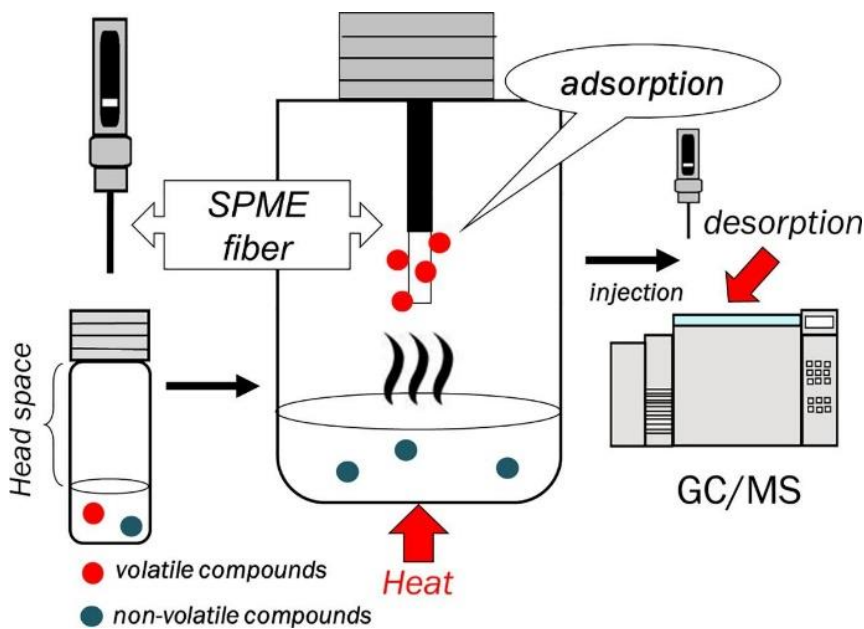


Figure 20 : Principe de la méthode d'extraction « HS-SPME ». Source : Saito et al. (2019)

Lors de l'extraction, il est possible d'agir sur différents paramètres comme le temps d'extraction, le temps d'adsorption sur la fibre, le temps de désorption, ainsi que les différentes températures de chaque étape afin d'optimiser l'extraction. Cette méthode permet d'éviter l'utilisation de solvants toxiques, de raccourcir considérablement l'étape de préparation des échantillons puisqu'ils peuvent être mis directement en poudre dans les flacons, et d'obtenir une meilleure reproductibilité des résultats. En revanche, la durée totale de l'analyse est rallongée, ce qui peut engendrer un coût supplémentaire, et seuls les composés volatiles sont détectés. La fibre utilisée pour ces travaux de thèse est une fibre Divinylbenzene/Carboxen/Polydimethylsiloxane (DVB/CAR/PDMS) généraliste qui permet l'adsorption d'une large gamme de composés. La colonne utilisée est une colonne capillaire de faible polarité (OPTIMA 5 MS Accent – 0.25 µm). Enfin, l'appareil GC-MS utilisé est un FOCUS GC gas chromatography system couplé à un spectromètre de masse « DSQ II Electron Impact-Single Quadrupole (EI-Q) » de chez ThermoScientific (MA, USA). L'« Electron Impact Ionization », ou ionisation électrique (EI), est une ionisation basée sur l'accélération des électrons grâce à une énergie cinétique de 70 eV, qui permet de bombarder les molécules dans la source et de générer des ions chargés positivement et instables. Cette instabilité conduit les ions à se dégrader et à produire plusieurs fragments qui seront ensuite analysés et détectés.

6.1.3.3 La RMN

La spectroscopie de Résonance Magnétique Nucléaire (RMN) repose sur le phénomène de résonance magnétique nucléaire de certains noyaux soumis à un champ magnétique externe.

Sous l'action du champ magnétique, ces noyaux peuvent prendre plusieurs orientations correspondant à différents niveaux d'énergie, on parle alors de résonance du noyau lors de la transition entre ses différentes orientations et niveaux d'énergie. Le signal ainsi émis est détecté, puis une transformation de Fourier est appliquée pour transformer ce signal en un signal dépendant de la fréquence, ce qui aboutit à un spectre RMN avec des signaux correspondant aux différents protons de l'échantillon analysé. Cette technique est majoritairement appliquée au proton (¹H) et au carbone (¹³C) dont l'environnement proche au sein d'une molécule va impacter la fréquence de résonance. En effet, le champ magnétique externe appliqué impacte aussi les électrons autour du noyau qui vont avoir une circulation créant un champ magnétique interne qui va modifier le champ externe (phénomène de blindage et de déblindage). Plus le phénomène de déblindage est intense et moins le proton doit être soumis à un champ magnétique externe fort pour que se produise la résonance. Ceci se traduit par un déplacement, appelé déplacement chimique des signaux sur le spectre RMN vers la gauche. Les déplacements chimiques sont exprimés par rapport à une référence de déplacement chimique à 0,0 ppm, souvent le tétraméthylsilane (TMS) et pour les travaux de cette thèse le triméthylsilylpropanoate (TMSP). Par ailleurs, l'analyse par RMN nécessite une étape préliminaire de solubilisation des extraits dans un solvant deutéré dont un ou plusieurs de leurs atomes d'hydrogènes sont remplacés par l'isotope stable du deutérium. Pour les analyses métabolomiques (comme c'est le cas pour cette thèse), un tampon (i.e. tampon phosphate) est souvent ajouté et permet de fixer le pH des différents échantillons.

6.1.4 Pré-traitement des données

6.1.4.1 La LC-MS et la GC-MS

Les chromatogrammes, les spectres de masses et les intensités des ions sont contenus dans des fichiers bruts qu'il est nécessaire de convertir pour réaliser leur pré-traitement. Pour cette thèse, les fichiers ont été convertis au format mzML grâce au logiciel MSconvert de la librairie Proteowizard (Chambers et al., 2012). Le pré-traitement consiste ensuite à convertir l'ensemble des données liées aux pics et aux molécules détectés en valeurs numériques (variables) exploitables statistiquement grâce à plusieurs étapes. Les données issues de la LC-MS ont été pré-traitées en ligne via la plateforme Worflow4Metabolomics (W4M) sur le portail Galaxy (Giacomoni et al., 2015 ; Guitton et al., 2017) qui est une plateforme en ligne utilisant les codes R du logiciel XCMS. Les données de GC-MS ont été pré-traitées via MzMine 2.53, un logiciel utilisant ses propres algorithmes (Pluskal et al., 2010).

Les étapes réalisées sur W4M sont : (1) l'extraction des ions de chaque échantillon, la filtration et l'intégration des pics (« xcms findChromPeaks »), (2) la combinaison des fichiers issus de la première étape en un seul fichier (« xcms findChromPeaks Merger »), (3) le groupement des pics représentant un même analyte au sein d'un échantillon selon des valeurs de m/z se chevauchant et par rapport à la distribution des pics selon leur temps de rétention (« xcms groupChromPeaks »), cette étape permettant aussi d'éliminer les pics détectés dans un nombre insuffisant d'échantillons, (4) la correction des dérives de temps de rétention (« xcms adjustRtime »), (5) un second groupement une fois les temps de rétention corrigés (« xcms groupChromPeaks ») et, (6) l'intégration des aires des pics manquants (« xcms fillChromPeaks »). Une étape additionnelle permet d'annoter les résultats et de fournir des statistiques (t-test et p-value) (« CAMERA.annotate ») permettant ensuite la correction par les blancs et par les pools d'échantillons (« Generic Filter » « Quality Metrics »).

Via MzMine 2.53, ces étapes sont : (1) la détection et création d'une liste de masses (« Features detection/Mass detection »), (2) la création d'un chromatogramme à partir de la liste de masses pour chaque échantillon (« Feature detection/ADAP Chromatogram builder »), (3) la séparation des pics pour chaque chromatogramme (« Feature detection/Chromatogram deconvolution »), (4) la déconvolution spectrale, étape spécifique à la GC-MS qui permet de combiner des pics similaires et de re-construire un spectre de pseudo-fragmentation en utilisant les intensités des pics (« Spectral deconvolution/Hierarchical clustering ») et enfin, (5) l'alignement des spectres de pseudo-fragmentation créés à l'étape précédente (« Alignement/ADAP Aligner (GC) »). Une étape additionnelle permet de rechercher et trouver les pics manquants et de combler l'absence d'éventuels pics n'ayant pas été détectés du fait de leur faible intensité dans les chromatogrammes (« Gap filling/Peak Finder (multitreaded) »).

Après ces pré-traitements, les données sont exportées pour constituer une matrice qui contient les variables en lignes, les échantillons en colonnes (ou inversement selon les logiciels de traitement) et les aires mesurées pour chaque variable dans chaque échantillon (**Figure 21**).

A	B	C	D	E	F	G	H	I	J	K	L	M	N	O	P	Q
1 name	17663208.8	17460551.1	17273023.1	17644433.0	17367483.9	18434826.3										
2 M117773	17821202.3	17051638.7	18587489.2	16707113.8	16740342.8	19139444.2										
3 M121725	2096540.28	782088.17	2204634.04	110560.88	1347154.93	2152799.51										
4 M127167	11836636.1	11714482	11653872.5	11333264	11722209	11625914.8	12396457	11737324.6	11802355.9	11895836.6	11223187.9	11791785.6	12021680.5			
5 M127765	3815377.39	4571170.05	3839026.8	3471905.94	3828545.6	3538481.13	3742923.94	3572706.18	4829616.03	4177308.02	4149392.43	3573856.15	2970816.63	3261314.44	3424172.18	2668380.7
6 M127745	11077969	7921536.2	13639574.4	13658083.9	14116358.9	13290920.6	13050410.7	11603750.4	11783203.3	11818963.2	10979058.1	13783937.6	13619078.3	12656138.9	14343762.2	12775021
7 M12976	12837418	12474914.4	12610946.1	12295065.1	12654970	12521128.5	13575063.3	12729446.4	12673048.9	12876209.2	12087691.1	12661828.4	13014436	12935407.1	12554134.2	12530535
8 M12975	3238088.12	2887985.17	3995777.16	3037216.88	4422776.67	3290426.58	4508840.5	2940510.9	4850924.06	3444789.7	5376147.69	3927186.98	2866880.2	3329219.73	3361258.53	1826326.2
9 M13075	5420430.2	4195993.76	7106453.02	4809369.97	701252.54	5563822.09	6070259.21	5356423.7	7636099.12	5311915.93	765125.86	4727502.85	5265922.22	5293103.87	5614231.96	6050423.8
10 M13075	5799376.33	5311196.76	7506548.4	5464608.21	6343288.29	6404521.94	7744069.89	5675566.82	9073923.27	6500364.67	8331302.89	7231519.91	6370556.51	6361746.47	6133504.19	6587937.4
11 M	4133288.86	2920594.37	4707667.76	4515731.06	2852581.9				1	4309306.44	4013811.33	4635084.82	4312380.09	4369516.85	3902538.85	3739937.6
12 M	6164288.56	6889508.79	6193402.3	5979928.1					5	6141155.83	6583737.4	6417084.49	6722239.94	4633279.13	6425462.91	4565939.2
13 M	4834647.42	3020731.24	4168124.61	405828.25	3937322.9				1	3842171.71	4586603.9	4660558.89	4166484.75	3824632.97	2941183.27	3360821.2
14 M	21059416.1	20901146.6	20092446.4	21042486.2	20763158	22289854.7	20459906.7	2102069.3	21221362	19936924.8	20898101.9	20839675.4	19099415.7	2020632		
15 M	8131623.29	6275346.58	7278057.99	6074288.67	6981087.07	5062774.09	5158209.78	6088774.78	6535428.46	6264809.24	6159289.23	7851764.68	6705493.58	5489356.66	12942383	
16 M17376	18674155.3	17461105.2	12262259.6	11425316.4	12318798.3	11906182.6	13542579.1	20841990.5	20226406.6	17959379.7	18413926.9	11723797.7	11296295.5	12655232.1	11367817	12962096
17 M17375	10698479.1	10652815.1	12593734	12383630.9	11321548.9	12737292.5	12755074	6609448.85	6793411.03	5482386.92	12049128.9	12169734.5	11334650.8	6269579.66	6675638.01	12740156
18 M18377	5639134.14	5631211.92	4214989.43	4449706.12	6638916.47	5401035.2	7799899.89	5900037.13	6412123.97	5251144.07	5498977.67	7314438.48	4995084.29	5234971.63	509492.92	4793781.7
19 M18374	146391.218	3214230.16	3858843.02	3464255.8	3591908.2	3725603.28	3108798.95	4335840.25	418550.57	3878300.28	3484079.89	3340186.33	3415067.14	3851625.47	3765207.65	3477656.5
20 M18374	5348950.91	5075072.04	5242935.7	5045711.06	5211608.94	5138218.6	5373590.16	5198024.82	5388928.78	5458106.91	5195958.46	5227976.78	5066496.25	4910245.02	5292938.66	5263517.1
21 M18374	3156580.56	29399368.5	29807510.8	30038050.5	30204159.3	3139874.2	33465155.1	34969296.6	35490527.8	31202237.7	31106203.3	28251414.8	29491541.2	32786254.3	31615349.5	3252194
22 M19373	4868509.48	4784507.96	5192317.47	4750723.13	4950816.93	4849042.69	5011526.89	5126758.73	5329248.07	5168732.9	4988664.66	5040413.26	4963129.35	5004934.36	4895829.24	4698585.5
23 M19373	41706335.8	38466503.6	40068610.7	40135731.3	40490534.4	40543280.1	44618632.9	44709971.2	41318239.2	40352576.6	37766299.26	39647811.5	42187121.1	42435159.3	42521780	
24 M19373	20599408.5	19126847.4	1950774.3	19723532.8	19673323.8	20260759.3	21898826.2	22543178.3	22940396.1	20188034.9	2008523.2	18635281	19350878.4	21050866.7	20915594.6	21053040
25 M19911	4552981.39	4241627.13	4397278.3	4402280.1	4416354.86	4450870.85	4915025.97	4874133.14	4867290.66	4517676.32	4421565.01	4156818.39	4324316.56	4652118.81	4617077.37	4627547.5
26 M19911	4501631.92	4806555.85	5033087.05	4945926.99	4913791.66	4863469.05	5091571.57	4719533.13	5071190.5	4833706.82	4557543.34	5015674.08	4767636.98	5163589.5	4935659.28	5015519.5
27 M2087306																

Figure 21 : Exemple de matrice après pré-traitement de données acquises en LC-MS

6.1.4.2 La RMN

En métabolomique les spectres RMN acquis sont souvent complexes par la diversité des signaux mais aussi par leur nombre lié à l'absence d'étape de séparation des métabolites en amont de l'analyse. Le pré-traitement consiste en différentes étapes successives principalement de (1) correction de la référence, (2) correction de la ligne de base, (3) alignement des différents spectres et, (4) bucketing. Dans le cadre de ma thèse l'algorithme de bucketing utilisé est le « bucketing intelligent » (Lefebvre et al., 2004). Cette dernière étape consiste à découper le spectre de manière optimisée « intelligente » en évitant de couper au milieu d'un signal (Figure 22), ce qui n'est pas le cas avec les méthodes de bucketing classiques qui découpent le spectre de manière régulière sans tenir compte des signaux. L'aire sous les pics est calculée et constituera le corps de la matrice.

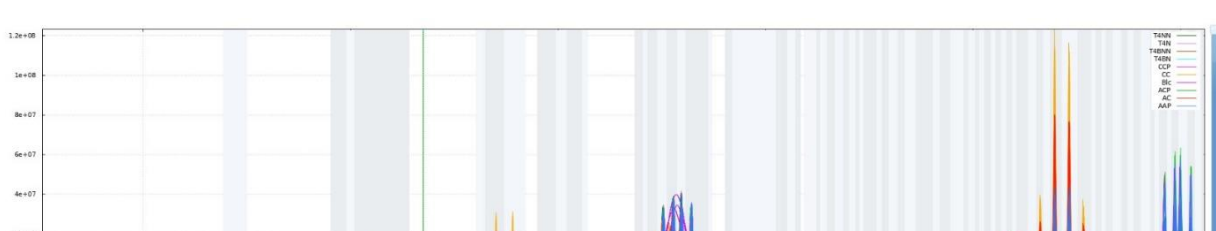


Figure 22 : Exemple de bucketing intelligent réalisé sur un ensemble de spectres RMN d'extraits polaires d'anguille

6.2 Le métabarcoding

Le metabarcoding est une technique de séquençage à haut-débit, qui permet d'identifier l'ensemble des organismes présents dans un échantillon grâce à l'étude de leur ADN. Il est possible de cibler un groupe d'organismes (tel que le microbiota), et d'étudier la composition de la communauté, en amplifiant une région des ADN des représentants du groupe avec des amorces spécifiques lors d'une réaction en chaîne par polymérase (PCR). Dans le cas de cette thèse, les communautés bactériennes des algues ont été étudiées grâce à l'amplification d'une région du gène de l'ARN ribosomique 16S (Klindworth et al., 2013). Le workflow est assez similaire à celui de la métabolomique. Il est d'abord nécessaire de réaliser l'extraction de l'ADN contenu dans les échantillons en plusieurs étapes : la lyse des cellules, la purification puis la précipitation et l'éluition des acides nucléiques. Ensuite, des étapes d'amplification et de séquençage sont réalisées. Le séquençage aujourd'hui le plus utilisé est le séquençage avec la technologie MiSeq (Illumina) qui permet de séquencer plusieurs millions de fragments d'ADN. Ce séquençage est réalisé en plusieurs étapes. D'abord des adaptateurs sont ligaturés aux brins d'ADN, puis ces brins sont fixés sur une « flowcell » et amplifiés en PCR « bridge ». La polymérisation est réalisée avec des nucléotides marqués avec une sonde fluorescente. Les nucléotides sont déterminés en fonction de la longueur d'onde et de l'intensité du signal émis après excitation. Ensuite, un pré-traitement est réalisé, permettant le nettoyage et l'annotation des séquences à partir de séquences de référence dont la taxonomie est connue (Callahan et al., 2016). La matrice finale est composée, pour chaque échantillon analysé, des « amplicon sequence variants » (ASVs), du nombre de séquences pour chaque ASV et des annotations à différents rangs taxonomiques (phylum, classe, ordre, famille et genre). Ensuite, comme pour la métabolomique, des outils statistiques et multivariés sont utilisés afin d'étudier deux niveaux de diversité, la diversité alpha (diversité intra-échantillons, en termes de nombre et d'abondances des ASVs) et la diversité beta (diversité inter-échantillons, en termes de similarités ou de différences des communautés bactériennes). La diversité alpha est ici étudiée grâce à trois indices, les indices de Chao1 (richesse spécifique en nombre d'ASVs), d'équitabilité (0= déséquilibre des abondances avec un seul ASV dominant, à 1= ASVs présents en abondances identiques), et de Shannon qui prend en compte les deux indices précédents (0= peuplement homogène constitué d'une seule espèce, >0 nombre d'espèces différentes dans le peuplement qui augmente). La diversité beta est étudiée à l'aide d'outils statistiques multivariés tels que présentés dans « **7. Outils statistiques** ». Enfin, certains outils comme Tax4Fun2

(Wemheuer et al., 2020) permettent de prédire les fonctions associées à l’assemblage bactérien en comparant les séquences des ASV avec une base de données de génomes.

6.3 La transcriptomique

La transcriptomique est une technique d’analyse qui permet l’analyse quantitative relative de l’ensemble des ARNs ou transcrits formant le transcriptome au sein d’un échantillon. L’analyse transcriptomique débute donc par l’extraction des ARN totaux contenus dans l’échantillon suivie de leur séquençage. Actuellement, la technique de séquençage la plus utilisée est le RNA-seq. Cette méthode de séquençage est composée de deux grandes étapes (1) la création des librairies de séquençage (= fragments d’ADNc) par transcription inverse et (2) le séquençage, avec la méthode Illumina telle que décrite dans le « **6.2 Métabarcoding** ». Les séquences (= reads) ainsi obtenues sont alignées sur un génome de référence ou sur un transcriptome annoté et le nombre de « reads » (ou nombre de fois qu’un même transcrit a été séquencé) permet de déterminer l’expression relative des gènes (**Figure 23**).

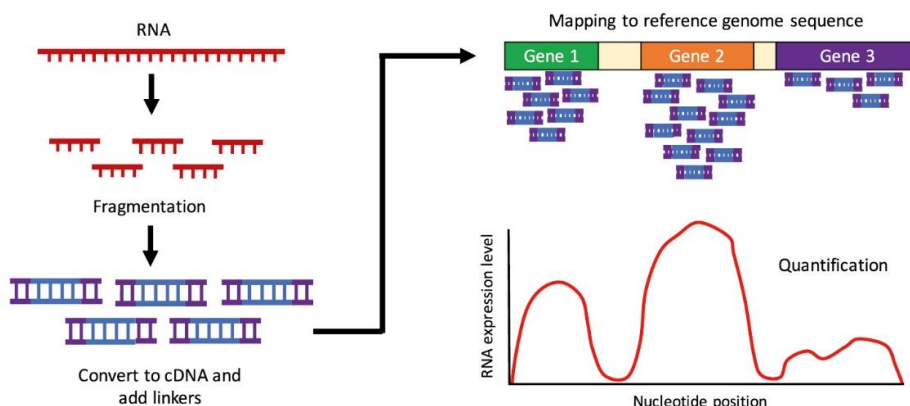


Figure 23 : Schéma des grandes étapes d’une analyse transcriptomique. Source : Adapté de Rogawski et al. (2017)

La matrice finale est composée, pour chaque échantillon, des gènes, du nombre de « reads » pour chaque gène et des éventuelles annotations. L’analyse de cette matrice est ensuite généralement réalisée en deux étapes avec d’abord l’étude des gènes différentiellement exprimés entre les différentes conditions expérimentales, suivie d’une analyse fonctionnelle qui regroupe les gènes en grandes fonctions biologiques et permet l’interprétation à une échelle plus globale.

7. Les outils statistiques

7.1 Normalisation des données

Selon le questionnement à l'origine d'une analyse, il peut être nécessaire de normaliser les données. En effet, les matrices obtenues en fin de pré-traitement peuvent contenir des variables dont l'aire (métabolomique) ou le nombre de comptage (métabarcoding, transcriptomique) est majoritaire. De plus, il peut exister des variables pour lesquelles la variance est très différente entre échantillons de même conditions expérimentales. Or les analyses multivariées (**7.3 Analyses multivariées**) donnent plus de « poids » aux variables avec une grande variance et ces variables ne sont pas nécessairement plus importantes selon la question biologique. En métabolomique, lorsque l'objectif est d'identifier des marqueurs discriminants entre plusieurs échantillons ou conditions, il est important d'appliquer une normalisation sur les données afin de limiter le « poids » des variables avec une grande variance lors de l'analyse. En revanche, lors d'analyses de la composition de communautés bactériennes, il peut être intéressant de ne pas normaliser les données pour identifier les espèces bactériennes dominantes et qui structurent l'ensemble de la communauté.

Il existe de nombreuses méthodes de normalisation des données utilisant des formules mathématiques différentes, l'une des plus utilisées consiste à centrer (« centering ») et réduire (« scaling ») les données en soustrayant aux valeurs leur espérance et en divisant par l'écart-type. Ainsi les données auront les mêmes moyennes et dispersion égales à 1.

7.2 Analyses univariées

Les analyses statistiques univariées permettent d'étudier la relation entre une valeur expliquée et une valeur explicative, par exemple, la croissance (valeur expliquée) mesurée d'une anguille est-elle différente entre la condition A et B (valeur explicative) ? Ces relations sont étudiées au travers de tests statistiques qui permettent de rejeter ou pas une hypothèse nulle (souvent l'absence de différence entre deux variables). Il existe de nombreux tests statistiques qui peuvent être paramétriques ou non paramétriques. Les tests paramétriques reposent sur plusieurs hypothèses dont la principale est que les échantillons ont une distribution continue, souvent selon une loi normale qu'il est nécessaire de vérifier (test de Shapiro). Ces tests sont généralement plus puissants et sensibles que les tests non paramétriques. Les tests paramétriques les plus utilisés sont le t-test (comparaison de moyenne entre deux variables explicatives) et l'ANOVA (ANalysis Of Variance) (comparaison de variance entre trois

variables explicatives ou plus). L'ANOVA permet de rejeter ou non l'hypothèse nulle, ensuite un test « Post-Hoc » (ex : test de Tukey) à comparaisons multiples est souvent utilisé pour identifier les valeurs explicatives qui diffèrent. Les équivalents non-paramétriques des t-tests et ANOVA sont les tests de Wilcoxon-Mann-Whitney et de Kruskal-Wallis respectivement et l'équivalent du test de Tukey est le test Nemenyi. Les tests donnent une valeur statistique la *p-value*, correspondant à la probabilité que l'hypothèse nulle soit vraie. Généralement, des valeurs de probabilités inférieures ou égales à 0,05 sont considérées comme suffisamment faibles pour que l'hypothèse nulle soit vraie et donc cette hypothèse nulle est rejettée.

7.3 Analyses multivariées

Les analyses statistiques multivariées visent à étudier la distribution de plusieurs variables. On distingue les analyses multivariées dites non-supervisées, des analyses supervisées.

7.3.1 Non supervisées

Les analyses non supervisées ont pour objectif d'évaluer la variance d'un ensemble de variables sans « guide ». Ces analyses sont descriptives et ont pour but de simplifier les données souvent en réduisant les dimensions du tableau de données. Je ne présenterai ensuite que l'ACP et l'analyse de classification hiérarchique avec les représentations en dendrogramme et en « heatmap » qui sont les analyses qui ont été utilisées dans cette thèse.

L'ACP est l'analyse la plus utilisée, elle permet de réduire l'information contenue dans le tableau de données en de nouvelles variables synthétiques appelées les composantes principales. Des pourcentages sont associés à ces composantes principales et représentent le pourcentage de variance expliqué par chaque composante. La réduction en quelques composantes principales peut induire une perte d'information, ainsi, plus le pourcentage de variance expliqué cumulé par les premières composantes (souvent les deux ou trois premières) est élevé, et plus l'information est conservée. Ces composantes principales peuvent être représentées graphiquement sous forme d'axes et les échantillons peuvent être projetés sur ce graphique (= scores plot). Ce graphique permet alors d'étudier la répartition globale des échantillons selon les composantes principales. D'autres types de représentations permettent d'explorer l'information contenue dans le tableau de données initial avec par exemple la projection des variables qui permet cette fois d'étudier la contribution des variables aux composantes principales ou encore le cercle des corrélations qui représente les corrélations des variables entre elles.

L'analyse de classification hiérarchique est une méthode statistique qui utilise des mesures de distance (Euclidienne, Spearman, Pearson...) et des algorithmes de partitionnement (Ward, Average, Complete...) pour regrouper des individus similaires. Le dendrogramme et la heatmap (ou carte de chaleur) sont deux types de représentations graphiques (**Figure 24A, B**) qui utilisent ce type d'analyse. Alors que le dendrogramme ne représente que les relations unidimensionnelles (par exemple entre individus ou entre variables) (**Figure 24A**), la heatmap est une représentation tridimensionnelle (**Figure 24B**) comprenant les individus et les variables qui peuvent être représentés selon une classification hiérarchique ainsi que l'intensité de ces variables pour chaque individu.

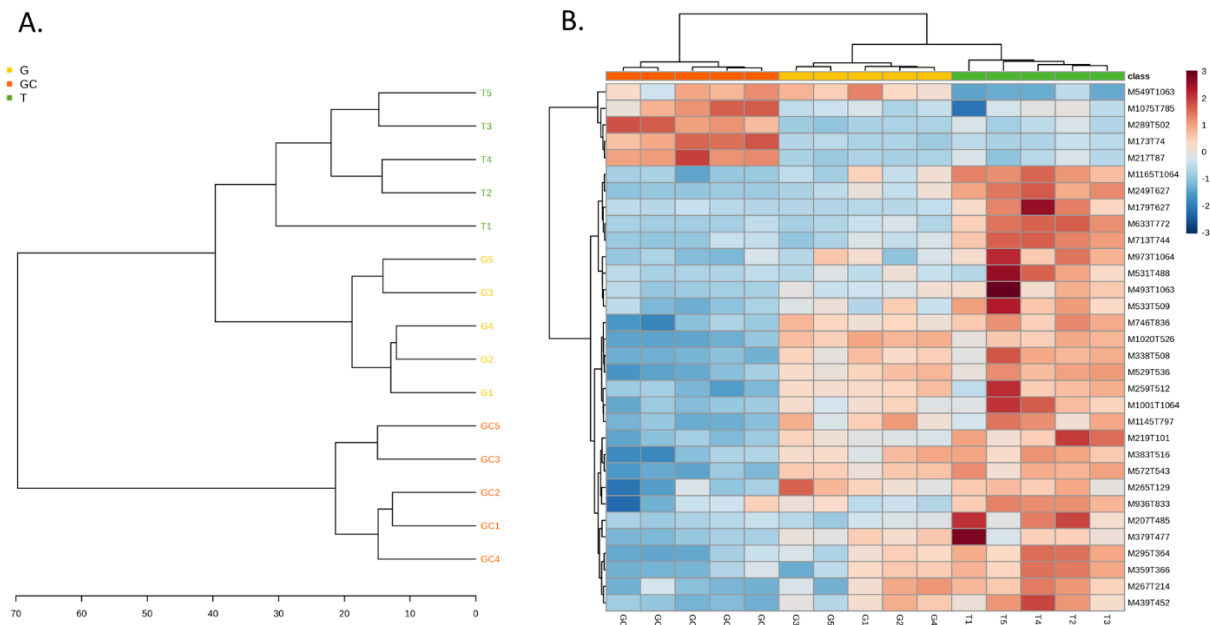


Figure 24 : Dendrogramme (A) et Heatmap (B) représentant le métabolome des échantillons des trois stades du cycle de vie d'*A. armata*. Distance : Euclidienne, Partitionnement : Ward.

7.3.2 Supervisées

Les outils statistiques « supervisés » permettent d'optimiser la séparation entre différents groupes d'échantillons et d'identifier les variables explicatives qui contribuent le plus à cette séparation. La PLS-DA pour Partial Least Squares Discriminant Analysis, en français « analyse discriminante des moindres carrés partiels » est l'une des analyses les plus utilisées. Cette méthode est basée sur la régression PLS qui construit un modèle de régression linéaire dont le but est de relier un bloc de variables à expliquer X à un bloc de variables explicatives Y. Des méthodes de validation des modèles ont été mises au point afin d'éliminer la possibilité d'un

bon modèle créé de manière aléatoire. Pour les travaux de cette thèse, les modèles PLS-DA ont été validés à l'aide de plusieurs paramètres qui sont l'accuracy qui représente la justesse de chaque composante en fonction de la précision de la prédiction, le R² qui indique la variation expliquée par les composantes, et le Q² qui indique la prédictibilité du modèle à partir de validations croisées. Une valeur de Q² proche de la valeur de R² est donc signe d'un bon modèle. Globalement, une valeur de Q² > 50 % est dite acceptable pour les études de métabolomique (Wiklund, 2008). La validation des PLS-DA a également été testée avec un test de significativité par permutation basé sur une validation croisée (Westerhuis et al., 2008). Dans ce test de validation, n échantillons sont séparés en $n-x$ échantillons pour la construction du modèle et les échantillons restants permettent de tester la performance du modèle. Le processus est répété k fois et donne un « classification error rate » (CER) correspondant au taux d'erreurs de classification des échantillons tests et une p-value pour évaluer le « pouvoir discriminant » du facteur utilisé.

7.4 Analyses « multiblock »

Le développement des technologies et notamment –omiques ont rendu possible les analyses intégratives. Pour permettre le traitement de ces données complémentaires, des outils statistiques dits « multiblock », qui permettent d'intégrer plusieurs jeux de données acquis sur un même échantillon, ont été élaborés. Certains de ces outils utilisent des approches non supervisées, c'est le cas de l'analyse en « composantes communes et poids spécifiques » (« Common Components and specific weights analysis (CCSWA) ») maintenant aussi appelée analyse « ComDim » (Cariou et al., 2019). Cette analyse consiste à déterminer un espace commun pour tous les tableaux de données inclus dans l'analyse, dont chacun a une contribution spécifique (= salience) à la détermination de chaque dimension de l'espace commun. Ceci est réalisé en extrayant le maximum de variance totale dans l'ensemble des tableaux de données. D'autres outils sont l'extension de méthodes supervisées comme DIABLO (Data Integration Analysis for Biomarker discovery using Latent variable approaches for Omics studies) qui est une analyse basée sur la PLS-DA (Singh et al., 2019). Les composantes du modèle sont construites de manière à maximiser les covariances entre toutes les paires d'ensembles de données.

7.5 Analyses de survie

L'analyse de survie permet de calculer une probabilité de survie d'individus. Ces probabilités peuvent ensuite être représentées en fonction du temps et permettre la comparaison de la survie

de plusieurs populations. L'estimateur de Kaplan-Meier est couramment utilisé et permet de prendre en compte la disparition d'individus (mortalité) qui se traduit sur la représentation graphique par des traits verticaux (**Figure 25**).

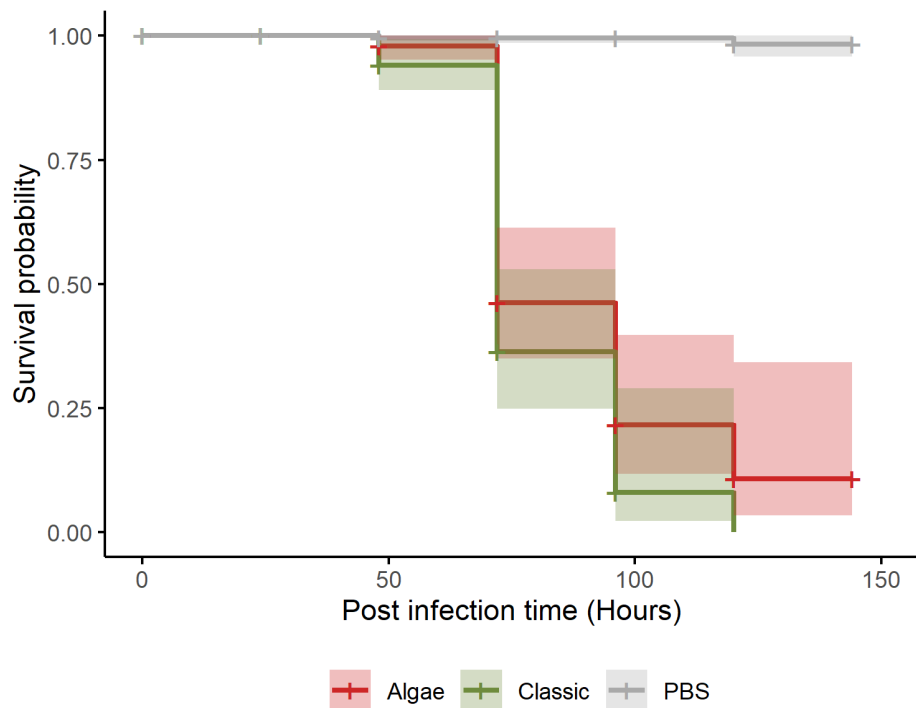


Figure 25 : Exemple de courbes de survie selon l'estimateur Kaplan-Meier.

Chapitre I : Développement d'une approche métabolomique « multiblock » pour explorer les variations des métabolites de deux algues du genre *Asparagopsis* liées à des facteurs interspécifiques et temporels

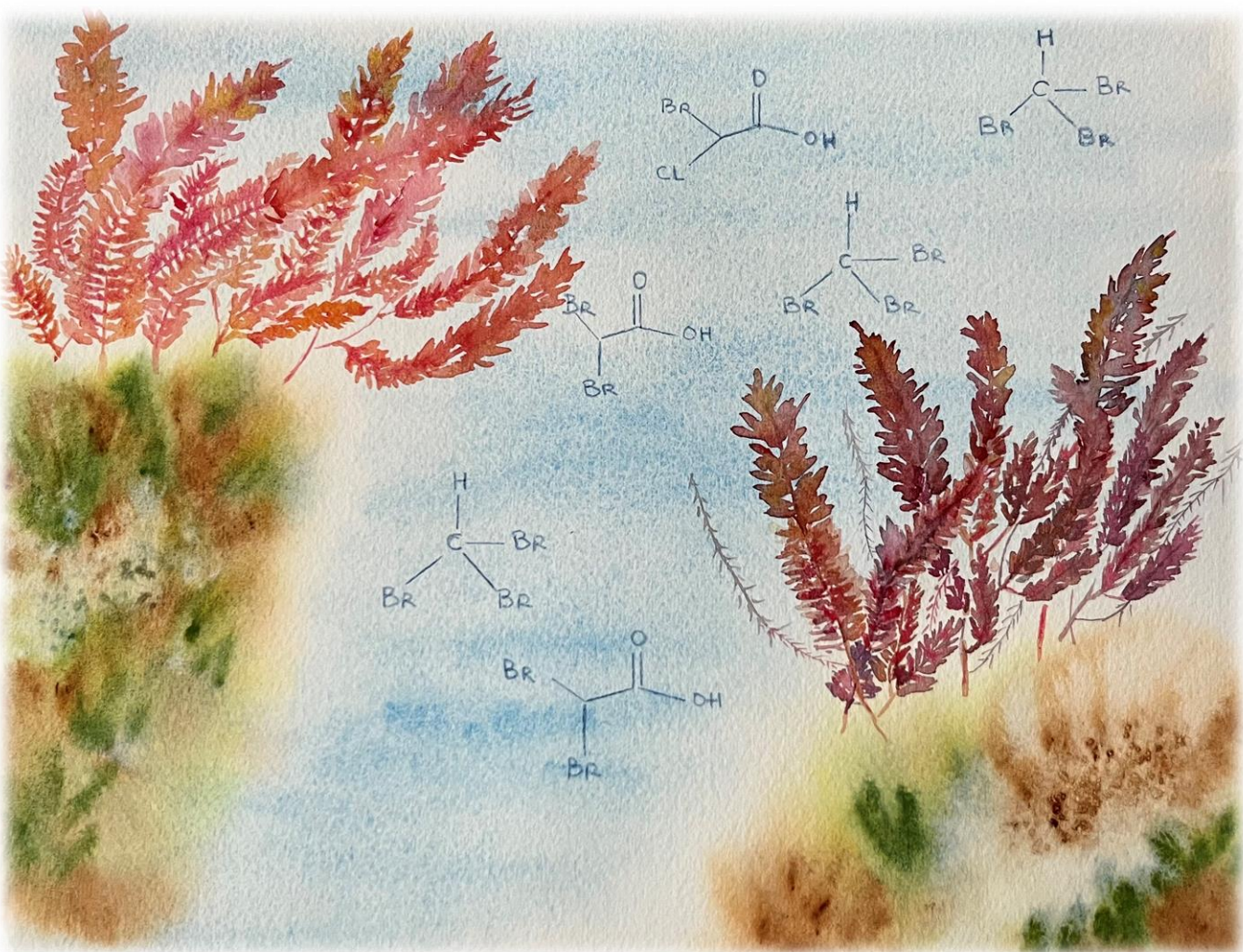


Illustration à l'aquarelle réalisée par Michèle Parchemin

1. Avant-Propos

Development of a Multiblock Metabolomics Approach to Explore Metabolite Variations of two Algae of the Genus *Asparagopsis* Linked to Interspecies and Temporal Factors

Christelle Parchemin, Delphine Raviglione, Hikmat Ghosson, Marie-Virginie Salvia, Corentine Goossens, Pierre Sasal, Elisabeth Faliex, Nathalie Tapissier-Bontemps

Publication

L’article ci-après a été publié dans le journal “Algal Research” le 13/05/2023.

Parchemin, C., Raviglione, D., Ghosson, H., Salvia, M.V., Goossens, C., Sasal, P., Faliex, E and Tapissier-Bontemps, N., (2023). Development of a Multiblock Metabolomics Approach to Explore Metabolite Variations of two Algae of the Genus *Asparagopsis* Linked to Interspecies and Temporal Factors. *Algal Research* 72, 103138. <https://doi.org/10.1016/j.algal.2023.103138>
IF : 5.276.

Contexte

Dans l’**Etat de l’art**, j’ai pu montrer l’intérêt de la métabolomique pour explorer et caractériser les variations métaboliques d’un organisme impacté par différents facteurs. J’ai également présenté la biologie et la chimie des deux espèces d’algues du genre *Asparagopsis*. Brièvement, la composition chimique de ces algues a été largement étudiée par GC-MS et plus récemment par LC-MS. Il a été montré que les extraits de ces algues présentaient une variabilité de leur composition chimique temporelle et spatiale. Cependant, le manque de connaissance sur la relation existant entre facteurs environnementaux et production des molécules, notamment celles qui sont actives, par les deux espèces peut présenter un frein à leur valorisation. L’objectif de ce **Chapitre I** est donc d’explorer les différences interspécifiques et temporelles (annuelles et saisonnières) de la composition chimique et des activités biologiques d’*A. armata* et d’*A. taxiformis*.

Méthodologie générale

Pour cela, une approche de métabolomique, intégrant les outils analytiques complémentaires que sont la LC-HRMS, la ^1H -RMN et la HS-SPME-GC-MS qui permettent d'obtenir l'image la plus exhaustive possible du métabolome des deux espèces, a été développée. Des échantillons des deux espèces ont été collectés en 2020 et 2021 dans 5 sites différents : Banyuls-sur-Mer (9 collectes) (*A. armata*), Marseille (3 collectes, au large) (*A. armata* et *A. taxiformis*), détroit de Messine (1 collecte) (*A. armata* et *A. taxiformis*), Portsall (Ploudalmézau) (2 collectes) (*A. armata*) et Moorea (9 collectes) (*A. taxiformis*). Une extraction biphasique a été réalisée sur chaque échantillon, la phase apolaire a été analysée en LC-HRMS et la phase polaire en ^1H -RMN. En parallèle la poudre d'algue a été analysée en HS-SPME-GC-MS. Les données ont été pré-traitées séparément. Les variations interspécifique et temporelle du métabolome ont été étudiées par une analyse statistique « multiblock ». Cette analyse a permis de créer un modèle incluant l'ensemble des jeux de données pour aboutir à une image globale du métabolome de chaque échantillon d'algue. La contribution de chaque jeu de données a été évaluée afin d'étudier la pertinence de chaque type d'analyse en fonction des variations étudiées. Des analyses statistiques supervisées ont été utilisées pour mettre en évidence des marqueurs d'espèces et de temporalité. En parallèle, la variation temporelle de l'activité antibactérienne des phases apolaires et des phases polaires a également été étudiée et a été correlée aux analyses métabolomiques pour faire le lien entre chimie et activité biologique des algues.

Contribution

Dans l'étude qui suit, j'ai réalisé toutes les collectes d'algues à Banyuls-sur-Mer ainsi que les extractions de tous les échantillons d'algues. Les auteurs des collectes d'algues dans les autres lieux apparaissent dans les remerciements à la fin de ce chapitre. Les analyses métabolomiques ont été réalisées sur la plateforme Bio2mar Métabolites Secondaires Xénobiotiques Métabolomique Environnementale (MSXM) à l'Université de Perpignan Via Domitia (<https://bio2mar-msxm.univ-perp.fr/>). Chaque méthodologie d'analyse des échantillons a été développée avec l'aide de Nathalie Tapissier-Bontemps et Delphine Raviglione ainsi que Hikmat Ghosson pour la HS-SPME-GC-MS et Marie-Virginie Salvia et Corentine Goossens pour la ^1H -RMN. J'ai ensuite réalisé l'ensemble des pré-traitements des données brutes, les analyses statistiques ainsi que l'interprétation des résultats.

Disponibilité des données

Les données brutes issues des analyses RMN et GC-MS ont été déposées sur la plateforme Mendeley Data, V1, et sont disponibles à : doi : 10.17632/zw3mbcp4r2.1. Les données issues des analyses LC-MS ont été déposées sur la plateforme MassIVE, et sont disponibles au numéro : MSV000091631.

Annexes

Les « Supplementary Materials » relatifs à ce chapitre débutent à la page **319** de ce manuscrit (Annexes ; 2. Annexe Chapitre I).

2. Article

Development of a Multiblock Metabolomics Approach to Explore Metabolite Variations of two Algae of the Genus *Asparagopsis* Linked to Interspecies and Temporal Factors

Christelle Parchemin^{*,1,2}, Delphine Raviglione¹, Hikmat Ghosson¹, Marie-Virginie Salvia¹, Corentine Goossens¹, Pierre Sasal¹, Elisabeth Faliex², Nathalie Tapissier-Bontemps¹

¹ Centre de Recherches Insulaires et Observatoire de l'Environnement (CRIODE), UAR 3278 UPVD-EPHE-CNRS, Université de Perpignan - Via Domitia, 52 Av. Paul Alduy, 66860 Perpignan CEDEX, France

² CEntre de Formation et de Recherche sur les Environnements Méditerranéens (CEFREM), UMR 5110 UPVD-CNRS, Université de Perpignan - Via Domitia, 52 Av. Paul Alduy, 66860 Perpignan CEDEX, France

2.1 Highlights

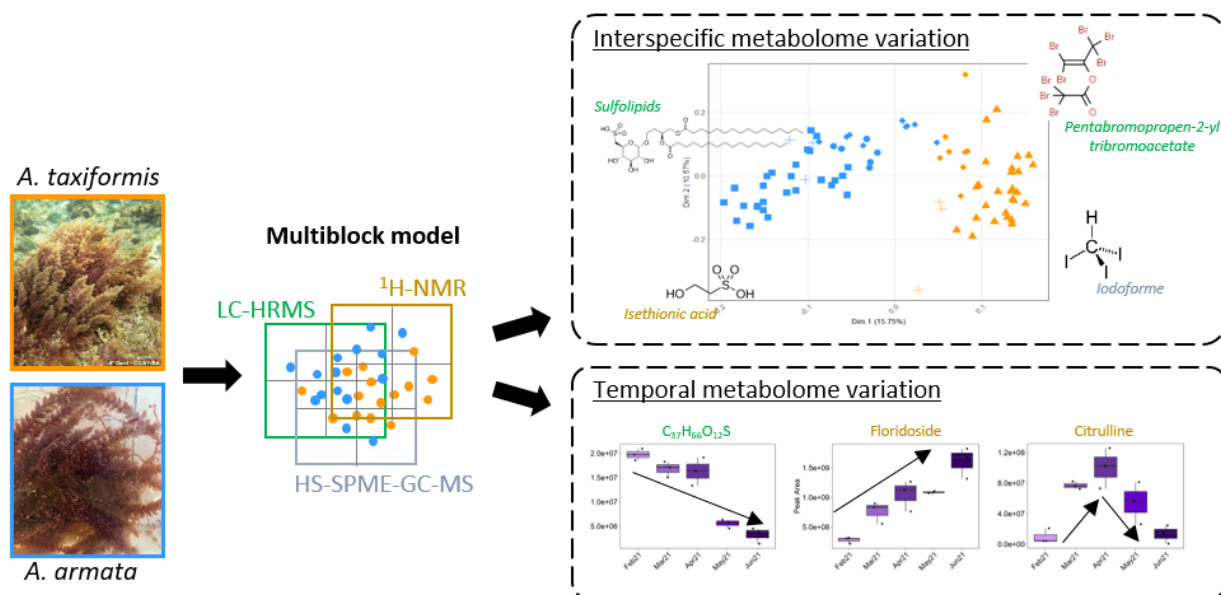
- The use of multiblock analysis allowed a better discrimination of the algal metabolome
- Interspecies and temporal discrimination of *Asparagopsis* spp. metabolome
- A perbrominated molecule was identified as a potential chemotaxonomic marker
- In *A. armata* extracts, floridoside, citrulline and SQDG intensities varied over time
- The antibacterial activity of both species is constant throughout the year

2.2 Abstract

Metabolomics, the science that describes a full range of small molecules in a sample at a time point, is a powerful tool to evaluate patterns in metabolites variations affected by environmental factors. We developed a multiblock metabolomics approach using LC-HRMS, HS-SPME-GC-MS and ¹H-NMR to study the interspecies and temporal metabolites variations of two red algae species from the genus *Asparagopsis* well-known for their broad range of biological activities. Samples were collected over two years at 5 sites. For each sample, a biphasic extraction was performed to allow distinct analyses of apolar phases by LC-HRMS and of polar phases by ¹H-NMR. The remaining lyophilized algal powder was analysed using a HS-SPME-GC-MS method. Temporal variation of antibacterial activities of extracts of the two algae was also studied and its potential covariation with algae metabolome was evaluated. On the one hand, the multiblock analysis allowed the interspecies and temporal discrimination of the two species,

and putative identification of potential chemotaxonomic markers including highly halogenated molecules. Organosulfur compounds enriched in *A. armata* samples could be detected with both ¹H-NMR (taurine and isethionic acid) and LC-HRMS (sulfolipids). On the other hand, the variation in several metabolites intensities could be related to temporal effects, probably linked to environmental factors. It is the case of floridoside, a major carbohydrate, and citrulline (¹H-NMR) that both can have antioxidant properties, but also of various sulfolipids (LC-HRMS). The antibacterial activity of extracts of both species was constant throughout the year and did not co-vary with metabolome. This work is also the first to report the study of the metabolome of the two different species of the genus *Asparagopsis* by ¹H-NMR and HS-SPME-GC-MS.

2.3 Graphical Abstract



Keywords: red algae, *Asparagopsis* spp., metabolomics, chemotaxonomic markers, antibacterial activities

2.4 Introduction

Marine natural products represent an important reservoir of active molecules with a broad range of application in health, industrial and food sector or agriculture (Fusetani, 2010). The production of these molecules by organisms is highly dependent of environmental and biological conditions that require to be described (Reverter et al., 2020). Among marine organisms, algae are known for their abilities to adapt to highly changing environment and to produce a high diversity of molecules.

Metabolomics, consists in the analysis of complex mixtures of small molecules present in a sample at a given time. By providing this overview, this approach is a powerful tool to evaluate patterns in metabolites variations impacted by several factors (Bayona et al., 2022; Viant, 2007). In previous studies, metabolomics has been used to describe chemical interactions between algae and their microbiota (Paix et al., 2019, 2020); or corals (Greff et al., 2017a), to identify spatial or temporal patterns (Gaubert et al., 2019b; Surget et al., 2017) and to evaluate the impact of environmental parameters or pollutants (Felline et al., 2019; Gaubert et al., 2019b, 2020; Ritter et al., 2014). Metabolomics has proven to be a powerful tool to explore the chemical diversity of macroalgae (Gaubert et al., 2019a; Hughes et al., 2021).

Asparagopsis armata and *A. taxiformis* are red algae belonging to the Bonnemaisoniaceae family. The two species have a different distribution, with *A. taxiformis* occurring in tropical waters and *A. armata* in more temperate waters. They are also found in sympatry in some areas such as the Mediterranean Sea. Morphologically, the two species are only distinguishable by the presence of long hooked stolons for *A. armata* (Andreakis et al., 2004). Lot of studies report on their high range of activities including antioxidant, anticancer, antimicrobial, antiviral, enzyme inhibition, immunostimulation properties (Ponte et al., 2022; Reverter et al., 2016; Thépot et al., 2022) and thus their high biotechnological potential (Pinteus et al., 2018; Zanolla et al., 2022a). Moreover, both species are considered invasive and their culture is in development which guarantees the availability of the biomass (Zanolla et al., 2022a). Their chemistry has long time been investigated, mainly by GC-MS, which has allowed the detection of a high diversity of halogenated molecules with potential and confirmed biological activities (Burreson et al., 1975, 1976; Greff et al., 2014; McConnell and Fenical, 1977; Paul et al., 2006a; Woolard et al., 1976, 1979). In the literature, other secondary metabolites with potential biological activities were also described including polysaccharides (Haslin et al., 2000), sterols (Combaut et al., 1979; El Hattab et al., 2006; Lopes et al., 2011) or mycosporine-like amino acids (MAAs) (Figueroa et al., 2008; Lalegerie et al., 2019).

Only a relatively small number of studies on biological activities and chemical composition were simultaneously performed on both species. Genovese et al. (2009) reported differences in biological activities of the two species with lower IC50 and IC90 for *A. taxiformis* than for *A. armata* in *in vitro* antimicrobial susceptibility assays against *Leishmania donovani*. Conversely, no significant difference in the measured bioactivity of extracts of the two species collected in Spain and evaluated against *Alvibrio fischeri* were found (Greff et al., 2017b). However, the metabolomes of the same samples of *A. armata* and *A. taxiformis* were significantly different

but no clear chemotaxonomic markers were highlighted (Greff et al., 2017b). These results show that differences in chemical composition between the two species need to be more investigated to learn about their individual biotechnological potential.

Finally, several studies reported temporal and spatial variations (Salvador et al., 2007) in the antibacterial activity of *A. taxiformis* and *A. armata* extracts, with absence of activity (Genovese et al., 2012; Marino et al., 2016; Salvador et al., 2007) or significantly higher activity depending on the sampling month (Genovese et al., 2012). Thus, the chemical composition of *A. taxiformis* and *A. armata* is expected to vary with time, space and individual properties and only limited proportion of data are available particularly for *A. armata*. Using a metabolomics approach, a work allowed the significant differentiation of metabolome fingerprinting of *A. taxiformis* collected at different sites but no spatial markers could be identified (Greff et al., 2017b). The same authors (Greff et al., 2017b) reported temporal variability in the chemical composition of *A. taxiformis* collected in different months of the year in La Réunion as well as in the South of France. Moreover, this observed temporal variability was greater for samples from La Réunion than from the South of France and seemed to correspond to a seasonal pattern. However, no chemical marker for this observed seasonality could be identified (Greff et al., 2017b). To our knowledge this is the only study on the temporality of the chemical composition of samples collected in situ. Factors of variation in chemical composition or biological activities are important parameters to consider when developing biotechnology applications, and should also be further investigated.

In this context, we developed a multiblock metabolomics approach using LC-HRMS, ¹H-NMR and HS-SPME-GC-MS, the latter technique allowing the study of the volatilome without the need of using any solvent. Both ¹H-NMR and HS-SPME-GC-MS have never been employed for a metabolomics analysis of these two red algae. This approach has been developed to study the interspecies and temporal variations of the metabolites of *A. armata* and *A. taxiformis* by considering the widest range of chemical compounds. Finally, we also evaluated the temporal variation of the antibacterial activity of polar and apolar extracts of both species and its potential covariation with the metabolome.

2.5 Materials and methods

2.5.1 Chemicals

For sample preparation, tert-methyl-butyl-ether (MTBE) HPLC grade was purchased from Honeywell Riedel de Haen™ (Germany), and Methanol (MeOH) HPLC grade and Water

HPLC grade VWR™ (Fontenay-sous-Bois, France). D₂O containing 0.002% TMSP D4 was purchased from Eurisotop and phosphate buffer from SIGMA DIAGNOSTICS (Saint Louis, France). For UHPLC-HRMS analysis, Water LC-MS grade was purchased from VWR™ (Fontenay-sous-Bois, France), and Acetonitrile LC-MS grade was purchased from Carlo Erba (Val de Reuil, France). Formic acid 99% (for LC-MS analysis) was obtained from Carlo Erba (Val de Reuil, France). Chemical standards for compounds characterization were purchased from Sigma-aldrich® (Saint Louis, USA) for Taurine, L-Citrulline and L-Glutamine and Thermo scientific™ (Waltham, MA, USA) for Isethionic acid.

2.5.2 Biological materials

Algae were collected at different sites in France: Bretagne (48.554113; -4.706051), Banyuls-sur-Mer (42.482230; 3.137175), Marseille (43.09583; 5.36220), Moorea (French Polynesia, -17.48262; -149.87213) and in Italy, Straits of Messina (38.15136; 15.36112) from 2020 to 2021 (**Table S13**). Algae physically contiguous were pooled and considered as one single individual. For each site, 3 individuals (biological replicates) distant from at least one meter were collected and processed separately. Immediately after collection, algae were cleaned of epiphytes, freeze-dried and stored at -25°C until extraction and analysis. Physico-chemical parameters at Banyuls-sur-Mer were obtained from the "Service d'Observation en Milieu Littoral (SOMLIT)" database at: www.somlit.fr. In Moorea, sea water temperature was extracted from a thermograph located at 8m depth.

2.5.3 Algae extracts preparation

Each sample of freeze-dried algae was ground to obtain a homogeneous powder. Firstly, 50 mg of crushed algae were placed in 20 mL glass vial (ThermoFisher Scientific) and sealed with pre-assembled 20 mm caps and septa for GC-MS analysis. In parallel, 50mg of powder was extracted using an adapted biphasic extraction method (Matyash et al., 2008) as follows: crushed algae was extracted with a mixture of 800 µL of MeOH and 2.2 mL MTBE and vortexed. Then, 100 µL of a solution of Diclofenac (0.1 mg/mL in MeOH) was added as an internal reference standard. H₂O (1.4 mL) was added and the whole solution was vortexed. Extraction was further performed with an ultrasonic bath for 5 minutes. This mixture was centrifuged (4400 rpm, 4°C, 10 minutes) to obtain two phases. Finally, phases were separately collected (700 µL of apolar and 1mL of polar phases) for each sample. Solvent was evaporated with a centrifugal vacuum evaporator GENEVAC EZ-2™ (SP Scientific, Warminster, PA 18974, USA) and the dried samples were stored at -20°C until LCMS and NMR analyses.

Quality control (QC) samples were prepared by pooling equal volume from all extracts or crushed samples.

2.5.4 Metabolomics analyses

2.5.4.1 LC-HRMS

Apolar extracts were solubilized in 1mL MeOH. Metabolites separation were performed on a C18 UHPLC column (Luna® Omega 1.6 μ m Polar C18 100 A LC Column 100 x 2.1 mm, Phenomenex, CA, USA). LC-HRMS analyses were performed with a Vanquish UHPLC system from ThermoScientific (MA, USA) equipped with a Q Exactive™ Plus mass spectrometer with an electrospray ionization source. The mobile phase consisted in a mixture of H₂O + 0.1% formic acid (solvent A) and acetonitrile + 0.1% formic acid (solvent B). The flow rate was 400 μ L/min. The program was set up at 2% B during 1 min, followed by a linear gradient to reach 100% B in 10 min, then maintained 5 min in isocratic mode (100% B). The analysis was followed by a return to initial conditions for column equilibration during 4 min for a total runtime of 20 min. Extracts were randomly injected alternating the quality control sample injections every 5 samples.

The mass spectrometer analyser parameters were set as follows: sheath gas flow rate, auxiliary gas and sweep gas flow rate at 45 arbitrary units (a.u.), 15 a.u. and 2 a.u. respectively, capillary and gas temperature to 320 °C and 250 °C respectively, the S-lens RF level and spray voltage to 60 V and 3.20 kV respectively. MS/MS acquisition consisted of one full scan mass spectrum and 5 data-dependent MS/MS scans, parameters for the Full MS experiments were set as follows: the resolution was 70,000, the Automatic Gain Control was 3E6 ions, the maximum Injection Time (IT) was 100ms and a scan mass window of 100–1500 *m/z* was used. For the dd-MS2/dd-SIM experiments, the resolution was 17,500, AGC target was 1e5 ions, maximum IT 50 ms, for each MS/MS scans top 5 most intense ions taking into account an isolation window of 4.0 *m/z* and a fixed first mass of 50.0 *m/z*. Three Normalized Collision EnergyTM (NCE) values were applied in order to obtain a combination of 3 fragmentation spectra (thus more fragments and structural information). The applied NCE values were 25 eV, 35 eV and 45 eV, normalized to a reference ion of mass 500 *m/z* and charge 1.

2.5.4.2 ¹H-NMR

The ¹H-NMR spectra were obtained on a 500 MHz ECZR JEOL spectrometer (Tokyo, Japan). Polar phases were dissolved in 1 mL of 0.1M phosphate buffered D₂O containing 0.002%

TMSP. A presaturation of the water peak was performed and the following parameters were used for data acquisitions: 16 scans, 65K data points, T=25°C. The TMSP half peak width was set up to maximum 0.8 Hz and its variability that of the signal-over-noise ratio across all samples did not exceed 10% (Deborde et al., 2019). 2D DQF-COSY spectra were acquired to help with the identification (**Figure S14, S15**). A presaturation of the water peak was also performed and the following parameters were used for data acquisitions: 8 scans, 1024 X_points and 256 Y_points

2.5.4.3 HS-SPME-GC-MS

Volatile compound analyses were performed using a FOCUS GC gas chromatography system coupled to a DSQ II Electron Impact-Single Quadrupole (EI-Q) mass spectrometer (Thermo Scientific, MA, USA). Samples were extracted using a Divinylbenzene/Carboxen/Polydimethylsiloxane (DVB/CAR/PDMS) fiber that was conditioned according to manufacturer instructions. Samples were incubated for 20min at 60°C in a TriPlus™ RSH Autosampler (ThermoFisher Scientific), then the fiber was exposed for 30 min and desorbed in the GC injection port at 230°C for 1 min at a helium flow rate of 1 mL·min⁻¹ under splitless conditions. Chromatographic separation was achieved on a capillary column (OPTIMA 5 MS Accent – 0.25 µm). The oven temperature was maintained at T=50°C for 2 min, increased to 280°C at 10°C/min and held at that temperature for 2 min. Helium was used as the carrier gas with a constant flow rate of 1 mL/min. The detector transfer line and ion source temperatures were 290 and 210 °C, respectively. The MS operated in the full scan mode at 70eV electron ionization, with 5 scans/sec and 30-400 amu as mass range. Pooled powders were analysed every 7 samples to control repeatability.

2.5.5 Metabolomics data processing

2.5.5.1 LC-MS

Data acquisitions were performed using Xcalibur 4.1.31.9 (Thermo Fisher Scientific). Raw data were converted to mzML files with MSconvert (version 3.0, from Proteowizard library) (M. C. Chambers et al., 2012). mzML files were uploaded and processed using the Galaxy web platform (version 3.3) (Giacomoni et al., 2015; Guitton et al., 2017). The workflow used for data pre-processing and used parameters are published on the Galaxy Workflow4Metabolomics platform at:

https://workflow4metabolomics.usegalaxy.fr/u/christelle_parchemin/w/workflowparcheminal gaeand are available in the **Supplementary Methods 2**. Briefly, the preprocessing consisted of

a chromatographic peak detection (Galaxy Version 3.12+galaxy0), a peak grouping, a loess/non-linear “PeakGroups” retention time adjustment, a peak filling and “CAMERA” peak annotation. A matrix of features with peak intensity, *m/z* value and retention time was generated. A clean-up step was performed in order to eliminate all features that are significantly detected in blanks. Then, an “inter/intra-batch” signal correction was applied using the “Batch correction” function with a “loess” regression model (van Der Klo et al., 2009). This step was followed by a second clean-up according to feature's CV in pool QC injections (Thévenot et al., 2015). Finally, redundancies due to isotopes were manually eliminated (only monoisotopic mass was kept). For identification, most probable molecular formula was determined using Sirius (v4.9.15 (Dührkop et al., 2019)), MetLin database, characteristics isotopic clusters, MS/MS spectra and comparison with literature.

2.5.5.2 $^1\text{H-NMR}$

Spectra were automatically Fourier-transformed and were processed using NMRProcFlow v1.4.14 (Jacob et al., 2017). They were calibrated to the internal standard ($\text{TMSP} = 0.0 \text{ ppm}$) and a global intermediate correction of the baseline was applied. An intelligent bucketing was applied with a resolution factor of 0.5 and a signal-to-noise ratio (SNR) threshold of 0.2 in order to get the final matrix. Spectra were visualized using MestReNova v14.2.3-29241 and putatively annotated by comparing chemical shifts of molecules in Chenomx profiler v9.02. 2D experiments, and comparisons with literature data were also used. Identification of interesting features was confirmed using chemical standards.

2.5.5.3 GC-MS

Raw data were converted to mzML files with MSconvert (version 3.0, Proteowizard) (Chambers et al., 2012). MzML files were processed in MZmine v2.53, the detailed used parameters for the data processing are available in the **Supplementary Methods 3** (Pluskal et al., 2010). Briefly, mass lists were created using the mass detection module, the ADAP chromatogram builder module (Myers et al., 2017) was used to create peak lists. The peak lists were deconvoluted using the algorithm wavelets (ADAP). A spectral deconvolution was applied using the hierarchical clustering algorithms to build pseudo fragmentation spectra. Finally, the peak lists were aligned using the ADAP aligner module. Most intense and interesting compounds were putatively identified using NIST MS Search 2.2 (National Institute of Standards and Technology, Gaithersburg, U.S.) and literature data.

2.5.6 Antibacterial assays

Polar and apolar phases were tested on several bacterial species. The recent promising studies on the potential for aquaculture of *A. armata* and *A. taxiformis* (Castanho et al., 2017; Manilal et al., 2012; Reverter et al., 2016; Thépot et al., 2021a, 2021b, 2022) led us to select fish pathogenic bacteria for our tests: *Vibrio anguillarum* (CIP63.36T), *Pseudomonas anguilliseptica* (CIP106711T), *Edwardsiella anguillarum* (DSMZ-27202) three Gram-negative bacteria, and *Lactococcus garvieae* (CIP102507T) a representative Gram-positive bacterium. They were maintained at -80°C respectively in Marine Broth, Marine Broth, Luria Broth and Brain Heart Infusion Broth (**Supplementary Methods 4**) supplemented with 30% (v/v) glycerol. Prior to use, all bacteria were revived from glycerol stocks and grown for 24 h at 26 °C on agar plates (except *L. garvieae* that grows at 37°C and *P. anguilliseptica* that grows for 48 h). An isolated colony was then cultivated in the above-mentioned liquid medium for 24h (or 48 h). Agar plates were flooded with bacterial broth ($OD_{620nm}=0.1$) and were set aside to dry. Assays of extracts were performed using the disc diffusion method (Bauer, 1966). Briefly, 10 µL of extract was pipetted onto a 0.6 cm sterile paper disc (final concentration: 0.1 mg/disc for the apolar phase and 1 mg/disc for the polar phase (higher concentration due to salt). Discs were placed under the hood to allow evaporation of the solvent. Following evaporation, the discs were placed onto the surface of the inoculated agar. The plates were incubated for 24 h at 26°C or 37°C. Discs soaked with antibiotics: Erythromycine 10 µg (Conda pronadisa ref 7234) or Kanamycine 30 µg (Condalab ref 7053) were used as positive control and MeOH was used as negative control. Areas of inhibited bacterial growth were observed as clear halos (zones) around the discs. The diameter of the zone of bacterial growth inhibition was measured, each reported measurement including the size of the disc.

2.5.7 Statistical analyses

Statistical analyses were performed using RStudio environment v2022.02.3 (R v4.2.0) and MetaboAnalyst 5.0 (Pang et al., 2021). An autoscaling normalization was applied on the data. Multiblock modelling was used to perform unsupervised analysis of data. A ComDim analysis ({MBAnalysis} Package (Mangamana et al., 2019, 2021) was used to evaluate the global dispersion of algae metabolome and the contribution of global and each dataset to components. In ComDim Analysis, the “percentage of explained variation” represents the percentages of inertia explained for each block, the “contribution” is the contribution of each block to the determination of global components, the “salience” represents the specific weight of the

different blocks of variables on global components (Mangamana et al., 2019). Permutation tests based on cross model validation (MVA.test, pairwise.MVA.test {RVAideMemoire}) were applied to validate the significance of the discriminations according to defined factors and global differences between groups. Datasets were then separately analysed and PLS-DA ({mixOmics} Package (Rohart et al., 2017)) was used for detection of features contributing the most to the model. Putative identification of the features was performed as mentioned in “2.5 Data treatment”. A Shapiro test was performed on data and, depending on the results, a T-test or an ANOVA followed by TukeyHSD post-hoc or Kruskall-Wallis followed by Nemenyi post-hoc were used ({Stats}{PMCMRplus} Packages) to test the significance of the differences of VIP features intensity among groups and the differences in antibacterial activity of the extracts. Dendograms and Heatmaps (Distance Measure: Euclidean; Clustering Algorithm: Ward) were drawn on MetaboAnalyst 5.0 to evaluate the grouping of samples and for visual detection of temporal variation pattern among VIP features. The correlations between the temporal variations of the metabolome of the two species and the variation of seawater temperature were calculated via a Mantel test using Spearman correlation and a permutation test (Vegan and Stat software packages). Mantel tests were also used to study the covariation between antibacterial activities and metabolome variations. A distance-based redundancy analysis (db-RDA)(Vegan package) was performed to reveal whether antibacterial activity, temperature and year of sampling have some significant impact on the (dis)similarities derived from the metabolomics data (Legendre and Anderson, 1999; McArdle and Anderson, 2001).

2.6 Results

2.6.1 Chemical nature of detected metabolites

Each instrumental analysis contributed to the detection of a large panel of metabolites of various chemical nature. The apolar extracts of *A. armata* and *A. taxiformis* were analysed by UHPLC-ESI⁻-HRMS which allowed the detection of halogenated molecules characteristic of the algae. Chromatographic profiles obtained with ESI⁺ mode were less informative that is why only the ESI⁻ mode was selected for the further analyses. Most intense ions obtained in ESI⁻ were putatively annotated (**Figure 1A**). The identified variables were: halogenated compounds, including di and tri halomethanes, haloacetic acids, haloforms, halogenated acetones and polar lipids including fatty acids and sulfolipids (**Table S1**). The polar phases of *A. armata* and *A. taxiformis* were analysed by ¹H-NMR. Spectra were annotated and about thirty molecules were putatively identified (**Figure S3**). Most intense signals displayed on the spectra were located

between δ_{H} 3.5 and 4 ppm (**Figure 1B**), which corresponds to the area of chemical shifts of methylene protons surrounded by hydroxyl groups of glycoside derivatives. Based on the comparison of chemical shifts of red algal carbohydrates reported in the literature and the presence of a characteristic doublet of an anomeric proton at δ_{H} 5.15 ppm, the major carbohydrate was identified as floridoside (**Figure 1B**). Two triplets at δ_{H} 3.15 and 3.95 ppm were assigned to methylene protons of an organosulfur compound identified as isethionic acid and confirmed by the use of a chemical standard. Most of the remaining signals were assigned to amino acids (**Figure S3**). Finally, the volatilome of powdered *A. armata* and *A. taxiformis* was analysed by HS-SPME-GC-MS. The most abundant compounds were putatively identified and were exclusively halogenated molecules including haloforms, carbon tetrahalides and halogenated acetones (**Figure 1C, Table S2**).

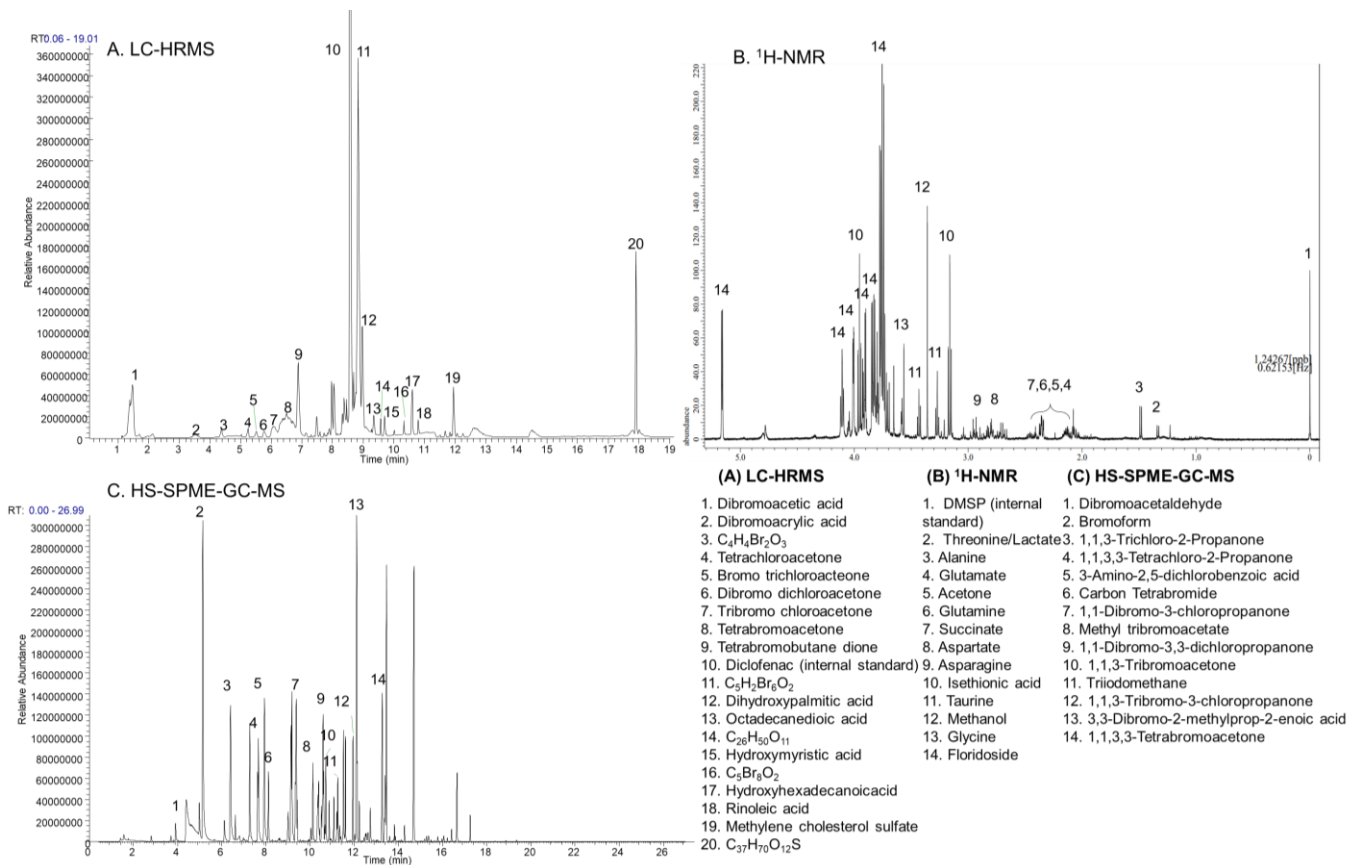


Figure 1: Annotated chromatograms of a quality control sample analysed with the UHPLC-ESI-HRMS spectrometer (A), ^1H -NMR representative spectrum (0-5 ppm) of *A. armata* (B) and annotated chromatogram of a quality control sample analysed with the HS-SPME-GC-MS spectrometer (C). Only the most intense ions or signals that could putatively be annotated are referenced. Additional information on retention time, chemical shifts, m/z are available in **Table S1, S2, and Figure S1**.

2.6.2 Interspecies variability of the metabolome

2.6.2.1 Multiblock unsupervised analysis

After data pre-processing, the matrices obtained from LC-HRMS, NMR and GC-MS analyses respectively included 262, 258 and 272 features. A ComDim multiblock method was applied to evaluate the global dispersion of algae metabolome and the contribution of each dataset in the construction of the model. On Dim.1 the greatest contribution and salience (specific weight of the different blocks of variables) were explained by the LC-MS dataset (twice those of NMR and GC-MS) while NMR dataset provided the highest Contribution and Salience on Dim.2 (**Table 1**).

Table 1 : Selected parameters on Dim.1 and Dim.2 of the built multiblock model following a Common Dimension Analysis (ComDim) applied on merged matrix containing LC-HRMS, NMR and GC-MS variables of *A. armata* and *A. taxiformis*.

	Dim.1			Dim.2		
	LC-MS	NMR	GC-MS	LC-MS	NMR	GC-MS
% of explained variation ^a	22.17	13.37	11.79	2.59	27.35	1.78
Contribution ^b	46.85	28.24	24.91	8.18	86.23	5.6
Saliences ^c	0.61	0.22	0.17	0.01	0.99	0

^a the “percentage of explained variation” represents the percentages of inertia explained for each block

^b the “contribution” is the contribution of each block to the determination of global components

^c the “salience” represents the specific weight of the different blocks of variables on global components

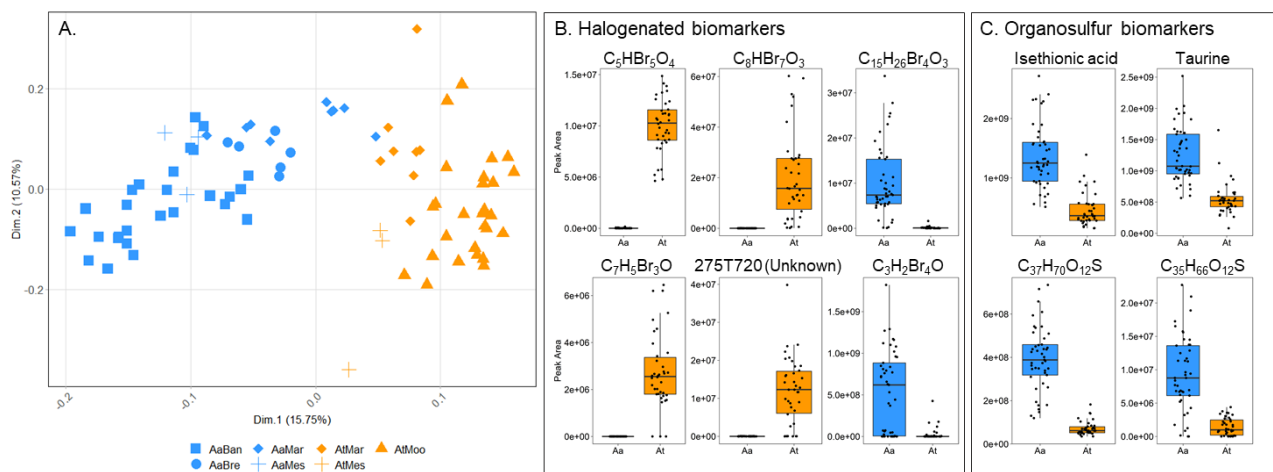


Figure 2: Scores plot of the global dataset built with a ComDim method. Dot shapes represent the sampling sites and the colours correspond to the species. Aa in blue = *A. armata* and At in orange = *A. taxiformis*. AaBan = *A. armata* Banyuls; AaBre = *A. armata* Bretagne; AaMar = *A. armata* Marseille; AaMes = *A. armata* Messina; AtMar = *A. taxiformis* Marseille; AtMes = *A. taxiformis* Messina, AtMoo = *A. taxiformis* Moorea. Boxplots of discriminating halogenated VIP features in one of the algae species (*A. armata* (Aa) in blue or *A. taxiformis* (At) in orange) (B) and discriminating organosulfur molecules (C). All groups are significantly different from each other (t-test, p <0.001).

The two first common components of the global dataset explained 26.32 % of variance. The scores plot showed a separation of algal samples according to the species along the first dimension even for samples collected in Marseille and Messina where both species live in sympatry (**Figure 2A**). Hierarchical clustering dendograms were also built to evaluate the clustering of the samples using each analytical method separately (**Figures S4, S5, S6**) and the multiblock matrix (**Figure S7**). The hierarchical clustering analysis using the multiblock matrix showed a better clustering of samples by species than that obtained from each analytical method separately. However, 5 (out of 9) samples of *A. armata* collected in Marseille are grouped with samples of *A. taxiformis*. This can also be observed on scores plot (**Figure 2A**) where some samples of both species collected in Marseille, are grouped in the centre of the plot showing the influence of the environment on the metabolome variation.

2.6.2.2 PLS-DA supervised analysis

To determine which features were responsible for the discrimination between *A. armata* and *A. taxiformis* a PLS-DA model was applied on the individual dataset obtained from each analytical method. A permutation test based on cross-model validation was applied to determine the significance of the discrimination. Classification error rates (CER) were low ($CER_{LC-MS}=0.007$, $CER_{RMN}=0.039$, $CER_{GC-MS}=0.028$) and $p=0.001$ for each dataset indicating a predictive model and a significant difference between chemical fingerprints of the two species (**Figure S8**).

The PLS-DA model obtained from the LC-MS data was the most predictive ($CER_{LC-MS}=0.007$) which is consistent with unsupervised analysis where the greatest contribution and salience on Dim.1 was provided by LC-MS dataset (**Table 1**). Thus, all features with VIP scores >1.25 (66 features) from the LC-MS analysis were considered, while only top 30 VIP from NMR and GC-MS were included. Finally, after redundancy cleaning, a total of 86 VIP features were considered. They were significantly different considering the defined factor species ($p<0.01$). Most of the discriminating features were more intense in *A. armata* extracts (50 over 84) than in *A. taxiformis* extracts. The discriminant features highlighted by LC-MS and GC-MS analyses were mostly abundant in *A. armata* (LCMS 26 over 43, GC-MS 16 over 25), while discriminant features revealed by NMR were mostly abundant in *A. taxiformis* (11 over 16). Using appropriate databases, 44 VIP features were putatively identified (**Table S3, S4, S5**).

In order to identify potential chemotaxonomic markers, mean intensity and ratio of VIP features between species were calculated. Six features presented high ratio (>100) and presence/absence-like pattern (**Figure 2B**). The analysis of the spectra of each molecule

allowed the detection of characteristic isotopic clustering indicating the presence of several bromines. They were detected by LC-MS and GC-MS and their molecular formulas were calculated in relation to exact mass, isotopic clusters and NIST Mass Research library. Among the four more abundant features found in *A. taxiformis* extracts, three were successfully annotated as C₅HBr₅O₄, C₈HBr₇O₃ and, C₇H₅Br₃O. The feature assigned to C₅HBr₅O₄ which presented the highest VIP scores (2.16) among other redundant VIP features at the same retention time, appeared to correspond to fragments of a perbrominated molecule identified as pentabromopropen-2-yl tribromoacetate (C₅Br₈O₂) previously isolated by our research team (Reverter et al., 2022). It was confirmed by comparison of its retention time, and fragmentation patterns that occurred in the mass spectrometer ionization chamber (Reverter et al., 2022). The two remaining features, C₁₅H₂₆Br₄O₃ and C₃H₂Br₄O were found more abundant in *A. armata* extracts than in *A. taxiformis* extracts (**Figure 2C**).

Most of the other putatively identified VIPs, which had lower ratios, were halogenated molecules, organosulfur compounds and fatty acids. Organosulfur compounds were mainly found in higher amount in *A. armata* extracts than in *A. taxiformis* extracts. Isethionic acid and Taurine were detected by NMR (**Figure 2C**). Their identifications could be confirmed by comparison with commercial standards. Other discriminating organosulfur compounds detected by LC-MS (**Table S3**) and found more abundant in *A. armata* apolar extracts than in *A. taxiformis* apolar extracts consisted mainly of sulfolipids, such as sulfoquinovosyl diacylglycerol (SQDG). Exploitation of MS/MS spectra allowed identification of common fragments in all VIP sulfolipids with *m/z* of 80.9649, 225.0078 and 537.2744 corresponding to [SO₃]⁻, [C₆H₉O₇S]⁻ and [M-H-C₁₅H₃₁COOH]⁻ (palmitic acid chain (C16:0)) fragments (**Figure S9**). The other fatty acid chain was variable among SQDG. C₃₇H₇₀O₁₂S and C₃₅H₆₆O₁₂S, the two most discriminating SQDGs (**Figure S9**), could correspond to a lauric acid chain (C12:0) and a decanoid acid chain (C10:0) according to the exploitation of other MS/MS fragments.

2.6.3 Temporal variability of the metabolome

2.6.3.1 Multiblock unsupervised analysis

All samples of *A. armata* collected in Banyuls on the one hand and *A. taxiformis* collected in Moorea on the other hand were compared in order to evaluate temporal metabolites variability. A ComDim multiblock analysis was computed. For *A. armata*, contribution and salience were equivalent for all datasets on Dim.1 while on Dim.2 NMR dataset clearly presented the highest contribution and salience (75 % and 0.95). For *A. taxiformis*, on Dim.1 the greatest contribution

and salience was for NMR dataset (62.1 % and 0.84) while GC-MS dataset provided the highest Contribution and Salience on Dim.2 (51.8 % and 0.68) (**Table 2**).

Table 2: Selected parameters on Dim.1 and Dim.2 of the built multiblock model following a Common Dimension Analysis (ComDim) applied on merged matrix containing LC-HRMS, NMR and GC-MS variables of *A. armata* collected in Banyuls and *A. taxiformis* collected in Moorea in 2020 and 2021.

	Dim.1			Dim.2		
	LC-MS	NMR	GC-MS	LC-MS	NMR	GC-MS
<i>A. armata</i>						
% of explained variation ^a	18.7	16.53	15.06	5.38	28.1	3.95
Contribution ^b	37.2	32.9	30	14.4	75.1	10.6
Saliences ^c	0.41	0.32	0.27	0.03	0.95	0.02
<i>A. taxiformis</i>						
% of explained variation ^a	13.45	36.78	8.96	13.73	7.62	22.95
Contribution ^b	22.7	62.1	15.2	31	17.32	51.8
Saliences ^c	0.11	0.84	0.05	0.24	0.08	0.68

^athe “percentage of explained variation” represents the percentages of inertia explained for each block

^bthe “contribution” is the contribution of each block to the determination of global components

^cthe “salience” represents the specific weight of the different blocks of variables on global components

Samples were projected on the two first common components of the global dataset that explained 29.4 % and 34.5 % of the total variation for *A. armata* and *A. taxiformis* respectively (**Figure 3A, B**). For *A. armata*, the scores plot showed an equivalent temporal repartition from the left to the right along Dim1 for the samples collected in 2020 and 2021 (**Figure 3A**). Hierarchical clustering dendograms were built to evaluate the clustering of the samples using each analytical method separately (**Figures S10, S11, S12**) and the multiblock matrix (**Figure S13**). The hierarchical clustering analysis using the multiblock matrix showed a better clustering of samples with a temporal repartition from the top to the bottom compared to that obtained from each analytical method separately. For *A. taxiformis* no clear temporal pattern could be observed on the scores plot or on the dendograms (**Figures S14, S15, S16**) but we observed higher intragroup variabilities than for *A. armata* (**Figure 3B**).

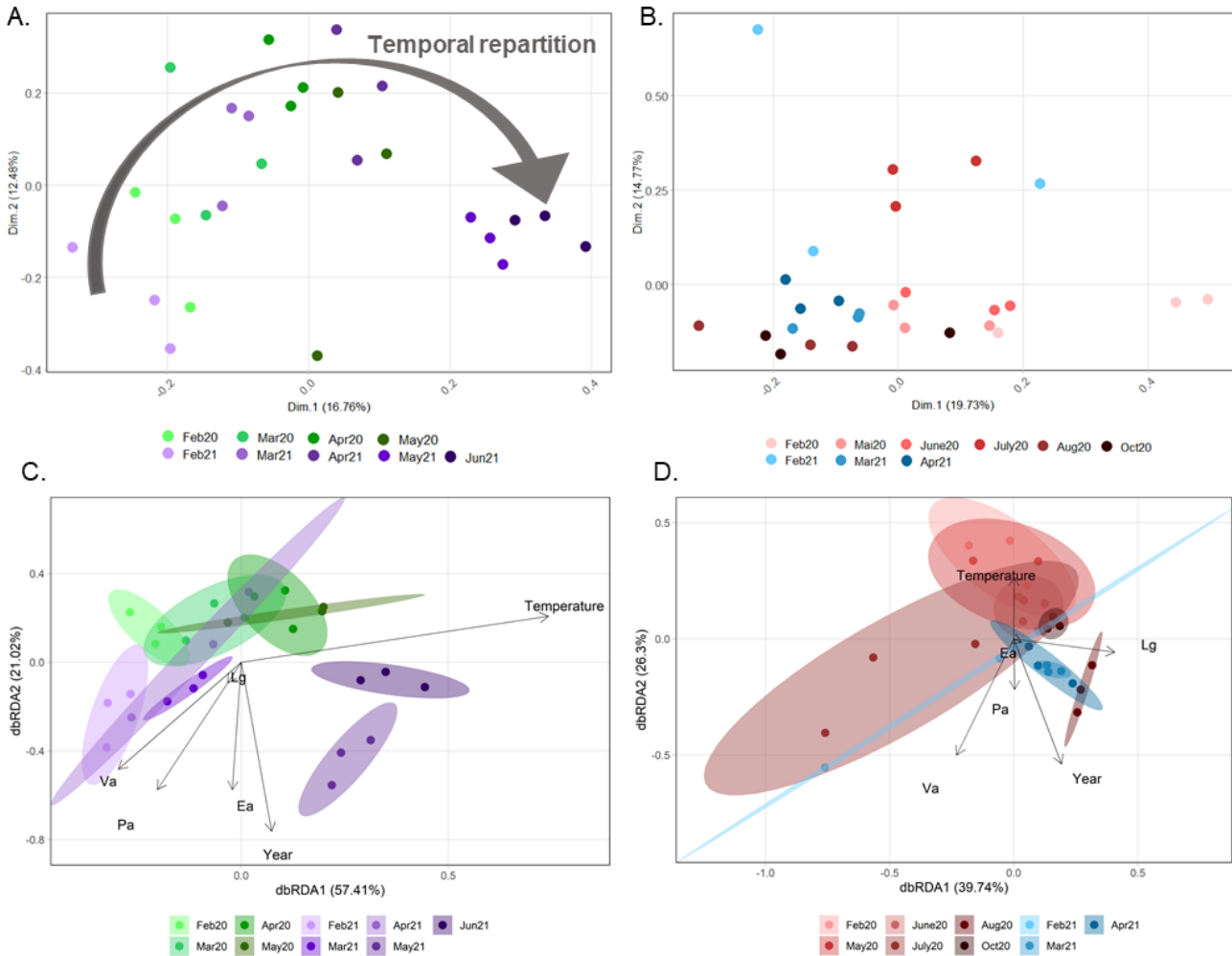


Figure 3: Scores plot of the two first common dimension of the ComDim model based on seasonal variability of *A. armata* collected in Banyuls (A) and *A. taxiformis* collected in Moorea (B) and Distance-Based Redundancy Analysis (db-RDA) plots constructed with the metabolome fingerprints of the apolar phase of *A. armata* collected in Banyuls (C) and *A. taxiformis* collected in Moorea (D) and sea water temperature, year of collection and antibacterial activity against Ea (*Edwardsiella angillarum*), Lg (*Lactococcus garvieae*), Pa (*Pseudomonas anguilliseptica*) and Va (*Vibrio angillarum*) as explaining variables. On A, arrow represents the observed temporal repartition according to the unsupervised clustering of samples. On A and C, the green colour gradient corresponds to 2020 samples, and the purple colour gradient to the 2021 samples. On B and D, the pink colour gradient corresponds to 2020 samples and the blue colour gradient to the 2021 samples.

2.6.3.2 PLS-DA Supervised analysis

As a consequence of low number of replicates (3) for the different groups, classification error rates (CER) were high ($\text{AaCER}_{\text{LC-MS}}=0.604$, $\text{AaCER}_{\text{RMN}}=0.676$, $\text{AaCER}_{\text{GC-MS}}=0.719$ and $\text{AtCER}_{\text{LC-MS}}=0.693$, $\text{AtCER}_{\text{RMN}}=0.744$, $\text{AtCER}_{\text{GC-MS}}=0.712$) but $p<0.01$ indicating that even if models were not predictive, for both species there were significant differences between metabolome fingerprints of samples collected at different months. For *A. armata*, top 30 features from each dataset were examined and heatmaps were used to visualize temporal

variations (**Figures S17, S18**). Three types of temporal variations could be detected. The first showed a pattern of features with a constant increasing intensity over time. Most of these features, detected in the polar extract with the NMR analysis (**Figure S17**) were redundant buckets of floridoside. The increase in floridoside intensity over time is more evident for samples collected in 2021 ($p_{2021}=0.02$) (**Figure 4A, B**). The second pattern consisted in a pattern of features with a constant decreased intensity among time. Most of top 30 VIP features from the apolar extract analysed by LC-MS presented this variation. They were mainly sulfolipids annotated on the basis of their characteristic MS² fragments (80.9649; 225.0078; 537.2738 *m/z*) (**Table S6**). As an example, C₃₇H₆₆O₁₂S is presented in **Figure 4C, D**. Its intensity decreased over time and was significantly different between the months of February and May/June ($p_{2020}=0.02$; $p_{2021}=0.01$). Finally, the third type of temporal variation was more complex. For example, Citrulline, detected in the polar extract with NMR and assigned by comparison with commercial standards, exhibited increase until April and decrease from April to June ($p_{2020}=0.02$; $p_{2021}=0.02$) (**Figures 4E, F**). No clear temporal gradient could be observed for features detected by GC-MS analysis (**Figure S18**).

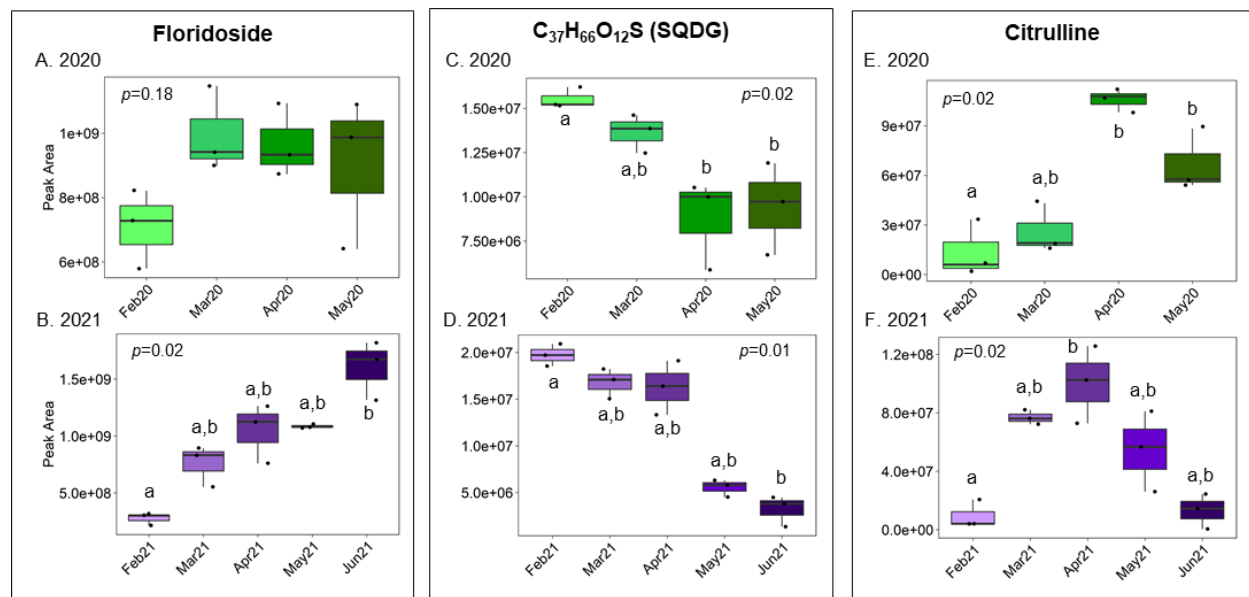


Figure 4: Box plot of Floridoside (A, B), C₃₇H₆₆O₁₂S (SQDG representative variation) (C, D) and Citrulline (E, F) Peak Area exhibiting temporal variations in 2020 (top green box plots) and 2021 (bottom purple boxplots) from February on the left to June on the right. P-value following a Kruskall-Wallis test is displayed at the corner of each plot and letters represent the differences between sampling months (Nemenyi Post Hoc).

2.6.4 Influence of environmental parameters

The influence of seawater temperature on temporal metabolome variation of *A. armata* in Banyuls-sur-Mer and *A. taxiformis* in Moorea was studied (**Tables S7, S8**). In general, we observed a lower seawater temperature variation in Moorea ($28.3 \pm 0.9^\circ\text{C}$ on average and 3% of coefficient of variation) than in Banyuls ($14.5 \pm 2.3^\circ\text{C}$ on average and 15.7% of coefficient of variation) (**Table S9**). We used a Mantel test to study the co-variation between metabolome of both species and seawater temperature. For *A. armata* in Banyuls, correlations of seawater temperature and metabolome variations were significantly positive for all analytical methods ($r=0.5$ on average, $p<0.05$) (**Table S10**). For *A. taxiformis* in Moorea, correlations were significant for all analytical methods ($p<0.05$) but the r coefficient of Pearson was closer to 0 (0.20 on average) meaning no co-variation (**Table S11**).

2.6.5 Temporal variability of the antibacterial activity

Then, the temporal variation of the antibacterial activity of apolar and polar extracts of *A. armata* collected in Banyuls and *A. taxiformis* collected in Moorea was also studied. Antibacterial activity assays were performed on 4 different fish pathogenic bacteria, three gram-negative (*E. anguillarum*, *V. anguillarum*, *P. anguilliseptica*) and one gram-positive (*L. garvieae*). While the polar phases did not show any activity at the dose tested (final 1 mg/disc), the apolar phases (final 0.1mg/disc) exhibited antibacterial activity (**Table 3**). For all apolar extracts, only slight variations of activity were observed and were not statistically significant ($p>0.05$) (**Table S12**). The same observation was made for each bacterial species.

Table 3: Average annual diameter of inhibition (including the size of the discs – 0.6 cm) measured as indicator of the antibacterial activity of extracts of *A. armata* collected in Banyuls-sur-Mer (three replicates for nine sampling month) and *A. taxiformis* collected in Moorea (three replicates for nine sampling month) against four different bacterial species. Letters (a, b, c) represent distinct groups based on Nemenyi Post Hoc between algal stages for each bacterium ($p < 0.05$).

Phase	Polar phases		Apolar phases		
	Species	Aa	At	Aa	At
Ea		$0.6 \pm 0^{\text{a}}$	$0.6 \pm 0^{\text{a}}$	1.7 ± 0.1	1.5 ± 0.1
Lg		$0.6 \pm 0^{\text{a}}$	$0.6 \pm 0^{\text{a}}$	0.9 ± 0.4	1.1 ± 0.0
Pa		$0.6 \pm 0^{\text{a}}$	$0.6 \pm 0^{\text{a}}$	2.9 ± 0.3	2.3 ± 0.1
Va		$0.6 \pm 0^{\text{a}}$	$0.6 \pm 0^{\text{a}}$	2.6 ± 0.3	2.2 ± 0.2

^aThe reported measurements include the size of the discs (0.6cm), thus all values 0.6cm mean no activity.

A distance based-redundancy analysis was performed to explore the relationship between the metabolome fingerprints of the apolar algal extracts with, the antibacterial activity measured against the 4 bacterial species, the sea water temperature, and, the year of collection as explaining variables (**Fig 3C, D**). As expected with the results of the Mantel test, temperature is highly correlated with the first RDA axis (biplot scores on dbRDA1=0.93) and with the metabolome of *A. armata* collected in April-May 2020 and May-June 2021. The antibacterial activity measured against Ea, Pa, and Va appeared to correlate with the second RDA axis (**Figure 3C**) as does the year of collection variable (biplot scores on dbRDA2= Year: -0.95; Ea: -0.729; Pa: -0.718; Va: -0.603). For the *A. taxiformis* dbRDA analysis also, antibacterial activities (dbRDA2 biplot scores: Ea: -0.019; Pa: -0.272; Va: -0.626) were negatively correlated with the temperature variable (dbRDA2 biplot scores: 0.333) and appeared more correlated with the year of collection (dbRDA2 biplot scores: -0.674) as for *A. armata* samples (**Figure 3D**). In both analyses, antibacterial activity of the apolar extracts against Lg was not correlated with either the temperature or year of collection. The use of Mantel tests confirmed the absence of covariation between metabolome dataset and antibacterial activities of apolar extracts ($r \sim 0$, $p < 0.05$) for both species

2.7 Discussion

A. armata and *A. taxiformis* are two red algae presenting a broad range of biological activities. Their chemistry has been studied since 70' and their richness in halogenated molecules has been highlighted (Burreson et al., 1975, 1976; Kladi et al., 2004; McConnell and Fenical, 1977). However, few studies have compared the two algae and few data were available on interspecies, spatial or temporal metabolites specificities. GC-MS was the most commonly used analytical technique to characterize the chemistry of these two algae, followed more recently by LC-MS (Greff et al., 2017b; Pinto et al., 2022; Thapa et al., 2020). Few studies were performed by NMR. Metabolomics, the science that describes a full range of small molecules in a sample at a time point, is a powerful tool to evaluate patterns in metabolites variations affected by environmental factors. Thus the aim of this study was to develop a complementary metabolomics approach based on three analytical methods: LC-HRMS, ^1H -NMR and HS-SPME-GC-MS in order to explore the interspecies and temporal metabolome variabilities.

The combination of these three analytical techniques allowed the detection of a wide range of chemical compounds. As reported in the literature, low molecular weight halogenated molecules could be detected with GC-MS (Burreson et al., 1975, 1976; McConnell and Fenical,

1977). Bromoform and dibromoacetic acid have been described to be some of the most abundant compounds in *A. armata* and *A. taxiformis* extracts (Machado et al., 2016; Paul et al., 2006a). In this study, bromoform could be detected using both LC-MS and HS-SPME-GC-MS, and intense dibromoacetic acid ion was also detected in LC-MS. Bromoform has recently received more attention because of its ability to reduce methane production (Roque et al., 2019, 2021). The use of HS-SPME-GC-MS could allow to quantify it without using any solvent and therefore in a greener way. The more recent chemical analyse of *Asparagopsis* spp. allowed description of pentabrominated mahorones (Greff et al., 2014) and hexabrominated derivatives (Thapa et al., 2020). Mahorones could not be detected in this study but an intense hexabrominated ion at m/z 572.5021 corresponding to the one reported recently (Thapa et al., 2020) was detected, as well as about ten other ions showing isotopic clustering indicators of the presence of more than 5 bromine atoms in the molecules. Therefore, we showed that the use of LC-HRMS allowed the detection of heavy halogenated molecules which may be responsible for some of the biological activities reported for extracts of this genus as described for mahorones (Greff et al., 2014). Unlike small halogenated molecules such as bromoform and dibromoacetic acid, which could repel herbivores and serve to control epiphytic bacterial communities through their release at the algal surface (Paul et al., 2006a; Vergés et al., 2008), the ecological role of more halogenated molecules remains to be elucidated. They could be precursors of smaller active halogenated molecules (Thapa et al., 2020).

To date, polar compartment of *Asparagopsis* spp. has received little attention. NMR has only been used to elucidate structures of isolated compounds (Burreson et al., 1976; Greff et al., 2014; McConnell and Fenical, 1977) or to study polysaccharides composition (Garon-Lardière, 2004). Our study is the first to report a “picture” of a polar complex mixture of the two species of the genus. The extract contained a majority of amino acids and carbohydrates identified by 2D NMR and for some, confirmed using chemical standards. Major carbohydrate was identified as floridoside, a heterosid especially found in red algae, which plays a role in carbon fixation and osmoregulation (Karsten et al., 1993; Martinez-Garcia and van der Maarel, 2016). Other major signals were those corresponding to an organosulfur compound, isethionic acid which has already been described in red algae with a large panel of possible ecological roles: anti-settlement, anti-quorum sensing or osmoregulation activities (Barrow et al., 1993; Hellio et al., 2004; Liu et al., 2008; Simon-Colin et al., 2002). Finally, amino acids: taurine, glycine, alanine, glutamine, asparagine were identified as a part of the natural central metabolic pathways of macroalgae as described in 2014 (Gupta et al., 2014). In this study, we report for the first time

the presence of floridoside, isethionic acid and taurine in the two species of the genus *Asparagopsis*.

The differences in the metabolome of the two species were assessed with a multiblock metabolomics approach. We could see with the dendograms, that the use of the multiblock analysis allowed a better discrimination of the samples than the use of an analytical method alone. The chemometric study of the data also showed that the greatest source of variability in the samples was species related. We detected six molecules exhibiting a "presence-absence"-like pattern using LC-MS and GC-MS. These molecules could therefore be specific to one or the other species. They are all halogenated. One of them, which presented the highest VIP scores was a fragment of an octabrominated compound named Pentabromopropen-2-yl tribromoacetate, and was first described in 1990 (Sugano et al., 1990) and recently reported as antibacterial agent against Flavobacteriaceae (Reverter et al., 2022). We also showed that many organosulfur molecules detected by NMR and LC-MS, in particular isethionic acid, taurine and sulfolipids, were discriminating and found in higher amounts in *A. armata* apolar extracts than in *A. taxiformis* apolar extracts. Red algae are known to contain high concentrations of taurine compared to green or brown algae but its ecological roles remain unclear and have been linked to osmoregulation process (Kawasaki et al., 2017; Kendel et al., 2013; Terriente-Palacios and Castellari, 2022). The exploitation of the MS/MS fragmentation patterns allowed qualifying sulfolipids as sulfoquinovosyldiacyl glycerol lipids (SQDG). The intensities of all detected SQDG between the two species were compared and we have observed that they were all in higher intensities in *A. armata* apolar extracts than in *A. taxiformis* apolar extracts. Their presence was not surprising as their role is to preserve the functions and structures of the membrane (Harwood, 1998). SQDG detected in the extracts all shared a fatty acid chain of the same length corresponding to palmitic acid (C16:0). These results are consistent with those of El Baz et al. (2013) who characterized the structure of sulfolipids in several algae species, determined fatty acids composition and found high proportion of palmitic acid. In addition, various studies reported that palmitic acid was the major fatty acid found in *A. armata* (Pereira et al., 2012; Pinto et al., 2022) and it has been shown that sulfolipids represent an important source of fatty acids (da Costa et al., 2019). In order to study the robustness of markers regardless of where the species is collected and to avoid over-influence of marked geographical environmental parameters on interspecies variability, this study included different sampling sites where the two species live in sympatry (Marseille and Messina). The highlighted interspecies markers were the same on sites with algae in sympatry but also at more distant

sites. Thus, these molecules could be proposed as chemotaxonomic markers regardless of the sampling site, the differences in the metabolome of the two species being probably due to genetic or gene expression differences. *A. armata* and *A. taxiformis* are genetically distinct (Andreakis et al., 2004). This could be due to or explain their generally different geographical distribution, *A. armata* living generally in more temperate water than *A. taxiformis* (Andreakis et al., 2004; Zanolla et al., 2022a). Temperate waters may be subjected to greater variations in environmental parameters such as temperature, which would explain the greater abundance of some molecules such as sulfolipids and taurine in *A. armata* extract.

The temporal variability of the metabolome of *A. armata* collected in Banyuls-sur-Mer and *A. taxiformis* collected in Moorea was then studied. Here again, we could see with the dendograms, that the use of the multiblock analysis allowed a better discrimination of the samples than the use of an analytical method alone. We have highlighted a temporal pattern for *A. armata* that was repeated over the two years of collection. No clear temporal pattern could be identified for *A. taxiformis*, which may be due to greater intra-group variability, particularly because collections were made between -5 and -15 m depth as opposed to 0 and -1 m for *A. armata*, but also to less seasonality in the Pacific. The visualization of the markers contributing the most to temporality allowed us to identify three types of gradients “increasing”, “decreasing” and “intermediate”. These patterns could be related to environmental conditions since we showed a significant covariation of metabolome and sea water temperature. Temperature has already been described as a factor influencing the growth and chemical composition of *Asparagopsis* spp. (Mata et al., 2017). In addition, *in situ*, a gradual yellowing of the algae was observed during the collections, particularly in May and June when water temperatures are used to rise sharply. Our results therefore suggest a stronger relationship between the variation of *A. armata* metabolome and the variation of seawater temperature in Banyuls which varies more. These observations could be a first explanation for the more marked temporality of the metabolome in Banyuls (Mediterranean Sea) than in Moorea (Pacific Ocean).

We have then identified several molecules with temporal variations. Floridoside intensity was maximum in May and June, especially in 2021. Several studies reported temporal variation of floridoside content in algae, with a maximum in summer months (Diehl et al., 2019; Karsten et al., 1993; Rødde et al., 2004). Floridoside is an antioxidant molecule that can be accumulated by the algae during stressful conditions such as an increase in temperature or osmotic stress (Karsten et al., 1993). We also detected that citrulline, an amino acid already detected in red algae (Impellizzeri et al., 1975; Mandalka et al., 2022) was maximal in April for both sampling

years. This antioxidant molecule can be accumulated under drought period (Akashi et al., 2001) or desiccation (Huang et al., 2021). Its accumulation in March and April could be an initial strategy set up by the algae in response to changing environmental conditions. In contrast, we found that the intensity of sulphated lipids decreased from February to June for both sampling years. In brown algae, it has been reported that some SQDG were more abundant in winter than in spring and summer (da Costa et al., 2019; Moreira et al., 2020), and that sulfolipids are more abundant in periods of low light irradiance and shorter light periods (Schmid et al., 2017). The temporal variations of some of the molecules identified here gave a better view of the mechanisms set up by the alga during the year. This knowledge is essential, particularly for the valorisation of these algae. Experiments under controlled conditions would allow to learn more about the variations in the production of molecules from these algae.

Finally, we evaluated the temporal variation of the antibacterial activity of apolar and polar extracts of both species. In contrast to the apolar extracts, the polar extracts showed no antibacterial activity. These results are consistent with our chemical analyses and with the literature. Indeed, Bansemir et al. (2006) reported that among dichloromethane, methanol and water extracts, only dichloromethane extracts showed significant antibacterial activity. Furthermore, most of the antibacterial activities of these red algae are attributed to halogenated molecules (Paul et al., 2006a; Ponte et al., 2022) which were detected in the apolar phase exhibiting the antibacterial activity. By performing a db-RDA analysis, we found out that the slight variations of antibacterial activity could be seen as a factor directly or indirectly correlated with the factor “year of collection” and with the metabolome of the 2021 samples. The 2021 samples may be more active than the 2020 samples, due to different environmental or stress parameters, other than temperature. The mantel tests performed confirmed that antibacterial activity and metabolome do not covariate. In our chemical analysis, the molecules with the most pronounced temporality were, in the apolar phase, the sulfolipids and, in the polar phase, several other molecules that are not known to have antibacterial activities. However, as other activities are reported for these molecules e.g. antiviral (El Baz et al., 2013) or anti-quorum sensing activities (Liu et al., 2008), we could expect to observe temporal variability effects by performing other assays such as antioxidant activity assays. A summary of the chemistry and antibacterial activity findings is presented in (**Table 3**).

Table 3: Summary of the 3 matrices analysed by different techniques, the main molecules identified, temporal variation of their chemical composition, antimicrobial activity and temporal variation.

Nature of the matrice	Analytical method	Molecules identified	Temporal variation of chemical composition	Antibacterial activity	Temporal variation of antibacterial activity
Apolar phase	UHPLC-ESI(-)-HRMS/MS	Halogenated ^a (di/tri halomethanes, haloacetic acids, haloforms, halogenated acetones); Hydroxy-fatty acids; SQDG	Yes (mainly SQDG)	Yes	No
Polar phase	¹ H-NMR	Carbohydrates; Organosulfur compounds; Amino acids	Yes	No	No
Powder	HS-SPME-GC-MS	Halogenated ^b (di/tri halomethanes, haloforms, carbon tetrahalides, acetaldehydes)	No	NA ^c	NA ^c

^aIncluding molecules with more than 4 bromines; ^bIncluding molecules with less than 4 bromines. ^cData not acquired.

2.8 Conclusion

To conclude, in this study we showed that the use of unsupervised multiblock analyses allowed (1) to explore the contribution of each analytical technic to the global model and (2) to highlight the complementarity of these techniques to answer different biological questions. The interspecies metabolome variability of *A. armata* and *A. taxiformis* was greater than the spatial metabolome variability and may be due to genetic or gene expression differences. We have identified some halogenated molecules as potential chemotaxonomic markers. The variation in several metabolites intensities could be related to temporal effects, probably linked to environmental factors. Finally, despite significant temporal variability in the metabolome of both species, we have shown that the antibacterial activity of the extracts of the two algae against fish pathogenic bacteria did not show any temporal variation. This is important as it means that the molecules responsible for algal activity are produced at a constant level throughout the year which may allow the annual biomass availability of algae for a potential use as fish feed complement. *In vivo* feeding experiments have also been undertaken in our laboratory on healthy and experimentally infected fish to allow investigations regarding efficiency and toxicity of this alternative way to prevent or treat bacterial fish diseases.

2.9 Acknowledgments

This work was supported by the Occitanie Region, France. Authors would like to thank Dr Erwan Ar Gall and its collaborators, Dr Stephane Greff, Dr Thierry Perez and their collaborators, Dr Giuseppa Genovese, Damiano Spagnuolo and their collaborators and Guillaume Iwankow for providing algae samples respectively from Bretagne, Marseille, Messina and Moorea. Acknowledgments to Adolfo Botana and Bernard Banaigs for their help in ¹H-NMR and 2D-NMR method's development. Thanks to Dr. Florence Nicolé and Dr. Florence Mehl for their help in statistical analysis. The LC-Q/Orbitrap, NMR and HS-SPME-GC-MS methods developments and analyses were performed using the Biodiversité et Biotechnologies Marines (Bio2Mar) facilities – Métabolites Secondaires Xénobiotiques Métabolomique Environnementale (MSXM) platform at the Université de Perpignan Via Domitia (<https://bio2mar-msxm.univ-perp.fr/>).

3. Ce qu'il faut retenir

L'objectif du travail réalisé dans ce chapitre était d'explorer différentes sources de variations (interspécifique et temporelle) du métabolome d'*A. armata* et d'*A. taxiformis* en développant une approche de métabolomique dite « multiblock » intégrant les données issues de trois méthodes analytiques complémentaires : la LC-HRMS, la RMN et la HS-SPME-GC-MS.

Pour cela, 84 échantillons d'algues provenant de 5 sites ont été collectés puis extraits selon une méthode biphasique permettant ensuite d'analyser les phases apolaires en LC-HRMS et les phases polaires en RMN. En parallèle, les poudres d'algues lyophilisées ont été analysées en HS-SPME-GC-MS. Après pré-traitement des données acquises, des analyses statistiques « multiblock » ont été réalisées permettant de construire un modèle intégrant les 3 jeux de données et d'estimer l'apport de chaque technique pour la création de ce modèle. En parallèle, la variation temporelle de l'activité antibactérienne des deux espèces a été évaluée et reliée aux résultats de l'analyse métabolomique.

(1) Les données acquises montrent une grande diversité chimique pour les deux espèces. La poudre d'algue extraite et analysée pour la première fois en HS-SPME-GC-MS contient une majorité de molécules volatiles halogénées de faible masse moléculaire. La phase apolaire analysée en LC-HRMS est constituée de lipides polaires et de molécules halogénées de plus haute masse moléculaire dont certaines avec plus de 5 bromes. Enfin, la phase polaire analysée en RMN est principalement composée d'acides aminés et de glucide dont certains sont décrits pour la première fois dans les espèces du genre *Asparagopsis*.

(2) Pour chaque variation du métabolome étudiée (interspécifique et temporelle), la séparation des groupes est meilleure pour la matrice intégrant les 3 jeux de données pour celles obtenues avec chaque technique analytique prise isolément. Ici encore, ce résultat montre la complémentarité et l'intérêt de combiner différents outils analytiques pour une meilleure compréhension des phénomènes étudiés. En revanche, si la discrimination globale est meilleure avec la matrice « multiblock », à la fois pour la discrimination interspécifique et pour la discrimination temporelle, l'utilisation d'un ou de deux outils analytiques expliquent davantage de variation que les autres. Ainsi, pour la discrimination interspécifique, la LC-HRMS contribue le plus au modèle, et pour la discrimination temporelle, la RMN et la LC-HRMS contribuent le plus au modèle.

(3) J'ai pu montrer une différence significative du métabolome des deux espèces. Cette différence est dûe d'une part à certaines molécules halogénées (détectées en LC-HRMS ou en HS-SPME-GC-MS) comme le tribromoacetate de pentabromopropen-2-yle ($C_5Br_8O_2$) non-détecté chez *A. armata* ou encore la 1,1,3,3-Tetrabromoacetone plus abondante chez *A. armata* que chez *A. taxiformis* et d'autre part à des molécules organosulfurées détectées en LC-HRMS (sulfolipides) et en RMN (taurine et acide iséthionique) abondantes chez *A. armata*.

(4) Les échantillons d'*A. armata* collectés entre février et juin en 2020 ainsi qu'en 2021 ont une variation temporelle de leur composition chimique beaucoup plus marquée que les échantillons d'*A. taxiformis* collectés entre février et octobre en 2020 et 2021. Le métabolome d'*A. armata* co-varie avec la température de l'eau. Le floridoside, la citrulline et les sulfolipides, sont quelques exemples de molécules identifiées dans les échantillons d'*A. armata* dont l'abondance varie avec la saison.

(5) Enfin, contrairement aux phases apolaires actives pour les 2 espèces d'algues contre les 4 espèces de bactéries, aucune activité antibactérienne n'a été détectée pour les phases polaires. L'activité des phases apolaires ne présentait pas de variation temporelle. Combinés aux résultats des données de métabolomique, ces résultats permettent de souligner qu'aucune molécule de la phase polaire ou présentant une variation temporelle ne peut être responsable de l'activité antibactérienne des extraits.

4. Résultats non intégrés à l'article

Outre les variations interspécifiques et temporelles, la variabilité spatiale est un autre facteur important de variation du métabolome qui n'a pas été mentionné dans l'article ci-dessus en raison d'une diversité de lieux de collecte jugée insuffisante. Toutefois, des résultats préliminaires suggèrent des tendances et indiquent des différences statistiquement significatives de la composition chimique en fonction des lieux de collectes. Ainsi la composition chimique des échantillons d'*A. armata* collectés à Banyuls-sur-Mer se distingue de la composition chimique des échantillons de la même espèce, collectés dans 3 autres sites (**Figure 26 A**). Le floridoside est l'une des molécules discriminantes de ces différents sites en étant plus abondant chez *A. armata* collectée à Banyuls-sur-Mer que dans les autres lieux. De manière similaire, la composition chimique des échantillons d'*A. taxiformis* collectés à Moorea se distingue de celle des échantillons collectés à Marseille et à Messine (**Figure 26B**). Une molécule putativement identifiée comme de l'acide gamma-aminobutyrique est absente des échantillons d'*A. taxiformis* collectés à Moorea.

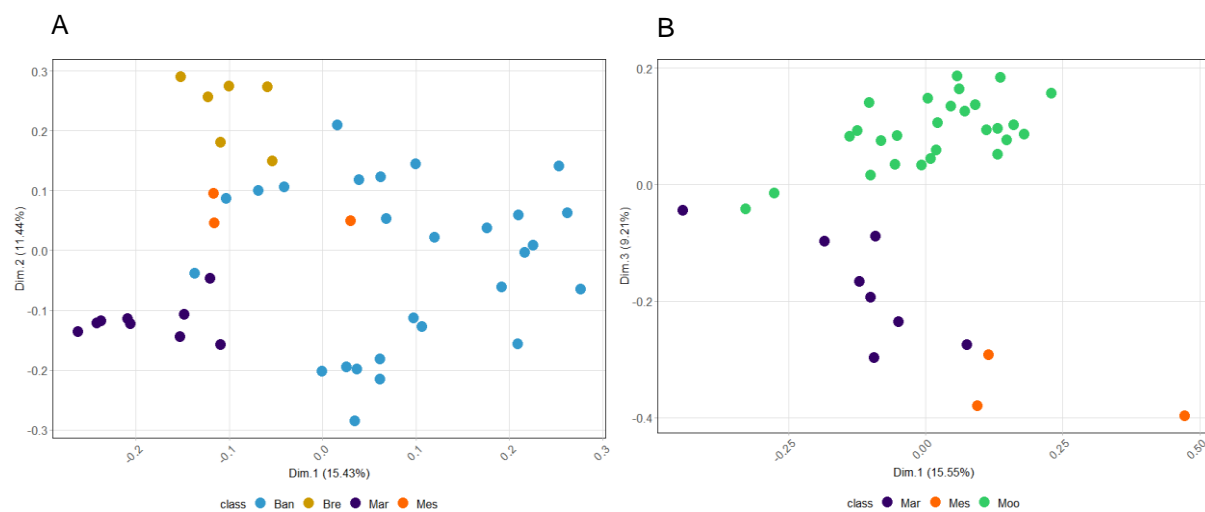


Figure 26 : ACP des deux premières dimensions communes déterminées avec l'analyse ComDim de la variabilité spatiale du métabolome d'*A. armata* (A) et de la première et troisième dimension commune de la variabilité spatiale du métabolome *A. taxiformis* (B). Les couleurs représentent des lieux de collectes différents. Ban=Banyuls, Bre=Bretagne, Mar=Marseille, Mes=Messina, Moo=Moorea.

Par ailleurs, peu de variabilité spatiale de l'activité antibactérienne des extraits des deux espèces a été mesurée contre Ea et Lg (**Tableau 3**). En revanche, la variabilité spatiale de l'activité antibactérienne des deux espèces contre Pa et Va était plus prononcée (**Tableau 3**). Ces résultats préliminaires indiquent qu'il existe des spécificités géographiques influençant le métabolome et les activités antibactériennes des deux espèces. Il serait nécessaire d'élargir le champ des

lieux de récolte et de collecter, en parallèle, des données environnementales afin d'en faciliter l'interprétation. Par ailleurs, même si vraisemblablement les échantillons de France métropolitaine appartiennent aux mêmes lignées, et que seuls les échantillons de Moorea correspondent à une lignée différente, il serait intéressant de lier les données de chimie à des données de génétiques en identifiant les lignées collectées.

Tableau 3 : Diamètre d'inhibition moyen (incluant la taille des disques – 0,6 cm) mesuré comme indicateur de l'activité antibactérienne des extraits d'*A. armata* (Aa) de Banyuls-sur-Mer (n = 9x3), Bretagne (n = 4x3), Messine (n = 3) et Marseille (n = 3x3), et de ceux d'*A. taxiformis* (At) de Moorea (n = 9x3), Messine (n = 3) et Marseille (n = 3x3) contre quatre espèces bactériennes différentes.

Sp	Aa				At			
	Site	Banyuls	Bretagne	Messine	Marseille	Moorea	Messine	Marseille
Ea		1,7 ± 0,2	1,4 ± 0,2	1,5 ± 0,1	1,5 ± 0,1	1,4 ± 0,2	1,8 ± 0,0	1,4 ± 0,1
Lg		0,7 ± 0,4	0,6 ^a ± 0,4	0,3 ^a ± 0,6	0,5 ^a ± 0,4	1,0 ± 0,1	1,1 ± 0,1	1,0 ± 0,1
Pa		2,9 ± 0,5	1,8 ± 0,2	2,2 ± 0,0	2,6 ± 0,5	2,2 ± 0,4	3,1 ± 0,7	1,9 ± 0,3
Va		2,6 ± 0,6	1,8 ± 0,4	2,2 ± 0,2	2,3 ± 0,5	2,1 ± 0,4	3,5 ± 0,3	1,7 ± 0,2

^aLes mesures incluent la taille des disques, donc les valeurs égales ou inférieures à 0,6 signifient une absence d'activité.

Chapitre II : Activité anti-quorum sensing des algues du genre *Asparagopsis*



Illustration à l'aquarelle réalisée par Michèle Parchemin de l'effet anti-quorum sensing

1. Avant Propos

Anti-Quorum Sensing Activities of *Asparagopsis* Algae

Christelle Parchemin, Théo Périon, Loic Maurice, Delphine Raviglione, Emilie Adouane, Pierre Sasal, Elisabeth Faliex, Raphaël Lami, Nathalie Tapissier-Bontemps

Publication

En l'état, l'article présenté dans ce chapitre n'a pas vocation à être publié mais il sera soumis pour publication lorsque les molécules responsables de l'activité décrite seront identifiées et que leur activité sera confirmée.

Contexte

Le quorum sensing (QS) est un mode de communication bactérien basé sur la densité cellulaire et la concentration en molécules inductrices (« auto-inductrices ») (le plus souvent des *N*-acyl homosérines lactones=AHLs) qui déclenchent l'expression de certains gènes liés à divers mécanismes tels que la formation de biofilm ou la virulence (Kalia, 2013 ; Miller and Bassler, 2001). Dans **l'Etat de l'art**, j'ai défini l'activité anti-quorum sensing et présenté le fait que l'espèce *A. taxiformis* est déjà connue pour ce type d'activité (Jha et al., 2013). En revanche, la molécule potentiellement responsable de cette activité n'ayant pas été isolée, son activité n'a pas pu être confirmée. Enfin, l'espèce sœur *A. armata* n'a à ce jour fait l'objet d'aucune étude. Une collaboration, débutée avant cette thèse entre Nathalie Tapissier-Bontemps et Raphaël Lami du Laboratoire de Biodiversité et Biotechnologies Microbiennes (LBBM) de l'Observatoire Océanologique de Banyuls-sur-Mer avait permis de confirmer l'activité anti-QS d'extraits bruts de l'espèce *A. taxiformis* collectée à Moorea (Polynésie Française). Au cours de l'année 2021, j'ai répondu à un appel à projet de l'école doctorale 305 de l'UPVD, ayant pour objectif de financer des projets complémentaires au projet doctoral à hauteur de 3000€, afin de poursuivre le travail entrepris sur l'activité anti-QS des deux espèces d'algues. Ce financement m'a été accordé et a permis la réalisation des travaux présentés dans ce chapitre.

Méthodologie générale

Les activités anti-QS d'organismes marins sont étudiées au LBBM grâce à un protocole de routine et à l'utilisation de 3 biosenseurs (des souches rapportrices, qui détectent naturellement les auto-inducteurs mais qui sont génétiquement modifiées pour ne plus les produire) : *Chromobacterium violaceum* CV026, *Pseudomonas putida* F117 and *Escherichia coli* MT102 (Andersen et al., 2001 ; McClean et al., 1997 ; Riedel et al., 2001). En présence d'AHLs, CV026 produit un pigment violet tandis que F117 et MT102 émettent de la fluorescence (GFP). En présence d'AHLs de synthèse et d'extraits d'organismes d'intérêts, l'activité anti-QS peut ainsi être détectée soit par l'absence de production de pigment soit par l'absence d'émission de fluorescence. La difficulté de ce type de test est de distinguer une activité anti-QS d'une activité bactéricide (déjà connue et éprouvée chez les algues du genre *Asparagopsis* (Jha et al., 2013). Dans ce travail, l'activité anti-QS des deux espèces d'*Asparagopsis* a été étudiée sur des extraits bruts et des fractions selon une méthodologie classique de fractionnement bioguidé.

Contribution

J'ai mis au point la méthode de fractionnement, « la mise en place et la réalisation des tests anti-QS au CRIOBE à partir des extraits et des fractions d'algues des deux espèces d'*Asparagopsis*. Théo Périon et Loic Maurice (stagiaires de M1 que j'ai encadrés) ont réalisé les extractions et le fractionnement des deux algues à plus grande échelle. Delphine Raviglione a fourni un appui pour la réalisation des analyses en LC-HRMS. Emilie Adouane et Raphaël Lami ont fourni les biosenseurs et les protocoles pour la réalisation des tests et ont participé à l'exploitation des résultats. Pierre Sasal, Elisabeth Faliex, Nathalie Tapissier-Bontemps ont participé à la mise en place du design expérimental et à l'exploitation des résultats.

Disponibilité des données

Les données LC-MS issues des travaux présentés dans ce chapitre n'ont pas été déposées sur une plateforme de partage.

2. Article

Anti-Quorum Sensing Activities of *Asparagopsis* Algae

C. Parchemin^{1,2}, T. Périon¹, L. Maurice¹, D. Raviglione¹, E. Adouane³, P. Sasal¹, E. Faliex², R. Lami³, N. Tapissier-Bontemps¹

¹ Centre de Recherches Insulaires et Observatoire de l'Environnement (CRIOBE), Université de Perpignan - Via Domitia, 52 Av. Paul Alduy, 66860 Perpignan CEDEX

² CEntre de Formation et de Recherche sur les Environnements Méditerranéens (CEFREM), Université de Perpignan - Via Domitia, 52 Av. Paul Alduy, 66860 Perpignan CEDEX

³ Laboratoire de Biodiversité et Biotechnologies Microbiennes (LBBM), UAR 3579 Sorbonne Université-CNRS, Observatoire Océanologique de Banyuls, Sorbonne Université, 66650 Banyuls-sur-Mer

2.1 Abstract

Quorum Sensing (QS) is a density-dependent bacterial mode of communication. It is a new target for controlling pathogens and diseases, as its inhibition slows down the development of antibiotic-resistant bacteria. In nature, a wide range of organisms produce molecules that disrupt signals and inhibit QS, enabling them to regulate epiphytic and foreign bacterial populations, including those that may be pathogenic. A study has reported the activity of extract from *A. taxiformis* against *Chromobacterium violaceum* but the potential molecule responsible for the activity has not been isolated, and no studies have been conducted on the anti-QS activity of *A. armata*. In this study, we evaluated the anti-QS activity of extracts and fractions from both *A. taxiformis* and *A. armata* against three biosensors: *Chromobacterium violaceum* CV026, *Pseudomonas putida* F117 and *Escherichia coli* MT102. Anti-QS activity was found to be similar for both species against the three biosensors, with activity concentrated in halogenated and polar lipids-containing fractions.

Keywords: red algae, bacterial communication, antibacterial activity, quorum quenching

2.2 Introduction

The rise of antibiotic-resistant bacteria has prompted the search for new methods to control bacterial diseases. Many of these diseases are linked to the formation and growth of bacteria within biofilms, which are regulated by a form of bacterial communication called quorum sensing (QS). QS is a process that regulates certain bacterial genes in response to an increase in bacterial density and the production of autoinducer molecules (Kalia, 2013), such as *N*-acyl

homoserine lactones (AHLs), butyrolactones or some cyclic peptides. The inhibition of QS or biofilm formation has become a new target for drug discovery, as it could help slow down the development of resistant-bacteria to active molecules (Taylor et al., 2014).

Several organisms, including bacteria, fungi, microalgae, sponges, and macroalgae produce molecules that resemble self-inducers and disrupt the QS signal (Dobretsov et al., 2009). *Delisea pulchra* was the first macroalgae and the first marine organism to be described with anti-QS activity, which comes from halogenated furanones produced by the algae that are structurally analogs to AHLs (Dobretsov et al., 2009; Dworjanyn et al., 1999; Maximilien et al., 1998). Other anti-QS activities have been reported from macroalgae and their epiphytic isolated microorganisms (Dahms and Dobretsov, 2017; Dobretsov et al., 2009; Tourneroche et al., 2019). Macroalgae-derived anti-QS molecules include hypobromous acid (*Laminaria digitata*), galactitol (*Spatoglossum* sp.) or floridoside, betonicine, and isethionic acid (*Ahnfeltiopsis flabelliformis*) (Dahms and Dobretsov, 2017; Kim et al., 2007; Liu et al., 2008).

Another study reported the anti-QS activity of thirty algal species from India, with only *Asparagopsis taxiformis* exhibiting anti-QS activity (Jha et al., 2013). The extract was fractionated and, based on a Fourier Transform Ion Cyclotron Resonance Mass Spectrometry analysis (ICR-FT/MS) of the active fraction, the authors identified a candidate compound responsible for the activity with the molecular formula C₁₄H₂₇O₅S, which may correspond to a 2-dodecanoyloxyethanesulfonate. However, the proposed molecule has not yet been isolated and its activity still needs to be confirmed. Furthermore, to date, no research has been conducted to explore the potential anti-QS activity of the sister species *A. armata*, which is already known for its various antibacterial and antifouling activities (Pinteus et al., 2015, 2018).

Therefore, the objective of the present study was to explore the anti-QS activities of both species of the genus *Asparagopsis* against the strain used in previous work (*Chromobacterium violaceum* CV026) and two others biosensors: *Pseudomonas putida* F117 and *Escherichia coli* MT102, in order to broader the possibility of anti-QS activity and to (1) evaluate the potential activity of *A. armata*, (2) compare the activity of the two species and (3) isolate molecules responsible for the activity.

2.3 Materials and Methods

2.3.1 Materials

2.3.1.1 Chemicals

For sample extraction, Methanol (MeOH) HPLC grade and Dichloromethane (DCM) HPLC grade were purchased from VWR™ (Fontenay-sous-Bois, France). Water used for fractionation was ultra-pure water, obtained by purification of water with a PURELAB Chorus 1 system (ELGA LabWater, Lane End, HP14, UK). Dimethylsulfoxide (DMSO) was purchased from Honeywell Riedel de Haen™. For assays, C6-HSLs and 3-oxoC10-HSLs were purchased from Sigma-Aldrich® (Saint Louis, USA) and cinnamaldehyde from Thermo Scientific™ (Waltham, MA, USA). Sea salts, peptone, yeast extract and agar for the composition of LB medium were all purchased from Sigma-Aldrich® (Saint Louis, USA). For the UHPLC-HRMS analysis, Water LC-MS grade was purchased from VWR™ (Fontenay-sous-Bois, France), and Acetonitrile (ACN) LC-MS grade was purchased from Carlo Erba (Val de Reuil, France). Formic acid (FA) 99% (for analysis) was obtained from Carlo Erba (Val de Reuil, France).

2.3.1.2 Algae

Asparagopsis armata and *A. taxiformis* were sampled in different months of the year 2020 in Banyuls-sur-Mer (lat. 42.482230°; long. 3.137175°) and Moorea (French Polynesia, lat. -17.48262°; long. -149.87213°) respectively. Immediately after collection, algae were manually cleaned of epiphytes, freeze-dried and stored at -25°C until use.

2.3.1.3 Biosensors strains

The biosensors strains *Chromobacterium violaceum* CV026, *Pseudomonas putida* F117 (pRK-C12; Kmr; ppuI :: npt) and *Escherichia coli* MT102 (pJBA132) were used in this study (Andersen et al., 2001; McClean et al., 1997; Riedel et al., 2001). In presence of AHLs, CV026 produces violacein, a purple pigment, while F117 and MT102 emit fluorescence (GFP). *P. putida* F117 is used for the detection of long-chain AHLs (8 carbons in the acyl side chain) (Andersen et al., 2001) while *C. violaceum* CV026 and *E. coli* MT102 are used for the detection of short chain AHLs (\leq 8 carbons in the acyl side chain) (McClean et al., 1997; Riedel et al., 2001). They were maintained at -80 °C in reconstituted Luria Broth supplemented with 30% (v/v) glycerol.

2.3.2 Algal extraction

Samples of each species collected throughout 2020 were pooled (73 g for *A. taxiformis* and 100 g for *A. armata*) and crude extracts (12.47 g for *A. taxiformis* and 17.64 g for *A. armata*) were obtained by three successive overnight maceration under agitation of algae powder in a mixture of MeOH:DCM (1:1). Then, crude extracts were fractionated on a C18-column (45g) (Interchim, puriflash IR 60, C18 50 µm, Montluçon, France) using a step gradient of 100% H₂O (F1), 90% H₂O-MeOH (F2), 80% H₂O-MeOH (F3), 70% H₂O-MeOH (F4), 60% H₂O-MeOH (F5), 40% H₂O-MeOH (F6), 30% H₂O-MeOH (F7), 20% H₂O-MeOH (F8), 10% H₂O-MeOH (F9), 100% MeOH (F10) and 100% EtoAc (F11) to give 11 fractions for each species. The resulting fractions were evaporated, weighed, and resuspended in MeOH at 5 mg/mL for petri dish assays. For microplates assays, fractions were resuspended in a mix of H₂O:DMSO (3:1) at 2.5 mg/mL in order to reach a non-toxic DMSO concentration of 2.5% once in each well.



Figure 1: Macerate of algae powder in MeOH:DCM (A) and ten of the eleven fractions obtained after fractionation of the crude extract (B)

2.3.3 Anti-QS effect on *Chromobacterium violaceum* CV026

The assays with the CV026 biosensor were performed either by visually observing pigment production on Petri dish or by measuring the optical density using microplates. However, the microplate assays were unsuccessful, so the assays were performed on Petri dishes instead. Before the assay, the Petri dishes were prepared with Luria agar containing 0.2 µM C6-HSL. CV026 was then revived from glycerol stocks and grown overnight at 26 °C in liquid LB medium. Culture was then diluted to 1/100 again in LB medium. Agar plates were flooded with bacterial broth and were set aside to dry. Algal fractions (10 µL) were deposited onto 6 mm sterile paper discs (final concentration: 0.05 mg/disc). MeOH was used as negative control and cinamaldehyde diluted 1/200e in DMSO was used as positive control. Discs were placed under the hood to allow evaporation of the solvent. Following evaporation, the discs were placed onto

the surface of the inoculated agar. The plates were incubated for 24 h at 26°C. Areas of inhibited bacterial growth were observed as clear halos (zones) around the discs while areas of QS inhibition were observed as yellowish zones around discs or around areas of inhibited bacterial growth (**Figure 2**). The diameter of the zone of inhibition of bacterial growth were measured to the nearest mm, each reported measure including the size of the disc (0.6 cm in diameter).

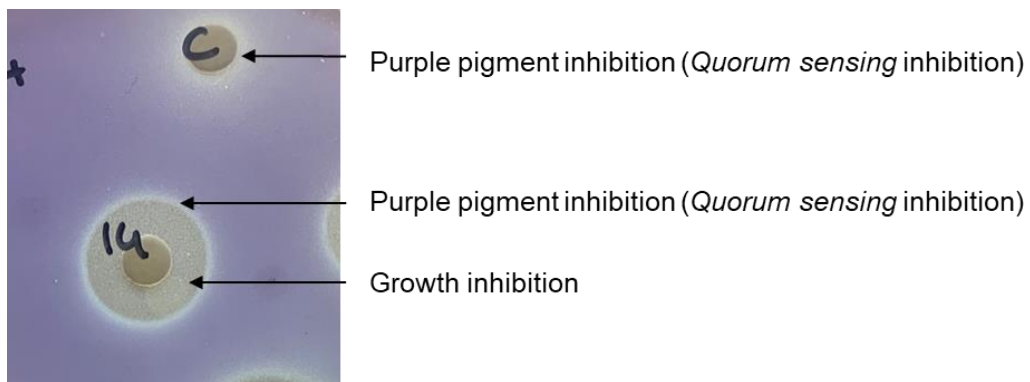


Figure 2: Differentiation between bacterial growth inhibition (toxicity) and pigment production inhibition (quorum sensing inhibition)

2.3.4 Anti-QS effect on *Pseudomonas putida* F117 and *Escherichia coli* MT102

Assays with biosensors F117 and MT102 were performed using microplates and adapted from Doberva et al. (2017). As for CV026 assays, F117 and MT102 were revived from glycerol stocks and grown overnight at 30°C and 37°C in liquid LB medium respectively. Culture was then diluted to 1/50 in LB medium and C6-HSL (F117) or OxoC10-HSL (MT102) (50 µL of 2 µM diluted in DMSO solutions) were added. Fresh culture (180 µL) was dispensed into 96-well microplates. Then, 20 µL of algal fractions (final concentration: 0.25 mg/mL) or controls were added in triplicates. Fresh culture without AHLs (no fluorescence), fresh culture with AHLs with DMSO (no inhibition of fluorescence) and medium (no fluorescence, no growth) were used as negative controls. Fresh culture with AHLs only (fluorescence) and fresh culture with AHLs and cinnamaldehyde (inhibition of fluorescence) were used as positive controls. Microplates were incubated at 30 °C and 37 °C and fluorescence (GFP) was determined after 24h of incubation using a Varioskan™ LUX spectrophotometer (Thermo Scientific) at an excitation and detection wavelength of 485nm and 535nm respectively. Optical density at 620nm was also measured to control bacterial growth. A fraction was considered positive for anti-QS activity when the percentage of fluorescence emission was reduced of 20% (percentage corresponding to that of the positive control).

The percentage of fluorescence was calculated as:

$$\frac{\left(\frac{\delta\text{FluoControl}}{\delta\text{DOControl}}\right) - \left(\frac{\delta\text{Fluo}}{\delta\text{DO}}\right)}{\frac{\delta\text{FluoControl}}{\delta\text{DOControl}}} = \% \text{ of fluorescence inhibition}$$

with $\delta\text{Fluo} = \text{Fluo}_{\text{measured}} - \text{Fluo}_{\text{Medium}}$ and $\delta\text{DO} = \text{DO}_{\text{measured}} - \text{DO}_{\text{medium}}$.

2.3.5 LC-HRMS analysis of the fractions

Fractions were concentrated at 0.5mg/mL in MeOH prior to analysis. LC-HRMS analyses were performed with a Vanquish UHPLC system from ThermoScientific (MA, USA) equipped with a Q Exactive™ Plus mass spectrometer with an electrospray ionization source. Metabolites separation was performed on a C18 UHPLC column (Luna® Omega 1.6µm Polar C18 100 A LC Column 100 x 2.1 mm, Phenomenex, CA, USA). The mobile phase consisted in a mixture of H₂O + 0.1% FA (solvent A) and ACN + 0.1% FA (solvent B). The flow rate was 400 µL/min. The elution program was set up at 2% B during 1 min, followed by a linear gradient up to 100% B during 10 min, then maintained 5 min in isocratic mode. The analysis was followed by a return to initial conditions for column equilibration during 4 min for a total runtime of 20 min.

The mass spectrometer analyzer parameters were set as follows: sheath gas flow rate, auxiliary gas and sweep gas flow rate at 45 arbitrary units (a.u.), 15 a.u. and 2 a.u. respectively, capillary and gas temperature to 320 °C and 250 °C respectively, the S-lens RF level and spray voltage to 60 V and 3.20 kV respectively. Parameters for the Full MS experiments were set as follows: the resolution was 70,000, the Automatic Gain Control was 3E6 ions, the maximum Injection Time (IT) was 100ms and a scan mass window of 100–1500 *m/z* was used.

2.4 Results

2.4.1 Anti-QS effect on *Chromobacterium violaceum* CV026

Anti-QS activity assays were conducted on crude extract and fractions from the species *A. armata* and *A. taxiformis* using CV026 as the test subject. The control (MeOH), showed no bactericidal nor anti-QS activities. On the other hand, variations in the anti-QS activity of cinnamaldehyde, which was used as the positive control, were observed. This variability may due to its volatility and slight bactericidal activity (**Table 1, Figure 3**). Cinnamaldehyde displayed clear anti-QS activity, as evidenced by the absence of purple pigment and the presence of bacterial mat surrounding the discs. Extracts from both species displayed a similar range of antibacterial activity, which was indicated by the presence of clear and transparent zones around impregnated discs (2.25 cm ± 0.1) (**Table 1, Figure 3**).

Table 1: Summary of results of the quorum sensing inhibition bioassay of crude extracts of *A. armata* and *A. taxiformis*. The results of bioassay were expressed as: + positive anti-QS effect, - No effect. The bioassays were conducted in triplicates. MeOH=Methanol; Cinna=Cinnamaldehyde. The diameter of the zone of inhibitions of bacterial growth were measured to the nearest mm, and each reported measurement including the size of the disc (0.6 cm in diameter).

Algae	Effects	MeOH	Cinna	Extract
<i>A. armata</i>	Antibacterial activity zone	-	Light	2.3±0.1
	Anti-QS zone	-	+	+
<i>A. taxiformis</i>	Antibacterial activity zone	-	Light	2.2±0.1
	Anti-QS zone	-	+	+



Figure 3: Results of the anti-QS assays of *A. armata* and *A. taxiformis* crude extracts on CV026.

The fractions of the algae were assayed the same manner. We observed differential growth and production of the pigment throughout the assays, for example between plate A, B and C where after 24h of culture, pigment in A was darker than in B and C (**Figure 4A, B, C**). We also observed that the inhibition of the pigment production around impregnated discs was most pronounced during early observations (<24 hours) as observed on plate B and C, and then slowly decreased. This could therefore affect the reading of the results and their interpretation. Similar activities were found between the fractions of the two species (**Figure 4A, B, C, D, E, F; Table 2**). No fractions exhibited only anti-QS activity, but for both species, most of them (F2 (90% H₂O-MeOH), F3 (80% H₂O-MeOH), F4 (70% H₂O-MeOH), F5 (60% H₂O-MeOH), F6 (40% H₂O-MeOH), F7 (30% H₂O-MeOH), F8 (20% H₂O-MeOH), F9 (10% H₂O-MeOH)) presented bactericidal activity surrounded by a light halo of QS activity (**Figure 4; Table 2**). Unlike for *A. armata*, fraction F1 (100% H₂O) of *A. taxiformis* also presented bactericidal activity surrounded by a light halo of QS activity. For both species, the fraction with the largest zone of inhibition was the one obtained with 40% H₂O-MeOH (**Figure 4B, E; Table 2**).

Table 2: Summary of the results of the quorum sensing inhibition bioassay of fractions of *A. armata* and *A. taxiformis*. The results of bioassay were expressed as: “+” positive anti-QS effect, “-“ No effect. The bioassays were conducted in triplicates. MeOH=Methanol; Cinna=Cinnamaldehyde. The diameter of the zones of inhibition of bacterial growth were measured to the nearest mm, each reported measurement including the included size of the disc (0.6 cm in diameter).

Algae	Effects	MeOH	Cinna	100H ₂ O	90	80	70	60
<i>A. armata</i>	Antibacterial activity zone	-	-	-	1.1±0.05	1.6±0.0	1.7±0.1	2.1±0.1
	Anti-QS zone	-	+	-	+	+	+	+
<i>A. taxiformis</i>	Antibacterial activity zone	-	-	1.5±0.1	1.8±0.0	1.5±0.0	1.5±0.1	1.1±0.0
	Anti-QS zone	-	+	+	+	+	+	+

Table 2: (suite)

Algae	Effects	40	30	20	10	100 MeOH	100 EtoAc
<i>A. armata</i>	Antibacterial activity zone	3.3±0.2	3.0±0.0	0.8±0.1	0.7±0.0	-	0.7±0.0
	Anti-QS zone	+	+	+	+	-	+
<i>A. taxiformis</i>	Antibacterial activity zone	3.2±0.1	1.9±0.1	2.2±0.1	1.1±0.1	0.8±0.0	0.8±0.0
	Anti-QS zone	+	+	+	-	-	-

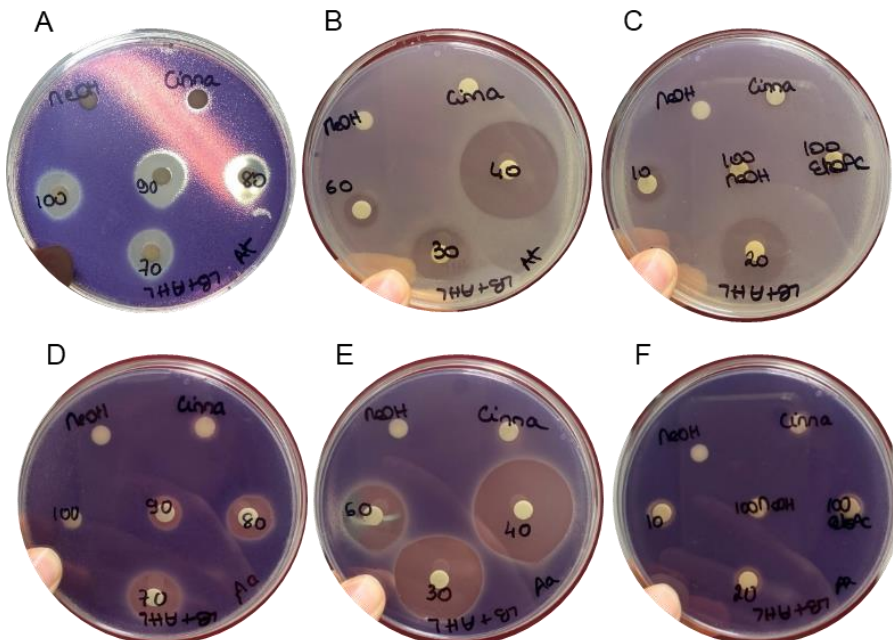


Figure 4: Results of the anti-QS assays of *A. taxiformis* (A, B, C) and *A. armata* (D, E, F) fractions on biosensor CV026.

2.4.2 Anti-QS effect on *Pseudomonas putida* F117 and *Escherichia coli* MT102

With regard to the results against CV026, we hypothesized that the majority of the bactericidal activity of the crude extracts could cover the anti-QS activity, so we directly tested the activity of the fractions against biosensors F117 and MT102. Anti-QS activity was measured through the reduction of the fluorescence emission of the two biosensors. We encountered variability in the activity of the cinnamaldehyde, our positive control, with inhibition of approximately 20% of fluorescence in each assay except for the assay of *A. taxiformis* fractions against F117 where cinnamaldehyde seemed to promote fluorescence (**Figure 5A and 6B**). As cinnamaldehyde is highly volatile and may result in inconsistent results, we still exploited the microplates essays results, but these results need to be confirmed. All fractions reducing the fluorescence emission of the biosensor by 20% were considered to have an anti- QS activity. Against F117, fractions F4 to F8 of *A. armata* all reduced fluorescence emission by more than 25% (**Figure 5A**) indicating a significant anti-QS activity. Approximately the same *A. taxiformis* fractions were active, except for F8 but with F2 in addition. However, fractions F9, F10 and F11 tended to increase fluorescence (**Figure 5A**), which was associated with increased bacterial growth. Different results were found against MT102, as for both species, fractions F2 to F6 tended to increase fluorescence, while fractions F7 to F11 inhibited fluorescence emission in similar range (>30%) signifying an anti-QS activity (**Figure 5B**).

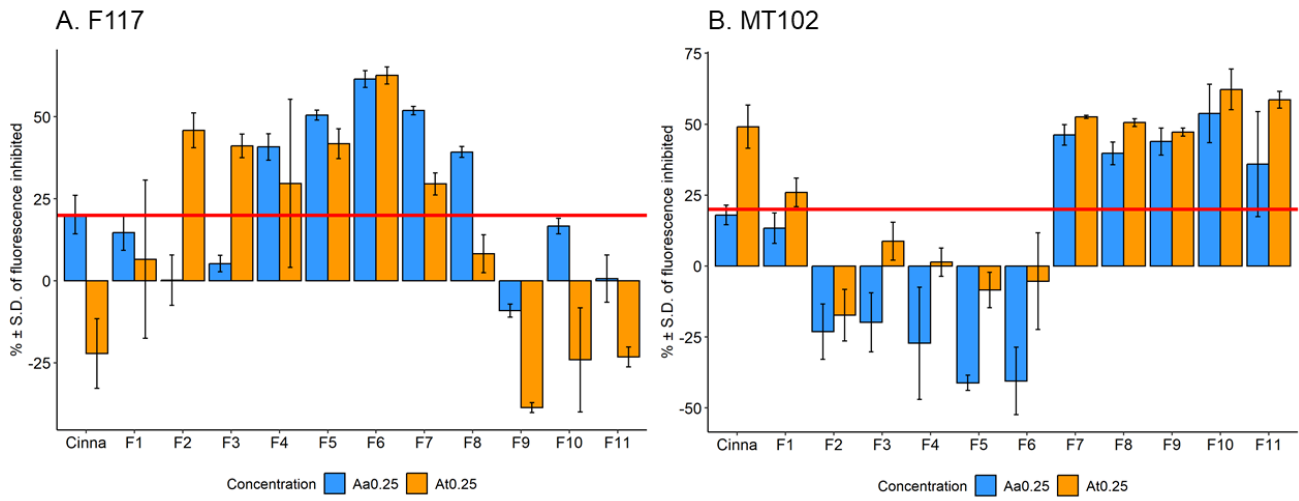


Figure 5: % ± S.D. of inhibited fluorescence by fractions of *A. taxiformis* (At) and *A. armata* (Aa) at 0.25 mg/mL on biosensors F117 (A) and MT102 (B). The red horizontal line represents the threshold (20%) to validate an anti-QS activity.

We also evaluated the effect of a dilution (1:9) of the fractions (resulting in a concentration of 0.025 mg/mL) on the anti-QS activity on biosensor F117 (**Figure 6A, B**). For *A. armata*'s fractions F3 to F6 at 0.025 mg/mL (**Figure 6A**), there was a decrease in anti-QS activity compared to those at 0.25 mg/mL (**Figure 5A**). Except for F6, this was less marked for *A. taxiformis*. Interestingly, for both species, fraction F9 which did not show any anti-QS activity and tended to promote fluorescence at 0.25 mg/mL, exhibited a strong inhibition of F117 fluorescence at 0.025 mg/mL (**Figure 6A, B**). A similar observation can be made for F10 with an increase in F117 fluorescence inhibition at 0.025 mg/mL but, for *A. taxiformis*, without reaching the 20% threshold (**Figure 6A, B**).

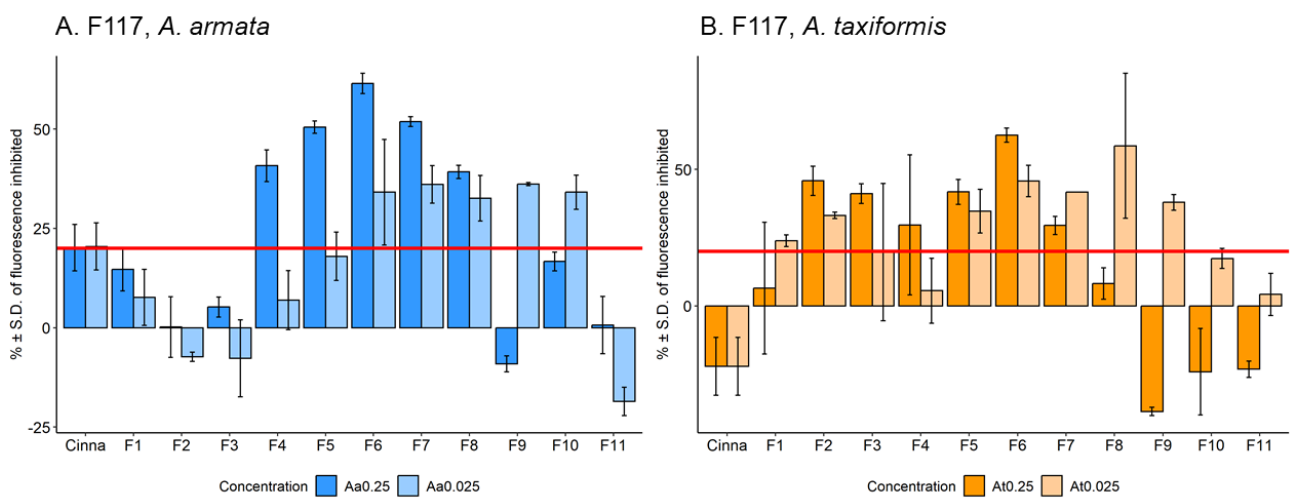


Figure 6: % ± S.D. of inhibited fluorescence by fractions of *A. taxiformis* (At) and *A. armata* (Aa) at 0.25 mg/mL and 0.025 mg/mL on biosensor F117. The red horizontal line represents the threshold (20%) to validate an anti-QS activity.

2.4.3 LC-HRMS analysis of the fractions

All fractions were analysed with LC-HRMS. In fraction F1 the presence of an intense ion corresponding to dibromoacetic acid (monoisotopic m/z 170.8454 [$M-H^-$], most intense m/z 172.8432 [$M-H^-$]) was detected. In addition, fraction F1 also contained an ion that was possibly floridoside (monoisotopic m/z 253.0936 [$M-H^-$]). This was confirmed with the 1H -NMR spectrum of F1 in which we detected peaks at δ_H 4.95 ppm characteristic of floridoside. We also detected two triplets at δ_H 2.95 and 3.75 ppm that corresponded to methylene protons of isethionic acid (**Figure 7**).

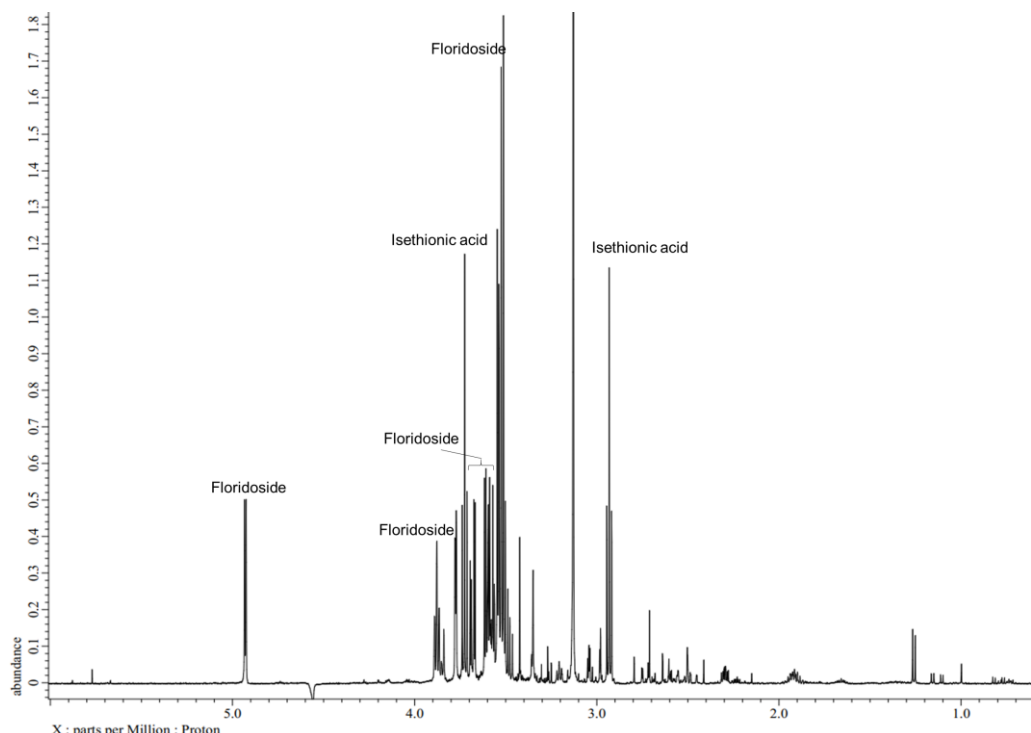
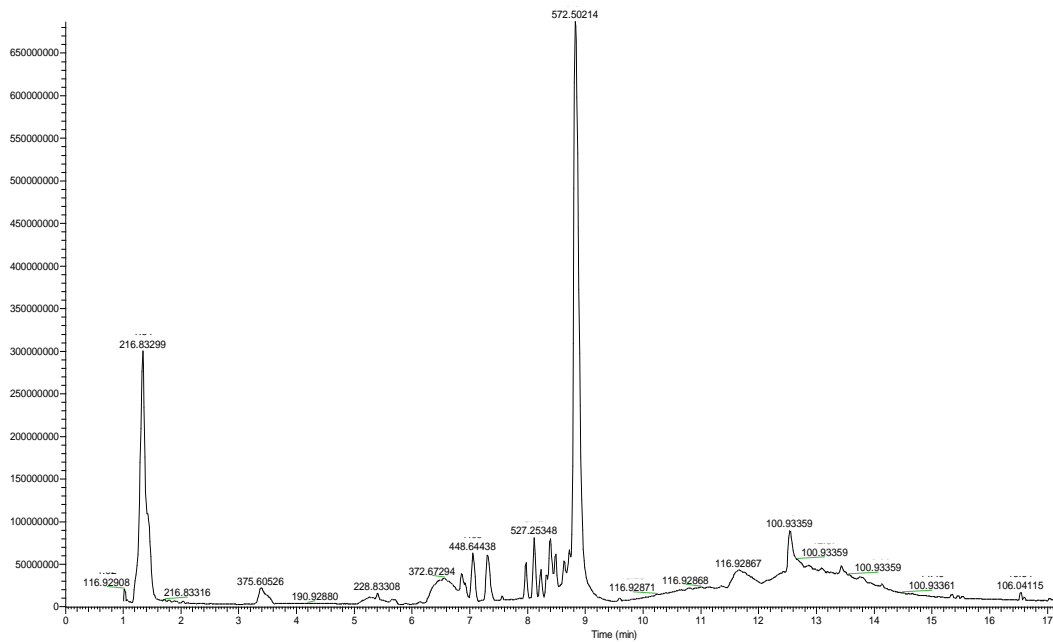


Figure 7: Annotated chromatograms of Fraction F1 (100% H₂O) of *A. armata* with the 1H -NMR spectrometer (0-5.5 ppm).

The highly active fractions F6 (40% H₂O-MeOH) against CV026 and F117 contained two intense ions with monoisotopic m/z of 488.5982 and 566.5085 [$M-H^-$] whose molecular formulas were determined as C₅H₃Br₅O₂ and C₅H₂Br₆O₂ in relation to exact mass, isotopic clusters and literature comparison (Parchemin et al., 2023, minor revision; Thapa et al., 2020). Fractions F9 to F11 mainly contained polar lipids. The molecule C₁₄H₂₇O₅S reported in Jha et al. (2013) was not detected in any of the fractions.

A. A. armata

RT: 0.00 - 19.01 SM: 3B



B. A. taxiformis

RT: 0.00 - 17.01 SM: 3B

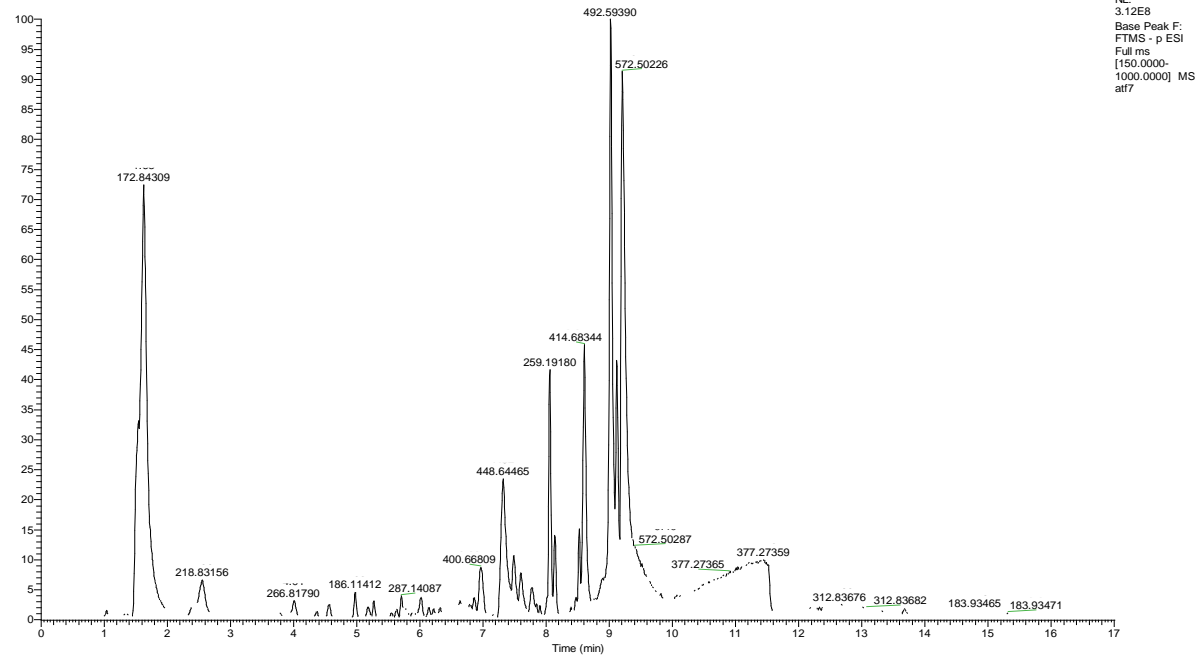


Figure 8: Chromatograms of the most active fraction “F6” (40% H₂O-MeOH) of *A. armata* (A) and *A. taxiformis* (B) analysed with the UHPLC-ESI-HRMS spectrometer.

2.4.4 Discussion

The anti-quorum sensing activity of *A. taxiformis* against *C. violaceum* has been previously reported (Jha et al., 2013) but the potential responsible molecule(s) identified by Jha et al. (2013) has not been isolated, and its activity needs to be confirmed. To date, there has been no exploration of the anti-QS potential of *A. armata* which is known for its various antibacterial and antifouling activities (Pinteus et al., 2015, 2018). In this study, fractions from both species showed predominantly bactericidal activities, accompanied by evidences of QS inhibition. Our fractionation method did not allow us to distinguish between bactericidal and anti-QS active molecules, as we observed large bactericidal zones around the impregnated discs, particularly for the fractions eluted with 40 (F6) and 30 % (F7) of H₂O (60 and 70 % of MeOH). These results are similar to those of Jha and collaborators, who also used a C18 SPE cartridge and a MeOH gradient to fractionate their extract and found their highest bactericidal activity in fractions eluted with 70 % and 80 % of methanol (Jha et al., 2013). However, they were able to separate the anti-QS activity that they found in the fraction eluted with 10% methanol. Further fractionation of the most active fractions and/or optimization of the concentrations used could potentially lead to the separation the two types of activity, as we showed that a dilution of some fractions against F117 resulted in different activities, suggesting a dose-dependent mode of action for these active compounds.

In previous study the active fraction corresponded to fraction eluted with 100 % H₂O (Jha et al., 2013). In our study, only the F1 fraction (eluted with the same percentage of solvent) from *A. taxiformis* extract showed bactericidal and anti-QS activity against CV026. Against F117 and MT102, this same fraction from both species was only slightly active without reaching the 20 % threshold except for *A. taxiformis* at low concentration (0.025 mg/mL). We therefore observed variability in activity between the two species for this fraction. The molecule C₁₄H₂₇O₅S reported in Jha et al. (2013) was not detected in any of the fractions. However, using LC-HRMS and ¹H-NMR analysis we detected, in F1, the presence of floridoside and isethionic acid. A study reported the anti-QS activity of a mixture of these two molecules isolated from another red algal species (Liu et al., 2008). Thus, floridoside and isethionic acid may be responsible for the slight activity observed in F1 but also in previous studies (Jha et al., 2013). Liu et al. (2008) also showed that a variation in the content of one of the two molecules had an impact on the activity. We have previously reported variation in the abundance of isethionic acid abundance between *A. armata* and *A. taxiformis* but not in floridoside (Parchemin et al., 2023, minor revision). The variation in their content in the two species may be a first

explanation in the variation of the activities observed for F1 in this study. Their dosage would support this hypothesis.

Anti-QS activity was found in different fractions against F117 and MT102. The QS of these biosensors is dependent on AHLs with different chain lengths (Andersen et al., 2001; Riedel et al., 2001). Our results suggest that different molecules may interact with different receptors and thereby inhibit the QS of various bacterial species. The most active fractions against F117 were F4 to F8. These fractions contained halogenated molecules such as C₅H₃Br₅O₂ and C₅H₂Br₆O₂. *Delisea pulchra*, another red algae, produces halogenated furanones with anti-QS activity (Dworjanyn et al., 1999; Maximilien et al., 1998). Therefore, halogenated molecules produced by *Asparagopsis* spp. may not only have bactericidal activity (Greff et al., 2014; Paul et al., 2006a; Reverter et al., 2022) but also disrupt bacterial communication. Finally, against MT102, the most active fractions were F7 to F11. Fractions 9 and 10 were also active at lower concentrations against F117. These fractions are mainly composed of polar lipids (such as hydroxyl fatty acids and sulfo lipids) as previously reported (Parchemin et al., 2023, minor revision). The role of fatty acids produced by algae in defense against bacteria has already been documented. They can inhibit growth but also act on QS, as demonstrated for palmitoleic and myristoleic acids against *Acinetobacter baumannii* and lyngbyoic acid isolated from a marine cyanobacterium against *Pseudomonas aeruginosa* (Kwan et al., 2011; Nicol et al., 2018; Zhou et al., 2016, 2017).

In conclusion, this study demonstrated that *A. taxiformis* and *A. armata* exhibit similar anti-QS activities against three different biosensors. These activities are probably linked to the production of different types of molecules as activity was found in fractions with molecules of various polarities. These molecules may be produced by the algae itself and/or by its microbiota.

3. Ce qu'il faut retenir

Ce chapitre rapporte l'étude de l'activité antibactérienne et anti-quorum sensing d'extraits et de fractions d'*A. armata* et d'*A. taxiformis* collectés respectivement à Banyuls-sur-Mer et à Moorea (Polynésie Française) contre *Chromobacterium violaceum* CV026 (la même souche sur celle utilisée dans l'étude reportant l'activité anti-QS d'*A. taxiformis* (Jha et al., 2013), *Pseudomonas putida* F117 et *Escherichia coli* MT102.

Les résultats majeurs sont :

- (1) Les extraits bruts et les fractions des deux espèces présentent des activités bactéricide et anti-QS globalement similaires.
- (2) Les extraits bruts et les fractions ont une activité bactéricide importante sur CV026 qui paraît masquer l'activité anti-QS. Aucune fraction n'a présenté uniquement de l'activité anti-QS.
- (3) Les fractions d'algues, testées sur F117 et MT102, ont une activité anti-QS qui inhibe l'émission de fluorescence. Les fractions anti-QS actives sur F117 ne sont pas les mêmes que celles qui sont actives sur MT102.
- (4) L'activité anti-QS de certaines fractions d'algues testées à 0.25 mg/mL et à 0.025 mg/mL sur F117 diffère selon la concentration.
- (5) Les fractions présentant une activité bactéricide sur CV026 et une activité anti-QS sur F117 correspondent aux fractions pour lesquelles les ions majoritaires détectées en LC-MS correspondent aux molécules aux formules brutes C₅H₃Br₅O₂ et C₅H₂Br₆O. Les fractions avec une activité anti-QS contre MT102 contiennent majoritairement des lipides polaires.

Chapitre III : Activités antibactériennes et cycle de vie d'*Asparagopsis armata* : implications du métabolome et du microbiote

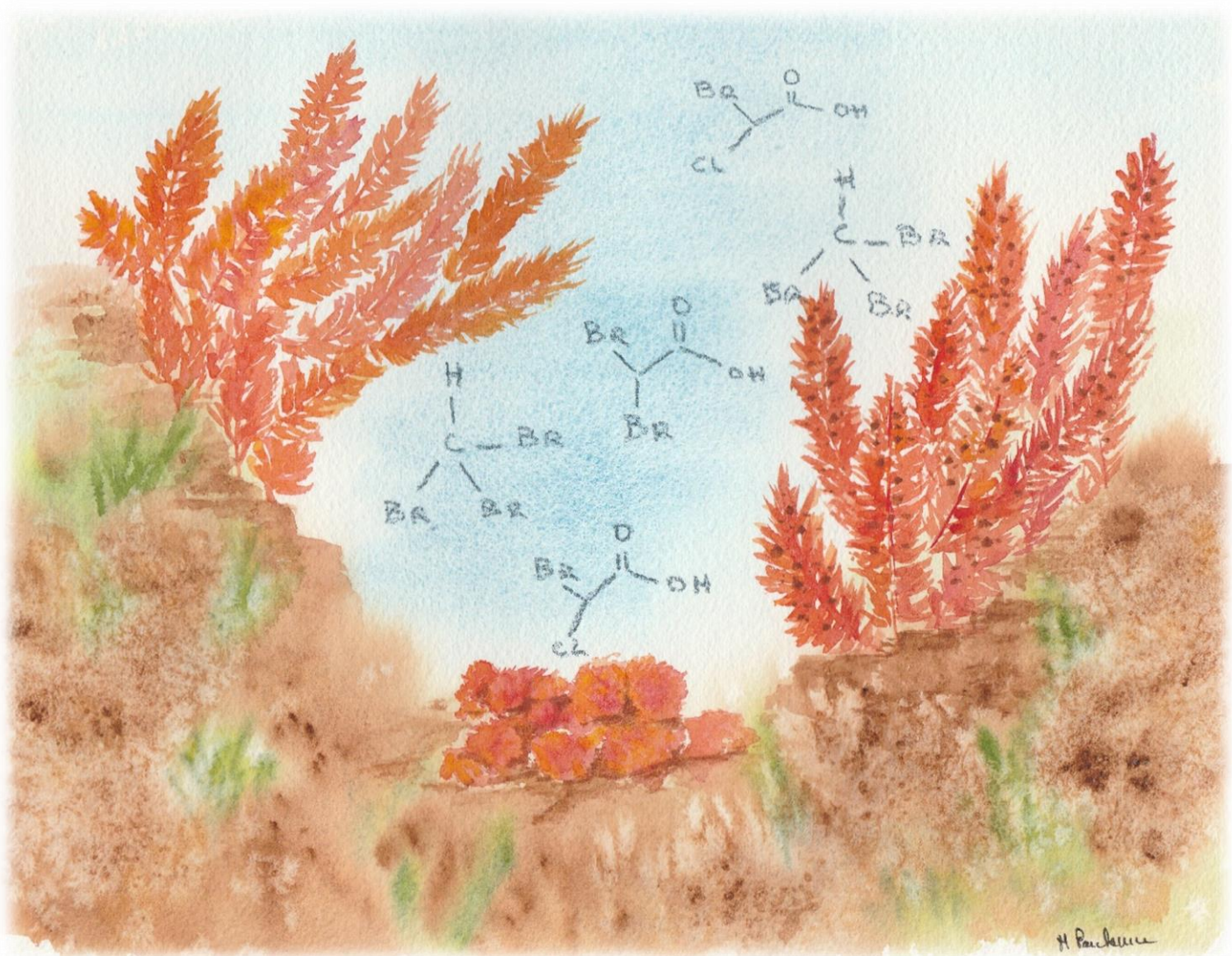


Illustration à l'aquarelle des différents stades du cycle de vie réalisée par Michèle Parchemin.

1. Avant propos

Antibacterial Activities and Life Cycle Stages of *Asparagopsis armata*: Implications of the Metabolome and Microbiome

Christelle Parchemin, Delphine Raviglione, Anouar Mejait, Camille Clerissi, Pierre Sasal,
Elisabeth Faliex, Nathalie Tapissier-Bontemps

Publication

L'article cité ci-après a été publié dans le journal "Marine Drugs" dans la Special Issue « *Marine Metabolomics and Microbiomics for Investigations of Secondary Metabolites* » le 17/06/2023.

Parchemin, C., Raviglione, D., Mejait, A., Sasal, P., Faliex, E., Clerissi, C., and Tapissier-Bontemps, N., (2023). Antibacterial Activities and Life Cycle Stages of *Asparagopsis armata*: Implications of the Metabolome and Microbiome. *Marine Drugs*, 21, 363.
<https://doi.org/10.3390/md21060363> IF : 6.085

Contexte

Les algues du genre *Asparagopsis* ont un cycle de vie hétéromorphe trigénétique haplodiplophasique. Comme abordé dans l'**Etat de l'art**, les extraits des stades gamétophytes et tétrasporophytes, qui sont les deux stades macroscopiques de ce cycle de vie, sont décrits comme actifs contre une grande diversité de bactéries. Ces deux stades pourraient donc être valorisés en industrie. Cependant, les extraits du gamétophyte ont été décrits comme plus actifs que ceux du tétrasporophyte. Il est donc nécessaire de mieux caractériser les différences de composition chimique à l'origine des différences d'activités biologiques observées. Des études ont décris, par GC-MS, des variations d'abondance de certaines molécules halogénées ciblées (bromoforme et acide dibromoacétique) entre les stades gamétophyte et térasporophyte. Ces variations pourraient être liées à des différences d'expression de gènes conduisant à la production différentielle de molécules halogénées, ou encore à des différences dans la composition des communautés microbiennes entre les différents stades du cycle de vie de l'algue. En effet, il est aujourd'hui largement admis que le microbiote a un impact sur la

composition chimique de l’algue et inversement (Egan et al., 2013). L’objectif de cette seconde étude est d’explorer à la fois les variations du métabolome, des activités antibactériennes mais aussi de la composition bactérienne au cours du cycle de vie d’*A. armata*, dont les différents stades du cycle de vie sont abondants à Banyuls-sur-Mer, et ainsi d’étudier les interactions possibles entre les différents stades de vie de cette algue et leur microbiote.

Méthodologie générale

Des échantillons correspondant à trois stades (gamétophyte, gamétophyte avec cystocarpes développés, et tétrasporophyte) du cycle de vie d’*A. armata* ont été collectés à Banyuls-sur-Mer en mai 2022. Une partie de chaque type d’échantillon a été lyophilisée pour l’analyse métabolomique et l’autre conservée à -80°C pour l’analyse des communautés bactériennes par métabarcoding. Une extraction biphasique des échantillons a été réalisée et les extraits apolaires ont été analysés par LC-HRMS selon la méthodologie décrite dans le **Chapitre I**. Des analyses statistiques multi- et univariées ont été effectuées pour évaluer les différences du métabolome entre les stades et identifier des marqueurs chimiques. L’activité antibactérienne des extraits des trois stades a été évaluée en boîte de pétri. Un fractionnement bioguidé a ensuite été réalisé pour isoler les molécules responsables de l’activité. Les ADN bactériens présents dans les échantillons d’algues ont été extraits et séquencés avec la méthode Illumina. Des analyses statistiques ont été effectuées pour identifier des différences dans la composition des communautés bactériennes entre les stades de vie de l’algue. Enfin, une analyse multi-omique a été réalisée afin d’étudier les éventuelles corrélations entre métabolites et bactéries.

Contribution des auteurs

Dans ce chapitre, j’ai réalisé la collecte des échantillons à Banyuls-sur-Mer ainsi que les extractions pour l’analyse métabolomique. L’extraction d’ADN pour l’analyse métabarcoding a été réalisée par Anouar Mejait. Comme pour le **Chapitre I**, j’ai réalisé les analyses de métabolomique sur la plateforme Bio2mar Métabolites Secondaires Xénobiotiques Métabolomique Environnementale (MSXM) à l’Université de Perpignan *Via Domitia* (<https://bio2mar-msxm.univ-perp.fr/>) sous la supervision de Delphine Raviglione. La technique d’analyse par LC-HRMS, développée avec Delphine Raviglione et Nathalie Tapissier-Bontemps est la même que celle utilisée dans le **Chapitre I** et n’a donc pas nécessité davantage de développement. J’ai réalisé le pré-traitement des données de métabolomique. Le séquençage d’ADN a été « sous-traité » au Canada. Le pré-traitement des données de métabarcoding a été réalisé par Camille Clerissi. J’ai ensuite réalisé l’ensemble des analyses statistiques et des

interprétations biologiques avec l'appui des différents auteurs. Pierre Sasal, Elisabeth Faliex, Nathalie Tapissier-Bontemps ont participé à la conceptualisation de l'étude et à l'exploitation des résultats.

Disponibilité des données

Les données brutes issues de l'analyse LC-HRMS ont été déposées sur la plateforme MassIVE sous le numéro MSV000091636 et seront rendues publiques dès publication de l'article. Les données brutes de métacodage des séquences sont disponibles dans la base de données Sequence Read Archive (BioProject ID PRJNA948342).

Annexes

Les « Supplementary Materials » relatifs à ce chapitre débutent à la page **351** de ce manuscrit (Annexes ; 3. Annexe Chapitre III).

2. Article

Antibacterial Activities and Life Cycle Stages of *Asparagopsis armata*: Implications of the Metabolome and Microbiome

Christelle Parchemin^{*,1,2}, Delphine Raviglione¹, Anouar Mejait¹, Pierre Sasal¹, Elisabeth Faliex², Camille Clerissi¹, Nathalie Tapissier-Bontemps¹

¹ Centre de Recherches Insulaires et Observatoire de l'Environnement (CRIODE), Ecole Pratique des Hautes Etudes (EPHE), Université PSL, UPVD, CNRS, UAR 3278, 52 Av. Paul Alduy, 66860 Perpignan CEDEX, France

² CEntre de Formation et de Recherche sur les Environnements Méditerranéens (CEFREM), UMR 5110 UPVD-CNRS, Université de Perpignan - Via Domitia, 52 Av. Paul Alduy, 66860 Perpignan CEDEX, France

2.1 Abstract

The red alga *Asparagopsis armata* is a species with a haplodiplophasic life cycle alternating between morphologically distinct stages. The species is known for its various biological activities linked to the production of halogenated compounds, which are described as having several roles for the algae such as the control of epiphytic bacterial communities. Several studies have reported differences in targeted halogenated compounds (using gas chromatography–mass spectrometry analysis (GC-MS)) and antibacterial activities between the tetrasporophyte and the gametophyte stages. To enlarge this picture, we analysed the metabolome (using liquid chromatography–mass spectrometry (LC-MS)), the antibacterial activity and the bacterial communities associated with several stages of the life cycle of *A. armata*: gametophytes, tetrasporophytes and female gametophytes with developed cystocarps. Our results revealed that the relative abundance of several halogenated molecules including dibromoacetic acid and some more halogenated molecules fluctuated depending on the different stages of the algae. The antibacterial activity of the tetrasporophyte extract was significantly higher than that of the extracts of the other two stages. Several highly halogenated compounds, which discriminate algal stages, were identified as candidate molecules responsible for the observed variation in antibacterial activity. The tetrasporophyte also harboured a significantly higher specific bacterial diversity, which is associated with a different bacterial community composition than the other two stages. This study provides elements that could help in understanding the processes that take place throughout the life cycle of *A. armata* with different potential energy investments between the development of reproductive elements, the production of halogenated molecules and the dynamics of bacterial communities.

Keywords: red algae, bacterial diversity, halogenated secondary metabolites, metabolomics, metabarcoding, multi-omics

2.2 Introduction

Unlike terrestrial plants, marine algae are known for their ability to produce halogenated compounds linked to the particular availability of bromine, iodine and chlorine in marine environments (Kladi et al., 2004; Paul and Pohnert, 2011). Particularly, a high number of halogenated compounds have been isolated from red algae that harbour biosynthetic pathways for their production (Kladi et al., 2004). This production could be related to various ecological roles including chemical defences against grazing or regulation of bacterial communities (also named microbiota) (Egan et al., 2013; Kladi et al., 2004; Paul and Pohnert, 2011). For example, halogenated furanones produced by *Delisea pulchra* (Dworjanyn et al., 1999; Maximilien et al., 1998), bromoform and dibromoacetic acid produced by *Asparagopsis armata* (Paul et al., 2006a), polyhalogenated 2-heptanoone produced by *Bonnemaisonia hamifera* (Nylund et al., 2008), and bromophycollides produced by *Callophyicus serratus* (Lane et al., 2009) were reported as factors constraining bacterial communities.

Amongst the red algae known to produce halogenated compounds, those of the genus *Asparagopsis* have been extensively studied leading to the identification of a wide variety of these molecules, mainly using gas chromatography-mass spectrometry (GC-MS) (Burreson et al., 1975, 1976; McConnell and Fenical, 1977; Paul et al., 2006a; Woolard et al., 1976, 1979) and more recently liquid chromatography-mass spectrometry (LC-MS) (Pinto et al., 2022; Thapa et al., 2020). Both species of this genus (*A. armata* and *A. taxiformis*) have a heteromorphic haplodiplophasic life cycle with different alternating stages: the plumose male or female gametophyte stage, the microscopic carposporophyte stage that develops on the female gametophyte and is protected inside gametophyte tissues called cystocarps, and the filamentous tetrasporophyte stage. Based on results from GC-MS analyses, several studies have reported differences in the composition of halogenated molecules, between the tetrasporophyte and the gametophyte stages of *A. armata* (Bruneau et al., 1978; Paul et al., 2006a; Vergés et al., 2008). Thus, Paul et al. (2006a) demonstrated that the levels of bromoform, dibromoacetic acid and bromochloroacetic acid were higher in the tetrasporophytes than in the gametophytes. Another study also reported that female gametophytes exhibited a higher abundance of bromoform than male gametophytes, particularly in the cell wall of the cystocarps (Vergés et al., 2008). These authors suggested an ecological role of these compounds via their potential to prevent grazing by herbivores. Indeed, it has been shown that the sea slug *Aplysia parvula*

avoided consuming the female gametophytes of *A. armata* and, particularly, the cystocarps containing carposporophytes (Vergés et al., 2008). It has also been shown that halogenated compounds produced by *A. armata* were involved in the control of epiphytic bacterial densities at the surface of this algae (Paul et al., 2006a). Several molecules isolated from this algae, such as bromoform and the recently described mahorones, have been reported as having antibacterial activities (Greff et al., 2014; Paul et al., 2006a). To our knowledge, only two studies concerning the antibacterial activity of several algae has included different stages of the *A. armata* life cycle. Both studies demonstrated high antibacterial activity for both stages and a significantly higher antibacterial activity for the extract obtained from the gametophyte than for the tetrasporophyte (Bansemir et al., 2006; Salvador et al., 2007). However, the authors did not carry out any analyses of the chemical composition. These studies clearly suggested possible interactions between bacterial communities and the halogenated molecules produced by the algae. In other words, we can hypothesise that the variation in the composition of halogenated molecules between the different stages of the algae could induce a variation in the composition of the bacterial communities. To our knowledge, only one study has focused on the differences in bacterial assemblages between different stages of the same algal species. It was conducted on gametophytes and sporophytes of several brown algal species of the genus *Mastocarpus* and highlighted distinct bacterial communities between the two stages (Lemay et al., 2018). Morphology and chemical composition were two factors put forward by the authors to explain the observed variation, although no chemical investigations have been conducted to confirm this hypothesis (Lemay et al., 2018). Regarding the characterisation of bacterial communities associated with *A. armata*, few data are available to date. For example, Aires et al. (2016) described bacterial communities associated with *A. armata* and *A. taxiformis* using metabarcoding and found that the two species harboured distinct bacterial communities, although they were collected at the same place. This study also highlighted functional genes associated with bacteria and particularly linked to production of secondary metabolites but not necessarily halogenated molecules, which could emphasize the role of microorganisms in the defence process of these algae (Aires et al., 2016). Another study reported the identification of bacteria associated with the gametophyte stage of *A. armata* and their antitumor and antibacterial activities (Horta et al., 2019).

In this context, the main objective of our study was to explore the composition of the metabolome and bacterial communities between the different stages of *A. armata* in order to provide elements that could help in understanding the processes that take place throughout the

life cycle of the algae. We used a metabolomics approach and a biphasic extraction focusing on apolar extracts that we previously reported as exhibiting antibacterial activity and containing high diversity of halogenated molecules (Parchemin et al., 2023). We also evaluated the variation of the antibacterial activity of algae extracts and used a bioguided fractionation combined with the calculation of the Pearson correlation to identify bioactive compounds. Then, we studied bacterial communities associated with the different stages of the life cycle of this algal species. Finally, we used multiblock statistical tools to evaluate correlations between metabolome and microbiota in order to highlight potential roles of the metabolites produced by the algae for the control of bacterial communities or, conversely, the role of bacteria in the production of bioactive metabolites.

2.3 Materials and methods

2.3.1 Chemicals

For sample preparation, methyl-tert-butyl-ether (MTBE) of HPLC grade was purchased from Honeywell Riedel de Haen™ (Germany), and methanol (MeOH) of HPLC grade, dichloromethane (DCM) and water of HPLC grade were purchased from VWR™ (Fontenay-sous-Bois, France). Water used for fractionation was ultra-pure water (18.2 MΩ.m, total organic carbon <10 ppb and <10 CFU/mL) obtained by purifying water with a PURELAB Chorus 1 system (ELGA LabWater, Lane End, HP14, UK). For UHPLC-HRMS analysis, ultra-pure water was used, and acetonitrile LC-MS grade was purchased from Carlo Erba (Val de Reuil, France). Formic acid 99% (for LC-MS analysis) was obtained from Carlo Erba (Val de Reuil, France).

2.3.2 Biological materials

For metabolomics, metabarcoding analyses and evaluation of antibacterial activity, five replicates for each of the three stages of the algal life cycle (**Supplementary method 1**) were sampled in May 2022 in the natural marine reserve in Banyuls-sur-Mer, France (lat. 42.482230°; long. 3.137175°) where the species is invasive. These stages include, samples of tetrasporophyte (T), and two sample types of gametophyte, without cystocarps (G) and with developed cystocarps (GC) (**Supplementary method 1**). Physically contiguous algae were pooled and considered to be one single individual while individuals separated by at least one meter from others are considered as different individuals. Five individuals (biological replicates) for each algal life cycle were collected and processed separately. Immediately after

collection, algae were cleaned of epiphytes. One part was stored at -80°C for metabarcoding analysis, and the other part was freeze-dried and stored at -20°C until subsequent analyses.

Due to a limited amount of algal material collected in 2022, the bioguided fractionation was performed on a pool of *A. armata* (gametophyte) samples collected between February and May 2021 in Banyuls-sur-Mer (lat. 42.482230° ; long. 3.137175°) and processed as indicated above

2.3.3 Algal extraction

Freeze-dried algae were ground to obtain a homogeneous powder. For metabolomics, samples were extracted as described in Parchemin et al. (2023). A biphasic extraction method was used. Briefly, 50 mg of each dried and crushed algae sample (5 replicates for each algal stage) was extracted with a mixture of MeOH and MTBE and vortexed. Then, H₂O was added, and the whole solution was vortexed. Extraction was performed in an ultrasonic bath, and the final mixture was centrifuged to obtain two phases. Equal volume of apolar phase was collected for each sample. Solvent was evaporated with a centrifugal vacuum evaporator GENEVAC EZ-2™ (SP Scientific, Warminster, PA, USA), and the dried samples were stored at -20°C until LCMS analyses. Quality control (QC) samples were prepared by pooling equal volume from all extracts. For the antibacterial activity assays only 3 replicates for each algal stages were extracted using the same biphasic extraction but using 250 mg of algae in order to obtain sufficient material for the assays.

Finally, for bioguided fractionation and to facilitate the extraction of larger quantities of algae, *A. armata* powder (100 g dry weight) was extracted by three successive macerations in MeOH:DCM (1:1).

2.3.4 Metabolomics

2.3.4.1 Chemical Analyses

Extract were analysed following the protocol described in Parchemin et al. (2023). Apolar extracts were solubilised in 1 mL MeOH. LC-HRMS analyses were performed with a Vanquish UHPLC system from ThermoScientific (MA, USA) equipped with a Q Exactive™ Plus mass spectrometer with an electrospray ionization source. Metabolite separation were performed on a C18 UHPLC column (Luna® Omega 1.6 μm Polar C18 100 A LC Column 100 x 2.1 mm, Phenomenex, CA, USA). The mobile phase consisted in a mixture of H₂O + 0.1% formic acid (solvent A) and acetonitrile + 0.1% formic acid (solvent B). The flow rate was 400 $\mu\text{L}/\text{min}$. The program was set up at 2% B during 1 min, followed by a linear gradient up to 100% B for

10 min, then maintained for 5 min in isocratic mode. The analysis was followed by a return to initial conditions for column equilibration for 4 min for a total runtime of 20 min. Extracts were randomly injected, alternating the quality control sample injections every 5 samples.

The mass spectrometer analyser parameters were set as follows: sheath gas flow rate, auxiliary gas and sweep gas flow rate set to 45 arbitrary units (a.u.), 15 a.u. and 2 a.u., respectively; capillary and gas temperature were set to 320 °C and 250 °C, respectively; the S-lens RF level and spray voltage were set to 60 V and 3.20 kV, respectively. MS/MS acquisition consisted of one full scan mass spectrum and 5 data-dependent MS/MS scans. Parameters for the full MS experiments were set as follows: the resolution was 70,000, the automatic gain control was 3E6 ions, the maximum injection time (IT) was 100 ms, and a scan mass window of 100–1500 m/z was used. For the dd-MS2/dd-SIM experiments, the resolution was 17,500, AGC target was 1e5 ions, and maximum IT was 50 ms. For each MS/MS scan, the top 5 most intense ions, taking into account an isolation window of 4.0 m/z and a fixed first mass of 50.0 m/z , were fragmented. Finally, normalized collision energy™ (NCE) ranged between 25,35 and 45 eV.

2.3.4.2 Data treatment

Data acquisitions were performed using Xcalibur 4.1.31.9 (Thermo Fisher Scientific). Raw data were converted to mzML files with MSconvert (version 3.0, from Proteowizard library). mzML files were uploaded and processed using the Galaxy web platform (version 3.3) (Giacomoni et al., 2015; Guitton et al., 2017). The workflow used for data pre-processing and used parameters are published on the Galaxy Workflow4Metabolomics platform at: https://workflow4metabolomics.usegalaxy.fr/u/christelle_parchemin/w/workflowparcheminal_gae and are available in the **Supplementary Method 2**. Briefly, the pre-processing consisted in a chromatographic peak detection (Galaxy Version 3.12+galaxy0) followed by a peak grouping, a loess/non-linear “PeakGroups” retention time adjustment, a peak filling and “CAMERA” peak annotation. A matrix of features with peak intensity, m/z value and retention time was generated. A clean-up step was performed in order to eliminate all features that are significantly detected in blanks. Then, an “intra-batch” signal correction was applied using the “Batch correction” function with a “loess” regression model (van Der Kloet et al., 2009). This step was followed by a second clean-up according to feature's CV in pool QC injections (Thévenot et al., 2015). Finally, redundancies due to isotopes were manually eliminated (only monoisotopic mass was kept). For identification, most probable molecular formula was determined using Sirius (v4.9.15 (Böcker et al., 2009; Böcker and Dürkop, 2016; Djoumbou

Feunang et al., 2016; Dürkop et al., 2015, 2019, 2021; Hoffmann et al., 2021; Kim et al., 2021)), characteristics isotopic clusters, MS/MS spectra and comparison with literature.

2.3.4.3 Multivariate and statistical analyses

Statistical analyses were performed using RStudio environment v2022.02.3 (R v4.2.0) and MetaboAnalyst 5.0 (Pang et al., 2021). Autoscaling was applied on data. Principal Component Analysis (PCA) (`prcomp {stats}`) was used to evaluate the global dispersion of algae metabolome. Permutation tests (`Adonis 2 {VEGAN}` and `pairwise.perm.manova {RVAideMemoire }`) were used to test the discrimination between groups. PLS-DA (`plsda {mixOmics}`) (Rohart et al., 2017)) was used for detection of features contributing the most to the model and putative identification of the features was performed as mentioned in “4.4.2 Data treatment”. Permutation test based on cross model validation (`MVA.test` and `pairwise.MVA.test {RVAideMemoire}`) was applied to validate PLS-DA model and to test the significance of the discriminations according to defined factors. Kruskall-Wallis followed by Nemenyi Post Hoc were used (`{Stats}{PMCMRplus}`) to test the significance of the differences of VIP features intensity among groups. Dendograms and Heatmaps (distance measure: Euclidean, clustering algorithm: Ward) were drawn on MetaboAnalyst 5.0 (Pang et al., 2021) to evaluate the grouping of samples and variables.

2.3.5 Antibacterial activity

Apolar phase antibacterial activity was tested on several bacterial species. The recent promising studies on the potential for aquaculture of *A. armata* and *A. taxiformis* (Castanho et al., 2017; Manilal et al., 2012; Reverter et al., 2016; Thépot et al., 2022, 2021a, 2021b) led us to select fish pathogenic bacteria for our tests: *Edwardsiella anguillarum* (DSMZ-27202, “Ea”, Gram -), *Lactococcus garvieae* (CIP102507T, “Lg”, Gram +), *Tenacibaculum maritimum* (CIP103528T, “Tm”, Gram -), *Vibrio anguillarum* (CIP63.36T, “Va”, Gram -), *V. harveyi* (CIP103192T, “Vh”, Gram -) and *Yersina ruckeri* (CIP82.80T, “Yr”, Gram -). They were maintained at -80°C respectively in liquid media (**Supplementary method 3**) supplemented with 30% (v/v) glycerol. Prior to use, all bacteria were revived from glycerol stocks and grown for 24 h at 26 °C on agar plates (except *Lg*, which grows at 37°C). An isolated colony was then cultivated in liquid medium for 12 h. Agar plates were flooded with fresh bacterial broth ($DO_{620nm} = 0.1$) and were set aside to dry. Assays of extracts were performed using the disc diffusion method (Bauer, 1966). Briefly, 10 µL of extract was placed onto a 0.6 cm sterile paper disc (final concentration: 0.1 mg/disc). Discs were placed under the hood to allow evaporation

of the solvent. Following evaporation, the discs were placed onto the surface of the inoculated agar. The plates were incubated for 24 h at 26 °C or 37 °C. Discs soaked with antibiotics (**Supplementary method 3**) were used as positive control, and MeOH was used as negative control. Areas of inhibited bacterial growth were observed as clear halos (zones) around the discs. The diameter of the zone of bacterial growth inhibition was measured, and each reported measurement including the size of the disc. Kruskal–Wallis tests followed by Nemenyi post hoc tests were used to test the significance of the differences in antibacterial activity among groups.

For faster testing of a larger number of samples, fractions from the bioguided fractionation (see “2.3.6”) were assayed in 96-well microplates and were only tested against *E. anguillarum*. Fractions were first solubilised at a concentration of 20 mg/mL in 100% DMSO and then diluted in sterilised water to reach a concentration of 5 mg/mL. Next, 180 µL of fresh 12 hours’ bacterial culture ($OD_{620\text{ nm}} = 0.1$) was deposited in the well, to which 20 µL of fraction was added (final concentration of fraction 0.5 mg/mL and 2.5% of DMSO). Bacterial culture, medium, and solvent (DMSO) were also deposited in wells to serve as controls. After 24 h of growth, optical density at 620 nm was measured. Percentage of growth inhibition was calculated as follows: $((OD_{\text{bacteria+solvent}} - OD_{\text{medium}}) - (OD_{\text{bacteria+fraction}} - OD_{\text{medium}})) / (OD_{\text{bacteria+solvent}} - OD_{\text{medium}}) \times 100$.

2.3.6 Bioguided fractionation and identification of a candidate molecule responsible for the antibacterial activity

Bioguided fractionation was performed on 100 g (dry weight) samples of *A. armata* gametophytes to obtain 17.6 g of crude extracts via three successive macerations of algal powder in MeOH:DCM (1:1). Then, each crude extract was fractionated by flash chromatography under vacuum on a C-18 pre-packed column (45 g) (Interchim, puriflash IR 60, C18 50 UM, Montluçon, France) using a step gradient of 100% H₂O, 90% H₂O-MeOH, 80% H₂O-MeOH, 70% H₂O-MeOH, 60% H₂O-MeOH, 30% H₂O-MeOH, 20% H₂O-MeOH, 10% H₂O-MeOH, 100MeOH and 100EtoAc to create 11 fractions. The resulting fractions were evaporated, weighed and re-suspended in MeOH at the concentration to be tested and assayed for antibacterial activity. The most active fractions were combined and further fractionated using an HPLC (Waters 1525) coupled to a UV detector (Waters 2487) set to 220 and 330 nm. Metabolite separations were performed on a reverse-phase column (Luna® 5µ PFP (2) 100 A, LC Column 250 × 10 mm, Phenomenex, Torrance, USA). The mobile phase consisted of a mixture of H₂O + 0.1% formic acid (solvent A) and acetonitrile + 0.1% formic acid (solvent

B). The flow rate was 2.5 mL/min. The program was set up at 40% B for 4 min, followed by a linear gradient up to 100% B for 21 min and then maintained for 5 min in isocratic mode. The analysis was followed by a return to initial conditions for column equilibration for 8 min for a total runtime of 40 min. The fractionation resulted in 14 fractions. All fractions were assayed and analysed by LC-HRMS/MS as described in 4.4.1—Chemical Analyses. The peaks of the most intense ions on the chromatograms were manually integrated, and the correlation between the area of each peak and the activity measured in all fractions was assessed using a Pearson correlation {stats}.

2.3.7 Metabarcoding

2.3.7.1 DNA extraction, PCR and sequencing

DNA extractions were conducted on approximately 1 cm² of each of the five replicates of the three algal stages using the ZymoBIOMICS DNA Miniprep Kit (ref. D4300, ZYMO RESEARCH, California, USA) according to the manufacturer’s protocol. The 16S rRNA gene of bacterial communities was amplified and sequenced using the variable V3V4 loops (341F: 5'-CCTACGGGNGGCWGCAG-3'; 805R: 5'-GACTACHVGGGTATCTAATCC-3') (Klindworth et al., 2013). Paired-end sequencing (300 bp read length) was performed at the Dalhousie University (Integrated Microbiome Resource, Halifax, Nova Scotia, Canada) on the MiSeq system (Illumina) using the v3 chemistry according to the manufacturer’s protocol. Raw sequence data are available in the Sequence Read Archive database (BioProject ID PRJNA948342).

2.3.7.2 Sequence analyses

The DADA2 package (Callahan et al., 2016) (truncLen=c(260,230); maxN=0; maxEE=c(2,2); truncQ=2) was used to define amplicon sequence variant (ASVs), and computed taxonomic affiliations using Silva database (release 138, December 2019). The dataset was filtered for singletons. Rarefaction curves of species richness were computed using the {phyloseq} R package and the ggrare function. The rarefy_even_depth function was used to subsample datasets. The estimate_richness function was used to compute alpha diversity metrics (Chao1, Evenness and Shannon). Lastly, the tax_glm function was used to obtain abundances at different taxonomic ranks (from genus to phylum).

2.3.8 Multivariate and statistical analyses

We performed a non-parametric Kruskal–Wallis test (because normality of residuals was rejected (Shapiro test)) to compare alpha diversity metrics between life stages. We then computed pairwise comparisons between group levels (post hoc analyses) using the Nemenyi test (`kwAllPairsNemenyiTest {PMCMR plus}`). Principal coordinate analysis (hereafter named PCoA) (ordinate, `{phyloseq}`) was computed to describe compositions of amplicon sequence variants (ASV) between samples using Bray–Curtis dissimilarities. Average distance to median was studied with the `betadisper` function `{VEGAN}`. Permutational multivariate analysis of variance (hereafter named PERMANOVA) was used to compare bacterial composition between life stages using 999 permutations (`adonis2, {vegan}`). Then, pairwise comparisons between group levels were computed using pairwise PERMANOVA (`pairwise.perm.manova{RVAideMemoire}`). We used variant abundances with default parameters to predict functional profiles using Tax4Fun2 (Wemheuer et al., 2020). This analysis provided a table of relative KEGG ortholog (KO) abundances. The reconstruct tool from KEGG Mapper (available at <https://www.genome.jp/kegg/mapper/reconstruct.html>, accessed on 19 December 2022) was used to identify metabolite pathways associated with the predicted functions. We used an indicator value index (hereafter named IndVal) and 999 permutations (`indval, {labdsv}`) (Cáceres and Legendre, 2009) to identify specific taxa and functions associated with the different life stages. Heatmaps of relative abundances of specific ASVs and predicted functions were computed using the function `heatmap` (`{stats}`). For all analyses, the threshold significance level was set at 0.05.

2.3.9 Multi-omics

The correlation between the variation of the metabolome and the variation of the bacterial community composition of each of the five replicates of the three algal stages was calculated via a Mantel test using Spearman correlation and a permutation test (`mantel` and `vegdist` `{Vegan}`). Correlation between the two datasets was further explored using the multiblock model DIABLO from the MixOmics package (Singh et al., 2019). DIABLO allows the creation of a model that maximizes the covariance between datasets in order to identify the most correlated and discriminating variables according to a defined factor. Here, the model allows the identification of most correlated ASVs and metabolites involved in the discrimination of each algal stage. Optimal number of components (2) was determined with the `perf()` function. Number of metabolites (60) and ASVs (32) were determined using the `tune.block.splsda()`

function. Finally, the model was validated by a cross validation test (DIABLO.cv()), {RVAidememoire}).

2.4 Results

2.4.1 Variation of the metabolome of the three life stages

Metabolome variations were analysed via a metabolomics study on the apolar extracts of five replicates of each of the three following life stages of *A. armata*: the tretrasporophyte (T), the gametophyte (G) and the gametophyte with developed cystocarpes (GC) collected in Banyuls-sur-Mer where the species is invasive. After data processing and filtering, the matrix obtained from the LC-ESI-HRMS analysis included 261 features. A PCA was performed to evaluate the global variation of algal metabolome. The two first principal components (PC) explained 56.82% of the total variation. The scores plot showed a separation of GC from the two other stages along PC1, while T and G were separated along PC2 (**Figure 1A**). Each stage harboured a different metabolomic fingerprint ($p = 0.012$ for each pair). The hierarchical clustering analysis (**Figure S1**) of the matrix showed a similar clustering to that observed on the PCA score plot with two clusters, with one containing G and T samples and the other one containing GC samples.

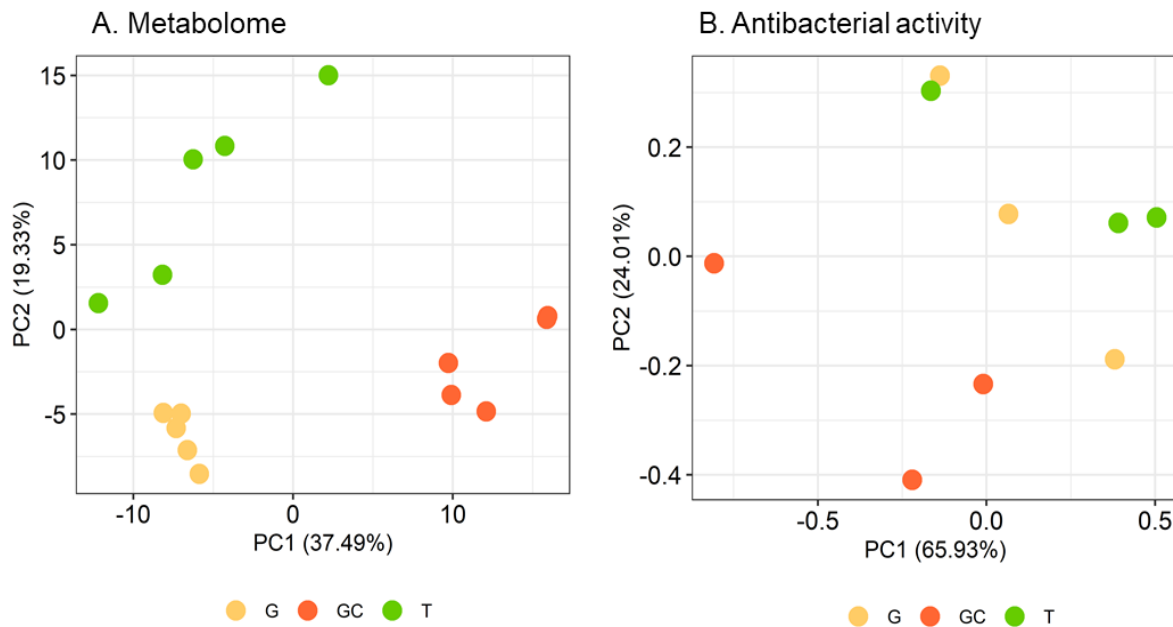


Figure 1: (A) Metabolome and (B) antibacterial activity scores plots of *A. armata* gametophyte “G”, with developed cystocarpes “GC”, and tetrasporophyte “T” stages. (B) refers to results mentioned in 2.2.

We then performed a supervised statistical analysis using a PLS-DA model to determine which features mostly discriminated the three phases. The classification error rate (CER) of the model was low ($CER = 0.01$, $p = 0.001$), indicating a predictive model.

Variables with a high importance in projection, called VIP, with a score > 1.25 (77 variables) were selected, and, after redundancy elimination (fragments and adducts), a total of 32 features were considered. A molecular formula was proposed for most of the features based on exact mass, isotopic patterns, MS/MS fragmentation and Sirius annotation (**Table S1**). The exploitation of the isotopic patterns allowed us to determine that most of the molecules were halogenated (23 over 32, 72%). Visualisation using a heatmap of the clustering of samples according to the relative abundance of these 32 molecules allowed the identification of three groups of discriminating molecules, most of which were common to G and T and more abundant than in GC (**Figure 2A**). For example, a molecule with the molecular formula $C_5H_2Br_6O_2$ (compound **1**, **Figure 3**), which also displayed the highest ion intensity on chromatograms (**Figure S2**), and another molecule that could be an analogue with the replacement of a bromine ion with a chlorine ion ($C_5H_2Br_5ClO_2$, compound **2**, **Figure 3**) were more abundant in G and T than in GC (**Figure 2B**). The identified molecules that were more abundant in GC were mainly low halogenated molecules containing bromines such as a dibromo acid derivative, bromochloroacetic acid and dibromoacetic acid (compound **3**, **Figure 3**) (**Figure 2C**). Finally, some features (i.e. M179T626, $C_{15}H_{22}Br_6O_2$, and $C_{15}H_{23}Br_5O_2$) were mostly detected in T (**Figure 2A**). Among them, both M179T626 (**Figure 2D**) and M451T626 (**Table S1**), barely detected in G and GC, corresponded to in-source fragments of pentabromopropen-2-yl tribromoacetate ($C_5Br_8O_2$, compound **4**, **Figure 3**) previously isolated by our research team (Reverter et al., 2022).

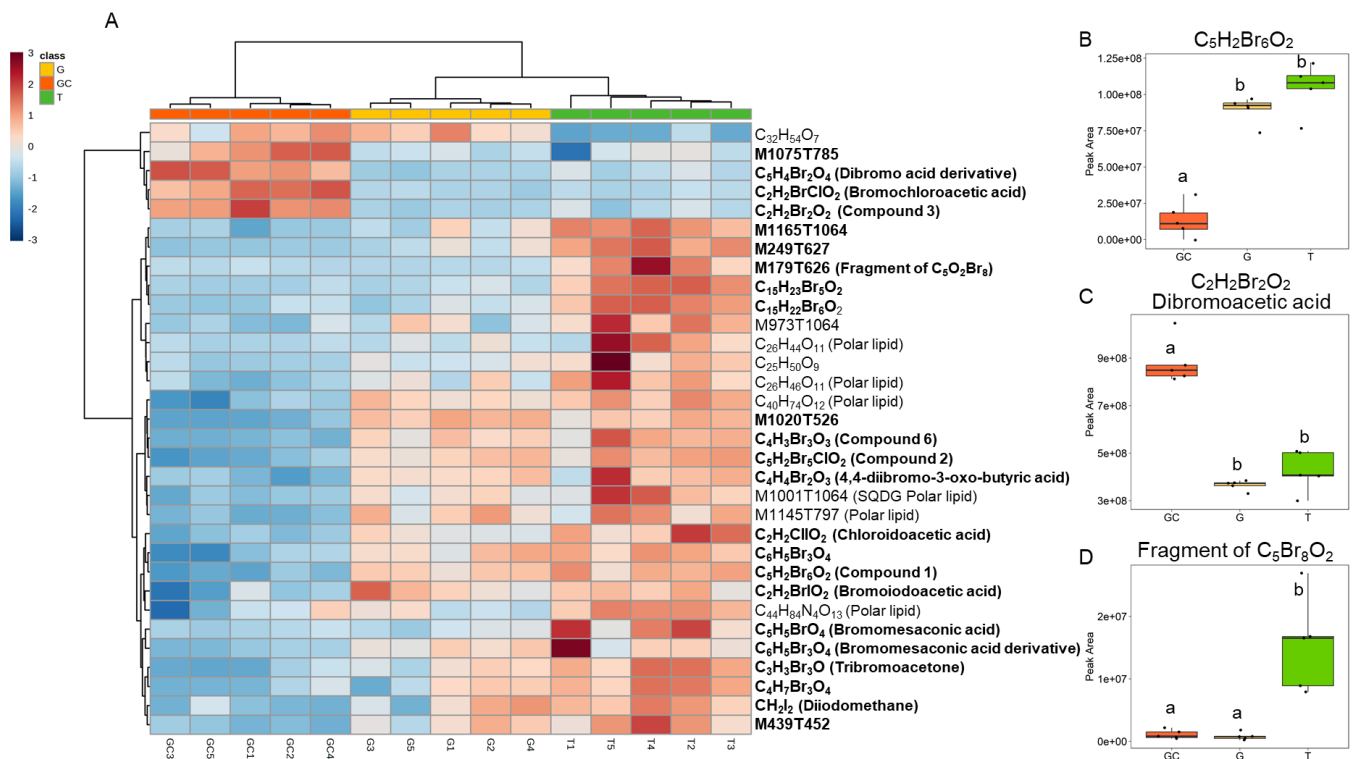


Figure 2: (A) Heatmap representation of top 33 VIP features for the discrimination of the three algal stages (the gametophyte, “G”; the gametophyte with cystocarps, “GC”; and the tetrasporophyte, “T”) detected with LC-HRMS and their putative identification. Clustering: ward. Distance: Euclidean. Putative identification in bold represents halogenated molecules. (B) On the right, box plots of peak area of $C_5H_2Br_6O_2$, (C) dibromoacetic acid and (D) $C_5Br_8O_2$ in the three types of samples. Letters a and b represent distinct groups based on Nemenyi post hoc tests between algal stages ($p < 0.05$).

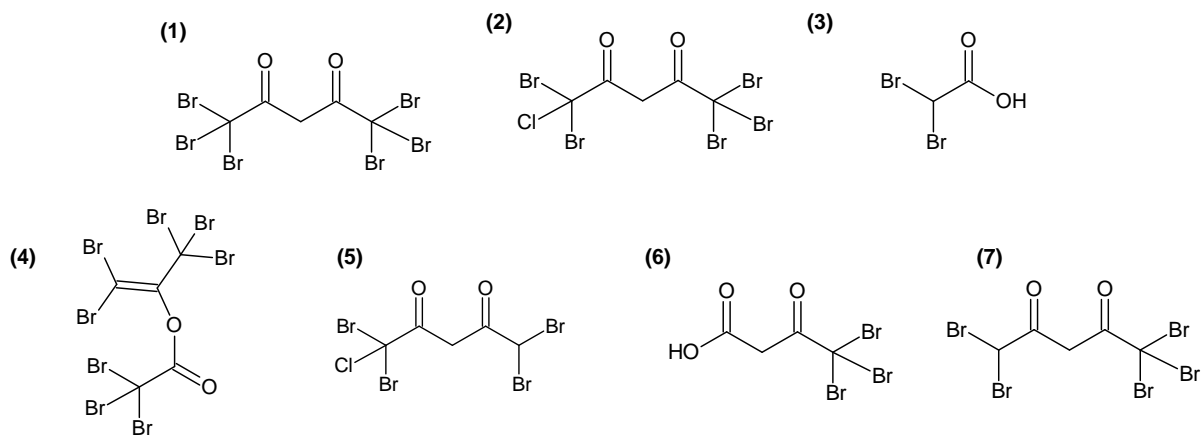


Figure 3: Chemical structures of molecules involved in the discrimination of the three algal stages (1-4) and of molecules with a correlation >0.8 (Pearson coefficient) with the bioactivity of *A. armata* fractions (1,2,5-7).

2.4.2 Variation in the antibacterial activity of the three life stages

The antibacterial activity of the apolar extracts (0.5 mg/discs) of the samples of the three algal stages (5 biological replicates) was evaluated against 6 fish pathogenic bacteria: *Edwardsiella anguillarum* (Ea) (Gram–), *Lactococcus gerviaeae* (Lg) (Gram+), *Tenacibaculum maritimum* (Tm) (Gram–), *Vibrio anguillarum* (Va) (Gram–), *V. harveyi* (Vh) (Gram–) and *Yersina ruckeri* (Yr) (Gram–). The extracts displayed antibacterial activity against all 6 bacteria (**Table 1**). The antibacterial activity of the three stages was significantly different for all bacteria, except for the two *Vibrio* spp. (**Table 1**). In addition, GC activity tended to be lower than that of the other stages, especially against Ea, Tm and Yr (**Table 1**). Against Lg, the measured inhibition diameters were much smaller than against the other bacterial species. Only T extracts showed activity against this bacterium, while G extracts showed very low and variable activity, and GC extracts showed no activity (**Table 1**).

Table 1: Diameter of inhibition (including the size of the discs – 0.6 cm) measured as indicator of the antibacterial activity of extracts of the 3 types of algal stages (the gametophyte with cystocarps “GC” ; the gametophyte “G”; and the tetrasporophyte “T”) against 6 different bacterial species. Letters (a and b) represent distinct groups based on Nemenyi Post Hoc between algal stages for each bacterium ($p < 0.05$).

	GC	G	T	<i>p</i>
Ea	1.7 ± 0.2 ^a	2 ± 0.06 ^{a,b}	2.2 ± 0.1 ^b	0.034
Lg*	0.6 ± 0	0.6 ± 0.06	0.8 ± 0	0.030
Tm	1.6 ± 0.1 ^a	2 ± 0.06 ^b	1.9 ± 0.1 ^{a,b}	0.050
Va	2.0 ± 0.06	2.1 ± 0.06	2.0 ± 0.06	0.141
Vh	1.4 ± 0.4	1.2 ± 0.4	1.1 ± 0.4	0.610
Yr	1.4 ± 0.1 ^a	1.6 ± 0.1 ^{a,b}	1.7 ± 0.06 ^b	0.042

*For Lg, although a Kruskall-Wallis test indicated significant differences among groups, the groups were not significantly different with each other according to the Nemenyi post hoc tests.

A PCA was performed to evaluate the global variation of algal antibacterial activity (**Figure 1B**). The two first PCs explained 89.94 % of the total variation. The scores plot showed a similar separation to that observed for the algal metabolome (**Figure 1A**) with the separation of the gametophyte with the developed cystocarps (GC) from the two other stages along PC1 and PC2 (**Figure 1B**). The covariation of the antibacterial activity and the metabolome was studied with a Mantel test and showed positive correlation ($r=0.41$, $p=0.025$).

2.4.3 Identification of candidate molecules responsible for antibacterial activity

The identification of candidate molecules responsible for the antibacterial activities was performed by bioguided (with *E. anguillarum*) fractionation on 100 g (dry weight) of powder of gametophyte of *A. armata*. To facilitate the extraction of large quantities of algae, extractions were realised by three successive macerations in MeOH:DCM (1:1). Like the apolar extract, this crude extract showed antibacterial activity against *E. anguillarum*, and the measured bacterial growth inhibition zone was 2.3 ± 0.1 cm. A bioguided fractionation was then performed on this extract using reverse-phase chromatography. Fractions eluted with 40% and 30% H₂O-MeOH, from the first fractionation, exhibited $98.9 \pm 0.4\%$ and $97.6 \pm 0.8\%$ of bacterial growth inhibition, respectively (**Table S2**), evaluated on 96-well plates (0.5 mg/mL). The LC-HRMS analyses of all fractions revealed that the two most active fractions harboured several intense ions (**Figure S3**) with monoisotopic masses at *m/z* 214.8352 [M-H]⁻ corresponding to compound **3** (**Figure 3**), 527.2532 [M-H]⁻ (C₂₃H₄₄O₁₁S), 555.2844 [M-H]⁻ (C₂₅H₄₈O₁₁S) and 566.5085 [M-H]⁻, corresponding to compound **1** (**Figure 3**). Peak integrations were manually performed, and the correlations between the determined peak areas and the bioactivity of the fractions were calculated for 14 major ions detected in active fractions (**Table S3**). Finally, five ions with monoisotopic masses at *m/z* of 444.6488 (C₅H₃Br₄ClO₂) (compound **5**, **Figure 3**), 334.7556 (C₄H₃Br₃O₃) (compound **6**, **Figure 3**), 488.5982 (C₅H₃Br₅O₂) (compound **7**, **Figure 3**) and masses corresponding to compound **1**, and **2** (**Figure 3**) exhibited strong correlation (*r*>0.8) with the bioactivity (**Table S3**). These molecules were seemingly structure-related as, on MS/MS spectra (**Figures S4, S5, S6, S7, S8**), **1**, **2**, **6** and **7** displayed a fragment with a monoisotopic mass at *m/z* 248.7552 [M-H]⁻ corresponding to [CBr₃]⁻ ion fragment, and **2** and **5** displayed a fragment with a monoisotopic mass at *m/z* 204.8066 [M-H]⁻, corresponding to [CBr₂Cl]⁻ ion fragment. A comparison with recent published data (Thapa et al., 2020) led us to assign structures for **1**, **2**, **5** and **7** as polyhalogenated 2,4-diones (**Figure 3**). For compound **6**, which was not observed by Thapa et al. (2020), we proposed the most probable structure based on fatty acid biosynthetic pathway coherence and fragmentation patterns (**Figure S5**).

Active fractions were further fractionated by semi-preparative HPLC leading to 14 fractions of which two, F9 and F10, induced $99\pm0.0\%$ and $93.7\pm0.3\%$ of bacterial growth inhibition, respectively (**Table S4**). These fractions still presented the same ions (**Figure S9**) that were highly correlated with the bioactivity (**Table S5**). However, while most of the ions presented a similar range of intensity between the first and second fractionation, a loss of intensity (**Figure**

S10) was observed for the one corresponding to compound **1**. At this stage, and despite a subsequent fractionation by semi-preparative HPLC, we did not achieve the purification of any of the halogenated compounds present in the active fraction.

2.4.4 Analysis of bacterial communities associated with *A. armata* stages

The variations of the bacterial communities associated with the same five replicates for each of the three algal stages for which metabolome and antibacterial activity were described in 2.4.1 and in 2.4.2 were then assessed. The metabarcoding sequencing of the 16S rRNA gene resulted in a dataset of 2,235,756 reads. After filtering and rarefying to the lowest number of sequences (24,710) (**Table S6; Figure S11**), the final dataset was finally composed of 3,075 Amplicon Sequence Variant (ASV). The α -diversity indices were calculated. No significant differences were observed between the three stages for evenness (**Table 2**). In contrast, T displayed significantly higher values than the other algal stages for Chao1 and Shannon indices (**Table 2**).

Table 2: α -diversity indices: Chao1, evenness and Shannon, of the three type of algal stages (the gametophyte with cystocarps, “GC”; the gametophyte, “G”; and the tetrasporophyte, “T”. Letters (a and b) represent distinct groups based on Nemenyi Post Hoc between algal stages ($p < 0.05$).

	GC	G	T	<i>p</i>
Evenness	0.78 ± 0.03	0.80 ± 0.04	0.84 ± 0.02	0.069
Chao1	$513.4 \pm 92.4^{\text{a}}$	$632.5 \pm 235.4^{\text{a,b}}$	$920.7 \pm 186.6^{\text{b}}$	0.031
Shannon	$4.87 \pm 0.3^{\text{a}}$	$5.1 \pm 0.5^{\text{a,b}}$	$5.7 \pm 0.3^{\text{b}}$	0.021

Differences in β -diversity were assessed using Bray-Curtis dissimilarities. The PCoA showed a separation of bacterial communities in accordance with the different stages (**Figure 4A**). The average distance to median (GC=0.1855, G=0.2476, T=0.2611) indicated no significant difference in the intragroup (intra-stage) bacterial composition ($p=0.39$). The T samples were separated from the other two stages according to PCo1 (**Figure 4A**) and showed a significantly different bacterial composition from G and GC ($p_{(GC_T)}=0.015$ and $p_{(G_T)}=0.015$) which did not separate according to PCo2 and the result of the pairwise permanova test ($p_{(GC_G)}=0.189$). By taking a closer examination of the structure of bacterial communities, we established that the sequences belonged to 283 genera corresponding to 156 families, 87 orders, 35 classes, and 21 phyla. The α -proteobacteria and γ -proteobacteria (Pseudomonadota) and Bacteroidia (Bacteroidota) dominated the bacterial communities in all algal stages at the class level (**Figure**

4B). At the family taxonomic rank (**Figure S12**), Saprospiraceae (Bacteroidia) dominated in similar range in all algal stages, representing 26 % on average of the ASVs (GC: 7,517 sequences, G: 6,402 sequences and T: 5,080 sequences out of 24,710 in total). Abundances in other families were more variable among the different algal stages, with Flavobacteriaceae (Flavobacteriia) representing 11% on average (2637 sequences out of 24,710 in total) of the total sequences of T and only 2% on average (GC: 531 sequences, G: 549 sequences out of 24,710 in total) in the two other algal stages. In a similar way, “Other” families (representing families with an abundance <0.02%, i.e., five sequences or less) accounted for 31% on average (7761 sequences out of 24,710 in total) of the total sequence of T and less than 15% on average (GC: 2603 sequences, G: 3355 sequences out of 24,710 in total) of that of the other two algal stages. In contrast, other families such as Thiotrichaceae were more represented in GC and C than in T samples with 14%, 11% and 5% on average of the ASVs for GC (3350 sequences), G (2778 sequences) and T (1313 sequences), respectively (**Figure S12**).

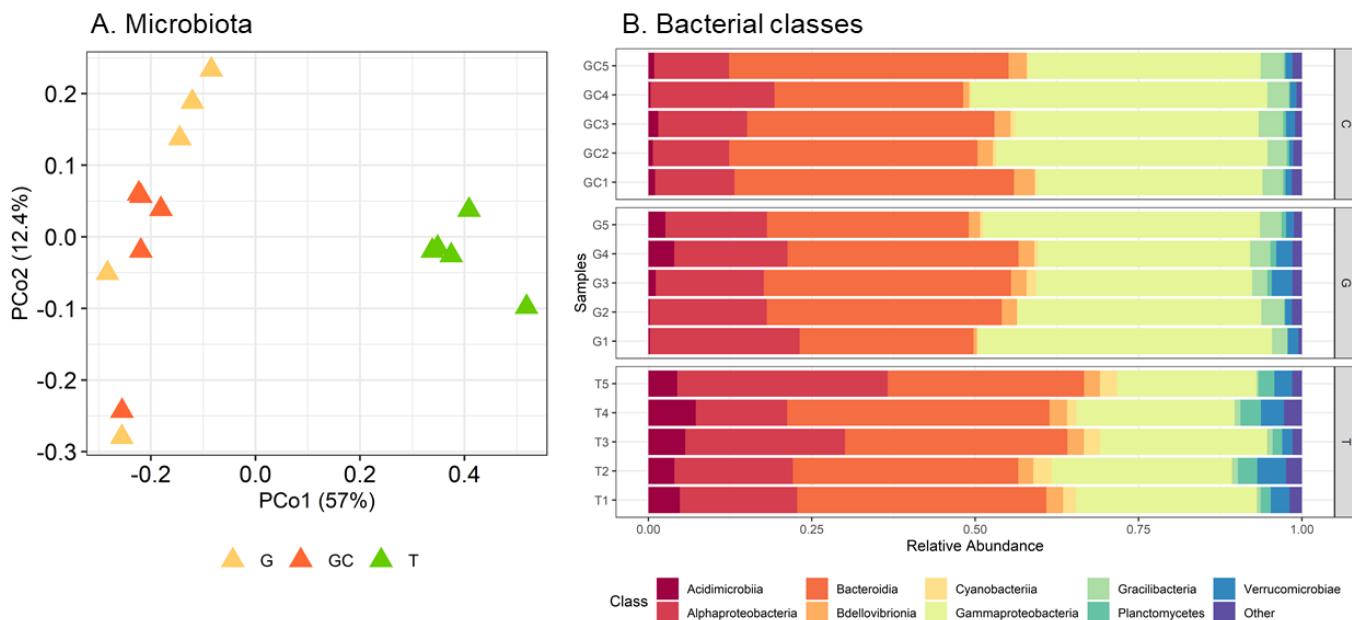


Figure 4: (A) Scores plot of microbiota of the three *A. armata* stages. (B) Relative abundance of bacterial classes associated with the three *A. armata* stages (the gametophyte, “G”; the gametophyte with cystocarps, “GC”; and the tetrasporophyte, “T”).

By calculating the indicator value index, we revealed that the majority of the discriminant ASVs (311 belonging to 39 distinct families) were significantly associated with T, while only 40 ASVs and 63 ASVs were significantly associated with G and GC, respectively (**Table S7**). Furthermore, the most abundant discriminating ASVs (representing >1 % of the total sequences) (**Table S7**) were almost equally associated with the three algal stages, with eight

ASVs associated with GC, six with G and five with T (**Table S7**). The clustering of samples on the heatmap representation of these most abundant discriminating ASVs showed a clustering similar to the projection of samples of each algal stage with the PCoA (**Figure 4A**). GC and G samples clustered together, and T samples were in a second group and harboured very specific bacterial ASV (**Figure 5**). Three Cellvibrionaceae with an unidentified genus (ASV_13, ASV_27, and ASV_38) were in very low abundance in T (0.06 % on average) compared to their abundances in G and GC (0.9 % and 2 % on average). In a similar way, the *Thiotrichaceae* family, were more abundant in G and GC (0.9 % and 1 % on average) than in T (0.03 %) samples. Conversely, a *Roseobacter* genus (Rhodobacteraceae) (ASV_83) and a *Lewinella* genus (Sapropiraceae)(ASV_18) were not sequenced at all in C and GC samples (**Figure 5, Table S7**), but represented an average of 1 % and 6 % of the total sequences in T samples, respectively. Finally, two genera of Flavobacteriaceae, *Winogradskyella* and *Croceitalea*, were also significantly associated with T samples.

The potential functional profile of bacterial communities associated with the algae was explored using the predictive metagenomics tool Tax4Fun2. It allowed the prediction of a total of 6625 functions. The indicator value index was used and 433, 1201 and 4306 predicted functions were associated with GC, G and T, respectively. According to the KEGG Mapper reconstruct tool, they were mostly associated with global and overview maps (mainly metabolic pathways; biosynthesis of secondary metabolites; and bacterial metabolism in diverse environments), carbohydrate metabolism, and amino acid metabolism (**Table S8**). We then focused on the most abundant predicted functions (abundance > 0.1%) (108 GC, 107G and 107T) of which 28 were associated with GC, 72 were associated with G and 24 were associated with T (IndVal). None of the predicted functions associated with the bacterial diversity of GC were involved in secondary metabolites but rather in metabolic pathways and membrane transport. In contrast, the functional diversity associated with the bacterial community of both G and T was mostly involved in metabolic pathways and the biosynthesis of secondary metabolites (**Figure S13**). Some specific predicted functions with a lower abundance (<0.1%) associated with the bacterial diversity of T were involved in the breakdown of macroalgal polysaccharides (beta-agarase, alpha-agarase, kappa-carrageenase, lambda-carrageenase, iota-carrageenase and oligo-alginate lyase). Finally, the predicted functions involved in dehalogenase production were associated with the bacterial diversity of G and GC (2-haloacid dehalogenase for GC; haloacetate dehalogenase for G).

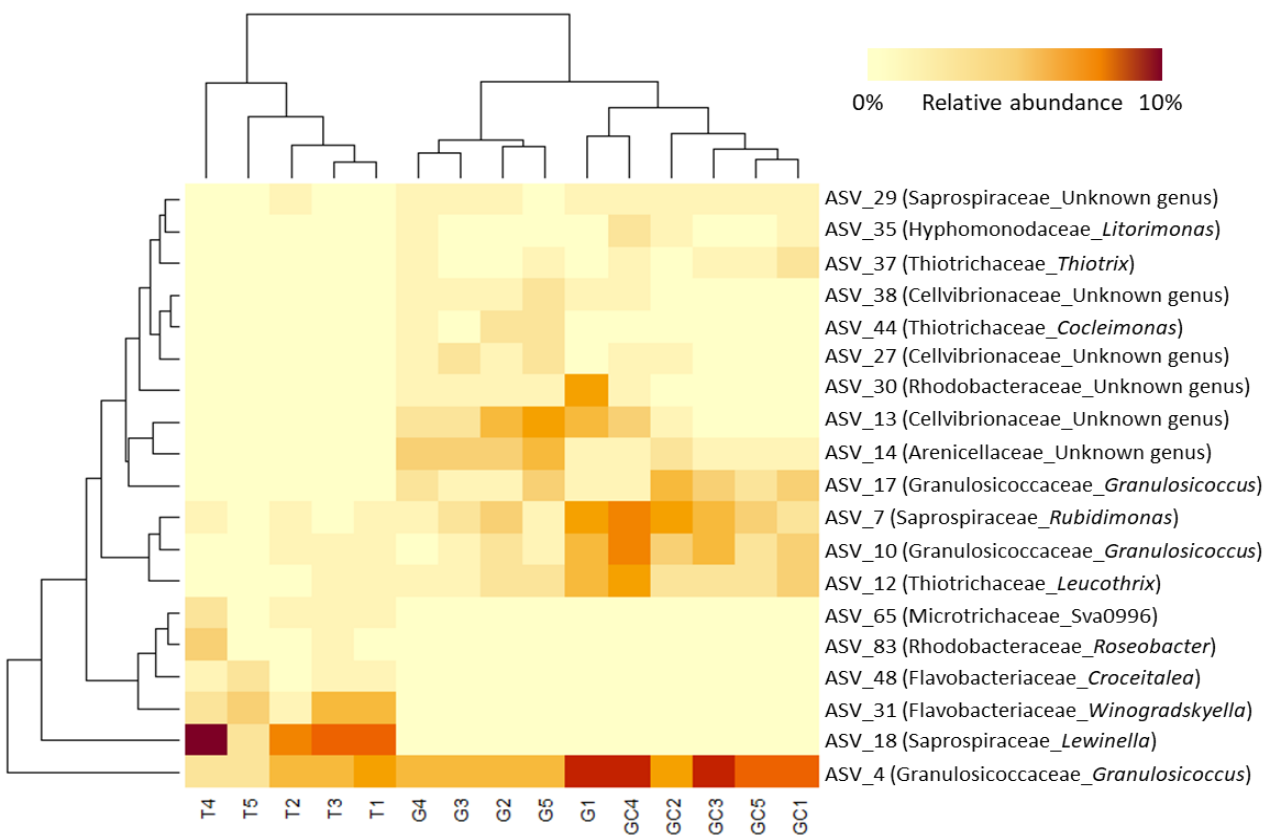


Figure 5: Heatmap of the most abundant (>1 % of the total number of sequences) and discriminant ASV (IndVal index) of the three *A. armata* stages (the gametophyte “G”; the gametophyte with cystocarps “GC” and the tetrasporophyte “T”). The lines represent the ASV, the columns the samples and the colours represent the relative abundance of each ASV in each sample.

2.4.5 Correlation between metabolite and bacterial compositions in algal stages

The correlation between metabolite and bacterial compositions of the five replicates of each of the algal stages was assessed by a Mantel test and a multiblock PLS-DA (DIABLO). The Mantel test showed no significant covariation between both datasets ($r = 0.16, p > 0.05$). In contrast, the scores plot (**Figure S14**) and correlation scores (0.93 on dimension 1 and 0.89 on dimension 2, **Figure S15**) of the multiblock PLS-DA analysis between the datasets showed good congruence and covariation between bacterial community and the metabolite compositions for each algal stage. The three algal stages were well discriminated with the built model ($CER=0.06, p=0.001$). The first dimension discriminated T from the other groups, while the second component discriminated GC from G (**Figure 1C**). A clustered image map was built to observe the clustering of the 60 metabolites and 32 ASV selected by the model. Three clusters were distinguishable, with (1) 41 variables discriminating G, (2) 32 discriminating T and, finally, (3) 19 discriminating GC (**Figure S16**). The cluster of the variables discriminating G

was mostly composed of ASVs (29) (**Figure S16**), while the clusters of the variables discriminating T and GC were mostly composed of 28 and 14 metabolites, respectively.

The three clusters can also be observed on the correlation network, which was built with the most discriminant variables that were highly positively or negatively correlated (threshold=0.7) (**Figure 6**).

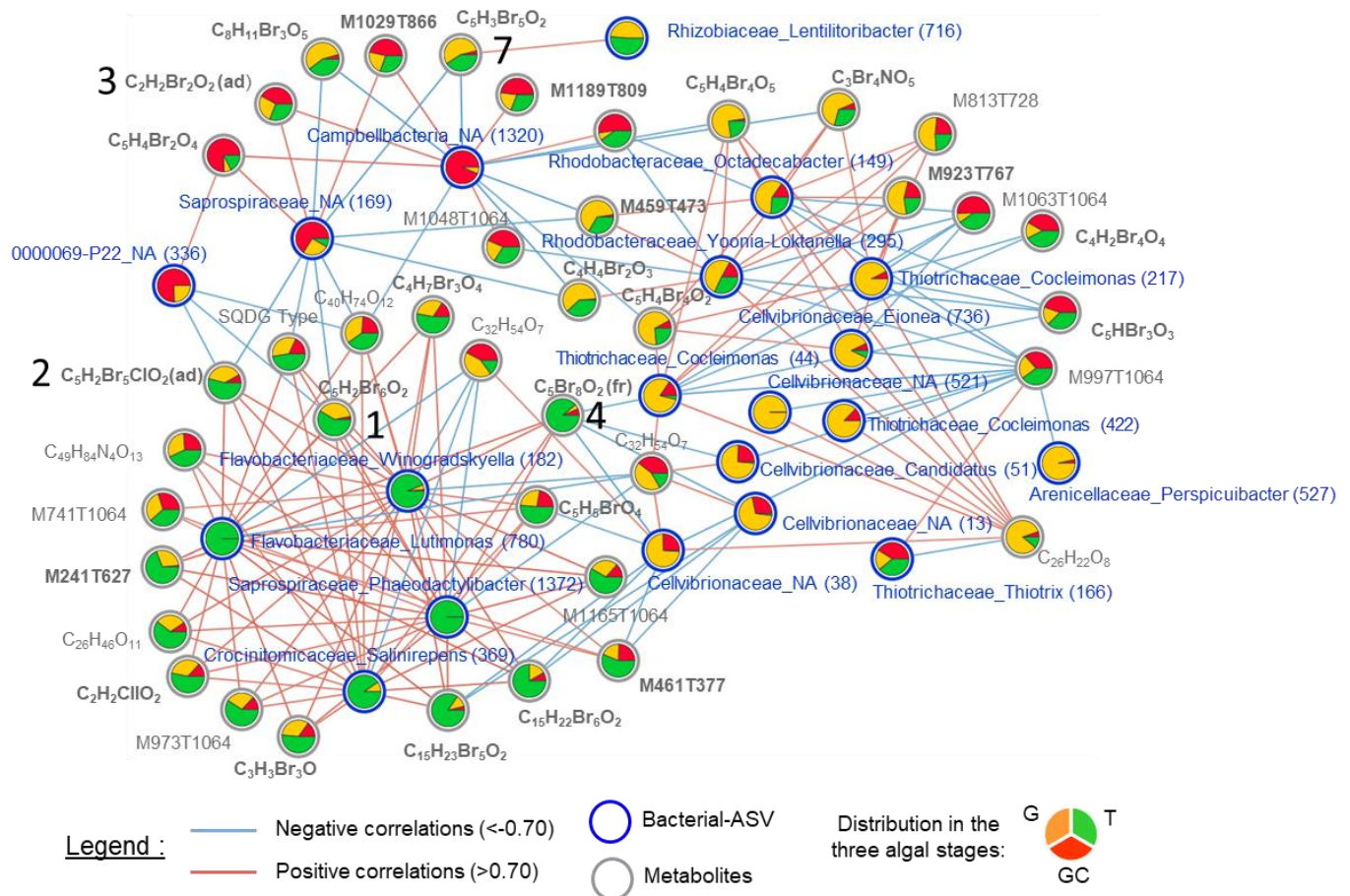


Figure 6: Correlation network of metabolites (grey circles and names) and ASVs (blue circles and names) selected by the DIABLO (multiblock sPLS-DA) analysis with a correlation threshold of 0.7. Negative correlations are represented by the blue lines, and positive correlations are represented by the red lines. Relative abundance in each algal stage (the gametophyte, “G”; the gametophyte with cystocarps, “GC” and the tetrasporophyte, “T”) is represented with the pie charts. Metabolite names in bold represent halogenated compounds. The numbers in brackets in Bacterial-ASV names represent the ASV number (see Table S7). The numbers **1**, **2**, **3**, **4** and **7** refer to the metabolites in **Figure 3**.

Notably, three clusters contained halogenated (including compounds **1**, **2**, **3**, **4** and **7**) and non-halogenated metabolites. Regarding the ASVs present in the correlation network, with the exception of ASV_38 (Cellvibrionaceae_NA), ASV_13 (Cellvibrionaceae_NA) and ASV_44 (Thiotrichaceae_Cocleimonas), all other ASVs that were correlated with metabolites

(halogenated or not) had a relatively low abundance (<1%) in the algal samples (**Table S9**). The cluster of the variables discriminating T was mainly composed of positively correlated variables, whereas the correlations were more mixed for the cluster of variables discriminating G and GC. Some halogenated molecules including compounds 1, 2 and 4 were positively correlated with the four ASVs discriminating T, all of which were Flavobacteriales (ASV_182, ASV_369, ASV_780 and ASV_1372). They were also strongly negatively correlated with some ASVs. We can distinguish compounds 1 and 2 but also 7, that were negatively correlated with ASVs discriminating GC, such as a Campbellbacteria variant (ASV_1320), a Saprospiraceae variant (ASV_169) and a 0000069-P22 variant (ASV_363) and those, including compound 4, negatively correlated with ASVs discriminating G, such as three Cellvibrionaceae variants (ASV_13, ASV_38 and ASV_51) (**Figure 6**).

2.5 Discussion

Asparagopsis armata and *A. taxiformis* are two red algae known for their production of halogenated molecules (Félix et al., 2021; Ponte et al., 2022; Zanolla et al., 2022a). Several studies reported differences in the concentration of some targeted halogenated molecules between the different life stages of the genus (Bruneau et al., 1978; Paul et al., 2006a; Vergés et al., 2008). In this study, we first aimed at exploring the metabolome and antibacterial activity variation of the different life stages of *A. armata*. Secondly, we performed a bioguided fractionation in order to identify the molecule(s) responsible for the antibacterial activity. Thirdly, we studied the variation of microbiota composition between the three algal stages, and finally, we assessed the complex interactions between the chemistry and the microbiota datasets.

2.5.1 The three stages of the life cycle of *A. armata* harboured distinct metabolome compositions

Using a metabolomics approach, we discovered that the three collected stages harboured different metabolome compositions. By studying the most discriminating molecules and their isotopic patterns, we were able to highlight that they were mainly halogenated molecules (25 over 33). Among them, haloacetic acids such as dibromoacetic acid, bromochloroacetic acid and dibromomethyl succinic acid were more abundant in GC (gametophyte with developed cystocarps) than in the other two stages, the contents of these molecules not being significantly different between G and T. These results differ from those of Paul et al. (2006a) who quantified targeted halogenated molecules contents in *A. armata* and found consistently higher levels of

dibromoacetic acid and bromochloroacetic acid in T compared to G. These differences may suggest that the location and the collection period could have an impact on the results found. In GC, the abundance of the three above-cited molecules could be linked to the development of the cystocarps on the female gametophyte. Indeed, Vergès et al. (2008) suggested that the accumulation of not only bromoform but also dibromoacetic acid, both of which were reported to be correlated (Paul et al., 2006a), in the cystocarps walls of *A. armata* may be related to the need to protect the fragile parts of this alga, such as its reproductive elements (Vergés et al., 2008). In their study, the cystocarp walls were the least consumed parts of the algae in preference tests performed on the sea slug *Aplysia parvula* (Vergés et al., 2008). A monitoring of the metabolome during the gradual transition from the G to the GC stage could reveal the increased abundance of these molecules and help to better understand their roles.

Then, we discovered that highly halogenated molecules, such as compounds **1** ($C_5H_2Br_6O_2$) and **2** ($C_5H_2Br_5ClO_2$), were significantly more abundant in G and T than in GC. The structures of molecules **1** and **2** were established by comparing the data obtained by Thapa et al. (2020) who proposed them on the basis of MS^n fragmentation patterns and suggested that they may be precursors of smaller halogenated molecules, such as dibromomethane and chlorodibromomethane, by hydrolytic cleavage. We could hypothesise that, in G and T, these molecules could be part of the storing strategy of halogenated resources, while in GC, these molecules could have undergone the transformations mentioned above, leading to a high abundance of small deterrent halogenated molecules. Thapa et al. (2020) also reported the presence of vanadate-dependant haloperoxidases in *A. taxiformis*, which could be involved in the production of bromoform by the algae (Thapa et al., 2020; Zhu et al., 2021), but also other halogenated compounds as these enzymes are known to catalyse the biosynthesis of halogenated molecules (Butler and Carter-Franklin, 2004; Paul and Pohnert, 2011; Theiler et al., 1978). Then, we discovered that compound **4** ($C_5Br_8O_2$) was only detected in T. In a previous study, we have proposed this perbrominated compound as a potential chemotaxonomic marker of the gametophyte stage of *Asparagopsis* spp. as it was only detected in the gametophyte samples of *A. taxiformis* (Parchemin et al., 2023, minor revision). It was thus interesting to observe the presence of this molecule in the tetrasporophyte stage of this species. A differential expression of haloperoxidases, which could then lead to the differential production of halogenated molecules, could explain the observed differences in the abundance of not only compound **4** but also other halogenated compounds. The preferential expression of a gene encoding for bromoperoxidase was already reported in the sporophyte stage of the red

algae *Pyropia yezoensis* (Matsuda et al., 2015). The authors showed that it was actively expressed in filamentous sporophytes, leading to bromoform production, but repressed in leafy gametophytes under normal growth conditions, which is in accordance with our hypothesis.

2.5.2 Highly halogenated molecules may be responsible for some antibacterial activity

By the screening of the antibacterial activity of the apolar extracts of the stages of the alga against six pathogenic bacteria of marine organisms, we found significant differences between the targeted stages. These results are in line with those of Salvador et al. (2007) who studied the antibacterial activity against human pathogens of several Iberian algae, including the tetrasporophyte and the gametophyte stages of *A. armata*, and significantly different antibacterial activity between the two stages (Salvador et al., 2007). However, in contrast to our study, a higher antibacterial activity was found for the gametophyte than for the tetrasporophyte. Similarly, the activity of the extracts from different stages of 26 cultivable algae species, including the gametophyte and tetrasporophyte stages of *A. armata*, was studied against pathogenic bacteria in aquaculture (Bansemir et al., 2006). In this study, dichloromethane extracts of both stages of *A. armata* were among the most active of algal extracts. The authors also measured higher inhibition diameters for the gametophyte than for the tetrasporophyte stage (Bansemir et al., 2006). The differences in activity observed between these studies and our study could be related to the composition of the extracts, which depends on the extraction method used, and the extraction method differed between all the studies. Indeed, we used a biphasic extraction, whereas the results mentioned above were obtained with aqueous extracts (Salvador et al., 2007) and dichloromethane extracts (Bansemir et al., 2006). The antibacterial activity of the GC extracts was significantly lower than that of the T extracts against three of the bacteria. Moreover, the extracts of GC and G were not active against Lg. In general, the inhibition diameters measured against this bacterium were much lower than those measured against the other bacteria. We could hypothesise that this may be related to the fact that Lg is a Gram-positive bacterium. However, in the literature, several studies on the antibacterial activity of *A. armata*, which included both Gram-positive and Gram-negative bacteria, did not report major differences or a higher activity of the algae when measuring activity against Gram-positive compared to Gram-negative bacteria (Paul et al., 2006a; Salvador et al., 2007). Thus, the observed lower activity may be more species-related, with Lg likely being less sensitive to our algal extracts than those of other bacteria.

The metabolomics analyses allowed us to discover that highly halogenated molecules were in higher abundance in G and T than in GC. The antibacterial activity of highly halogenated

molecules, isolated from *A. taxiformis*, was already described. This is the case for compound **4**, which has already been reported for its antibacterial activity against two strains of bacteria belonging to Flavobacteriaceae (Reverter et al., 2022) and pentabrominated mahorones (Greff et al., 2014). In addition, via bioguided fractionation and the calculation of the Pearson correlation, we identified structurally related halogenated compounds (**1,2 and 5-7**) as being potential responsible for the observed antibacterial activity. Compounds **1** and **2** also appeared as VIPs for the discrimination of algal stages. Unfortunately, and despite the precautions taken, like Thapa et al. (2020), who have already tried to isolate compound **1** to confirm its structure but did not succeed because of its lability, we failed to complete the purification of the active molecules. Regarding compound **1**, we also observed a decrease in the corresponding chromatographic peak during the successive fractionation steps, which suggests the instability of this compound in our purification conditions. Therefore, we could not confirm the activity of the molecules cited above; however, with the correlations measured and the activities already described for other molecules, we could consider that highly halogenated molecules may be involved in some of the variations in the antibacterial activity observed in vitro. Their ecological roles remain to be determined. The localisation of these molecules in the algal tissues by MALDI imaging mass spectrometry and the analysis of *Asparagopsis* exometabolome by LC-MS may provide some answers by indicating whether these molecules are stored in the specialized cells already observed in *A. armata* (Marshall et al., 2003; Paul et al., 2006a) and released on the algal surface and the immediate surrounding environment.

2.5.3 Microbiota composition differs throughout the three stages of the life cycle of *A. armata*

We then studied the composition of the microbiota of the same samples of the three algal stages as in Section 3.1 using metabarcoding analysis. Pseudomonadota (α -proteobacteria and γ -proteobacteria) and Bacteroidota (Bacteroidia) were the dominant phyla (and classes) of the bacterial communities, which is consistent with what is commonly found in macroalgae (Egan et al., 2013). Similarly, α -proteobacteria (Rhodobacterales, Rhizobiales) were also found to be dominant in the tetrasporophyte of *A. taxiformis* in previous studies (Zhao et al., 2022, preprint). Saprospiraceae (Bacteroidia) was the most represented family (26%) in our samples. This was in accordance with previous studies that reported that this family was very abundant in samples of *Asparagopsis* spp. and could be a constitutive part of the microbiota of the genus *Asparagopsis* (Aires et al., 2016).

The comparison of bacterial communities between the different stages of *A. armata* clearly showed that the alpha diversity (evenness, Chao1 and Shannon indices) of the T samples was significantly higher than that of the GC and G samples, for which there was no significant difference. This specific bacterial diversity of T was associated with a greater number of predicted functions, which were calculated using Tax4Fun 2 (Wemheuer et al., 2020), than for the GC and G stages. These observations are in line with those of another study that explored the microbiota of the gametophyte and sporophyte of *Mastocarpus* spp. and found that the specific diversity of the bacterial community of the two stages of the alga was different. However, unlike our study, the sporophyte samples of *Mastocarpus* spp. presented a lower Chao1 index and, thus, a lower specific diversity than the gametophyte samples (Lemay et al., 2018). The genetic host identity (Tabrett and Horton, 2020), the microbial communities analysed (surface microbial communities compared to whole microbial communities in our study), and the collection site (Queen Charlotte Basin in British Columbia compared to the Mediterranean Sea in our study) could be some explanations for the observed differences between both studies. Indeed, it is well known that the environment and the location of the samples have an influence on microbial composition (Paix et al., 2021b).

The molecules produced by the algae could also impact the composition of the bacterial community (Egan et al., 2013). In our study, we found no correspondence between the clustering analyses of the molecular composition and the bacterial community composition of the different algal stages nor any covariation between the molecular composition and bacterial community composition (Mantel test). These results suggest that there is no relationship between chemical composition and bacterial community composition for any algal stage. Nevertheless, there may be correlations between specific metabolites and specific bacteria as seen in our study and further discussed below. We can also hypothesise that other molecules, not observed in our study, could be involved in bacterial colonization. As an example, polysaccharides that constitute the cell walls of macroalgae are sources of nutrients that some bacteria can break down (Egan et al., 2013) and their composition may differ between gametophytes and tetrasporophytes (Waaland, 1975). In our study, among the predicted functions of the identified bacterial communities, some, significantly associated with T, were involved in the degradation of polysaccharides for which T composition differed from that of the gametophyte (Haslin et al., 2000). However, the most abundant bacteria associated with the tetrasporophyte were Flavobacteriaceae, which are known for their ability to degrade algal polysaccharides (Mann et al., 2013; Michel et al., 2006; Thomas et al., 2017). Apart from the

predicted functions involved in the degradation of polysaccharides, some of the most abundant predicted functions (>0.1%) associated with the bacterial community diversity of G and T were involved in the biosynthesis of secondary metabolites, which was not the case for GC. This could be an additional explanation for the differences in antibacterial activity observed between G, T and GC. However, the functions were predicted using Tax4Fun2, and further metabolic details would be revealed by metagenomics combined with metatranscriptomics (Aires et al., 2016).

Apart from chemistry, the morphology may influence bacterial composition (Lemay et al., 2018, 2021). The gametophyte and the tetrasporophyte of *A. armata* have very distinct morphologies to the point that they were long considered to belong to different genera until the life cycle of the algae was unravelled (Zanolla et al., 2022a). The tetrasporophyte has a pompom-like shape and measures 2 to 3 cm maximum, whereas the gametophyte, bearing numerous branches, can measure up to 40 cm (Zanolla et al., 2014). Due to these different morphologies, the two algal stages interact differently with their surrounding environment and with water flow, which also influences biofilm formation and potentially provides a diversity of habitats for bacterial communities (Rusconi et al., 2014; Rusconi and Stocker, 2015).

Among the most abundant and discriminant ASVs associated with tetrasporophytes, Flavobacteriaceae were well represented, notably with the genera *Croceitalea* and *Winogradskyella*. The above-mentioned bacterial genera were also encountered in the older basal parts of the brown algae *Taonia atomaria*, which, compared to medial and apical parts, also harboured the highest bacterial density and diversity (Paix et al., 2020). The author hypothesised that the basal part of the algae may be subjected to a longer period of exposure to bacterial communities and thus may be exposed to a high succession of communities, which could explain the higher bacterial density and diversity. Given that, in Banyuls-sur-Mer, the tetrasporophyte is persistent throughout the year, whereas the gametophyte is only present from late January to June, these features could explain the great bacterial diversity of *A. armata* tetrasporophyte.

2.5.4 The overall analyses performed suggest complex interactions between the host and its microbiota

Although the unsupervised analysis suggested no significant relationship between chemical and bacterial community compositions, the supervised multi-omics analysis allowed us to identify discriminant variables that correlated with each other in both datasets. The discriminant ASVs

identified in the model were correlated with both halogenated and non-halogenated molecules. These ASVs were mostly present in a low abundance in the algal samples, meaning that more than just the most abundant bacteria are potentially involved in chemical interactions with the host.

In this study, among ASVs negatively correlated with compounds 1, 2 and 7 and with other halogenated molecules, three were abundant in GC: a Saprospiraceae variant (Bacteroidota), a Campbellbacteria (Patescibacteria) variant and a 0000069-P22 variant (Patescibacteria). Compound 4 was negatively correlated with three Cellvibrionaceae (Pseudomonadota) variants that were abundant in G. The genus of these ASVs is unknown, and, as the genome of these bacteria has not yet been sequenced, we lack information to hypothesise their potential functional roles. However, dehalogenase functions have been predicted and associated with GC (2-haloacid dehalogenase) and G (haloacetate dehalogenase). This is of particular interest as compound 4 is a haloacetate and was negatively correlated with ASVs that were abundant in G. Thus, in our study, bacteria that are negatively correlated with halogenated molecules could produce specific enzymes that could perform dehalogenation and recycle halogenated molecules, which would lead to a decrease in the abundance of halogenated molecules and could explain negative correlations. In the literature, these types of enzymes were also found in the Flavobacteria *Zobellia galactanivorans* (Bacteroidota) (Grigorian et al., 2021), in a Rhodobacteraceae (Pseudomonadota) (Novak et al., 2014) and in *Psychromonas ingrahamii* (Pseudomonadota) (Novak et al., 2013). Negative correlations may also be explained by a potential susceptibility of the above-cited genera to halogenated molecules, which were therefore less sequenced in the life stages producing these molecules.

It was interesting to observe the positive correlations of compound 4 with Flavobacteriaceae as, in a previous study performed by our research team, the antibacterial activity of this molecule against the species of this family was reported (Reverter et al., 2022). We could have, therefore, observed negative correlations instead. This could be explained by differences in susceptibility at the species level. The general observation of the high abundance of this family in samples of the tetrasporophyte is interesting as some genera of this family were reported as potential causative agents for algal disease partly because of their ability to degrade polysaccharides (Hudson and Egan, 2022; Kumar et al., 2016; Zozaya-Valdes et al., 2015). However, the Flavobacteriaceae family is composed of a high number of genera, which are probably not all pathogenic for the algae. Apart from the two Flavobacteriaceae, two other members of the Flavobacteriales were also present in the T cluster and positively correlated with halogenated

molecules. It is not excluded that members of this bacterial order could be involved in the biosynthesis of halogenated molecules by the algae, which could explain the positive correlations. However, the interpretation of the observed correlations is risky and must be fastidious because they could be related to different causes as mentioned. The cultivation of the identified bacteria of interest could be used to test the different hypotheses but is not always possible. The use of metagenomics combined with metatranscriptomics could also help by providing data on the link between bacterial community structures and functions in these communities (Aires et al., 2016; Burke et al., 2011).

Finally, the main results and hypotheses are summarized in **Table 3**.

Table 3: Summary of the main findings and hypotheses.

Algal stages	Metabolome	Antibacterial activity	Microbiota diversity and composition	Conclusions and hypotheses
General observation	Significant differences between GC-G, GC-T and G-T	Significant differences between GC-T	Significant Differences between GC-T and G-T	Highly halogenated molecules may be responsible of a part of the antibacterial activity No major covariation between metabolome and microbiota (Mantel) Correlations between specific metabolites and ASV
GC	Abundance in $C_2H_2Br_2O_2$, $C_2H_2BrClO_2$, $C_5H_4Br_2O_4$	Lower than T	Lower diversity than T Bacterial community dominated by the same ASVs as G	Distinct metabolome that may be related to the development and the protection of reproductive elements
G	Composition similar to T with abundance in highly brominated molecules ($C_5H_2Br_6O_2$, $C_5H_2Br_5ClO_2$)	Not significantly different from the two others (but closer to T)	Intermediate diversity between GC and T Bacterial community dominated by the same ASVs as GC	$C_5H_2Br_6O_2$ and $C_5H_2Br_5ClO_2$ may be responsible for a part of the antibacterial activities
T	Abundance in $C_5Br_8O_2$ barely detected in GC and G	Higher than GC, not significantly different from G	Diversity higher than GC and G Harbours some specific ASV not shared with GC or G	Morphology and annual persistence as major factors influencing microbiota composition? Differences in chemical composition involved in the bacterial diversity or conversely? Greater differences in gene expression involved in specific biosynthethic pathways?

2.6 Conclusion

To conclude, we have explored conjointly, for the first time, the variations of the metabolome composition, the antibacterial activity and the bacterial community composition of three stages of the life cycle of *A. armata*. We have shown that there were variations between the algal stages but no covariations between the metabolome and the bacterial community composition. Gametophyte harbouring developed cystocarps (GC) was associated with the overexpression of low halogenated molecules, lower bacterial diversity and lower antibacterial activity, in contrast to the tetrasporophyte stage (T). We have shown that an abundance of highly halogenated molecules was different between algal stages and could be involved for part of the variation of the antibacterial activity between the different algal stages. However, their ecological roles remain to be determined. The tetrasporophyte stage harboured a significantly higher specific bacterial diversity, which was associated with a greater number of and diversity between predicted functions than that of the GC and G samples. While the Saprospiraceae appeared to be a constitutive part of the microbiota of the three stages, Flavobacteriaceae were very specific to the tetrasporophyte, but their functions for this stage remain to be determined. Finally, this study provided cues that could help in understanding the processes that take place throughout the life cycle of *A. armata* by building a hypothesis regarding the different energetic investments between cystocarps development, the production of halogenated molecules and bacterial community dynamics.

2.7 Acknowledgements

This work was supported by the Occitanie Region, France. Authors would like to thank Guillaume Iwankow for providing algae samples from Mo'orea. The LC-Q/Orbitrap methods developments and analyses were performed using the Biodiversité et Biotechnologies Marines (Bio2Mar) facilities – Métabolites Secondaires Xénobiotiques Métabolomique Environnementale (MSXM) platform at the Université de Perpignan Via Domitia (<https://bio2mar-msxm.univ-perp.fr/>).

3. Ce qu'il faut retenir

L'objectif du travail réalisé dans ce chapitre était d'étudier les variations du métabolome, des activités antibactériennes et de la composition de la communauté bactérienne de trois stades du cycle de vie *d'A. armata* (gamétophyte, gamétophyte avec cystocarpes développés et tétrasporophyte). Pour cela, des échantillons des trois stades (x5 pour chaque stade) ont été collectés à Banyuls-sur-Mer en mai 2022. Le métabolome a été étudié en LC-HRMS tandis que la composition de la communauté bactérienne a été étudiée par métabarcoding.

Les principaux résultats sont :

(1) Les trois stades du cycle de vie ont une composition chimique différente. Les molécules bromées de faible masse moléculaire comme l'acide dibromoacétique et l'acide bromochloroacétique sont plus abondantes dans le gamétophyte avec des cystocarpes développés (GC) que dans les deux autres stades. Des molécules comportant un nombre plus important d'halogènes (ex : $C_5H_2Br_6O_2$ et $C_5H_2Br_5ClO_2$) sont abondantes dans les extraits du gamétophyte (G) et du térasporophyte (T). Enfin quelques molécules comme le tribromoacetate de pentabromopropen-2-yle ($C_5Br_8O_2$) sont particulièrement présentes dans T et proches du seuil de détection dans GC et G.

(2) Les extraits des trois stades du cycle de vie montrent des activités antibactériennes contre les six espèces de bactéries, à l'exception des extraits de GC et G qui sont inactifs contre *Lactococcus garvieae*. Les activités antibactériennes mesurées sont significativement différentes entre les différents stades du cycle de vie *d'A. armata* contre 4 bactéries. En particulier, T présente une activité antibactérienne plus importante que GC contre les espèces *Edwardsiella angillarum* et *Yersina ruckeri*.

(3) Plusieurs molécules correspondant à des pentan-2,4-diones polyhalogées et dérivés, de formules brutes $C_5H_3Br_4ClO_2$, $C_5H_2Br_5ClO_2$, $C_5H_2Br_6O_2$, $C_5H_3Br_5O_2$ mais aussi $C_4H_3Br_3O_3$ sont fortement corrélées à l'activité des fractions d'algue.

(4) T présente une diversité spécifique de sa communauté bactérienne plus importante que les deux autres stades dont les communautés bactériennes ne sont pas différentes. De manière générale, les Flavobacteriaceae sont particulièrement abondantes dans T et les Thiotrichaceae sont abondantes dans G et GC. Parmi les ASVs abondants et discriminants des différents stades de vie, les Flavobacteriaceae, les Granulosicoccaceae et les Cellvibrionaceae sont discriminants de T, GC et G respectivement.

(5) Le métabolome et la composition bactérienne ne covarient pas entre les différents stades du cycle de vie de l’algue. L’analyse multi-omique supervisée a mis en évidence des corrélations positives et négatives entre certains genres bactériens dans les différents stades de l’algue et certaines molécules halogénées mais aussi non halogénées. En particulier, le pentabromopropen-2-yl tribromoacétate ($C_5Br_8O_2$), négativement corrélé à des ASVs abondants chez G. Certaines fonctions prédictes de la communauté bactérienne de G sont associées à des haloacétate déhalogenases.

4. Résultats non intégrés à l'article

En comparant les gamétophytes des deux espèces (**Chapitre I**), nous avons observé que le pentabromopropen-2-yl tribromoacetate était détecté uniquement chez *A. taxiformis*. En analysant les différents stades de vie d'*A. armata*, nous avons observé ce composé dans le térasporophyte (**Chapitre III**). Il paraissait donc intéressant de vérifier la présence de cette molécule dans le térasporophyte d'*A. taxiformis*. Pour cela, des échantillons de térasporophytes et gamétophytes (avec des cystocarpes développés) d'*A. taxiformis* ont été collectés par Jean-Pascal Quod à la Réunion. Les échantillons ont été extraits et analysés selon les protocoles utilisés dans cette thèse (**Chapitre I et III**). La molécule a été détectée à des intensités équivalentes dans les deux stades d'*A. taxiformis* (**Figure 27, Figure 28**). On peut donc penser qu'il existe au stade gamétophyte d'*A. armata*, des processus qui aboutissent à l'altération de la voie de biosynthèse du pentabromopropen-2-yl tribromoacetate ou à sa dégradation. Des analyses de transcriptomique pour comparer l'expression des gènes liés aux halopéroxydases (biosynthèse) et aux déhalogénases (dégradation) entre les différents stades du cycle de vie d'*A. armata* pourraient apporter des éléments d'information quant au(x) processus impliqué(s).

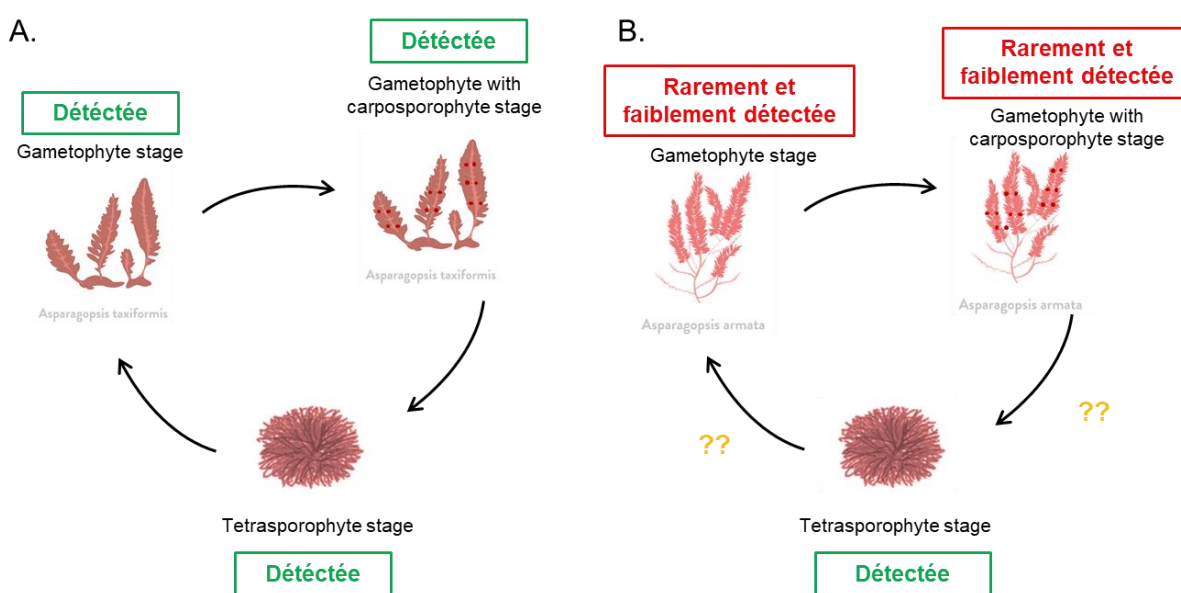


Figure 27 : Schéma général de détection de la molécule ($C_5Br_8O_2$) dans les différents stades de vie d'*A. taxiformis* (A) et *A. armata* (B).

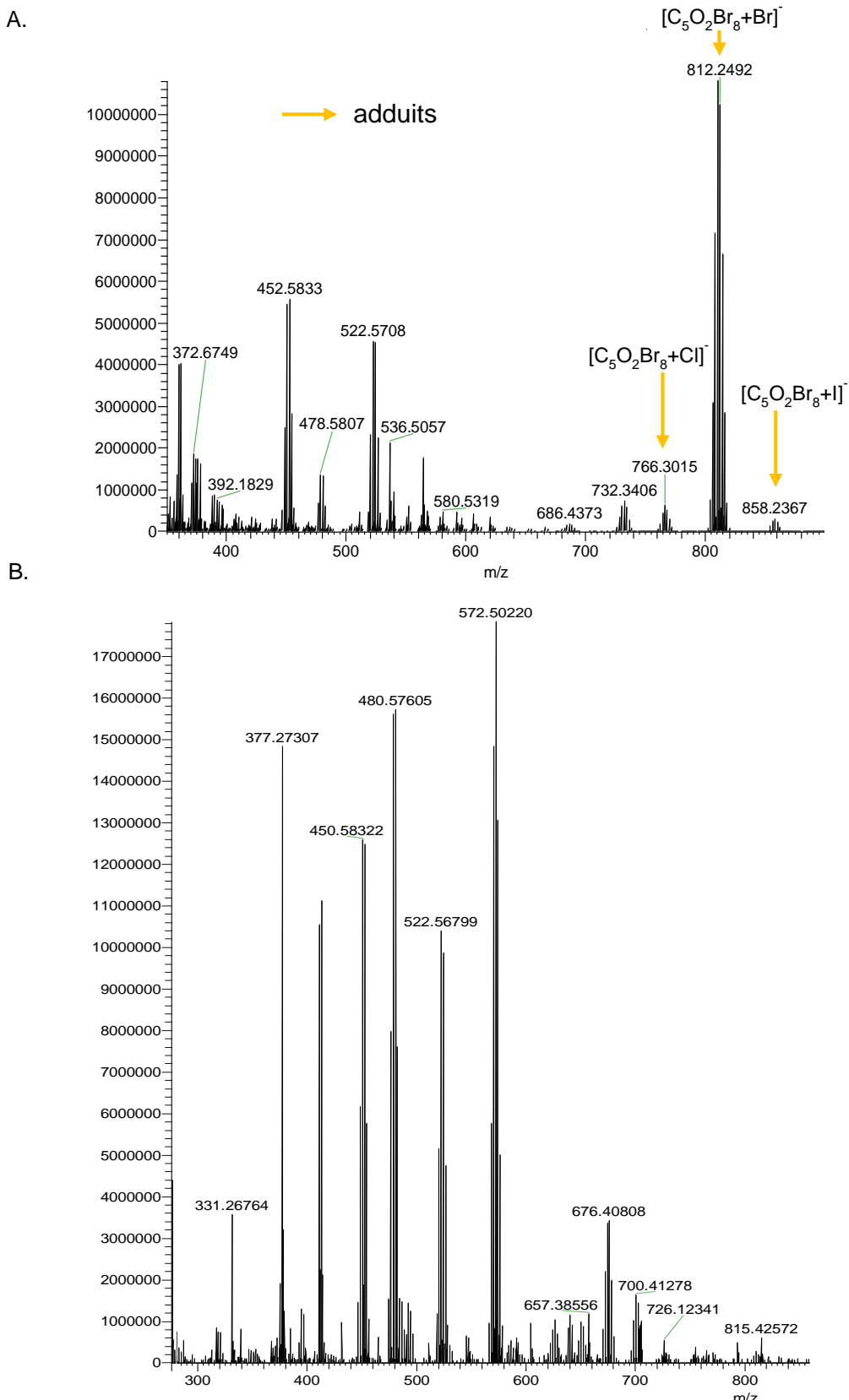


Figure 28 : Spectre de masse présentant des fragments caractéristiques et des ions pseudomoléculaires de la molécule $C_5Br_8O_2$ purifiée et avec des conditions d'analyses optimisées (A) et spectre de masse présentant des fragments caractéristiques de la molécule $C_5Br_8O_2$ en mélange dans un extrait d'un tétrasporophyte d'*A. taxiformis* collectée à la Réunion (B).

Chapitre IV : *Asparagopsis* spp. comme complément alimentaire pour une espèce en danger critique d'extinction ? Effet sur l'anguille européenne (*Anguilla anguilla*) et sur ses pathogènes



Illustration à l'aquarelle des interactions algue-parasite et algue-anguille, réalisée par
Michèle Parchemin

1. Avant propos

Asparagopsis spp. as feed supplement for a critically endangered species? Effect on the European eel (*Anguilla anguilla*) and on its pathogens

Christelle Parchemin, Gaël Simon, Edouard Jobet, Cristian Chaparro, Marie-Christine Carpentier, Elsa Amilhat, Nathalie Tapissier-Bontemps, Pierre Sasal, Elisabeth Faliex

Publication

L'article est en préparation en vue d'une soumission dans le journal *Fish and Shellfish Immunology*.

Parchemin, C., Simon, G., Jobet, E., Chaparro, C., Carpentier, M., C., Amilhat, E., Tapissier-Bontemps, N., Sasal, P., and Faliex, E., (2023). *Asparagopsis* spp. as feed supplement for a critically endangered species? Effect on the European eel (*Anguilla anguilla*) and on its pathogens. Soumission prevue dans *Fish and Shellfish Immunology*. IF : 4.622

Contexte

Comme explicité dans l'**Etat de l'art (revue)**, il existe un réel enjeu pour le développement d'alternatives aux antibiotiques permettant de traiter les pathogènes, particulièrement en aquaculture. Parmi celles proposées, la vaccination est possible, mais cette solution permet de lutter contre un nombre limité de pathogènes, bien que des vaccins « multi-cibles » soient développés. Le développement de préparations à base de produits naturels ajoutés à l'alimentation des poissons pour stimuler leur immunité et augmenter leur résistance aux maladies, est une seconde alternative. Il existe déjà quelques études sur l'impact de ce type d'alimentation sur l'anguille mais ces études concernent principalement l'anguille japonaise. De plus, aucun de ces travaux n'a étudié l'effet de ce type d'alimentation sur des pathogènes autres que d'origine bactérienne.

Dans les **Chapitres I et III** j'ai pu montrer l'activité des extraits d'*A. armata* et d'*A. taxiformis* contre des bactéries avérées pathogènes de l'anguille européenne telles que *Edwardsiella angillarum*, *Lactococcus garvieae*, *Pseudomonas anguilliseptica*, *Tenacibaculum maritimum*, *Vibrio angillarum*, *V. harveyi* et *Yersina ruckeri*, ainsi que l'absence de variations saisonnières

de ces activités. *Asparagopsis armata* et *A. taxiformis* ont aussi déjà été incorporées dans l'alimentation de poissons d'intérêt aquacole comme la daurade, le platax ou le saumon. Des résultats prometteurs ont été recensés avec, par exemple, une croissance des poissons plus importante, une surexpression de certains paramètres liées à l'immunité ou encore une diminution du nombre d'espèces bactériennes potentiellement pathogènes dans les intestins des poissons traités.

Ainsi, l'objectif du travail présenté dans ce chapitre est, tout d'abord, de compléter les études sur l'effet *in vitro* d'extraits des deux espèces du genre *Asparagopsis* sur les pathogènes de l'anguille européenne des **Chapitres I et III** par leur effet sur le parasite *Anguillicola crassus*, un autre pathogène de l'anguille européenne. Puis, d'évaluer *in vivo* l'effet d'une alimentation complémentée en algue sur la physiologie de l'anguille européenne, au travers de sa croissance et des changements au sein de son transcriptome, et sur *A. crassus* et *E. anguillarum*, au travers de la réussite d'infestation et le développement du parasite, et la résistance de l'anguille à l'infection bactérienne.

Méthodologie générale

Pour la réalisation des tests *in vitro* sur le parasite *A. crassus*, une extraction biphasique a été réalisée sur des échantillons d'*A. armata* collectés à Banyuls-sur-Mer et des échantillons d'*A. taxiformis* collectés à Moorea. Les parasites adultes ont été récupérés à partir d'anguilles sauvages infestées, pêchées dans la lagune de Canet. Le test a consisté à mettre les parasites en contact avec les extraits d'algues à différentes concentrations et à observer leur mouvement et leur mortalité par comparaison avec un contrôle. Etant limitée par le nombre de parasites disponibles et considérant que seules les phases apolaires ont montré une activité bactéricide, elles seules ont été testées sur le parasite.

Pour la réalisation des tests *in vivo*, deux expériences ont été réalisées au cours lesquelles des anguilles ont été nourries pendant quatre semaines avec une nourriture complémentée en poudre d'algue. Après quatre semaines, une partie des anguilles a été prélevée, mesurée et pesée avant congélation de leur corps à -80 °C pour la réalisation des analyses transcriptomiques. L'autre partie a été, soit infestée expérimentalement avec *A. crassus* (Expérience 1), soit infectée avec *E. anguillarum* (Expérience 2). Dans le cas de l'expérience 1, après 6 semaines post-infestation, les anguilles ont été pesées, mesurées, sacrifiées, les vessies gazeuses ont été prélevées, et les corps des anguilles (moins leur vessie gazeuse), ont été conservés à -80 °C. Les vessies gazeuses ont été disséquées sous loupe binoculaire et le nombre de parasites, leur sexe ainsi que leur

stade de développement ont été déterminés afin d'évaluer l'effet de l'algue sur la réussite de l'infestation et le développement du parasite. Dans le cas de l'expérience 2, un suivi de la mortalité des anguilles post-infection a été réalisé pendant une semaine afin d'évaluer l'effet préventif d'une nourriture complémentée avec l'algue sur le pathogène bactérien. L'effet de l'algue sur la physiologie de l'anguille a été évalué aux travers de paramètres de croissance (gain de taille et de poids) et d'une analyse transcriptomique.

Contribution des auteurs

J'ai réalisé avec l'aide de Gaël Simon (et avec l'appui de Pierre Sasal, Elisabeth Faliex et Nathalie Tapissier-Bontemps) l'élevage des anguilles de 2020 à 2021. J'ai réalisé les extractions d'algues pour les tests *in vitro* et mis au point le protocole de test sur le parasite. J'ai réalisé avec Gaël Simon et Edouard Jobet les pêches de copécopes à Villeneuve de la Raho pour le déroulement du cycle expérimental du parasite. Les infestations des copécopes avec le parasite *A. crassus* puis des anguilles, ainsi que les infections bactériennes ont été réalisées en équipe avec l'ensemble des co-auteurs (sauf Marie-Christine Carpentier et Cristian Chaparro). Le sexe et le stade de développement de chaque parasite a été déterminé par Elisabeth Faliex. J'ai effectué l'ensemble des analyses statistiques sur les données issues des différentes expériences citées ci-dessus. Les extractions d'ADN pour les analyses transcriptomiques ont été réalisées par Edouard Jobet. Le séquençage a été réalisé sur la plateforme Bioenvironnement de l'Université de Perpignan *Via Domitia*. Les pré-traitements et analyses bioinformatiques des données transcriptomiques ont été réalisés par Marie-Christine Carpentier et Cristian Chaparro. Enfin, j'ai réalisé l'ensemble des interprétations avec l'appui de Nathalie Tapissier-Bontemps, Pierre Sasal et Elisabeth Faliex.

Disponibilité des données

Les données brutes issues du séquençage seront déposées sur Sequence Read Archive et rendues publiques dès soumission de l'article.

Annexes

Les « Supplementary Materials » relatifs à ce chapitre débutent à la page **379** de ce manuscrit (Annexes ; 4. Annexe Chapitre IV).

2. Article

Asparagopsis spp. as feed supplement for a critically endangered species? Effect on the European eel (*Anguilla anguilla*) and on its pathogens

Christelle Parchemin *^{1,2}, Gaël Simon², Edouard Jobet¹, Cristian Chaparro³, Marie-Christine Carpentier⁴, Elsa Amilhat², Nathalie Tapissier-Bontemps¹, Pierre Sasal¹, Elisabeth Faliex²

¹Centre de Recherches Insulaires et Observatoire de l'Environnement (CRIOBE), UAR 3278 UPVD-EPHE-CNRS, Université de Perpignan - Via Domitia, 52 Av. Paul Alduy, 66860 Perpignan CEDEX, France

²CEntre de Formation et de Recherche sur les Environnements Méditerranéens (CEFREM), UMR 5110 UPVD-CNRS, Université de Perpignan - Via Domitia, 52 Av. Paul Alduy, 66860 Perpignan CEDEX, France

³Interaction Hôtes Pathogènes Environnement (IHPE), UMR 5244, Université de Montpellier-CNRS-Ifremer-UPVD, Université de Perpignan - Via Domitia, 52 Av. Paul Alduy, 66860 Perpignan CEDEX, France

⁴Laboratoire Génome et Développement des Plantes (LGDP), UMR 5096, UPVD-CNRS, Université de Perpignan - Via Domitia, 52 Av. Paul Alduy, 66860 Perpignan CEDEX, France

2.1 Abstract

Anguilla anguilla is a critically endangered fish species. Infection by pathogens is considered a factor in the collapse of the eel population in the wild and a cause of losses in aquaculture. The use of plants and algae as immunostimulant to prevent diseases has received a growing interest these last years. In this context, we studied the potential effects of *Asparagopsis* spp. *in vitro* and *in vivo* on two pathogens of the European eel: *Anguillicola crassus* and *Edwardsiella anguillarum* and as immunostimulant through a transcriptomics analysis. *In vitro*, the survival of the parasite was heavily impacted by extracts of *A. armata* and *A. taxiformis*. *In vivo*, the algal supplemented diet had a negative impact on eel growth compared to a classic diet. When eels were challenged with a culture of *E. anguillarum*, we observed a tendency to delay mortality in eels fed with both algae. Then, we observed a higher infestation success both in terms of mean number of total parasites and mean number of larvae in eels fed an algal supplemented diet than in eels fed with a classic diet. This, combined with transcriptomics results, revealed that eels devote more energy on the detoxification processes related to their adaptation to the algal supplemented diet than on immunity. While there has been growing interest in the use of algae as an immunostimulant solution for aquaculture, few studies have so far investigated the impact of such feeding on pathogens other than bacteria. This is the first

time that the impact of an algal supplemented diet on the success of infestation and development of *A. crassus* has been reported.

Keywords: transcriptomics, growth, immunostimulation, disease, *Edwardsiella angillarum*, *Anguillicola crassus*

2.2 Introduction

The European eel *Anguilla anguilla* is a critically endangered species (Pike et al., 2020). Infection by pathogens (macroparasites, bacteria or viruses) is one of the plausible factors for the collapse of the eel population (Esteve and Alcaide, 2009; Kirk, 2003; van Beurden et al., 2012). Among pathogens, the bacterium *Edwardsiella angillarum* and the nematode parasite *Anguillicola crassus* are regularly cited to have deleterious effects on eel health (Alcaide et al., 2006; Joh et al., 2011; Kirk, 2003; Molnár et al., 1991). *Edwardsiella angillarum* is responsible for Edwardsiellosis causing hemorrhages, ulcerations, and septicemia (Griffin et al., 2020; Mohanty and Sahoo, 2007). *Anguillicola crassus* is a hematophagous nematode, originally a parasite of the swimbladders of Japanese eels, which was introduced into Europe in the 1980s (Koops and Hartmann, 1989). The parasite affects swimming, migration and breeding abilities through damages to the swimbladder (inflammations, reduction of elasticity and thickening) (Barry et al. 2014; Kirk 2003; Palstra et al. 2007). Both pathogens can cause damages to wild and farmed eels, causing a global weakening of the population and significant economic losses for eel farmers (Joh et al., 2011; Molnár et al., 1991; Sjöberg et al., 2009; van Banning and Haenen, 1990).

To treat these diseases, the classical approaches consist in chemical administration (antibiotics, antiviral and antiparasitic agents) through food or “bath” (Parchemin et al., 2022). These methods present high efficiency but studies highlighted that chemicals can induce pathogen resistances, impact fish and be ineffective in the long term (Buchmann 2011; Mellergaard 1990; Santos and Ramos 2018). In addition, treatments may be short-lived, only reducing the infection which will resume when they are stopped (Geets et al. 1992; Mellergaard 1990;). Finally, the use of chemicals can lead to the release of products and/or their persistence in the environment (Gothwal and Shashidhar 2015; Preena et al. 2020; Weston 1996). Thus, alternative treatment methods have been developed. Among them, vaccination and the development of plant-based preparations have received a growing interest since they could prevent diseases and also have less detrimental consequences on the environment (Gudding and Van Muiswinkel, 2013; Reverter et al., 2014, 2021). Vaccination has been used to prevent infection and development

of both *E. anguillarum* and *A. crassus* in *A. japonica* and *A. anguilla* (Guo et al., 2019; Knopf and Lucius, 2008; LiHua et al., 2019). Most recently developed vaccines consist of bacteria formalin killed cells, inactivated cells, but also specific outer membrane protein (OmpA of *E. anguillarum*) (Parchemin et al., 2022). Although the results were encouraging, with a reduction in mortality of up to 90% of eels infected with *E. anguillarum* after vaccination, in some cases the reduction was only 10% (He et al. 2021; Hossain et al. 2012; Jun et al. 2020; Jung et al. 2015; LiHua et al. 2019). To date, only one study has addressed the development of a vaccine against *A. crassus* by attenuating infective larvae (L3) using ¹³⁵Cs irradiation. The number of *A. crassus* adults was significantly reduced in immunized *A. japonica* but the treatment did not appear to be effective for *A. anguilla* (Knopf and Lucius, 2008). Thus vaccines may not be as efficient as chemical treatments, and studies on long-term effects are still sparse.

The use of plants, probiotics or natural products has increased exponentially in the last decades (Reverter et al., 2014). They can improve the growth of fish but also their immunity and thus protection against bacterial pathogens and parasites (Reverter et al., 2014, 2021). The potential of diet supplementation has also been explored on *Anguilla* spp., mainly on *A. japonica* but much less on *A. anguilla* (Parchemin et al., 2022). Probiotics and plants including probiotic bacteria (Chang and Liu, 2002; Lee et al., 2013, 2017), association of a bacterium and mannooligosaccharides (Lee et al., 2018), alternative protein sources (Garcia-Gallego et al., 1998), and various other natural product derivatives (Bae et al. 2008, 2012; Choi et al. 2008; Huang et al. 2020; Lee et al. 2018) have been tested. Various protocols were used with a feeding duration ranging from 2 to 20 weeks. In general, eels fed a supplemented diet and infected with a bacterial pathogen (*E. anguillarum*, *Vibrio anguillarum* or *Aeromonas hydrophila*) showed lower mortality rates than those whose diet was not supplemented. To date, no studies have investigated the effects of such feeding on viral or parasitic pathogens in eels.

Terrestrial plants are by far the most studied plants but the increased knowledge and accessibility of seaweed has also made it possible to test their effects as a dietary supplement for aquaculture (Thanigaivel et al., 2016). Thus, the number of studies using algae has also increased exponentially (Reverter et al., 2021). Algae are sources of proteins, dietary fibers, vitamins and minerals (Burtin, 2003; Wan et al., 2019). They also produce a wide variety of compounds, including secondary metabolites with activities against various pathogens (Shanmughapriya et al., 2008; Vatsos and Rebours, 2015). The critical point in the use of algae for aquaculture remains their availability. This is why invasive or cultivated algae are good candidates. The most studied algae species are *Sargassum* spp., *Ulva* spp. and *Grateloupia* spp.

Other studies include algae of the genus *Fucus* spp. or *Asparagopsis* spp. *Asparagopsis* genus contains two red algae species, *Asparagopsis armata* and *A. taxiformis*, both particularly interesting for aquaculture. They are invasive and their cultivation is already practiced in the wild (France) or is in development in several countries over the world (Pinteus et al., 2018; Zanolla et al., 2022a). They are also known for their *in vitro* antibacterial or antiparasitic activities (Bansemir et al. 2006; Genovese et al. 2009, 2012; Manilal et al. 2009; Marino et al. 2016; Pinteus et al. 2015; Soler et al. 2007; Vitale et al. 2015). Some studies have already used these algae in diet or balneation for fish (*Salmo salar*, *Siganus fuscescens*, *Sparus aurata*, and *Platax orbicularis*) (Castanho et al., 2017; Marino et al., 2016; Reverter et al., 2016; Thépot et al., 2021a, 2021b, 2022), and shrimp (Manilal et al., 2013). Enhanced growth rate, food intake and immune response were observed (Reverter et al., 2016; Thépot et al., 2021a, 2021b, 2022).

Thus in this study, we investigated the *in vitro* effects of both *A. taxiformis* and *A. armata* extracts on *A. crassus* survival. We also studied the potential protective and immunostimulant effects of *A. taxiformis* supplemented diet on European eel specimens through growth parameters and transcriptomic analysis as well as its impact on infestation success and development of *A. crassus* and on survival of eels after *E. anguillarum* infection.

2.3 Materials and methods

2.3.1 Rearing of eels

Parasite-free glass eels (from the same cohort, average weight 0.2 g/individual) were caught in February 2020 at the Grau de La Fourcade (lat. 43.456694°, long. 4.444013°) (East of the town of Saintes-Maries-de-la-Mer and West of the Rhône delta) by the “Observatoire des poisons migrateurs amphihalins Rhône-Méditerranée”. Glass eels were brought back to the lab in oxygenated tanks and transferred to aquaria (25 and 50 L) filled with artificial seawater (15 g/L using Instant Ocean – Aquarium systems Salt) for rearing. Room temperature was maintained at 25 °C for a water temperature around 19 °C. The photoperiod was modelled on the natural day and night periods. Water from each aquarium was filtered through a biological filter. Eels were fed daily to satiation with nauplii of artemia (*Artemia salina*) raised *in house* from commercial eggs (Ocean Nutrition). After few weeks of rearing, bloodworms (Ocean Nutrition) were included in the feed in order to gradually reduce the amount of artemia nauplii. Then in a same way, commercial fish pellets (Inicio plus M, Biomar) were included in the food and were mixed with bloodworms to form a paste. Eels were raised in this way for about 15 months to reach an average size of 14/15 cm and an average weight of 4/5 g before experimental

treatments (algae supplemented diet and/or experimental infections). The eels must be large enough to be infested by the parasitic nematode *A. crassus*. At each sampling point during the experiments, eels were put to sleep in water containing eugenol (5 mL eugenol (Sigma-aldrich®) diluted to 30 % in ethanol per 10 L water) then either woken up in oxygenated water (after infestation for example) or killed by overdosing with the same anesthetic for dissection and analytical processing.

2.3.2 Collection and extraction of algae

In vitro assays were performed with *A. taxiformis* collected in Moorea (lat. -17.48262°, long. -149.87213°) in September 2019 and *A. armata* collected in April 2019 in Banyuls (lat. 42.482230°, long. 3.137175°). Algae extracts were used for *in vitro* assays. The ground algae (20 g) were extracted as described in (Parchemin et al., 2023, minor revision). Briefly, a biphasic extraction method was used, ground algae samples were extracted with a mixture of Methanol (MeOH, HPLC grade, VWR™, Fontenay-sous-Bois, France) and Methyl tert-butyl ether (MTBE, HPLC grade, Honeywell Riedel de Haen™) and vortexed. Then, H₂O (HPLC grade VWR™, Fontenay-sous-Bois, France) was added and the whole solution was vortexed. Extraction was performed in an ultrasonic bath and the final mixture was centrifuged to obtain two phases. The apolar and polar phases were separately collected. Solvent was evaporated using a centrifugal vacuum evaporator GENEVAC EZ-2™ (SP Scientific, Warminster, PA 18974, USA) and solubilized in 100 % dimethylsulfoxide (DMSO, Honeywell Riedel de Haen™, Germany), for antiparasitic assays at three concentrations of 5, 50 and 100 mg/mL.

For *in vivo* assays, *A. taxiformis* was chosen instead of *A. armata* in regard of the *in vitro* results against *A. crassus* (cf. results) and following preliminary tests showing that appetite towards *A. armata* was lower than that towards *A. taxiformis* (unpublished data). Assays were performed with *A. taxiformis* collected in February 2021 in Moorea (lat. -17.48262°, long. -149.87213°). After collection, the algae was lyophilized, ground to obtain a homogeneous powder and stored at -20 °C until use. Due to practical aspects and available material, we decided to use ground algae instead of bioactive extracts for *in vivo* assays.

2.3.3 Antiparasitic activity of algae against *A. crassus*

2.3.3.1 *In vitro* experiments

Adult worms were isolated from naturally infected eels (Canet lagoon, France). Parasites were sexed and five parasites were randomly (with a constant number of male and female in each

conditions to avoid sex bias) deposited in petri dishes containing 20 mL of distilled water with 8 g/L NaCl. Then, 0.2 mL of extracts were added to the plates for a final concentration of 1 mg/mL, 0.5 mg/mL and 0.05 mg/mL and 10% DMSO. DMSO and NaCl solution (8 g/L) were used as negative control. Due to the limited number of parasites available, only apolar phases, already known for their antibacterial activities (Parchemin et al., 2023, minor revision), were tested. Movements of parasites were observed every 20 min for two hours (if necessary the Petri dished were gently shake to induce movement) and parasites were considered dead after two observations without movements. Then, the impact of the different treatments on the survival of parasites was studied (RStudio environment v2022.02.3 (R v4.2.0)) by creating a survival object and plotting it using the Kaplan-Meier method (Packages {survminer} (Kassambara et al., 2017) and {survival} (Therneau and Lumley, 2015)). Differences between survival curves graphs were assessed with a Pairwise Log-Rank test using the “pairwise_survdiff” function {survminer}.

2.3.3.2 *In vivo* experiments

2.3.3.2.1 Experimental design 1

Before the start of the experiment and after the rearing period, the absence of the parasite *A. crassus* was confirmed by sacrificing 18 eels and examining their swimbladders. Then, 234 eels were distributed in 18 aquaria of 50 L (13 eels/aquarium) divided into nine aquaria with a classic diet and nine others with an algal supplemented diet (**Figure 1A**). The diet consisted of a mixture of bloodworms and ground fish pellets (proportion 1:1) to which 3 % of *A. taxiformis* powder was added in the case of supplemented diet (concentration determined through preliminary (not published) experiments and previously published protocol) (Reverter et al., 2016; Thépot et al., 2022). Five grams of the paste (classic or algal supplemented diets paste depending on the experimental condition) were distributed in each aquarium. After four weeks of feeding (T4), three eels per aquarium of the two types of diets were randomly sampled (54 in total). Eels were measured and weighed, and swimbladders dissected and examined to confirm the absence of *A. crassus*. The remaining whole body of each eel was then labeled, immersed in liquid nitrogen and stored at -80°C for transcriptomic analyses. Then, 120 eels (60 from the supplemented and 60 from the classic diet) were experimentally infested with *A. crassus* (see 2.3.3.2.2 “Experimental life cycle of *A. crassus* and eel infestation protocol”) and were distributed in 12 aquaria of 50 L (10 eels/aquarium). Of these aquaria, eels from six aquaria were fed the supplemented diet and eels from the others six aquaria were fed the classic diet, resulting in the conditions APA and CPA and APC and CPC respectively (A= algal; C= classic;

P= parasitized) (**Figure 1A**). Eels not experimentally infested with *A. crassus* (30 from the supplemented and 30 from the classic diet) were distributed in six aquariums giving the AC and CC conditions (**Figure 1A**). From this point and after six weeks of rearing (T10), 10 eels from each aquarium were sampled and processed as explained above.

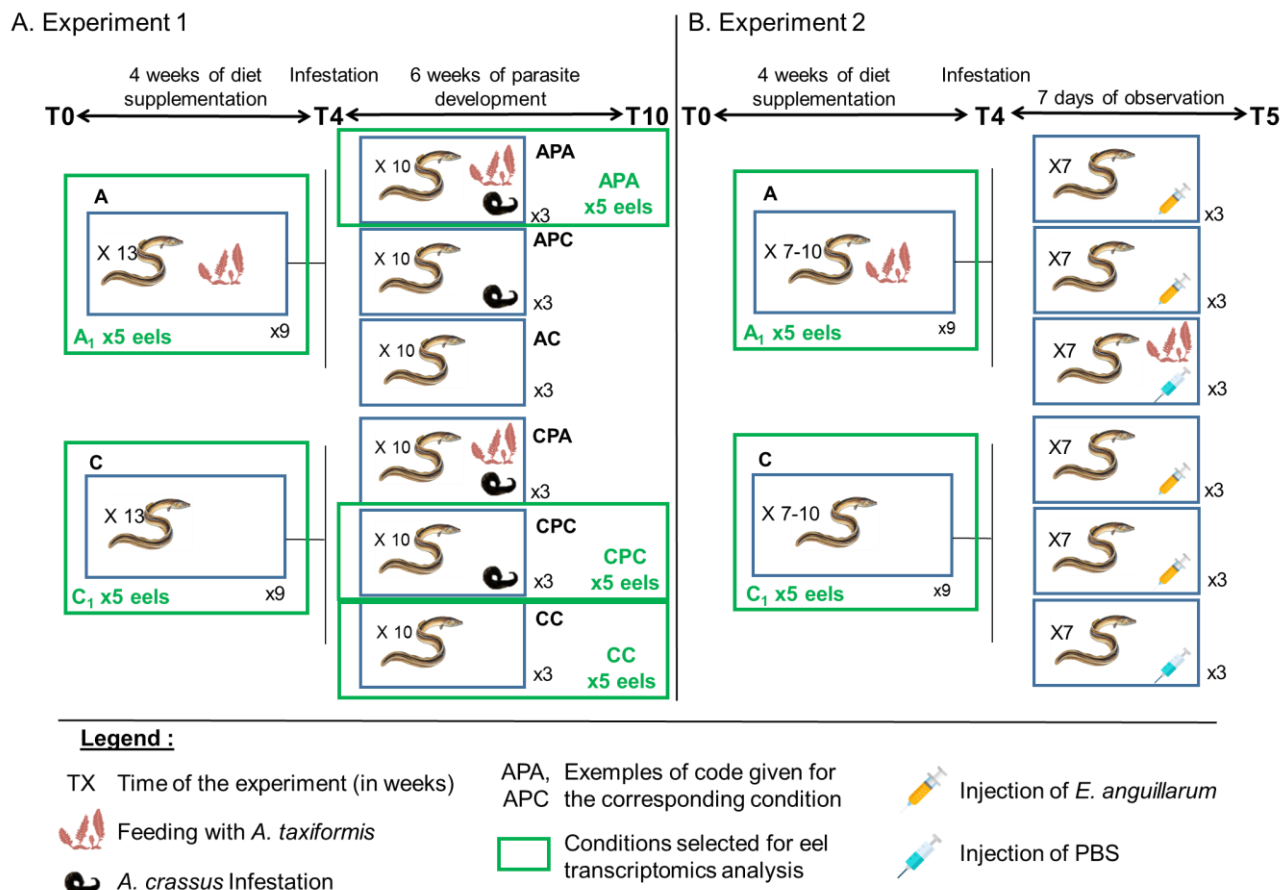


Figure 1: Experimental design for the *in vivo* studies of an algal supplemented diet on *A. crassus* (A) and *E. anguillarum* (B).

2.3.3.2.2 Experimental life cycle of *A. crassus* and eel infestation protocol

For the experimental infestation of eels, *A. crassus* larvae (L2) and eggs were isolated from naturally infected eels (provided by a fisherman from Canet lagoon, France). Eggs were incubated at 25 °C for 48 h to allow hatching. Copepods, first intermediate host of *A. crassus* life cycle, were collected in the lake of Villeneuve-de-La-Raho (lat. 42.628158°, long. 2.893990°), maintained in aquarium and fed with paramecia. Batches of 15 copepods were each placed in contact with 150 L2 larvae for 24 hours to allow infestation. Infected copepods were incubated at 25 °C for two weeks to allow development from L2 to L3 stage. Development to

the L3 stage was checked under the microscope and confirmed by the presence of a sclerified brace-shaped structure at the anterior end of the larvae, the so-called "mouth ornamentation" (Blanc et al., 1992). Then, copepods were lightly crushed to release the L3s. From there, 20 L3 larvae in 0.2 mL of saline solution were injected using a syringe equipped with a flexible cannula into the stomach of each eel previously anaesthetised. The eels were then quickly returned to their respective aquaria to allow them to wake up. Saline solution (0.2 mL) without parasites was injected in control eels.

2.3.3.2.3 Infestation success and parasite development

Swimbladders were sampled at T0, T4 and T10. The presence or absence of the parasite was observed under a stereomicroscope. In each sampled swimbladder, the total number and the developmental stage (Adults, L4, L3) of parasites were determined. Adults were sexed and attributed to male, female or undeterminable (in cases where sexes could not be determined because not clearly observable) sex groups. Necrotic parasites were also observed and considered as a group. The developmental stage of females and males was also assessed. Females were classified as gravid (uterus full of developing embryos to eggs containing L2), early-gravid (uterus containing only a few developing embryos and no eggs), non-gravid (young female with empty uterus) and males as young (rather small individuals, shortly after the last moult, whose digestive tract is not yet completely filled with digested blood) and mature (rather large individuals whose digestive tract is full of digested blood).

The differences in:

-Percentage of eels parasitized (%) = (Number of parasitized eels in one condition / Total number of eels in the condition) x 100

-Mean number of parasites per eel = Total number of parasites in one condition / Total number of eels in the condition

-Average infestation success (%) = [Total number of parasites in one condition /(Total number of eels in the condition x 20_{parasites deposited in stomach}] x 100

between the four conditions (APA, APC, CPC and CPA) were assessed in pairs, following a Shapiro test to evaluate the normality of residuals, using a Wilcoxon rank test (wilcox.test {stats}).

For the following statistical analyses, eels that were experimentally infested but had no parasites in their swimbladder were removed, so that statistical analyses were performed on eels exhibiting at least one parasite. The differences in the mean number of parasites according to their sex or stage of development (Total, TotalAdults, Female, Male, Undeterminable, Necrotic,

TotalLarvae, L3 and L4) between the different conditions APA, APC, CPC and CPA or , Classic and Algal supplemented diets were assessed with an ANOVA test followed by TukeyHSD post-hoc (aov {Stats}, TukeyHSD{PMCMRplus}) and a Student's t.test {stats} respectively. The differences in female or male development (Gravid, Early-Gravid, Non-Gravid, Mature male, Young male...) between the different conditions APA, APC, CPC and CPA or EarlySupplementation and NoorLateSupplementation were evaluated the same way. Barplots {ggplot2} (Wickham et al., 2016) were used for visual representation of the mean number of each parasite stage (\pm Standard Deviation (S.D.)) under the different conditions.

2.3.4 Antibacterial activity of algae against *E. anguillarum*

2.3.4.1 Experimental design 2

This experimental design 2 was performed in a similar way of the experimental design 1 but with 7-10 eels/aquarium of 25 L (**Figure 1B**). A total of 160 eels were distributed in 18 aquaria divided into nine aquaria with a classic diet and nine aquaria with an algal supplemented diet as described in “2.3.3.1”. However, unlike in “2.3.3.1”, the paste was distributed in each aquarium *ad libitum*. After four weeks of feeding (T4), 23 eels were sampled (11 on the classic diet and 12 on the supplemented diet) and the whole body (minus swimbladder) of each individual was labeled, immersed in liquid nitrogen and conserved at -80°C for transcriptomic analyses.

2.3.4.2 Bacterial challenge

An overnight culture of *E. anguillarum* diluted to reach 1×10^8 CFU.mL⁻¹ was centrifuged and resuspended in 1 mL of Phosphate Buffered Saline (PBS for cell culture, pH 7.4) (Sigma-aldrich®, Saint Louis, USA). In both feeding conditions, six eels died during the four weeks of feeding. On the remaining 137 eels, 78 were intraperitoneally injected with 0.1 mL/eel of the resuspended bacterial culture and distributed in 12 aquaria (7 eels/25 L aquarium) and 59 were intraperitoneally injected with 0.1 mL/eel of PBS and distributed in 6 aquaria (7eels/ 25 L aquarium) (**Figure 1B**). Eel mortality was monitored for 7 days.

2.3.5 Eels growth performance

The weight gain (WG), the size gain (SG) and the specific growth rate (SGR) related to size and weight were calculated according to the following equations:

$$\text{WG (\%)} = [(\text{final body weight} - \text{initial body weight})/\text{initial body weight}] * 100.$$

$$\text{SG (\%)} = [(\text{final size} - \text{initial size})/\text{initial size}] * 100.$$

$$\text{SGR}_{\text{weight}} (\% \text{ day}^{-1}) = [(\ln \text{ final weight} - \ln \text{ initial weight})/\text{number of days}] * 100.$$

$$\text{SGR}_{\text{size}} (\% \text{ day}^{-1}) = [(\ln \text{ final size} - \ln \text{ initial size})/\text{number of days}] * 100.$$

A Student's t.test was used to assess the differences in the above growth parameters between the eels fed the algal supplemented diet (A) and the eels fed with the classic diet (C).

2.3.6 Transcriptomic analysis

Transcriptomic analyses were performed on 35 eels of homogenous size and weight, in order to avoid growth bias, of the following conditions: eels fed an algal supplemented diet for four weeks (five eels "A₁" and five eels "A₂", **Figure 1A, B**), eels fed a classic diet for four weeks (five eels "C₁" and five eels "C₂", **Figure 1A, B**), eels experimentally infested and fed a classic diet for 10 weeks (five eels "CPC", **Figure 1A**), eels experimentally infested and fed an algal supplemented diet for 10 weeks (five eels "APA", **Figure 1A**), and not infested eels fed a classic diet for 10 weeks (five eels "CC" condition, **Figure 1A**). Eels infested with *A. crassus* were also selected according to the number of parasites in their swimbladder to maximize the effects on the parasite on the eel transcriptome and to facilitate interpretations.

Eel bodies (whole body minus swimbladder) were ground in liquid nitrogen using a TissueLyser (Qiagen). RNA was extracted by using TRIzolTM Reagent (InvitrogenTM) according to supplier's recommendations. RNA concentration and purity were checked using a Nanodrop ND-1000 spectrometer (Thermo Scientific), and their integrity was analysed by capillary electrophoresis on a BioAnalyzer 2100 (Agilent). RNA-seq library construction and sequencing as well as bio-informatics processing of the data were carried out by the Bio-environment platform (University of Perpignan, France). PolyA+ library was constructed using the NEBNext Ultra II Directional RNA library prep kit for Illumina (New England Biolabs) according to manufacturer's instructions, and sequenced on a NextSeq550 Instrument (single reads 75 bp).

For each library, reads were trimmed using Trimmomatic v0.39 (Bolger et al., 2014). Trimmed reads were mapped against *Anguilla* genome (GCF_013347855.1) with the gtf annotation file using Hisat2 v2.2.1 (Kim et al., 2019) with standard parameters. Only unique mapped reads were kept using samtools v1.13 with option '-q 10' (Danecek et al., 2021). Reads count by gene was performed by htseq-count in union v1.99.2 in 'union' mode (Anders et al., 2015). Differential expression analyses were performed using the Bioconductor R package DESeq2 (Love et al., 2014), with a false discovery rate of 0.05. P values were corrected for multiple tests by the Benjamin-Hochberg rule (adjusted P value).

A functional analysis was performed for the 31,062 genes present in the genome to identify biological functions enriched in the different conditions using Blastx (Camacho et al., 2009) against ncbi nr database and Interproscan (Paysan-Lafosse et al., 2023). These data were loaded into OmicsBox (Götz et al., 2008) where they were mapped and annotated producing the list of associated GO terms. A GO term enrichment analysis was performed using the GO_MWU program (Wright et al., 2015) using the $\log_{2}FC \geq \pm 1$ values and the absValue=1 while the authors suggested default values were kept for the other parameters.

2.4 Results

2.4.1 Effects of *Asparagopsis* sp. on eel pathogens

2.4.1.1 *In vitro* effects of *A. armata* and *A. taxiformis* extracts against *A. crassus*

The parasites survival was differently affected by the various treatments ($p <0.0001$) (**Figure 2A, B**). The survival curves of parasites in 8 g/L NaCl only or additionally exposed to 10 % DMSO were not significantly different ($p=0.6121$). For both algae species, the two highest extract concentrations (1 mg/mL and 0.5 mg/mL) had a negative impact on parasite survival. At a concentration of 1 mg/mL, the probability of parasite survival reached 0 after 30 min for *A. armata* and after 60 min for *A. taxiformis* (**Figure 2A, B**). At this concentration the effect on parasite survival did not differ between extracts of the two algae species ($p=0.9436$) (**Table S1**). At 0.5 mg/mL there was a significant difference on parasite survival between *A. armata* and *A. taxiformis* ($p<0.0001$) (**Figure 2A, B; Table S1**). Extract from *A. taxiformis* had a greater impact on the survival of *A. crassus* than that of *A. armata*. After 60 min of exposure, the probability of parasite survival reached 0 when exposed to 0.5 mg/ml of *A. taxiformis* extract while it was still close to 1 when exposed to the same concentration of *A. armata* extract (**Figure 2A, B**). The survival curves of parasites exposed to 1 mg/mL and 0.5 mg/mL of *A. taxiformis* extract were not significantly different ($p=0.0990$, **Table S1**). Finally, and for both algae species, the survival curves of parasites exposed to the lowest concentration of algal extract (0.05 mg/mL) did not differ significantly from each other and from the control and the solvent ($p=0.695$ and 0.276 for *A. armata*; $p=0.600$ and 0.966 for *A. taxiformis*, **Table S1**).

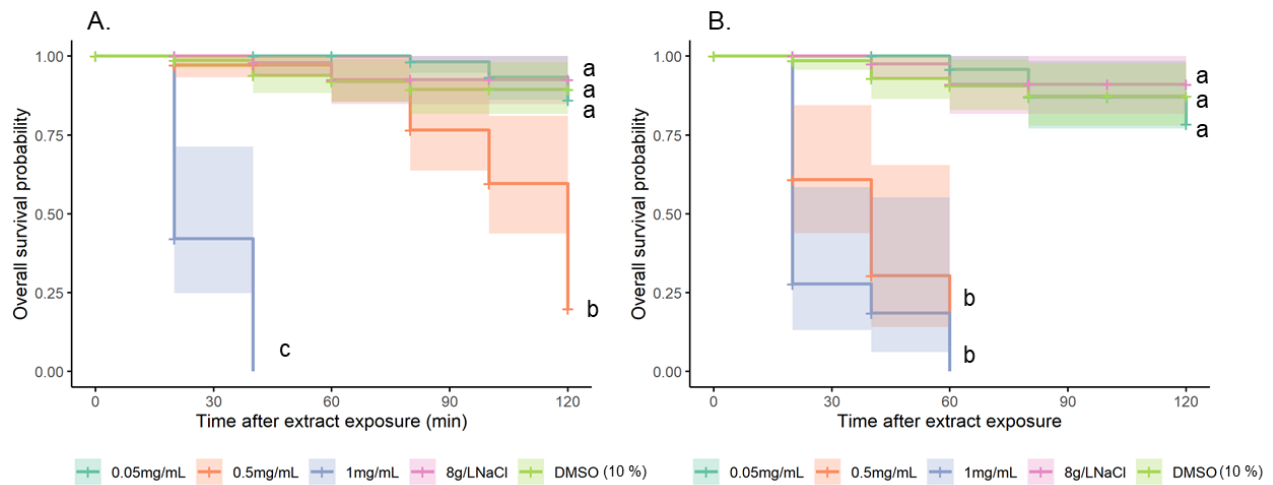


Figure 2: Kaplan-Meier survival curves of *A. crassus* adults in 8 g/L NaCl and exposed to different concentrations of *A. armata* extracts and 10 % DMSO (A) and of *A. taxiformis* extracts and 10 % DMSO (B). Letters indicate significant differences after a pairwise permutation test. Each treatment was carried out in triplicate.

2.4.1.2 *In vivo* effects of *A. taxiformis* supplemented diet on *A. crassus* infestation success and development

Eels were experimentally infested with *A. crassus* (20 L3 larvae per eel) four weeks after receiving an algal supplemented diet or a classic diet. Six weeks after infestation, eel swimbladders were collected and dissected to assess the impact of the different diets on infestation success and parasite development.

2.4.1.2.1 Infestation success

The percentage of parasitized eels were 97 %, 90 %, 87 % and 83 % for APA, APC, CPC and CPA respectively (**Table 1**). The mean number of parasites per eel and the mean infestation success were the lowest for the CPC group (3.5 ± 3.1 and 17.7 ± 15.3 % respectively) and the highest for the APA group (4.9 ± 3.4 and 24.7 ± 16.9 % respectively) without being significantly different (**Table 1**).

These conditions were then grouped into Algae (APA, APC, CPA) or Classic (CPC) and Early (APA, APC) or Late/No Supplementation (APC and CPC). The greatest difference in the percentage of parasitized eels was observed for the Early vs Late/No comparison with 93 % and 84.7 % of eels infested respectively. On the other hand, the greatest differences of the mean number of parasites per eel and in the average infestation success were observed for the Algae vs Classic comparison without being significant ($p=0.09$).

Table 1: Infestation success parameters

Condition	APA	APC	CPA	CPC	Algae ^a	Classic ^b	Early ^c	Late or No ^d
Percentage of parasitized eels (%) ^e	96.7	90	80	87	89.9	87	93	84.7
Mean number of parasites per eel ^f	4.9±3.4	4.7±3.6	4.5±4.1	3.5±3.1	4.7±3.7	3.5±3.1	4.8±3.5	4.0±3.6
Mean infestation success (%) ^g	24.7±16.9	23.3±18.1	22.6±20.4	17.7±15.3	23.5±18.3	17.7±15.3	24.0±17.4	20.08±18

^aAlgae condition includes APA, APC and CPA. ^bClassic condition includes CPC.^cEarly condition includes APA and APC. ^dLate or No includes CPA and CPC.^ePercentage of parasitized eels (%) = (Number of parasitized eels in the condition/Total number of eels in the condition) x100^fMean number of parasites per eel = Total number of parasites in one condition / Total number of eels in the condition^gAverage infestation success (%) = [Total number of parasites in one condition /(Total number of eels in the condition x 20_{parasites deposited in stomach}] x 100

2.4.1.2.2 Parasite development

At this point, eels that were experimentally infested but had no parasites in their swimbladder were removed from the analyses (1 APA, 3 APC, 5 CPA, 4 CPC), so that statistical analyses were performed on eels exhibiting at least one parasite. The effect of the different feed treatments on parasite development was studied. There was no difference in the mean number of total adult parasites in eels after the different feeding treatments ($p=0.91$) (**Figure 3A**). In a similar way, no significant difference was found for the mean number of female, male, undeterminable and necrotic parasites between the different feeding treatments ($p_{female}=0.18$, $p_{male}=0.38$, $p_{undeterminable}=0.72$, $p_{necrotic}=0.95$) (**Figure 3A**). Finally, the mean number of total larvae, as well as the mean numbers of L3 and L4, were not significantly different after the different feeding treatments ($p_{total larvae}=0.23$, $p_{L4}=0.57$, $p_{L3}=0.23$) (**Figure 3B**).

Then, we grouped data from the three diets including algal supplementation in order to study the overall impact of algal supplementation, irrespective of the timing of the supplementation. A tendency of a higher mean number of parasites in eels fed an algal supplemented diet was observed, but without being significant ($p=0.13$) (**Figure 3C**). No differences were found for any of the groups assigned to adults ($p_{adults Total}=0.55$, $p_{female}=0.81$, $p_{male}=0.56$, $p_{undeterminable}=0.81$, $p_{necrotic}=0.59$). The mean number of total larvae was significantly higher for eels fed an algal supplemented diet than those fed a classic diet (**p=0.026**) (**Figure 3D**). In particular, the number of L3 larvae was significantly higher in eels fed an algal supplemented diet than in those fed a classic diet (**p=0.016**) (**Figure 3D**). The same trend was observed for L4 larvae without being significant ($p=0.13$) (**Figure 3D**).

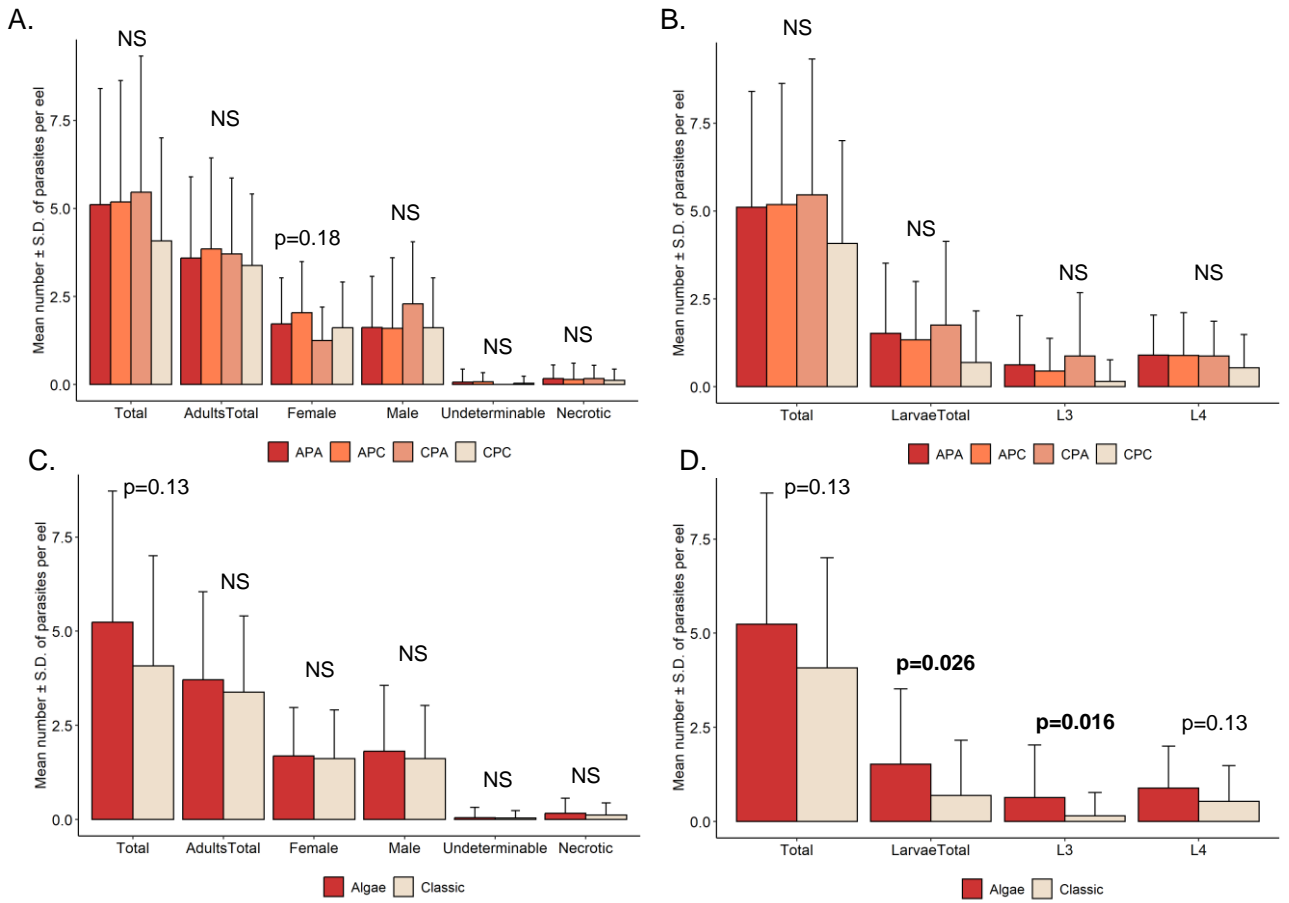


Figure 3: Mean number (\pm S.D.) of parasites per eel according to their development stage: adults (A, C) and larvae (B, D) fed the four different diet treatments (A, B), or grouped according to an algal diet or a classic diet (C, D). NS indicates not significant after either an ANOVA test (A and B) or a t-test (C and D). p -value under 0.2 are displayed and significant p -value (<0.05) are in bold.

Next, the developmental stages of male and female parasites were analysed. Females were divided into gravid, gravid at an early stage or non-gravid females, while males were divided in mature or young male (**Figure 4A, B**). The mean number of non-gravid females was significantly different between the different diet treatments (**$p=0.011$**). It was higher for the APC diet compared to CPA diet (**$p=0.015$**), and tended to be higher than the one of CPC diet ($p=0.09$). This number was clearly not different between APC-APA diet ($p=0.87$) and CPC-CPA ($p=0.83$). No significant differences were found for male development. We further explored the developmental stages of females and males by grouping conditions in “EarlySupplementation” (eels fed an algal supplemented diet four weeks before infestation, APA and APC) and “NoOrLateSupplementation” (eels fed a classic diet four weeks prior to infestation, and fed or not fed an algal supplemented diet after infestation, CPC and CPA) (**Figure 4C, D**). Using this grouping, we were able to detect that the mean number of non-gravid females (**$p=0.0014$**) was significantly higher in eels fed an early algal supplemented diet

compared to those fed a classic diet or a late algal supplemented diet. In addition, the mean number of females (“TotalFemale”) tended to be higher ($p=0.079$) and the mean number of gravid female tended to be lower ($p=0.059$) in eels fed an early algal supplemented diet compared to those fed a classic diet or a late algal supplemented diet. The mean number of males was not significantly different between the two grouping conditions; the mean number of young males tended to be lower in the “EarlySupplementation” grouping ($p=0.062$).

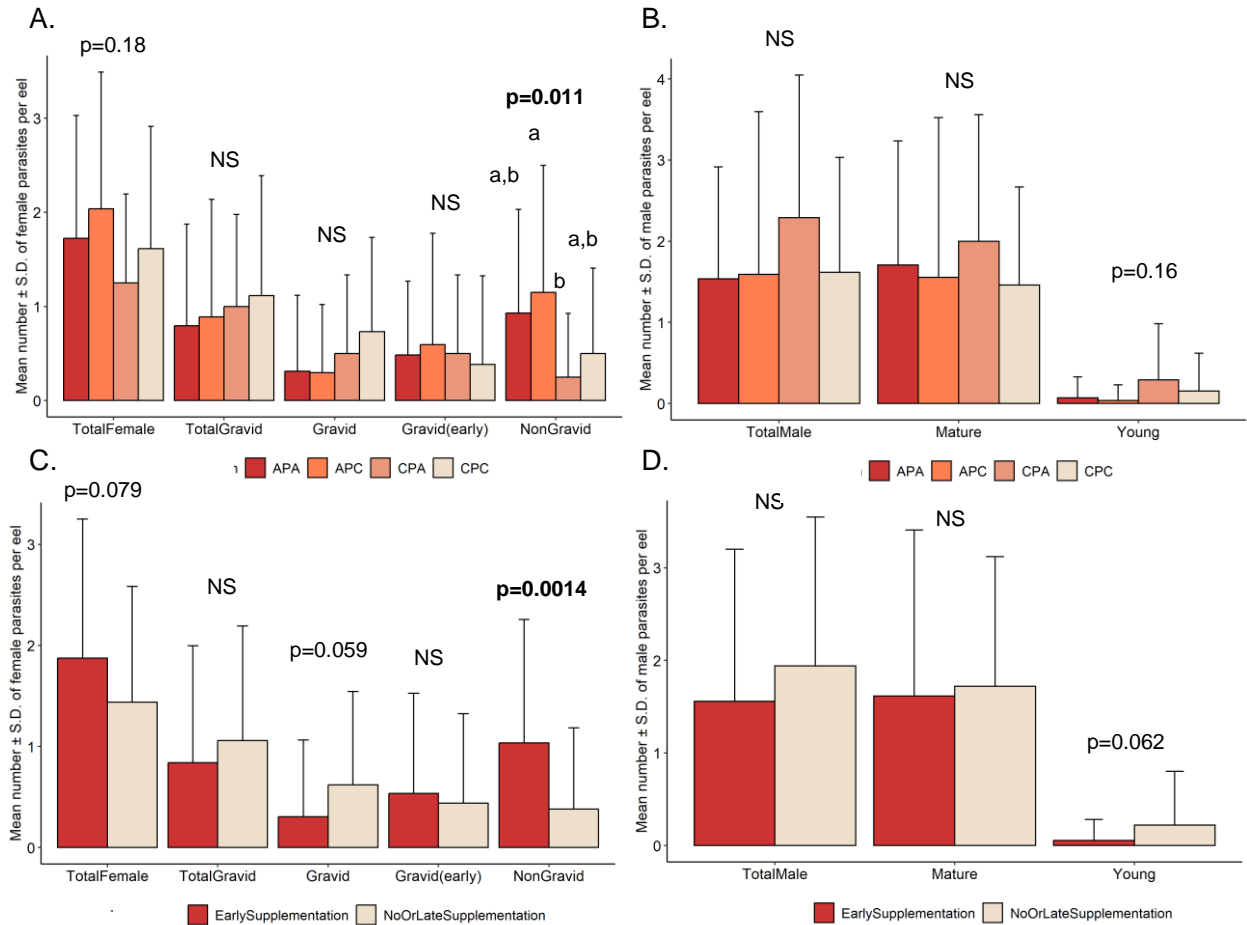


Figure 4: Mean number (\pm SD) of female or male parasites per eel according to their development stage: female (A, C) and male (B, D) fed the four different diet treatments (A, B), or grouped according to an EarlySupplementation diet (APA and APC) or NoOrLateSupplementation (CPC and CPA) (C, D). NS indicates not significant after either an ANOVA test (A and B) or a t-test (C and D). p-value under 0.2 are displayed and significant p-value (<0.05) are in bold.

2.4.1.3 *In vivo* effects of *A. taxiformis* supplemented diet on *E. anguillarum* through eel survival

Eels fed an algal supplemented diet or a classic diet for four weeks were challenged by an intraperitoneal injection of a 1×10^8 CFU.mL $^{-1}$ culture of *E. anguillarum*. Significant mortality occurred three and four days after the injection, resulting in the loss of almost 100 % of the eels. Although a trend towards delayed mortality could be observed for eels fed an algal supplemented diet, the survival probability curves of eels fed an algal supplemented diet or a classic diet were not significantly different (**Figure 5**, $p_{4\text{weeks}}=0.065$).

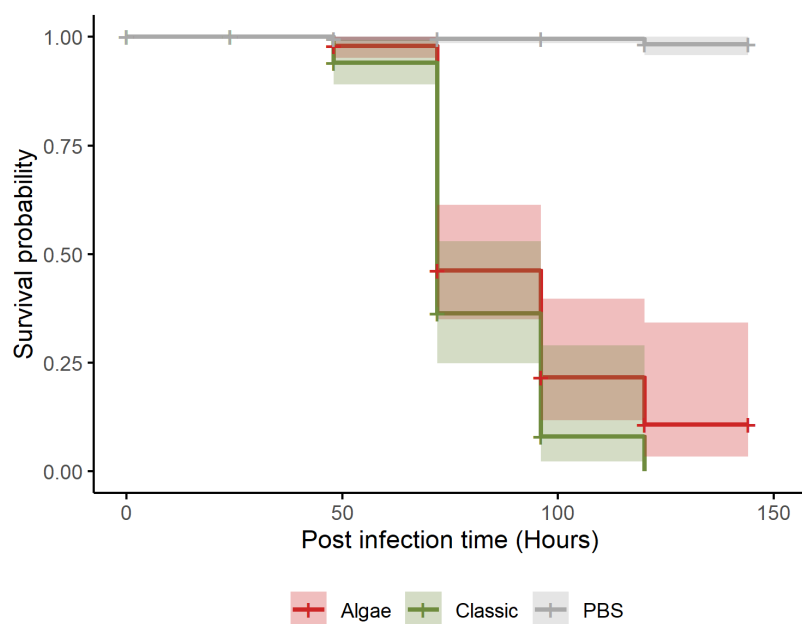


Figure 5: Kaplan-Meier survival curves of *A. anguilla* challenged with 0.1 mL of an *E. anguillarum* culture at 1×10^8 CFU.mL $^{-1}$ after 4 weeks of an algal supplemented diet or a classic diet. n=6 for the algal and classic treatments and n=3 for the PBS conditions.

2.4.2 *In vivo* effects of *A. taxiformis* supplemented diet on eel growth performance

2.4.2.1 Experiment 1

In this first experiment the eels were 13 per aquarium (50 L) and were fed daily with five g per aquarium of a paste supplemented with algae (supplemented diet) or without algae (classic diet). After four weeks of classic or supplemented diet, the average size and weight of eels were not significantly different between the two treatments (**Table 2**; $p=0.677$). The different parameters of the growth performance were not significantly different either (**Table 2**). After 4 weeks of feeding (supplemented or classic diet) the size gains (SG) were low and the weight gains (WG) were negative (**Table 2**).

Table 2: Growth performance of European eels fed for 4 weeks on an algae supplemented diet or a classic diet.

	T0 (N=252)	ClassicT4 (N=27)	Algae supplementedT4 (N=27)	p-value^e
Mean size (cm)	14.6±1.8	14.7±1.6	14.8±1.6	0.677
Mean weight (g)	4.6±1.7	4.2±1.4	4.3±1.4	0.786
SG (%) ^a	-	0.2±11.2	1.5±11	0.677
WG (%) ^b	-	-8.2±29.8	-6±30	0.786
SGR (size)(%) ^c	-	0.0±0.4	0.0±0.4	0.674
SGR (weight)(%) ^d	-	-0.5±1.3	-0.4±1.3	0.795

^aWG (%) = Weight Gain = [(final body weight - initial body weight)/initial body weight] * 100.^bSG (%) = Size Gain = [(final size - initial size)/initial size] * 100.^cSGR_{weight} (% day-1) = Specific Growth Rate_{weight} = [(ln final weight - ln initial weight)/number of days] * 100.^dSGR_{size} (% day-1) = Specific Growth Rate_{size} = [(ln final size - ln initial size)/number of days] * 100^et-test of the different parameters between the two diets ControlT4 and AlgaesupplementedT4

2.4.2.2 Experiment 2

The same growth parameters were measured during a second experiment in which eel were 7-10 eels per 25 L aquarium and food was distributed *ad libitum* in each aquarium. Size parameters were not significantly different between eels fed a supplemented diet and those fed a classic diet (**Table 3**, $p>0.05$). In both diets, parameters related to weight (WG and SGR_{weight}) were negative and significantly different between eels fed a supplemented and those fed a classic diet (**$p<0.05$**) (**Table 3**). Eels fed a supplemented diet exhibited greater weight loss and lower SGR_{weight} (-16±39.7 % and -1.1±1.9 % respectively) than those fed a classic diet (-0.6±46.8 % and -0.5±1.7 % respectively) (**Table 3**).

Table 3: Growth performance of European eels fed for 4 weeks on an algae supplemented diet or a classic diet.

	T0(N=156)	ClassicT4(N=77)	AlgaeT4(N=73)	p-value^e
Mean size (cm)	14.1±2.4	14.8±2.2	14.3±2.3	0.172
Mean weight (g)	4.3±2.2	4.3±2.0	3.6±1.7	0.033
SG (%) ^a	-	5.1±15.6	1.4±16.7	0.172
WG (%) ^b	-	-0.6±46.8	-16±39.7	0.033
SGR (size)(%) ^c	-	0.1±0.5	0.0±0.6	0.167
SGR (weight)(%) ^d	-	-0.5±1.7	-1.1±1.9	0.045

^aWG (%) = Weight Gain = [(final body weight - initial body weight)/initial body weight] * 100.^bSG (%) = Size Gain = [(final size - initial size)/initial size] * 100.^cSGR_{weight} (% day-1) = Specific Growth Rate_{weight} = [(ln final weight - ln initial weight)/number of days] * 100.^dSGR_{size} (% day-1) = Specific Growth Rate_{size} = [(ln final size - ln initial size)/number of days] * 100^et-test of the different parameters between the two diets ControlT4 and AlgaesupplementedT4

2.4.3 Impact of *A. taxiformis* and/or *A. crassus* on eel transcripts

A transcriptomic analysis was performed on 35 eels to explore the effect of *A. taxiformis* and/or *A. crassus* (five conditions) on eel gene expression. The sequencing resulted in 25,984,497 reads. After a pre-processing of the data, the final matrix was composed of 31,062 annotated transcripts.

The comparison of gene expression among the different conditions revealed a total of 6,589 differentially expressed genes (DEG) ($p<0.05$). Among them, 2,962 were up-regulated and

3,627 were down-regulated (**Table 4**). The log₂ fold change (log₂FC) ranged from -5.6 to 5.5. A functional analysis was also performed. Due to a low number of DE genes with a *p* < 0.05, all genes with a log₂FC ≥ ±1 were used for the detection of GO terms enriched. GO terms were all part of the domain “biological process”. The functional annotation led to identification of 62, 92, 22 and 44 significantly enriched biological functions in A₁vsC₁, A₂vsC₂, CPCvsCC and APAvsCPC respectively (**Table 5**).

2.4.4 Effect of the algal feeding

First, the impact of the algal supplementation on eel’s transcript was studied in experiments 1 and 2 (codes A₁vsC₁ and A₂vsC₂ conditions). In the first and second experiments, 6484 and 23 DEGs were found respectively (*p* < 0.05) (**Table 4**). Most DEGs were specific to each condition and 6 up-regulated and 6 down-regulated genes were shared by the two experiments (**Figure S1, Table S2**).

In eels fed an algal supplemented diet, two genes, with a high log₂FC > 1 and common to both experiments were significantly up-regulated: the up-regulator of cell proliferation-like and the cytochrome P450 2C20-like (**Table 4**). Another gene, a zonadhesin like was also significantly up-regulated in A₁ and A₂ but with a log₂FC < 1 (**Table 4**). In addition, and for the second experiment only (A₂vsC₂), some genes such as an apolipoprotein A-IV-like and a major histocompatibility complex class I related gene (both with log₂FC > 1) were significantly over-expressed in A₂ eels (**Table 4**). Finally, a high number of lectin-like genes with high negative log₂FC (-5.6 to -2.7) were significantly down-regulated in A₁ eels: fuclectin-3, galactose-binding lectin 1 1-like, fuclectin 7-like, and a C-type lectin domain family 4 member E-like (**Table 4**).

Then, the functional analysis and enrichment of functions, revealed 11 and 40 over-represented functions for A₁ and A₂ eels respectively (**Figure S2**). These functions were associated with transport processes with for example the “GO” terms transmembrane transport, calcium ion transmembrane transport, anion transport and cation transport over-represented in A₁ and A₂ eels (**Table 5, Figure S2**). Several biological functions related to stress response, stimulus response, or metabolic processes were under-represented in A₁ and A₂ eels (**Table 5, Figure S2**).

Table 4: Main DEGs in the different comparisons (\uparrow up-regulated; \downarrow down-regulated; no arrow for not DE). For every lines (except “Number of DEG”) the number displayed next to the arrow corresponds to the Log2FC. Log2FC values in bold corresponds to gene with a p-value <0.05.

Observed effect	Algal effect		Parasite effect	Combined algal and parasite effect
Codes	A ₁ vsC ₁ (5 eels)	A ₂ vsC ₂ (5 eels)	CPCvsCC (5 eels)	APAvsCPC (5 eels)
Number of DEG	\uparrow 2904 \downarrow 3605	\uparrow 23 \downarrow 14	\uparrow 16 \downarrow 12	\uparrow 38 \downarrow 11
Examples of DEG (Log2FC displayed, p-value<0.05)				
up-regulator of cell proliferation-like	\uparrow 2.8	\uparrow 2.7	-1.8	-1.5
cytochrome P450 2C20-like	\uparrow 1.2	\uparrow 1.6	-0.1	\uparrow 1.7
zonadhesin like	\uparrow 0.9	\uparrow 0.8	0.6	\uparrow 0.7
apolipoprotein A-IV-like	-0.9	\uparrow 1.3	-0.03	\uparrow 3.1
major histocompatibility complex class I	-0.1	\uparrow 1.1	\downarrow -1.4	1.2
fucoselectin-3	\downarrow -5.6	-1.3	\uparrow 5.5	\downarrow -4.9
galactose-binding lectin 11-like	\downarrow -4.7	-0.3	\uparrow 4.3	-2.2
fucoselectin 7-like	\downarrow -3.6	-0.2	1.7	-1.6
C-type lectin domain family 4 member E-like	\downarrow -2.9	0.5	0.0	\downarrow -1.5
microfibril-associated glycoprotein 4-like	-1.8	-0.3	\uparrow 2.2	\downarrow -1.5
activator of 90 kDa heat shock protein ATPase homolog 1-like,	0.2	-0.2	\downarrow -0.4	0.1
DnaJ family of heat shock proteins (Hsp40) member B4	-0.8	0.3	\downarrow -1.4	0.8
hypoxia inducible factor 1 subunit alpha, like 2, transcript variant X1	0.6	0.1	\downarrow -1.3	0.7

Table 5: Summary of GO terms enriched in the different comparisons (\uparrow over-represented; \downarrow under-represented; - not enriched)

Observed effect	Algal effect		Parasite effect	Combined algal and parasite effect
Codes	A ₁ vsC ₁ (5 eels)	A ₂ vsC ₂ (5 eels)	CPCvsCC (5 eels)	APAvsCPC (5 eels)
Number of GO terms enriched	$\uparrow 11 \downarrow 51$	$\uparrow 40 \downarrow 52$	$\uparrow 6 \downarrow 16$	$\uparrow 17 \downarrow 27$
Examples of enriched GO terms (number of genes with a log₂FC $\geq \pm 1$ in the GO category/the total number of genes in the GO category)				
Transmembrane transport	$\uparrow 56/785$	$\uparrow 21/788$	-	$\uparrow 37/787$
Calcium ion transmembrane transport	$\uparrow 2/57$	$\uparrow 1/57$	-	-
Cation transport	$\uparrow 21/389$	$\uparrow 9/389$	-	-
Anion transport	$\uparrow 22/417$	-	$\downarrow 10/147$	$\uparrow 18/417$
Stress response	$\downarrow 21/163$	$\downarrow 10/164$	$\uparrow 8/162$	$\downarrow 12/162$
Stimulus response	$\downarrow 43/289$	$\downarrow 19/290$	$\uparrow 19/288$	$\downarrow 22/288$
Immune system process	$\downarrow 21/119$	-	$\uparrow 10/119$	$\downarrow 8/119$
Macromolecules biosynthetic process	$\downarrow 22/256$	$\downarrow 10/255$	-	$\downarrow 9/257$
Biosynthetic processes	-	$\downarrow 18/639$	$\downarrow 13/637$	-
Examples of genes in GO “term immune system process” (Log2FC displayed)				
Interleukin 21	$\downarrow -1.02$	-	$\uparrow 0.7$	$\downarrow -1.5$
Tumor necrosis factor a	$\downarrow -0.6$	$\uparrow 0.6$	$\uparrow 0.8$	$\downarrow -0.6$
Tumor necrosis factor b	$\downarrow -0.7$	-	$\uparrow 1$	$\downarrow -0.6$
Tumor necrosis factor superfamily 18	$\downarrow -0.6$	$\downarrow -0.9$	$\uparrow 1$	$\downarrow -1$
Chemokine (C-C motif) ligand 34a, duplicate 3	$\downarrow -1.1$	-	$\uparrow 0.7$	$\downarrow -0.8$
Chemokine (C-C motif) ligand 19b	-	$\downarrow -0.6$	$\uparrow 0.6$	$\downarrow -1$
C-C motif chemokine 20-like	$\downarrow -0.9$	-	$\uparrow 0.5$	$\downarrow -1.1$
C-C motif chemokine 26-like	$\downarrow -0.6$	$\downarrow -1.3$	$\uparrow 1.4$	$\downarrow -1$

2.4.5 Effect of the parasite

When comparing infested eels *vs* non-infested ones (CPCvsCC conditions), 28 DEGs were found, of which 16 were significantly up-regulated and 12 significantly down-regulated. Most DEGs were specific and 5 up-regulated and 4 down-regulated genes were shared with the other conditions (**Figure S1**). In parasitized eels (CPC), lectin-related genes, such as fucoslectin-3 and galactose-binding lectin 1 1-like, were detected as significantly up-regulated with log₂FC >4 (**Table 4**). In addition, a microfibril-associated glycoprotein 4-like was also up-regulated in CPC eels. In contrast, the activator of 90 kDa heat shock protein ATPase homolog 1-like, the B4 member of the DnaJ family of heat shock proteins (Hsp40), the major histocompatibility

complex class I gene-related protein (transcript variant X5) and the alpha 2-like subunit of hypoxia-inducible factor 1 (transcript variant X1) were down-regulated (**Table 4**).

The gene enrichment analysis allowed the identification of several biological processes over-represented in parasitized eels. They were related to stress response, stimulus response and immune system. In contrast, in non-parasitized control eels (CC), enriched GO terms were more related to metabolic processes (biosynthetic processes **Table 5**) (**Figure S2**).

2.4.6 Combined effect of the algal feeding and the parasite

When comparing eels parasitized and fed a supplemented diet (APA) *vs* eels parasitized and fed a classic diet (CPC), 49 DEGs were found, of which 38 and 11 were significantly up- and down-regulated respectively (**Table 4**). Among them, 11 up-regulated and 6 down regulated genes were shared with other conditions (**Figure S1**).

For example, a cytochrome P450 2C20-like and a zonadhesin-like were both up-regulated in APA eels as well as in eels fed the algal supplemented diet (A₁*vs*C₁, A₂*vs*C₂) (**Table 4**). In contrast, the fucolactin-3, already observed to be down-regulated in A₁ (A₁*vs*C₁) and up-regulated in CPC (CPC*vs*CC), was significantly down-regulated in APA eels (**Table 4**). In a similar way, the microfibril-associated glycoprotein 4-like found up-regulated in CPC eels (CPC*vs*CC), was down-regulated in APA eels (**Table 4**). Finally, A C-type lectin (domain family 4 member E-like), found down-regulated in A₁ eels was also found down-regulated in APA eels.

The functions over-represented in APA eels were similar to those over-represented in eels fed the algal supplemented diet (A₁*vs*C₁, A₂*vs*C₂): transmembrane transport and anion transport were over-represented while stress response, stimulus response, immune systems process and macromolecules biosynthetic process GO terms were under-represented (**Table 5, Figure S2**). By further exploring genes with a log₂FC $\geq\pm 1$ in the over-represented immune systems process GO term, we found that a high number of cytokines (interleukines and tumor necrosis factor) and chemokines were down-regulated in eels from A₁*vs*C₁, A₂*vs*C₂, APA*vs*CPC and up-regulated in CPC*vs*CC (**Table 5**).

2.5 Discussion

A. anguilla is a critically endangered species. Pathogens may be one of the factors driving the collapse of the eel population. In response to the need for more environmentally friendly treatments, we thus evaluated in this paper 1) the *in vitro* effect of *Asparagopsis* spp. extract on

the eel parasite, *A. crassus*, 2) the *in vivo* effect of a diet supplemented with *A. taxiformis* extract on eels physiology through their growth and transcriptome and 3) the potential immunostimulating effect *in vivo* of a diet supplemented with an extract of *A. taxiformis* on eels infested with *A. crassus* or *E. anguillarum*.

2.5.1 *Asparagopsis* spp. extract significantly reduced *Anguillicolae crassus* survival *in vitro*

In a previous study we reported antibacterial activity of apolar extracts of *A. armata* and *A. taxiformis* on several eel pathogens including *E. anguillarum*, *Vibrio anguillarum*, *Pseudomonas anguilliseptica* and *Lactococcus garvieae* and the absence of temporal variation of this biological activity (Parchemin et al., 2023, minor revision). In the present work, we showed that the survival of another eel pathogen the parasite *A. crassus*, was negatively impacted by the highest concentrations (1 mg/mL and 0.5 mg/mL) of both *A. taxiformis* and *A. armata* extracts. Other studies reported antiparasitic activities of extracts and fractions of *Asparagopsis* spp. against the protozoan *Leishmania* with low IC₅₀ (10 to >40 µg/mL) and LD₅₀ (25 to 9 µg/mL) (Genovese et al. 2009; Vitale et al. 2015) or against the ectoparasitic monogenean *Neobenedenia* sp., with the extract inhibiting embryonic development and reducing hatching success (Hutson et al., 2012). The results of our study increase knowledge on the activities of the two algal species against parasites and in particular for the first time against a nematode. We also highlighted a differential effect of the extracts of the two algae species as the survival probability of parasites in contact with *A. taxiformis* extract was 0 % while it was still above 75 % for parasites in contact with *A. armata* extract after 60 minutes of exposure to a concentration of 0.5 mg/mL. Such differences in activity between *A. armata* and *A. taxiformis* extracts have already been reported with lower IC₅₀ and IC₉₀ for *A. taxiformis* extracts than for *A. armata* extracts against *Leishmania* (Genovese et al., 2009). This could be related to differences in the chemical composition of the two extracts as we have shown in another study (Parchemin et al., 2023, minor revision).

2.5.2 *A. taxiformis* diet supplementation impacted negatively eel growth and physiology

Following *in vitro* assays, we performed two feeding experiments with different food quantities, to evaluate the potential effects of a supplemented diet with *A. taxiformis* eel growth and physiology. The impact on eel growth after 4 weeks of feeding was assessed through two experiments. In the first experiment, overall size and weight gain were not different between the different diet conditions. This result is in agreement with a study performed on *Dicentrarchus labrax* and *Sparus aurata* in which neither whole *A. taxiformis* supplementation

nor algal extract had a significant impact on fish growth (Marino et al. 2016). However, compared to other studies using *A. taxiformis* or performed on eels, all growth parameters observed in this work were very low or even negatives. For example, the growth of Atlantic salmon fed twice a day for four weeks with 6% *A. taxiformis* extract was increased by up to 33% (Thépot et al., 2022), juvenile *Siganus fuscescens* fed twice daily for four weeks with 6% *A. taxiformis* extract increased by up to 40% (Thépot et al., 2021b) as did weight gain of *Platax orbicularis* (+18% increase after 3 weeks of supplemented diet with the whole algae) (Reverter et al., 2016). Similarly, European eels fed a mixture of Chinese herbal medicines for 42 days twice a day exhibited a weight gain of over 60% (Huang et al., 2020) and Japanese eels fed with 0.5% propolis twice a day for 12 weeks gained up to 148.9% in weight (Bae et al., 2012). In our study, we observed dominance and competition for food, which resulted in large and small fish explaining the large standard deviations associated with the growth parameters. We also only fed the eels once a day, with a food paste that disintegrated very quickly in the water. Thus, the difficulties encountered in controlling food intake as well as the dominance/competition phenomena observed could explain the low weight and size gains noticed in our experiment. We hypothesized that decreasing the number of fish per aquarium, increasing the quantity of feed or the number of feed intakes per day, and using pellets instead of food paste in future experiments could potentially improve the growth performance of eels.

The growth parameters measured in the second experiment, in which the food quantity was higher than in the first experiment, allowing better access to food and less competition, were consistent with these assumptions. Indeed, we found a slightly higher gain in size and weight than in the first experiment. However, if the weight gain was significantly different between classic and algal supplemented diets, the greatest weight loss was observed for eels fed the supplemented diet. This was again in contrast to what has been found in previous studies as mentioned above (Reverter et al., 2016; Thépot et al., 2021b, 2022). Thus, in our work, algae supplementation had a negative impact on the growth of the European eels. In this experiment, we used a 3% algae supplementation following optimal results obtained in Reverter et al. (2016) for *Platax orbicularis* and a preliminary not published study. In a future study, we could try other proportions with the aim of optimising the most suitable one for eel, as the results obtained in this work could be related to a dose-response effect as highlighted by Marino et al. (2016). We could also use the extract that led to better results than with algal powder (Thépot et al., 2021b, 2022).

Next, the impact of algal supplementation diet on eel physiology was assessed at the molecular level by transcriptomic analysis. Overall, few genes were found to be significantly differentially expressed under the different conditions, which is most likely related to a high variation in gene expression between individuals in the same groups. Thus, the functional analysis performed on all genes with a $\log_{2}FC \geq \pm 1$ allowed us to complete findings of the differential expression profiles (DEseq) analysis and to interpret transcriptomic change at a higher functional level. Most of DEGs were specific to the experimental conditions and very few were common. Among them, a zonadhesin-like and a cytochrome P450 2C20-like were over-expressed in the three conditions in which eels were fed the algal supplemented diet. In fish, zonadhesin and a zonadhesin-like expressions were evaluated in a variety of tissues of Atlantic salmon and were found expressed in liver and gut (midgut, hindgut and foregut) (Hunt et al., 2005). However, their function in fish remains unclear. Cytochromes P450 are enzymes involved in the detoxification and metabolism of various exogenous and endogenous metabolites (Andersson and Förlin, 1992; Uno et al., 2012). Then, an apolipoprotein A-IV-like was also found highly over-expressed in eels fed with the alga. Apolipoprotein A-IV is an endogenous anti-oxidant and anti-inflammatory protein involved in various physiological processes such as lipid and glucose metabolism, and was also associated with satiety in fish (Wang et al., 2015). Both zonadhesin and apolipoprotein A-IV-like were already found to be up-regulated in Japanese elvers exposed to stressful conditions such as air exposure (Yada et al., 2018). In our study, an up-regulator of cell proliferation-like (URGCP-like) was also an up-regulated gene associated to *A. taxiformis* diet supplementation. In fish, the up-regulation of this gene was described as associated with stress exposure. Indeed, it was found to be up-regulated in the gills of *Trematomus bernacchii* 72h after sublethal heat exposure (Greco et al., 2022) and in head kidney of juvenile common carp exposed to glyphosate (Liu et al., 2021). Thus, the above cited up-regulated genes in eels fed the algal supplemented diet are seemingly related to stressful conditions. The enrichment of functions confirmed these first observations. Indeed, the GO terms enrichment analysis showed that the biological processes over-represented in eels fed with the algae were linked to transport, including transmembrane transport and ion transport. Various studies reported an enrichment in transmembrane transport GO terms in case of fish acclimation to changing environment including high temperature, low salinity or high altitude (Gibbons et al., 2017; Logan and Somero, 2010; Tong et al., 2015). Conversely, functions linked to biosynthetic processes, such as macromolecules biosynthetic process were under-represented compared to control eels. Overall, the up-regulated genes and over-represented

functions suggest the establishment of stress and detoxification processes at the expense of metabolic biosynthetic processes in response to the feeding with the algae.

2.5.3 *A. taxiformis* supplemented diet seemed to favour infestation by *A. crassus* and did not improve *A. anguilla* survival challenged with *E. anguillarum*

The effect of the algal supplemented diet was evaluated on the success of infestation and development of *A. crassus*. We showed a higher percentage of parasitized eels in APA and APC conditions and observed a trend towards a higher mean number of parasites in all conditions where eels were fed with the algal supplemented diet. These results were in agreement with some works in the literature, which point out a reduction of the immune response in *Dicentrarchus labrax* and *Sparus aurata* fed with a diet supplemented with *A. taxiformis* (Marino et al. 2016). However, more research has shown an increased immune response in fish fed with the same algal species (Reverter et al. 2016 in *Platax orbicularis*; Thépot et al. 2021b in *Siganus fuscescens* and Thépot et al. 2022 in *Salmo salar*). We can hypothesise here that the algal supplemented diet could, instead of stimulating the immune response in eels, lead to a depression of this response and thus to higher rates of parasitism. Furthermore, we found that the mean number of larvae, and in particular L3 larvae, was significantly higher in all conditions where eels were fed the algal supplemented diet. Finally, we also highlighted that the mean number of non-gravid females was significantly higher in eels that received early algal supplementation (APA and APC conditions) than those receiving a late or no algal supplementation. These last results could indicate that if the algal supplemented diet appears to favour infestation, it could also induce delays in the development of the parasite, both in the moult of the L3 larva into L4 and in the maturity of the females (non-gravid vs gravid). We could assume here a toxic effect of the alga on the parasite insofar as, this one being hematophagous, it could ingest, via the blood of the eel, compounds harmful to its normal development. This would be all the more marked in females who are led to consume a large quantity of blood due to a high energy demand for their development. These hypotheses could be consistent with what is shown in the literature, in particular the inhibition of embryonic development in the monogeneous ectoparasite *Neodenedenia* sp. (Hutson et al. 2012). Indeed, the L3 larvae and non-gravid females studied here belonging to a group of parasites (Nematodes) known to possess a thick and solid body wall and being at more advanced stages of development than those of *Neodenedenia* sp. embryos, could be less affected by the potential toxicity of the algae and suffer only delays rather than inhibition of their development.

Regarding the effect of the algal supplementation on the survival of eels challenged with *E. anguillarum*, the survival probability curves of eels were not significantly different between those fed the classic diet and those fed the algal supplemented diet. Overall, when challenged with *E. anguillarum*, the eels died very quickly, regardless of the administered diet. The quick mortality observed in this work was unexpected and in contradiction with the literature. Indeed, previous studies have shown the efficiency of supplemented diets in eels challenged with pathogens resulting in reduced mortality (Bae et al., 208, 2012; Chang and Liu, 2002; Lee et al., 2018). In these studies, the bacteria used was *E. tarda* that is now considered an ambiguous species with the recent re-affiliation of some *E. tarda* strains to the species *E. anguillarum* and *E. piscida* (Buján et al., 2018; da Costa et al., 2022), the latter causing less mortality than *E. anguillarum* (Rahmawaty et al., 2022). This can cause difficulties in comparing results. Still, the dose for the bacterial infection used in the above cited studies ranged between 1×10^6 CFU.mL $^{-1}$ and 3.5×10^8 CFU.mL $^{-1}$ (Bae et al., 2008, 2012; Chang and Liu, 2002; Lee et al., 2013; Lee et al., 2018). The dose chosen in our work (1×10^8 CFU.mL $^{-1}$), rather located in the high concentration range, could therefore explain our result of a faster and higher mortality than in the cited studies. It should be noted that the choice of the bacterial dose injected here was made following experiments to select the optimal dose (unpublished results), in which no effect was observed for a dose of 1×10^7 CFU.mL $^{-1}$. Finally, the *E. anguillarum* strain (DSMZ-27202) used in this study, originally isolated from a diseased *A. japonica* (Shao et al., 2015), may be a too virulent a strain for *A. anguilla* to produce a "natural" infection as expected.

The transcriptomic analysis provided important insights into the understanding of the observed phenotypic traits particularly on the infestation success and parasite development. Indeed, several genes were found down regulated in eels fed the algal supplemented diet but up-regulated in eels parasitized and fed with the classic diet. This was particularly the case for many lectin-like genes including in particular fucosidase-3 and the galactose-binding lectin l-1-like. Lectins are proteins that play a role in pathogen recognition in fish and may play an important role in the innate immune response (da Silva Lino et al., 2014). These proteins may also play a role in the immune response in case of parasitic infestation (Alvarez-Pellitero, 2008; Buchmann, 2001). Immune system process, stress and stimulus responses were GO terms that were under-represented in eels fed the algal supplemented diet. These same biological functions were over-represented in eels infested with *A. crassus* and fed the classic diet. This was consistent with a study of immune genes expression in the spleen and head kidney of European eels infested with *A. crassus*, in which 18 of 32 enriched GO terms belonged to "immune system

process” or “response to stimulus” (Bracamonte et al., 2019). By further exploring genes in these GO terms, we found out that, in addition to lectins, several types of cytokines: interleukins, tumor necrosis factor, and chemokines, that also are involved in the innate immune responses, including against parasites (Alvarez-Pellitero, 2008) were down-regulated in eels fed the algal supplemented diet and up-regulated in eels parasitized but fed with the classic diet. Conversely, and interestingly, among genes down-regulated in eels parasitized and fed with a classic diet, two coded for heat shock proteins, one for major histocompatibility complex class I, and the last for hypoxia inducible factor 1. The two first are mostly up-regulated in case of heat stress and stress response in general (Li et al., 2022). They were also described as having a role in immunity as they were differentially expressed in Japanese flounder after a *E. tarda* injection (Li et al., 2022; Yan et al., 2021). Major histocompatibility complex class I, were also found down-regulated in another study in which eels were experimentally infected with *A. crassus* (Bracamonte et al., 2019). These molecules are part of the adaptive immune system, playing a role in the recognition of pathogens (Mokhtar et al., 2023; Yamaguchi and Dijkstra, 2019). Then, the hypoxia inducible factor 1 that is usually up-regulated in hypoxia condition was also recently associated with mandarin fish immune response against viral diseases (He et al., 2019). In our study, the down-regulation of these genes, involved in stress or immunity, provide new insights on the impact of *A. crassus*, at a molecular level, on its host.

Thus, our results regarding the success of infestation and development of *A. crassus* in eels and their resistance to *E. anguillarum* are in agreement with the transcriptomic analysis. It can therefore be assumed that eels invest more in detoxification processes related to the adaptation to the algal supplemented diet than to immunity, resulting in higher infestation rates and numbers of *A. crassus* and a lack of resistance to *E. anguillarum*. To our knowledge, this is the first time that the impact of an algal supplementation diet on the success of infestation and development of *A. crassus* has been reported.

2.6 Conclusion

To conclude this study, we reported an *in vitro* high activity of algae extracts of the genus *Asparagopsis* on adults *A. crassus* impacting their survival. *In vivo*, we did not observe any promoting effects on growth performance between eels fed the algal supplemented diet and those fed the classic diet. Transcriptomic and epidemiological analyses of eels infested with *A. crassus* highlighted that supplementation with *A. taxiformis* could lead to an energetic trade-off between detoxification and immunity processes leading to higher parasites numbers in eels fed the algal supplemented diet. We also did not observe any differences in resistance to infection

against *E. anguillarum* in eels fed the algal supplemented diet or fed the classic diet. The use of plants as an immunostimulant solution for aquaculture has received a growing interest and might be very promising in reducing bacterial infection. However, few studies investigate the impact of such feeding on other pathogens than bacteria. This study shows that attention should be paid to many pathogens and their interactions with their fish host in feeding assay as a solution for aquaculture since, as we have shown, the use of an algal supplemented diet may, contrary to what is expected, have no immunostimulatory effect and/or promote infection. Indeed, we demonstrated here that the use of *A. taxiformis* may not be suitable as diet supplementation for the critically endangered European eel.

2.7 Acknowledgements

This work was supported by the Occitanie Region, France and the “Bonus Qualité Recherche” grant from University of Perpignan *Via Domitia*. Authors are very grateful to Dr. Delphine Nicolas, Jordane Lambremon and Pierre Campton from the “Observatoire des poisons migrateurs amphihalins Rhône-Méditerranée” for supplying glass eels. Authors would also like to thank professional fishermen, Jean Claude Pons and Hervé Turc, for providing adults eels. Thanks to Dr. Raphaël Lagarde for his help in statistical analysis. Thanks to Jennifer Sola for her help during observation of *A. crassus* movement and to Florent Tintillier for his help in *Artemia* breeding.

3. Ce qu'il faut retenir

L'objectif de l'étude présentée dans ce chapitre était d'étudier les effets potentiels d'*Asparagopsis armata* et *A. taxiformis* sur deux pathogènes de l'anguille européenne : *Anguilllicola crassus* et *Edwardsiella anguillarum* et l'effet d'une supplémentation de l'alimentation à 3 % avec *A. taxiformis* sur la physiologie de l'anguille au travers de sa croissance et des variations au sein de son transcriptome.

Pour cela, des tests *in vitro* de survie de parasites exposés à des extraits des deux espèces d'*Asparagopsis* ont été réalisés. Deux expériences de supplémentation de l'alimentation d'anguilles européennes avec 3% d'*A. taxiformis* ont ensuite été réalisées. L'effet de cette alimentation sur la physiologie de l'anguille a été étudié au travers de sa croissance et des variations au sein de son transcriptome. Enfin, sur les deux pathogènes cités plus haut, l'effet de cette alimentation a été évalué au travers du succès de l'infestation et du développement du parasite et de la survie d'anguilles confrontées à *E. anguillarum*.

Les résultats majeurs sont :

(1) *In vitro*, les deux espèces d'algues ont un effet négatif sur la survie du parasite *A. crassus*. *Asparagopsis taxiformis* présente une activité plus importante que *A. armata* à la concentration de 0.5 mg/ml. Il existe des effets dose-dépendants puisque les extraits à 0.05 mg/ml n'ont pas d'effets sur les parasites.

(2) Le pourcentage d'infestation par le parasite *A. crassus* est supérieur pour les anguilles ayant été alimentées avec la nourriture supplémentée en algue avant l'infestation. Les vessies gazeuses de ces mêmes anguilles contiennent un plus grand nombre de femelles, en particulier de femelles non gravides que les anguilles ayant été nourries avec l'alimentation supplémentée en algue après l'infestation. De manière générale, toutes les anguilles ayant été nourries avec l'alimentation supplémentée en algue présentent un plus grand nombre de larves de parasites et une tendance à un plus grand nombre de parasite total que les anguilles ayant été nourries avec l'alimentation classique.

(3) Une tendance (non significative) à un ralentissement de la mortalité des anguilles infectées avec *E. anguillarum* et ayant été nourries avec l'alimentation supplémentée en algue est observée chez les anguilles

(4) Sur les deux expériences menées, la croissance des anguilles après quatre semaines d'alimentation est globalement négative avec une perte de poids mesurée pour les anguilles

nourries avec l'alimentation supplémentée en algue et avec l'alimentation classique. Cette perte de poids n'est pas significativement différente entre les deux conditions d'alimentation dans l'expérience 1. Dans l'expérience 2, une perte de poids est également observée pour les deux conditions. Les anguilles nourries avec l'alimentation supplémentée en algue ont perdu significativement plus de poids que les anguilles nourries avec l'alimentation classique.

(5) L'étude transcriptomique montre que des gènes sont différemment exprimés entre les différentes conditions. Des gènes liés à la détoxicification sont sur-exprimés chez les anguilles ayant reçu l'alimentation supplémentée en algue (i.e. cytochrome P450). Les fonctions enrichies avec l'analyse fonctionnelle, sur-représentées chez les anguilles ayant eu de l'algue sont essentiellement liées au transport membranaire d'ions. A l'inverse, des gènes liés à l'immunité (lectines et cytokines) sont sous-exprimés chez les anguilles ayant reçu l'alimentation supplémentée en algue. Les fonctions liées à l'immunité, aux réponses aux stress ou aux stimuli sont également sous-représentées dans ces anguilles. En condition de nourriture classique, les anguilles parasitées montrent une sur-représentation de ces mêmes fonctions et gènes.

4. Résultats non intégrés à l'article

Une étude métabolomique en LC-HRMS (mode positif et mode négatif) et en RMN a été menée sur les mêmes échantillons d'anguilles que ceux analysés en transcriptomique. Les corps d'anguilles ont été extraits selon la méthode biphasique décrite dans le **Chapitre I**. Seules les phases polaires ont été analysées, les phases apolaires ont été conservées : riches en lipides, elles pourront être analysées dans le cadre de collaborations futures. Les phases polaires sont quant à elles riches en acides aminés et en sucres. Les analyses en RMN ont révélé une abondance importante de signaux pouvant correspondre à la créatine ou à la créatinine (déplacement chimique proche), de carnitine, de glycine ou encore de taurine (**Figure 29**).

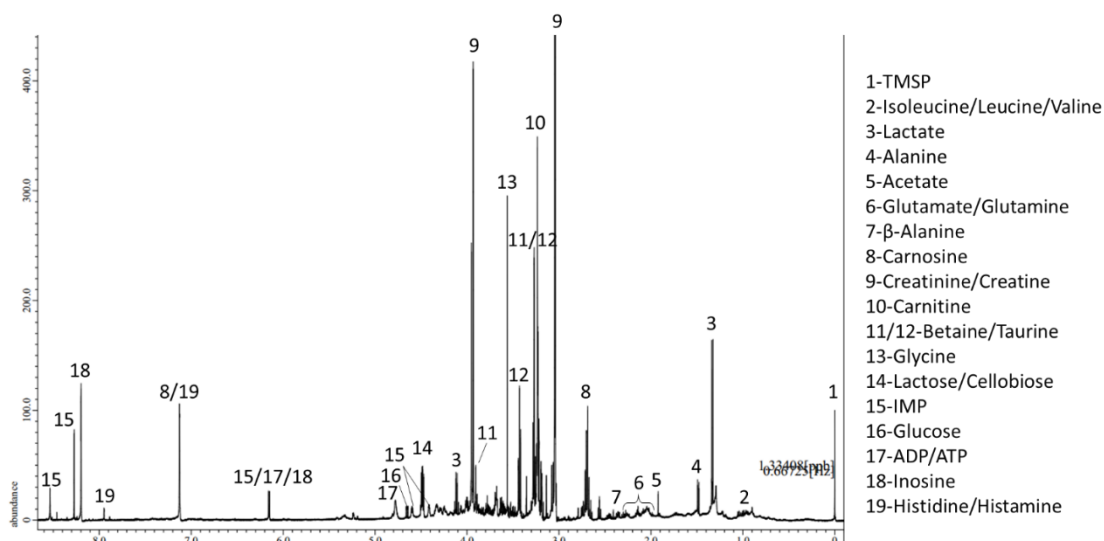


Figure 29 : Spectre RMN ^1H représentatif de la phase polaire d'extraits d'anguilles. Seuls les signaux les plus intenses qui ont pu être putativement annotés sont référencés.

Une analyse « multiblock » a été utilisée pour intégrer et analyser les trois jeux de données. Les résultats préliminaires ont montré une grande variabilité intra-groupe (**Figure 30A, B, C, D**) du métabolome des anguilles rendant les modèles statistiques non prédictifs ($\text{CER} > 0.1$). Les analyses univariées préliminaires, réalisées avec les données issues de la RMN ont permis d'identifier quelques molécules spécifiques des conditions telles que le lactate, plus abondant chez les anguilles non parasitées et nourries avec l'alimentation classique (CC et C₁) (**Figure 31**). Ce résultat est surprenant car le lactate est plutôt connu comme molécule marqueur de stress chez les poissons (Santos et al., 2010 ; Wells and Pankhurst, 1999). On pourrait donc s'attendre à une augmentation de son abondance chez les anguilles parasitées et chez celles nourries avec l'alimentation supplémentée en algues, ce qui n'est pas le cas. Outre le lactate,

l'abondance d'autres molécules, non identifiées, mais dont certaines présentent des signaux caractéristiques de glucides, est également significativement différente entre les conditions. L'abondance de nombreux autres métabolites détectés en RMN et en LC-MS est également significativement différente entre les conditions. Un travail d'annotation et d'identification est en cours.

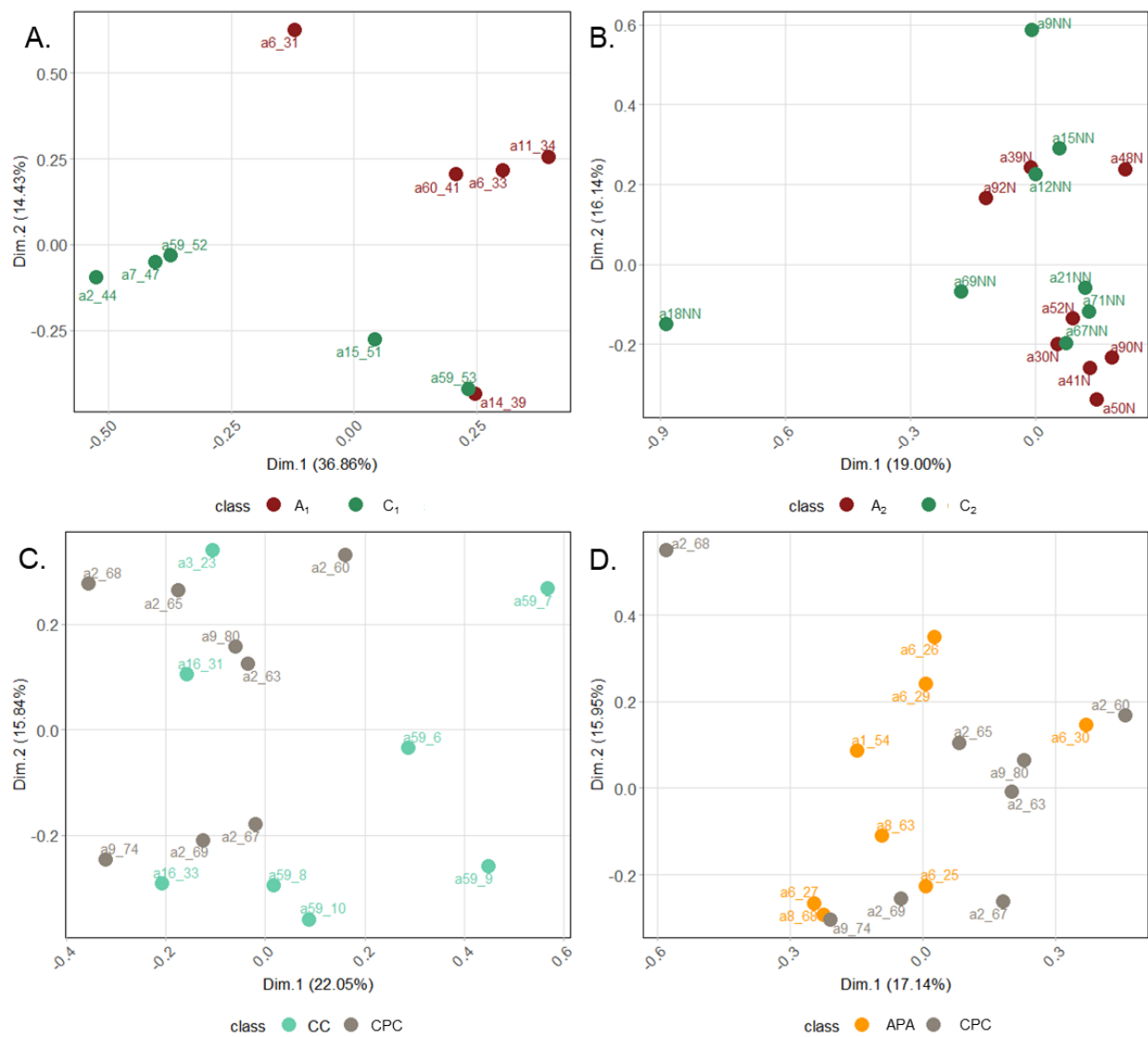


Figure 30 : ACP des deux premières dimensions communes déterminées avec l'analyse ComDim pour les comparaisons anguilles nourries avec une alimentation supplémentée en algues (Code : A) et anguilles nourries avec une alimentation classique (Code : C) dans la première expérimentation (A) et la deuxième expérimentation (B) et pour les comparaisons anguilles parasitées (Code : CPC) et non parasitées (Code : CC) (C) et anguilles parasitées soit nourries avec une alimentation supplémentée en algues (Code : APA) soit avec une alimentation classique (CPC). Les couleurs correspondent aux différentes conditions.

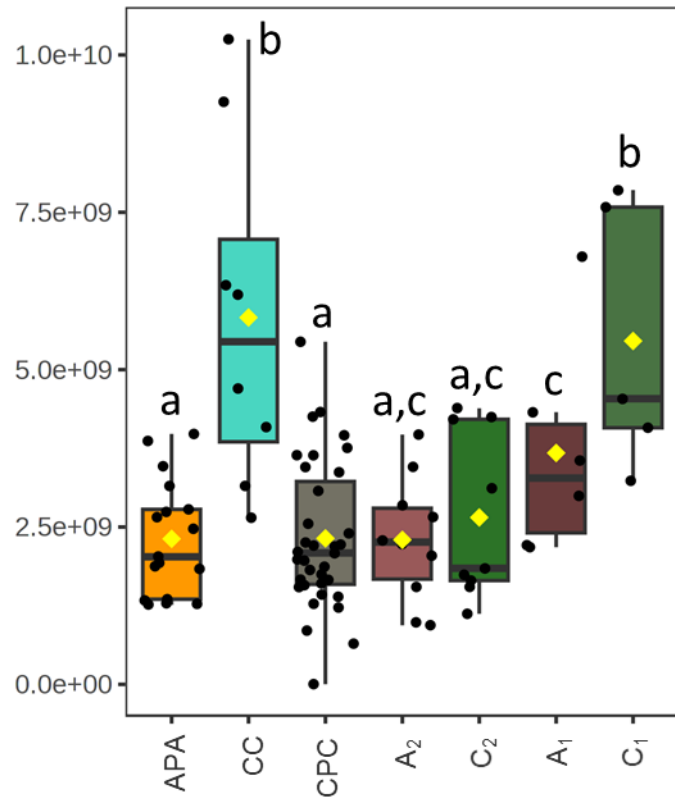


Figure 31 : Abondance relative du lactate dans les différentes conditions.

Les données issues de ce travail pourront être combinées aux données issues de l’analyse transcriptomique et analysées par une approche multi-omique, ce qui pourrait permettre d’identifier des voies de biosynthèse impactées par les différentes conditions.

Conclusion générale et perspectives



Illustration à l'aquarelle réalisée par Michèle Parchemin

L'anguille européenne (*Anguilla anguilla*), connaît depuis les années 1970 un effondrement de sa population et est considérée en danger critique d'extinction. Les pathogènes pourraient être l'une des causes de cet effondrement. Depuis quelques années, des traitements alternatifs aux antibiotiques, préventifs et plus respectueux de l'environnement sont en développement, tels que les préparations à base de plantes terrestres ou d'algues. Des études ont montré le potentiel bénéfice des algues du genre *Asparagopsis* en aquaculture puisque leur inclusion dans l'alimentation de certains poissons a permis d'augmenter la croissance et l'expression de certains gènes liés à l'immunité (Reverter et al., 2016 ; Thépot et al., 2021a, 2021b, 2022). En Méditerranée, *A. armata* et *A. taxiformis* sont considérées comme envahissantes et représentent une biomasse peu valorisée dans ce cadre. Ainsi, ce travail de thèse avait pour objectif principal d'évaluer les effets de deux espèces d'algues rouges du genre *Asparagopsis* sur la physiologie de l'anguille européenne et sur certains de ses pathogènes.

Améliorer les connaissances sur les 2 espèces d'algue : un préalable indispensable pour juger de leur potentiel

Une nouvelle approche intégrative pour la connaissance du métabolome

Si *A. taxiformis* et *A. armata* ont été principalement étudiées par GC-MS, très récemment, des études par LC-HRMS ont montré que de nouvelles molécules, notamment halogénées, pouvaient être détectées par cette technique (Pinto et al., 2022 ; Thapa et al., 2020). Par ailleurs, la spectrométrie de RMN, principalement utilisée pour caractériser les molécules isolées, n'a jamais été utilisée pour l'analyse plus globale du métabolome de ces algues.

Dans cette thèse, nous avons exploré pour la première fois, par une approche non-ciblée en RMN, l'ensemble des métabolites polaires de ces algues. Ceci nous a conduit à mettre en évidence l'importance de molécules comme la taurine, le floridoside ou encore l'acide iséthionique, communes chez les algues rouges, mais qui n'avaient pas encore été décrites chez le genre *Asparagopsis*.

Nous avons également développé, pour la première fois sur *Asparagopsis*, une méthode alternative d'extraction sans solvant (HS-SPME) préalable à l'analyse en GC-MS pour explorer les molécules volatiles.

Enfin, l'approche de métabolomique non-ciblée choisie dans cette thèse associe l'utilisation de ces techniques (LC-HRMS, HS-SPME-GC-MS et RMN) et la combinaison des données par

une analyse « multiblock » pour atteindre la vision la plus complète possible du métabolome de ces algues. Nous avons montré que cette approche, appliquée pour la première fois à l'étude de deux algues rouges, a permis une meilleure discrimination des échantillons en fonction de l'espèce et de la temporalité qu'en exploitant les données de chaque méthode analytique séparément.

Un métabolome lié à l'espèce ?

Dans la littérature, des différences d'activités biologiques ont été reportées entre les deux espèces mais peu d'études sur la composition chimique ont été réalisées conjointement sur les deux algues.

Ainsi, lors de cette thèse, nous avons mis en évidence, en LC-MS, la présence d'un marqueur chimiotaxonomique de l'espèce *A. taxiformis*: une molécule perhalogénée originale, le pentabromopropen-2-yl tribromoacétate, abondante chez le gamétophyte d'*A. taxiformis* mais rarement détectable et en très faible abondance chez le gamétophyte d'*A. armata*. Son rôle biologique reste à élucider.

Par ailleurs, nous avons montré, en RMN, que d'autres molécules halogénées ainsi que des molécules soufrées telles que des sulfolipides l'acide iséthionique et la taurine, sont plus abondantes dans les extraits d'*A. armata* que dans ceux d'*A. taxiformis*. Nous avons émis l'hypothèse qu'une adaptation environnementale liée à la répartition géographique de chaque espèce peut expliquer cette différence.

Contrairement à la phase polaire inactive aux concentrations testées, la phase apolaire des deux espèces a montré une activité contre *Edwardsiella anguillarum*, *Lactococcus garvieae*, *Pseudomonas anguilliseptica* et *Vibrio anguillarum*, 4 bactéries pathogènes de l'anguille européenne et de poissons en général.

Variation saisonnière du métabolome et des activités antibactériennes ?

Les échantillons d'*A. armata* collectés à Banyuls-sur-Mer montrent une temporalité de leur composition chimique plus marquée que celle des échantillons d'*A. taxiformis* collectés à Moorea. Nous avons émis l'hypothèse de conditions environnementales plus variables en surface (*A. armata*) qu'en profondeur (*A. taxiformis*). Parmi les molécules présentant des patrons de variations saisonnières significatives, nous avons pu identifier, en RMN, le

floridoside et la citrulline dont l'abondance est corrélée à l'augmentation de la température de l'eau. L'abondance des sulfolipides, détectés en LC-HRMS est également variable et diminuait de Février à Juin. En revanche, les molécules détectées par GC-MS ne variaient pas significativement au cours des saisons. Ces molécules, principalement volatiles et halogénées, peuvent être davantage impliquées dans des rôles de défense face à des stress biotiques. Nous avons ainsi réalisé la première étude, par métabolomique, permettant d'évaluer les variations chimiques temporelles d'*A. armata*.

Dans la littérature, des études avaient reporté une variabilité marquée de l'activité antibactérienne d'extraits d'*A. taxiformis* avec notamment l'absence d'activité à certains mois de collecte (Genovese et al., 2012 ; Marino et al., 2016). Dans notre étude et pour les deux espèces, seule la phase apolaire a montré une activité avec une faible variation temporelle non significative. L'activité antibactérienne des extraits d'algues que nous avons analysés est donc stable dans le temps, ce qui laisse envisager des collectes de l'algue pour leur valorisation quand elle est présente, quelle que soit la saison. De plus, notre approche non-ciblée pourrait confirmer que les composés halogénés d'*A. taxiformis*, mais également d'*A. armata*, sont responsables des activités antibactériennes reportées dans la littérature.

Une autre stratégie de lutte contre les infections bactériennes : l'anti-quorum sensing ?

L'inhibition de la communication bactérienne (quorum-sensing) est considérée comme une cible prometteuse car, en plus de permettre la lutte contre certains mécanismes de pathogénicité, elle permettrait de limiter les phénomènes de résistance bactérienne. Si l'espèce *A. taxiformis* est déjà connue pour ce type d'activité (Jha et al., 2013), qu'en est-il pour l'espèce *A. armata* ? Par des tests *in vitro*, nous avons montré que des extraits obtenus à partir des deux espèces ont des activités bactéricides et anti-quorum sensing comparables. Les résultats obtenus restent préliminaires et le travail est à poursuivre pour tenter d'identifier les molécules responsables de cette activité. Par ailleurs, il est à noter que la molécule candidate proposée par Jha et al. (2013) sur la base d'une analyse par ICR-FT/MS, de formule brute C₁₄H₂₇O₅S qui pourrait correspondre à du 2-dodecanoxyloxyethanesulfonate, n'a été détectée dans aucune de nos fractions actives. Nos résultats suggèrent donc la nécessité d'explorer d'autres pistes.

Activités antibactériennes et stades du cycle de vie d'*A. armata*. Implications du métabolome et du microbiome ?

Dans la littérature, les extraits du gamétophyte ont été décrits comme plus actifs que ceux du tétrasporophyte (Bansemir et al., 2006 ; Salvador et al., 2007). Les données comparatives de composition chimique de ces deux stades de vie ont été principalement acquises par GC-MS (Bruneau et al., 1978 ; Paul et al., 2006a ; Vergés et al., 2008). Par ailleurs, il est aujourd’hui largement décrit que les communautés bactériennes associées aux algues interviennent dans les processus de biosynthèse de certaines molécules retrouvées dans l’algue (Egan et al., 2013).

Dans ce contexte, nous avons souhaité étudier les variations du métabolome, des activités antibactériennes et du microbiote, associés à trois stades de vie d'*A. armata* (tétrasporophyte (T), gamétophyte (G) et gamétophyte avec cystocarpes développés (GC)). La LC-MS a été utilisée pour l’analyse du métabolome afin d’élargir la fenêtre d’analyse à des molécules peu prises en compte dans les travaux existants.

Ainsi, le profil chimique des échantillons du GC se distingue de celui des deux autres stades. Les molécules associées au GC pourraient être liées au développement des tissus fragiles reproducteurs qu’il est nécessaire de protéger (Vergés et al., 2008). Un suivi du métabolome lors du passage progressif du stade G au stade GC pourrait révéler l’augmentation de l’abondance de ces molécules et aider à mieux appréhender leur rôle.

L’activité antibactérienne diffère significativement en fonction des stades du cycle de vie de l’algue. Les extraits de G et T sont plus actifs que ceux du GC. Le fractionnement bioguidé réalisé à partir d’extraits du gamétophyte d'*A. armata* et les corrélations mesurées ensuite, entre l’aire des ions abondants dans les fractions et l’activité des fractions, laissent penser que des 2,4-diones polyhalogénées, dont certaines, sur-exprimées chez G et T, pourraient être impliquées dans l’activité antibactérienne. Comme nous ne sommes pas parvenus à purifier ces molécules, il serait judicieux de poursuivre ce travail à partir d’une biomasse algale plus importante ou de mettre au point leur synthèse pour obtenir des molécules pures et confirmer leur structure et leur activité. Cependant, la diminution de leur stabilité au fur et à mesure de leur purification laisse entrevoir des difficultés pour atteindre ces objectifs.

Par ailleurs, le pentabromopropen-2-yl tribromoacétate ($C_5Br_8O_2$), détecté dans le gamétophyte d'*A. taxiformis* mais quasiment pas dans celui d'*A. armata*, est présent, de manière surprenante, dans le stade tétrasporophyte de cette dernière. Il existerait donc des processus qui aboutissent à l’altération de la voie de biosynthèse de cette molécule ou à sa dégradation au cours du cycle

de vie d'*A. armata*. Des analyses de transcriptomique pour comparer l'expression des gènes liées aux halopéroxydases (biosynthèse) et aux déhalogénases (dégradation) entre les différents stades du cycle de vie d'*A. armata* pourraient apporter des éléments d'information quant au(x) processus impliqué(s).

Le stade tétrasporophyte d'*A. armata* abrite également une communauté bactérienne à la diversité spécifique plus élevée, associée à un plus grand nombre et à une plus grande diversité de fonctions prédites que celle des échantillons de GC et G. A ce stade, la morphologie du T, sa persistance annuelle dans l'environnement ou encore des différences de composition chimique pourraient expliquer ces différences. Cependant, aucune covariation entre métabolome et microbiote n'a pu être mise en évidence. Ainsi, le métabolome analysé ne paraît pas être le facteur majeur influençant la composition de la communauté bactérienne et inversement. Pour autant, des corrélations entre certaines molécules et certaines bactéries ont pu être mises en évidences grâce à l'analyse multi-omique DIABLO. Des molécules, notamment halogénées sont négativement corrélées à des genres bactériens abondants chez GC et G. Ces corrélations négatives pourraient être expliquées par des fonctions (prédites) de déhalogénéation associées aux communautés bactériennes de GC et G. L'utilisation de la métatéronomique combinée à la métatranscriptomique permettraient de compléter ces données en fournissant des informations sur les liens entre composition et expression des gènes liées aux fonctions des communautés bactériennes (Burke et al., 2011 ; Cardenas and Tiedje, 2008).

Asparagopsis spp. : effet bénéfique ou néfaste sur la physiologie de l'anguille européenne et sur ses pathogènes ?

Effets *in vitro* des deux espèces d'algues sur les principaux pathogènes de l'anguille ?

Les extraits apolaires des deux espèces montrent des activités antibactériennes sur au moins quatre bactéries pathogènes de l'anguille européenne : *E. anguillarum*, *L. garvieae*, *P. anguilliseptica* et *V. anguillarum*. En outre, pour la première fois, nous avons montré que les extraits apolaires des deux algues ont également un effet significatif sur la survie du parasite *A. crassus*. Il serait intéressant de déterminer les concentrations minimales inhibitrices afin de comparer l'efficacité des extraits des deux algues avec celles de produits antibactériens et antiparasitaires commerciaux, et de les tester sur d'autres parasites pathogènes pour les poissons ou pour l'homme.

Effet d'une complémentation en algue sur la physiologie de l'anguille européenne ?

Une expérience d'appétence entre des anguilles alimentées par une nourriture supplémentée avec *A. armata* ou avec *A. taxiformis* a été menée. De manière surprenante une différence de comportement a été observée avec beaucoup plus de refus d'alimentation pour les anguilles dont la nourriture était supplémentée avec *A. armata* qu'avec *A. taxiformis*. Ces observations ont été confirmées par une meilleure croissance pour les anguilles dont la nourriture était supplémentée (3 %) avec *A. taxiformis*.

Les expérimentations réalisées ensuite ont révélé que le gain de poids des anguilles nourries avec l'alimentation supplémentée en algue est très inférieur (-15 %) à celui des anguilles nourries avec une alimentation non supplémentée (-1 %). Cela signifie que, dans les conditions de notre étude et contrairement à la plupart des résultats publiés récemment sur d'autres espèces de poissons, la supplémentation avec *A. taxiformis* n'induit pas de gain de croissance chez l'anguille européenne. Etant donné que dans la littérature, les poissons nourris avec une alimentation supplémentée en extrait plutôt qu'en poudre ont un gain de poids plus important (Thépot et al., 2021b, 2022), il serait peut-être judicieux de tester une alimentation supplémentée en extrait. En effet, cela pourrait permettre d'éviter d'administrer des composés potentiellement toxiques tout en privilégiant ceux qui ont un effet positif. En revanche, l'utilisation d'extrait nécessiterait davantage de matière première et une formulation adaptée de l'aliment pour éviter la possible dégradation des composés actifs.

Les résultats de l'étude transcriptomique soulignent, chez les anguilles nourries avec l'alimentation supplémentée en algues, une sur-représentation de gènes et de fonctions biologiques associées à des processus de détoxicification et une sous-représentation de ceux associés à l'immunité. Une analyse complémentaire utilisant une approche métabolomique est en cours et pourrait permettre, couplée à la transcriptomique d'identifier des voies métaboliques impactées par les différentes conditions.

Effets *in vivo* d'une alimentation complémentée en algue sur *E. anguillarum* et *A. crassus* ?

Deux infestations expérimentales d'anguilles européennes ont été réalisées, après quatre semaines d'alimentation enrichie en *A. taxiformis*, l'une avec le parasite *A. crassus* et l'autre avec la bactérie *E. anguillarum*.

Dans toutes les conditions testées, l'infection d'anguilles avec *E. anguillarum* a conduit à une mortalité très rapide et exponentielle de celles-ci, contrairement à ce qui est rapporté dans la littérature pour des espèces de poissons du genre *Anguilla*. Nous avons montré qu'il n'y avait aucun effet préventif de ce type d'alimentation contre cette bactérie pathogène. A notre connaissance, il s'agit de la première expérience portant sur l'effet d'une alimentation supplémentée avec *A. taxiformis* sur la survie de poissons expérimentalement exposés à des pathogènes bactériens. Cependant nos résultats sont à relativiser du fait de la possible virulence de la souche bactérienne utilisée, ainsi que de la dose choisie et du mode d'injection, non représentatifs de phénomènes naturels d'infection. Il nous paraît donc nécessaire, sur ce modèle, de trouver les conditions optimales pour apprécier le potentiel préventif et curatif d'*A. taxiformis*.

Les anguilles expérimentalement infestées avec le parasite *A. crassus* et nourries avec une alimentation supplémentée en *A. taxiformis* hébergent plus de parasites que celles nourries avec une alimentation non supplémentée. Ces résultats, corrélés aux observations sur la croissance des anguilles et aux données de transcriptomique laissent penser que les anguilles dont l'alimentation était enrichie en algue, investiraient davantage d'énergie dans la détoxication (sur-expression du gène codant pour le cytochrome P450 2C20-like et de gènes impliqués dans les réponses au stress) au détriment de leur immunité (sous-expression des gènes codant pour des lectines et des cytokines).

Ainsi, cette thèse, ciblée sur le potentiel des algues du genre *Asparagopsis* permet d'enrichir les connaissances sur le métabolome des deux espèces et sa variabilité. Les approches modernes utilisant des technologies de pointe et des outils permettant l'intégration de plusieurs jeux de données montrent que des molécules peu étudiées ou récemment décrites jouent un rôle dans la variabilité chimique et les activités biologiques de ces espèces. Ce travail a permis de révéler qu'en plus de leurs effets bactéricides, les extraits apolaires d'*A. armata* et *A. taxiformis* inhibent la communication bactérienne et sont parasiticides sur *A. crassus*. Cependant, les résultats obtenus relatifs à l'administration d'une nourriture supplémentée à 3% d'*A. taxiformis* chez l'anguille européenne mettent en évidence une toxicité de cette algue pour cette espèce sans effet préventif ni curatif vis-à-vis de ses pathogènes. Les résultats de cette thèse montrent la pertinence des expérimentations *in vivo* qui sont primordiales pour estimer, de manière réaliste, le potentiel de substances naturelles ou d'extraits actifs *in vitro*, sur le pathogène et sur l'hôte.

Nous avons également montré l'importance de la prise en considération de l'espèce hôte dans la démarche de recherche de solutions alternatives puisque, chez l'anguille européenne, les effets bénéfiques de l'alimentation supplémentée en *A. taxiformis* décrits chez d'autres poissons, ne sont pas retrouvés. Pour envisager l'utilisation de cette algue en aquaculture, il conviendra donc de tester préalablement son impact spécifique sur l'espèce ciblée, à différents stades de développement (jeune et adulte par exemple) et à court et long terme.

Enfin, contrairement aux études précédentes ayant évaluées les effets d'une supplémentation sur des paramètres ciblés de l'hôte (gènes et activités enzymatiques liées à l'immunité, paramètres sanguins, croissance...), nous avons, lors de cette thèse, caractérisé la réponse globale de l'organisme. Avec cette vision large, des effets majeurs, tels que la toxicité, ont pu émerger. Cette approche intégrative apparaît donc appropriée pour identifier les avantages et les risques de l'ajout d'*Asparagopsis* dans l'alimentation des poissons pour augmenter leur capacité à lutter contre les pathogènes en aquaculture ou pour réduire la production de méthane par les ruminants.

Références

- Adams, A., Thompson, K.D., 2011. Development of diagnostics for aquaculture: challenges and opportunities. *Aquaculture Research* 42, 93–102. <https://doi.org/10.1111/j.1365-2109.2010.02663.x>
- Ador, M.A.A., Haque, M.S., Paul, S.I., Chakma, J., Ehsan, R., Rahman, A., 2021. Potential Application of PCR Based Molecular Methods in Fish Pathogen Identification: A Review. *Aquaculture Studies* 22(1), AQUAST621. <https://doi.org/10.4194/2618-6381/AQUAST621>
- Aires, T., Serrão, E.A., Engelen, A.H., 2016. Host and environmental specificity in bacterial communities associated to two highly invasive marine species (genus *Asparagopsis*). *Frontiers in Microbiology* 7, 559. <https://doi.org/10.3389/fmicb.2016.00559>
- Akashi, K., Miyake, C., Yokota, A., 2001. Citrulline, a novel compatible solute in drought-tolerant wild watermelon leaves, is an efficient hydroxyl radical scavenger. *Febs Letters* 508, 438–442. [https://doi.org/10.1016/S0014-5793\(01\)03123-4](https://doi.org/10.1016/S0014-5793(01)03123-4)
- Alcaide, E., Blasco, M.-D., Esteve, C., 2004. Occurrence of Drug-Resistant Bacteria in Two European Eel Farms. *Applied and Environmental Microbiology* 71, 3348–3350. <https://doi.org/10.1128/AEM.71.6.3348-3350.2005>
- Alcaide, E., Herraiz, S., Esteve, C., 2006. Occurrence of *Edwardsiella tarda* in wild European eels *Anguilla Anguilla* from Mediterranean Spain. *Diseases of Aquatic Organisms* 73, 77–81. <https://doi.org/10.3354/dao073077>
- Almeida, M., Filipe, S., Humanes, M., Maia, M.F., Melo, R., Severino, N., Da Silva, J.A.L., da Silva, J.F., Wever, R., 2001. Vanadium haloperoxidases from brown algae of the Laminariaceae family. *Phytochemistry* 57, 633–642. [https://doi.org/10.1016/S0031-9422\(01\)00094-2](https://doi.org/10.1016/S0031-9422(01)00094-2)
- Altinok, İ., Kurt, İ., 2003. Molecular diagnosis of fish diseases: a review. *Turkish Journal of Fisheries and Aquatic Sciences* 3, 131–138.
- Alvarado, V., Stanislawski, D., Boehm, K.H., Schlotfeldt, H.J., 1989. First isolation of *Flexibacter columnaris* in eel (*Anguilla anguilla*) in northwest Germany (Lower Saxony). *Bulletin of the European Association of Fish Pathologists* 9, 96–99.
- Alvarez-Mora, I., Bolliet, V., Lopez Herguedas, N., Olivares, M., Mathilde, M., Etxebarria, N., 2023. Metabolomics to Study the Sublethal Effects of Diazepam and Irbesartan on Glass Eels (*Anguilla anguilla*). <https://dx.doi.org/10.2139/ssrn.4325876>
- Alvarez-Pellitero, P., 2008. Fish immunity and parasite infections: from innate immunity to immunoprophylactic prospects. *Veterinary Immunology and Immunopathology* 126, 171–198. <https://doi.org/10.1016/j.vetimm.2008.07.013>
- Amaro, C., Biosca, E.G., Fouz, B., Alcaide, E., Esteve, C., 1995. Evidence that water transmits *Vibrio vulnificus* biotype 2 infections to eels. *Applied and Environmental Microbiology* 61, 1133–1137. <https://doi.org/10.1128/aem.61.3.1133-1137.1995>
- Amaro, C., Biosca, E.G., 1996. *Vibrio vulnificus* biotype 2, pathogenic for eels, is also an opportunistic pathogen for humans. *Applied and Environmental Microbiology* 62, 1454–1457. <https://doi.org/10.1128/aem.62.4.1454-1457.1996>
- Anders, S., Pyl, P.T., Huber, W., 2015. HTSeq—a Python framework to work with high-throughput sequencing data. *Bioinformatics* 31, 166–169. <https://doi.org/10.1093/bioinformatics/btu638>
- Andersen, J.B., Heydorn, A., Hentzer, M., Eberl, L.E.O., Geisenberger, O., Christensen, B.B., Molin, S., Givskov, M., 2001. gfp-based N-acyl homoserine-lactone sensor systems for detection of bacterial communication. *Applied and Environmental Microbiology* 67, 575–585. <https://doi.org/10.1128/AEM.67.2.575-585.2001>
- Andersson, T., Förlin, L., 1992. Regulation of the cytochrome P450 enzyme system in fish. *Aquatic Toxicology* 24, 1–19. [https://doi.org/10.1016/0166-445X\(92\)90014-E](https://doi.org/10.1016/0166-445X(92)90014-E)
- Andreakis, N., Procaccini, G., Kooistra, W.H., 2004. *Asparagopsis taxiformis* and *Asparagopsis armata* (Bonnemaisoniales, Rhodophyta): genetic and morphological identification of Mediterranean populations. *European Journal of Phycology* 39, 273–283. <https://doi.org/10.1080/0967026042000236436>

- Andreakis, N., Costello, P., Zanolla, M., Saunders, G.W., Mata, L., 2016. Endemic or introduced? Phylogeography of *Asparagopsis* (Florideophyceae) in Australia reveals multiple introductions and a new mitochondrial lineage. *Journal of Phycology* 52, 141–147. <https://doi.org/10.1111/jpy.12373>
- Andree, K.B., Rodgers, C.J., Furones, D., Gisbert, E., 2013. Co-Infection with *Pseudomonas anguilliseptica* and *Delftia acidovorans* in the European eel, *Anguilla anguilla* (L.): a case history of an illegally trafficked protected species. *Journal of Fish Diseases* 36, 647–656. <https://doi.org/10.1111/jfd.12066>
- Aoyama, J., 2009. Life history and evolution of migration in catadromous eels (genus *Anguilla*).
Arai, T., 2014. Do we protect freshwater eels or do we drive them to extinction? *SpringerPlus* 3, 1–10. <https://doi.org/10.1186/2193-1801-3-534>
- Assefa, A., Abunna, F., 2018. Maintenance of fish health in aquaculture: review of epidemiological approaches for prevention and control of infectious disease of fish. *Veterinary Medicine International* 218, 5432497. <https://doi.org/10.1155/2018/5432497>
- Austin, B., Austin, D.A., Austin, B., Austin, D.A., 2012. *Bacterial fish pathogens*. Springer.
- Austin, B., 2017. The value of cultures to modern microbiology. *Antonie Van Leeuwenhoek* 110, 1247–1256. <https://doi.org/10.1007/s10482-017-0840-8>
- Bae, J.-Y., Han, K.-M., Lee, J.-H., Kim, S.-E., Lee, J.-Y., Bai, S.-C.C., 2008. Effects of dietary quartz porphyry and feed stimulants, BAISM supplementation on growth performance and disease resistance of juvenile eel *Anguilla japonica*. *Journal of Aquaculture* 21, 26–33.
- Bae, J.-Y., Park, G.H., Lee, J.-Y., Okorie, O.E., Bai, S.C., 2012. Effects of dietary propolis supplementation on growth performance, immune responses, disease resistance and body composition of juvenile eel, *Anguilla japonica*. *Aquaculture International* 20, 513–523. <https://doi.org/10.1007/s10499-011-9482-4>
- Bansemir, A., Blume, M., Schröder, S., Lindequist, U., 2006. Screening of cultivated seaweeds for antibacterial activity against fish pathogenic bacteria. *Aquaculture* 252, 79–84. <https://doi.org/10.1016/j.aquaculture.2005.11.051>
- Barrow, K.D., King, R.J., Karsten, U., 1993. Isethionic acid from the marine red alga *Ceramium flaccidum*. *Phytochemistry* 34, 1429–1430.
- Barry, J., Mcleish, J., Dodd, J.A., Turnbull, J.F., Boylan, P., Adams, C.E., 2014. Introduced parasite *Anguillicoloides crassus* infection significantly impedes swim bladder function in the European eel *Anguilla anguilla* (L.). *Journal of Fish Diseases* 37, 921–924. <https://doi.org/10.1111/jfd.12215>
- Barry, J., Newton, M., Dodd, J.A., Evans, D., Newton, J., Adams, C.E., 2017. The effect of foraging and ontogeny on the prevalence and intensity of the invasive parasite *Anguillicoloides crassus* in the European eel *Anguilla anguilla*. *Journal of Fish Diseases* 40, 1213–1222. <https://doi.org/10.1111/jfd.12596>
- Barse, A.M., Secor, D.H., 1999. An exotic nematode parasite of the American eel. *Fisheries* 24, 6–10. [https://doi.org/10.1577/1548-8446\(1999\)024<0006:AENPOT>2.0.CO;2](https://doi.org/10.1577/1548-8446(1999)024<0006:AENPOT>2.0.CO;2)
- Batista, M.M., 2020. *Reproduction And Cultivation Of Asparagopsis taxiformis* (Delile) Trevisan (PhD Thesis). Universidade do Algarve (Portugal).
- Bauer, A.W., 1966. Antibiotic susceptibility testing by a standardized single disc method. *American Journal of Clinical Pathology* 45, 149–158.
- Bayona, L.M., de Voogd, N.J., Choi, Y.H., 2022. Metabolomics on the study of marine organisms. *Metabolomics* 18, 1–24. <https://doi.org/10.1007/s11306-022-01874-y>
- Békési, L., Horvath, I., Kovacs-Gayer, E., Csaba, G., 1986. Demonstration of herpesvirus like particles in skin lesions of European eel (*Anguilla anguilla*). *Journal of Applied Ichthyology* 2, 190–192. <https://doi.org/10.1111/j.1439-0426.1986.tb00662.x>
- Bellec, L., Cabon, J., Bergmann, S., de Boisseson, C., Engelsma, M., Haenen, O., Morin, T., Olesen, N.J., Schuetze, H., Toffan, A., 2014. Evolutionary dynamics and genetic diversity from three genes of Anguillid rhabdovirus. *Journal of General Virology* 95, 2390–2401. <https://doi.org/10.1099/vir.0.069443-0>
- Beregi, A., Molnár, K., Békési, L., Székely, C.S., 1998. Radiodiagnostic method for studying swimbladder inflammation caused by *Anguillicoloides crassus* (Nematoda: Dracunculoidea). *Diseases of Aquatic Organisms* 34, 155–160. <https://doi.org/10.3354/dao034155>

- Bergmann, S.M., Fichtner, D., Skall, H.F., Schlotfeldt, H.-J., Olesen, N.J., 2003. Age-and weight-dependent susceptibility of rainbow trout *Oncorhynchus mykiss* to isolates of infectious haematopoietic necrosis virus (IHNV) of varying virulence. Diseases of Aquatic Organisms 55, 205–210. <https://doi.org/10.3354/dao055205>
- Bierman, S.M., Tien, N.S.H., Van de Wolfshaar, K.E., Winter, H.V., De Graaf, M., 2012. Evaluation of the Dutch Eel Management Plan 2009-2011. IMARES.
- Biosca, E.G., Amaro, C., Esteve, C., Alcaide, E., Garay, E., 1991. First record of *Vibrio vulnificus* biotype 2 from diseased European eel, *Anguilla anguilla* L. Journal of Fish Diseases 14, 103–109. <https://doi.org/10.1111/j.1365-2761.1991.tb00581.x>
- Blanc, G., Bonneau, S., Biagiotti, S., Petter, A.J., 1992. Description of the larval stages of *Anguilllicola crassus* (Nematoda, Dracunculoidea) using light and scanning electron microscopy. Aquatic Living Resources 5, 307–318. <https://doi.org/10.1051/alr:1992029>
- Böcker, S., Letzel, M.C., Lipták, Z., Pervukhin, A., 2009. SIRIUS: decomposing isotope patterns for metabolite identification. Bioinformatics 25, 218–224. <https://doi.org/10.1093/bioinformatics/btn603>
- Böcker, S., Dührkop, K., 2016. Fragmentation trees reloaded. Journal of Cheminformatics 8, 1–26. <https://doi.org/10.1186/s13321-016-0116-8>
- Bolger, A.M., Lohse, M., Usadel, B., 2014. Trimmomatic: a flexible trimmer for Illumina sequence data. Bioinformatics 30, 2114–2120. <https://doi.org/10.1093/bioinformatics/btu170>
- Boudouresque, C.F., Verlaque, M., 2002. Biological pollution in the Mediterranean Sea: invasive versus introduced macrophytes. Marine Pollution Bulletin 44, 32–38. [https://doi.org/10.1016/S0025-326X\(01\)00150-3](https://doi.org/10.1016/S0025-326X(01)00150-3)
- Bracamonte, S.E., Johnston, P.R., Knopf, K., Monaghan, M.T., 2019. Experimental infection with *Anguilllicola crassus* alters immune gene expression in both spleen and head kidney of the European eel (*Anguilla anguilla*). Marine Genomics 45, 28–37. <https://doi.org/10.1016/j.margen.2018.12.002>
- Bruneau, Y., Codomier, L., Combaut, G., Teste, J., 1978. Etude comparative des composés halogénés du *Falkenbergia rufolanesa* (HARV.) SCHMITZ et de l'*Asparagopsis armata* (HARV.): Rhodophycees Bonnemaisoniales. Compte Rendu de l'Académie des Sciences à Paris 286, 603–605.
- Bruslé, J., 1990. Pathogenesis of the eel in culture. Pathology in Marine Science 441.
- Bruslé, J., 1994. L'anguille européenne *Anguilla anguilla*, un poisson sensible aux stress environnementaux et vulnérable à diverses atteintes pathogènes. Bulletin Français de la Pêche et de la Pisciculture 237–260. <https://doi.org/10.1051/kmae:1994015>
- Buchmann, Køie, Mellergarr, 1987. *Pseudodactylogyirus* infections in eel: a review. Diseases of Aquatic Organisms 3, 51–57. <https://doi.org/10.3354/dao003051>
- Buchmann, K., 2001. Lectins in fish skin: do they play a role in host–monogenean interactions? Journal of Helminthology 75, 227–231. <https://doi.org/10.1079/JOH200155>
- Buchmann, K., 2011. *Pseudodactylogyirus anguillae* and *P. bini*. Chapter 12. In Woo, PTK and Buchmann, K (eds), Fish Parasites: Pathobiology and Protection. UK: CABI, pp. 209–224. <https://doi.org/10.1079/9781845938062.0209>
- Buján, N., Mohammed, H., Balboa, S., Romalde, J.L., Toranzo, A.E., Arias, C.R., Magariños, B., 2018. Genetic studies to re-affiliate *Edwardsiella tarda* fish isolates to *Edwardsiella piscicida* and *Edwardsiella anguillarum* species. Systematic and Applied Microbiology 41, 30–37. <https://doi.org/10.1016/j.syapm.2017.09.004>
- Burke, C., Steinberg, P., Rusch, D., Kjelleberg, S., Thomas, T., 2011. Bacterial community assembly based on functional genes rather than species. Proceedings of the National Academy of Sciences 108, 14288–14293. <https://doi.org/10.1073/pnas.1101591108>
- Burreson, B.J., Moore, R.E., Roller, P., 1975. Haloforms in the essential oil of the alga *Asparagopsis taxiformis* (Rhodophyta). Tetrahedron Letters 16, 473–476.
- Burreson, B.J., Moore, R.E., Roller, P.P., 1976. Volatile halogen compounds in the alga *Asparagopsis taxiformis* (Rhodophyta). Journal of Agricultural and Food Chemistry 24, 856–861.
- Burtin, P., 2003. Nutritional value of seaweeds. Electronic Journal of Environmental Agricultural and Food Chemistry 2, 498–503.

- Butler, A., Carter-Franklin, J.N., 2004. The role of vanadium bromoperoxidase in the biosynthesis of halogenated marine natural products. *Natural Product Reports* 21, 180–188. <https://doi.org/10.1039/B302337K>
- Byrd, A.L., Segre, J.A., 2016. Adapting Koch's postulates. *Science* 351, 224–226. <https://doi.org/10.1126/science.aad6753>
- Cáceres, M.D., Legendre, P., 2009. Associations between species and groups of sites: indices and statistical inference. *Ecology* 90, 3566–3574. <https://doi.org/10.1890/08-1823.1>
- Callahan, B.J., McMurdie, P.J., Rosen, M.J., Han, A.W., Johnson, A.J.A., Holmes, S.P., 2016. DADA2: High-resolution sample inference from Illumina amplicon data. *Nature Methods* 13, 581–583. <https://doi.org/10.1038/nmeth.3869>
- Camacho, C., Coulouris, G., Avagyan, V., Ma, N., Papadopoulos, J., Bealer, K., Madden, T.L., 2009. BLAST+: architecture and applications. *BMC Bioinformatics* 10, 1–9. <https://doi.org/10.1186/1471-2105-10-421>
- Cannell, R.J., 1993. Algae as a source of biologically active products. *Pesticide Science* 39, 147–153.
- Cao, H., Long, X., Lu, L., Yang, X., Chen, B., 2016. *Citrobacter freundii*: a causative agent for Tail Rot Disease in freshwater cultured Japanese Eel *Anguilla japonica*. *The Israeli Journal of Aquaculture-Bamidgeh, IJA* 68.2016.1271.
- Cardenas, E., Tiedje, J.M., 2008. New tools for discovering and characterizing microbial diversity. *Current Opinion in Biotechnology* 19, 544–549. <https://doi.org/10.1016/j.copbio.2008.10.010>
- Cariou, V., Bouveresse, D.J.-R., Qannari, E.M., Rutledge, D.N., 2019. ComDim methods for the analysis of multiblock data in a data fusion perspective, in: *Data Handling in Science and Technology*. Elsevier, pp. 179–204. <https://doi.org/10.1016/B978-0-444-63984-4.00007-7>
- Caruso, C., Peletto, S., Gustinelli, A., Arsieni, P., Mordenti, O., Modesto, P., Acutis, P.L., Masoero, L., Fioravanti, M.L., Prearo, M., 2014. Detection of a phylogenetically divergent eel virus European X (EVEX) isolate in European eels (*Anguilla anguilla*) farmed in experimental tanks in Italy. *Aquaculture* 434, 115–120. <https://doi.org/10.1016/j.aquaculture.2014.07.024>
- Castanho, S., Califano, G., Soares, F., Costa, R., Mata, L., Pousão-Ferreira, P., Ribeiro, L., 2017. The effect of live feeds bathed with the red seaweed *Asparagopsis armata* on the survival, growth and physiology status of *Sparus aurata* larvae. *Fish physiology and biochemistry* 43, 1043–1054. <https://doi.org/10.1007/s10695-017-0351-6>
- Castric, J., Chastel, C., 1980. Isolation and characterization attempts of three viruses from European eel, *Anguilla anguilla*: preliminary results, in: *Annales de l'Institut Pasteur/Virologie*. Elsevier, pp. 435–448. [https://doi.org/10.1016/0769-2617\(80\)90042-8](https://doi.org/10.1016/0769-2617(80)90042-8)
- Castric, J., Rasschaert, D., Bernard, J., 1984. Evidence of lyssaviruses among rhabdovirus isolates from the European eel *Anguilla anguilla*, in: *Annales de l'Institut Pasteur/Virologie*. Elsevier, pp. 35–55. [https://doi.org/10.1016/S0769-2617\(84\)80038-6](https://doi.org/10.1016/S0769-2617(84)80038-6)
- Castric, J., Jeffroy, J., Bearzotti, M., Kinkelin, P. de, 1992. Isolation of viral haemorrhagic septicaemia virus (VHSV) from wild elvers *Anguilla anguilla*. *Bulletin of the European Association of Fish Pathologists* 12, 21–23.
- Chambers, M.C., Maclean, B., Burke, R., Amodei, D., Ruderman, D.L., Neumann, S., Gatto, L., Fischer, B., Pratt, B., Egertson, J., 2012. A cross-platform toolkit for mass spectrometry and proteomics. *Nature Biotechnology* 30, 918–920. <https://doi.org/10.1038/nbt.2377>
- Chambers, S.M., Qi, Y., Mica, Y., Lee, G., Zhang, X.-J., Niu, L., Bilsland, J., Cao, L., Stevens, E., Whiting, P., 2012. Combined small-molecule inhibition accelerates developmental timing and converts human pluripotent stem cells into nociceptors. *Nature Biotechnology* 30, 715–720. <https://doi.org/10.1038/nbt.2249>
- Chang, C.-I., Liu, W.-Y., 2002. An evaluation of two probiotic bacterial strains, *Enterococcus faecium* SF68 and *Bacillus toyoi*, for reducing edwardsiellosis in cultured European eel, *Anguilla anguilla* L. *Journal of Fish Diseases* 25, 311–315. <https://doi.org/10.1046/j.1365-2761.2002.00365.x>
- Chen, Q., Gong, H., Yang, J., 2011. Isolation and identification of *Edwardsiella tarda* in *Anguilla anguilla*. *Chinese Journal of Zoonoses* 27, 7–10.
- Choi, S.-H., Park, K.-H., Yoon, T.-J., Kim, J.-B., Jang, Y.-S., Choe, C.H., 2008. Dietary Korean mistletoe enhances cellular non-specific immune responses and survival of Japanese eel

(*Anguilla japonica*). Fish & Shellfish Immunology 24, 67–73.
<https://doi.org/10.1016/j.fsi.2007.08.007>

- Clark, B.R., Mizobe, M., Kaluhiwa, J.L., Leong, J.-A., Borris, R.P., 2018. Chemical and genetic differences between Hawaiian lineages of the alga *Asparagopsis taxiformis*. Journal of Applied Phycology 30, 2549–2559. <https://doi.org/10.1007/s10811-018-1474-6>
- Coleman, S.S., Melanson, D.M., Biosca, E.G., Oliver, J.D., 1996. Detection of *Vibrio vulnificus* biotypes 1 and 2 in eels and oysters by PCR amplification. Applied and Environmental Microbiology 62, 1378–1382. <https://doi.org/10.1128/aem.62.4.1378-1382.1996>
- Collado, R., Fouz, B., Sanjuán, E., Amaro, C., 2000. Effectiveness of different vaccine formulations against vibriosis caused by *Vibrio vulnificus* serovar E (biotype 2) in European eels *Anguilla anguilla*. Diseases of Aquatic Organisms 43, 91–101. <https://doi.org/10.3354/dao043091>
- Combaut, G., Bruneau, Y., Codomier, L., Teste, J., 1979. Comparative sterols composition of the red alga *Asparagopsis armata* and its tetrasporophyte *Falkenbergia rufolanosa*. Journal of natural products 42, 150–151.
- Cone, D.K., Marcogliese, D.J., Watt, W.D., 1993. Metazoan parasite communities of yellow eels (*Anguilla rostrata*) in acidic and limed rivers of Nova Scotia. Canadian Journal of Zoology 71, 177–184. <https://doi.org/10.1139/z93-024>
- Crean, S.R., Dick, J.T.A., Evans, D.W., Elwood, R.W., Rosell, R.S., 2003. Anal redness in European eels as an indicator of infection by the swimbladder nematode, *Anguillicola crassus*. Journal of Fish Biology 62, 482–485. <https://doi.org/10.1046/j.1095-8649.2003.00034.x>
- Cresci, A., 2020. A comprehensive hypothesis on the migration of European glass eels (*Anguilla anguilla*). Biological Reviews 95, 1273–1286. <https://doi.org/10.1111/brv.12609>
- da Costa, A.R., Chideroli, R.T., Lanes, G.C., Ferrari, N.A., Chicoski, L.M., Batista, C.E., Pandolfi, V.C.F., Ware, C., Griffin, M.J., Dos Santos, A.R., 2022. Multiplex PCR assay for correct identification of the fish pathogenic species of *Edwardsiella* genus reveals the presence of *E. angillarum* in South America in strains previously characterized as *E. tarda*. Journal of Applied Microbiology 132, 4225–4235. <https://doi.org/10.1111/jam.15538>
- da Costa, E., Domingues, P., Melo, T., Coelho, E., Pereira, R., Calado, R., Abreu, M.H., Domingues, M.R., 2019. Lipidomic signatures reveal seasonal shifts on the relative abundance of high-valued lipids from the brown algae *Fucus vesiculosus*. Marine drugs 17, 335. <https://doi.org/10.3390/md17060335>
- da Silva Lino, M.A., Bezerra, R.F., da Silva, C.D.C., Carvalho, E., Coelho, L., 2014. Fish lectins: a brief review. Advances in zoology research. Nova Science, Hauppauge 95–114.
- Dahms, H.U., Dobretsov, S., 2017. Antifouling compounds from marine macroalgae. Marine drugs 15(9), 265. <https://doi.org/10.3390/md15090265>
- Dalsgaard, I., Høi, L., Siebeling, R.J., Dalsgaard, A., 1999. Indole-positive *Vibrio vulnificus* isolated from disease outbreaks on a Danish eel farm. Diseases of Aquatic Organisms 35, 187–194. <https://doi.org/10.3354/dao035187>
- Danecek, P., Bonfield, J.K., Liddle, J., Marshall, J., Ohan, V., Pollard, M.O., Whitwham, A., Keane, T., McCarthy, S.A., Davies, R.M., 2021. Twelve years of SAMtools and BCFtools. Gigascience 10, giab008. <https://doi.org/10.1093/gigascience/giab008>
- Danne, L., Horn, L., Feldhaus, A., Fey, D., Emde, S., Schütze, H., Adamek, M., Hellmann, J., 2022. Virus infections of the European Eel in North Rhine Westphalian rivers. Journal of Fish Diseases 45, 69–76. <https://doi.org/10.1111/jfd.13536>
- Davis, J.F., Hayasaka, S.S., 1983. Pathogenic bacteria associated with cultured American eels, *Anguilla rostrata* Le Sueur. Journal of Fish Biology 23, 557–564. <https://doi.org/10.1111/j.1095-8649.1983.tb02935.x>
- De Charleroy, D., Grisez, L., Thomas, K., Belpaire, C., Ollevier, F., 1990. The life cycle of *Anguillicola crassus*. Diseases of Aquatic Organisms 8, 77–84.
- De Noia, M., Poole, R., Kaufmann, J., Waters, C., Adams, C., McGinnity, P., Llewellyn, M., 2022. Towards an in-situ non-lethal rapid test to accurately detect the presence of the nematode parasite, *Anguillicoloides crassus*, in European eel, *Anguilla anguilla*. Parasitology 1–29. <https://doi.org/10.1017/S0031182021002146>
- Deborde, C., Fontaine, J.-X., Jacob, D., Botana, A., Nicaise, V., Richard-Forget, F., Lecomte, S., Decourt, C., Hamade, K., Mesnard, F., 2019. Optimizing 1D ¹H-NMR profiling of plant

- samples for high throughput analysis: extract preparation, standardization, automation and spectra processing. *Metabolomics* 15, 1–12. <https://doi.org/10.1007/s11306-019-1488-3>
- Defoirdt, T., Sorgeloos, P., Bossier, P., 2011. Alternatives to antibiotics for the control of bacterial disease in aquaculture. *Current Opinion in Microbiology* 14, 251–258. <https://doi.org/10.1016/j.mib.2011.03.004>
- Dekker, W., 2008. Coming to grips with the eel stock slip-sliding away. International governance of fisheries ecosystems: learning from the past, finding solutions for the future. American Fisheries Society, Bethesda, Maryland 335–355.
- Demain, A.L., Fang, A., 2000. The natural functions of secondary metabolites. *History of Modern Biotechnology* I, 1–39. https://doi.org/10.1007/3-540-44964-7_1
- Dezfuli, B.S., Maestri, C., Lorenzoni, M., Carosi, A., Maynard, B.J., Bosi, G., 2021. The impact of *Anguillicoloides crassus* (Nematoda) on European eel swimbladder: histopathology and relationship between neuroendocrine and immune cells. *Parasitology* 148, 612–622. <https://doi.org/10.1017/S0031182021000032>
- Diehl, N., Michalik, D., Zuccarello, G.C., Karsten, U., 2019. Stress metabolite pattern in the eulittoral red alga *Pyropia plicata* (Bangiales) in New Zealand—mycosporine-like amino acids and heterosides. *Journal of Experimental Marine Biology and Ecology* 510, 23–30. <https://doi.org/10.1016/j.jembe.2018.10.002>
- Dijoux, L., Viard, F., Payri, C., 2014. The more we search, the more we find: discovery of a new lineage and a new species complex in the genus *Asparagopsis*. *PloS one* 9, e103826. <https://doi.org/10.1371/journal.pone.0103826>
- Dixon, P.F., Hill, B.J., 1984. Rapid detection of fish rhabdoviruses by the enzyme-linked immunosorbent assay (ELISA). *Aquaculture* 42, 1–12. [https://doi.org/10.1016/0044-8486\(84\)90308-9](https://doi.org/10.1016/0044-8486(84)90308-9)
- Dixon, P.S., 1964. *Asparagopsis* in Europe. *Nature* 204, 902–902.
- Djoumbou Feunang, Y., Eisner, R., Knox, C., Chepelev, L., Hastings, J., Owen, G., Fahy, E., Steinbeck, C., Subramanian, S., Bolton, E., 2016. ClassyFire: automated chemical classification with a comprehensive, computable taxonomy. *Journal of cheminformatics* 8 (61). <https://doi.org/10.1186/s13321-016-0174-y>
- Doberva, M., Stien, D., Sorres, J., Hue, N., Sanchez-Ferandin, S., Eparvier, V., Ferandin, Y., Lebaron, P., Lami, R., 2017. Large diversity and original structures of acyl-homoserine lactones in strain MOLA 401, a marine Rhodobacteraceae bacterium. *Frontiers in Microbiology* 8, 1152. <https://doi.org/10.3389/fmicb.2017.01152>
- Dobretsov, S., Teplitski, M., Paul, V., 2009. Mini-review: quorum sensing in the marine environment and its relationship to biofouling. *Biofouling* 25, 413–427. <https://doi.org/10.1080/08927010902853516>
- Drouineau, H., Durif, C., Castonguay, M., Mateo, M., Rochard, E., Verreault, G., Yokouchi, K., Lambert, P., 2018. Freshwater eels: A symbol of the effects of global change. *Fish and Fisheries* 19, 903–930. <https://doi.org/10.1111/faf.12300>
- Dührkop, K., Shen, H., Meusel, M., Rousu, J., Böcker, S., 2015. Searching molecular structure databases with tandem mass spectra using CSI: FingerID. *Proceedings of the National Academy of Sciences* 112(41), 12580–12585. <https://doi.org/10.1073/pnas.1509788112>
- Dührkop, K., Fleischauer, M., Ludwig, M., Aksnov, A.A., Melnik, A.V., Meusel, M., Dorrestein, P.C., Rousu, J., Böcker, S., 2019. SIRIUS 4: a rapid tool for turning tandem mass spectra into metabolite structure information. *Nature Methods* 16, 299–302. <https://doi.org/10.1038/s41592-019-0344-8>
- Dührkop, K., Nothias, L.-F., Fleischauer, M., Reher, R., Ludwig, M., Hoffmann, M.A., Petras, D., Gerwick, W.H., Rousu, J., Dorrestein, P.C., 2021. Systematic classification of unknown metabolites using high-resolution fragmentation mass spectra. *Nature Biotechnology* 39, 462–471. <https://doi.org/10.1038/s41587-020-0740-8>
- Dworjanyn, S.A., De Nys, R., Steinberg, P.D., 1999. Localisation and surface quantification of secondary metabolites in the red alga *Delisea pulchra*. *Marine Biology* 133, 727–736. <https://doi.org/10.1007/s002270050514>

- Dzido, J., Rolbiecki, L., Izdebska, J.N., Bednarek, R., 2020. Checklist of the parasites of European eel *Anguilla anguilla* (Linnaeus, 1758) (Anguillidae) in Poland. Biodiversity data journal 8:e52346. <https://doi.org/10.3897%2FBDJ.8.e52346>
- Egan, S., Harder, T., Burke, C., Steinberg, P., Kjelleberg, S., Thomas, T., 2013. The seaweed holobiont: understanding seaweed–bacteria interactions. FEMS Microbiology Reviews 37(3), 462–476. <https://doi.org/10.1111/1574-6976.12011>
- Egusa, S., 1970. Brachchionephritis prevailed among eel populations in farm-ponds in the winter of 1969-70. Fish Pathology 5, 51–66.
- Egusa, S., 1979. Notes on the culture of the European eel (*Anguilla anguilla* L.) in Japanese eel-farming ponds. Rapports et Proces-Verbaux des Reunions, Conseil Internationale pour l'Exploration de la Mer 174, 51–58.
- Egusa, S., Tanaka, M., Ogami, H., Oka, H., 1989. Histopathological observations on an intense congestion of the gills in cultured Japanese eel, *Anguilla japonica*. Fish Pathology 24, 51–56. <https://doi.org/10.3147/jsfp.24.51>
- Ehrenfeld, J.G., 2010. Ecosystem consequences of biological invasions. Annual Review of Ecology, Evolution, and Systematics 41, 59–80. <https://doi.org/10.1146/annurev-ecolsys-102209-144650>
- El Baz, F.K., El Baroty, G.S., Abd El Bakry, H.H., Abd El-Salam, O.I., Ibrahim, E.A., 2013. Structural characterization and biological activity of sulfolipids from selected marine algae. Grasas y Aceites 64, 5.
- El Hattab, N., Daghbouche, Y., El Hattab, M., Piovetti, L., Garrigues, S., de la Guardia, M., 2006. FTIR-determination of sterols from the red alga *Asparagopsis armata*: Comparative studies with HPLC. Talanta 68, 1230–1235. <https://doi.org/10.1016/j.talanta.2005.07.023>
- El-Baroty, G.S., Moussa, M.Y., Shallan, M.A., Ali, M.A., Sabh, A.Z., Shalaby, E.A., 2007. Contribution to the aroma, biological activities, minerals, protein, pigments and lipid contents of the red alga: *Asparagopsis taxiformis* (Delile) Trevisan. J. Appl. Sci. Res 3, 1825–1834.
- Elie, P., Rigaud, C., 1987. L'impact d'un barrage d'estuaire sur la migration des poissons amphihalins: le cas de l'anguille et du barrage d'Arzal. La Houille Blanche 99–108. <https://doi.org/10.1051/lhb/1987010>
- Ellis, A.E., Dear, G., Stewart, D.J., 1983. Histopathology of Sekiten-byo' caused by *Pseudomonas anguilliseptica* in the European eel, *Anguilla anguilla* L., in Scotland. Journal of Fish Diseases 6, 77–79. <https://doi.org/10.1111/j.1365-2761.1983.tb00053.x>
- Esteve, C., Alcaide, E., Herráiz, S., Canals, R., Merino, S., Tomás, J.M., 2007. First description of nonmotile *Vibrio vulnificus* strains virulent for eels. FEMS microbiology letters 266, 90–97. <https://doi.org/10.1111/j.1574-6968.2006.00519.x>
- Esteve, C., Biosca, E.G., Amaro, C., 1993. Virulence of *Aeromonas hydrophila* and some other bacteria isolated from European eels *Anguilla anguilla* reared in fresh water. Diseases of Aquatic Organisms 16, 15–20.
- Esteve, C., Amaro, C., Garay, E., Santos, Y., Toranzo, A.E., 1995. Pathogenicity of live bacteria and extracellular products of motile *Aeromonas* isolated from eels. Journal of Applied Bacteriology 78, 555–562. <https://doi.org/10.1111/j.1365-2672.1995.tb03099.x>
- Esteve, C., Alcaide, E., 2009. Influence of diseases on the wild eel stock: the case of Albufera Lake. Aquaculture 289, 143–149. <https://doi.org/10.1016/j.aquaculture.2008.12.015>
- Esteve, C., Alcaide, E., Ureña, R., 2012. The effect of metals on condition and pathologies of European eel (*Anguilla anguilla*): In situ and laboratory experiments. Aquatic Toxicology 109, 176–184. <https://doi.org/10.1016/j.aquatox.2011.10.002>
- Esteve-Gassent, M.D., Fouz, B., Amaro, C., 2004a. Efficacy of a bivalent vaccine against eel diseases caused by *Vibrio vulnificus* after its administration by four different routes. Fish & Shellfish Immunology 16, 93–105. [https://doi.org/10.1016/S1050-4648\(03\)00036-6](https://doi.org/10.1016/S1050-4648(03)00036-6)
- Esteve-Gassent, M.D., Fouz, B., Barrera, R., Amaro, C., 2004b. Efficacy of oral reimmunisation after immersion vaccination against *Vibrio vulnificus* in farmed European eels. Aquaculture 231, 9–22. <https://doi.org/10.1016/j.aquaculture.2003.10.006>
- FAO, 2021. Fishery and Aquaculture Statistics 2019/FAO annuaire. Statistiques des pêches et de l'aquaculture 2019/FAO anuario.

- Feldmann, J., 1939. Algology. On the development of carpospores and alteranation of generations of Harvey. *Asparagopsis armata*. Comptes Rendus Hebdomadaires des Séances de L'Académie des Sciences 208, 1240–1242.
- Feldmann, J., Feldmann, G., 1942. Recherches sur les Bonnemaisoniacés et leur alternance de générations. Annales des sciences naturelles Botanique 11, 75–175.
- Félix, R., Dias, P., Félix, C., Cerqueira, T., Andrade, P.B., Valentão, P., Lemos, M.F., 2021. The biotechnological potential of *Asparagopsis armata*: What is known of its chemical composition, bioactivities and current market? Algal Research 60, 102534. <https://doi.org/10.1016/j.algal.2021.102534>
- Felline, S., Del Coco, L., Kaleb, S., Guarnieri, G., Fraschetti, S., Terlizzi, A., Fanizzi, F.P., Falace, A., 2019. The response of the algae *Fucus virsoides* (Fucales, Ochrophyta) to Roundup® solution exposure: A metabolomics approach. Environmental Pollution 254, 112977. <https://doi.org/10.1016/j.envpol.2019.112977>
- Feng, J., Lin, P., Guo, S., Jia, Y., Wang, Y., Zadlock, F., Zhang, Z., 2017. Identification and characterization of a novel conserved 46 kD maltoporin of *Aeromonas hydrophila* as a versatile vaccine candidate in European eel (*Anguilla anguilla*). Fish & Shellfish Immunology 64, 93–103. <https://doi.org/10.1016/j.fsi.2017.03.010>
- Feunteun, E., 2002. Management and restoration of European eel population (*Anguilla anguilla*): an impossible bargain. Ecological engineering 18, 575–591. [https://doi.org/10.1016/S0925-8574\(02\)00021-6](https://doi.org/10.1016/S0925-8574(02)00021-6)
- Figueroa, F.L., Bueno, A., Korbee, N., Santos, R., Mata, L., Schuenhoff, A., 2008. Accumulation of Mycosporine-like Amino Acids in *Asparagopsis armata* Grown in Tanks with Fishpond Effluents of Gilthead Sea Bream, *Sparus aurata*. Journal of the World Aquaculture Society 39, 692–699. <https://doi.org/10.1111/j.1749-7345.2008.00199.x>
- Foscarini, R., 1989. Induction and development of bacterial gill disease in the eel (*Anguilla japonica*) experimentally infected with *Flexibacter columnaris*: pathological changes in the gill vascular structure and in cardiac performance. Aquaculture 78, 1–20. [https://doi.org/10.1016/0044-8486\(89\)90002-1](https://doi.org/10.1016/0044-8486(89)90002-1)
- Fournier, J.-B., Leblanc, C., 2014. Halogenation and vanadium haloperoxidases. Outstanding Marine Molecules 225–242. <https://doi.org/10.1002/9783527681501.ch10>
- Fouz, B., Esteve-Gassent, M.D., Barrera, R., Larsen, J.L., Nielsen, M.E., Amaro, C., 2001. Field testing of a vaccine against eel diseases caused by *Vibrio vulnificus*. Diseases of Aquatic Organisms 45, 183–189. <https://doi.org/10.3354/dao045183>
- Frans, I., Michiels, C.W., Bossier, P., Willems, K.A., Lievens, B., Rediers, H., 2011. *Vibrio anguillarum* as a fish pathogen: virulence factors, diagnosis and prevention. Journal of Fish Diseases 34, 643–661. <https://doi.org/10.1111/j.1365-2761.2011.01279.x>
- Fries, L.T., Williams, D.J., Johnson, S.K., 1996. Occurrence of *Anguillicola crassus*, an exotic parasitic swim bladder nematode of eels, in the southeastern United States. Transactions of the American Fisheries Society 125, 794–797. [https://doi.org/10.1577/1548-8659\(1996\)125%3C0794:NOOCAE%3E2.3.CO;2](https://doi.org/10.1577/1548-8659(1996)125%3C0794:NOOCAE%3E2.3.CO;2)
- Frisch, K., Davie, A., Schwarz, T., Turnbull, J.F., 2016. Comparative imaging of European eels (*Anguilla anguilla*) for the evaluation of swimbladder nematode (*Anguillicoloides crassus*) infestation. Journal of Fish Diseases 39, 635–647. <https://doi.org/10.1111/jfd.12383>
- Fusetani, N., 2010. Biotechnological potential of marine natural products. Pure and Applied Chemistry 82, 17–26. <https://doi.org/10.1351/PAC-CON-09-01-11>
- Galinier, R., van Beurden, S., Amilhat, E., Castric, J., Schoehn, G., Verneau, O., Fazio, G., Allienne, J.-F., Engelsma, M., Sasal, P., 2012. Complete genomic sequence and taxonomic position of eel virus European X (EVEX), a rhabdovirus of European eel. Virus Research 166, 1–12. <https://doi.org/10.1016/j.virusres.2012.02.020>
- Garcia-Gallego, M., Akharbach, H., De la Higuera, M., 1998. Use of protein sources alternative to fish meal in diets with amino acids supplementation for the European eel (*Anguilla anguilla*). Animal science 66, 285–292. <https://doi.org/10.1017/S1357729800009073>
- Garon-Lardiére, S., 2004. Etude structurale des polysaccharides pariétaux de l'algue rouge *Asparagopsis armata* (Bonnemaisoniales) (PhD Thesis). Université de Bretagne Occidentale.

- Gatesoupe, F.J., 1999. The use of probiotics in aquaculture. *Aquaculture* 180, 147–165. [https://doi.org/10.1016/S0044-8486\(99\)00187-8](https://doi.org/10.1016/S0044-8486(99)00187-8)
- Gaubert, J., Greff, S., Thomas, O.P., Payri, C.E., 2019a. Metabolomic variability of four macroalgal species of the genus *Lobophora* using diverse approaches. *Phytochemistry* 162, 165–172. <https://doi.org/10.1016/j.phytochem.2019.03.002>
- Gaubert, J., Payri, C.E., Vieira, C., Solanki, H., Thomas, O.P., 2019b. High metabolic variation for seaweeds in response to environmental changes: a case study of the brown algae *Lobophora* in coral reefs. *Scientific reports* 9, 993. <https://doi.org/10.1038/s41598-018-38177-z>
- Gaubert, J., Rodolfo-Metalpa, R., Greff, S., Thomas, O.P., Payri, C.E., 2020. Impact of ocean acidification on the metabolome of the brown macroalgae *Lobophora rosacea* from New Caledonia. *Algal Research* 46, 101783. <https://doi.org/10.1016/j.algal.2019.101783>
- Geets, A., Liewes, E.W., Ollevier, F., 1992. Efficacy of some anthelmintics against the swimbladder nematode *Anguillicola crassus* of eel *Anguilla anguilla* under saltwater conditions. *Diseases of Aquatic Organisms* 13, 123–128. <https://doi.org/10.3354/dao013123>
- Genovese, G., Tedone, L., Hamann, M., Morabito, M., 2009. The Mediterranean red alga *Asparagopsis*: a source of compounds against *Leishmania*. *Marine drugs* 7, 361–366. <https://doi.org/10.3390/md7030361>
- Genovese, G., Faggio, C., Gugliandolo, C., Torre, A., Spanò, A., Morabito, M., Maugeri, T.L., 2012. *In vitro* evaluation of antibacterial activity of *Asparagopsis taxiformis* from the Straits of Messina against pathogens relevant in aquaculture. *Marine Environmental Research* 73, 1–6. <https://doi.org/10.1016/j.marenvres.2011.10.002>
- Gérard, C., Trancart, T., Amilhat, E., Faliex, E., Virag, L., Feunteun, E., Acou, A., 2013. Influence of introduced vs. native parasites on the body condition of migrant silver eels. *Parasite* 20:38. <https://doi.org/10.1051%2Fparasite%2F2013040>
- Giacomoni, F., Le Corguille, G., Monsoor, M., Landi, M., Pericard, P., Petera, M., Duperier, C., Tremblay-Franco, M., Martin, J.-F., Jacob, D., 2015. Workflow4Metabolomics: a collaborative research infrastructure for computational metabolomics. *Bioinformatics* 31, 1493–1495. <https://doi.org/10.1093/bioinformatics/btu813>
- Giari, L., Ruehle, B., Fano, E.A., Castaldelli, G., Poulin, R., 2020. Temporal dynamics of species associations in the parasite community of European eels, *Anguilla anguilla*, from a coastal lagoon. *International Journal for Parasitology: Parasites and Wildlife* 12, 67–75. <https://doi.org/10.1016/j.ijppaw.2020.05.001>
- Giari, L., Castaldelli, G., Gavioli, A., Lanzoni, M., Fano, E.A., 2021. Long-term ecological analysis of *Anguillicola crassus* occurrence and impact on the European eel population in a Mediterranean lagoon (North Italy). *Estuarine, Coastal and Shelf Science* 249, 107117. <https://doi.org/10.1016/j.ecss.2020.107117>
- Gibbons, T.C., Metzger, D.C., Healy, T.M., Schulte, P.M., 2017. Gene expression plasticity in response to salinity acclimation in threespine stickleback ecotypes from different salinity habitats. *Molecular Ecology* 26, 2711–2725. <https://doi.org/10.1111/mec.14065>
- Glasson, C.R., Kinley, R.D., de Nys, R., King, N., Adams, S.L., Packer, M.A., Svenson, J., Eason, C.T., Magnusson, M., 2022. Benefits and risks of including the bromoform containing seaweed *Asparagopsis* in feed for the reduction of methane production from ruminants. *Algal Research* 64, 102673. <https://doi.org/10.1016/j.algal.2022.102673>
- Gothwal, R., Shashidhar, T., 2015. Antibiotic pollution in the environment: a review. *Clean–Soil, Air, Water* 43, 479–489. <https://doi.org/10.1002/clen.201300989>
- Götz, S., García-Gómez, J.M., Terol, J., Williams, T.D., Nagaraj, S.H., Nueda, M.J., Robles, M., Talón, M., Dopazo, J., Conesa, A., 2008. High-throughput functional annotation and data mining with the Blast2GO suite. *Nucleic acids research* 36(10), 3420–3435. <https://doi.org/10.1093/nar/gkn176>
- Greco, S., Gaetano, A.S., Furlanis, G., Capanni, F., Manfrin, C., Giulianini, P.G., Santovito, G., Edomi, P., Pallavicini, A., Gerdol, M., 2022. Gene Expression Profiling of *Trematomus bernacchii* in Response to Thermal and Stabiling Stress. *Fishes* 7(6), 387. <https://doi.org/10.3390/fishes7060387>

- Greff, S., Zubia, M., Genta-Jouve, G., Massi, L., Perez, T., Thomas, O.P., 2014. Mahorones, highly brominated cyclopentenones from the red alga *Asparagopsis taxiformis*. Journal of natural products 77, 1150–1155. <https://doi.org/10.1021/np401094h>
- Greff, S., 2016. Métabolomique, effets biologiques et caractère invasif de la macroalgue *Asparagopsis taxiformis* (PhD Thesis). Aix-Marseille.
- Greff, S., Aires, T., Serrão, E.A., Engelen, A.H., Thomas, O.P., Pérez, T., 2017a. The interaction between the proliferating macroalga *Asparagopsis taxiformis* and the coral *Astroides calycularis* induces changes in microbiome and metabolomic fingerprints. Scientific reports 7, 1–14. <https://doi.org/10.1038/srep42625>
- Greff, S., Zubia, M., Payri, C., Thomas, O.P., Perez, T., 2017b. Chemogeography of the red macroalgae *Asparagopsis*: metabolomics, bioactivity, and relation to invasiveness. Metabolomics 13, 33. <https://doi.org/10.1007/s11306-017-1169-z>
- Griffin, M.J., Soto, E., Wise, D.J., 2020. Edwardsiellosis., in: Climate Change and Infectious Fish Diseases. CABI Wallingford UK, pp. 235–264. <https://doi.org/10.1079/9781789243277.0235>
- Grigorian, E., Groisillier, A., Thomas, F., Leblanc, C., Delage, L., 2021. Functional characterization of a L-2-haloacid dehalogenase from *Zobellia galactanivorans* DsijT suggests a role in haloacetic acid catabolism and a wide distribution in marine environments. Frontiers in Microbiology 12:725997. <https://doi.org/10.3389/fmicb.2021.725997>
- Guan, R., Xiong, J., Huang, W., Guo, S., 2011. Enhancement of protective immunity in European eel (*Anguilla anguilla*) against *Aeromonas hydrophila* and *Aeromonas sobria* by a recombinant *Aeromonas* outer membrane protein. Acta Biochimica et Biophysica Sinica 43, 79–88. <https://doi.org/10.1093/abbs/gmq115>
- Gudding, R., Van Muiswinkel, W.B., 2013. A history of fish vaccination: science-based disease prevention in aquaculture. Fish & Shellfish Immunology 35, 1683–1688. <https://doi.org/10.1016/j.fsi.2013.09.031>
- Guitton, Y., Tremblay-Franco, M., Le Corguillé, G., Martin, J.-F., Pétéra, M., Roger-Mele, P., Delabrière, A., Goulitquer, S., Monsoor, M., Duperier, C., 2017. Create, run, share, publish, and reference your LC–MS, FIA–MS, GC–MS, and NMR data analysis workflows with the Workflow4Metabolomics 3.0 Galaxy online infrastructure for metabolomics. The International Journal of Biochemistry & Cell Biology 93, 89–101. <https://doi.org/10.1016/j.biocel.2017.07.002>
- Guo, C., Huang, X., Yang, M., Wang, S., Ren, S., Li, H., Peng, X., 2014. GC/MS-based metabolomics approach to identify biomarkers differentiating survivals from death in crucian carps infected by *Edwardsiella tarda*. Fish & Shellfish Immunology 39, 215–222. <https://doi.org/10.1016/j.fsi.2014.04.017>
- Guo, S., Hu, L., Feng, J., Lin, P., He, L., Yan, Q., 2019. Immunogenicity of a bivalent protein as a vaccine against *Edwardsiella anguillarum* and *Vibrio vulnificus* in Japanese eel (*Anguilla japonica*). MicrobiologyOpen 8, e00766. <https://doi.org/10.1002/mbo3.766>
- Guo, S., He, L., Wu, L., Xiao, Y., Zhai, S., Yan, Q., 2020. Immunization of a novel bivalent outer membrane protein simultaneously resisting *Aeromonas hydrophila*, *Edwardsiella anguillarum* and *Vibrio vulnificus* infection in European eels (*Anguilla anguilla*). Fish & Shellfish Immunology 97, 46–57. <https://doi.org/10.1016/j.fsi.2019.12.044>
- Guo, S.-L., Wang, Y., Guan, R.-Z., Feng, J.-J., Yang, Q.-H., Lu, P.-P., Hu, L.-L., Zhao, J.-P., 2013. Immune effects of a bivalent expressed outer membrane protein to American eels (*Anguilla rostrata*). Fish & Shellfish Immunology 35, 213–220. <https://doi.org/10.1016/j.fsi.2013.04.027>
- Guo, S.-L., Lu, P.-P., Feng, J., Zhao, J., Lin, P., Duan, L., 2015. A novel recombinant bivalent outer membrane protein of *Vibrio vulnificus* and *Aeromonas hydrophila* as a vaccine antigen of American eel (*Anguilla rostrata*). Fish & Shellfish Immunology 43, 477–484. <https://doi.org/10.1016/j.fsi.2015.01.017>
- Gupta, V., Thakur, R.S., Baghel, R.S., Reddy, C.R.K., Jha, B., 2014. Seaweed metabolomics: a new facet of functional genomics, in: Advances in Botanical Research. Elsevier, pp. 31–52. <https://doi.org/10.1016/B978-0-12-408062-1.00002-0>
- Gutierrez, M.A., Miyazaki, T., Hatta, H., Kim, M., 1993. Protective properties of egg yolk IgY containing anti-*Edwardsiella tarda* antibody against paracolpo disease in the Japanese eel,

- Anguilla japonica* Temminck & Schlegel. Journal of Fish Diseases 16, 113–122. <https://doi.org/10.1111/j.1365-2761.1993.tb00854.x>
- Gutierrez, M.A., Miyazaki, T., 1994. Responses of Japanese eels to oral challenge with *Edwardsiella tarda* after vaccination with formalin-killed cells or lipopolysaccharide of the bacterium. Journal of Aquatic Animal Health 6, 110–117. [https://doi.org/10.1577/1548-8667\(1994\)006<0110:ROJETO>2.3.CO;2](https://doi.org/10.1577/1548-8667(1994)006<0110:ROJETO>2.3.CO;2)
- Haenen, O.L.M., Davidse, A., 2001. First isolation and pathogenicity studies with *Pseudomonas anguilliseptica* from diseased European eel *Anguilla anguilla* (L.) in The Netherlands. Aquaculture 196, 27–36. [https://doi.org/10.1016/S0044-8486\(00\)00566-4](https://doi.org/10.1016/S0044-8486(00)00566-4)
- Haenen, O., van Ginneken, V., Engelsma, M., van den Thillart, G., 2009. Impact of eel viruses on recruitment of European eel, in: Spawning Migration of the European Eel. Springer, pp. 387–400. <https://doi.org/10.1007/978-1-4020-9095-0>
- Haenen, O.L.M., Lehmann, J., Engelsma, M.Y., Stürenberg, F.-J., Roozenburg, I., Kerkhoff, S., Breteler, J.K., 2010. The health status of European silver eels, *Anguilla anguilla*, in the Dutch River Rhine Watershed and Lake IJsselmeer. Aquaculture 309, 15–24. <https://doi.org/10.1016/j.aquaculture.2010.08.026>
- Haenen, O.L.M., Mladineo, I., Konecny, R., Yoshimizu, M., Groman, D., Munoz, P., Saraiva, A., Bergmann, S.M., Van Beurden, S.J., 2012. Diseases of eels in an international perspective: Workshop on Eel Diseases at the 15th International Conference on Diseases of Fish and Shellfish, Split, Croatia, 2011. Bulletin of the European Association of Fish Pathologists 32, 109–115.
- Haenen, O.L.M., Van Zanten, E., Jansen, R., Roozenburg, I., Engelsma, M.Y., Dijkstra, A., Boers, S.A., Voorbergen-Laarman, M., Möller, A.V.M., 2014. *Vibrio vulnificus* outbreaks in Dutch eel farms since 1996: strain diversity and impact. Diseases of Aquatic Organisms 108, 201–209. <https://doi.org/10.3354/dao02703>
- Haenen, O., 2019. Major eel diseases in Europe: the past 30 years, in: Eels Biology, Monitoring, Management, Culture and Exploitation: Proceedings of the First International Eel Science Symposium. 5m Books Ltd.
- Hah, Y.-C., Hong, S.-W., Oh, H.-B., Fryer, J.L., Rohovec, J.S., 1984. Isolation and characterization of bacterial pathogens from eels (*Anguilla japonica*) cultured in Korea. Korean Journal of Microbiology 22, 41–48.
- Hanek, G., Threlfall, W., 1970. Metazoan parasites of the American eel (*Anguilla rostrata* (Le Sueur)) in Newfoundland and Labrador. Canadian Journal of Zoology 48, 597–600. <https://doi.org/10.1139/z70-105>
- Hangalapura, B.N., Zwart, R., Engelsma, M.Y., Haenen, O.L., 2007. Pathogenesis of *Herpesvirus anguillae* (HVA) in juvenile European eel *Anguilla anguilla* after infection by bath immersion. Diseases of Aquatic Organisms 78, 13–22. <https://doi.org/10.3354/dao01849>
- Harvey, W.H., 1855. Some account of the marine botany of the colony of Western Australia. The Transactions of the Royal Irish Academy 22, 525–566.
- Harwood, J.L., 1998. Membrane lipids in algae, in: Lipids in Photosynthesis: Structure, Function and Genetics. Springer, pp. 53–64. https://doi.org/10.1007/0-306-48087-5_3
- Haslin, C., Lahaye, M., Pellegrini, M., 2000. Chemical composition and structure of sulphated water-soluble cell-wall polysaccharides from the gametic, carposporic and tetrasporic stages of *Asparagopsis armata* Harvey (Rhodophyta, Bonnemaisoniaceae). Botanica marina 43, 475–482. <https://doi.org/10.1515/BOT.2000.048>
- Hayasaka, S.S., Sullivan, J., 1981. Furunculosis in cultured American eel *Anguilla rostrata* (Le Sueur). Journal of Fish Biology 18, 655–659. <https://doi.org/10.1111/j.1095-8649.1981.tb03807.x>
- Hayward, C.J., Iwashita, M., Crane, J.S., Ogawa, K., 2001. First report of the invasive eel pest *Pseudodactylogyrus bini* in North America and in wild American eels. Diseases of Aquatic Organisms 44, 53–60. <https://doi.org/10.3354/dao044053>
- He, J., Yu, Y., Qin, X.-W., Zeng, R.-Y., Wang, Y.-Y., Li, Z.-M., Mi, S., Weng, S.-P., Guo, C.-J., He, J.-G., 2019. Identification and functional analysis of the Mandarin fish (*Siniperca chuatsi*) hypoxia-inducible factor-1 α involved in the immune response. Fish & Shellfish Immunology 92, 141–150. <https://doi.org/10.1016/j.fsi.2019.04.298>

- He, L., Wu, L., Lin, P., Zhai, S., Guo, S., Xiao, Y., Wan, Q., 2020. First expression and immunogenicity study of a novel trivalent outer membrane protein (OmpII-UA) from *Aeromonas hydrophila*, *Vibrio vulnificus* and *Edwardsiella anguillarum*. *Aquaculture* 519, 734932. <https://doi.org/10.1016/j.aquaculture.2020.734932>
- He, W., Wu, L., Li, S., Guo, S., 2021. Transcriptome RNA-seq revealed lncRNAs activated by *Edwardsiella anguillarum* post the immunization of OmpA protecting European eel (*Anguilla anguilla*) from being infected. *Fish & Shellfish Immunology* 118, 51–65. <https://doi.org/10.1016/j.fsi.2021.08.027>
- Hellio, C., Simon-Colin, C., Clare, A., Deslandes, E., 2004. Isethionic acid and floridoside isolated from the red alga, *Grateloupia turuturu*, inhibit settlement of *Balanus amphitrite* cyprid larvae. *Biofouling* 20, 139–145. <https://doi.org/10.1080/08927010412331279605>
- Hiney, M., 2001. Validation of non-culture-based pathogen detection systems: theoretical problems and practical considerations. Risk analysis in aquatic animal health. World Organisation for Animal Health (OIE), Paris 259–264.
- Hnath, J.G., 1983. Infectious pancreatic necrosis. A Guide to Integrated Fish Health Management in the Great Lakes Basin 18, 169–173.
- Hoffman, G.L., 2019. Parasites of North American freshwater fishes. Cornell University Press.
- Hoffmann, M.A., Nothias, L.-F., Ludwig, M., Fleischauer, M., Gentry, E.C., Witting, M., Dorrestein, P.C., Dührkop, K., Böcker, S., 2021. Assigning confidence to structural annotations from mass spectra with COSMIC. *BioRxiv* 2021–03. <https://doi.org/10.1101/2021.03.18.435634>
- Höglund, J., Pilström, L., 1994. Purification of adult *Anguilllicola crassus* whole-worm extract antigens for detection of specific antibodies in serum from the European eel (*Anguilla anguilla*) by ELISA. *Fish & Shellfish Immunology* 4, 311–319. <https://doi.org/10.1006/fsim.1994.1027>
- Høi, L., Dalsgaard, I., DePaola, A., Siebeling, R.J., Dalsgaard, A., 1998. Heterogeneity among isolates of *Vibrio vulnificus* recovered from eels (*Anguilla anguilla*) in Denmark. *Applied and Environmental Microbiology* 64, 4676–4682. <https://doi.org/10.1128/AEM.64.12.4676-4682.1998>
- Horta, A., Alves, C., Pinteus, S., Lopes, C., Fino, N., Silva, J., Ribeiro, J., Rodrigues, D., Francisco, J., Rodrigues, A., 2019. Identification of *Asparagopsis armata*-associated bacteria and characterization of their bioactive potential. *MicrobiologyOpen* e00824. <https://doi.org/10.1002/mbo3.824>
- Hossain, M.M.M., Kawai, K., 2009. Stability of effective *Edwardsiella tarda* vaccine developed for Japanese eel (*Anguilla japonica*). *Journal of Fisheries and Aquatic Science* 4, 296–305. <https://doi.org/10.3923/jfas.2009.296.305>
- Hossain, M.M.M., Kawai, K., Duston, J., Oshima, S., 2012. Comparison of the efficacy of selected bacterins against *Edwardsiella tarda* in immunized Japanese eel (*Anguilla japonica*). *Journal of the Bangladesh Agricultural University* 10, 355–366. <http://dx.doi.org/10.3329/jbau.v10i2.14680>
- Hossain, M.M.M., Kawai, K., Oshima, S., 2011a. Immunogenicity of pressure inactivated *Edwardsiella tarda* bacterin to *Anguilla japonica* (Japanese eel). *Pakistan Journal of Biological Sciences: PJBS* 14, 755–767. <https://doi.org/10.3923/pjbs.2011.755.767>
- Hossain, M.M.M., Kawai, K., 2011b. Pathogenicity of *Aeromonas hydrophila* and some other bacteria isolated from Japanese eels (*Anguilla japonica*) reared farm water. *Bangladesh Research Publications Journal* 5, 22–30.
- Huang, L., Peng, L., Yan, X., 2021. Multi-omics responses of red algae *Pyropia haitanensis* to intertidal desiccation during low tides. *Algal Research* 58, 102376. <https://doi.org/10.1016/j.algal.2021.102376>
- Huang, Z., Lu, J., Ye, Y., Xu, A., Li, Z., 2020. Effects of dietary Chinese herbal medicines mixture on growth performance, digestive enzyme activity and serum biochemical parameters of European eel, *Anguilla anguilla*. *Aquaculture Reports* 18, 100510. <https://doi.org/10.1016/j.aqrep.2020.100510>
- Hudson, E.B., Bucke, D., Forrest, A., 1981. Isolation of infectious pancreatic necrosis virus from eels, *Anguilla anguilla* L., in the United Kingdom. *Journal of Fish Diseases* 4, 429–431. <https://doi.org/10.1111/j.1365-2761.1981.tb01153.x>

- Hudson, J., Egan, S., 2022. Opportunistic diseases in marine eukaryotes: Could Bacteroidota be the next threat to ocean life? *Environmental Microbiology* 24, 4505–4518. <https://doi.org/10.1111/1462-2920.16094>
- Hughes, A.H., Magot, F., Tawfike, A.F., Rad-Menéndez, C., Thomas, N., Young, L.C., Stucchi, L., Carettoni, D., Stanley, M.S., Edrada-Ebel, R., 2021. Exploring the chemical space of macro- and micro-algae using comparative metabolomics. *Microorganisms* 9(2), 311. <https://doi.org/10.3390/microorganisms9020311>
- Hunt, P.N., Wilson, M.D., Von Schalburg, K.R., Davidson, W.S., Koop, B.F., 2005. Expression and genomic organization of zonadhesin-like genes in three species of fish give insight into the evolutionary history of a mosaic protein. *BMC Genomics* 6, 1–15. <https://doi.org/10.1186/1471-2164-6-165>
- Hutson, K.S., Mata, L., Paul, N.A., De Nys, R., 2012. Seaweed extracts as a natural control against the monogenean ectoparasite, *Neobenedenia* sp., infecting farmed barramundi (*Lates calcarifer*). *International Journal for Parasitology* 42, 1135–1141. <https://doi.org/10.1016/j.ijpara.2012.09.007>
- Iida, T., Yonekura, H., Izumiya, M., Wakabayashi, H., 1991. Indirect enzyme-linked immunosorbent assay (ELISA) for the detection of eel serum antibody. *Fish Pathology* 26, 201–205. <https://doi.org/10.3147/jsfp.26.201>
- Impellizzeri, G., Mangiafico, S., Oriente, G., Piattelli, M., Sciuto, S., Fattorusso, E., Magno, S., Santacroce, C., Sica, D., 1975. Amino acids and low-molecular-weight carbohydrates of some marine red algae. *Phytochemistry* 14, 1549–1557. [https://doi.org/10.1016/0031-9422\(75\)85349-0](https://doi.org/10.1016/0031-9422(75)85349-0)
- Inui, T., Ushikoshi, R., Nogami, S., Hirose, H., 1999. A competitive-ELISA for the serodiagnosis of anguillicolosis in Japanese eel, *Anguilla japonica*. *Fish Pathology* 34, 25–31. <https://doi.org/10.3147/jsfp.34.25>
- IUCN, 2022. The IUCN Red List of Threatened Species. Version 2021-3. <https://www.iucnredlist.org>. Accessed on 30/01/2022.
- Jacob, D., Deborde, C., Lefebvre, M., Maucourt, M., Moing, A., 2017. NMRProcFlow: A graphical and interactive tool dedicated to 1D spectra processing for NMR-based metabolomics. *Metabolomics* 13, 36. <https://doi.org/10.1007/s11306-017-1178-y>
- Jacoby, D.M., Casselman, J.M., Crook, V., DeLucia, M.-B., Ahn, H., Kaifu, K., Kurwie, T., Sasal, P., Silfvergrip, A.M., Smith, K.G., 2015. Synergistic patterns of threat and the challenges facing global anguillid eel conservation. *Global Ecology and Conservation* 4, 321–333. <https://doi.org/10.1016/j.gecco.2015.07.009>
- Jakob, E., Hanel, R., Klimpel, S., Zumholz, K., 2009. Salinity dependence of parasite infestation in the European eel *Anguilla anguilla* in northern Germany. *ICES Journal of Marine Science* 66, 358–366. <https://doi.org/10.1093/icesjms/fsn160>
- Jakob, E., Walter, T., Hanel, R., 2016. A checklist of the protozoan and metazoan parasites of European eel (*Anguilla anguilla*): checklist of *Anguilla anguilla* parasites. *Journal of Applied Ichthyology* 32, 757–804. <https://doi.org/10.1111/j.1439-0426.2009.01345.x>
- Jaruboonyakorn, P., Tejangkura, T., Chontananarth, T., 2022. Multiplex PCR development for the simultaneous and rapid detection of two pathogenic flukes, *Dactylogyrus* spp. and *Centrocestus formosanus*, in ornamental fishes. *Aquaculture* 548, 737660. <https://doi.org/10.1016/j.aquaculture.2021.737660>
- Jha, B., Kavita, K., Westphal, J., Hartmann, A., Schmitt-Kopplin, P., 2013. Quorum sensing inhibition by *Asparagopsis taxiformis*, a marine macro alga: separation of the compound that interrupts bacterial communication. *Marine Drugs* 11, 253–265. <https://doi.org/10.3390/md11010253>
- Joh, S.J., Kweon, C.H., Kim, M.J., Kang, M.S., Jang, H., Kwon, J.H., 2010. Characterization of *Yersinia ruckeri* isolated from the farm-cultured eel *Anguilla japonica* in Korea. *Korean Journal of Veterinary Research* 50, 29–35.
- Joh, S.-J., Kim, M.-J., Kwon, H.-M., Ahn, E.-H., Jang, H., Kwon, J.-H., 2011. Characterization of *Edwardsiella tarda* isolated from farm-cultured eels, *Anguilla japonica*, in the Republic of Korea. *Journal of Veterinary Medical Science* 73, 7–11. <https://doi.org/10.1292/jvms.10-0252>
- Joh, S.-J., Ahn, E.-H., Lee, H.-J., Shin, G.-W., Kwon, J.-H., Park, C.-G., 2013. Bacterial pathogens and flora isolated from farm-cultured eels (*Anguilla japonica*) and their environmental waters in

- Korean eel farms. Veterinary Microbiology 163, 190–195. <https://doi.org/10.1016/j.vetmic.2012.11.004>
- Johnson, C.H., Ivanisevic, J., Siuzdak, G., 2016. Metabolomics: beyond biomarkers and towards mechanisms. Nature reviews Molecular Cell Biology 17, 451–459. <https://doi.org/10.1038/nrm.2016.25>
- Jørgensen, P.E.V., Castric, J., Hill, B., Ljungberg, O., De Kinkelin, P., 1994. The occurrence of virus infections in elvers and eels (*Anguilla anguilla*) in Europe with particular reference to VHSV and IHNV. Aquaculture 123, 11–19. [https://doi.org/10.1016/0044-8486\(94\)90115-5](https://doi.org/10.1016/0044-8486(94)90115-5)
- Jousseaume, T., Roussel, J.-M., Beaulaton, L., Bardouillet, A., Faliex, E., Amilhat, E., Acou, A., Feunteun, E., Launey, S., 2021. Molecular detection of the swim bladder parasite *Anguilllicola crassus* (Nematoda) in fecal samples of the endangered European eel *Anguilla anguilla*. Parasitology Research 120, 1897–1902. <https://doi.org/10.1007/s00436-021-07100-3>
- Jun, J.W., Kang, J.W., Giri, S.S., Yun, S., Kim, H.J., Kim, S.G., Kim, S.W., Han, S.J., Kwon, J., Oh, W.T., 2020. Immunostimulation by starch hydrogel-based oral vaccine using formalin-killed cells against edwardsiellosis in Japanese eel, *Anguilla japonica*. Vaccine 38, 3847–3853. <https://doi.org/10.1016/j.vaccine.2020.03.046>
- Jung, S.-H., Kwon, M.-G., Seo, J.-S., Hwang, J.Y., 2015. Effect of Immersion and Oral Vaccination using Formalin-killed *Edwardsiella tarda* against Eel *Anguilla japonica*. Journal of Fisheries and Marine Sciences Education 27, 672–681. <https://doi.org/10.13000/JFMSE.2015.27.3.672>
- Kaifu, K., Mochioka, N., Yamaoka, M., Kurota, H., Yoshida, T., 2018. Current activities and challenges for conservation and sustainable harvest of Japanese eel in Japan. Japanese Journal of Ecology 68, 43–57.
- Kaifu, K., Yokouchi, K., 2019. Increasing or decreasing? -Current status of the Japanese eel stock. Fisheries Research 220, 105348. <https://doi.org/10.1016/j.fishres.2019.105348>
- Kalia, V.C., 2013. Quorum sensing inhibitors: an overview. Biotechnology Advances 31, 224–245. <https://doi.org/10.1016/j.biotechadv.2012.10.004>
- Karsten, U., Barrow, K.D., King, R.J., 1993. Floridoside, L-isofloridoside, and D-isofloridoside in the red alga *Porphyra columbina* (seasonal and osmotic effects). Plant Physiology 103(2), 485–491. <https://doi.org/10.1104/pp.103.2.485>
- Kassambara, A., Kosinski, M., Biecek, P., Fabian, S., 2017. Package ‘survminer.’ Drawing Survival Curves using ‘ggplot2’(R package version 03 1).
- Kawasaki, A., Ono, A., Mizuta, S., Kamiya, M., Takenaga, T., Murakami, S., 2017. The taurine content of Japanese seaweed, in: Taurine 10. Springer, pp. 1105–1112. https://doi.org/10.1007/978-94-024-1079-2_88
- Kempter, J., Hofsoe, P., Panicz, R., Bergmann, S.M., 2014. First detection of anguillid herpesvirus 1 (AngHV1) in European eel (*Anguilla anguilla*) and imported American eel (*Anguilla rostrata*) in Poland. Bulletin of the European Association of Fish Pathologists 34, 87–94.
- Kendel, M., Couzinet-Mossion, A., Viau, M., Fleurence, J., Barnathan, G., Wielgosz-Collin, G., 2013. Seasonal composition of lipids, fatty acids, and sterols in the edible red alga *Grateloupia turuturu*. Journal of Applied Phycology 25, 425–432. <https://doi.org/10.1007/s10811-012-9876-3>
- Kennedy, C.R., Fitch, D.J., 1990. Colonization, larval survival and epidemiology of the nematode *Anguilllicola crassus*, parasitic in the eel, *Anguilla anguilla*, in Britain. Journal of Fish Biology 36, 117–131. <https://doi.org/10.1111/j.1095-8649.1990.tb05588.x>
- Kennedy, C.R., 2007. The pathogenic helminth parasites of eels. Journal of Fish Diseases 30, 319–334. <https://doi.org/10.1111/j.1365-2761.2007.00821.x>
- Kikuchi, H., 1929. Two new species of Japanese trematodes belonging to Gyrodactylidae. Annotationes zoologicae Japonenses 12, 175–186.
- Kim, D., Paggi, J.M., Park, C., Bennett, C., Salzberg, S.L., 2019. Graph-based genome alignment and genotyping with HISAT2 and HISAT-genotype. Nature Biotechnology 37, 907–915. <https://doi.org/10.1038/s41587-019-0201-4>
- Kim, H.W., Wang, M., Leber, C.A., Nothias, L.-F., Reher, R., Kang, K.B., Van Der Hooft, J.J., Dorrestein, P.C., Gerwick, W.H., Cottrell, G.W., 2021. NPClassifier: A deep neural network-based structural classification tool for natural products. Journal of Natural Products 84, 2795–2807. <https://doi.org/10.1021/acs.jnatprod.1c00399>

- Kim, J.S., Kim, Y.H., Seo, Y.W., Park, S., 2007. Quorum sensing inhibitors from the red alga, *Ahnfeltiopsis flabelliformis*. Biotechnology and Bioprocess Engineering 12, 308–311. <https://doi.org/10.1007/BF02931109>
- Kim, S.M., Ko, S.M., Jin, J.H., Seo, J.S., Lee, N.S., Kim, Y.S., Gu, J.H., Bae, Y.R., 2018. Characteristics of Viral Endothelial Cell Necrosis of Eel (VECNE) from Culturing Eel (*Anguilla japonica*, *Anguilla bicolor*) in Korea. Korean Journal of Ichthyology 30, 185–193. <https://doi.org/10.35399/ISK.30.4.1>
- Kirk, R.S., Kennedy, C.R., Lewis, J.W., 2000. Effect of salinity on hatching, survival and infectivity of *Anguillicola crassus* (Nematoda: Dracunculoidea) larvae. Diseases of Aquatic Organisms 40, 211–218. <https://doi.org/10.3354/dao040211>
- Kirk, R.S., 2003. The impact of *Anguillicola crassus* on European eels. Fisheries Management and Ecology 10, 385–394. <https://doi.org/10.1111/j.1365-2400.2003.00355.x>
- Kladi, M., Vagias, C., Roussis, V., 2004. Volatile halogenated metabolites from marine red algae. Phytochemistry Reviews 3, 337–366. <https://doi.org/10.1007/s11101-004-4155-9>
- Klindworth, A., Pruesse, E., Schweer, T., Peplies, J., Quast, C., Horn, M., Glöckner, F.O., 2013. Evaluation of general 16S ribosomal RNA gene PCR primers for classical and next-generation sequencing-based diversity studies. Nucleic acids research 41 (1), e1. <https://doi.org/10.1093/nar/gks808>
- Knights, B., 2003. A review of the possible impacts of long-term oceanic and climate changes and fishing mortality on recruitment of anguillid eels of the Northern Hemisphere. Science of the Total Environment 310, 237–244. [https://doi.org/10.1016/S0048-9697\(02\)00644-7](https://doi.org/10.1016/S0048-9697(02)00644-7)
- Knopf, K., Naser, K., Van der Heijden, M.H.T., Taraschewski, H., 2000. Humoral immune response of European eel *Anguilla anguilla* experimentally infected with *Anguillicola crassus*. Diseases of Aquatic Organisms 42, 61–69. <https://doi.org/10.3354/dao043039>
- Knopf, K., Mahnke, M., 2004. Differences in susceptibility of the European eel (*Anguilla anguilla*) and the Japanese eel (*Anguilla japonica*) to the swim-bladder nematode *Anguillicola crassus*. Parasitology 129, 491. <https://doi.org/10.1017/S0031182004005864>
- Knopf, K., 2006. The swimbladder nematode *Anguillicola crassus* in the European eel *Anguilla anguilla* and the Japanese eel *Anguilla japonica*: differences in susceptibility and immunity between a recently colonized host and the original host. Journal of Helminthology 80, 129. <https://doi.org/10.1079/JOH2006353>
- Knopf, K., Lucius, R., 2008. Vaccination of eels (*Anguilla japonica* and *Anguilla anguilla*) against *Anguillicola crassus* with irradiated L3. Parasitology 135, 633. <https://doi.org/10.1017/S0031182008004162>
- Kobayashi, T., Miyazaki, T., 1996. Rhabdoviral dermatitis in Japanese eel, *Anguilla japonica*. Fish Pathology 31, 183–190.
- Kobayashi, T., Shiino, T., Miyazaki, T., 1999. The effect of water temperature on rhabdoviral dermatitis in the Japanese eel, *Anguilla japonica* Temminck and Schlegel. Aquaculture 170, 7–15. [https://doi.org/10.1016/S0044-8486\(98\)00390-1](https://doi.org/10.1016/S0044-8486(98)00390-1)
- Køie, M., 1991. Swimbladder nematodes (*Anguillicola* spp.) and gill monogeneans (*Pseudodactylogyrus* spp.) parasitic on the European eel (*Anguilla anguilla*). ICES Journal of Marine Science 47, 391–398. <https://doi.org/10.1093/icesjms/47.3.391>
- Køie, M., 1988. Parasites in European eel *Anguilla anguilla* (L.) from Danish Freshwater, Brackish and Marine Localities. Ophelia 29, 93–118. <https://doi.org/10.1080/00785326.1988.10430822>
- König, G.M., Wright, A.D., 1993. Algal secondary metabolites and their pharmaceutical potential. ACS Publications 19, pp 276-293. <https://doi.org/10.1021/bk-1993-0534.ch019>
- Koops, H., Hartmann, F., 1989. *Anguillicola*-infestations in Germany and in German eel imports. Journal of Applied Ichthyology 5, 41–45. <https://doi.org/10.1111/j.1439-0426.1989.tb00568.x>
- Kumar, V., Zozaya-Valdes, E., Kjelleberg, S., Thomas, T., Egan, S., 2016. Multiple opportunistic pathogens can cause a bleaching disease in the red seaweed *Delisea pulchra*. Environmental microbiology 18, 3962–3975. <https://doi.org/10.1111/1462-2920.13403>
- Kusuda, R., Kawai, K., Salati, F., Banner, C.R., Fryer, J.L., 1991. *Enterococcus seriolicida* sp. nov., a fish pathogen. International Journal of Systematic and Evolutionary Microbiology 41, 406–409. <https://doi.org/10.1099/00207713-41-3-406>

- Kusuda, R., Ono, K., Salati, F., 1991. Passive immunization of glass eel, *Anguilla japonica* against Edwardsiellosis. Aquaculture Science 39, 259–262. <https://doi.org/10.11233/aquaculturesci1953.39.259>
- Kwan, J.C., Meickle, T., Ladwa, D., Teplitski, M., Paul, V., Luesch, H., 2011. Lyngbyoic acid, a “tagged” fatty acid from a marine cyanobacterium, disrupts quorum sensing in *Pseudomonas aeruginosa*. Molecular BioSystems 7, 1205–1216. <https://doi.org/10.1039/C0MB00180E>
- Lalegerie, F., Lajili, S., Bedoux, G., Taupin, L., Stiger-Pouvreau, V., Connan, S., 2019. Photo-protective compounds in red macroalgae from Brittany: Considerable diversity in mycosporine-like amino acids (MAAs). Marine environmental research 147, 37–48. <https://doi.org/10.1016/j.marenvres.2019.04.001>
- Lamson, H.M., Cairns, D.K., Shiao, J.-C., Iizuka, Y., Tzeng, W.-N., 2009. American eel, *Anguilla rostrata*, growth in fresh and salt water: implications for conservation and aquaculture. Fisheries Management and Ecology 16, 306–314. <https://doi.org/10.1111/j.1365-2400.2009.00677.x>
- Lane, A.L., Stout, E.P., Lin, A.-S., Prudhomme, J., Le Roch, K., Fairchild, C.R., Franzblau, S.G., Hay, M.E., Aalbersberg, W., Kubanek, J., 2009. Antimalarial bromophycolides J- Q from the Fijian red alga *Callophycus serratus*. The Journal of Organic Chemistry 74, 2736–2742. <https://doi.org/10.1021/jo900008w>
- Larrat, S., Marvin, J., Lair, S., 2012. Low sensitivity of antemortem gill biopsies for the detection of subclinical *Pseudodactylogyrus bini* infestations in American eels (*Anguilla rostrata*). Journal of Zoo and Wildlife Medicine 43, 190–192. <https://doi.org/10.1638/2011-0150.1>
- Le, H., LiHua, D., JianJun, F., Peng, L., SongLin, G., 2018. Immunogenicity study of an expressed outer membrane protein U of *Vibrio vulnificus* in Japanese eel (*Anguilla japonica*). Journal of Applied Microbiology 125, 1642–1654. <https://doi.org/10.1111/jam.14068>
- Lee, J.-S., Cheng, H., Damte, D., Lee, S.-J., Kim, J.-C., Rhee, M.-H., Suh, J.-W., Park, S.-C., 2013. Effects of dietary supplementation of *Lactobacillus pentosus* PL11 on the growth performance, immune and antioxidant systems of Japanese eel *Anguilla japonica* challenged with *Edwardsiella tarda*. Fish & Shellfish Immunology 34, 756–761. <https://doi.org/10.1016/j.fsi.2012.11.028>
- Lee, S., Katya, K., Park, Y., Won, S., Seong, M., Bai, S.C., 2017. Comparative evaluation of dietary probiotics *Bacillus subtilis* WB60 and *Lactobacillus plantarum* KCTC3928 on the growth performance, immunological parameters, gut morphology and disease resistance in Japanese eel, *Anguilla japonica*. Fish & Shellfish Immunology 61, 201–210. <https://doi.org/10.1016/j.fsi.2016.12.035>
- Lee, S., Katya, K., Hamidoghi, A., Hong, J., Kim, D.-J., Bai, S.C., 2018. Synergistic effects of dietary supplementation of *Bacillus subtilis* WB60 and mannanoligosaccharide (MOS) on growth performance, immunity and disease resistance in Japanese eel, *Anguilla japonica*. Fish & Shellfish Immunology 83, 283–291. <https://doi.org/10.1016/j.fsi.2018.09.031>
- Lee, S.H., Lee, Y.K., Katya, K., Park, J.K., Bai, S.C., 2018. Natural dietary additive yellow loess as potential antibiotic replacer in Japanese eel, *Anguilla japonica*: Effects on growth, immune responses, serological characteristics and disease resistance against *Edwardsiella tarda*. Aquaculture Nutrition 24, 1034–1040. <https://doi.org/10.1111/anu.12641>
- Lefebvre, B., Golotvin, S., Schoenbachler, L., Beger, R., Price, P., Megyesi, J., Safirstein, R., 2004. Intelligent bucketing for metabolomics-part 1. Metabolic Profiling: Pathways in Discovery.
- Legendre, P., Anderson, M.J., 1999. Distance-based redundancy analysis: testing multispecies responses in multifactorial ecological experiments. Ecological Monographs 69, 1–24. [https://doi.org/10.1890/0012-9615\(1999\)069\[0001:DBRATM\]2.0.CO;2](https://doi.org/10.1890/0012-9615(1999)069[0001:DBRATM]2.0.CO;2)
- Lehmann, J., Mock, D., Stürenberg, F.-J., Bernardet, J.-F., 1991. First isolation of *Cytophaga psychrophila* from a systemic disease in eel and cyprinids. Diseases of Aquatic Organisms 10, 217–220. <https://doi.org/10.3354/dao010217>
- Lemay, M.A., Martone, P.T., Hind, K.R., Lindstrom, S.C., Wegener Parfrey, L., 2018. Alternate life history phases of a common seaweed have distinct microbial surface communities. Molecular ecology 27, 3555–3568. <https://doi.org/10.1111/mec.14815>
- Lemay, M.A., Chen, M.Y., Mazel, F., Hind, K.R., Starko, S., Keeling, P.J., Martone, P.T., Parfrey, L.W., 2021. Morphological complexity affects the diversity of marine microbiomes. The ISME Journal 15, 1372–1386. <https://doi.org/10.1038/s41396-020-00856-z>

- Li, L., Liu, Z., Quan, J., Sun, J., Lu, J., Zhao, G., 2022. Comprehensive proteomic analysis to elucidate the anti-heat stress effects of nano-selenium in rainbow trout (*Oncorhynchus mykiss*). Ecotoxicology and Environmental Safety 241, 113736. <https://doi.org/10.1016/j.ecoenv.2022.113736>
- Li, N., Yu, L., Fu, X., Liu, L., Lin, Q., Zhang, D., Shi, C., Wu, S., 2014. Immune efficacy of *Edwardsiella tarda* ghosts vaccine for European eel (*Anguilla anguilla*) by 3 kinds of inoculation routes. Journal of Fisheries of China 38, 1910–1916.
- Li, W., Arnott, S.A., Jones, K.M., Braicovich, P.E., De Buron, I., Wang, G., Marcogliese, D.J., 2015. First record of paratenic hosts of the swimbladder nematode *Anguillicoloides crassus* in North America. Journal of Parasitology 101, 529–535. <https://doi.org/10.1645/15-774>
- Lieke, T., Meinelt, T., Hoseinifar, S.H., Pan, B., Straus, D.L., Steinberg, C.E., 2020. Sustainable aquaculture requires environmental-friendly treatment strategies for fish diseases. Reviews in Aquaculture 12, 943–965. <https://doi.org/10.1111/raq.12365>
- LiHua, D., JianJun, F., Peng, L., SongLin, G., Le, H., YiQun, X., 2019. Evaluation of an outer membrane protein as a vaccine against *Edwardsiella anguillarum* in Japanese eels (*Anguilla japonica*). Aquaculture 498, 143–150. <https://doi.org/10.1016/j.aquaculture.2018.08.012>
- Lin, M., Wu, X., Yan, Q., Ma, Y., Huang, L., Qin, Y., Xu, X., 2016. Incidence of antimicrobial-resistance genes and integrons in antibiotic-resistant bacteria isolated from eels and aquaculture ponds. Diseases of Aquatic Organisms 120, 115–123. <https://doi.org/10.3354/dao03013>
- Liu, H.B., Koh, K.P., Kim, J.S., Seo, Y., Park, S., 2008. The effects of betonicine, floridoside, and isethionic acid from the red alga *Ahnfeltiopsis flabelliformis* on quorum-sensing activity. Biotechnology and Bioprocess Engineering 13, 458–463. <https://doi.org/10.1007/s12257-008-0145-x>
- Liu, J.-B., Chen, K., Liu, T.-B., Wang, Z.-Y., Wang, L., 2021. Global transcriptome profiling reveals antagonizing response of head kidney of juvenile common carp exposed to glyphosate. Chemosphere 280, 130823. <https://doi.org/10.1016/j.chemosphere.2021.130823>
- Logan, C.A., Somero, G.N., 2010. Transcriptional responses to thermal acclimation in the eurythermal fish *Gillichthys mirabilis* (Cooper 1864). American Journal of Physiology-Regulatory, Integrative and Comparative Physiology 299, R843–R852. <https://doi.org/10.1152/ajpregu.00306.2010>
- Lopes, G., Sousa, C., Bernardo, J., Andrade, P.B., Valentão, P., Ferreres, F., Mouga, T., 2011. Sterol profiles in 18 macroalgae of the portuguese coast 1. Journal of Phycology 47, 1210–1218. <https://doi.org/10.1111/j.1529-8817.2011.01028.x>
- Love, M., Anders, S., Huber, W., 2014. Differential analysis of count data—the DESeq2 package. Genome Biology 15, 10–1186.
- Low, C.-F., Rozaini, M.Z.H., Musa, N., Syarul Nataqain, B., 2017. Current knowledge of metabolomic approach in infectious fish disease studies. Journal of Fish Diseases 40, 1267–1277. <https://doi.org/10.1111/jfd.12610>
- Machado, L., Magnusson, M., Paul, N.A., de Nys, R., Tomkins, N., 2014. Effects of marine and freshwater macroalgae on *in vitro* total gas and methane production. PLoS One 9. <https://doi.org/10.1371/journal.pone.0085289>
- Machado, L., Magnusson, M., Paul, N.A., Kinley, R., de Nys, R., Tomkins, N., 2016. Identification of bioactives from the red seaweed *Asparagopsis taxiformis* that promote antimethanogenic activity *in vitro*. Journal of Applied Phycology 28, 3117–3126. <https://doi.org/10.1007/s10811-016-0830-7>
- Mandalka, A., Cavalcanti, M.I.L.G., Harb, T.B., Toyota Fujii, M., Eisner, P., Schweiggert-Weisz, U., Chow, F., 2022. Nutritional Composition of Beach-Cast Marine Algae from the Brazilian Coast: Added Value for Algal Biomass Considered as Waste. Foods 11, 1201. <https://doi.org/10.3390/foods11091201>
- Mangamana, E.T., Cariou, V., Vigneau, E., Kakai, R.L.G., Qannari, E.M., 2019. Unsupervised multiblock data analysis: A unified approach and extensions. Chemometrics and Intelligent Laboratory Systems 194, 103856. <https://doi.org/10.1016/j.chemolab.2019.103856>
- Mangamana, E.T., Kakai, R.G., Qannari, E.M., 2021. A general strategy for setting up supervised methods of multiblock data analysis. Chemometrics and Intelligent Laboratory Systems 217, 104388. <https://doi.org/10.1016/j.chemolab.2021.104388>

- Manilal, A., Sujith, S., Kiran, G.S., Selvin, J., Shakir, C., Gandhimathi, R., Lipton, A.P., 2009a. Antimicrobial potential and seasonality of red algae collected from the southwest coast of India tested against shrimp, human and phytopathogens. *Annals of Microbiology* 59, 207–219. <https://doi.org/10.1007/BF03178319>
- Manilal, A., Sujith, S., Selvin, J., Shakir, C., Kiran, G.S., 2009b. Antibacterial activity of *Falkenbergia hillebrandii* (Born) from the Indian coast against human pathogens. *Phyton* 78, 161.
- Manilal, A., Selvin, J., George, S., 2012. *In vivo* therapeutic potentiality of red seaweed, *Asparagopsis* (Bonnemaisoniales, Rhodophyta) in the treatment of Vibriosis in *Penaeus monodon* Fabricius. *Saudi Journal of Biological Sciences* 19, 165–175. <https://doi.org/10.1016/j.sjbs.2011.12.003>
- Manilal, A., Selvin, J., Sugathan, S., 2013. Immuno-Modulatory Efficacy of Indian Red Algae, *Asparagopsis taxiformis*, in *Penaeus monodon*. *Journal of Applied Aquaculture* 25, 81–93. <https://doi.org/10.1080/10454438.2013.763514>
- Mann, A.J., Hahnke, R.L., Huang, S., Werner, J., Xing, P., Barbeyron, T., Huettel, B., Stüber, K., Reinhardt, R., Harder, J., 2013. The genome of the alga-associated marine flavobacterium *Formosa agariphila* KMM 3901T reveals a broad potential for degradation of algal polysaccharides. *Applied and Environmental Microbiology* 79, 6813–6822. <https://doi.org/10.1128/AEM.01937-13>
- Marino, F., Di Caro, G., Gugliandolo, C., Spanò, A., Faggio, C., Genovese, G., Morabito, M., Russo, A., Barreca, D., Fazio, F., 2016. Preliminary study on the *in vitro* and *in vivo* effects of *Asparagopsis taxiformis* bioactive phycoderivates on teleosts. *Frontiers in Physiology* 7, 459. <https://doi.org/10.3389/fphys.2016.00459>
- Marshall, R.A., Hamilton, J.T., Dring, M.J., Harper, D.B., 2003. Do vesicle cells of the red alga *Asparagopsis* (*Falkenbergia* stage) play a role in bromocarbon production? *Chemosphere* 52, 471–475. [https://doi.org/10.1016/S0045-6535\(03\)00197-8](https://doi.org/10.1016/S0045-6535(03)00197-8)
- Martinez-Garcia, M., van der Maarel, M.J., 2016. Floridoside production by the red microalga *Galdieria sulphuraria* under different conditions of growth and osmotic stress. *AMB Express* 6, 71. <https://doi.org/10.1186/s13568-016-0244-6>
- Mata, L., Lawton, R.J., Magnusson, M., Andreakis, N., de Nys, R., Paul, N.A., 2017. Within-species and temperature-related variation in the growth and natural products of the red alga *Asparagopsis taxiformis*. *Journal of Applied Phycology* 29, 1437–1447. <https://doi.org/10.1007/s10811-016-1017-y>
- Matsuda, R., Ozgur, R., Higashi, Y., Takechi, K., Takano, H., Takio, S., 2015. Preferential expression of a bromoperoxidase in sporophytes of a red alga, *Pyropia yezoensis*. *Marine Biotechnology* 17, 199–210. <https://doi.org/10.1007/s10126-014-9608-6>
- Matyash, V., Liebisch, G., Kurzchalia, T.V., Shevchenko, A., Schwudke, D., 2008. Lipid extraction by methyl-tert-butyl ether for high-throughput lipidomics. *Journal of Lipid Research* 49, 1137–1146. <https://doi.org/10.1194/jlr.D700041-JLR200>
- Maximilien, R., de Nys, R., Holmström, C., Gram, L., Givskov, M., Crass, K., Kjelleberg, S., Steinberg, P.D., 1998. Chemical mediation of bacterial surface colonisation by secondary metabolites from the red alga *Delisea pulchra*. *Aquatic Microbial Ecology* 15, 233–246. <https://doi.org/10.3354/ame01523>
- McAllister, P.E., Nagabayashi, T., Wolf, K., 1977. Viruses of eels with and without stomatopapillomas [*Anguilla anguilla*, *A. vulgaris*]. *Annals of the New York Academy of Sciences*, 298, 233–244. <https://doi.org/10.1111/j.1749-6632.1977.tb19268.x>
- McArdle, B.H., Anderson, M.J., 2001. Fitting multivariate models to community data: a comment on distance-based redundancy analysis. *Ecology* 82, 290–297. [https://doi.org/10.1890/0012-9658\(2001\)082\[0290:FMMTC\]2.0.CO;2](https://doi.org/10.1890/0012-9658(2001)082[0290:FMMTC]2.0.CO;2)
- McClean, K.H., Winson, M.K., Fish, L., Taylor, A., Chhabra, S.R., Camara, M., Daykin, M., Lamb, J.H., Swift, S., Bycroft, B.W., 1997. Quorum sensing and *Chromobacterium violaceum*: exploitation of violacein production and inhibition for the detection of N-acylhomoserine lactones. *Microbiology* 143, 3703–3711. <https://doi.org/10.1099/00221287-143-12-3703>
- McConnell, O., Fenical, W., 1977. Halogen chemistry of the red alga *Asparagopsis*. *Phytochemistry* 16, 367–374. [https://doi.org/10.1016/0031-9422\(77\)80067-8](https://doi.org/10.1016/0031-9422(77)80067-8)
- McConville, J., Fringuelli, E., Evans, D., Savage, P., 2018. First examination of the Lough Neagh European eel (*Anguilla anguilla*) population for eel virus European, eel virus European X and

- Anguillid Herpesvirus-1 infection by employing novel molecular techniques. *Journal of Fish Diseases* 41, 1783–1791. <https://doi.org/10.1111/jfd.12885>
- Mellergaard, S., Dalsgaard, I., 1987. Disease problems in Danish eel farms. *Aquaculture* 67, 139–146. [https://doi.org/10.1016/0044-8486\(87\)90019-6](https://doi.org/10.1016/0044-8486(87)90019-6)
- Mellergaard, S., 1990. Mebendazole treatment against *Pseudodactylogyrus* infections in eel (*Anguilla anguilla*). *Aquaculture* 91, 15–21. [https://doi.org/10.1016/0044-8486\(90\)90174-L](https://doi.org/10.1016/0044-8486(90)90174-L)
- Michel, C., Bernardet, J.F., Dinand, D., 1992. Phenotypic and genotypic studies of *Pseudomonas anguilliseptica* strains isolated from farmed European eels (*Anguilla anguilla*) in France. *Fish Pathology* 27, 229–232. <https://doi.org/10.3147/jsfp.27.229>
- Michel, G., Nyval-Collen, P., Barbeyron, T., Czjzek, M., Helbert, W., 2006. Bioconversion of red seaweed galactans: a focus on bacterial agarases and carrageenases. *Applied Microbiology and Biotechnology* 71, 23–33. <https://doi.org/10.1007/s00253-006-0377-7>
- Miller, M.B., Bassler, B.L., 2001. Quorum sensing in bacteria. *Annual Reviews in Microbiology* 55, 165–199. <https://doi.org/10.1146/annurev.micro.55.1.165>
- Minegishi, Y., Aoyama, J., Inoue, J.G., Miya, M., Nishida, M., Tsukamoto, K., 2005. Molecular phylogeny and evolution of the freshwater eels genus *Anguilla* based on the whole mitochondrial genome sequences. *Molecular Phylogenetics and Evolution* 34, 134–146. <https://doi.org/10.1016/j.ympev.2004.09.003>
- Miyazaki, T., Egusa, S., 1976a. Histopathological Studies of Edwardsiellosis of the Japanese Eel (*Anguilla japonica*)—II Suppurative hepatitis form. *Fish Pathology* 11, 67–75. <https://doi.org/10.3147/jsfp.11.33>
- Miyazaki, T., Egusa, S., 1976b. Histopathological Studies of Edwardsiellosis of the Japanese Eel (*Anguilla japonica*)—I. *Fish Pathology* 11, 33–43. <https://doi.org/10.3147/jsfp.11.67>
- Miyazaki, T., Egusa, S., 1976c. Histopathological Studies of Edwardsiellosis of the Japanese Eel (*Anguilla japonica*)—III. *Fish Pathology* 11, 127–131. <https://doi.org/10.3147/jsfp.11.127>
- Mizutani, T., Sayama, Y., Nakanishi, A., Ochiai, H., Sakai, K., Wakabayashi, K., Tanaka, N., Miura, E., Oba, M., Kurane, I., 2011. Novel DNA virus isolated from samples showing endothelial cell necrosis in the Japanese eel, *Anguilla japonica*. *Virology* 412, 179–187. <https://doi.org/10.1016/j.virol.2010.12.057>
- Mohanty, B.R., Sahoo, P.K., 2007. Edwardsiellosis in fish: a brief review. *Journal of Biosciences* 32, 1331–1344. <https://doi.org/10.1007/s12038-007-0143-8>
- Moigne, J.Y., 1998. Use of algae extracts as antibacterial and/or antifungal agent and composition containing same. PCT Patent Appl WO 1998010656, A1.
- Mokhtar, D.M., Zaccone, G., Alesci, A., Kuciel, M., Hussein, M.T., Sayed, R.K., 2023. Main Components of Fish Immunity: An Overview of the Fish Immune System. *Fishes* 8(2), 93. <https://doi.org/10.3390/fishes8020093>
- Molnár, K., Székely, C., Baska, F., 1991. Mass mortality of eel in Lake Balaton due to *Anguilllicola crassus* infection. *Bulletin of the European Association of Fish Pathologists* 11, 211–212.
- Molnár, K., Baska, F., Csaba, G., Glávits, R., Székely, C., 1993. Pathological and histopathological studies of the swimbladder of eels *Anguilla anguilla* infected by *Anguilllicola crassus* (Nematoda: Dracunculoidea). *Diseases of Aquatic Organisms* 15, 41–50.
- Monni, G., Cognetti-Varriale, A.M., 2002. Antigenicity of *Pseudodactylogyrus anguillae* and *P. bini* (Monogenea) in the European eel (*Anguilla anguilla*, L.) under different oxygenation conditions. *Fish & Shellfish Immunology* 13, 125–131. <https://doi.org/10.1006/fsim.2001.0387>
- Mooney, H.A., Drake, J.A., 2012. Ecology of biological invasions of North America and Hawaii. Springer Science & Business Media.
- Moreira, A.S., da Costa, E., Melo, T., Sulpice, R., Cardoso, S.M., Pitarma, B., Pereira, R., Abreu, M.H., Domingues, P., Calado, R., 2020. Seasonal plasticity of the polar lipidome of *Ulva rigida* cultivated in a sustainable integrated multi-trophic aquaculture. *Algal Research* 49, 101958. <https://doi.org/10.1016/j.algal.2020.101958>
- Moriarty, C., 1990. Eel management practice in three lake systems in Ireland, in: Proceedings of a Symposium Organised by the European Inland Fisheries Advisory Commission, Goteborg, Sweden. pp. 262–269.
- Moriarty, C., Dekker, W., 1997. Management of the European eel. *Fisheries Bulletin*. Marine Institute.

- Muñoz, P., Barcala, E., Peñalver, J., Romero, D., 2019. Can inorganic elements affect herpesvirus infections in European eels? Environmental Science and Pollution Research 26, 35266–35269. <https://doi.org/10.1007/s11356-019-06617-6>
- Muroga, K., Jo, Y., Yano, M., 1973. Studies on red spot disease of pond-cultured eels—I The occurrence of the disease in eel culture ponds in Tokushima prefecture in 1972. Fish Pathology 8, 1–9. <https://doi.org/10.3147/jsfp.8.1>
- Myers, O.D., Sumner, S.J., Li, S., Barnes, S., Du, X., 2017. One step forward for reducing false positive and false negative compound identifications from mass spectrometry metabolomics data: new algorithms for constructing extracted ion chromatograms and detecting chromatographic peaks. Analytical Chemistry 89, 8696–8703. <https://doi.org/10.1021/acs.analchem.7b00947>
- Nagabayashi, T., Wolf, K., 1979. Characterization of EV-2, a virus isolated from European eels (*Anguilla anguilla*) with stomatopapilloma. Journal of Virology 30, 358–364. <https://doi.org/10.1128/jvi.30.1.358-364.1979>
- Nagasawa, K., Kim, Y.G., Hirose, H., 1994. *Anguillicola crassus* and *A. globiceps* (Nematoda: Dracunculoidea) parasitic in the swimbladder of eels (*Anguilla japonica* and *A. anguilla*) in East Asia: a review. Folia Parasitologica 41, 127–137.
- Nagasawa, K., Katahira, H., 2017. A revised and updated checklist of the parasites of eels (*Anguilla* spp.) (Anguilliformes: Anguillidae) in Japan (1915–2017). Biosphere Science 56, 33–69.
- Nakai, T., Muroga, K., 1982. *Pseudomonas anguilliseptica* isolated from European eels (*Anguilla anguilla*) in Scotland. Fish Pathology 17, 147–150. <https://doi.org/10.3147/jsfp.17.147>
- Nakai, T., Kanemori, Y., Nakajima, K., Muroga, K., 1985. The fate of *Pseudomonas anguilliseptica* in artificially infected eels *Anguilla japonica*. Fish Pathology 19, 253–258. <https://doi.org/10.3147/jsfp.19.253>
- Neukirch, M., 1985. Isolation of an orthomyxovirus like agent from European eel (*Anguilla anguilla*). Bulletin of the European Association of Fish Pathologists 5, 12–13.
- Newbold, L.R., Hockley, F.A., Williams, C.F., Cable, J., Reading, A.J., Auchterlonie, N., Kemp, P.S., 2015. Relationship between European eel *Anguilla anguilla* infection with non-native parasites and swimming behaviour on encountering accelerating flow. Journal of Fish Biology 86, 1519–1533. <https://doi.org/10.1111/jfb.12659>
- Nguyen, T.T., Jin, Y., Kiełpińska, J., Bergmann, S.M., Lenk, M., Panicz, R., 2017. Detection of *Herpesvirus anguillae* (Ang HV-1) in European eel *Anguilla anguilla* (L.) originating from northern Poland—assessment of suitability of selected diagnostic methods. Journal of Fish Diseases 40, 1717–1723. <https://doi.org/10.1111/jfd.12689>
- Nicol, M., Alexandre, S., Luizet, J.-B., Skogman, M., Jouenne, T., Salcedo, S.P., Dé, E., 2018. Unsaturated fatty acids affect quorum sensing communication system and inhibit motility and biofilm formation of *Acinetobacter baumannii*. International Journal of Molecular Sciences 19, 214. <https://doi.org/10.3390/ijms19010214>
- Nikolic, N., Liu, S., Jacobsen, M.W., Jónsson, B., Bernatchez, L., Gagnaire, P.-A., Hansen, M.M., 2020. Speciation history of European (*Anguilla anguilla*) and American eel (*A. rostrata*), analysed using genomic data. Molecular Ecology 29, 565–577. <https://doi.org/10.1111/mec.15342>
- Nishimura, T., Toba, M., Ban, F., Okamoto, N., Sano, T., 1981. Eel rhabdovirus, EVA, EVEX and their infectivity to fishes. Fish Pathology 15, 173–184. <https://doi.org/10.3147/jsfp.15.173>
- Noga, E.J., 2010. Fish disease: diagnosis and treatment. John Wiley & Sons. 2nd ed. Wiley-Blackwell
- Novak, H.R., Sayer, C., Panning, J., Littlechild, J.A., 2013. Characterisation of an 1-haloacid dehalogenase from the marine psychrophile *Psychromonas ingrahamii* with potential industrial application. Marine biotechnology 15, 695–705. <https://doi.org/10.1007/s10126-013-9522-3>
- Novak, H.R., Sayer, C., Isupov, M.N., Gotz, D., Spragg, A.M., Littlechild, J.A., 2014. Biochemical and structural characterisation of a haloalkane dehalogenase from a marine Rhodobacteraceae. FEBS letters 588, 1616–1622. <https://doi.org/10.1016/j.febslet.2014.02.056>
- Nylund, G.M., Cervin, G., Persson, F., Hermansson, M., Steinberg, P.D., Pavia, H., 2008. Seaweed defence against bacteria: a poly-brominated 2-heptanone from the red alga *Bonnemaisonia hamifera* inhibits bacterial colonisation. Marine Ecology Progress Series 369, 39–50. <https://doi.org/10.3354/meps07577>

- Okazaki, S., Manabe, H., Omatsu, T., Tsuchiaka, S., Yamamoto, T., Chow, S., Shibuno, T., Watanabe, K., Ono, S., Kuwada, H., 2015. Detection of Japanese eel endothelial cells-infecting virus (JEECV) in the Japanese eel *Anguilla japonica* (Temminck & Schlegel), living in natural habitats. *Journal of Fish Diseases* 38, 849–852. <https://doi.org/10.1111/jfd.12294>
- Okazaki, S., Yasumoto, S., Koyama, S., Tsuchiaka, S., Naoi, Y., Omatsu, T., Ono, S., Mizutani, T., 2016. Detection of Japanese eel endothelial cells-infecting virus in *Anguilla japonica* elvers. *Journal of Veterinary Medical Science* 78, 705–707. <https://doi.org/10.1292/jvms.15-0515>
- Okazaki-Terashima, S., Kurogi, H., Chow, S., Yamamoto, T., Matsuya, N., Ijiri, S., Mochioka, N., Tsuchiaka, S., Naoi, Y., Sano, K., 2016. Detection of Japanese eel endothelial cells-infecting virus (JEECV) in mature Japanese eel *Anguilla japonica* caught from their spawning area. *Fish Pathology* 51, 64–66. <https://doi.org/10.3147/jsfp.51.64>
- Ono, S., Wakabayashi, K., Nagai, A., 2003. Sequence of genome segment A of a birnavirus isolated from cultured Japanese eel with viral endothelial cell necrosis of eel. *Journal of Marine Science and Technology* 1, 39–49.
- Paix, B., Othmani, A., Debroas, D., Culoli, G., Briand, J.-F., 2019. Temporal covariation of epibacterial community and surface metabolome in the Mediterranean seaweed holobiont *Taonia atomaria*. *Environmental Microbiology* 21, 3346–3363. <https://doi.org/10.1111/1462-2920.14617>
- Paix, B., Carriot, N., Barry-Martinet, R., Greff, S., Misson, B., Briand, J.-F., Culoli, G., 2020. A multi-omics analysis suggests links between the differentiated surface metabolome and epiphytic microbiota along the thallus of a Mediterranean seaweed holobiont. *Frontiers in Microbiology* 11, 494. <https://doi.org/10.3389/fmicb.2020.00494>
- Paix, B., Layglon, N., Le Poupon, C., D'onofrio, S., Misson, B., Garnier, C., Culoli, G., Briand, J.-F., 2021a. Integration of spatio-temporal variations of surface metabolomes and epibacterial communities highlights the importance of copper stress as a major factor shaping host-microbiota interactions within a Mediterranean seaweed holobiont. *Microbiome* 9, 1–19. <https://doi.org/10.1186/s40168-021-01124-8>
- Paix, B., Vieira, C., Potin, P., Leblanc, C., De Clerck, O., Briand, J.-F., Culoli, G., 2021b. French Mediterranean and Atlantic populations of the brown algal genus *Taonia* (Dictyotales) display differences in phylogeny, surface metabolomes and epibacterial communities. *Algal Research* 59, 102452. <https://doi.org/10.1016/j.algal.2021.102452>
- Palstra, A.P., Van Ginneken, V.J.T., Murk, A.J., Van Den Thillart, G., 2006. Are dioxin-like contaminants responsible for the eel (*Anguilla anguilla*) drama? *Naturwissenschaften* 93, 145. <https://doi.org/10.1007/s00114-005-0080-z>
- Palstra, A.P., Heppner, D.F.M., Van Ginneken, V.J.T., Székely, C., Van den Thillart, G., 2007. Swimming performance of silver eels is severely impaired by the swim-bladder parasite *Anguillicola crassus*. *Journal of Experimental Marine Biology and Ecology* 352, 244–256. <https://doi.org/10.1016/j.jembe.2007.08.003>
- Pang, Z., Chong, J., Zhou, G., de Lima Morais, D.A., Chang, L., Barrette, M., Gauthier, C., Jacques, P.-É., Li, S., Xia, J., 2021. MetaboAnalyst 5.0: narrowing the gap between raw spectra and functional insights. *Nucleic acids research* 49, W388–W396. <https://doi.org/10.1093/nar/gkab382>
- Parchemin, C., Tapissier-Bontemps, N., Sasal, P., Faliex, E., 2022. *Anguilla* sp. diseases diagnoses and treatments: The ideal methods at the crossroads of conservation and aquaculture purposes. *Journal of Fish Diseases* 45, 943–969. <https://doi.org/10.1111/jfd.13634>
- Parchemin, C., Ravaglione, D., Ghosson, H., Salvia, M.-V., Goossens, C., Sasal, P., Faliex, E., Tapissier-Bontemps, N., 2023. Development of a Multiblock Metabolomics Approach to Explore Metabolite Variations of two Algae of the Genus *Asparagopsis* Linked to Interspecies and Temporal Factors. *Algal Research* 72, 103138. <https://doi.org/10.1016/j.algal.2023.103138>
- Patwary, Z.P., Zhao, M., Wang, T., Paul, N.A., Cummins, S.F., 2023. A Proteomic Analysis for the Red Seaweed *Asparagopsis taxiformis*. *Biology* 12(2), 167. <https://doi.org/10.3390/biology12020167>
- Paul, C., Pohnert, G., 2011. Production and role of volatile halogenated compounds from marine algae. *Natural product reports* 28, 186–195. <https://doi.org/10.1039/C0NP00043D>

- Paul, N.A., de Nys, R., Steinberg, P.D., 2006a. Chemical defence against bacteria in the red alga *Asparagopsis armata*: linking structure with function. *Marine Ecology Progress Series* 306, 87–101. <https://doi.org/10.3354/meps306087>
- Paul, N.A., De Nys, R., Steinberg, P.D., 2006b. Seaweed–herbivore interactions at a small scale: direct tests of feeding deterrence by filamentous algae. *Marine Ecology Progress Series* 323, 1–9. <https://doi.org/10.3354/meps323001>
- Pawliszyn, J., 1997. Solid phase microextraction: theory and practice. John Wiley & Sons.
- Pawliszyn, J., 2012. Theory of solid-phase microextraction, in: *Handbook of Solid Phase Microextraction*. Elsevier, pp. 13–59. <https://doi.org/10.1016/B978-0-12-416017-0.00002-4>
- Paysan-Lafosse, T., Blum, M., Chuguransky, S., Grego, T., Pinto, B.L., Salazar, G.A., Bileschi, M.L., Bork, P., Bridge, A., Colwell, L., 2023. InterPro in 2022. *Nucleic Acids Research* 51, D418–D427. <https://doi.org/10.1093/nar/gkac993>
- Pellegrini, M., 1969. Contribution à l'étude chimique des Algues Méditerranéennes. *Botanica Marina* 12(1-4). <https://doi.org/10.1515/botm.1969.12.1-4.179>
- Pelster, B., 2015. Swimbladder function and the spawning migration of the European eel *Anguilla anguilla*. *Frontiers in Physiology* 5, 486. <https://doi.org/10.3389/fphys.2014.00486>
- Pereira, H., Barreira, L., Figueiredo, F., Custódio, L., Vizetto-Duarte, C., Polo, C., Rešek, E., Engelen, A., Varela, J., 2012. Polyunsaturated fatty acids of marine macroalgae: potential for nutritional and pharmaceutical applications. *Marine Drugs* 10, 1920–1935. <https://doi.org/10.3390/md10091920>
- Perrier, F., Bertucci, A., Pierron, F., Feurtet-Mazel, A., Simon, O., Klopp, C., Candaudap, F., Pokrovski, O., Etcheverria, B., Mornet, S., 2020. Transfer and Transcriptomic Profiling in Liver and Brain of European Eels (*Anguilla anguilla*) After Diet-borne Exposure to Gold Nanoparticles. *Environmental Toxicology and Chemistry* 39, 2450–2461. <https://doi.org/10.1002/etc.4858>
- PGA, 2018. Rapport Plan de Gestion Anguille de la France - Rapport de mise en oeuvre - Article 9 du R (CE) n°1100/2007. <https://professionnels.ofb.fr/sites/default/files/pdf/RapportPGA2018.pdf>.
- Pike, C., Crook, V., Gollock, M., 2020. *Anguilla anguilla*. The IUCN red list of threatened species 2020: e. T60344A152845178. International Union for Conservation of Nature 2020–2. <https://dx.doi.org/10.2305/IUCN.UK.2020-2.RLTS.T60344A152845178.en>
- Pinteus, S., Alves, C., Monteiro, H., Araújo, E., Horta, A., Pedrosa, R., 2015. *Asparagopsis armata* and *Sphaerococcus coronopifolius* as a natural source of antimicrobial compounds. *World Journal of Microbiology and Biotechnology* 31, 445–451. <https://doi.org/10.1007/s11274-015-1797-2>
- Pinteus, S., Rodrigues, A.N., Silva, J., Lokman, C., Lemos, M.F., Pedrosa, R., 2016. The marine invasive *Asparagopsis armata* (Harvey, 1855) as source of bioactive valuable compounds-Antioxidant potential enrichment by Vacuum liquid Chromatography. *Frontiers in Marine Science*.
- Pinteus, S., Lemos, M.F., Alves, C., Neugebauer, A., Silva, J., Thomas, O.P., Botana, L.M., Gaspar, H., Pedrosa, R., 2018. Marine invasive macroalgae: Turning a real threat into a major opportunity-the biotechnological potential of *Sargassum muticum* and *Asparagopsis armata*. *Algal Research* 34, 217–234. <https://doi.org/10.1016/j.algal.2018.06.018>
- Pinto, D.C., Lesenfants, M.L., Rosa, G.P., Barreto, M.C., Silva, A., Seca, A.M., 2022. GC- and UHPLC-MS Profiles as a Tool to Valorize the Red Alga *Asparagopsis armata*. *Applied Sciences* 12(2), 892. <https://doi.org/10.3390/app12020892>
- Pluskal, T., Castillo, S., Villar-Briones, A., Orešić, M., 2010. MZmine 2: modular framework for processing, visualizing, and analyzing mass spectrometry-based molecular profile data. *BMC Bioinformatics* 11, 1–11. <https://doi.org/10.1186/1471-2105-11-395>
- Ponte, J.M., Seca, A.M., Barreto, M.C., 2022. *Asparagopsis* Genus: What We Really Know About Its Biological Activities and Chemical Composition. *Molecules* 27(6), 1787. <https://doi.org/10.3390/molecules27061787>
- Preema, P.G., Swaminathan, T.R., Kumar, V.J.R., Singh, I.S.B., 2020. Antimicrobial resistance in aquaculture: a crisis for concern. *Biologia* 75, 1497–1517. <https://doi.org/10.2478/s11756-020-00456-4>
- Preuss, M., Nelson, W.A., D'Archino, R., 2022. Cryptic diversity and phylogeographic patterns in the *Asparagopsis armata* species complex (Bonnemaisoniales, Rhodophyta) from New Zealand. *Phycologia* 61, 89–96. <https://doi.org/10.1080/00318884.2021.2015223>

- Rahmawaty, A., Chen, M.-Y., Byadgi, O.V., Wang, P.-C., Chen, S.-C., 2022. Phenotypic and genotypic analysis of *Edwardsiella* isolates from Taiwan indicates wide variation with a particular reference to *Edwardsiella tarda* and *Edwardsiella anguillarum*. Journal of Fish Diseases 45, 1659–1672. <https://doi.org/10.1111/jfd.13688>
- Reverter, M., Bontemps, N., Lecchini, D., Banaigs, B., Sasal, P., 2014. Use of plant extracts in fish aquaculture as an alternative to chemotherapy: current status and future perspectives. Aquaculture 433, 50–61. <https://doi.org/10.1016/j.aquaculture.2014.05.048>
- Reverter, M., Saulnier, D., David, R., Bardon-Albaret, A., Belliard, C., Tapissier-Bontemps, N., Lecchini, D., Sasal, P., 2016. Effects of local Polynesian plants and algae on growth and expression of two immune-related genes in orbicular batfish (*Platax orbicularis*). Fish & Shellfish Immunology 58, 82–88. <https://doi.org/10.1016/j.fsi.2016.09.011>
- Reverter, M., Rohde, S., Parchemin, C., Tapissier-Bontemps, N., Schupp, P.J., 2020. Metabolomics and marine biotechnology: coupling metabolite profiling and organism biology for the discovery of new compounds. Frontiers in Marine Science 7, 1062. <https://doi.org/10.3389/fmars.2020.613471>
- Reverter, M., Tapissier-Bontemps, N., Sarter, S., Sasal, P., Caruso, D., 2021. Moving towards more sustainable aquaculture practices: a meta-analysis on the potential of plant-enriched diets to improve fish growth, immunity and disease resistance. Reviews in Aquaculture 13, 537–555. <https://doi.org/10.1111/raq.12485>
- Reverter, M., Tapissier-Bontemps, N., Banaigs, B., Sasal, P., Calvayrac, C., Mazzitelli, J.-Y., Tintillier, F., 2022. Composé antibactérien et antiparasitaire. French patent FR3117734, International extension WO2022/129453.
- Rickards, W.L., Gregg, F., 1978. A diagnostic manual of eel diseases occurring under culture conditions in Japan.
- Riedel, K., Hentzer, M., Geisenberger, O., Huber, B., Steidle, A., Wu, H., Høiby, N., Givskov, M., Molin, S., Eberl, L., 2001. N-acylhomoserine-lactone-mediated communication between *Pseudomonas aeruginosa* and *Burkholderia cepacia* in mixed biofilms. Microbiology 147, 3249–3262. <https://doi.org/10.1099/00221287-147-12-3249>
- Righton, D., Walker, A.M., 2013. Anguillids: conserving a global fishery. <https://doi.org/10.1111/jfb.12157>
- Rijsewijk, F., Pritz-Verschuren, S., Kerkhoff, S., Botter, A., Willemsen, M., van Nieuwstadt, T., Haenen, O., 2005. Development of a polymerase chain reaction for the detection of *Anguillid herpesvirus* DNA in eels based on the herpesvirus DNA polymerase gene. Journal of Virological Methods 124, 87–94. <https://doi.org/10.1016/j.jviromet.2004.11.007>
- Ritter, A., Dittami, S.M., Goulitquer, S., Correa, J.A., Boyen, C., Potin, P., Tonon, T., 2014. Transcriptomic and metabolomic analysis of copper stress acclimation in *Ectocarpus siliculosus* highlights signaling and tolerance mechanisms in brown algae. BMC plant biology 14, 1–17. <https://doi.org/10.1186/1471-2229-14-116>
- Rødde, R.S.H., Vårum, K.M., Larsen, B.A., Myklestad, S.M., 2004. Seasonal and geographical variation in the chemical composition of the red alga *Palmaria palmata* (L.) Kuntze. Botanica Marina 47(2). <https://doi.org/10.1515/BOT.2004.012>
- Rødsæther, M.C., Olafsen, J., Raa, J., Myhre, K., Steen, J.B., 1977. Copper as an initiating factor of vibriosis (*Vibrio anguillarum*) in eel (*Anguilla anguilla*). Journal of Fish Biology 10, 17–21. <https://doi.org/10.1111/j.1095-8649.1977.tb04037.x>
- Rogawski, D.S., Vitanza, N.A., Gauthier, A.C., Ramaswamy, V., Koschmann, C., 2017. Integrating RNA sequencing into neuro-oncology practice. Translational Research 189, 93–104. <https://doi.org/10.1016/j.trsl.2017.06.013>
- Rohart, F., Gautier, B., Singh, A., Lê Cao, K.-A., 2017. mixOmics: An R package for ‘omics feature selection and multiple data integration. PLoS computational biology 13, e1005752. <https://doi.org/10.1371/journal.pcbi.1005752>
- Romanazzi, D., Sanchez-Garcia, C., Svenson, J., Mata, L., Pes, K., Hayman, C.M., Wheeler, T.T., Magnusson, M., 2021. Rapid analytical method for the quantification of bromoform in the red seaweeds *Asparagopsis armata* and *Asparagopsis taxiformis* using gas chromatography–mass spectrometry. ACS Agricultural Science & Technology 1, 436–442. <https://doi.org/10.1021/acsagscitech.1c00161>

- Romero, J., Feijoó, C.G., Navarrete, P., 2012. Antibiotics in aquaculture—use, abuse and alternatives. *Health and Environment in Aquaculture* 159.
- Roque, B.M., Salwen, J.K., Kinley, R., Kebreab, E., 2019. Inclusion of *Asparagopsis armata* in lactating dairy cows' diet reduces enteric methane emission by over 50 percent. *Journal of Cleaner Production* 234, 132–138. <https://doi.org/10.1016/j.jclepro.2019.06.193>
- Roque, B.M., Venegas, M., Kinley, R.D., de Nys, R., Duarte, T.L., Yang, X., Kebreab, E., 2021. Red seaweed (*Asparagopsis taxiformis*) supplementation reduces enteric methane by over 80 percent in beef steers. *PLoS One* 16, e0247820. <https://doi.org/10.1371/journal.pone.0247820>
- Rusconi, R., Guasto, J.S., Stocker, R., 2014. Bacterial transport suppressed by fluid shear. *Nature Physics* 10, 212–217. <https://doi.org/10.1038/nphys2883>
- Rusconi, R., Stocker, R., 2015. Microbes in flow. *Current Opinion in Microbiology* 25, 1–8. <https://doi.org/10.1016/j.mib.2015.03.003>
- Saito, K., Kaneko, S., Furuya, Y., Asada, Y., Ito, R., Sugie, K., Akutsu, M., Yanagawa, Y., 2019. Confirmation of synthetic cannabinoids in herb and blood by HS-SPME-GC/MS. *Forensic Chemistry* 13, 100156. <https://doi.org/10.1016/j.forc.2019.100156>
- Salati, F., Ono, K., Kusuda, R., 1991. Oral vaccination of glass eel of *Anguilla japonica* against *Edwardsiella tarda* infection. *Fish and Shellfish Immunology* 1(4), 309–310. [https://doi.org/10.1016/S1050-4648\(05\)80068-3](https://doi.org/10.1016/S1050-4648(05)80068-3)
- Salvador, N., Gómez Garreta, M.A., Lavelli, L., Ribera Siguán, M.A., 2007. Antimicrobial activity of Iberian macroalgae. *Scientia Marina*, 71(1), 101–113. <https://doi.org/10.3989/scimar.2007.71n1101>
- Sano, M., Fukuda, H., Sano, T., 1990. Isolation and characterization of a new herpesvirus from eel. *Pathology in Marine Sciences* 15, 31.
- Sano, T., 1976. Viral diseases of cultured fishes in Japan. *Fish Pathology* 10, 221–226. <https://doi.org/10.3147/jsfp.10.221>
- Sano, T., Nishimura, T., Okamoto, N., Yamazaki, T., Hanada, H., Watanabe, Y., 1977. Studies on viral diseases of Japanese fishes. VI. Infectious hematopoietic necrosis (IHN) of salmonids in the mainland of Japan. *Journal of the Tokyo University of Fisheries* 63, 81–85.
- Santos, G.A., Schrama, J.W., Mamauag, R.E.P., Rombout, J., Verreth, J.A.J., 2010. Chronic stress impairs performance, energy metabolism and welfare indicators in European seabass (*Dicentrarchus labrax*): the combined effects of fish crowding and water quality deterioration. *Aquaculture* 299, 73–80. <https://doi.org/10.1016/j.aquaculture.2009.11.018>
- Santos, L., Ramos, F., 2018. Antimicrobial resistance in aquaculture: current knowledge and alternatives to tackle the problem. *International Journal of Antimicrobial Agents* 52, 135–143. <https://doi.org/10.1016/j.ijantimicag.2018.03.010>
- Schmid, M., Guihéneuf, F., Stengel, D.B., 2017. Plasticity and remodelling of lipids support acclimation potential in two species of low-intertidal macroalgae, *Fucus serratus* (Phaeophyceae) and *Palmaria palmata* (Rhodophyta). *Algal research* 26, 104–114. <https://doi.org/10.1016/j.algal.2017.07.004>
- Shanmugapriya, S., Manilal, A., Sujith, S., Selvin, J., Kiran, G.S., Natarajaseenivasan, K., 2008. Antimicrobial activity of seaweeds extracts against multiresistant pathogens. *Annals of Microbiology* 58, 535–541. <https://doi.org/10.1007/BF03175554>
- Shao, S., Lai, Q., Liu, Q., Wu, H., Xiao, J., Shao, Z., Wang, Q., Zhang, Y., 2015. Phylogenomics characterization of a highly virulent *Edwardsiella* strain ET080813T encoding two distinct T3SS and three T6SS gene clusters: Propose a novel species as *Edwardsiella anguillarum* sp. nov. *Systematic and Applied Microbiology* 38, 36–47. <https://doi.org/10.1016/j.syam.2014.10.008>
- Shchelkunov, I.S., Skurat, E.K., Sivolotskaia, V.A., Sapot'ko, K.V., Shimko, V.V., 1989. Rhabdovirus anguilla in eels in the USSR and its pathogenicity for fish. *Voprosy virusologii* 34, 81–84.
- Simon-Colin, C., Kervarec, N., Pichon, R., Bessières, M.-A., Deslandes, E., 2002. Characterization of N-methyl-L-methionine sulfoxide and isethionic acid from the red alga *Gratelouphia doryphora*. *Phycological Research* 50, 125–128. <https://doi.org/10.1046/j.1440-1835.2002.00265.x>
- Singh, A., Shannon, C.P., Gautier, B., Rohart, F., Vacher, M., Tebbutt, S.J., Lê Cao, K.-A., 2019. DIABLO: an integrative approach for identifying key molecular drivers from multi-omics assays. *Bioinformatics* 35, 3055–3062. <https://doi.org/10.1093/bioinformatics/bty1054>

- Sjöberg, N.B., Petersson, E., Wickström, H., Hansson, S., 2009. Effects of the swimbladder parasite *Anguillicola crassus* on the migration of European silver eels *Anguilla anguilla* in the Baltic Sea. *Journal of Fish Biology* 74, 2158–2170. <https://doi.org/10.1111/j.1095-8649.2009.02296.x>
- Soares, S.M., Walker, A., Elwenn, S.A., Bayliss, S., Garden, A., Stagg, H.E., Munro, E.S., 2019. First isolation of *Flavobacterium psychrophilum* associated with reports of moribund wild European eel (*Anguilla anguilla*) in Scotland. *Journal of Fish Diseases* 42, 1509–1521. <https://doi.org/10.1111/jfd.13069>
- Sokolowski, M.S., Dove, A.D., 2006. Histopathological examination of wild American eels infected with *Anguillicola crassus*. *Journal of Aquatic Animal Health* 18, 257–262. <https://doi.org/10.1577/H06-009.1>
- Solanki, K.S., Burton, I.W., MacKinnon, S.L., Walter, J.A., Dacanay, A., 2005. Metabolic changes in Atlantic salmon exposed to *Aeromonas salmonicida* detected by ¹H-nuclear magnetic resonance spectroscopy of plasma. *Diseases of Aquatic Organisms* 65, 107–114. <https://doi.org/10.3354/dao065107>
- Songlin, Y.Q.G., Ruizhang, G., Tianyi, Z.W.L.Y.W., 2012. Isolation and identification of pathogenic *Aeromonas veronii* from *Anguilla japonica*. *Biotechnology Bulletin* 07.
- Sprengel, G., Lüchtenberg, H., 1991. Infection by endoparasites reduces maximum swimming speed of European smelt *Osmerus eperlanus* and European eel *Anguilla anguilla*. *Diseases of Aquatic Organisms* 11, 31–35. <https://doi.org/10.3354/dao011031>
- Stengel, D.B., Connan, S., Popper, Z.A., 2011. Algal chemodiversity and bioactivity: sources of natural variability and implications for commercial application. *Biotechnology Advances* 29, 483–501. <https://doi.org/10.1016/j.biotechadv.2011.05.016>
- Stewart, D.J., Woldemariam, K., Dear, G., Mochaba, F.M., 1983. An outbreak of 'Sekiten-byo' among cultured European eels, *Anguilla anguilla* L., in Scotland. *Journal of Fish Diseases* 6, 75–76. <https://doi.org/10.1111/j.1365-2761.1983.tb00052.x>
- Stiger-Pouvreau, V., Zubia, M., 2020. Macroalgal diversity for sustainable biotechnological development in French tropical overseas territories. *Botanica Marina* 63, 17–41. <https://doi.org/10.1515/bot-2019-0032>
- Streftaris, N., Zenetos, A., 2006. Alien marine species in the Mediterranean-the 100 'Worst Invasives' and their impact. *Mediterranean Marine Science* 7, 87–118. <https://doi.org/10.12681/mms.180>
- Sugano, M., Sato, A., Nagak, H., Yoshiok, S., Shiraki, T., Horikoshi, H., 1990. Aldose reductase inhibitors from the red alga, *Asparagopsis taxiformis*. *Tetrahedron letters* 31, 7015–7016. [https://doi.org/10.1016/S0040-4039\(00\)97230-7](https://doi.org/10.1016/S0040-4039(00)97230-7)
- Sures, B., Knopf, K., Würtz, J., Hirt, J., 1999. Richness and diversity of parasite communities in European eels *Anguilla anguilla* of the River Rhine, Germany, with special reference to helminth parasites. *Parasitology* 119, 323–330. <https://doi.org/10.1017/S0031182099004655>
- Surget, G., Le Lann, K., Delebecq, G., Kervarec, N., Donval, A., Poullaouec, M.-A., Bihannic, I., Poupart, N., Stiger-Pouvreau, V., 2017. Seasonal phenology and metabolomics of the introduced red macroalga *Gracilaria vermiculophylla*, monitored in the Bay of Brest (France). *Journal of Applied Phycology* 29, 2651–2666. <https://doi.org/10.1007/s10811-017-1060-3>
- Tabrett, A., Horton, M.W., 2020. The influence of host genetics on the microbiome. *F1000Research* 9. <https://doi.org/10.12688%2Ff1000research.20835.1>
- Taraschewski, H., Renner, C., Mehlhorn, H., 1988. Treatment of fish parasites. *Parasitology Research* 74, 281–289. <https://doi.org/10.1007/BF00539579>
- Taylor, P.K., Yeung, A.T., Hancock, R.E., 2014. Antibiotic resistance in *Pseudomonas aeruginosa* biofilms: towards the development of novel anti-biofilm therapies. *Journal of Biotechnology* 191, 121–130. <https://doi.org/10.1016/j.jbiotec.2014.09.003>
- Terriente-Palacios, C., Castellari, M., 2022. Levels of taurine, hypotaurine and homotaurine, and amino acids profiles in selected commercial seaweeds, microalgae, and algae-enriched food products. *Food Chemistry* 368, 130770. <https://doi.org/10.1016/j.foodchem.2021.130770>
- Thanigaivel, S., Chandrasekaran, N., Mukherjee, A., Thomas, J., 2016. Seaweeds as an alternative therapeutic source for aquatic disease management. *Aquaculture* 464, 529–536. <https://doi.org/10.1016/j.aquaculture.2016.08.001>

- Thapa, H.R., Lin, Z., Yi, D., Smith, J.E., Schmidt, E.W., Agarwal, V., 2020. Genetic and biochemical reconstitution of bromoform biosynthesis in *Asparagopsis* lends insights into seaweed ROS enzymology. ACS Chemical Biology. <https://doi.org/10.1021/acschembio.0c00299>
- Theiler, R., Cook, J.C., Hager, L.P., Siuda, J.F., 1978. Halohydrocarbon synthesis by bromoperoxidase. Science 202, 1094–1096. <https://doi.org/10.1126/science.202.4372.1094>
- Thépot, V., Campbell, A.H., Paul, N.A., Rimmer, M.A., 2021a. Seaweed dietary supplements enhance the innate immune response of the mottled rabbitfish, *Siganus fuscescens*. Fish & Shellfish Immunology 113, 176–184. <https://doi.org/10.1016/j.fsi.2021.03.018>
- Thépot, V., Campbell, A.H., Rimmer, M.A., Paul, N.A., 2021b. Effects of a seaweed feed inclusion on different life stages of the mottled rabbitfish *Siganus fuscescens*. Aquaculture Research 52, 6626–6640. <https://doi.org/10.1111/are.15533>
- Thépot, V., Campbell, A.H., Rimmer, M.A., Jelocnik, M., Johnston, C., Evans, B., Paul, N.A., 2022. Dietary inclusion of the red seaweed *Asparagopsis taxiformis* boosts production, stimulates immune response and modulates gut microbiota in Atlantic salmon, *Salmo salar*. Aquaculture 546, 737286. <https://doi.org/10.1016/j.aquaculture.2021.737286>
- Therneau, T.M., Lumley, T., 2015. Package ‘survival.’ R Top Doc 128, 28–33.
- Thévenot, E.A., Roux, A., Xu, Y., Ezan, E., Junot, C., 2015. Analysis of the human adult urinary metabolome variations with age, body mass index, and gender by implementing a comprehensive workflow for univariate and OPLS statistical analyses. Journal of Proteome Research 14, 3322–3335. <https://doi.org/10.1021/acs.jproteome.5b00354>
- Thomas, F., Bordron, P., Eveillard, D., Michel, G., 2017. Gene expression analysis of *Zobellia galactanivorans* during the degradation of algal polysaccharides reveals both substrate-specific and shared transcriptome-wide responses. Frontiers in Microbiology 8, 1808. <https://doi.org/10.3389/fmicb.2017.01808>
- Tison, D.L., Nishibuchi, M., Greenwood, J.D., Seidler, R.J., 1982. *Vibrio vulnificus* biogroup 2: new biogroup pathogenic for eels. Applied and Environmental Microbiology 44, 640–646. <https://doi.org/10.1128/aem.44.3.640-646.1982>
- Tong, C., Zhang, C., Zhang, R., Zhao, K., 2015. Transcriptome profiling analysis of naked carp (*Gymnocypris przewalskii*) provides insights into the immune-related genes in highland fish. Fish & Shellfish Immunology 46, 366–377. <https://doi.org/10.1016/j.fsi.2015.06.025>
- Tournerche, A., Lami, R., Hubas, C., Blanchet, E., Vallet, M., Escoubeyrou, K., Paris, A., Prado, S., 2019. Bacterial–fungal interactions in the kelp endomicrobiota drive autoinducer-2 quorum sensing. Frontiers in microbiology 10, 1693. <https://doi.org/10.3389/fmicb.2019.01693>
- Triwibowo, R., Rachmawati, N., Dwiyitno, D., 2020. Rapid and Simultaneous Detection of *Vibrio parahaemolyticus*, *Salmonella* spp. and *Escherichia coli* in Fish by Multiplex PCR. Squalen Bulletin of Marine and Fisheries Postharvest and Biotechnology 15, 53–64. <https://doi.org/10.15578/squalen.v15i2.444>
- Uno, T., Ishizuka, M., Itakura, T., 2012. Cytochrome P450 (CYP) in fish. Environmental toxicology and pharmacology 34, 1–13. <https://doi.org/10.1016/j.etap.2012.02.004>
- Vailati-Riboni, M., Palombo, V., Loor, J.J., 2017. What are omics sciences?, in: Periparturient Diseases of Dairy Cows. Springer, pp. 1–7. https://doi.org/10.1007/978-3-319-43033-1_1
- Vallejos-Vidal, E., Reyes-López, F., Teles, M., MacKenzie, S., 2016. The response of fish to immunostimulant diets. Fish & Shellfish Immunology 56, 34–69. <https://doi.org/10.1016/j.fsi.2016.06.028>
- van Banning, P., Haenen, O.L.M., 1990. Effects of the swimbladder nematode *Anguillicola crassus* in wild and farmed eel, *Anguilla anguilla*. Pathology in marine science 317–330.
- van Beurden, S.J., Bossers, A., Voorbergen-Laarman, M.H., Haenen, O.L., Peters, S., Abma-Henkens, M.H., Peeters, B.P., Rottier, P.J., Engelsma, M.Y., 2010. Complete genome sequence and taxonomic position of anguillid herpesvirus 1. Journal of General Virology 91, 880–887. <https://doi.org/10.1099/vir.0.016261-0>
- van Beurden, S.J., Voorbergen-Laarman, M.A., Roozenburg, I., Boerlage, A.S., Haenen, O.L., Engelsma, M.Y., 2011. Development and validation of a two-step real-time RT-PCR for the detection of eel virus European X in European eel, *Anguilla anguilla*. Journal of Virological Methods 171, 352–359. <https://doi.org/10.1016/j.jviromet.2010.11.019>

- van Beurden, S.J., Engelsma, M.Y., Roozenburg, I., Voorbergen-Laarman, M.A., van Tulden, P.W., Kerkhoff, S., van Nieuwstadt, A.P., Davidse, A., Haenen, O.L., 2012. Viral diseases of wild and farmed European eel *Anguilla anguilla* with particular reference to the Netherlands. Diseases of Aquatic Organisms 101, 69–86. <https://doi.org/10.3354/dao02501>
- van Beurden, S.J., Voorbergen-Laarman, M.A., Roozenburg, I., van Tellingen, J., Haenen, O.L.M., Engelsma, M.Y., 2016. Development and validation of a real-time PCR assay for the detection of anguillid herpesvirus 1. Journal of Fish Diseases 39, 95–104. <https://doi.org/10.1111/jfd.12330>
- van Der Kloet, F.M., Bobeldijk, I., Verheij, E.R., Jellema, R.H., 2009. Analytical error reduction using single point calibration for accurate and precise metabolomic phenotyping. Journal of Proteome Research 8, 5132–5141. <https://doi.org/10.1021/pr900499r>
- van Ginneken, V.J.T., Haenen, O.L.M., Coldenhoff, K., Willemze, R., Antonissen, E., van Tulden, P.W., Dijkstra, S., Wagenaar, F., van den Thillart, G., 2004. Presence of virus infections in eel species from various geographic regions. Bulletin of the European Association of Fish Pathologists 24, 268–272.
- van Ginneken, V.J., Maes, G.E., 2005. The European eel (*Anguilla anguilla*, Linnaeus), its lifecycle, evolution and reproduction: a literature review. Reviews in Fish Biology and Fisheries 15, 367–398. <https://doi.org/10.1007/s11160-006-0005-8>
- van Nieuwstadt, A.P., Dijkstra, S.G., Haenen, O.L.M., 2001. Persistence of herpesvirus of eel *Herpesvirus anguillae* in farmed European eel *Anguilla anguilla*. Diseases of Aquatic Organisms 45, 103–107. <https://doi.org/10.3354/dao045103>
- Varvarigos, P., Vendramin, N., Cappellozza, E., Bovo, G., 2011. First confirmation of *Herpesvirus anguillae* (HVA) and infectious pancreatic necrosis (IPN) virus infecting European eels *Anguilla anguilla* farmed in Greece. Bulletin of the European Association of Fish Pathologists 31, 101–111.
- Vatsos, I.N., Rebours, C., 2015. Seaweed extracts as antimicrobial agents in aquaculture. Journal of Applied Phycology 27, 2017–2035. <https://doi.org/10.1007/s10811-014-0506-0>
- Vendrell, D., Balcázar, J.L., Ruiz-Zarzuela, I., De Blas, I., Gironés, O., Múzquiz, J.L., 2006. *Lactococcus garvieae* in fish: a review. Comparative immunology, microbiology and infectious diseases 29, 177–198. <https://doi.org/10.1016/j.cimid.2006.06.003>
- Vergés, A., Paul, N.A., Steinberg, P.D., 2008. Sex and life-history stage alter herbivore responses to a chemically defended red alga. Ecology 89, 1334–1343. <https://doi.org/10.1890/07-0248.1>
- Viant, M.R., 2007. Metabolomics of aquatic organisms: the new ‘omics’ on the block. Marine Ecology Progress Series 332, 301–306. <https://doi.org/10.3354/meps332301>
- Vitale, F., Genovese, G., Bruno, F., Castelli, G., Piazza, M., Migliazzo, A., Minicante, S.A., Manghisi, A., Morabito, M., 2015. Effectiveness of red alga *Asparagopsis taxiformis* extracts against *Leishmania infantum*. Open Life Sciences 10. <https://doi.org/10.1515/biol-2015-0050>
- Waaland, J.R., 1975. Differences in carrageenan in gametophytes and tetrasporophytes of red algae. Phytochemistry 14, 1359–1362. [https://doi.org/10.1016/S0031-9422\(00\)98626-6](https://doi.org/10.1016/S0031-9422(00)98626-6)
- Wakabayashi, H., Egusa, S., 1972. Characteristics of a *Pseudomonas* sp. from an epizootic of pond-cultured eels (*Anguilla japonica*). Bulletin of the Japanese Society of Scientific Fisheries 38(6), 577–587.
- Wakabayashi, H., Egusa, S., 1973. *Edwardsiella tarda* (*Paracolobactrum anguillimortiferum*) associated with pared-cultured eel disease. Bulletin of the Japanese Society of Scientific Fisheries, 39(9), 931–936. <https://doi.org/10.2331/suisan.39.931>
- Wan, A.H., Davies, S.J., Soler-Vila, A., Fitzgerald, R., Johnson, M.P., 2019. Macroalgae as a sustainable aquafeed ingredient. Reviews in Aquaculture 11, 458–492. <https://doi.org/10.1111/raq.12241>
- Wan, Q., Wu, L., Yang, Q., Lin, M., Guo, S., 2021. First identification and pathogenicity study of *Vibrio harveyi* isolated from diseased American eel (*Anguilla rostrata*) cultivated in freshwater. Aquaculture Research 53(4), 1240–1253. <https://doi.org/10.1111/are.15658>
- Wang, F., Kohan, A.B., Lo, C.-M., Liu, M., Howles, P., Tso, P., 2015. Apolipoprotein A-IV: a protein intimately involved in metabolism. Journal of Lipid Research 56, 1403–1418. <https://doi.org/10.1194/jlr.R052753>

- Wang, H.-M.D., Chen, C.-C., Huynh, P., Chang, J.-S., 2015. Exploring the potential of using algae in cosmetics. *Bioresource Technology* 184, 355–362. <https://doi.org/10.1016/j.biortech.2014.12.001>
- Wangensteen, O.S., Cebrian, E., Palacín, C., Turon, X., 2018. Under the canopy: Community-wide effects of invasive algae in Marine Protected Areas revealed by metabarcoding. *Marine Pollution Bulletin* 127, 54–66. <https://doi.org/10.1016/j.marpolbul.2017.11.033>
- Wells, R.M., Pankhurst, N.W., 1999. Evaluation of simple instruments for the measurement of blood glucose and lactate, and plasma protein as stress indicators in fish. *Journal of the World Aquaculture Society* 30, 276–284. <https://doi.org/10.1111/j.1749-7345.1999.tb00876.x>
- Wemheuer, F., Taylor, J.A., Daniel, R., Johnston, E., Meinicke, P., Thomas, T., Wemheuer, B., 2020. Tax4Fun2: prediction of habitat-specific functional profiles and functional redundancy based on 16S rRNA gene sequences. *Environmental Microbiome* 15, 1–12. <https://doi.org/10.1186/s40793-020-00358-7>
- Westerhuis, J.A., Hoefsloot, H.C., Smit, S., Vis, D.J., Smilde, A.K., van Velzen, E.J., van Duijnhoven, J.P., van Dorsten, F.A., 2008. Assessment of PLSDA cross validation. *Metabolomics* 4, 81–89. <https://doi.org/10.1007/s11306-007-0099-6>
- Weston, D.P., 1996. Environmental considerations in the use of antibacterial drugs in aquaculture.
- Wickham, H., Chang, W., Wickham, M.H., 2016. Package ‘ggplot2.’ Create elegant data visualisations using the grammar of graphics. Version 2, 1–189.
- Wiklund, S., 2008. Multivariate data analysis for Omics. Umea: Umetrics.
- Wiklund, T., Bylund, G., 1990. *Pseudomonas anguilliseptica* as a pathogen of salmonid fish in Finland. *Diseases of Aquatic Organisms* 8, 13–19. <https://doi.org/10.3354/dao008013>
- Wolf, K., Quimby, M.C., Pettijohn, L.L., Landolt, M.L., 1973. Fish viruses: isolation and identification of infectious hematopoietic necrosis in eastern North America. *Journal of the Fisheries Board of Canada* 30, 1625–1627. <https://doi.org/10.1139/f73-261>
- Woolard, F.X., Moore, R.E., Roller, P.P., 1976. Halogenated acetamides, but-3-en-2-ols, and isopropanols from *Asparagopsis taxiformis* (delile) trev. *Tetrahedron* 32(22), 2843–2846. [https://doi.org/10.1016/0040-4020\(76\)80134-2](https://doi.org/10.1016/0040-4020(76)80134-2)
- Woolard, F.X., Moore, R.E., Roller, P.P., 1979. Halogenated acetic and acrylic acids from the red alga *Asparagopsis taxiformis*. *Phytochemistry* 18, 617–620.
- Wright, J.T., Kennedy, E.J., de Nys, R., Tatsumi, M., 2022. Asexual propagation of *Asparagopsis armata* gametophytes: fragmentation, regrowth and attachment mechanisms for sea-based cultivation. *Journal of Applied Phycology* 1–10. <https://doi.org/10.1007/s10811-022-02763-6>
- Wright, R.M., Aglyamova, G.V., Meyer, E., Matz, M.V., 2015. Gene expression associated with white syndromes in a reef building coral, *Acropora hyacinthus*. *BMC genomics* 16, 1–12. <https://doi.org/10.1186/s12864-015-1540-2>
- Xiao, Y., Wu, L., He, L., Tang, Y., Guo, S., Zhai, S., 2022. Transcriptomic analysis using dual RNA sequencing revealed a Pathogen–Host interaction after *Edwardsiella anguillarum* infection in European eel (*Anguilla anguilla*). *Fish & Shellfish Immunology* 120, 745–757. <https://doi.org/10.1016/j.fsi.2021.12.051>
- Xu, B., Gong, H., Chen, X., Tian, D., Chen, Q., Chen, Y., Lin, T., 2012. Minimum dosage of *Vibrio vulnificus* OMP-ISCOMs for vaccinating *Anguilla anguilla*. *Fujian Journal of Agricultural Sciences* 27, 1280–1282.
- Yada, T., Mekuchi, M., Ojima, N., 2018. Molecular biology and functional genomics of immune-endocrine interactions in the Japanese eel, *Anguilla japonica*. *General and Comparative Endocrinology* 257, 272–279. <https://doi.org/10.1016/j.ygcen.2017.11.001>
- Yamaguchi, T., Dijkstra, J.M., 2019. Major histocompatibility complex (MHC) genes and disease resistance in fish. *Cells* 8, 378. <https://doi.org/10.3390/cells8040378>
- Yan, W., Qiao, Y., Qu, J., Liu, X., Zhang, Q., Wang, X., 2021. The hsp40 gene family in Japanese flounder: identification, phylogenetic relationships, molecular evolution analysis, and expression patterns. *Frontiers in Marine Science* 7, 596534. <https://doi.org/10.3389/fmars.2020.596534>
- Yi, S.-W., You, M.-J., Cho, H.-S., Lee, C.-S., Kwon, J.-K., Shin, G.-W., 2013. Molecular characterization of *Aeromonas* species isolated from farmed eels (*Anguilla japonica*). *Veterinary Microbiology* 164, 195–200. <https://doi.org/10.1016/j.vetmic.2013.02.006>

- Zanolla, M., Carmona, R., De la Rosa, J., Salvador, N., Sherwood, A.R., Andreakis, N., Altamirano, M., 2014. Morphological differentiation of cryptic lineages within the invasive genus *Asparagopsis* (Bonnemaisoniales, Rhodophyta). *Phycologia* 53, 233–242. <https://doi.org/10.2216/13-247.1>
- Zanolla, M., Carmona, R., Mata, L., De la Rosa, J., Sherwood, A., Barranco, C.N., Muñoz, A.R., Altamirano, M., 2022a. Concise review of the genus *Asparagopsis* Montagne, 1840. *Journal of Applied Phycology* 1–17. <https://doi.org/10.1007/s10811-021-02665-z>
- Zanolla, M., Romanazzi, D., Svenson, J., Sherwood, A., Stengel, D.B., 2022b. Bromoform, mycosporine-like amino acids and phycobiliprotein content and stability in *Asparagopsis armata* during long-term indoor cultivation. *Journal of Applied Phycology* 1–13. <https://doi.org/10.1007/s10811-022-02706-1>
- Zemke-White, W.L., Clements, K.D., 1999. Chlorophyte and rhodophyte starches as factors in diet choice by marine herbivorous fish. *Journal of Experimental Marine Biology and Ecology* 240, 137–149. [https://doi.org/10.1016/S0022-0981\(99\)00056-8](https://doi.org/10.1016/S0022-0981(99)00056-8)
- Zhang, A., Sun, H., Wang, P., Han, Y., Wang, X., 2012. Modern analytical techniques in metabolomics analysis. *Analyst* 137, 293–300. <https://doi.org/10.1039/C1AN15605E>
- Zhang, W., Liao, Z., Hu, F., Chen, X., Huang, X., 2019. Protective immune responses of recombinant outer membrane proteins OmpF and OmpK of *Aeromonas hydrophila* in European eel (*Anguilla anguilla*). *Aquaculture Research* 50, 3559–3566. <https://doi.org/10.1111/are.14311>
- Zhang, W., Zhu, Z., Chen, Z., Mei, J., Lin, X., 2010. Isolation and identification of the pathogen associated with skin cancer of Japanese eel (*Anguilla japonica*). *Freshwater Fisheries* 2, 41–46.
- Zhao, J., Wu, L., Zhai, S., Lin, P., Guo, S., 2020. Construction expression and immunogenicity of a novel trivalent outer membrane protein (OmpU-A-II) from three bacterial pathogens in Japanese eels (*Anguilla japonica*). *Journal of Fish Diseases* 43, 519–529. <https://doi.org/10.1111/jfd.13132>
- Zhao, M., Campbell, A.H., Patwary, Z.P., Wang, T., Lang, T., Webb, J., Zuccarello, G.C., Wegner, A., Heyne, D., McKinnie, L., 2022. The red seaweed *Asparagopsis taxiformis* genome and integrative-omics analysis. *Scientific Reports*. Preprint. <https://doi.org/10.21203/rs.3.rs-2232367/v1>
- Zhou, J., Lyu, Y., Richlen, M.L., Anderson, D.M., Cai, Z., 2016. Quorum sensing is a language of chemical signals and plays an ecological role in algal-bacterial interactions. *Critical reviews in plant sciences* 35, 81–105. <https://doi.org/10.1080/07352689.2016.1172461>
- Zhou, L., Zhang, L.-H., Cámarra, M., He, Y.-W., 2017. The DSF family of quorum sensing signals: diversity, biosynthesis, and turnover. *Trends in Microbiology* 25, 293–303. <https://doi.org/10.1016/j.tim.2016.11.013>
- Zhu, P., Li, D., Yang, Q., Su, P., Wang, H., Heimann, K., Zhang, W., 2021. Commercial cultivation, industrial application, and potential halocarbon biosynthesis pathway of *Asparagopsis* sp. *Algal Research* 56, 102319. <https://doi.org/10.1016/j.algal.2021.102319>
- Zozaya-Valdes, E., Egan, S., Thomas, T., 2015. A comprehensive analysis of the microbial communities of healthy and diseased marine macroalgae and the detection of known and potential bacterial pathogens. *Frontiers in Microbiology* 6, 146. <https://doi.org/10.3389/fmicb.2015.00146>
- Zubia, M., Fabre, M.-S., Kerjean, V., Deslandes, E., 2009. Antioxidant and cytotoxic activities of some red algae (Rhodophyta) from Brittany coasts (France). *Botanica Marina* 52, 268–277. <https://doi.org/10.1515/BOT.2009.037>

Annexes

1. Mini-Revue : Métabolomique et biotechnologies marines : coupler le profilage des métabolites et la biologie des organismes pour la découverte de nouveaux composés

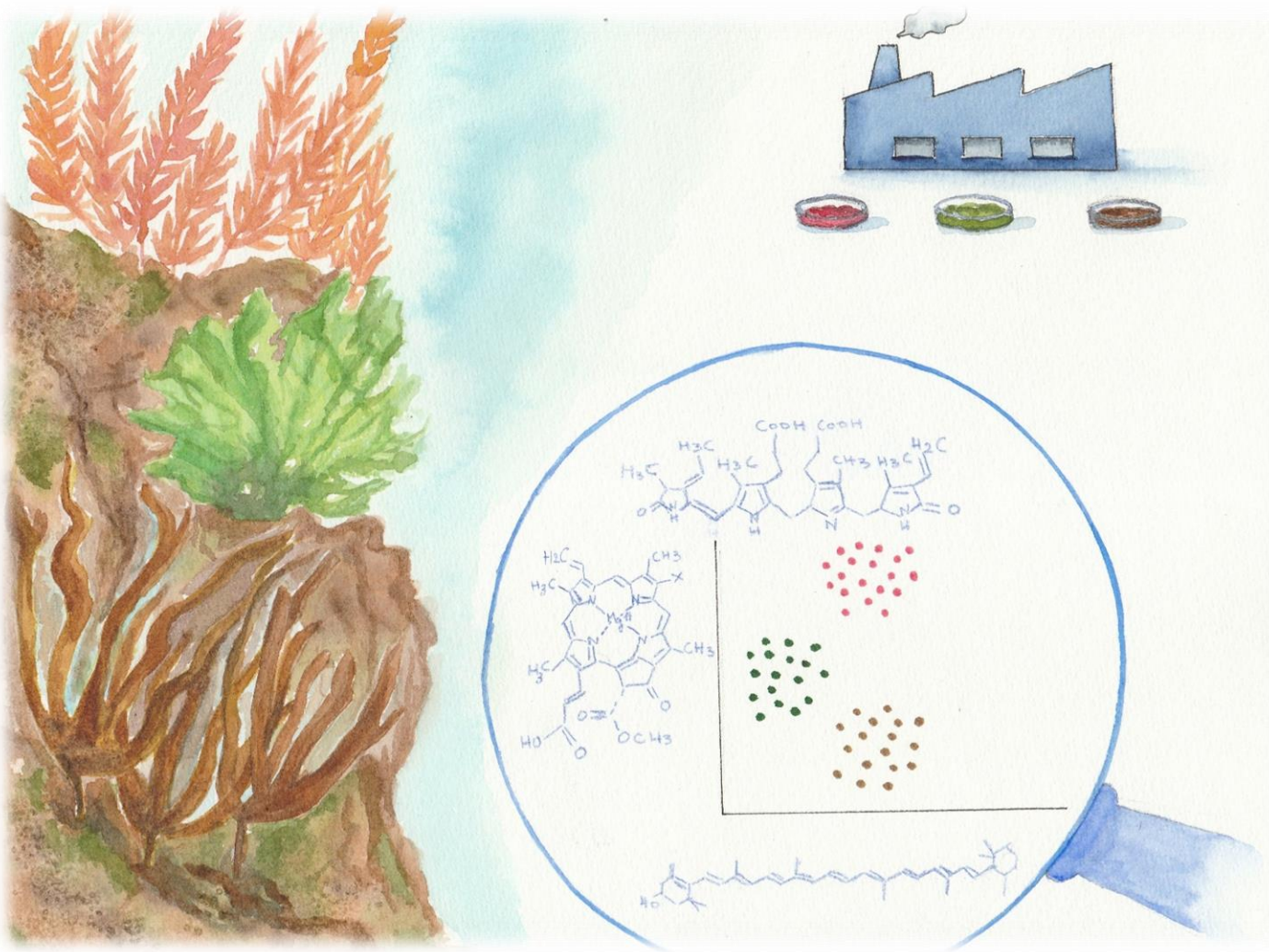


Illustration à l'aquarelle réalisée par Michèle Parchemin

Metabolomics and marine biotechnology: coupling metabolite profiling and organism biology for the discovery of new compounds

Miriam Reverter^{1*}, Sven Rohde¹, Christelle Parchemin², Nathalie Tapissier-Bontemps^{2,3}, Peter J. Schupp^{1,4}

¹Institute for Chemistry and Biology of the Marine Environment (ICBM) at the University of Oldenburg, Wilhelmshaven, Germany

²PSL Research University, UAR EPHE-UPVD-CNRS 3278, CRIobe, Université de Perpignan, 52 Avenue Paul Alduy, 66860, Perpignan Cedex, France

³Labex Corail, BP1013 Papetoai, 98729 Moorea, French Polynesia

⁴Helmholtz Institute for Functional Marine Biodiversity at the University of Oldenburg (HIFMB), D-26129 Oldenburg, Germany

1.1 Abstract

The high diversity of marine natural products represents promising opportunities for drug discovery, an important area in marine biotechnology. Within this context, high-throughput techniques such as metabolomics are extremely useful in unveiling unexplored chemical diversity at much faster rates than classical bioassay-guided approaches. Metabolomics approaches enable studying large sets of metabolites, even if they are produced at low concentrations. Although, metabolite identification remains the main metabolomics bottleneck, bioinformatic tools such as molecular networks can lead to the annotation of unknown metabolites and discovery of new compounds. A metabolic approach in drug discovery has two major advantages: It enables analyses of multiple samples, allowing fast dereplication of already known compounds and provides a unique opportunity to relate metabolite profiles to organisms' biology. Understanding the ecological and biological factors behind a certain metabolite production can be extremely useful in enhancing compound yields, optimizing compounds extraction or in selecting bioactive compounds. Metazoan-associated microbiota are often responsible for metabolite synthesis, however, classical approaches only allow studying metabolites produced from cultivatable microbiota, which often differ from the ones produced within the host. Therefore, coupling holobiome metabolomics with microbiome analysis can bring new insights to the role of microbiota in compound production. The ultimate potential of metabolomics is its coupling with other “omics” (i.e. transcriptomics, metagenomics). Although, such approaches are still challenging, especially in non-model species where genomes have not been annotated, this innovative approach is extremely valuable

in elucidating gene clusters associated with biosynthetic pathways and will certainly become increasingly important in marine drug discovery.

Keywords: metabolomics, marine natural products, marine biotechnology, systems biology, dereplication, marine chemical ecology.

1.2 Introduction

Natural products (i.e. compounds produced by living organisms) are key to drug development, and have proved especially useful in the development of anticancer and anti-infective agents (Liu et al., 2019; Rodrigues et al., 2016). The marine environment, which harbours a large and yet highly unexplored biodiversity, is an extremely rich source of novel and structurally unique compounds with antibacterial, antifungal, antiviral, antiparasitic, antitumor, anti-inflammatory, antioxidant and immunomodulatory activities (Abdelmohsen et al., 2017; Carroll et al., 2020; Mayer et al., 2019). Some marine organisms such as sponges are amongst the most prolific sources of natural products, suggesting the marine environment is a reservoir of natural products of high relevance for marine biotechnology and drug discovery (including against resistant pathogens) (Abdelmohsen et al., 2017; Liu et al., 2019; Thakur and Müller, 2004). The development of high-throughput techniques such as genomics and metabolomics (i.e. the study of all small molecules, < 2,000 Da, in an organism) promises to revolutionise natural product discovery, which according to some estimates, could outpace antibiotic discovery at its peak in the 1950s (Fortman and Mukhopadhyay, 2016). The use of these techniques, do not only offer an increase in the speed of natural product discovery and decrease in the re-discovery rate (Wolfender et al., 2019; van der Hooft et al., 2020), but provide a wide-array of unprecedented opportunities to discover unexplored chemical diversity and elucidate the biological and molecular mechanisms involved in metabolites production (e.g. (Cantrell et al., 2019; Mohanty et al., 2020). Here, we provide a synthetic overview of the advantages of using metabolomic approaches in marine natural product discovery and marine biotechnology. Metabolomics is a scientific field at the interface of different disciplines (chemistry, bioinformatics, ecology, microbiology, systems biology); therefore, this mini-review aims to illustrate how the multidisciplinarity of metabolomics is a key asset for the advancement of marine natural product discovery.

1.3 Speeding up molecule identification

Bioassay-guided fractionation (i.e. extract fractionation and purification based on targeted activities) has been classically used for the discovery of new natural products (El Menif et al., 2019; Kildgaard et al., 2017). However, this approach is not only time-consuming but often

results in the isolation of previously known compounds, since molecule dereplication is performed at the end of the workflow (Herath et al., 2019; Pereira et al., 2019). In recent years, metabolomics has arisen as a new tool to circumvent some of the bioassay-guided fractionation limitations and has shown its effectiveness in the discovery of new active compounds from marine sources (Stuart et al., 2020). Metabolomics approaches are based on the simultaneous screening (using different spectrometry and spectroscopy techniques such as LC-MS, GC-MS and NMR) of a large number of samples and the use of numerical analyses and databases to detect patterns and relevant metabolites, according to a previously defined biological question. By combining direct analysis of complex extracts with machine learning, metabolomics allows studying complex chemical mixtures, including minor compounds, whilst accelerating the dereplication process and decreasing the re-discovery rate (van Der Hooft et al., 2020; Wolfender et al., 2018). Combining large-scale biological screening with untargeted metabolomics of multiple organisms can lead to the fast identification of specimens producing unique compounds and their prioritization in further investigations (Luzzatto-Knaan et al., 2017; Réveillon et al., 2019). For example, the study of shallow water hydrothermal vent sponges by mass spectrometry-based metabolomics combined with cytotoxic activity bioassays led to the selection of three sponges harbouring a unique chemical diversity and the putative identification of a minor original compound cyclostellettamine P (Einarsdottir et al., 2017).

Metabolomic approaches, require however, method standardisation (same extraction and analytical conditions) between the different samples analysed, which can lead to metabolite losses (Gertsman and Barshop, 2018). Furthermore, data processing and curation may be fastidious and the identification of marine compounds remains challenging since marine databases are still scarce compared to terrestrial ones (Barbosa and Roque, 2019). The development of bioinformatics tools, such as mass spectrometry-based molecular networking, are emerging as approaches that could fill some of these gaps and facilitate dereplication (Ramos et al., 2019, **Figure 1**). In molecular networking (such as implemented by the GNPS platform, <https://gnps.ucsd.edu>), algorithms detect and group metabolites based on the similarity of their fragments (mass ion spectra from tandem mass spectrometry), allowing the identification of candidate molecule clusters (i.e. groups of molecules grouped together) (Wang et al., 2016). Then molecular networks can be annotated by identifying matching cluster members in existing databases or by using tools such as Unsupervised Substructure Discovery (MS2LDA, <http://ms2lda.org/>). For example, using this approach, two smenamide-related clusters containing unknown analogs with anti-proliferative activity against cancer cells were

identified in Caribbean sponges (Caso et al., 2019). Then, a targeted isolation can be performed to confirm the activity and the structure of the target compounds using NMR experiments (Li et al., 2018). For example, new pyrrole derived alkaloids were isolated from a marine bacterium and were identified with the analysis of their HRMS, MS/MS, and NMR data (Zhang et al., 2019). Molecular networking is also a powerful tool in minor natural product dereplication (Cantrell et al., 2019). For example, sarasinosides and melophlins were identified using molecular networking tools, despite only small amounts of sponges being available (Mohanty et al., 2020). Finally, a recent tool called “bioactivity-based molecular networking” allows to accelerate the identification of bioactive candidate molecules by integrating data on the activity of extracts/fractions directly into the network via a bioactivity score (Nothias et al., 2018). The use of such a tool led to the isolation of new decalinoylspirotetramic acid derivatives (pyrenosetis A–C) from a seaweed-derived fungus (Fan et al., 2019).

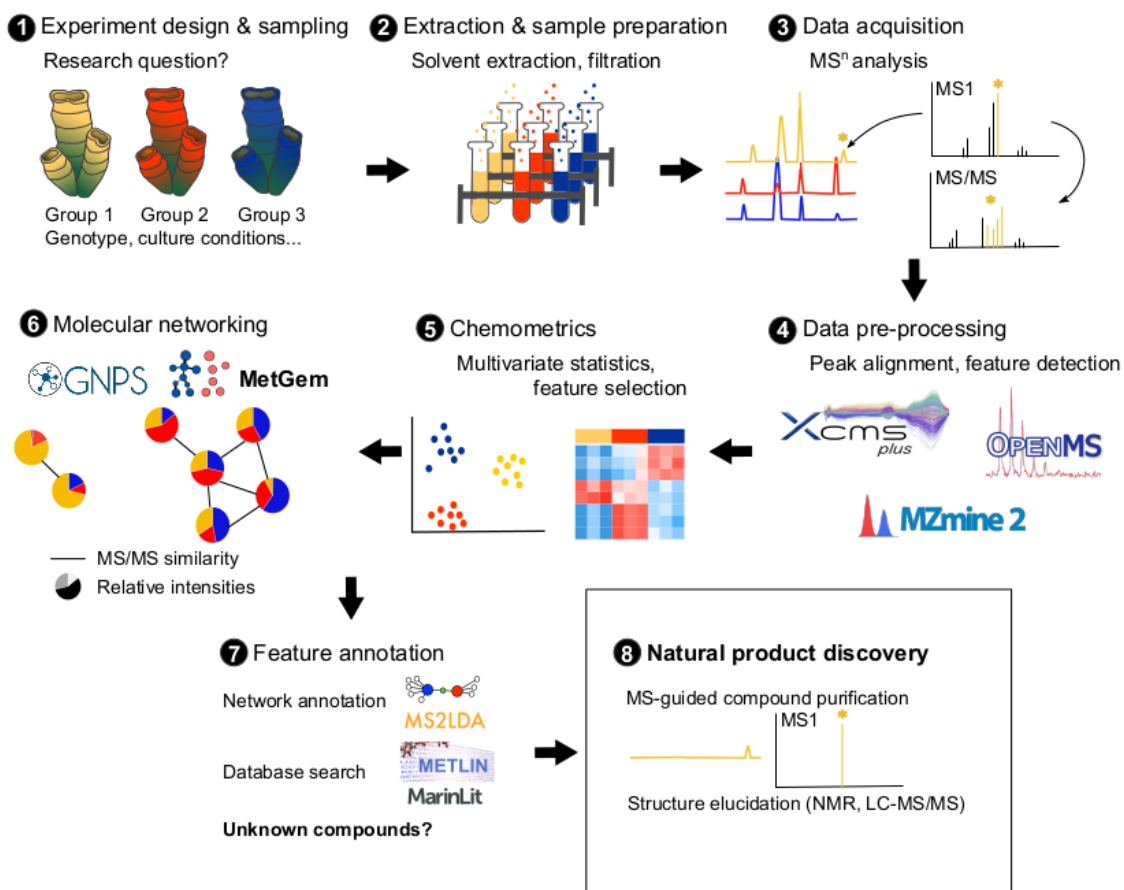


Figure 1. Metabolomics pipeline illustrating the different steps: experiment design according to the biological research question (1), sample extraction (2), MSⁿ analyses (3), pre-processing the raw MSⁿ data using softwares such as XCMS, mzMine2 or OpenMS (4), data numerical analyses to identify patterns and select interesting metabolites (5), molecular networking analysis using tools such as GNPS or MetGem (6), network and metabolite annotation using tools such as MS2LDA or databases (Metlin, MarinLit) (7) and purification and elucidation of new natural products (8).

1.4 Linking chemical diversity and ecology

Secondary metabolites are responsible for a diverse array of ecological functions. While most ecological studies focussing on the function of known natural products investigate defences against predators, allelopathy, or interactions with microbes (Puglisi and Becerro, 2018), metabolites are often involved in multiple additional life history traits such as reproduction, recruitment (Hay, 2009), or resistance against abiotic stressors (Pavia and Brock, 2000). As consequence of the diverse array of ecological functions, the biosynthesis of metabolites is highly variable and strongly affected by environmental and biological conditions. Consequently, biotechnological exploitation of natural products faces the challenge that metabolic variations occur at inter- and intraspecific scales, vary with time and space and as such make it difficult to interpret multiparametric responses. Before the emergence of metabolomics approaches, chemical ecologists relied on targeting few well-characterised compounds to identify metabolites ecological functions. For example, a study on the sponge *Styliasa massa* that investigated the variability of six major metabolites over various geographical scales and in response to biotic and abiotic conditions showed a high variation in metabolite concentrations, suggesting a partly genetic control, but most of the variability could not be assigned to specific factors (Rohde et al., 2012). The development of metabolomics, provides significant opportunities to investigate patterns in metabolite variation, expanding the focus from few to hundreds of metabolites, which could assist in unravelling the multiple pathways that are affected by environmental factors (Figure 1). A study of the metabolome of the red alga *Gracilaria vermiculophylla* in response to herbivory revealed 19 upregulated metabolites with some compounds increasing more than 100-fold in concentration, illustrating the broad spectrum of metabolites that are relevant in single interactions (Nylund et al., 2011). The study of the metabolome of the brown *Lobophora rosacea* showed that out of 262 features identified by LC-MS, the expression of 53 metabolites changed under different pH conditions (Gaubert et al., 2020).

Understanding the variability of metabolite production is not only relevant for ecological purposes, but is important for natural product research and potential drug development. For example, production of peloruside A (a metabolite with potent anticancer activity, Altmann and Gertsch, 2007), from large-scale aquaculture of the sponge *Mycale hentscheli* has been challenging, since its production is altered by parameters such as light and fouling intensity in the farm setting (Page et al., 2005; Page et al., 2005). Similarly, the production of specialized metabolites including the anticancer panicein A hydroquinone (Fiorini et al., 2015), displayed

marked temporal variations in *Haliclona* sponges, decreasing over 10-fold in the putative reproductive months (Reverter et al., 2018). Knowing and controlling the biological and ecological factors that affect metabolite production is thus essential for the harvest of high quantities of natural products. In fact, most microbiologists are nowadays using the “OSMAC” (One Strain Many Compounds) and co-culture approaches to produce differential compounds by modifying the abiotic or biotic culture conditions (Fan et al., 2019; Sproule et al., 2019).

Metabolomics have proven a powerful, even though mostly descriptive, tool to identify metabolic patterns and responses (e.g. Reverter et al., 2018; Gaubert et al., 2020). Still, bioassays are often needed to verify the functions of the identified chemomarkers. Therefore, the development of ecological realistic bioassays to identify the function of metabolites could also lead to the identification of suitable conditions promoting metabolite production with direct implications for bioprospecting (Ledoux and Antunes, 2018). Another aspect that metabolomic approaches, as well as traditional chemical ecology methods, have to cope with is the reproducibility of *in situ* experiments and possible associated artefacts of controlled laboratory experiments, since environmental factors that were not considered in such studies may also affect the metabolome, masking single factor effects. The causality of environmental conditions, metabolite production and ecological function further complicates when the producer itself is unclear. For example, the biosynthesis of some sponge-derived molecules by symbiotic microorganisms is well established (Wilson et al., 2014). These relations have shifted metabolome research from multicellular organisms to their associated microbes

1.5 Host-microbe interactions

Many animals and plants harbour exceptionally diverse communities of microorganisms (i.e. bacteria, fungi, viruses) that display vital functions in the holobiont (Bewley et al., 1996; Thomas et al., 2016; Wilkins et al., 2019). In marine organisms, associated microorganisms are often identified as the producers of the natural products found in their hosts (e.g. Morita and Schmidt, 2018; Rust et al., 2020; Wilson et al., 2014). For example, recent studies have demonstrated that many sponge-isolated compounds such as different polyketides, peptides and bromotyrosine-derived alkaloids, are in fact, produced by their associated microorganisms (Nicacio et al., 2017; Wilson et al., 2014). Another example includes γ -pyrones, which are often found in molluscs such as cone snails, and which were shown to be produced by the associated cultivable bacteria *Nocardiopsis alba* (Lin et al., 2013). Classical approaches used to investigate the contribution of host-associated microorganisms in natural product synthesis include isolation and host-independent culture of the microorganisms (Lin et al., 2013; Nicacio et al.,

2017). Host-associated culture with miniature incubation chambers inside the host has also been applied with varying success (Steinert et al., 2014). However, these approaches are unsuitable for uncultivable microorganisms, which for the prokaryotic phyla alone are proposed to be at least 70% of the known taxa (Achtman and Wagner, 2008). Furthermore, the holobiont comprises a complex network of microorganisms that are in constant communication and signalling, which regulates gene expression and metabolite synthesis (Hughes and Sperandio, 2008; Pande and Kost, 2017). Therefore, isolation and repeated culture of host-associated microorganisms can result in a loss of natural product production (Morita and Schmidt, 2018). Within this context, the combined study of the holobiont microbiome and metabolome provides new exciting opportunities to explore host-symbiont relationships. Identification of consistent co-associations between compounds and microorganisms using correlation tools can assist in metagenomics mining to search for natural product biosynthetic gene clusters (BGCs) in the holobionts (Paix et al., 2019; Reverter et al., 2020, **Figure 2**). For example, cyclic dipeptides found in the algae *Taonia atomaria* were found to be highly correlated with a BD1-7 clade bacterial taxon from the Alteromonadaceae family (Paix et al., 2019). Similarly, several haemoglobin-derived peptides found in the butterflyfish *Chaetodon lunulatus* were highly correlated to a Fusobacteriaceae strain (Reverter et al., 2020), suggesting a possible direct or indirect involvement of these bacteria in the production of the aforementioned compounds.

1.6 Multi-omics integration

Despite several natural product BGCs have been elucidated using metagenomics (e.g. Storey et al., 2020; Wakimoto et al., 2014), most of them have yet to be linked to the metabolites they encode (Amos et al., 2017). Metabolomics is considered the last link in the systems biology chain, therefore, its coupling with other high-throughput technologies, such as transcriptomics and genomics, provides a bridge to link molecular mechanisms with metabolite production (Amos et al., 2017; van Der Hooft et al., 2020). Such integration techniques provide a deeper understanding of the molecular mechanisms involved in the production of biologically active compounds through the identification of BGCs, gene expression patterns and enzymes related to the produced metabolites (Paul et al., 2019; van Der Hooft et al., 2020). For example, an integrated metabolomic-transcriptomic analysis of the sea urchin *Strongylocentrotus intermedius* allowed identification of critical genes related to eicosanoid acid biosynthesis (Wang et al., 2020). A study of Dysideidae sponges using mass spectrometry, molecular fragmentation and NMR spectroscopy identified a large-array of new polybrominated diphenyl ethers (PBDEs) in these sponges (Agarwal et al., 2015), and then by using metagenomics, the

genes responsible for PBDEs production were identified within the sponge cyanobacterial endosymbionts (Agarwal et al., 2017; Schorn et al., 2019). Similarly, integration of molecular networking and genome-mining of several marine *Salinispora* bacteria led to several molecular family-BGC pairings, including the characterization of a new cytotoxic depsipeptide (retimycin) and its link to gene cluster NRPS40 (Amos et al., 2017; Duncan et al., 2015). Metabologenomics, a term that defines these integrated approaches, can therefore contribute to accelerate the linking of unknown BGCs to metabolites as well as assist in extract prioritization for structure elucidation (Goering et al., 2016; van Der Hooft et al., 2020, **Figure 2**).

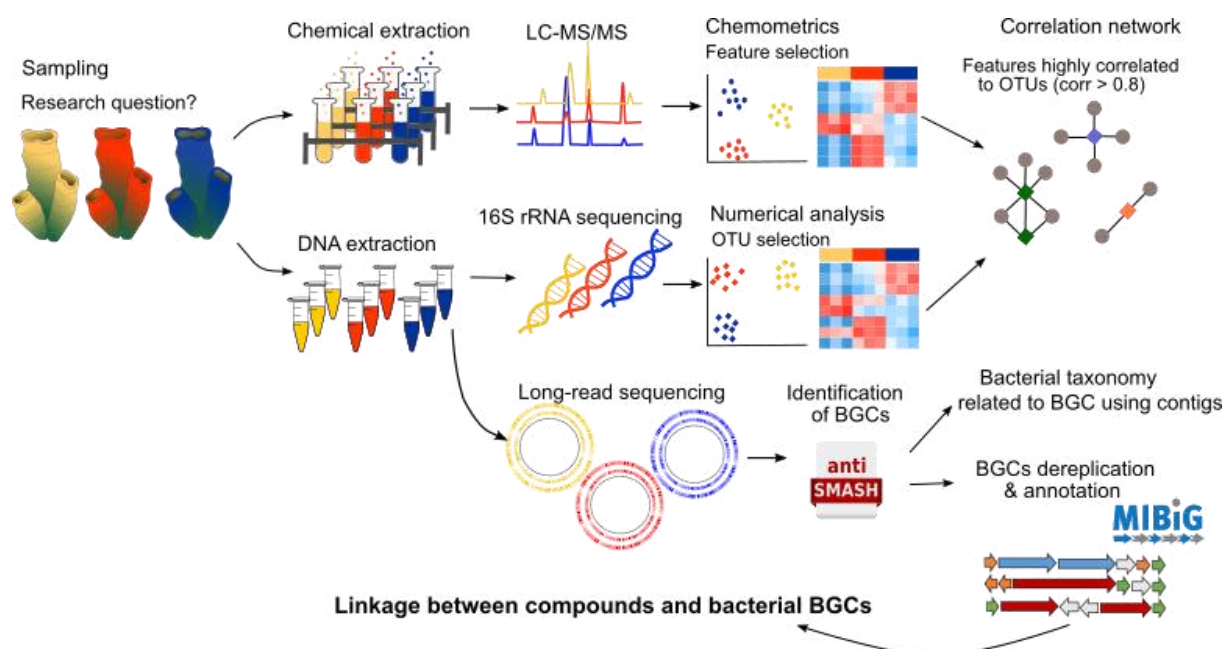


Figure 2. Pipeline illustrating the integration of metabolomics, microbiomics and metagenomics tools. The parallel metabolome and microbiome analysis allows the identification of metabolites of interest that are highly correlated to specific bacterial taxons. Then by performing long-read sequencing and genome mining (using tools such as AntiSMASH or similar) biosynthetic gene clusters (BGCs) can be identified and annotated manually or by using databases such as MIBiG. 16S contigs (i.e. continuous fragments of DNA sequence from an incomplete genome) can then be used to assign the BGCs to specific bacterial taxon genomes. The predicted compounds encoded by these BGCs can then be compared with the metabolome data in order to link produced metabolites with specific bacterial BGCs.

Natural products complexity is often a barrier in their synthesis and scale-up production, and harvest of the natural source (e.g. plants, marine macroorganisms or uncultivable microorganisms) might not be always a reliable or sustainable option (Paddon and Keasling, 2014). For example, 13 tonnes of the marine bryozoan *Bugula neritina* were harvested for the isolation of 18g of the potent anti-cancer compound bryostatin 1 for clinical phase 1 studies (Schaufelberger et al., 1991). In such cases, pairing interesting metabolites with their encoding genes provides new opportunities for the synthesis of natural products using synthetic biology

approaches such as insertion of biosynthetic genes in heterologous hosts (Ahmed et al., 2020; Amos et al., 2017; Zhang et al., 2019). However, despite the huge potential of these methods and the global effort in increasing the number of annotated and well-curated genome data from marine bacteria and symbionts (e.g. (Machado et al., 2015; Udwary et al., 2007), these tools are still in the infancy and need to be further developed for their widespread use in marine biotechnology.

1.7 Discussion

Amidst the increasing global concern over antimicrobial resistance, the SARS-CoV-2 virus pandemic, and the continuous need for anticancer and antiviral drugs, the natural product research field has attracted renewed attention as new tools such as metabolomics accelerate metabolite discovery and decrease re-discovery rates (Liu et al., 2019; Rodrigues et al., 2016). In particular, marine organisms arise as a prolific source of novel natural products (Abdelmohsen et al., 2017). Marine organisms have been much less studied than their terrestrial counterparts, while they produce an incredibly diverse array of molecules with new chemical features and modes of action (Abdelmohsen et al., 2017; Carroll et al., 2020). For example, the production of highly bioactive organohalogens seems to be a special feature widespread amongst marine organisms, which is much less common amongst terrestrial organisms (Gribble, 2009). Both the discovery of new species and improved taxonomic descriptions offer new natural product bioprospecting possibilities. However, it is nowadays apparent that not only taxonomy affects the production of metabolites but also that both biotic (e.g. life cycle, organisms interactions) and abiotic (e.g. environmental conditions) factors play determinant roles in the production of specialised metabolites (e.g. Gaubert et al., 2020; Nylund et al., 2011). Metabolomics arises therefore not only as a fast alternative to elucidate new biologically active metabolites, but also as an emerging tool in chemical ecology to study the variation of the organism's chemical diversity in response to different factors. Linking the production of biologically active metabolites to environmental or biological conditions could have direct implications for bioprospecting and scale-up metabolite production. Where scale-up metabolite production from whole organism culture is not possible, the linking of metabolomics with metagenomics approaches that identify responsible BGCs (either in the host or the associated microorganisms) also provides new opportunities for metabolite production through synthetic biology and bioengineering (Ahmed et al., 2020).

Despite the many advantages and huge potential of metabolomics approaches in the discovery of new marine biologically active compounds, the major drawback continues to be the poor

coverage of marine natural products in public databases (Barbosa and Roque, 2019; Pereira and Aires-de-Sousa, 2018). Such lack of public reference spectra (including fragmentation patterns) of marine-derived natural products prevents automated dereplication processes, and often results in the development of in-house libraries by the different research groups (by purifying and structural elucidating each of the metabolites), multiplying the efforts and slowing metabolite identification on the global level. Therefore, along with the constant development and improvement of metabolomics tools (e.g. hardware and workflows) to increase sensitivity, repeatability and allow comparison and integration of a larger number of datasets (Forsberg et al., 2018; Guitton et al., 2017), development of a free-access database with well-curated spectrometric data (e.g. MS¹, MS², UV, NMR) on marine natural products is urgently needed. This could be achieved, for example with the integration of known and new marine natural products (from both macro and microorganisms) into currently operational databases highly used in metabolomics such as GNPS.

1.8 Reference

- Abdelmohsen, U.R., Balasubramanian, S., Oelschlaeger, T.A., Grkovic, T., Pham, N.B., Quinn, R.J., et al. (2017). Potential of marine natural products against drug-resistant fungal, viral, and parasitic infections. *Lancet Infect. Dis.* 17(2), e30-e41. doi: 10.1016/S1473-3099(16)30323-1
- Achtman, M., and Wagner, M. (2008). Microbial diversity and the genetic nature of microbial species. *Nat. Rev. Microbiol.* 6(6), 431-440. doi: 10.1038/nrmicro1872
- Agarwal, V., Blanton, J.M., Podell, S., Taton, A., Schorn, M.A., Busch, J., et al. (2017). Metagenomic discovery of polybrominated diphenyl ether biosynthesis by marine sponges. *Nat. Chem. Biol.* 13(5), 537-543. doi: 10.1038/nchembio.2330
- Agarwal, V., Li, J., Rahman, I., Borgen, M., Aluwihare, L.I., Biggs, J.S., et al. (2015). Complexity of naturally produced polybrominated diphenyl ethers revealed via mass spectrometry. *Env. Sci. Technol.* 49(3), 1339-1346. doi: 10.1021/es505440j
- Ahmed, Y., Rebets, Y., Estévez, M.R., Zapp, J., Myronovskiy, M., and Luzhetskyy, A. (2020). Engineering of *Streptomyces lividans* for heterologous expression of secondary metabolite gene clusters. *Microb. Cell Fact.* 19(1), 5. doi: 10.1186/s12934-020-1277-8
- Altmann, K.H., and Gertsch, J. (2007). Anticancer drugs from nature - natural products as a unique source of new microtubule-stabilizing agents. *Nat. Prod. Rep.* 24, 327-357. doi: 10.1039/b515619j
- Amos, G.C.A., Awakawa, T., Tuttle, R.N., Letzel, A.-C., Kim, M.C., Kudo, Y., et al. (2017). Comparative transcriptomics as a guide to natural product discovery and biosynthetic gene cluster functionality. *Proc. Natl. Acad. Sci. U. S. A.* 114(52), E11121-E11130. doi: 10.1073/pnas.1714381115
- Aron, A. T., Gentry, E. C., McPhail, K. L., Nothias, L.-F., Nothias-Esposito, M., Bouslimani, A., et al. (2020). Reproducible molecular networking of untargeted mass spectrometry data using GNPS. *Nat. Protoc.* 15, 1954-1991. doi: 10.1038/s41596-020-0317-5

- Barbosa, A.J.M., and Roque, A.C.A. (2019). Free marine natural product databases for biotechnology and bioengineering. *Biotechnol. J.* 14(11), 1800607. doi: 10.1002/biot.201800607
- Bewley, C.A., Holland, N.D., and Faulkner, D.J. (1996). Two classes of metabolites from *Theonella swinhonis* are localized in distinct bacterial symbionts. *Experientia* 52(7), 716-722. doi: 10.1007/BF01925581
- Cantrell, T.P., Freeman, C.J., Paul, V.J., Agarwal, V., and Garg, N. (2019). Mass spectrometry-based integration and expansion of the chemical diversity harbored within a marine sponge. *J. Am. Soc. Mass Spectrom.* 30(8), 1373-1384. doi: 10.1007/s13361-019-02207-5
- Carroll, A.R., Copp, B.R., Davis, R.A., Keyzers, R.A., and Prinsep, M.R. (2020). Marine natural products. *Nat. Prod. Rep.* 37(2), 175-223. doi: 10.1039/C9NP00069K
- Caso, A., Esposito, G., Della Sala, G., Pawlik, J. R., Teta, R., Mangoni, A., et al. (2019). Fast detection of two smenamide family members using molecular networking. *Mar. Drugs* 17(11), 618. doi: 10.3390/md17110618
- Duncan, K.R., Crüsemann, M., Lechner, A., Sarkar, A., Li, J., Ziemert, N., et al. (2015). Molecular networking and pattern-based genome mining improves discovery of biosynthetic gene clusters and their products from *Salinispore* species. *Chem. Biol.* 22(4), 460-471. doi: 10.1016/j.chembiol.2015.03.010
- El Menif, E., Offret, C., Labrie, S., and Beaulieu, L. (2019). Identification of peptides implicated in antibacterial activity of snow crab hepatopancreas hydrolysates by a bioassay-guided fractionation Approach combined with mass spectrometry. *Probiotics Antimicrob. Proteins* 11, 1023–1033. doi: 10.1007/s12602-018-9484-x
- Einarsdottir, E., Magnusdottir, M., Astarita, G., Köck, M., Ögmundsdottir, H. M., Thorsteinsdottir, M., et al. (2017). Metabolic profiling as a screening tool for cytotoxic compounds: Identification of 3-alkyl pyridine alkaloids from sponges collected at a shallow water hydrothermal vent site north of Iceland. *Mar. Drugs* 15, 52. doi: 10.3390/md15020052
- Forsberg, E.M., Huan, T., Rinehart, D., Benton, P.H., Warth, B., Hilmers, B. et al. (2018). Data processing, multi-omic pathway mapping, and metabolite activity analysis using XCMS Online. *Nat. Prot.* 13, 633-651. doi: 10.1038/nprot.2017.151
- Fan, B., Parrot, D., Blümel, M., Labes, A., and Tasdemir, D. (2019). Influence of OSMAC-based cultivation in metabolome and anticancer activity of fungi associated with the brown alga *Fucus vesiculosus*. *Mar. drugs* 17, 67. doi: 10.3390/md17010067
- Fiorini, L., Aude-Tribalat, M.A., Sauvard, L., Cazareth, J., Lalli, E., Broutin, I., Thomas, O.P., and Mus-Veteau, I. (2015). Natural paniceins from Mediterranean sponge inhibit the multidrug resistance activity of patched and increase chemotherapy efficiency on melanoma cells. *Oncotarget* 6(26), 22282-22297. doi: 10.18632/oncotarget.4162
- Fortman, J.L., and Mukhopadhyay, A. (2016). The Future of antibiotics: emerging technologies and stewardship. *Trends Microbiol.* 24(7), 515-517. doi: 10.1016/j.tim.2016.04.003
- Gaubert, J., Rodolfo-Metalpa, R., Greff, S., Thomas, O.P., and Payri, C.E. (2020). Impact of ocean acidification on the metabolome of the brown macroalgae *Lobophora rosacea* from New Caledonia. *Algal Res.* 46, 101783. doi: 10.1016/j.algal.2019.101783
- Gertsman, I., and Barshop, B. A. (2018). Promises and pitfalls of untargeted metabolomics. *J. inherit. Metab. Dis.* 41, 355–366. doi: 10.1007/s10545-017-0130-7

- Goering, A.W., McClure, R.A., Doroghazi, J.R., Albright, J.C., Haverland, N.A., Zhang, Y., et al. (2016). Metabologenomics: correlation of microbial gene clusters with metabolites drives discovery of a nonribosomal peptide with an unusual amino acid monomer. *ACS Cent. Sci.* 2(2), 99-108. doi: 10.1021/acscentsci.5b00331
- Gribble, G.W. (2010). *Naturally Occurring Organohalogen Compounds – A Comprehensive Update*. Vienna: Springer.
- Guitton, Y., Tremblay-Franco, M., Le Corguillé, G., Martin, J-F., Pétéra, M., Mele, P.R., et al. (2017). Create, run, share, publish, and reference your LC-MS, FIA-MS, GC-MS and NMR data analysis workflows with the Workfloy4Metabolomics 3.0 Galaxy online infrastructure for metabolomics. *Int. J. Biochem. Cell Biol.* 93, 89-101. doi: 10.1016/j.biocel.2017.07.002
- Hay, M.E. (2009). Marine chemical ecology: chemical signals and cues structure marine populations, communities, and ecosystems. *Ann. Rev. Mar. Sci.* 1, 193-212. doi: 10.1146/annurev.marine.010908.163708
- Herath, H. M. P., Preston, S., Jabbar, A., Garcia-Bustos, J., Taki, A. C., Addison, R. S., et al. (2019). Identification of fromiamycalin and halaminol A from Australian marine sponge extracts with anthelmintic activity against *Haemonchus contortus*. *Mar. Drugs* 17, 598. doi: 10.3390/md17110598
- Hughes, D.T., and Sperandio, V. (2008). Inter-kingdom signalling: communication between bacteria and their hosts. *Nat. Rev. Microbiol.* 6(2), 111-120. doi: 10.1038/nrmicro1836
- Kildgaard, S., Subko, K., Phillips, E., Goidts, V., De la Cruz, M., Díaz, C., et al. (2017). A dereplication and bioguided discovery approach to reveal new compounds from a marine-derived fungus *Stilbella fimetaria*. *Mar. Drugs* 15, 253. doi: 10.3390/md15080253
- Ledoux, J.B., and Antunes, A. (2018). Beyond the beaten path: improving natural products bioprospecting using an eco-evolutionary framework - the case of the octocorals. *Crit. Rev. Biotechnol.* 38, 184-198. doi: 10.1080/07388551.2017.1331335
- Li, F., Janussen, D., Peifer, C., Pérez-Victoria, I., and Tasdemir, D. (2018). Targeted isolation of tsitsikammamines from the Antarctic deep-sea sponge *Latrunculia biformis* by molecular networking and anticancer activity. *Mar. Drugs* 16, 268. doi: 10.3390/md16080268
- Lin, Z., Torres, Joshua P., Ammon, Mary A., Marett, L., Teichert, Russell W., Reilly, Christopher A., et al. (2013). A Bacterial source for mollusk pyrone polyketides. *Chem. Biol.* 20(1), 73-81. doi: 10.1016/j.chembiol.2012.10.019
- Liu, M., El-Hossary, E.M., Oelschlaeger, T.A., Donia, M.S., Quinn, R.J., and Abdelmohsen, U.R. (2019). Potential of marine natural products against drug-resistant bacterial infections. *Lancet Infect. Dis.* 19(7), e237-e245. doi: 10.1016/S1473-3099(18)30711-4
- Luzzatto-Knaan, T., Garg, N., Wang, M., Glukhov, E., Peng, Y., Ackermann, G., et al. (2017). Digitizing mass spectrometry data to explore the chemical diversity and distribution of marine cyanobacteria and algae. *eLife* 6, e24214. doi: 10.7554/eLife.24214.001
- Machado, H., Sonnenschein, E.C., Melchiorsen, J., and Gram, L. (2015). Genome mining reveals unlocked bioactive potential of marine Gram-negative bacteria. *BMC Genomics* 16(1), 158. doi: 10.1186/s12864-015-1365-z
- Mayer, M.S., Guerrero, A.J., Rodriguez, A.D., Taglialatela-Scafati, O., Nakamura, F., Fusetani, N. (2020). Marine pharmacology in 2014-2015: marine compounds with antibacterial, antidiabetic, antifungal, anti-inflammatory, antiprotozoal, antituberculosis, antiviral and anthelmintic activities; affecting the immune and nervous systems, and other miscellaneous mechanisms of action. *Mar. Drugs* 18, 5. doi: 10.3390/md18010005

- Mohanty, I., Podell, S., Biggs, J.S., Garg, N., Allen, E.E., and Agarwal, V. (2020). Multi-omic profiling of *Melophlus* Sponges reveals diverse metabolomic and microbiome architectures that are non-overlapping with ecological neighbors. *Mar. Drugs* 18(2), 124. doi: 10.3390/md18020124
- Morita, M., and Schmidt, E.W. (2018). Parallel lives of symbionts and hosts: chemical mutualism in marine animals. *Nat. Prod. Rep.* 35(4), 357-378. doi: 10.1039/C7NP00053G
- Nicacio, K.J., Ióca, L.P., Fróes, A.M., Leomil, L., Appolinario, L.R., Thompson, C.C., et al. (2017). Cultures of the marine bacterium *Pseudovibrio denitrificans* Ab134 produce bromotyrosine-derived alkaloids previously only isolated from marine sponges. *J. Nat. Prod.* 80(2), 235-240. doi: 10.1021/acs.jnatprod.6b00838
- Nothias, L.-F., Nothias-Esposito, M., da Silva, R., Wang, M., Protsyuk, I., Zhang, Z., et al. (2018). Bioactivity-based molecular networking for the discovery of drug leads in natural product bioassay-guided fractionation. *J. Nat. Prod.* 81, 758–767. doi: 10.1021/acs.jnatprod.7b00737
- Nylund, G.M., Weinberger, F., Rempt, M., and Pohnert, G. (2011). Metabolomic assessment of induced and activated chemical defence in the invasive red alga *Gracilaria vermiculophylla*. *PLoS One* 6, e29359-e29359. doi: 10.1371/journal.pone.0029359
- Page, M., West, L., Northcote, P., Battershill, C., and Kelly, M. (2005a). Spatial and temporal variability of cytotoxic metabolites in populations of the New Zealand sponge *Mycale hentscheli*. *J. Chem. Ecol.* 31, 1161-1174. doi: 10.1007/s10886-005-4254-0
- Page, M.J., Northcote, P.T., Webb, V.L., Mackey, S., and Handley, S.J. (2005b). Aquaculture trials for the production of biologically active metabolites in the New Zealand sponge *Mycale hentscheli* (Demospongiae : Poecilosclerida). *Aquaculture* 250, 256-269. doi: 10.1016/j.aquaculture.2005.04.069
- Paix, B., Othmani, A., Debroas, D., Culoli, G., and Briand, J.F. (2019). Temporal covariation of epibacterial community and surface metabolome in the Mediterranean seaweed holobiont *Taonia atomaria*. *Environ. Microbiol.* doi: 10.1111/1462-2920.14617
- Pande, S., and Kost, C. (2017). Bacterial unculturability and the formation of intercellular metabolic networks. *Trends Microbiol.* 25(5), 349-361. doi: 10.1016/j.tim.2017.02.015
- Paul, V.J., Freeman, C.J., and Agarwal, V. (2019). Chemical Ecology of Marine Sponges: New Opportunities through "-Omics". *Integr. Comp. Biol.* 59, 765-776. doi: 10.1093/icb/icz014
- Pavia, H., and Brock, E. (2000). Extrinsic factors influencing phlorotannin production in the brown alga *Ascophyllum nodosum*. *Mar. Ecol. Prog. Ser.* 193, 285-294. doi: 10.3354/meps193285
- Pereira, F., and Aires-de-Sousa, J. (2018). Computational Methodologies in the Exploration of Marine Natural Product Leads. *Mar Drugs*. 16, 236. doi: 10.3390/md16070236
- Pereira, R. B., Pereira, D. M., Jiménez, C., Rodríguez, J., Nieto, R. M., Videira, R. A., et al. (2019). Anti-inflammatory effects of 5 α , 8 α -epidioxycholest-6-en-3 β -ol, a steroidal endoperoxide isolated from *Aplysia depilans*, based on bioguided fractionation and NMR analysis. *Mar. Drugs* 17, 330. doi: 10.3390/md17060330
- Puglisi, M.P., and Becerro, M.A. (2018). Chemical ecology: the ecological impacts of marine natural products. CRC Press.

- Ramos, A.E.F., Evanno, L., Poupon, E., Champy, P., and Beniddir, M.A. (2019). Natural products targeting strategies involving molecular networking: different manners, one goal. *Nat. Prod. Rep.* 36, 960-980. doi: 10.1039/c9np00006b
- Réveillon, D., Tunin-Ley, A., Grondin, I., Othmani, A., Zubia, M., Bunet, R., et al. (2019). Exploring the chemodiversity of tropical microalgae for the discovery of natural antifouling compounds. *J. Appl. Phycol.* 31, 319–333. doi: 10.1007/s10811-018-1594-z
- Reverter, M., Sasal, P., Suzuki, M.T., Raviglione, D., Inguimbert, N., Pare, A. et al. (2020). Insights into the natural defences of a coral reef fish against gill ectoparasites: integrated metabolome and microbiome approach. *Metabolites* 10, 227. doi: 10.3390/metabo10060227
- Reverter, M., Tribalat, M.-A., Pérez, T., and Thomas, O.P. (2018). Metabolome variability for two Mediterranean sponge species of the genus *Haliclona*: specificity, time, and space. *Metabolomics* 14(9), 114. doi: 10.1007/s11306-018-1401-5
- Rodrigues, T., Reker, D., Schneider, P., and Schneider, G. (2016). Counting on natural products for drug design. *Nat. Chem.* 8(6), 531-541. doi: 10.1038/nchem.2479
- Rohde, S., Gochfeld, D.J., Ankisetty, S., Avula, B., Schupp, P.J., and Slattery, M. (2012). Spatial variability in secondary metabolites of the Indo-Pacific sponge *Stylissa massa*. *J. Chem. Ecol.* 38, 463-475. doi: 10.1007/s10886-012-0124-8
- Rust, M., Helfrich, E.J.N., Freeman, M.F., Nanudorn, P., Field, C.M., Rückert, C., et al. (2020). A multiproducer microbiome generates chemical diversity in the marine sponge *Mycale hentscheli*. *Proc. Nat. Acad. Sci. U.S.A.* 117(17) 9508-9518. doi: 10.1073/pnas.1919245117
- Schaufelberger, D.E., Koleck, M.P., Beutler, J.A., Vatakis, A.M., Alvarado, A.B., Andrews, P., et al. (1991). The large-scale isolation of bryostatin 1 from *Bugula neritina* following current good manufacturing practices. *J. Nat. Prod.* 54(5), 1265-1270. doi: 10.1021/np50077a004
- Schorn, M.A., Jordan, P.A., Podell, S., Blanton, J.M., Agarwal, V., Biggs, J.S., et al. (2019). Comparative genomics of cyanobacterial symbionts reveals distinct, specialized metabolism in tropical *Dysideidae* sponges. *mBio* 10(3), e00821-00819. doi: 10.1128/mBio.00821-19
- Sproule, A., Correa, H., Decken, A., Haltli, B., Berrué, F., Overy, D. P., et al. (2019). Terrosamycins A and B, bioactive polyether ionophores from *Streptomyces* sp. RKND004 from Prince Edward Island sediment. *Mar. Drugs* 17, 347. doi: 10.3390/md17060347
- Steinert, G., Whitfield, S., Taylor, M.W., Thoms, C., Schupp, P.J. (2014). Application of diffusion growth chambers for the cultivation of marine sponge-associated bacteria. *Mar. Biotechnol.* 16, 594-603. doi: 10.1007/s10126-014-9575-y
- Storey, M.A., Andreassend, S.K., Bracegirdle, J., Brown, A., Keyzers, R.A., Ackerley, D.F., et al. (2020). Metagenomic exploration of the marine sponge *Mycale hentscheli* uncovers multiple polyketide-producing bacterial symbionts. *mBio* 11(2), e02997-02919. doi: 10.1128/mBio.02997-19
- Stuart, K. A., Welsh, K., Walker, M. C., and Edrada-Ebel, R. (2020). Metabolomic tools used in marine natural product drug discovery. *Expert Opin. Drug Discov.* 15, 499–522. doi: 10.1080/17460441.2020.1722636
- Thakur, N.L., and Müller, W.E.G. (2004). Biotechnological potential of marine sponges. *Curr. Sci.* 86(11), 1506-1512.

- Thomas, T., Moitinho-Silva, L., Lurgi, M., Björk, J.R., Easson, C., Astudillo-Garcia, C., et al. (2016). Diversity, structure and convergent evolution of the global sponge microbiome. *Nat. Comm.* 7, 11870. doi: 10.1038/ncomms11870
- Udwary, D.W., Zeigler, L., Asolkar, R.N., Singan, V., Lapidus, A., Fenical, W., et al. (2007). Genome sequencing reveals complex secondary metabolome in the marine actinomycete *Salinispora tropica*. *Proc. Natl. Acad. Sci. U. S. A.* 104(25), 10376-10381. doi: 10.1073/pnas.0700962104
- van der Hooft, J.J.J., Mohimani, H., Bauermeister, A., Dorrestein, P.C., Duncan, K.R., and Medema, M.H. (2020). Linking genomics and metabolomics to chart specialized metabolic diversity. *Chem. Soc. Rev. In press.* doi: 10.1039/D0CS00162G
- Wakimoto, T., Egami, Y., Nakashima, Y., Wakimoto, Y., Mori, T., Awakawa, T., et al. (2014). Calyculin biogenesis from a pyrophosphate protoxin produced by a sponge symbiont. *Nat. Chem. Biol.* 10(8), 648-655. doi: 10.1038/nchembio.1573
- Wang, M., Carver, J. J., Phelan, V. V., Sanchez, L. M., Garg, N., Peng, Y., et al. (2016). Sharing and community curation of mass spectrometry data with Global Natural Products Social Molecular Networking. *Nat. biotechnol.* 34, 828–837. doi: 10.1038/nbt.3597
- Wang, H., Ding, J., Ding, S., and Chang, Y. (2020). Integrated metabolomic and transcriptomic analyses identify critical genes in eicosapentaenoic acid biosynthesis and metabolism in the sea urchin *Strongylocentrotus intermedius*. *Sci. Rep.* 10(1), 1697. doi: 10.1038/s41598-020-58643-x
- Wilkins, L.G.E., Leray, M., O'Dea, A., Yuen, B., Peixoto, R.S., Pereira, T.J., et al. (2019). Host-associated microbiomes drive structure and function of marine ecosystems. *PLoS Biol.* 17(11), e3000533-e3000533. doi: 10.1371/journal.pbio.3000533
- Wilson, M.C., Mori, T., Rückert, C., Urias, A.R., Helf, M.J., Takada, K., et al. (2014). An environmental bacterial taxon with a large and distinct metabolic repertoire. *Nature* 506(7486), 58-62. doi: 10.1038/nature12959
- Wolfender, J.-L., Nuzillard, J.-M., van der Hooft, J.J.J., Renault, J.-H., and Bertrand, S. (2019). Accelerating metabolite identification in natural product research: toward an ideal combination of liquid chromatography–high-resolution tandem mass spectrometry and NMR Profiling, *in silico* databases, and chemometrics. *Anal. Chem.* 91(1), 704-742. doi: 10.1021/acs.analchem.8b05112
- Zhang, F., Braun, D. R., Chanana, S., Rajski, S. R., and Bugni, T. S. (2019). Phallusialides A–E, pyrrole-derived alkaloids discovered from a marine-derived *Micromonospora* sp. bacterium using MS-based metabolomics approaches. *J. Nat. Prod.* 82, 3432–3439. doi:10.1021/acs.jnatprod.9b00808
- Zhang, J.J., Tang, X., and Moore, B.S. (2019). Genetic platforms for heterologous expression of microbial natural products. *Nat. Prod. Rep.* 36, 1313-1332. doi:10.1039/C9NP00025A

2. Annexe Chapitre I

Supplementary materials for

Development of a Multiblock Metabolomics Approach to Explore
Metabolite Variations of two Algae of the Genus *Asparagopsis* Linked
to Interspecies and Temporal Factors

Christelle Parchemin^{*,1,2}, Delphine Raviglione¹, Hikmat Ghosson¹, Marie-Virginie Salvia¹,
Corentine Goossens¹, Pierre Sasal¹, Elisabeth Faliex², Nathalie Tapissier-Bontemps^{*,1}

¹ Centre de Recherches Insulaires et Observatoire de l'Environnement (CRIOBE), Ecole
Pratique des Hautes Etudes (EPHE), Université PSL, UPVD, CNRS, UAR 3278, 52 Av. Paul
Alduy, 66860 Perpignan CEDEX, France

² CEntre de Formation et de Recherche sur les Environnements Méditerranéens (CEFREM),
UMR 5110 UPVD-CNRS, Université de Perpignan - Via Domitia, 52 Av. Paul Alduy, 66860
Perpignan CEDEX, France

*Corresponding authors: Christelle Parchemin (christelle.parchemin@univ-perp.fr); Nathalie
Tapissier-Bontemps (nathalie.tapissier@univ-perp.fr)

2.1 Supplementary methods

Supplementary Method 1: Details of sampling events for the study of interspecies and temporal variation of the metabolome of *A. armata* and *A. taxiformis*.

Species	Site (Country)	Latitude	Longitude	Date
<i>A. armata</i>	Banyuls (France)	42.482230	3.137175	20/02/2020
				20/03/2020
				17/04/2020
				18/05/2020
				9/3/2021
				15/03/2021
				8/4/2021
				12/5/2021
				11/6/2021
				29/01/21
<i>A. taxiformis</i>	Portsall (France)	48.554113	-4.706051	2/5/2021
				29/01/2020
				22/05/2020
				15/06/2020
				6/7/2020
				Moorea (French Polynesia)
				-17.48262
				-149.87213
				24/08/2020
				6/10/2020
<i>A. taxiformis</i>	La Ciotat (France)	43.09583	5.36220	5/2/2021
				23/03/21
				9/6/2021
				26/02/2020
				15/06/2020
				6/7/2020
				Moorea (French Polynesia)
				-17.48262
				-149.87213
				24/06/2020
<i>A. taxiformis</i>	Messina (Italy)	38.15136	15.36112	15/03/2021
				16/04/21
				29/03/2021
				Marseille (France)
				43.09583
				5.36220
				23/03/21
				9/6/2021
				24/06/2020

Supplementary Method 2

Data acquisitions were performed using Xcalibur 4.1.31.9 (Thermo Fisher Scientific). Raw data were converted to mzML files with MSconvert (version 3.0, from Proteowizard library) (S. M. Chambers et al., 2012). mzML files were uploaded and processed using the Galaxy web platform (version 3.3) (Giacomoni et al., 2015; Guitton et al., 2017). The workflow used for data pre-processing and used parameters are published on the Galaxy Workflow4Metabolomics platform at: https://workflow4metabolomics.usegalaxy.fr/u/christelle_parchemin/w/workflowparcheminalgae. Briefly, the preprocessing consisted in a chromatographic peak detection (Galaxy Version 3.12+galaxy0) using the CentWave method with a minimum and maximum peak width of 5 and 60s, and 4 successive scans with an intensity above 5E5 as limit for consideration of region of interest. The chromatographic peak detection was followed by a peak grouping using the

PeakDensity method step, a loess/non-linear “PeakGroups” retention time adjustment (degree of smoothing: 0.8), a peak filling and “CAMERA” peak annotation. A matrix of features with peak intensity, *m/z* value and retention time was generated. A clean-up based on p-values and t-stat outputs generated by the “CAMERA” step was performed in order to eliminate all features that are significantly detected in blanks. Then, an “inter/intra-batch” signal correction was applied using the “Batch correction” function with a “loess” regression model (span = 0.8) (van Der Kloet et al., 2009). This step was followed by a second clean-up according to feature's CV in pool QC injections (all features with area relative standard deviation upper than 30% through pool QC injections were eliminated from the dataset) (Thévenot et al., 2015). Finally, redundancy due to adducts and isotopes was manually eliminated (only monoisotopic mass was kept). For identification, most probable molecular formula was determined using Sirius (v4.9.15 (Dürkop et al., 2019))), MetLin database, characteristics isotopic clusters, MS/MS spectra and comparison with literature.

Supplementary Method 3

Raw data were converted to mzML files with MSconvert (version 3.0, Proteowizard) (S. M. Chambers et al., 2012). MzML files were processed in MZmine v2.53 (Pluskal et al., 2010). Mass lists were created using the mass detection module with a noise level of 5E05. The ADAP chromatogram builder module (Myers et al., 2017) was used to create peak lists with a minimum group size in # of scans 5, a group intensity threshold and min highest intensity of 4E5 and an *m/z* tolerance of 0.5 Da. The peak lists were deconvoluted using the algorithm wavelets (ADAP) with the following parameters: S/N threshold 10, minimum feature height 4E5, coefficient/area threshold 30, peak duration time 0-2.5sec, RT wavelet range (0-10sec). A spectral deconvolution was applied using the hierarchical clustering algorithms and the following parameters: 0.05 min of minimum cluster distance, 3 as minimum cluster size, 100 as minimum cluster intensity, 0.02 as min edge-to-height ratio and min delta-to-height ratio, 10 as minimum sharpness and 35 for the shape-similarity tolerance to build pseudo fragmentation spectra. Finally, the peak lists were aligned using the ADAP aligner module with a minimum confidence of 0.2 a RT tolerance of 0.5 min, an *m/z* tolerance of 0.5 Da and a score threshold of 0.75 and score weight of 0.1. Most intense and compounds of interest were putatively identified using NIST MS Search 2.2 (National Institute of Standards and Technology, Gaithersburg, U.S.) and literature data.

Supplementary Methods 4: Composition of bacterial media. The quantities (in g) correspond to the preparation of 1L of medium.

	Marine Broth (MB)	Brain Heart Infusion Agar (BHIA)	Luria Broth (LB)
Reconstituted powder ^a	37.4	52	-
Yeast Extract ^b	-	-	5
Peptone ^c	-	-	10
Sea salts ^d	-	-	10
Bacteriological agar ^e	15	-	15

^aMB:Difco™ Marine Broth 2216 (Becton, Dickinson and Company, Sparks, USA); BHIA: Brain Heart Infusion Agar 70138-500G (Sigma-Aldrich®, Saint-Louis USA)

^bYeast Extract 70161-500G (Fluka Analytical, Sigma-Aldrich®, Saint-Louis USA)

^cPeptone from casein, pancreatic digest 70169-500G (Fluka Analytical, Sigma-Aldrich®, Saint-Louis USA)

^dSea salts S9883-500G (Sigma Life Science, Sigma-Aldrich®, Saint-Louis USA)

^eBacteriological agar A5306-250G (Sigma-Aldrich®, Saint-Louis USA)

2.2 Supplementary figures

Figure S1: 2D ^1H DQF-COSY spectrum of a representative polar extract of *A. taxiformis*.

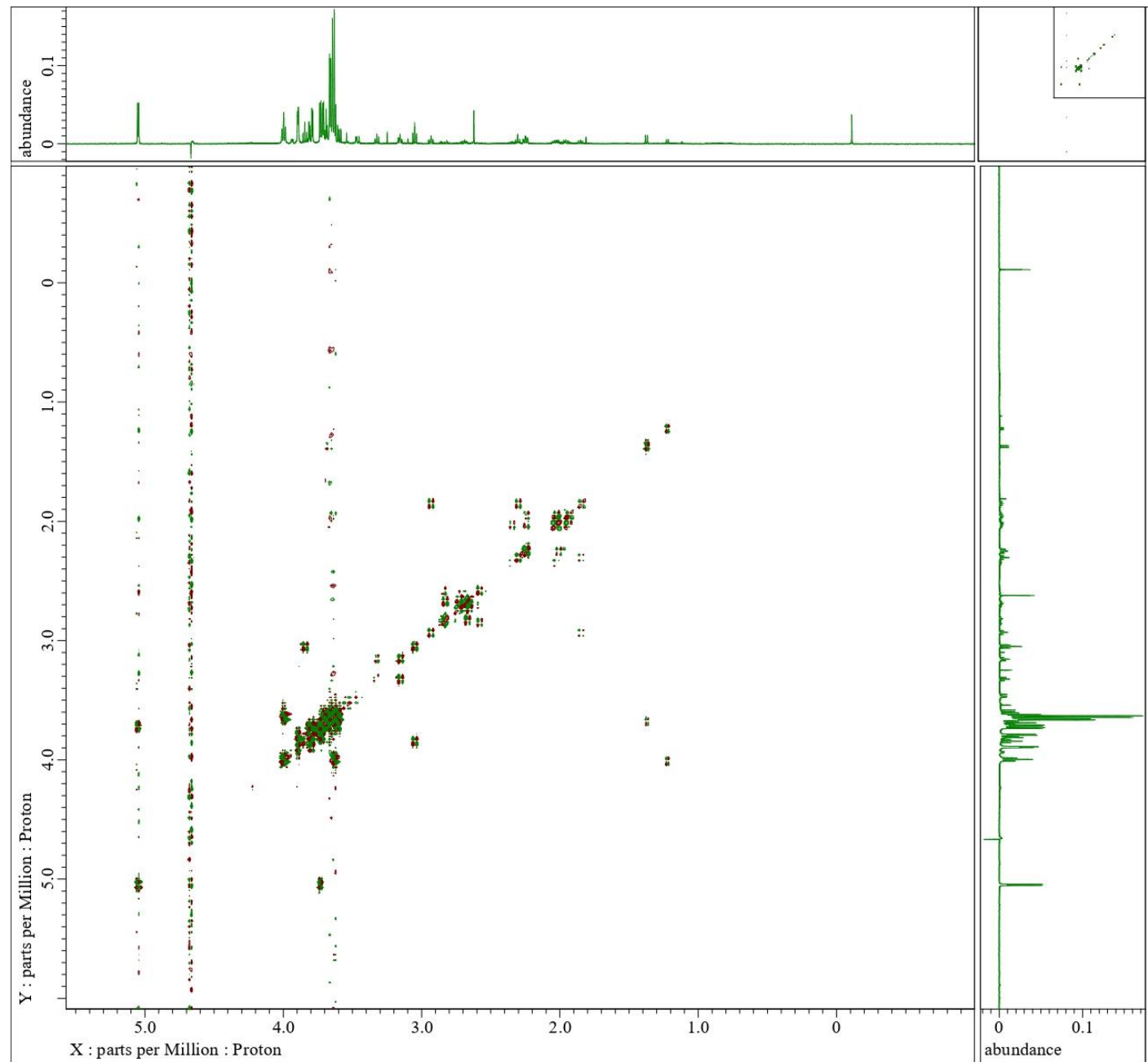


Figure S2: 2D ^1H DQF-COSY spectrum of a representative polar extract of *A. armata*

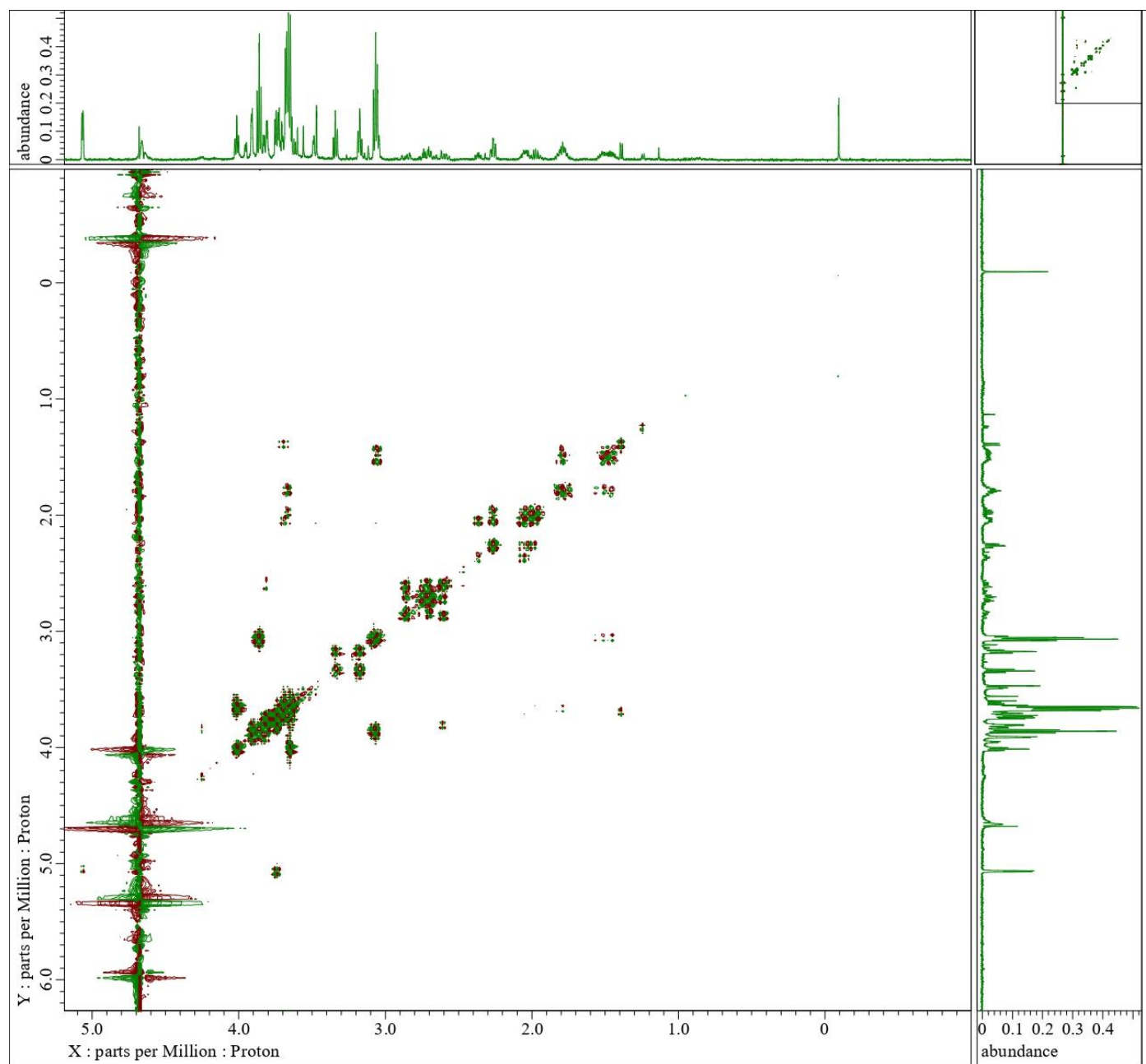


Figure S3: Detailed putative annotation of ^1H -NMR spectra of polar extracts of *A. armata* and *A. taxiformis* (representative spectrum from each species is overlaid). Annotation was performed with Chenomx profiler v9.02 and comparison of chemical shifts with literature data. Spectra were separated in three, top right: Amino acids regions, top left : Carbohydrates regions, bottom left : Aromatic region. The number in brackets refers to the annotated peaks on Fig1.B

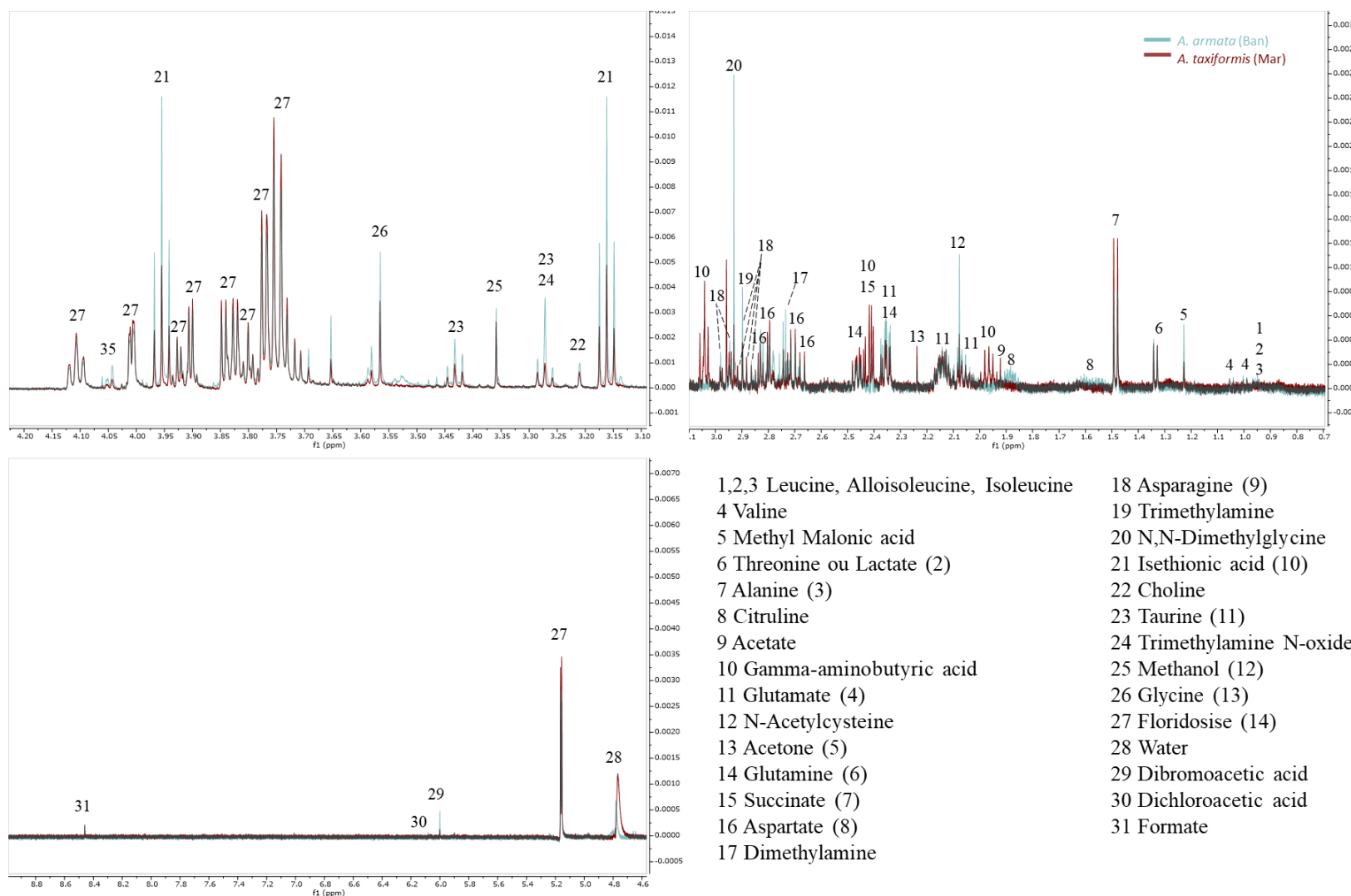


Figure S4: Hierarchical clustering analysis dendrogram of *Asparagopsis armata* and *Asparagopsis taxiformis* metabolome from different sites analysed in UHPLC-ESI—HRMS/MS (distance measure: Euclidean, clustering algorithm: Ward)

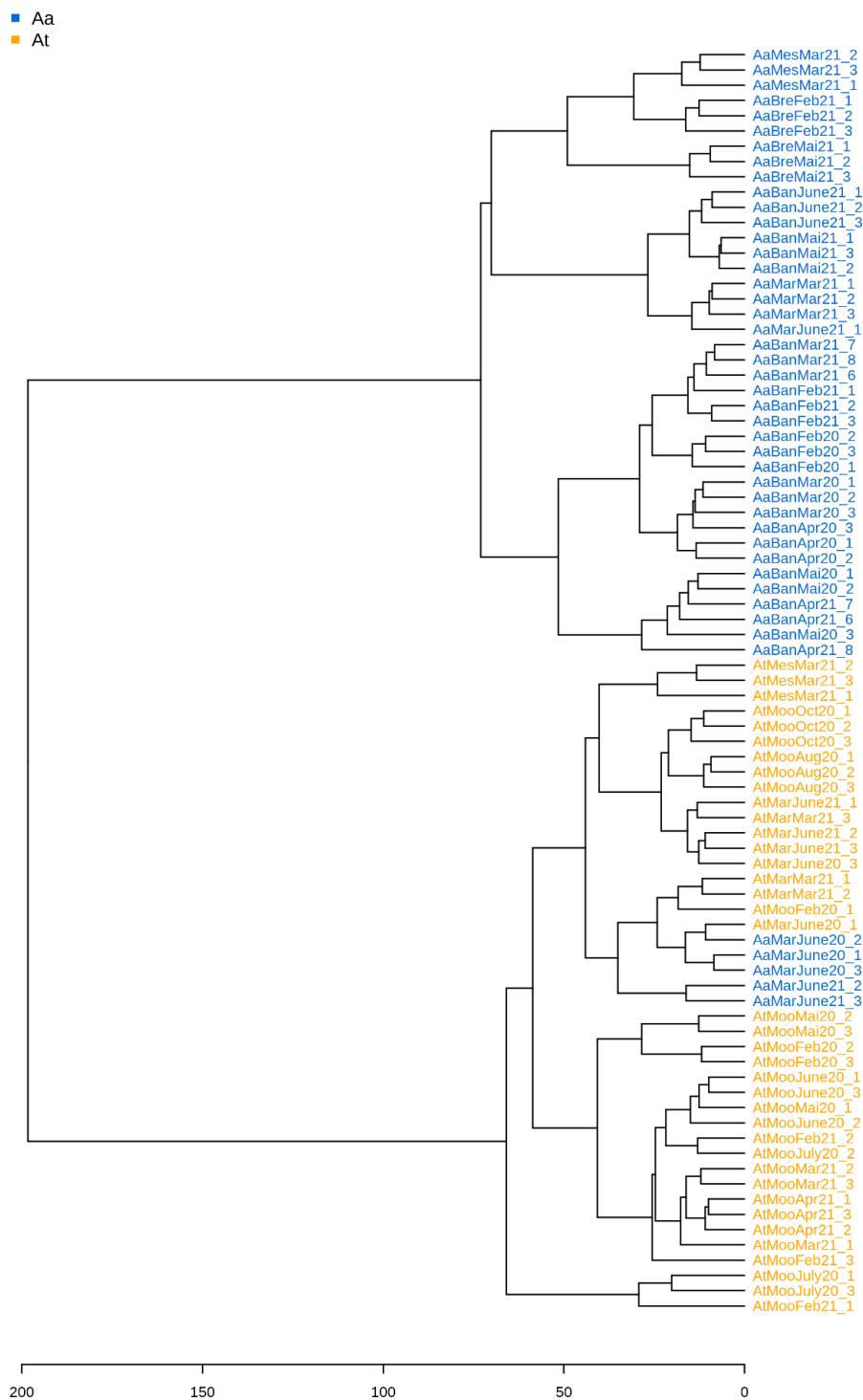


Figure S5: Hierarchical clustering analysis dendrogram of *Asparagopsis armata* and *Asparagopsis taxiformis* metabolome from different sites analysed in ^1H -NMR (distance measure: Euclidean, clustering algorithm: Ward)

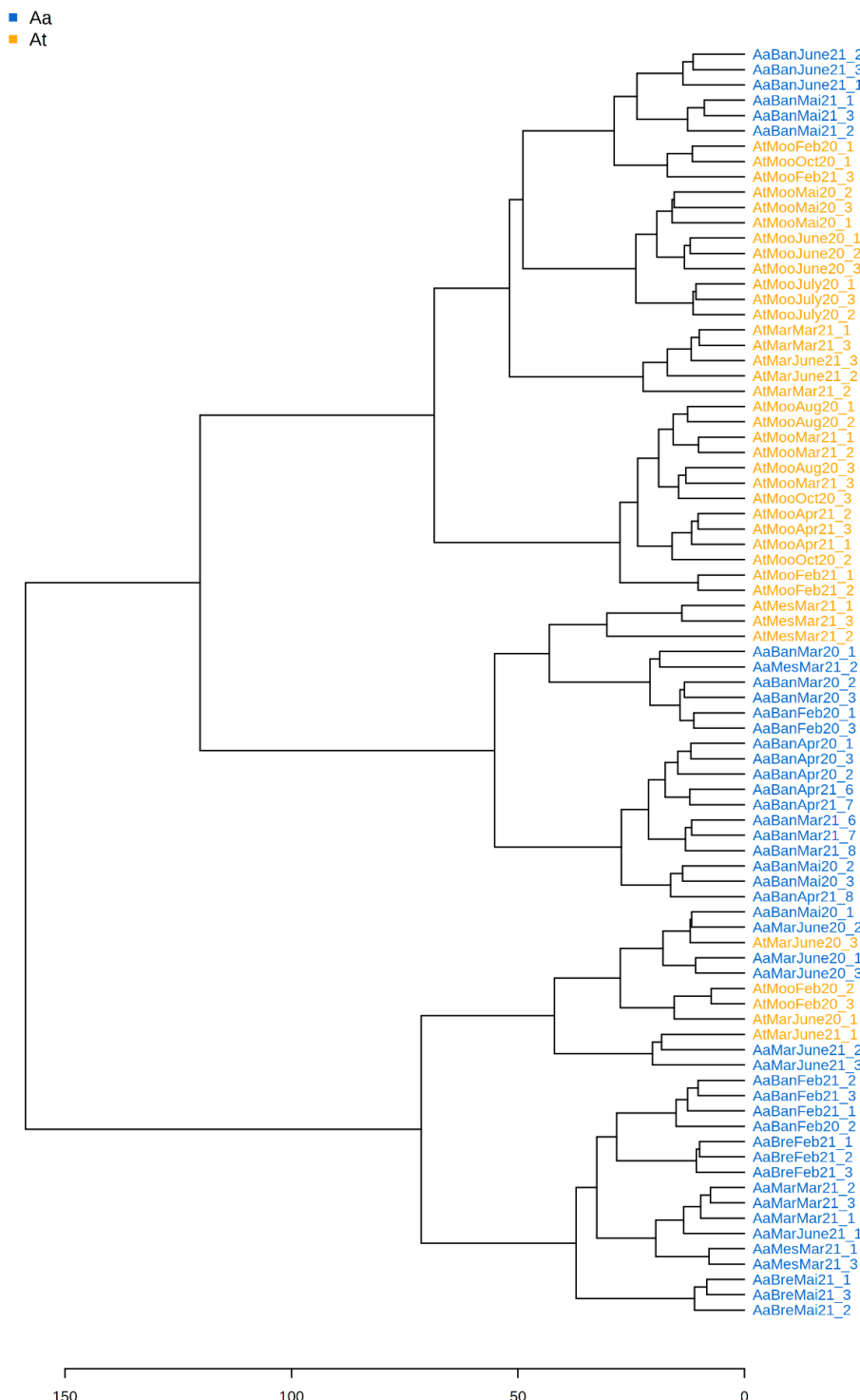


Figure S6: Hierarchical clustering analysis dendrogram of *Asparagopsis armata* and *Asparagopsis taxiformis* metabolome from different sites analysed in HS-SPME-GC-MS (distance measure: Euclidean, clustering algorithm: Ward)

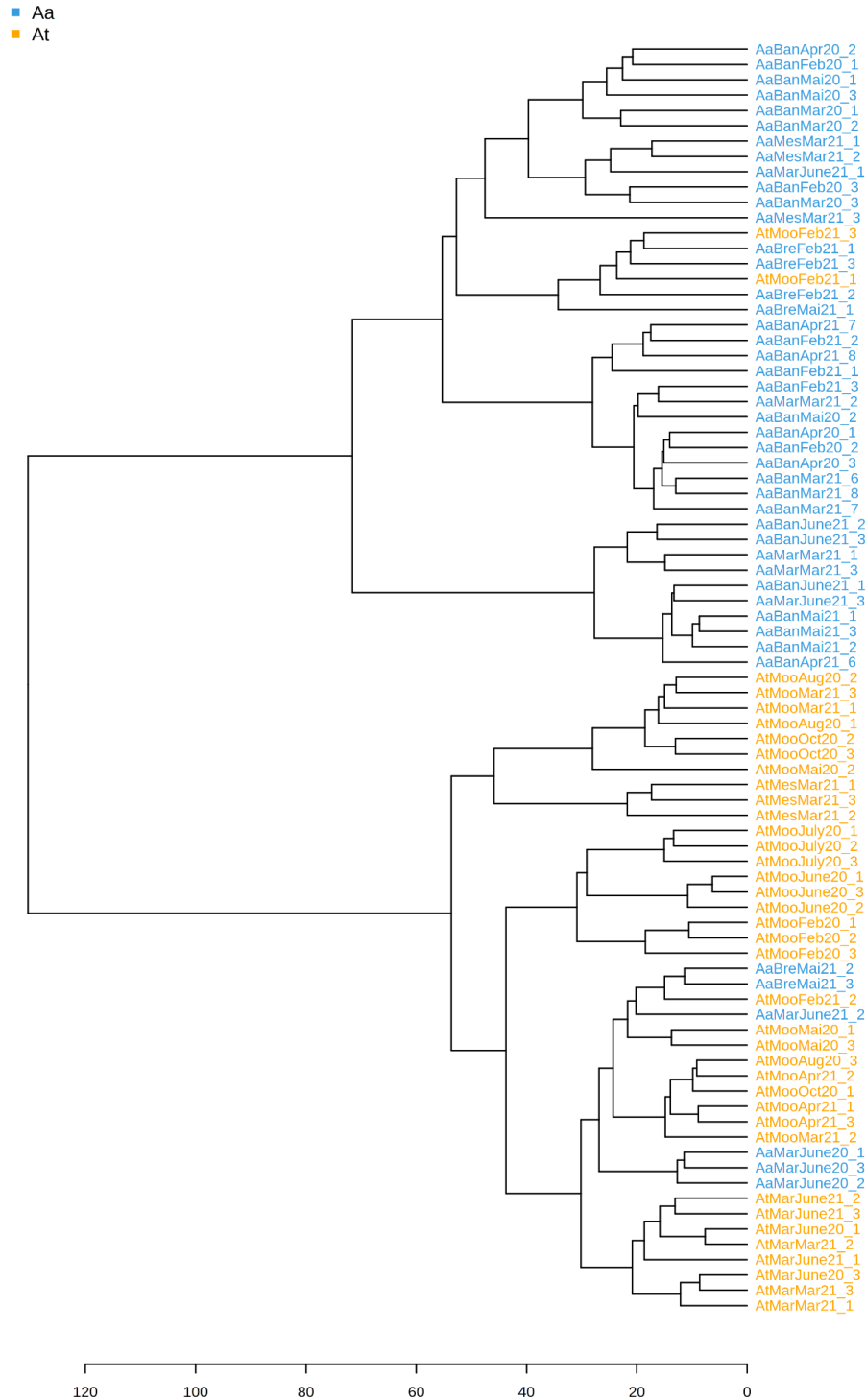


Figure S7: Hierarchical clustering analysis dendrogram of the multiblock matrix of *Asparagopsis armata* and *Asparagopsis taxiformis* metabolome from different sites (distance measure: Euclidean, clustering algorithm: Ward)

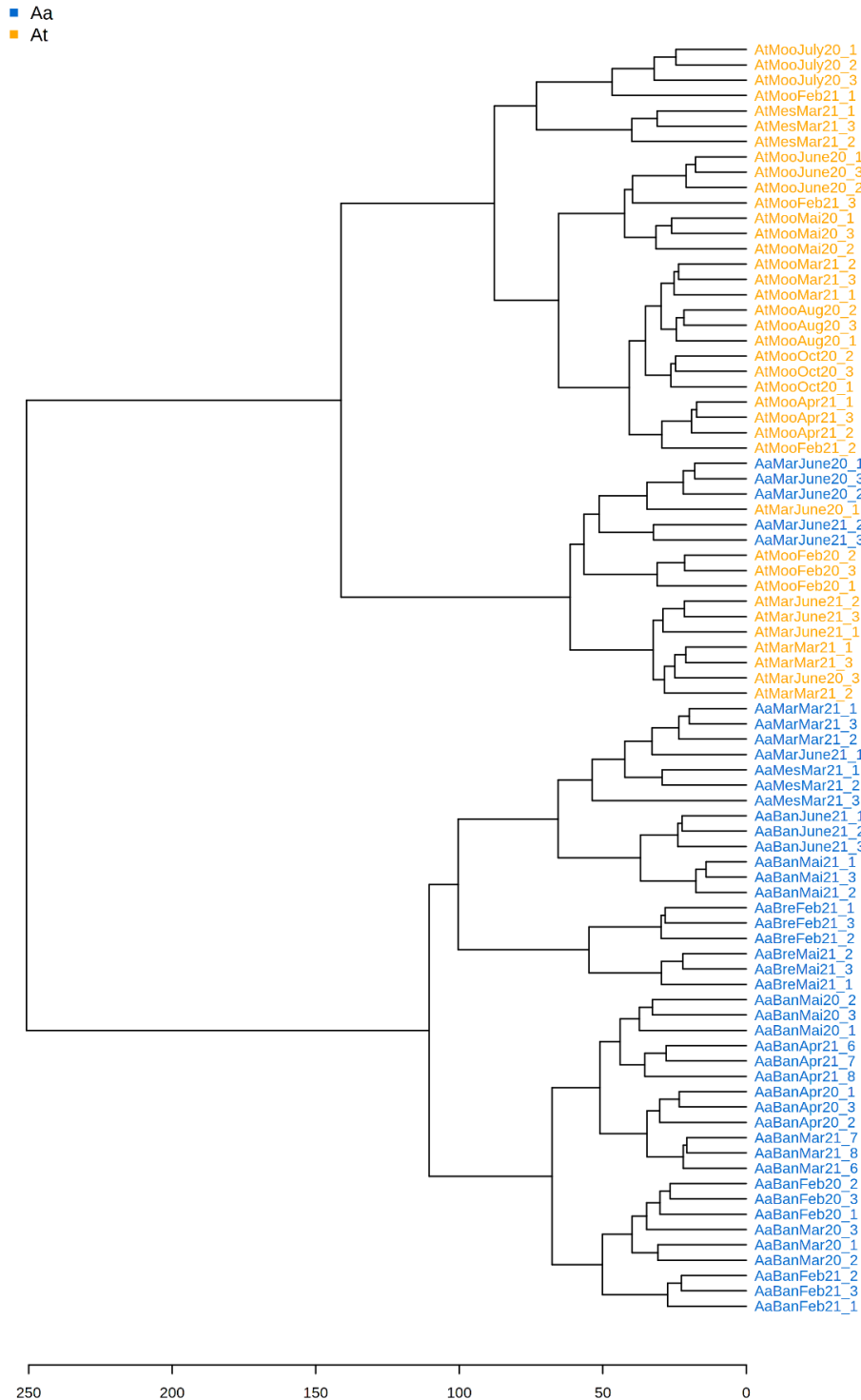


Figure S8: Scores plot of Partial Least-Squares-Discriminant Analysis (PLS-DA) of *A. armata* (Aa in blue) and *A. taxiformis* (At in orange) metabolome profiles obtained with the three different analytic methods : (a) LC-MS, (b) NMR, (c) GC-MS . CER = Mean classification error rate with p-value after double cross model validation.

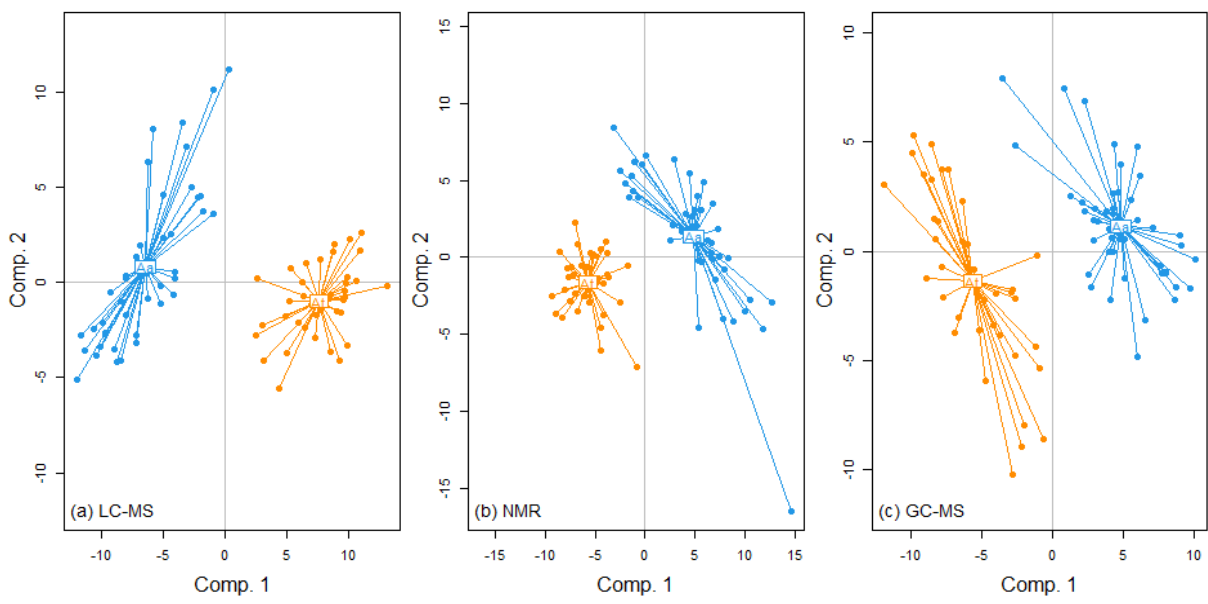


Figure S9: ESI-MS/MS spectrum of the VIP “M737T1066” with a m/z of 737.4503 [M-H] $^-$ and the possible fragmentation pattern

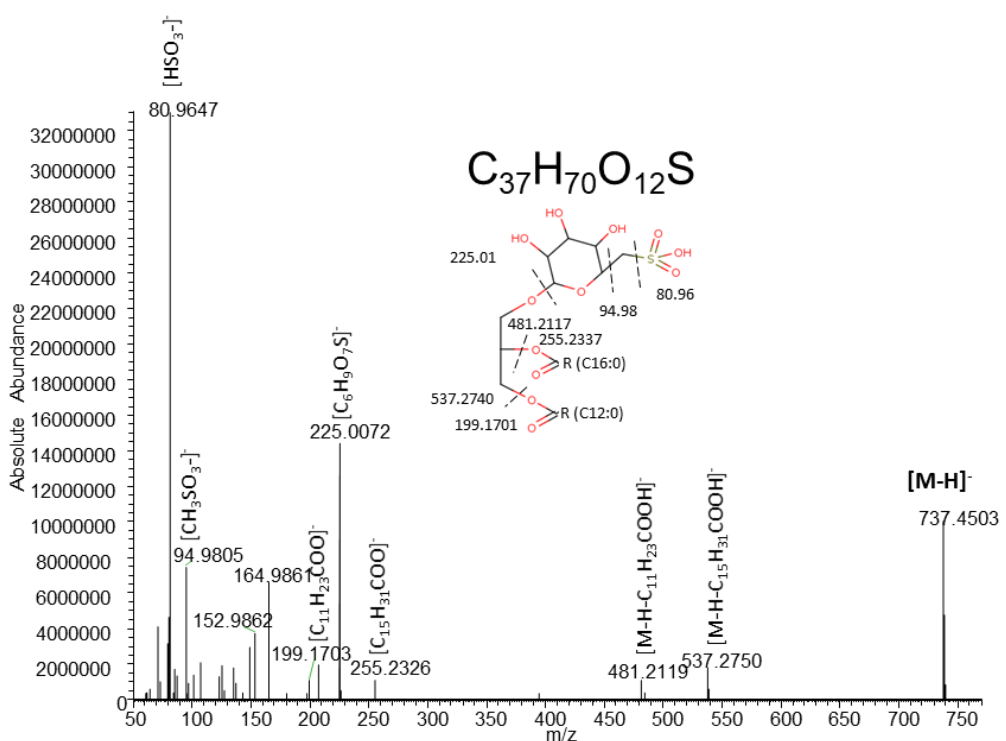


Figure S10: Hierarchical clustering analysis dendrogram of *Asparagopsis armata* metabolome sampled in Banyuls analysed in UHPLC-ESI—HRMS/MS (distance measure: Euclidean, clustering algorithm: Ward)

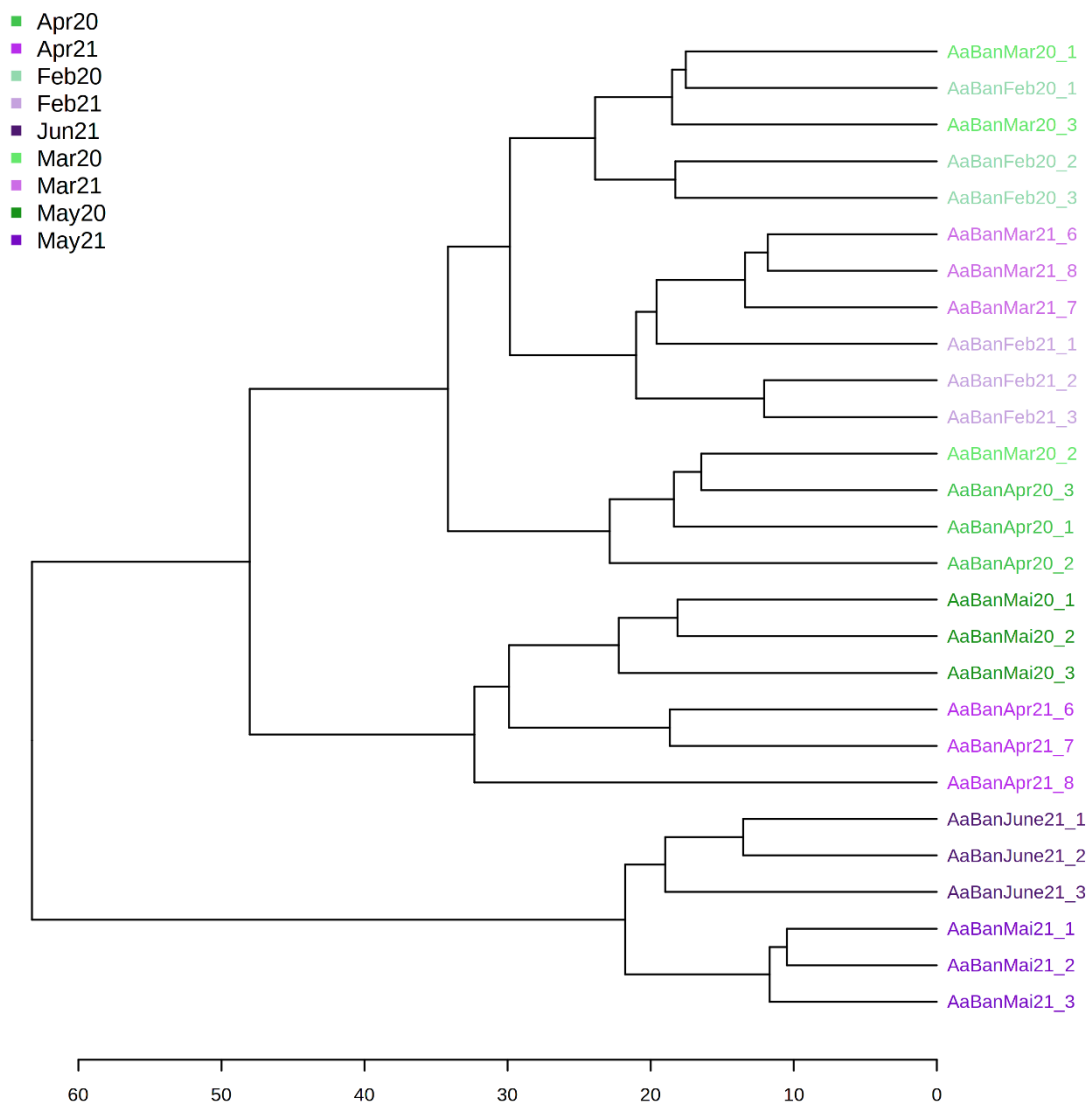


Figure S11: Hierarchical clustering analysis dendrogram of *Asparagopsis armata* metabolome sampled in Banyuls analysed in ^1H -NMR (distance measure: Euclidean, clustering algorithm: Ward)

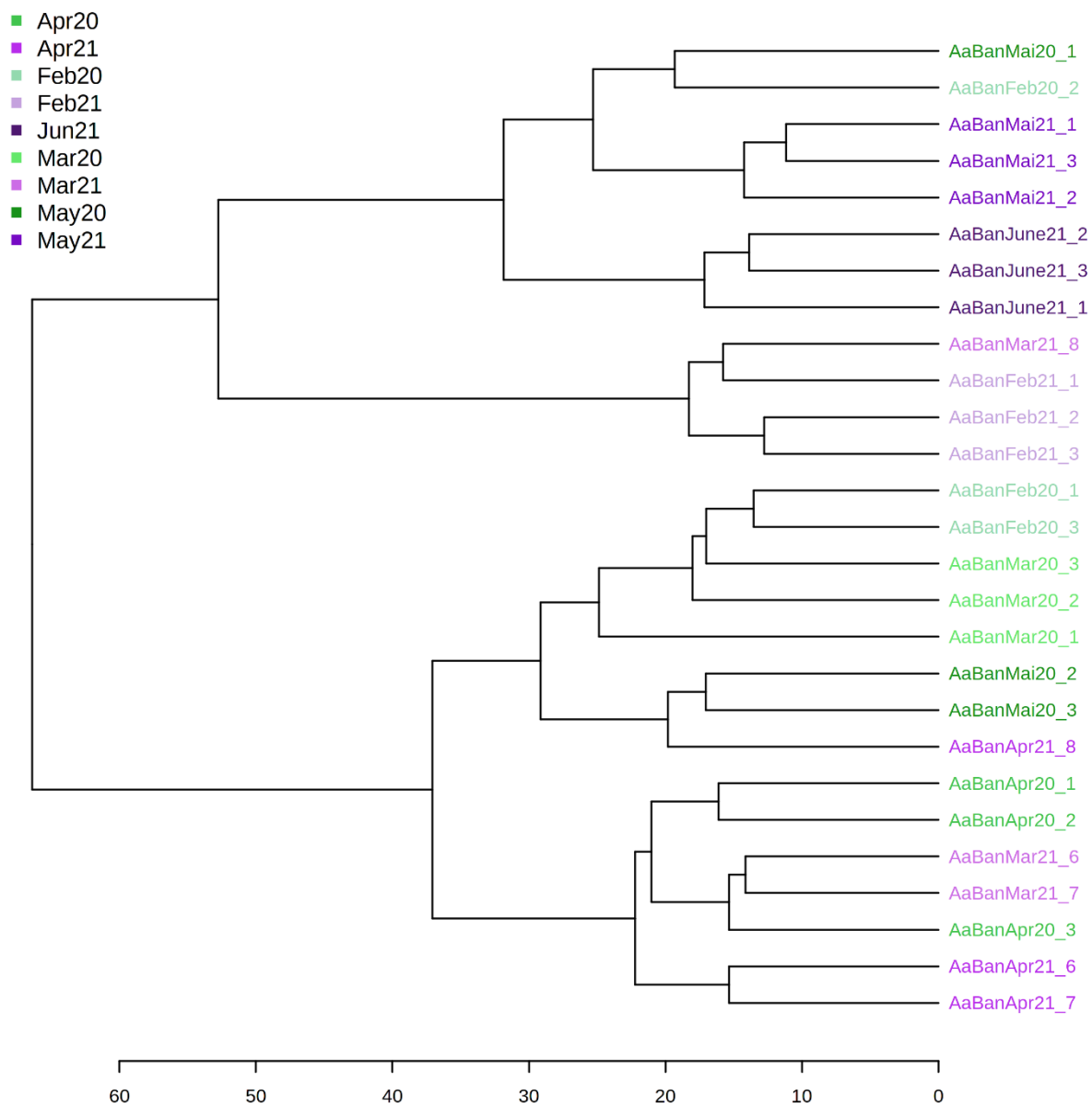


Figure S12: Hierarchical clustering analysis dendrogram of *Asparagopsis armata* metabolome sampled in Banyuls analysed in HS-SPME-GC-MS (distance measure: Euclidean, clustering algorithm: Ward)

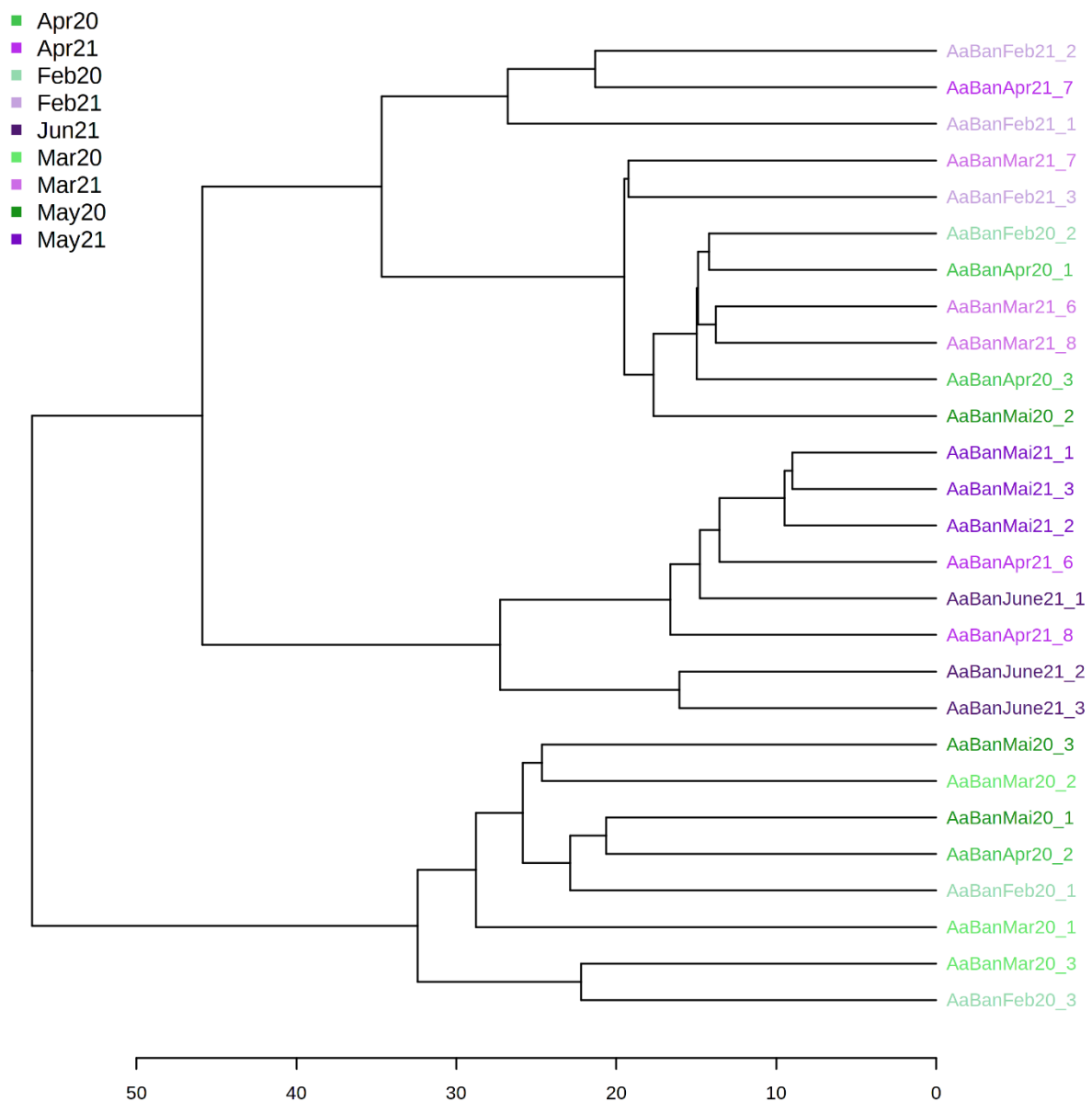


Figure S13: Hierarchical clustering analysis dendrogram of the multiblock matrix of *Asparagopsis armata* metabolome sampled in Banyuls (distance measure: Euclidean, clustering algorithm: Ward)

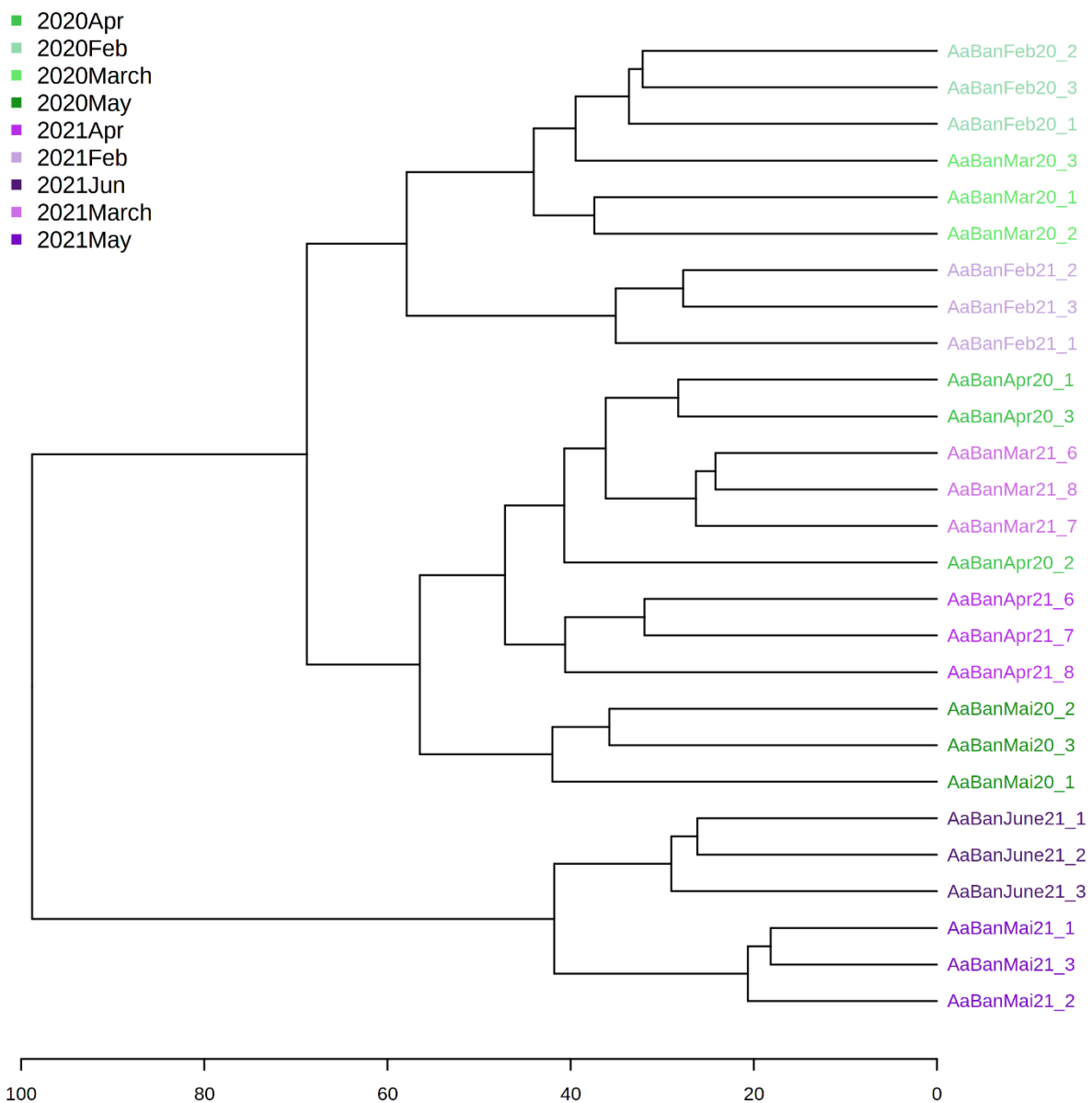


Figure S14: Hierarchical clustering analysis dendrogram of *Asparagopsis taxiformis* metabolome sampled in Moorea analysed in UHPLC-ESI—HRMS/MS (distance measure: Euclidean, clustering algorithm: Ward)

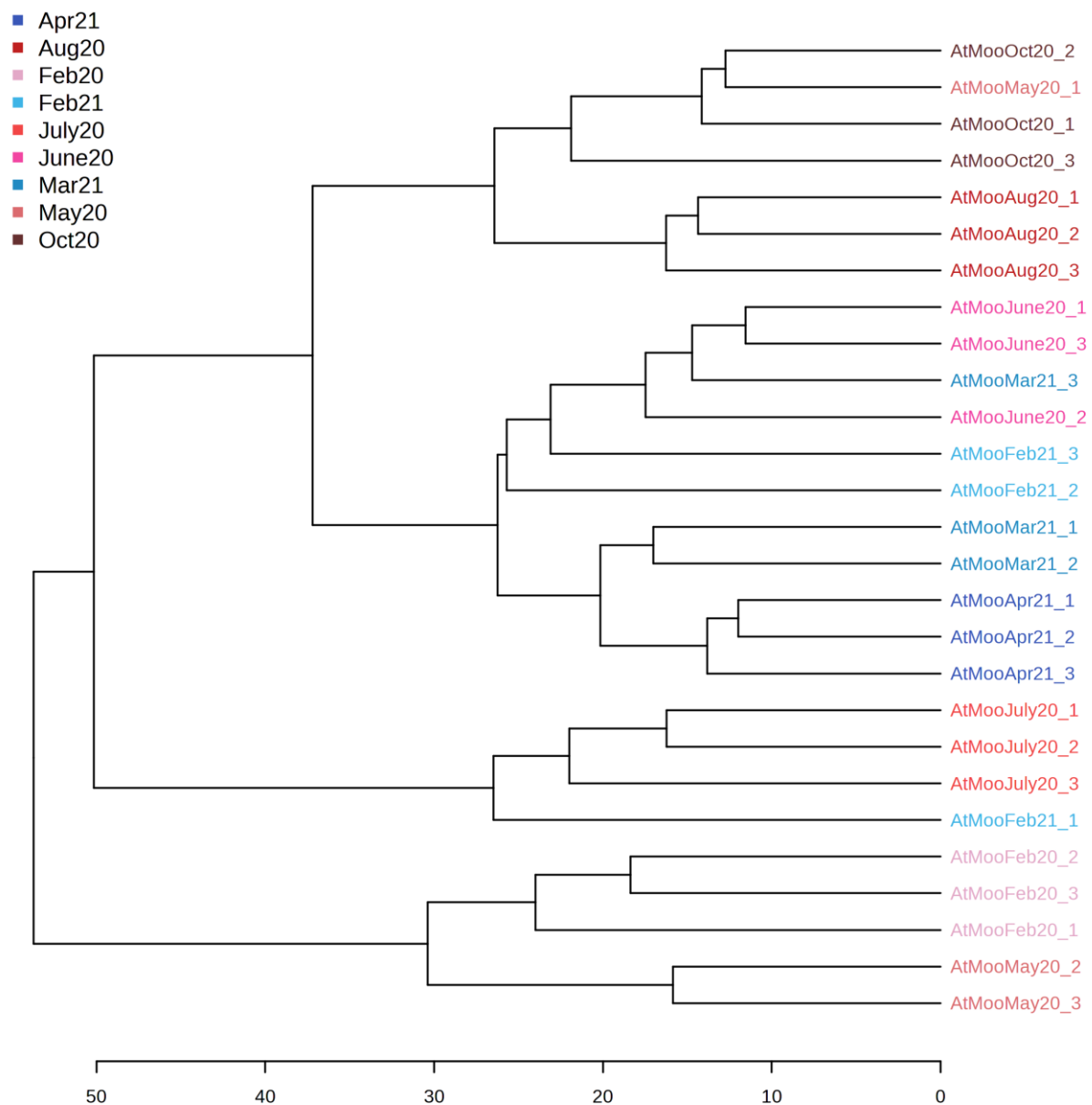


Figure S15: Hierarchical clustering analysis dendrogram of *Asparagopsis taxiformis* metabolome sampled in Moorea analysed in ^1H -NMR (distance measure: Euclidean, clustering algorithm: Ward)

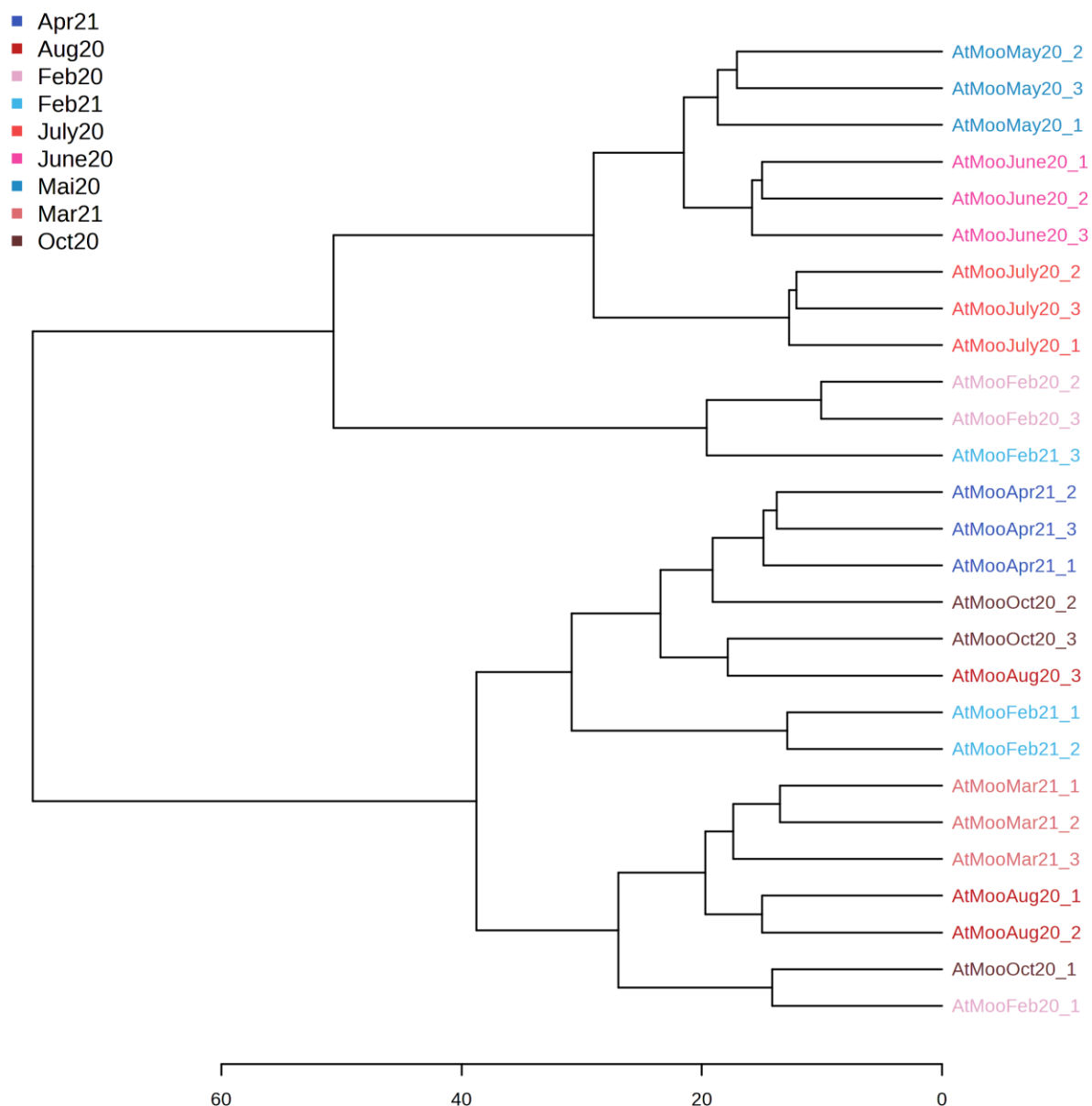


Figure S16: Hierarchical clustering analysis dendrogram of *Asparagopsis taxiformis* metabolome sampled in Moorea analysed in HS-SPME-GC-MS (distance measure: Euclidean, clustering algorithm: Ward)

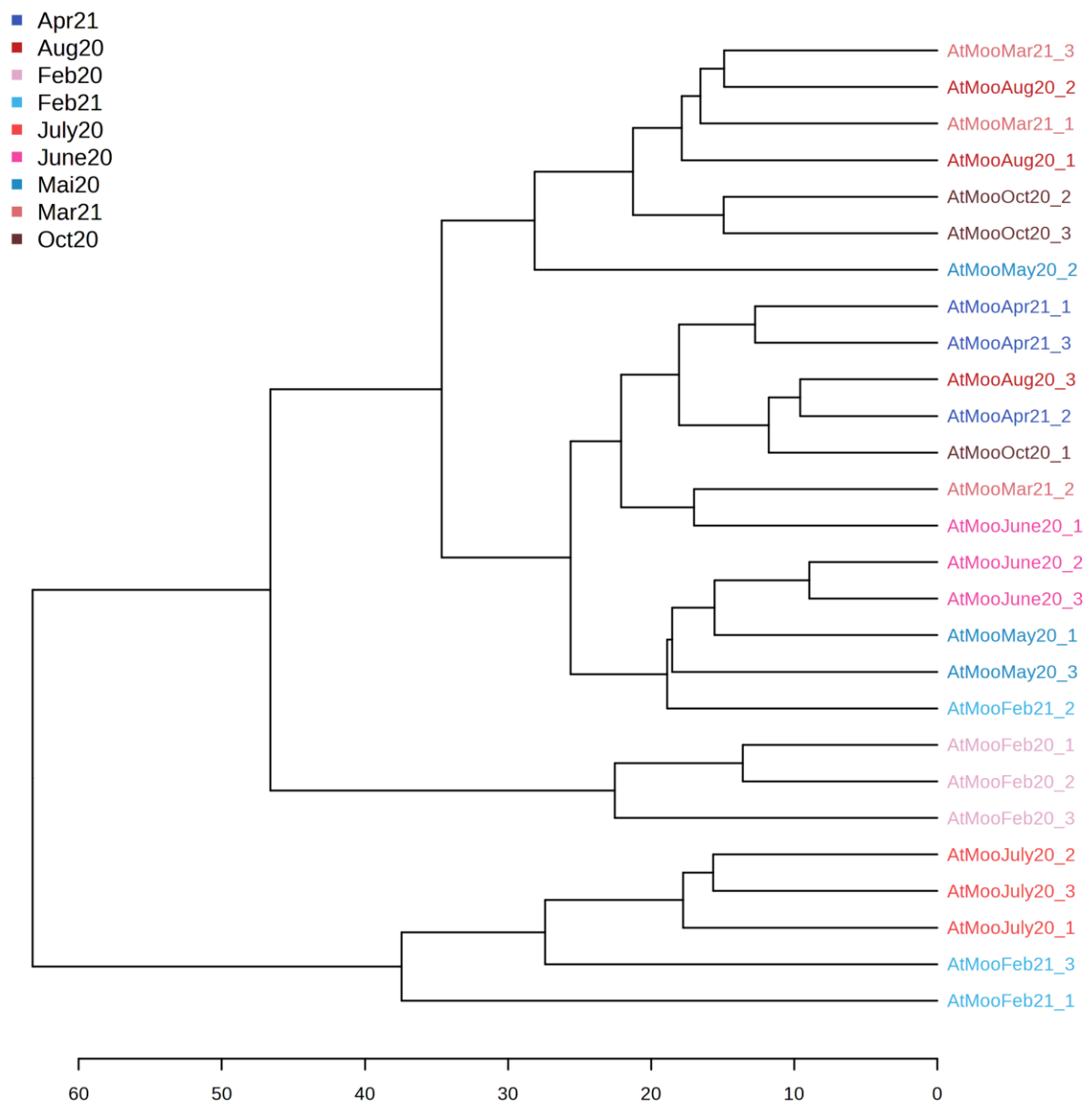


Figure S17: Heat Map of *Asparagopsis armata* metabolites intensity from February on the left to June on the right. Euclidian distance, no clustering, only top 30 VIP features based on PLS-DA model are shown. Features of the same group or molecule are framed. Arrows represent the global temporal intensity pattern

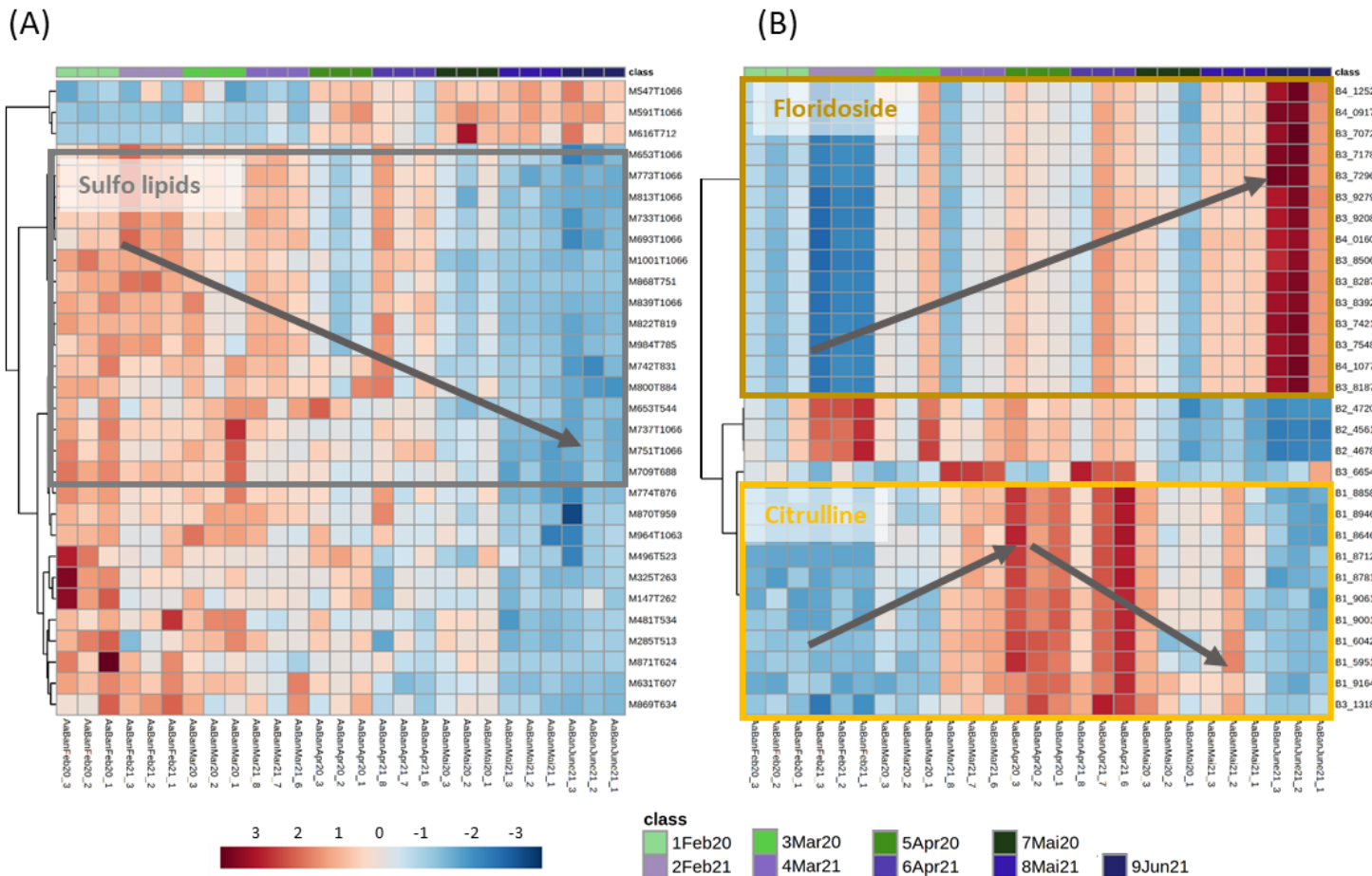
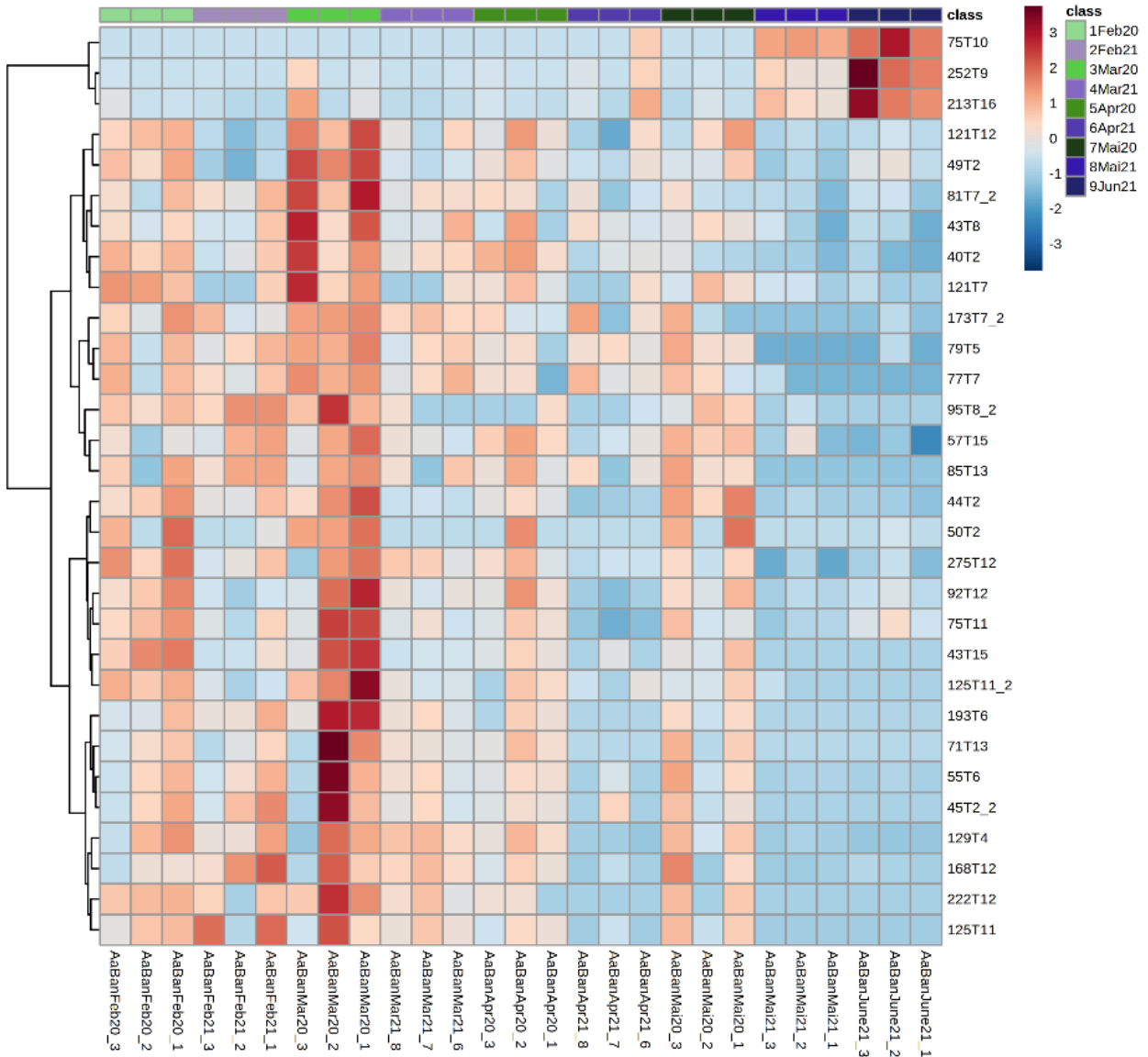


Figure S18: Heat Map of *Asparagopsis armata* metabolites intensity from February on the left to June on the right collected in 2020 and 2021 in Banyuls analysed with HS-SPME-GC-MS. Euclidian distance, no clustering, only top 30 features based on PLS-DA analysis are shown.



2.3 Supplementary tables

Table S1: Putative identification of most intense ions from the apolar phase of a pooled QC analysed by UHPLC-ESI-HRMS/MS. Abbreviations: Rt for Retention time; SQDG: sulfoquinovosyldiacylglycerol.

Monoisotopic (m/z)	Rt (min)	Calculated MF	Putative identification ^{a,b}	Sirius score	Isotope Score	Tree Score	Mass error (ppm)
214.835	1.32	C ₂ H ₂ Br ₂ O ₂	Dibromoacetic acid (1)	98.15	0	10.03	2.99
262.8211	1.99	C ₂ H ₂ BrIO ₂	Bromoiodoacetic acid	65.97	0	21.3	2.32
226.8351	3.39	C ₃ H ₂ Br ₂ O ₂	Dibromoacrylic acid (2)	99.73	0	13.9	3.27
256.8459	4.27	C ₄ H ₄ Br ₂ O ₃	(3)	89.97	0	9.34	3.80
192.8788	5.13	C ₃ H ₂ Cl ₄ O	Tetrachloroacetone (4)	-	-	-	3.22
236.8285	5.40	C ₃ H ₂ BrCl ₃ O	Bromo trichloroactone (5)	-	-	-	3.53
280.7778	5.66	C ₃ H ₂ Br ₂ Cl ₂ O	Dibromo dichloroacetone (6)	-	-	-	2.32
324.7276	5.98	C ₃ H ₂ Br ₃ ClO	Tribromo chloroacetone (7)	-	-	-	2.98
368.6771	6.45	C ₃ H ₂ Br ₄ O	Tetrabromoacetone (8)	99.9	0	6.7	2.66
396.6717	6.76	C ₄ H ₂ Br ₄ O ₂	Tetrabromobutane dione (9)	-	-	-	1.69
488.5982	7.00	C ₅ H ₃ Br ₅ O ₂	-	-	-	-	2.06
259.1913	7.90	C ₁₄ H ₂₈ O ₄	Ipurolic acid	100	5.2	47.9	1.31
294.0095	8.44	C ₁₄ H ₁₁ Cl ₂ NO ₂	Diclofenac (internal standard) (10)	-	-	-	2.09
566.5085	8.70	C ₅ H ₂ Br ₆ O ₂	(11)	-	-	-	1.40
287.223	8.85	C ₁₆ H ₃₂ O ₄	Dihydroxypalmitic acid (12)	100	5.7	49.4	2.57
267.1969	9.03	C ₁₆ H ₂₈ O ₃	Hexadecenoic acid	100	3.5	28.9	3.19
313.2385	9.22	C ₁₈ H ₃₄ O ₄	Octadecanedioic acid (13)	100	5.6	37.3	1.88
537.3287	9.44	C ₂₆ H ₅₀ O ₁₁	(14)	99.9	5.9	35.9	2.21
243.1965	9.57	C ₁₄ H ₂₈ O ₃	Hydroxymyristic acid (15)	100	3.5	23.3	1.86
446.5872	10.20	C ₅ Br ₈ O ₂	(Fragments of the molecular ion) (16)	-	-	-	1.28
271.2277	10.47	C ₁₆ H ₃₂ O ₃	Hydroxyhexadecanoic acid (17)	100	5.4	23	1.30
297.2434	10.67	C ₁₈ H ₃₄ O ₃	Rinoleic acid (18)	100	5.5	17.7	1.36
477.3041	11.77	C ₂₈ H ₄₆ O ₄ S	Methylene cholesterol sulfate (19)	-	-	-	0.46
773.5425	14.61	C ₄₂ H ₇₈ O ₁₂	-	99.9	8.3	36.36	1.25
769.5477	14.84	C ₄₃ H ₇₈ O ₁₁	-	99.9	8.6	75.3	1.41
801.5740	15.97	C ₄₄ H ₈₂ O ₁₂	-	93.7	0	41.3	1.46
737.4521	17.77	C ₃₇ H ₇₀ O ₁₂ S	SQDG type (20)	90.4	7.5	34.9	1.49
839.4991	17.77	C ₄₅ H ₇₆ O ₁₂ S	SQDG type	52.34	7.59	29.96	1.37
465.3136	17.90	C ₂₇ H ₄₇ O ₄ P	Cholesterol phosphate	28.6	6.3	15.2	0.44

^aIdentification after Sirius (v4.9.15) or manual interpretation of MS/MS spectra

^bThe number in brackets refers to the annotated peaks on **Fig1.A**

Table S2: List of putative identification of volatile compounds of a pooled QC analysed by HS-SPME-GC-MS. Abbreviations are Rt for Retention time, SI for Similarity index, RSI for Reversed Search Index, Prob for Probability.

Rt (min)	Putative identity ^{a,b}	SI	RSI	Prob (%)	Molecular Formula
1.74	Chloroacetaldehyde	737	756	89.3	C ₂ H ₃ ClO
2.79	Bromochloroacetaldehyde	892	904	94.42	C ₂ H ₂ BrClO
3.69	Chlorodibromomethane	876	916	72.76	CHBr ₂ Cl
3.91	Dibromoacetaldehyde (1)	866	900	85.32	C ₂ H ₂ Br ₂ O
4.99	1,3-Dichloroacetone	704	822	97.52	C ₃ H ₄ Cl ₂ O
5.15	Bromoform (2)	908	908	91.52	CHBr ₃
6.39	1,1,3-Trichloro-2-Propanone (3)	947	952	95.5	C ₃ H ₃ ClO
7.62	1,1,3,3-Tetrachloro-2-Propanone (4)	886	888	98.6	C ₂ H ₂ Cl ₄ O
7.93	3-Amino-2,5-dichlorobenzoic acid (5)	727	979	76.81	C ₇ H ₅ ClNO ₂
8.13	Carbon Tetrabromide (6)	953	960	97.97	CBr ₄
9.39	1,1-Dibromo-3-chloropropanone (7)	831	863	98.49	C ₃ H ₅ Br ₂ Cl
10.13	Methyl tribromoacetate (8)	910	953	98.44	C ₃ H ₃ Br ₃ O ₂
10.54	1,1-Dibromo-3,3-dichloropropanone (9)	819	866	88.64	C ₃ H ₂ Br ₂ Cl ₂ O
10.62	1,1,3-Tribromoacetone (10)	758	873	98.49	C ₃ H ₃ Br ₃ O
11.27	Triiodomethane (11)	777	856	96.87	CHI ₃
11.97	1,1,3-Tribromo-3-chloropropanone (12)	841	850	96.82	C ₃ H ₂ Br ₃ ClO
12.09	3,3-Dibromo-2-methylprop-2-enoic acid (13)	729	787	85.57	C ₄ H ₄ Br ₂ O ₂
13.28	1,1,3,3-Tetrabromoacetone (14)	808	821	85.58	C ₃ H ₂ Br ₄ O
13.41	Benzoic acid-2,2 bromoethyl – methoxy (15)	810	920	80.54	C ₁₄ H ₁₁ BrO ₃

^aIdentification using NIST MS Search 2.2 library

^bThe number in brackets refers to the annotated peaks on Fig1.C

Table S3: Top VIPs features for the intraspecific discrimination from the LC-MS analysis (after redundancy elimination) of *A. armata* and *A. taxiformis* apolar extracts. Abbreviations are: Rt for Retention time, FA chain.

Code	Rt (min)	Monoisotopic <i>m/z</i>	VIP Score	Mean Peak Area At ^a	Mean Peak Area Aa ^a	Ratio ^b	Molecular formula ^c	Mass error (ppm)	Sirius Score	Isotope Score	Tree Score	Br or Cl number ^d	MSMS fragments ^e	FA chain
M1001T1066	17.77	1001.3713	1.423	2.15E+07	4.15E+07	1.93			-	-	-		80.9649; 126.9052; 225.0078; 537.2738; 837.4833; 873.4612	
M129T69	1.14	128.8937	1.2822	2.06E+06	1.98E+07	9.62			-	-	-	Cl ₂		
M183T426	7.1	183.1028	1.4207	3.28E+05	6.68E+06	20.35	C ₁₀ H ₁₆ O ₃	3.56	-	-	-		139.1127; 182.8249	
M215T79	1.32	214.835	1.4061	6.42E+07	1.98E+08	3.09	C ₂ H ₂ Br ₂ O ₂	2.99	98.15	0	10.03		78.9184; 170.8449	
M219T91	1.52	218.8717	1.3584	1.93E+06	2.87E+07	14.88	C ₂ H ₂ ClO ₂	3.17	33.74	0	13.8			
M223T379	6.32	220.8739	1.5136	5.60E+06	1.33E+08	23.72			-	-	-	BrCl ₂		
M223T407	6.78	223.1011	1.27	7.57E+05	7.74E+06	10.22			-	-	-			
M241T496	8.27	236.7556	1.6654	1.80E+07	7.75E+05	23.22			-	-	-	Br ₃		
M247T392	6.53	246.9264	1.6058	2.60E+07	4.58E+06	5.67	C ₇ H ₅ IO ₂	3.12	-	-	-		112.9856; 126.9049; 246.9259	
M267T386	6.43	264.8233	1.562	2.01E+06	4.67E+07	23.25	C ₄ H ₂ BrCl ₃ O ₂	2.73	-	-	-		78.9184; 238.8348	
M273T504	8.4	273.2071	1.3723	1.02E+07	2.78E+06	3.65	C ₁₅ H ₃₀ O ₄	1.79	-	-	-		227.2016; 273.2069	
M287T492	8.2	286.8334	1.2755	2.54E+07	6.24E+07	2.46			-	-	-	Br ₂	78.9184; 258.8432; 286.8386	
M288T555	9.24	287.2228	1.3627	3.41E+06	1.28E+06	2.66	C ₁₆ H ₃₂ O ₄	1.88	100	3.7	44.3		241.2173; 287.2226	
M311T392	6.53	308.773	1.4557	8.95E+06	1.35E+06	6.65	C ₄ H ₂ Br ₂ Cl ₂ O ₂	3.03	49.98	0	6.4	Cl ₂ Br ₂	78.9184	
M327T475	7.92	327.1792	1.466	1.65E+06	4.71E+07	28.45			-	-	-			
M355T531	8.85	355.2107	1.5462	1.37E+07	5.13E+06	2.67			-	-	-			
M362T553	9.22	362.2372	1.3527	9.91E+05	3.04E+05	3.26	C ₁₈ H ₃₇ NO ₄ S	1.84	7.02	0	1.2		80.9648; 293.1791; 362.2371	
M368T679	11.32	368.3169	1.3034	1.19E+07	2.30E+06	5.18	C ₂₂ H ₄₃ NO ₃	1.10	100	5.3	16.3			
M373T456	7.6	372.8233	1.5566	4.61E+06	1.87E+06	2.47	C ₇ H ₄ I ₂ O ₂	2.75	-	-	-		126.9050; 372.8227	
M449T515	8.58	444.6481	1.5116	2.88E+06	2.04E+07	7.06			-	-	-			
M451T381	6.35	446.5873	1.7013	1.37E+07	5.04E+06	2.72	C ₃ HBr ₅ O	1.50	-	-	-	Br ₅	78.9184; 238.7534	
M525T612	10.2	518.5718	2.1601	9.95E+06	1.23E+04	806.99	C ₅ HBr ₅ O ₄	0.82	-	-	-	Br ₅		
M529T514	8.56	522.5585	1.3778	1.11E+08	6.04E+07	1.84	C ₅ H ₂ Br ₅ ClO ₂	0.53	-	-	-		78.9184; 206.8037; 250.7533; 272.7952	
M537T568	9.47	537.328	1.4406	5.67E+07	2.62E+07	2.17	C ₂₆ H ₅₀ O ₁₁	0.91	99.9	5.9	24.6		255.2328	

M549T700	11.67	549.3829	1.37	5.94E+06	1.55E+07	2.61	C ₃₂ H ₅₄ O ₇	6.81	98.5	0	21.7	183.1752; 229.1807; 319.1946; 549.3831
M555T735	12.25	550.8436	1.5075	1.24E+05	1.41E+07	112.90	C ₁₅ H ₂₆ Br ₄ O ₃	0.76	-	-	-	Br ₄ 78.9184; 326.2330
M579T307	5.12	574.8419	1.4975	4.75E+06	7.53E+05	6.31			-	-	-	Br ₃ 78.9184; 235.0822; 250.7530
M605T577	9.61	605.3542	1.3492	7.01E+06	3.37E+06	2.08	C ₃₀ H ₅₄ O ₁₂	0.78	99.9	0	59.9	255.2329; 605.3540
M633T753	12.55	628.7537	1.5036	5.49E+05	1.56E+07	28.34	C ₁₅ H ₂₃ Br ₅ O ₂	0.01	-	-	-	Br ₅ 78.9184; 250.7533
M647T657	10.95	642.7333	1.6616	1.92E+05	6.43E+06	33.42			-	-	-	Br ₅
M653T1066	17.77	653.3204	1.4268	1.25E+07	2.20E+07	1.76	C ₃₀ H ₅₄ O ₁₃ S	-0.48	38.79	5.6	36	80.9649; 164.9865; 225.0078; 537.2726; 397.0814; 653.3224 C16:0, C5:1
M653T544	9.1	653.321	1.2856	4.57E+06	8.98E+06	1.97	C ₃₀ H ₅₄ O ₁₃ S	-0.48	-	-	-	
M693T1066	17.77	693.3519	1.3998	3.08E+06	8.45E+06	2.74	C ₃₃ H ₅₈ O ₁₃ S	-0.16	59.09	4.1	35	
M702T594	9.9	696.413	1.5199	1.20E+07	1.81E+03	6622.06	C ₈ HBr ₇ O ₃	-0.19	-	-	-	Br ₇ 78.9184; 421.6619
M709T688	11.47	709.42	1.556	1.34E+06	1.12E+07	8.39	C ₃₅ H ₆₆ O ₁₂ S	0.42	95.34	5.5	33.9	80.9649; 164.9865; 225.0078; 453.1025; 537.2738; 709.3486 C16:0, C10:0
M711T727	12.12	706.6649	1.6804	5.99E+05	1.63E+07	27.16	C ₁₅ H ₂₂ Br ₆ O ₂	0.98	-	-	-	Br ₆ 78.9184; 250.7533
M733T1066	17.77	733.3831	1.3628	2.15E+06	5.59E+06	2.60	C ₃₇ H ₆₆ O ₁₂ S	-49.83	-	-	-	80.9649; 164.9865; 225.0078; 477.1445; 537.2738; 733.3846 C16:0, C12:2
M737T1066	17.77	737.4513	1.8868	8.40E+07	4.36E+08	5.19	C ₃₇ H ₇₀ O ₁₂ S	0.41	88.55	7.4	26.62	80.9649; 164.9865; 225.0078; 481.2117; 537.2738 C16:0, C12:0
M746T815	13.58	745.5108	1.6105	2.68E+06	1.19E+07	4.43	C ₄₀ H ₇₄ O ₁₂	0.77	99.1	8.4	20.9	
M751T1066	17.77	751.4661	1.3584	1.17E+07	2.64E+07	2.26	C ₃₈ H ₇₂ O ₁₂ S	-0.73	64.87	7.3	37.9	80.9649; 164.9865; 225.0078; 495.2296; 537.2738; 751.4692 C16:0, C13:0
M774T876	14.6	773.5416	1.6171	1.76E+07	4.87E+07	2.76	C ₄₂ H ₇₈ O ₁₂	0.09	99.97	8.26	36.36	
M795T712	11.87	786.5709	1.3012	9.15E+04	8.31E+06	90.83			-	-	-	Br ₆
M805T1068	17.8	805.439	1.8643	9.93E+05	7.77E+06	7.83			-	-	-	80.9649; 164.9865; 225.0078; 481.2117; 537.2738; 737.4526 C16:0, C12:0

^aArea in bold indicate in which group the variable is over-expressed

^bRatio of the Mean Peak Area of the two species

^cDetermined after Sirius (v4.9.15) or manual interpretation of MS/MS spectra and isotopic amats

^dDetermined with isotopic amats

^eFor some ion, MS/MS spectra were not acquired

Table S4: Top VIPs features with score >1.5 for the intraspecific discrimination from the ^1H -NMR analysis of *A. armata* and *A. taxiformis* polar extracts.

Code	Chemical shifts	VIP Scores	Mean Peak Area At ^a	Mean Peak Area Aa ^a	Ratio ^b	Identification	Molecular Formula
B5_8972	5.90	1.93	4.99E+07	3.04E+07	1.64		
B5_4484	5.45	1.6289	6.96E+06	6.39E+05	10.90		
B4_9781	4.98	2.1322	2.15E+07	4.58E+05	46.84		
B4_9682	4.97	1.7448	4.01E+07	1.58E+07	2.54		
B4_0285	4.02	1.52	1.74E+08	8.93E+07	1.95		
B3_9347	3.93	1.7322	3.10E+08	1.15E+08	2.69		
B3_9161	3.91	1.6692	2.50E+08	1.32E+08	1.89		
B3_8913	3.89	1.5578	1.96E+08	1.23E+08	1.59		
B3_2712	3.27	2.1327	7.49E+08	1.08E+09	1.44	Taurine ^c	C ₂ H ₇ NO ₃ S
B3_1481	3.15	2.2139	6.41E+08	1.13E+09	1.76	Isethionic acid ^c	C ₂ H ₆ O ₄ S
B3_1318	3.13	2.0125	8.68E+07	1.68E+08	1.93		
B2_9316	2.93	1.875	1.27E+08	3.53E+08	2.77		
B2_7581	2.76	1.9046	4.32E+07	6.50E+07	1.51		
B2_7262	2.73	1.5653	9.02E+07	4.16E+07	2.17		
B2_0292	2.03	1.8904	6.14E+07	1.95E+07	3.15		
B1_1603	1.16	1.5948	1.21E+07	3.63E+06	3.32		

^aArea in bold indicate in which group the variable is over-expressed

^bRatio of the Mean Peak Area of the two species.

^cThese two identifications were confirmed using reference standard, thus identification confidence is level 1 following the level system in Schymanski et al. (2014) Environ. Sci. Technol. 2014, 48, 4, 2097–2098

Table S5: Top VIPs features with score >1.5 for the intraspecific discrimination from the HS-SPME-GC-MS analysis of *A. armata* and *A. taxiformis* powder. Abbreviations are Rt for Retention time, SI for Similarity index, RSI for Reversed Search Index, Prob for Probability.

Code	Rt (min)	m/z	VIP Scores	Mean Peak area At ^a	Mean Peak Area Aa ^a	Ratio ^b	Identif ^c	MF	SI	RSI	Prob (%)
346T16	15.76	345.63	2.4128	2.43E+06	1.00E-06	>1000	1,3,5-Tribromo-2-methoxybenzene	C ₇ H ₅ Br ₃ O			
275T12	11.51	274.65	2.2303	1.00E+07	1.00E-10	>1000					
97T9	8.61	97.02	2.0786	9.73E+06	2.86E+07	2.94					
77T12	12.46	76.94	2.0393	1.07E+07	5.04E+08	47.06					
201T12_2	11.97	200.75	2.0134	1.55E+08	1.48E+09	9.56	1,1,3-Tribromo-3-chloropropanone	C ₃ H ₂ Br ₃ ClO	843	854	95.62
175T11	11.20	174.81	1.9718	4.46E+07	1.90E+07	2.34					
129T11	10.62	128.84	1.9446	8.76E+07	3.98E+08	4.54	1,3-Dibromo-1,3-dichloropropanone	C ₃ H ₂ Br ₂ Cl ₂ O	763	896	92.95
50T2	1.73	49.97	1.9431	1.61E+06	1.44E+07	8.96	Chloroacetaldehyde	C ₂ H ₃ ClO	808	823	98.16
94T2	2.14	93.89	1.9414	7.29E+05	1.12E+07	15.44					
267T11	11.24	266.72	1.9222	3.70E+07	2.43E+06	15.21	Iodoform	CHI ₃			
219T9	9.32	218.74	1.8862	3.97E+07	1.02E+07	3.92	Bromodiiodomethane	CHBrI ₂			
60T7	6.76	59.99	1.8511	4.76E+07	3.04E+07	1.56					
120T12	13.29	119.86	1.7997	2.53E+06	4.61E+08	182.02	1,1,3,3-Tetrabromoacetone	C ₅ H ₂ Br ₄ O	798	821	85.53
201T11	10.52	200.75	1.7926	7.00E+07	4.30E+08	6.15	1,1 Dibromo3,3 dichloropropanone	C ₅ H ₂ Br ₂ Cl ₂ O	823	882	89.96
173T9	9.40	172.75	1.7865	2.87E+07	2.84E+08	9.90	1,1 Dibromo-3-chloropropanone	C ₅ H ₃ Br ₂ ClO	865	913	98.44
120T11	10.58	119.86	1.7732	1.62E+07	5.51E+07	3.40	1,1,3-Tribromoacetone	C ₅ H ₃ Br ₃ O	685	902	93.67
120T12	12.24	119.87	1.7623	1.88E+06	4.32E+06	2.30					
77T11_2	10.93	76.96	1.7462	2.80E+06	7.98E+07	28.46					
201T13_2	12.94	200.75	1.7327	2.66E+08	1.30E+09	4.86					
213T12_2	12.10	212.76	1.6942	4.89E+08	9.40E+07	5.21					
121T14	13.61	120.89	1.6564	8.38E+06	4.40E+08	52.48					
251T8	8.10	250.65	1.6353	1.49E+08	6.02E+08	4.04	Carbon Tetrabromide	CBr ₄	955	958	96.67
121T11_2	10.60	120.90	1.5905	1.81E+07	6.12E+08	33.84	1,1,3-Tribromoacetone	C ₅ H ₃ Br ₃ O	685	902	93.67
198T13	13.33	197.76	1.5702	6.43E+05	3.41E+07	53.03					
127T11	11.13	126.85	1.5597	2.31E+07	6.12E+06	3.78					

^aArea in bold indicate in which group the variable is over-expressed

^bRatio of the Mean Peak Area of the two species

^cIdentification confidence of level 2 following level system in Schymanski et al. (2014) Environ. Sci. Technol. 2014, 48, 4, 2097–2098

Table S6: Putative annotation of top 30 VIPs features for the temporal discrimination from the LC-HRMS analysis of *A. armata* samples collected in Banyuls. Abbreviations are: Rt for Retention time. INC: Increase over time, DEC: Decrease over time, FA:Fatty acid

Code	Rt (min)	Monoisotopic m/z	VIP Score	Temporal pattern	Molecular formula ^a	Adducts	Sirius score	Isotope Score	Tree Score	Mass error (ppm)	MSMS fragments ^b	FA Chain
M1001T1066	17.77	1001.3713	2.0066	DEC			-	-	-		80.9649; 126.9052;225.0078;537.2738;837.4833;873.4612	C16, ?
M147T262	4.37	146.9064	1.6985	DEC	C ₃ HBrO ₂	[M-H]-	-	-	-	-12.11	78.9185	
M285T513	8.55	284.8403	1.6495	DEC	C ₅ H ₅ Br ₂ O ₄	[M-H]-	75.19	0	8.6	1.63	78.9185	
M325T263	4.39	322.7562	1.7949	DEC	C ₃ HBr ₃ O ₃	[M-H]-	-	-	-	2.37	78.9185;126.9052;180.8131;254.9070(Br2)	
M481T534	8.89	481.2577	1.6886	DEC	C ₂₃ H ₄₂ O ₈	[M+Cl]-	26.04	6.3	34.7	1.98	245.0433;253.2175;481.2556	
M496T523	8.71	488.5959	1.6447	DEC	C ₅ H ₅ Br ₂ O ₂	[M-H]-	-	-	-	-2.64	78.9185 ; 238.8353(Br2); 248.7556 (Br2)	
M547T1066	17.77	547.4031	1.6477	INC	C ₃₀ H ₆₀ O ₆ S	[M-H]-	52.14	0	20.8	-0.29	213.1862;227.2020;319.19; 333.2105;547.4042	
M591T1066	17.77	591.4293	1.9288	INC	C ₃₂ H ₆₄ O ₇ S	[M-H]-	77.57	4.6	22	-0.30	211.2068;257.2126;333.2112;349.2058;591.4304	
M616T712	11.86	616.4244	1.7638	INC			-	-	-		-	
M631T607	10.12	631.3254	2.033	DEC	C ₃₁ H ₅₃ O ₁₁ P	[M-H]-	19.74	6.4	41.5	1.03	69.0341;167.0715;253.2176;395.1117;631.3260	
M653T1066	17.77	653.3204	1.7435	DEC	C ₃₀ H ₅₄ O ₁₃ S	[M-H]-	38.79	5.6	36	-0.48	80.9649;164.9865; 225.0078; 537.2726;397.0814;653.3224	C16:0, C5:1
M653T544	9.07	653.321	1.638	DEC	C ₃₀ H ₅₄ O ₁₃ S	[M-H]-	-	-	-	-0.48	80.9649; 225.0078;400.7505; 537.2726;653.3224	C16:0, C5:1
M693T1066	17.77	693.3519	1.7486	DEC	C ₃₃ H ₅₈ O ₁₃ S	[M-H]-	59.09	4.1	35	-0.16	80.9649; 164.9865;225.0078;437.1116;537.2738;693.3535	C16:0, C8:2
M709T688	11.47	709.42	2.0703	DEC	C ₃₅ H ₆₆ O ₁₂ S	[M-H]-	95.34	5.5	33.9	0.42	80.9649; 164.9865;225.0078;453.1025;537.2738;709.3486	C16:0, C10:0
M733T1066	17.77	733.3831	1.7974	DEC	C ₃₇ H ₆₆ O ₁₂ S	[M-H]-	-	-	-	-49.83	80.9649; 164.9865;225.0078;477.1445;537.2738;733.3846	C16:0, C12:2
M737T1066	17.77	737.4513	1.9203	DEC	C ₃₇ H ₇₀ O ₁₂ S	[M-H]-	88.55	7.4	26.62	0.41	80.9649; 164.9865;225.0078;481.2117;537.2738;	C16:0, C12:0
M742T831	13.85	741.5155	1.897	DEC	C ₄ H ₄ O ₁₁	[M-H]-	99.58	8.5	65.3	0.25	75.0083;113.0245;227.2019;281.2490;741.5179	
M751T1066	17.77	751.4661	1.8234	DEC	C ₃₈ H ₇₂ O ₁₂ S	[M-H]-	64.87	7.3	37.9	-0.73	80.9649; 164.9865;225.0078;495.2296;537.2738;751.4692	C16:0, C13:0
M773T1066	17.77	773.416	1.827	DEC	C ₃₉ H ₆₆ O ₁₃ S	[M-H]-	-	-	-	1.79	80.9649;164.9865;225.0078;281.2489;517.1741;537.2738;773.4160	C16:0, C14:4
M774T876	14.6	773.5416	1.8633	DEC	C ₄₂ H ₇₈ O ₁₂	[M-H]-	99.97	8.26	36.36	0.09	227.2028;255.2341;281.2479;463.2872	
M800T884	14.73	799.5572	1.7207	DEC	C ₅₁ H ₇₆ O ₇	[M-H]-	95.71	0	42.3	7.36	227.2030;255.2341;281.2482;307.2668	
M813T1066	17.77	813.4457	1.843	DEC			-	-	-		-	
M822T819	13.65	821.542	1.847	DEC			-	-	-		255.2336;301.2177	
M839T1066	17.77	839.4979	1.9172	DEC	C ₄₅ H ₇₆ O ₁₂ S	[M-H]-	52.34	7.59	29.96	-0.06	80.9649;164.9865;225.0078;444.5057;583.2609;737.4526;839.4993	C16, C20:5
M868T751	12.52	867.526	1.885	DEC			-	-	-		-	
M869T634	10.57	869.4713	1.7158	DEC	C ₄₅ H ₇₄ O ₁₄ S	[M-H]-	-	-	-	-0.95	80.9649;164.9865;225.0078;255.2330;537.2738;615.2521;869.4726	C16, C20:6
M870T959	15.98	869.56	1.737	DEC	C ₄₇ H ₈₂ O ₁₄	[M-H]-	95.1	6.6	6	-3.05	112.9858	
M871T624	10.4	871.4872	1.6546	DEC	C ₄₅ H ₇₆ O ₁₄ S	[M-H]-	-	-	-	-0.66	80.9649; 126.9052;164.9865;225.0078;255.2330;537.2738;677.3585;871.4885	C16, C20:5
M964T1063	17.72	963.6252	1.7086	DEC	C ₅₇ H ₈₈ O ₁₂	[M-H]-	30.09	5.3	54.7	5.62	255.2340;281.2480;397.1337	
M984T785	13.08	983.5945	1.8161	DEC	C ₅₂ H ₈₈ O ₁₇	[M-H]-	99.87	9.3	207.1	0.15	255.2338;301.2165;397.1337	

^aDetermined after Sirius (v4.9.15) or manual interpretation of MS/MS spectra and isotopic amats

^bFor some ion, MS/MS spectra were not acquired

Table S7: Environmental parameters of sea water near Banyuls. NA : data not acquired due to COVID lockdown

Sampling date	Sea Temperature (°C) (daily mean)	Salinity (PSU)	pH
20/02/2020	12.9	37.22	7.93
20/03/2020	14 ^a	NA	NA
17/04/2020	15 ^a	NA	NA
18/05/2020	17.5	36.49	8.35
09/02/2021	11.8	37.64	7.93
15/03/2021	12.6	37.04	7.93
08/04/2021	13.5	37.71	8.29
12/05/21	14.4	37.89	8.22
11/06/2021	18.7	37.75	7.96

^aEstimated measurement from : <https://fr.seatemperature.net/monthly/banyuls-sur-mer-in-march-8075> and <https://fr.seatemperature.net/monthly/banyuls-sur-mer-in-april-8075>

Table S8: Daily mean sea water temperature measured at -8m (24 measurements) near Moorea.

Sampling date	Sea Temperature (°C) (daily mean)
26/02/2020	29.4
22/05/2020	28.9
15/06/2020	28.4
6/7/2020	27.8
24/08/2020	26.8
6/10/2020	27.2
5/2/2021	28.6
15/03/2021	29.2
16/04/21	28.7

Table S9: Mean, Standard deviation (SD) and Coefficient of variation (SD/mean*100) of the sea water temperature in Banyuls and Moorea.

Location	Mean (°C)	Standard deviation (SD)	Coefficient of variation (%)
Banyuls	14.5	2.3	15.7
Moorea	28.3	0.9	3.1

Table S10: Results of Mantel tests on the distance matrices of the metabolome of *A. armata* samples collected in Banyuls in 2021 and average sea water temperatures Correlation method = pearson; significance evaluated after 999 permutations of the dissimilarity matrix. Significant results are in bold.

	LC-MS		RMN		GC-MS	
	r	Significance	r	Significance	r	Significance
T (°C)	0.43	0.001	0.65	0.001	0.40	0.013

Table S11: Results of the Mantel test on the distance matrices of the metabolome of *A. taxiformis* samples collected in Moorea and average sea water temperature. Correlation method = pearson; significance evaluated after 999 permutations of the dissimilarity matrix. Significant results are in bold.

	LC-MS		RMN		GC-MS	
	r	Significance	r	Significance	r	Significance
T (°C)	0.19	0.032	0.21	0.011	0.21	0.009

Table S12: Mean diameter of bacterial inhibition of *A. armata* (Aa) and *A. taxiformis* (At) polar and apolar phases collected in Banyuls and Moorea in 2020 and 2021. The four bacteria of the assay are *Edwardsiella anguillarum* (Ea), *Vibrio anguillarum* (Va), *Pseudomonas anguilliseptica* (Pa) and *Lactococcus garvieae*. Negative and Positive controls are MeOH and Antibiotics (Erythromycine or Kanamycine depending on bacterial susceptibility).

Sp	Sampling month and year	Ea	Lg	Va	Pa
MeOH					
	For all	0.6 ^a	0.6 ^a	0.6 ^a	0.6 ^a
Antibiotics					
	Erythromycine	-	2.2 ± 0.1	-	-
	Kanamycine	1.1	0.1	1.3 ± 0.3	3.5 ± 0.6
Polar phases					
Aa	For all	0.6 ^a	0.6 ^a	0.6 ^a	0.6 ^a
At	For all	0.6 ^a	0.6 ^a	0.6 ^a	0.6 ^a
Apolar phases					
Aa	Feb 20	1.7 ± 0.1	1 ± 0.1	2.2 ± 0.2	2.9 ± 0.6
	Mar 20	1.5 ± 0	0.6 ^a ± 0.6	2.2 ± 0.2	2.3 ± 0.1
	Apr 20	1.7 ± 0	0.6 ^a ± 0.6	2.2 ± 0.2	2.5 ± 0.5
	Mai 20	1.5 ± 0.1	0.8 ± 0.1	2.3 ± 0.2	2.3 ± 0.3
	Feb 21	1.8 ± 0.1	0.8 ± 0.2	4.1 ± 0.1	3.8 ± 0.3
At	Mar 21	1.8 ± 0.1	0.9 ± 0.3	2.7 ± 0.5	3.2 ± 0.2
	Apr 21	1.5 ± 0.1	0.6 ^a ± 0.6	2.3 ± 0.2	2.5 ± 0.1
	Mai 21	1.8 ± 0.1	1 ± 0.2	2.6 ± 0.3	3 ± 0.3
	June 21	1.8 ± 0.1	0.6 ^a ± 0.6	2.6 ± 0.5	3.2 ± 0.2
	Feb 20	1.4 ± 0	1 ± 0.1	1.5 ± 0.1	1.5 ± 0.1
At	Mai 20	1.6 ± 0.1	1.1 ± 0	2.2 ± 0.3	2.2 ± 0.1
	June 2020	1.6 ± 0.1	1.1 ± 0.1	2.3 ± 0.2	3 ± 0.3
	July 20	1.5 ± 0.1	1 ± 0	2.4 ± 0.3	2.4 ± 0
	Aug 20	1.3 ± 0	1 ± 0	2 ± 0.3	1.8 ± 0
	Oct 20	1.4 ± 0	1 ± 0	1.8 ± 0.3	2.2 ± 0.2
At	Feb 21	1.5 ± 0.1	1.1 ± 0	2.4 ± 0.1	2.2 ± 0.1
	Mar 21	1.7 ± 0.1	1.1 ± 0	2.5 ± 0.2	2.9 ± 0.1
	Apr 21	1.5 ± 0.1	1.1 ± 0.1	2.3 ± 0.3	2.2 ± 0.1

^aThe reported measurements include the size of the discs (0.6cm), thus all values 0.6cm mean no activity.

3. Annexe Chapitre III

Supplementary materials for

Variation of Metabolome, Antibacterial Activities and Bacterial Communities in different Life Cycle Stages of *Asparagopsis armata* in relation to the Production of Halogenated Molecules

Christelle Parchemin^{*,1,2}, Delphine Raviglione¹, Anouar Mejait¹, Pierre Sasal¹, Elisabeth Faliex²,
Camille Clerissi¹, Nathalie Tapissier-Bontemps¹

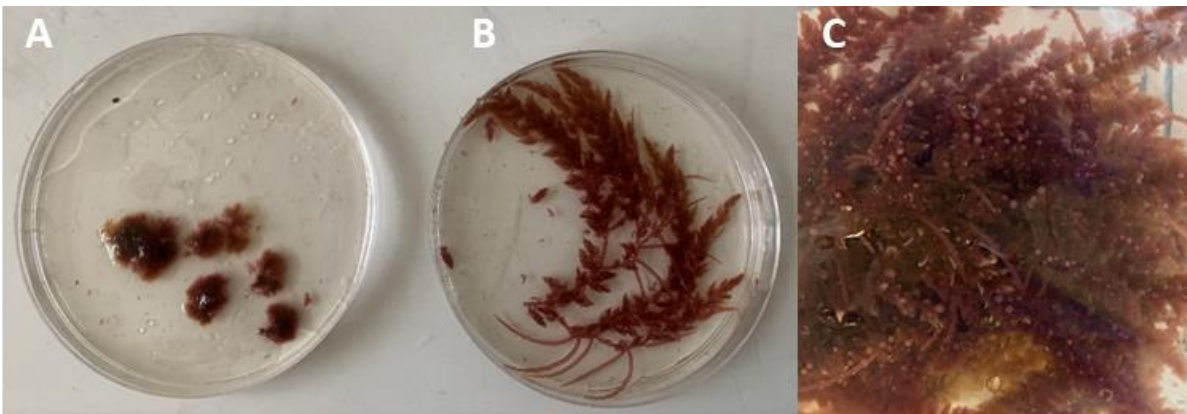
¹ Centre de Recherches Insulaires et Observatoire de l'Environnement (CRIOBE), UAR 3278
UPVD-EPHE-CNRS, Université de Perpignan - Via Domitia, 52 Av. Paul Alduy, 66860
Perpignan CEDEX, France

² CEntre de Formation et de Recherche sur les Environnements Méditerranéens (CEFREM),
UMR 5110 UPVD-CNRS, Université de Perpignan - Via Domitia, 52 Av. Paul Alduy, 66860
Perpignan CEDEX, France

*Corresponding authors: Christelle Parchemin (christelle.parchemin@univ-perp.fr); Nathalie Tapissier-Bontemps (nathalie.tapissier@univ-perp.fr)

3.1 Supplementary methods

Supplementary method 1: Pictures of the stages of *A. armata* life cycle collected in Banyuls-sur-Mer with the tetrasporophyte (A), the gametophyte without cystocarps (B) and the gametophyte with developed cystocarps (C)



Supplementary method 2:

Data acquisitions were performed using Xcalibur 4.1.31.9 (Thermo Fisher Scientific). Raw data were converted to mzML files with MSconvert (version 3.0, from Proteowizard library). mzML files were uploaded and processed using the Galaxy web platform (version 3.3) (Giacomoni et al., 2015; Guitton et al., 2017). The workflow used for data pre-processing and used parameters are published on the Galaxy Workflow4Metabolomics platform at: https://workflow4metabolomics.usegalaxy.fr/u/christelle_parchemin/w/workflowparcheminalgae. Briefly, the preprocessing consisted in a chromatographic peak detection (Galaxy Version 3.12+galaxy0) using the CentWave method with a minimum and maximum peak width of 5 and 60s, and 4 successive scans with an intensity above 500 000 as limit for consideration of region of interest. The chromatographic peak detection was followed by a peak grouping using the PeakDensity method step, a loess/non-linear “PeakGroups” retention time adjustment (degree of smoothing: 0.8), a peak filling and “CAMERA” peak annotation. A matrix of features with peak intensity, m/z value and retention time was generated. A clean-up based on p-Values and t-Stat outputs generated by the “CAMERA” step was performed in order to eliminate all features that are significantly detected in blanks. Then, an “inter/intra-batch” signal correction was applied using the “Batch correction” function with a “loess” regression model (span = 0.8) (van Der Kloet et al., 2009). This step was followed by a second clean-up according to feature's CV in pool QC injections (all features with area relative standard deviation upper than 30% through pool QC injections were

eliminated from the dataset) (Thévenot et al., 2015). Finally, redundancies due to isotopes were manually eliminated (only monoisotopic mass was kept). For identification, most probable molecular formula was determined using Sirius (v4.9.15 (Dührkop et al., 2019))), MetLin database, characteristics isotopic clusters, MS/MS spectra and comparison with literature.

Supplementary method 3: Composition of bacterial media. The quantities (in g) correspond to the preparation of 1 L of medium

Code	Strain	Medium	Culture temperature (°C)	Incubation time (h)	Susceptible to antibiotic
Ea	<i>Edwardsiella anguillarum</i> (DSMZ-27202)	Luria Broth ^a	27	24	Kanamycine
Lg	<i>Lactococcus garvieae</i> (CIP102507T)	Brain Heart Infusion ^b	37	24	Erythromycine
Tm	<i>Tenacibaculum maritimum</i> (CIP103528T)	Marine Broth ^c	27	24	Ampicilline
Va	<i>Vibrio anguillarum</i> (CIP 63.36T)	Marine Broth ^c	27	24	Kanamycine
Vh	<i>Vibrio harveyi</i> (CIP103192T)	Marine Broth ^c	27	24	Kanamycine
Yr	<i>Yersina ruckeri</i> (CIP82.80T)	Marine Broth ^c	27	24	Amoxicilline

^aLuria Broth = 5 g of yeast extract (Yeast Extract 70161-500G (Fluka Analytical, Sigma-Aldrich®, Saint-Louis USA)), 10g of peptone (Peptone from casein, pancreatic digest 70169-500G (Fluka Analytical, Sigma-Aldrich®, Saint-Louis USA)), 10g of sea salts (Sea salts S9883-500G (Sigma Life Science, Sigma-Aldrich®, Saint-Louis USA)) and 15 g of bacteriological agar (Bacteriological agar A5306-250G (Sigma-Aldrich®, Saint-Louis USA)).

^bBrain Heart Infusion Agar = 52 g for 1 L of medium (Brain Heart Infusion Agar 70138-500G (Sigma-Aldrich®, Saint-Louis USA))

^cMarine Broth = 37.4 g for 1 L of medium (Difco™ Marine Broth 2216 (Becton, Dickinson and Company, Sparks, USA))

3.2 Supplementary figures

Figure S1: Hierarchical clustering analysis of the metabolome of three stages of the life cycle of *A. armata* analysed in UHPLC-ESI(-)-HRMS/MS (distance measure: Euclidean, clustering algorithm: Ward)

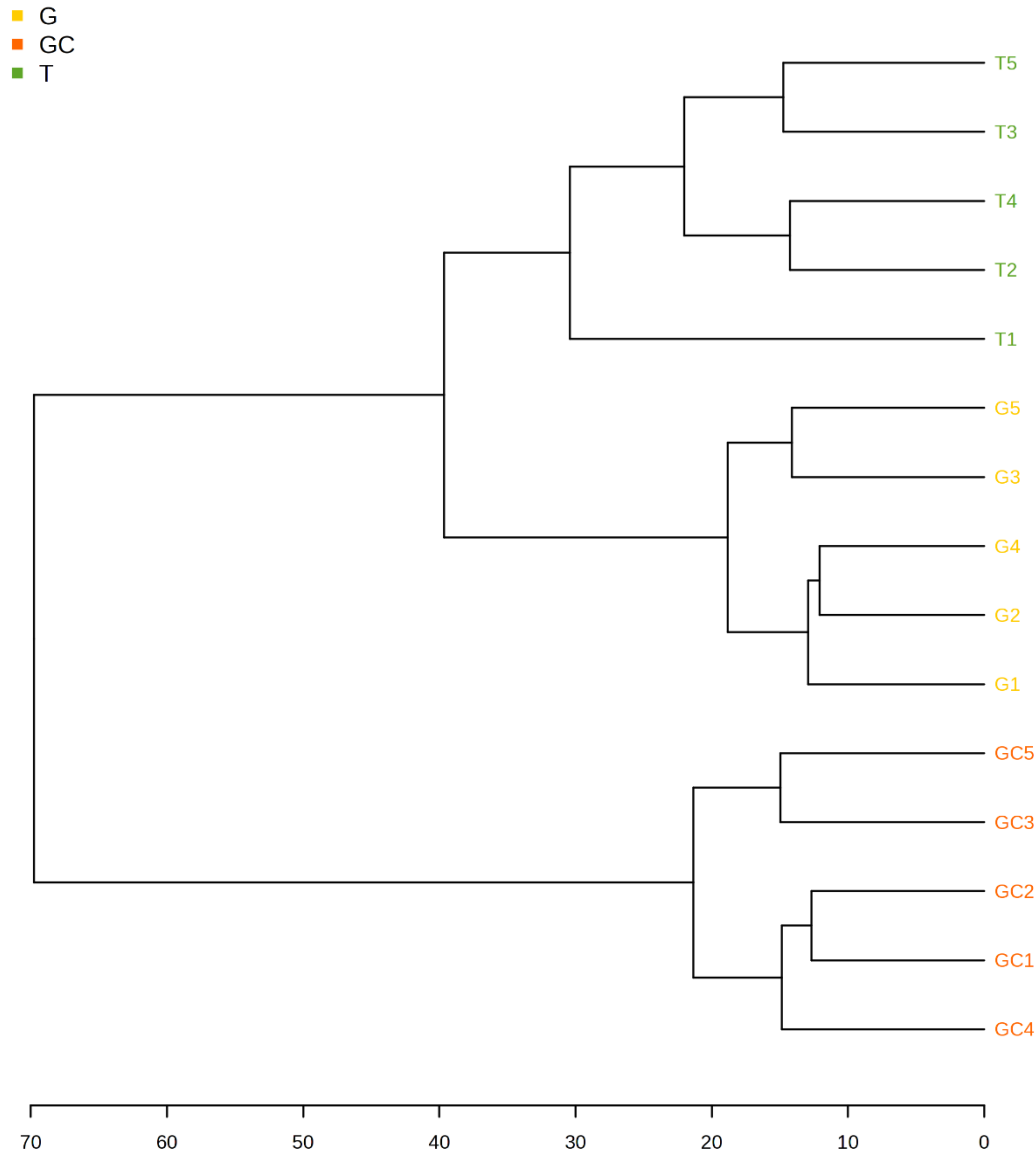


Figure S2: Chromatogram of a quality control sample analysed with the UHPLC-ESI⁻-HRMS spectrometer and displaying the ion at m/z 572.50134 [M-H]⁻ (most intense isotopic mass) of the molecule C₅H₂Br₆O₂ with the highest intensity on the chromatogram.

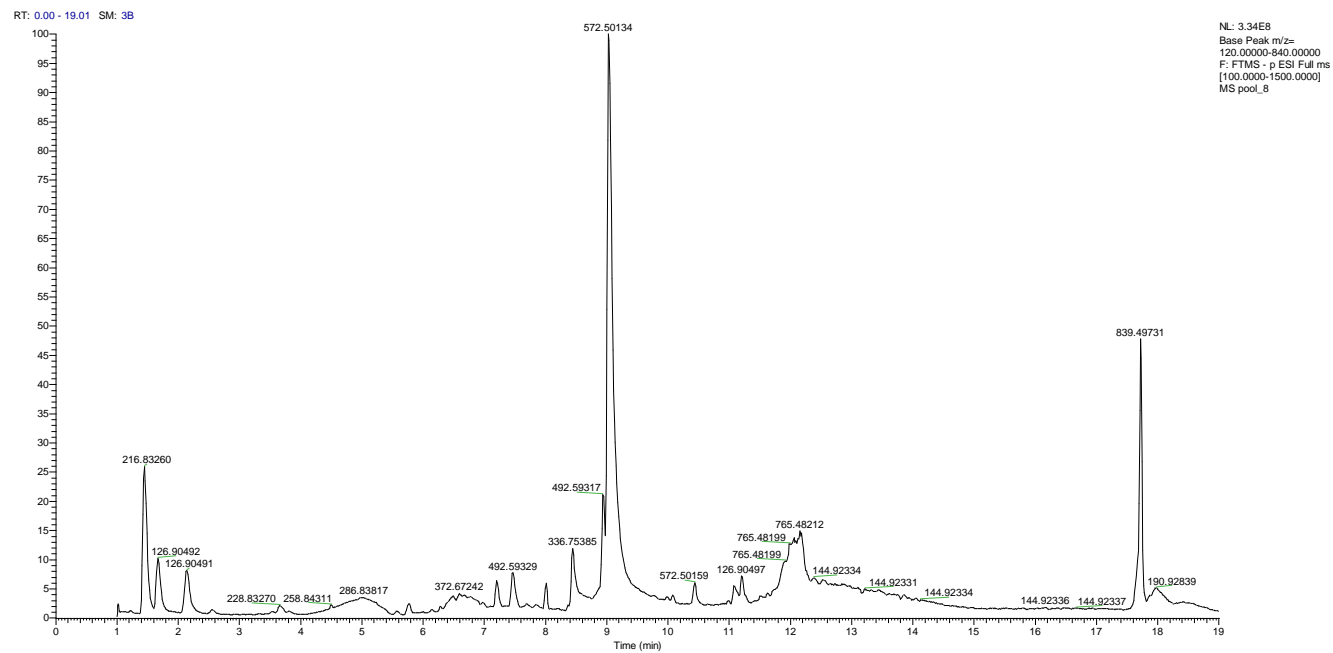
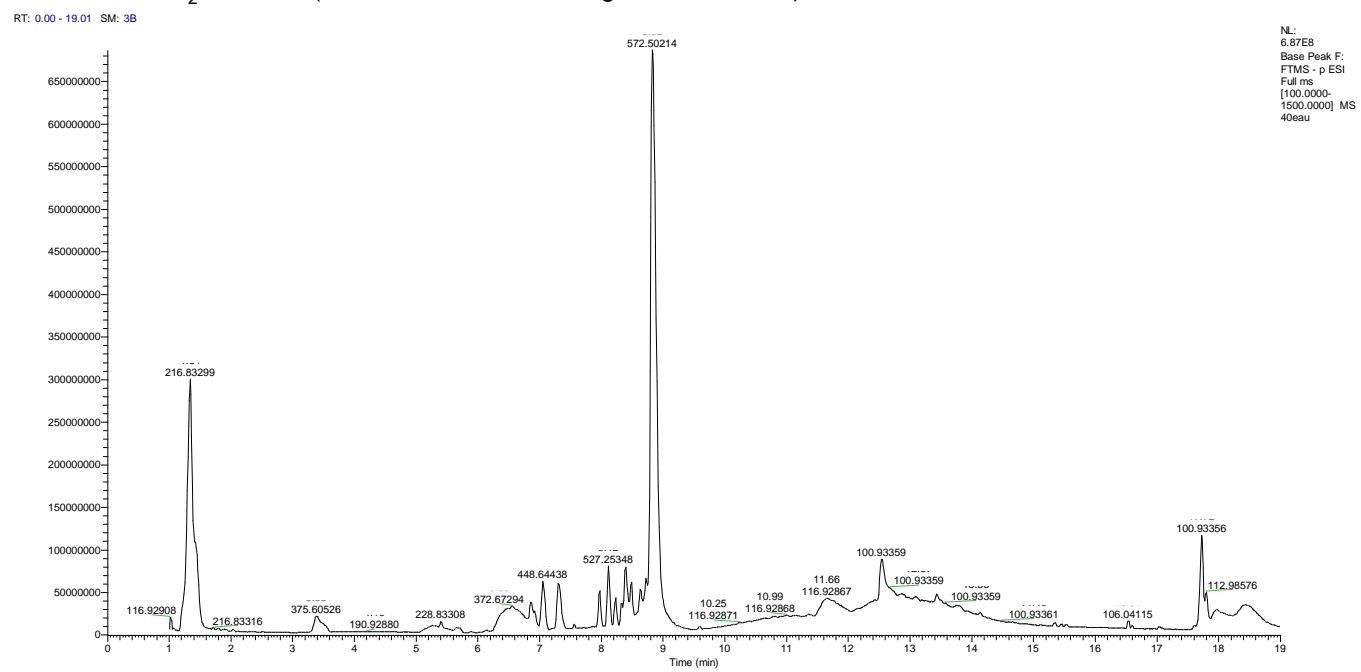


Figure S3: Chromatogram of the most active fractions (flash-chromatography fractionation) analysed by UHPLC-ESI(-)-HRMS/MS

A. 40 % H₂O-MeOH (98.9±0.4 % of bacterial growth inhibition)



B. 30 % H₂O-MeOH (97.6±0.8 % of bacterial growth inhibition)

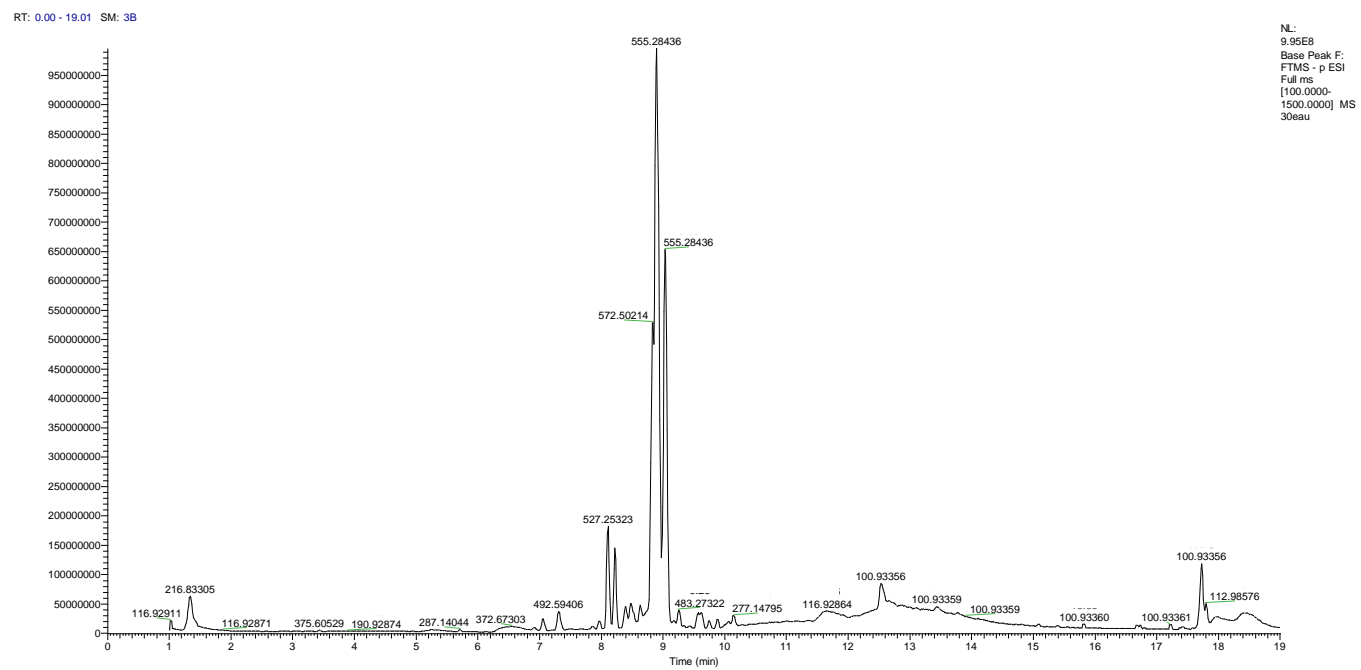


Figure S4: ESI(-)-MS/MS spectrum of $C_5H_2Br_6O_2$ (compound 1) and the possible fragmentation pattern.

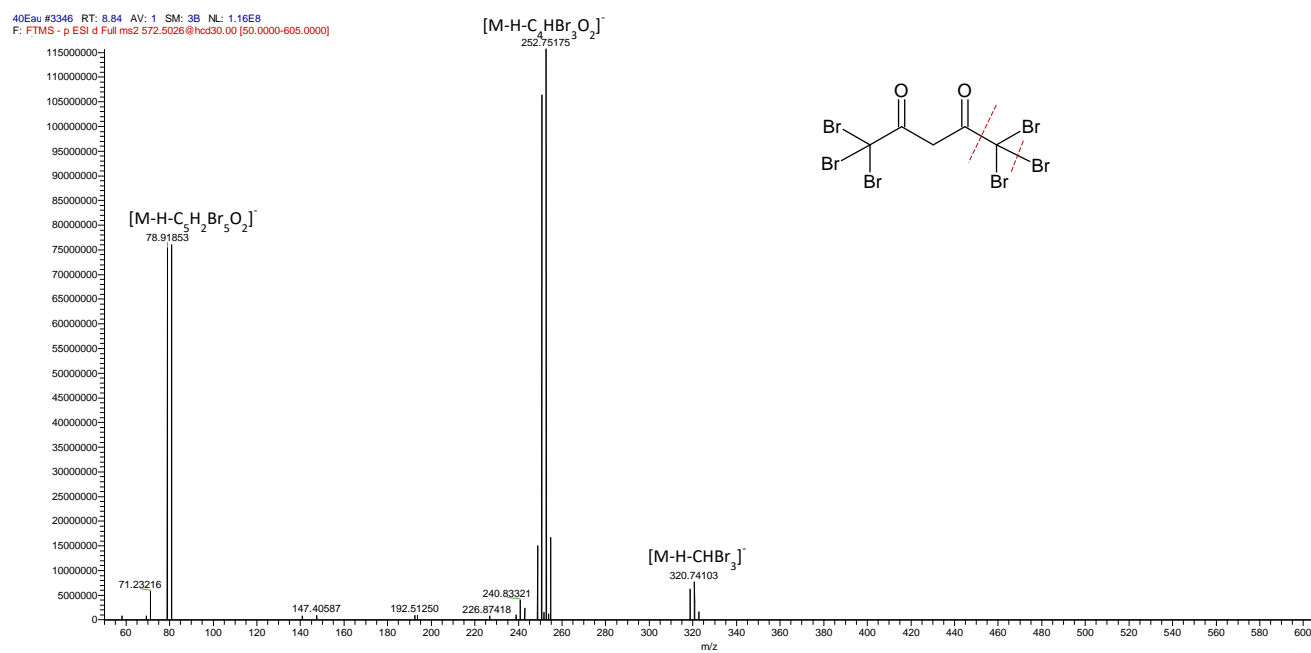


Figure S5: ESI(-)-MS/MS spectrum of $C_5H_2Br_5ClO_2$ (compound 2) and the possible fragmentation pattern.

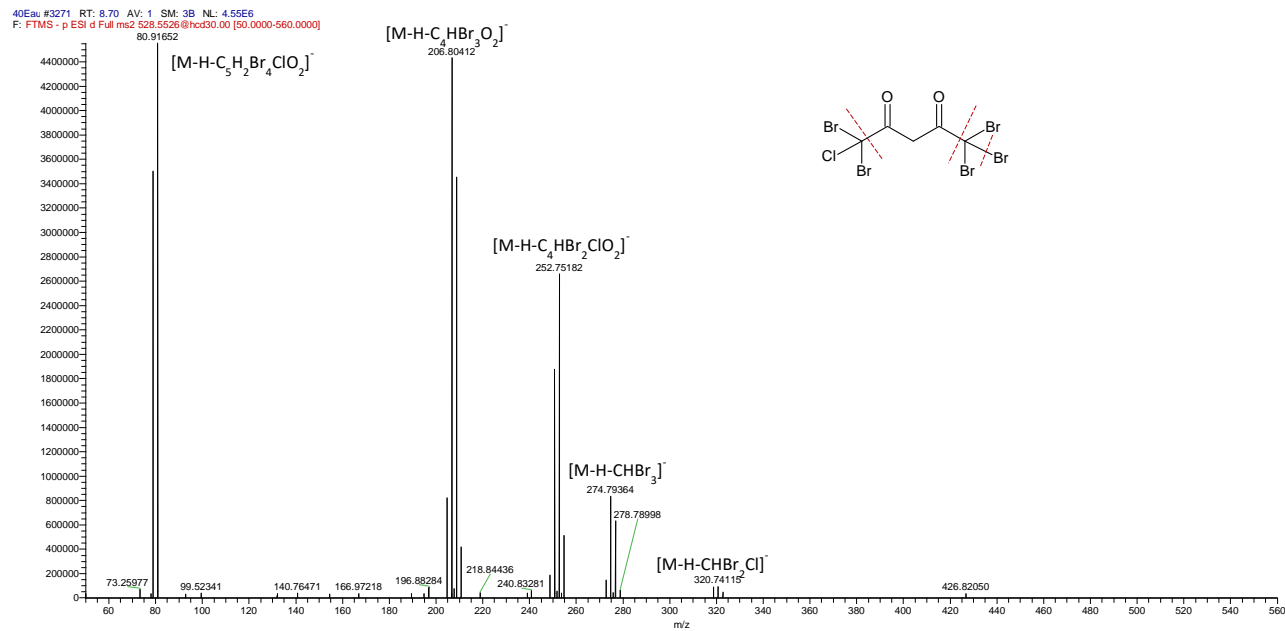


Figure S6: ESI(-)-MS/MS spectrum of $C_5H_3Br_4ClO_2$ (compound 5) and the possible fragmentation pattern.

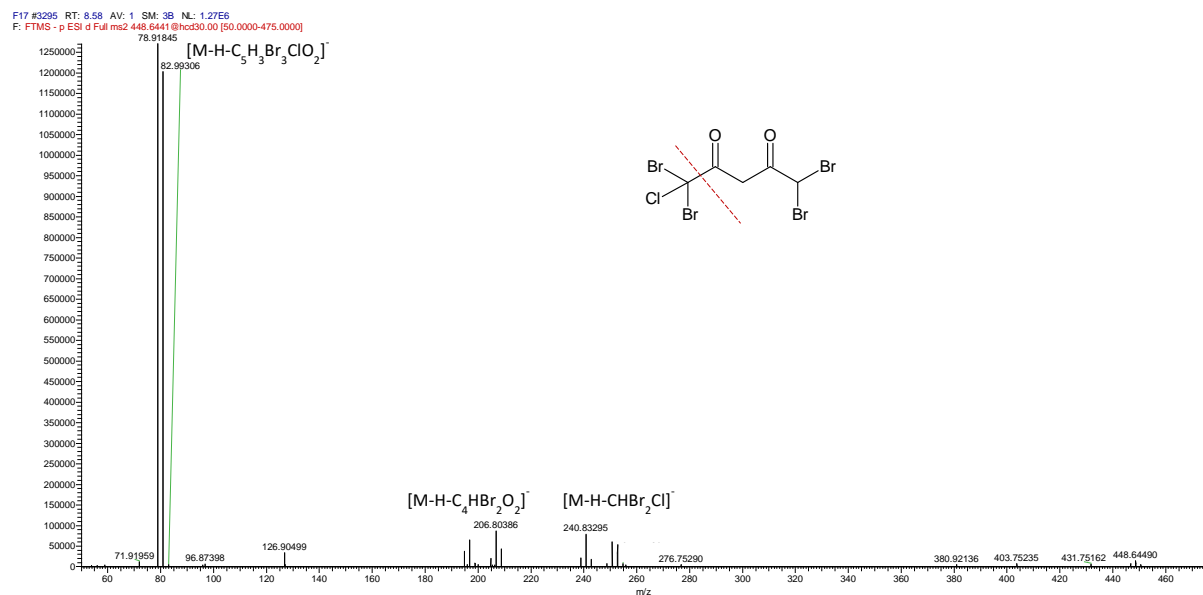


Figure S7: ESI(-)-MS/MS spectrum of $C_4H_3Br_3O_3$ (compound 6) and the possible fragmentation pattern.

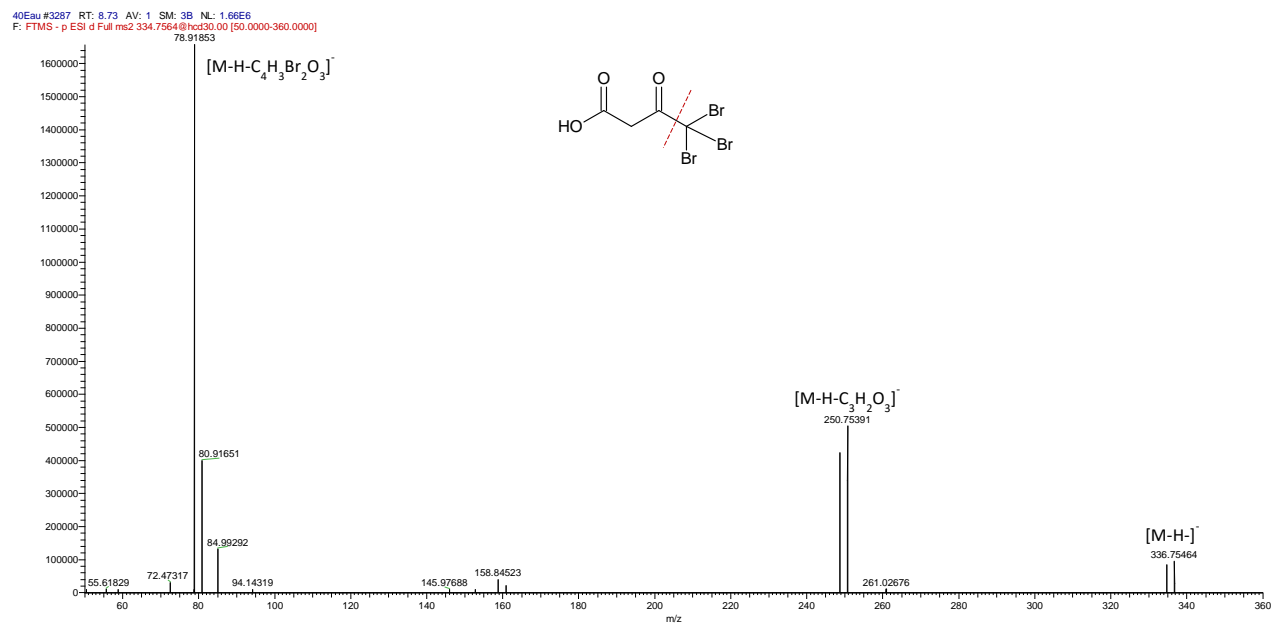


Figure S8: ESI(-)-MS/MS spectrum of $C_5H_3Br_5O_2$ (compound 7) and the possible fragmentation pattern.

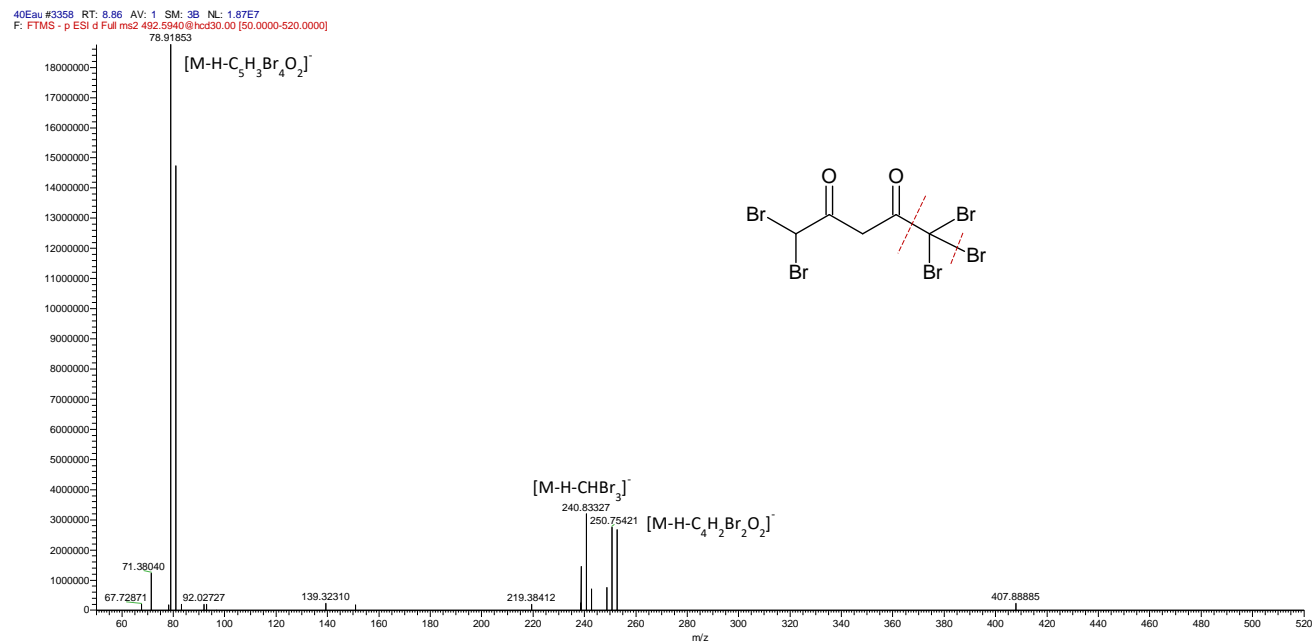
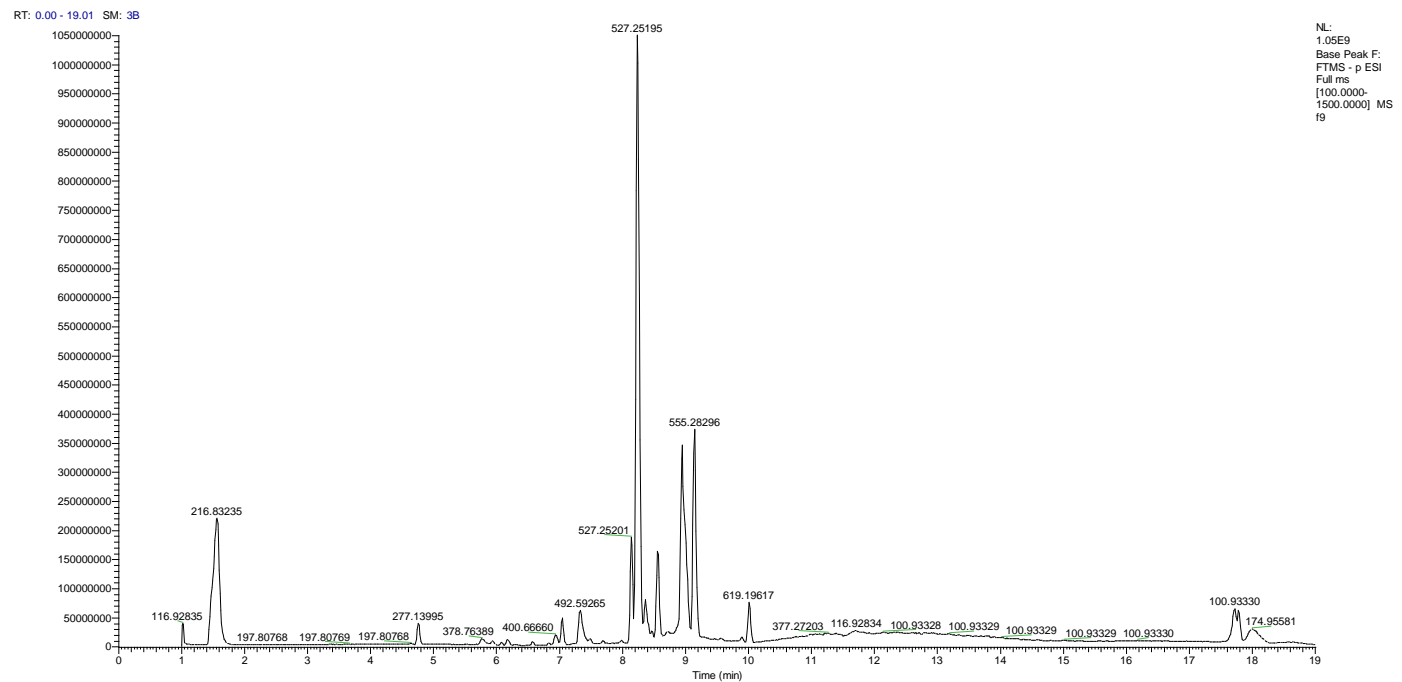


Figure S9: Chromatogram of the most active fractions of the second fractionation (HPLC (Waters 1525) coupled to a UV detector (Waters 2487)) analysed by UHPLC-ESI(-)-HRMS/MS

A. F9 (99±0.0 % of bacterial growth inhibition)



B. F10 (93.7 ± 0.3 % of bacterial growth inhibition)

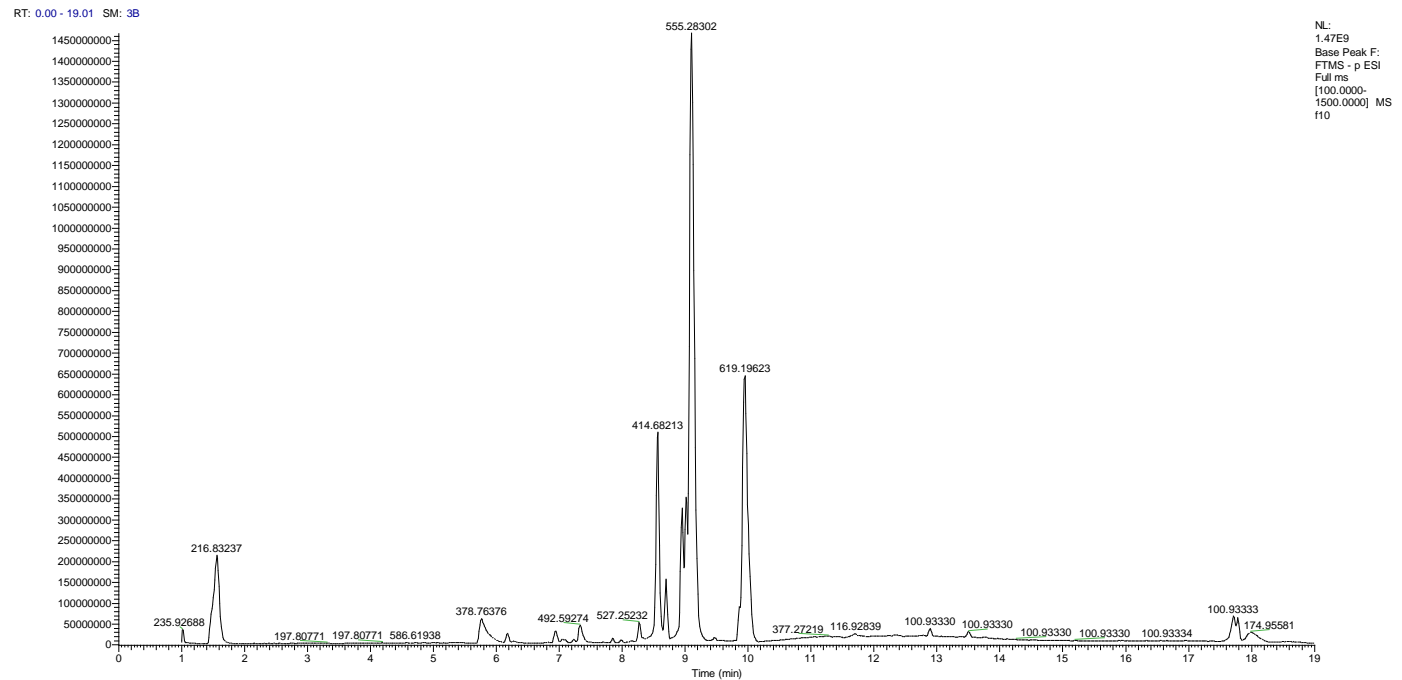
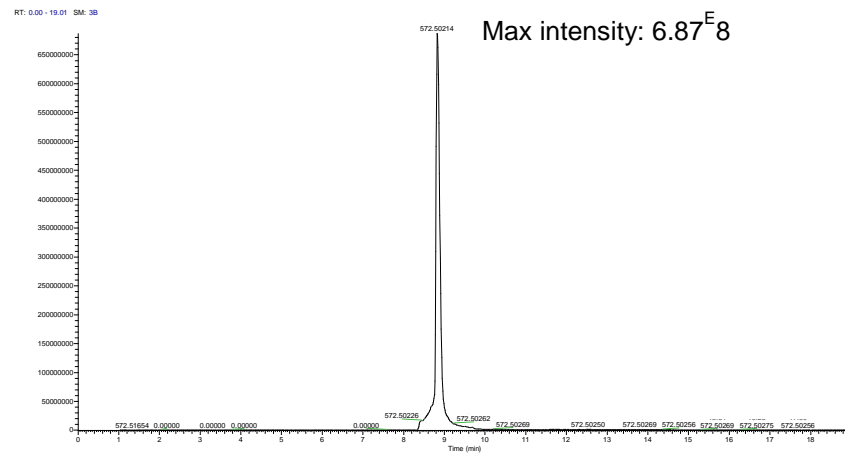
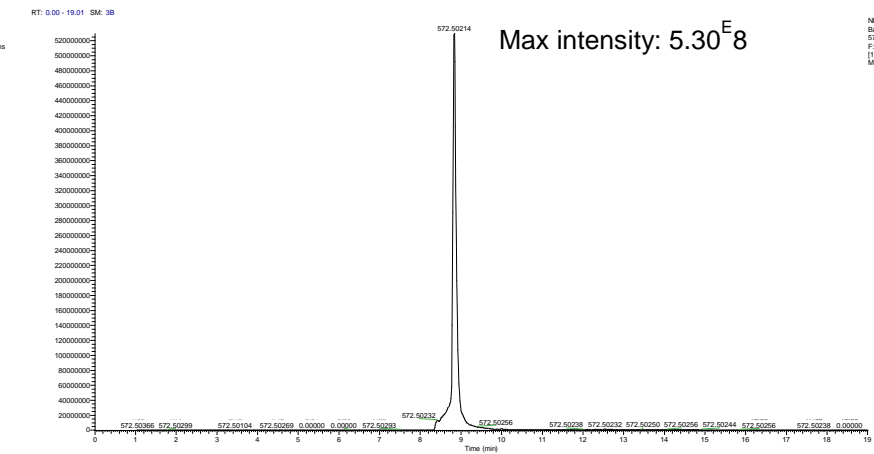


Figure S10: EIC of ion with a m/z 572.5021 (most abundant isotopic mass) corresponding to a monoisotopic m/z of 566.5085 in active fractions 40 % H₂O-MeOH (A), 30 % H₂O-MeOH (B), F9 (C) and F10 (D).

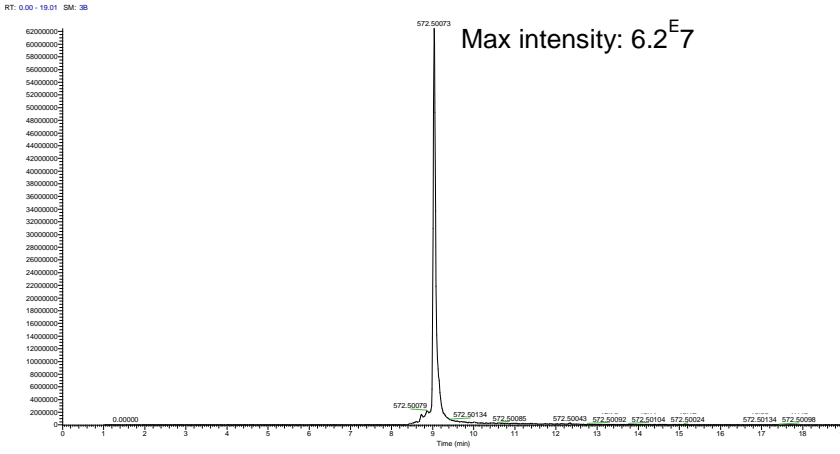
A. 40% H₂O-MeOH



B. 30% H₂O-MeOH



C. F9



D. F10

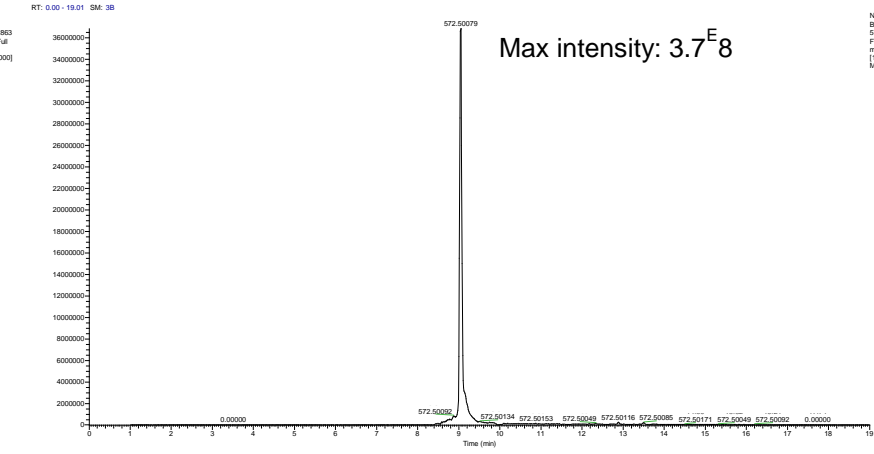


Figure S11: Rarefaction curves of 16S rRNA gene sequences for the gametophyte with developed cystocarps (A), the gametophyte (B) and the tetrasporophyte (C) samples.

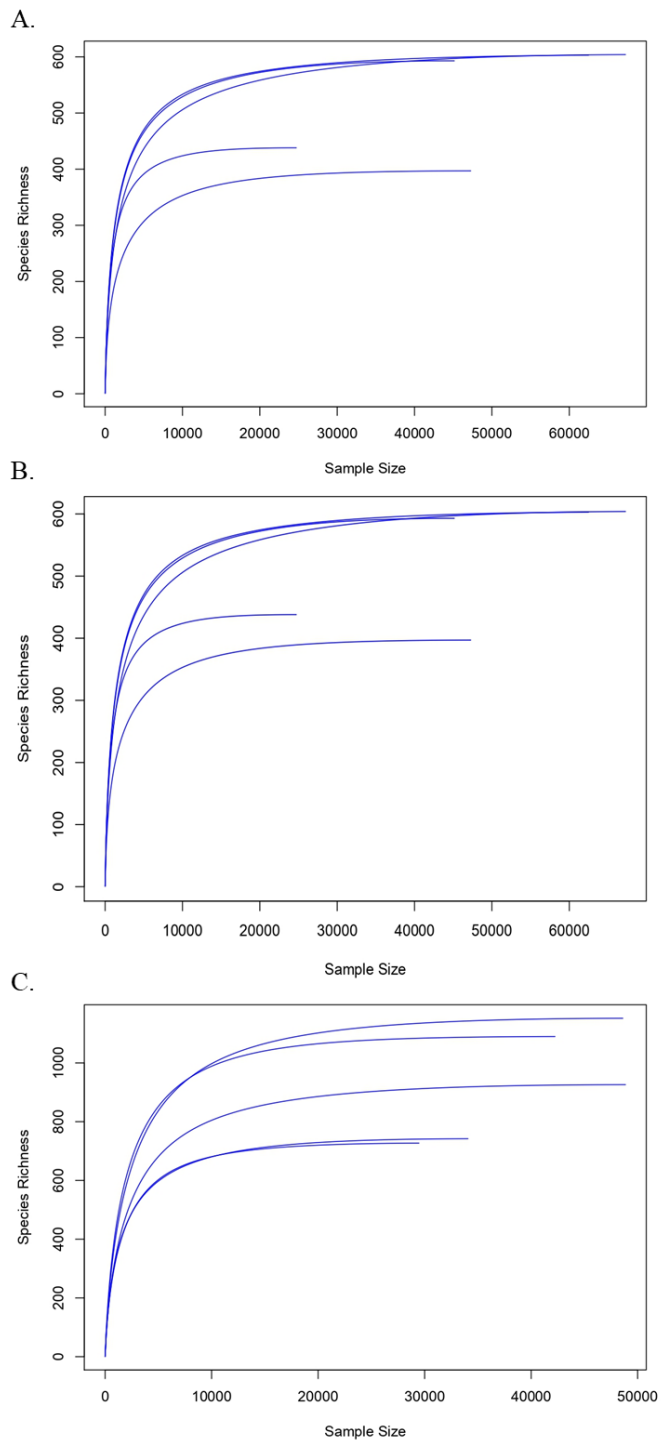


Figure S12: Relative abundance of bacterial families associated with the three *A. armata* stages. Codes “C” represents samples of the gametophyte with developed cystocarps, “G” the gametophyte samples and “T” the tetrasporophyte samples.

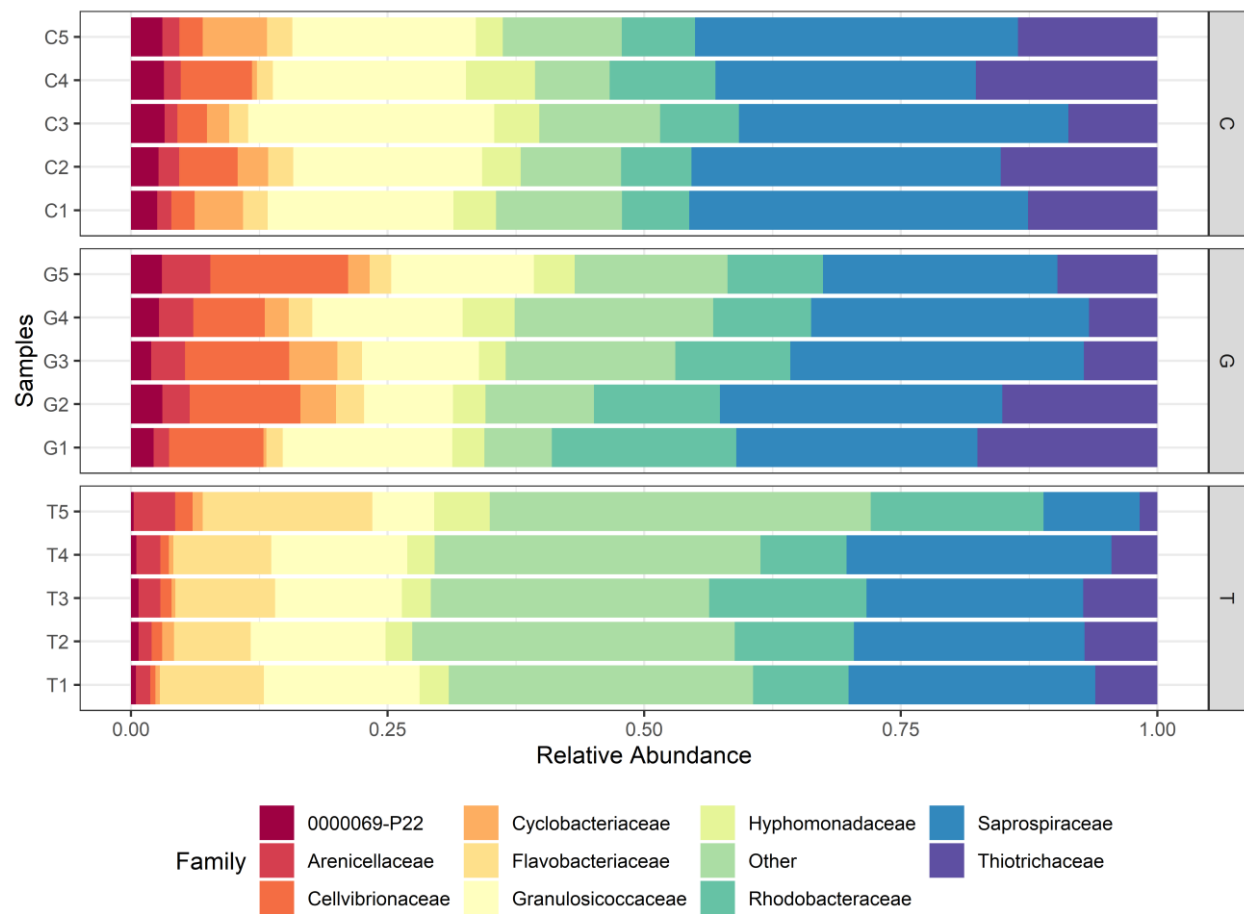
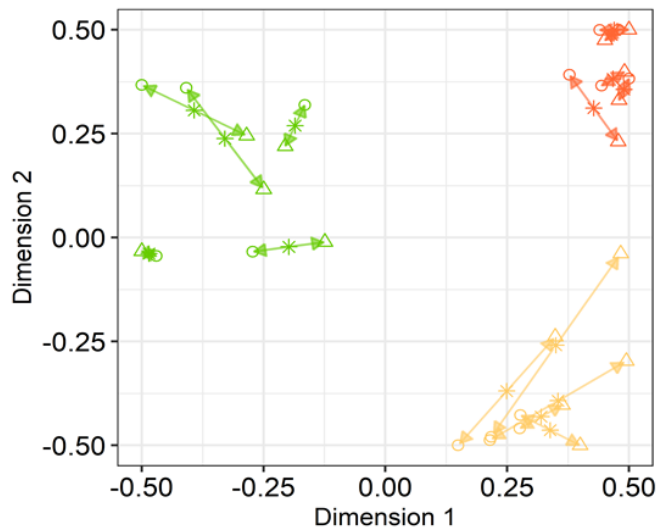


Figure S13: KO pathways of the most abundant functions associated with GC (A), G (B) and T (C).

A. GC	B. G
Metabolism	Metabolism
Global and overview maps 01100 Metabolic pathways (4)	Global and overview maps 01100 Metabolic pathways (25)
Carbohydrate metabolism 00040 Pentose and glucuronate interconversions (1)	01110 Biosynthesis of secondary metabolites (12)
00650 Butanate metabolism (1)	01120 Microbial metabolism in diverse environments (15)
Energy metabolism 00920 Sulfur metabolism (1)	01200 Carbon metabolism (7)
Nucleotide metabolism 00230 Purine metabolism (1)	01210 2-Oxocarboxylic acid metabolism (1)
Amino acid metabolism 00260 Glycine, serine and threonine metabolism (1)	01212 Fatty acid metabolism (8)
Environmental Information Processing	01230 Biosynthesis of amino acids (2)
Membrane transport 02010 ABC transporters (5)	01240 Biosynthesis of cofactors (1)
Signal transduction 02020 Two-component system (2)	Carbohydrate metabolism 00010 Glycolysis / Gluconeogenesis (2)
Cellular Processes	00053 Ascorbate and aldarate metabolism (1)
Cell growth and death 04113 Melosis - yeast (1)	00060 Pyruvate metabolism (5)
Cellular community - prokaryotes 02024 Quorum sensing (1)	00630 Glyoxylate and dicarboxylate metabolism (5)
02025 Biofilm formation - <i>Pseudomonas aeruginosa</i> (1)	00640 Propanoate metabolism (6)
02026 Biofilm formation - <i>Escherichia coli</i> (1)	00650 Butanate metabolism (6)
Organismal Systems	00660 C5-Branched dibasic acid metabolism (1)
Aging 04213 Longevity regulating pathway - multiple species (1)	Energy metabolism 00720 Carbon fixation pathways in prokaryotes (3)
Human Diseases	00680 Methane metabolism (1)
Drug resistance: antimicrobial 01503 Cationic antimicrobial peptide (CAMP) resistance (1)	00610 Nitrogen metabolism (1)
C. T	00620 Sulfur metabolism (1)
Metabolism	00661 Fatty acid biosynthesis (3)
Global and overview maps 01100 Metabolic pathways (6)	00071 Fatty acid degradation (8)
01110 Biosynthesis of secondary metabolites (5)	00120 Primary bile acid biosynthesis (1)
01120 Microbial metabolism in diverse environments (3)	00551 Glycerolipid metabolism (1)
01200 Carbon metabolism (3)	00592 alpha-Linolenic acid metabolism (1)
01212 Fatty acid metabolism (1)	Amino acid metabolism 00250 Alanine, aspartate and glutamate metabolism (2)
01230 Biosynthesis of amino acids (1)	00260 Glycine, serine and threonine metabolism (1)
01250 Biosynthesis of nucleotide sugars (1)	00280 Valine, leucine and isoleucine degradation (11)
01240 Biosynthesis of cofactors (2)	00290 Valine, leucine and isoleucine biosynthesis (1)
Carbohydrate metabolism 00010 Glycolysis / Gluconeogenesis (2)	00310 Lysine degradation (5)
00020 Citrate cycle (TCA cycle) (2)	00220 Arginine biosynthesis (3)
00052 Galactose metabolism (1)	00330 Arginine and proline metabolism (1)
00520 Amino sugar and nucleotide sugar metabolism (1)	00340 Histidine metabolism (1)
00620 Pyruvate metabolism (2)	00350 Tyrosine metabolism (1)
00630 Glyoxylate and dicarboxylate metabolism (1)	00380 Tryptophan metabolism (4)
00640 Propanoate metabolism (1)	Metabolism of other amino acids 00410 beta-Alanine metabolism (3)
00562 Inositol phosphate metabolism (1)	00480 Glutathione metabolism (1)
Energy metabolism 00680 Methane metabolism (1)	Metabolism of cofactors and vitamins 00760 Nicotinate and nicotinamide metabolism (1)
Lipid metabolism 00061 Fatty acid biosynthesis (1)	00770 Pantothenate and CoA biosynthesis (2)
Amino acid metabolism 00260 Glycine, serine and threonine metabolism (2)	Metabolism of terpenoids and polyketides 00900 Terpenoid backbone biosynthesis (1)
00270 Cysteine and methionine metabolism (1)	00981 Insect hormone biosynthesis (1)
00280 Valine, leucine and isoleucine degradation (1)	00903 Limonene and pinene degradation (2)
00310 Lysine degradation (1)	00281 Geraniol degradation (2)
00380 Tryptophan metabolism (1)	Xenobiotics biodegradation and metabolism 00362 Benzene degradation (4)
Glycan biosynthesis and metabolism 00541 O-Antigen nucleotide sugar biosynthesis (1)	00627 Aminobenzoate degradation (1)
Metabolism of cofactors and vitamins 00780 Biotin metabolism (1)	00625 Choroidal and chloralkene degradation (1)
Biosynthesis of other secondary metabolites 00521 Streptomyycin biosynthesis (1)	00642 Ethylbenzene degradation (1)
00333 Prodiginosin biosynthesis (1)	00791 Atrazine degradation (1)
Environmental Information Processing	00930 Caprolactam degradation (2)
Membrane transport 02010 ABC transporters (3)	00980 Metabolism of xenobiotics by cytochrome P450 (1)
Signal transduction 02020 Two-component system (4)	00982 Drug metabolism - cytochrome P450 (1)
04070 Phosphatidylinositol signaling system (1)	00983 Drug metabolism - other enzymes (1)
Cellular Processes	Genetic Information Processing
Cell growth and death 04112 Cell cycle - <i>Caulobacter</i> (2)	Translation 00970 Aminocetyl-tRNA biosynthesis (1)
Cellular community - prokaryotes 02025 Biofilm formation - <i>Pseudomonas aeruginosa</i> (1)	Environmental Information Processing
Cell motility 02030 Bacterial chemotaxis (2)	Membrane transport 02010 ABC transporters (18)
02040 Flagellar assembly (1)	Signal transduction 02020 Two-component system (3)
Organismal Systems	Cellular Processes
	Transport and catabolism 04145 Peroxisome (2)
	Cell growth and death 04216 Ferroptosis (1)
	04217 Necroptosis (1)
	Cellular community - prokaryotes 02024 Quorum sensing (14)
	Organismal Systems
	Endocrine system 04920 Cytokine signaling pathway (1)
	04921 PPAR signaling pathway (2)
	Digestive system 04975 Fat digestion and absorption (1)
	Nervous system 04724 Glutamatergic synapse (1)
	04727 GABAergic synapse (1)
	Aging 04212 Longevity regulating pathway - worm (1)
	Environmental adaptation 04714 Thermogenesis (1)
	Human Diseases
	Cancer: overview 05200 Pathways in cancer (1)
	05204 Chemical carcinogenesis - DNA adducts (1)
	05207 Chemical carcinogenesis - receptor activation (1)
	05208 Chemical carcinogenesis - reactive oxygen species (1)
	Cancer specific types 05225 Hepatocellular carcinoma (1)
	Cardiovascular disease 05418 Fluid shear stress and atherosclerosis (1)
	Endocrine and metabolic disease 04936 Alcoholic liver disease (2)
	Drug resistance: antimicrobial 01501 beta-Lactam resistance (2)
	Drug resistance: antineoplastic 01524 Platinum drug resistance (1)

Figure S14: Scores plot of the multiblock PLS-DA analysis (DIABLO) of *A. armata* gametophyte (*G*), with developed cystocarps (*GC*), and tetrasporophyte (*T*) stages.

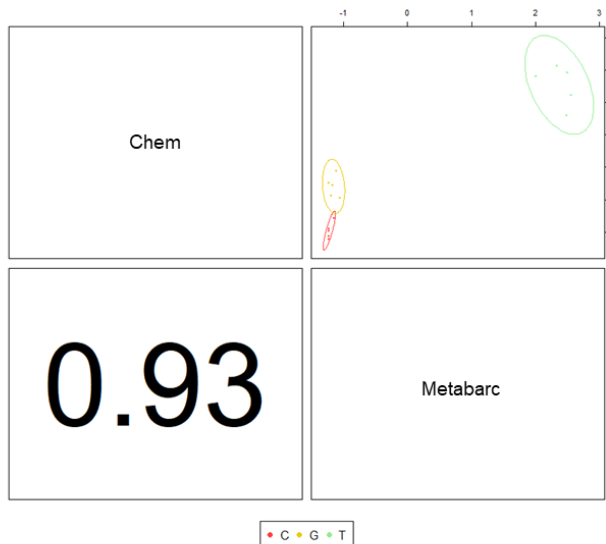


Legend

- | | |
|--|----------------------|
| ● Gametophyte (G) | ○ Chemistry dataset |
| ● Gametophyte with developed cystocarps (GC) | △ Microbiota dataset |
| ● Tetrasporophyte (T) | * Centroid |

Figure S15: Correlations between the first dimension (A) and the second dimension (B) of each dataset (Chem=Chemistry; Metabarc=Metabarcoding) for the two PLS models. Codes “C” represents samples of the gametophyte with developed cystocarps, “G” the gametophyte samples and “T” the tetrasporophyte samples.

A. Dimension 1



B. Dimension 2

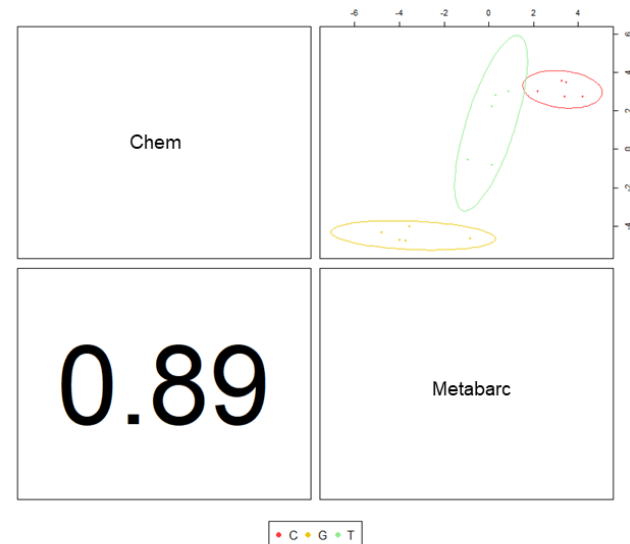
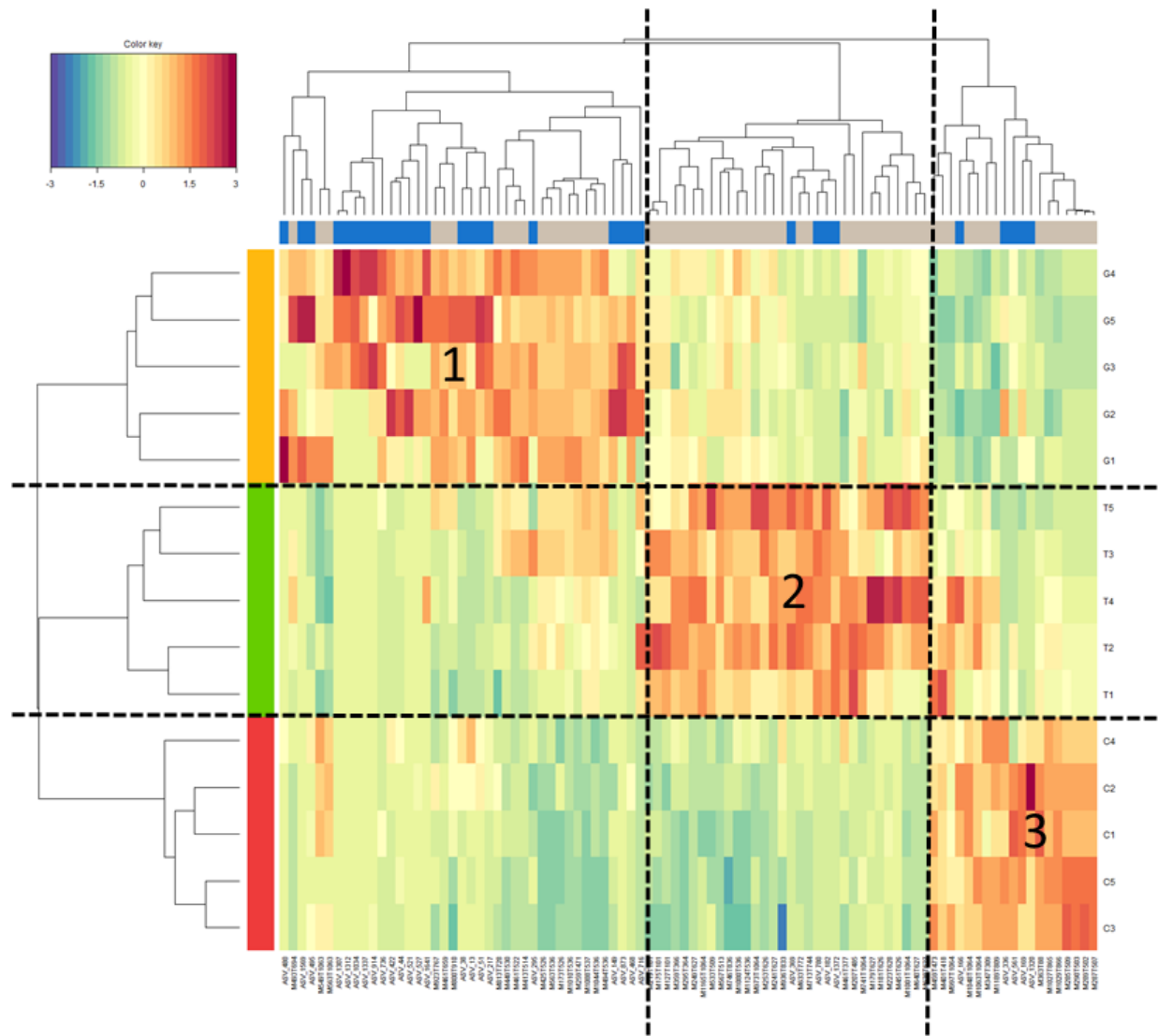


Figure S16: Heatmap of significant ASV and metabolites of the three stages of *A. armata* (“C” represents samples of the gametophyte with developed cystocarps, “G” the gametophyte samples and “T” the tetrasporophyte samples)



3.3 Supplementary tables

Table S1: Putative annotation of top VIPs features for the discrimination of *A. armata* stages from the UHPLC-ESI(-)-HRMS/MS analysis of samples collected in Banyuls-Sur-Mer. Abbreviations are: Rt for Retention time.

Code	Related redundant VIP (score >1.25) ^a	Rt (min)	Monoisotopic m/z	VIP Score	Pattern ^b	Possible bromine number ^c	Molecular formula ^c	Mass error (ppm)	Annotation	Sirius Score ^d	Tree Score ^d	MS/MS fragments (monoisotopic m/z)
M173T74		1.2	170.8853	1.5	GC	Br	C ₂ H ₂ BrClO ₂	2.5	Bromochloroacetic acid	39.13	16.14	78.9183; 130.8904; 146.9610
M179T627	[M451T626]	10.5	178.8439	1.3	T	Br ₁	(fragment of C ₅ O ₂ Br ₈)					78.9183; 99.9255
M207T485		8.1	206.9297	1.4	T	Br ₁	C ₅ H ₅ BrO ₄	1.82	Bromomesaconic acid	99.98	18.45	78.9184; 162.9826
M217T87	[M161T87; M173T87; M217T87; M286T87; M332T87; M374T87; M433T87; M435T87; M468T87]	1.5	214.8347	1.4	GC	Br ₂	C ₂ H ₂ Br ₂ O ₂	1.6	Dibromoacetic acid			78.9183; 172.8427
M219T101	[M175T101]	1.7	218.8712	1.6	T	-	C ₂ H ₂ ClIO ₂	0.89	Chloriodoacetic acid			
M249T627	[M253T626; M241T627; M640T627; M223T628]	10.5	248.7561	1.7	T	Br ₃	-					78.9183; 248.7560
M259T512	[M257T517]	8.5	256.8452	1.4	G,T	Br ₂	C ₄ H ₄ Br ₂ O ₃	1.09	4,4-diibromo-3-oxo-butyric acid			78.9184; 219.8454
M265T129	[M219T129]	2.2	262.8208	1.3	G,T	Br	C ₂ H ₂ BrIO ₂	1.18	Bromoiodoacetic acid			
M267T214		3.6	266.8168	1.4	G,T	-	CH ₂ I ₂	0.02	Diiodomethane			126.9049; 220.8289
M289T502	[M1080T502; M289T502; M573T502; M621T502; M290T503]	8.4	284.8399	1.4	GC	Br ₂	C ₅ H ₄ Br ₂ O ₄	0.23	Dibromo acid derivative			78.9184; 118.9140; 258.8428
M295T364		6.1	290.7661	1.6	G,T	Br ₃	C ₃ H ₃ Br ₃ O	1.71	Tribromoacetone			78.9184; 158.8450

M338T508		8.5	334.7557	1.6	G,T	Br ₃	C ₄ H ₃ Br ₃ O ₃	0.8	4,4,4-tribromo-3-oxo-butyric acid (composé 6)				78.9185; 248.7556
M359T366		6.1	354.7823	1.5	G,T	Br ₃	C ₄ H ₇ Br ₃ O ₄	1.84					78.9183
M379T477		8.0	376.7662	1.3	G,T	Br ₃	C ₆ H ₅ Br ₃ O ₄	0.54	Bromomesaconic acid derivative	99.85	8.5		78.9184; 127.0036; 248.7554
M383T516		8.6	378.7642	1.5	G,T	Br ₃	C ₆ H ₅ Br ₃ O ₄	1.6					78.9183; 127.0036; 248.7559
M439T452		7.5	436.6887	1.5	G,T	Br ₃ /Br ₅	-						78.9184; 126.9048; 146.9062; 180.8268; 363.2800
M493T1063		17.7	493.3354	1.4	T	-	C ₂₅ H ₅₀ O ₉	-4.61					-
M529T536	[M1044T536; M1080T536; M1124T536]	8.9	522.5574	1.6	G,T	Br ₅	C ₅ H ₂ Br ₅ ClO ₂	-1.57	1,1,1,5,5-pentabromo-5-chloro- pentan-2,4-dione (composé 2)				78.9183; 204.8059; 248.7559; 272.7961
M531T488		8.1	531.2811	1.3	T	-	C ₂₆ H ₄₄ O ₁₁	1.01		99	20.9		281.2483
M533T509		8.5	533.2963	1.6	T	-	C ₂₆ H ₄₆ O ₁₁	0.16	Polar lipid	99.87	18.45		251.2013
M549T1063		17.7	549.3827	1.4	GC,G	-	C ₃₂ H ₅₄ O ₇	6.44		98.5	22.08		188.1752; 229.1807; 319.1946
M572T543	[M638T512; M1168T692; M1168T692]	9.1	566.5072	1.3	G,T	Br ₆	C ₅ H ₂ Br ₆ O ₂	-0.89	1,1,1,5,5-hexabromo pentan-2,4-dione (composé 1)				78.9183; 248.7554; 318.7425
M633T772		12.9	628.7534	1.6	T	Br ₅	C ₁₅ H ₂₃ Br ₅ O ₂	-0.47					-
M713T744		12.4	706.664	1.6	T	Br ₆	C ₁₅ H ₂₂ Br ₆ O ₂	-0.29					78.9183; 252.7512
M746T836		13.9	745.5084	1.6	G,T	-	C ₄₀ H ₇₄ O ₁₂	-2.45	Polar lipid	78.25	23.69		301.2168; 397.1346; 415.1451
M936T833		13.9	935.5935	1.4	T	-	C ₄₉ H ₈₄ N ₄ O ₁₃	2.34	Polar lipid	55.24	70.3		80.9647; 126.9049; 225.0074; 255.2327; 537.2708;
M973T1064		17.7	973.3403	1.5	T	-	-						-
M1001T1064		17.7	1001.3688	1.5	G,T	-	-		SQDG polar lipid				80.9647; 126.9049; 225.0072; 537.2728;

														837.4813; 873.4576
M1020T526		8.8	1014.3014	1.4	G,T	Br ₇	-							-
M1075T785		13.1	1073.347	1.3	GC	Br			Polar lipid (C>50)					78.9183; 126.9049
M1145T797		13.3	1145.4697	1.4	G,T	-	-		Polar lipid					-
M1165T1064		17.7	1163.2484	1.7	T	Br	-							-

^aAnd not displayed on the Heatmap (Figure 2)

^bPattern showing in which algal stages features are more abundant, GC is for the gametophyte with developed cystocarps, G for the gametophyte and T for the tetrasporophyte

^cDetermined after Sirius (v4.9.15) or manual interpretation of MS/MS spectra and isotopic amats

^dFor some ion, MS/MS spectra were not acquired

Table S2: Bacterial growth inhibition results (n=3) of the fractions at 0.5 mg/mL obtained from the fractionation of 17.48 g of algae crude extract. Green cells represent most active fractions.

Fractions	Weight (mg)	Activity
100% H ₂ O	9,017	-7.3±12.4
90%	1,011	-4.7±12.0
80%	175.2	1.2±14.4
70%	232	37.5±4.4
60%	183.5	50.8±4.8
40%	252.4	98.9±0.4
30%	179.1	97.6±0.8
20%	441.5	-5.6±7.1
10%	368.2	-14±2.6
100% MeOH	617.6	-23.1±3.8
100% EtoAc	256.4	-32.1±1.3

Table S3: Table of the manually integrated surface area of the 14 most intense ions in the algal fractions and the calculated correlation (Pearson correlation) of these areas with the bioactivity of the fractions (first fractionation). *m/z* displayed is the mass of the most intense ions. High correlations ($r>0.8$) are in red and bold. Abbreviation: RT= Retention Time

Fractions	Bioactivity	572.502 (RT=8.85 min)	527.2532 (RT=8.11 min)	527.2536 (RT=8.24 min)	555.2843 (RT=8.96 min)	555.2843 (RT=9.03 min)	492.5941 (RT=7.31 min)	492.5939 (RT=8.8 min)	216.8329 (RT=1.34 min)	297.1275 (RT=6.85 min)	448.6444 (RT=7.06 min)	293.1762 (RT=7.98 min)	336.7544 (RT=8.39 min)	414.6835 (RT=8.49 min)	528.5526 (RT=8.72 min)
100% H ₂ O	-7.3±12.4	7.6E+05	6.9E+04	5.4E+04	3.5E+05	1.8E+05	9.4E+04	1.3E+05	1.3E+08	0.0E+00	4.5E+04	1.7E+08	3.3E+04	0.0E+00	0.0E+00
9.0E-01	-4.7±12.0	9.6E+05	9.0E+04	8.2E+04	4.6E+05	2.0E+05	2.9E+05	2.5E+05	4.8E+08	0.0E+00	5.7E+04	2.3E+08	4.1E+04	1.1E+06	0.0E+00
8.0E-01	1.2±14.4	1.3E+06	3.4E+05	1.3E+06	1.3E+07	3.3E+06	7.0E+06	9.8E+07	2.1E+09	0.0E+00	4.1E+06	2.9E+08	1.2E+05	1.3E+08	2.9E+04
7.0E-01	37.5±4.4	1.7E+08	3.6E+05	7.5E+05	1.1E+07	5.0E+06	9.8E+07	1.2E+09	3.6E+09	4.2E+05	1.1E+08	1.3E+08	6.2E+06	5.2E+08	6.8E+06
6.0E-01	50.8±4.8	1.1E+09	7.6E+06	3.7E+06	1.1E+07	6.7E+06	5.2E+07	4.9E+08	2.0E+09	1.3E+09	1.2E+08	1.3E+08	5.8E+07	1.5E+08	1.1E+08
4.0E-01	98.9±0.4	3.9E+09	2.4E+08	1.3E+08	5.2E+07	2.1E+07	2.7E+08	6.1E+08	1.6E+09	1.2E+08	2.6E+08	1.6E+08	2.3E+08	2.0E+08	2.6E+08
3.0E-01	97.6±0.8	2.4E+09	5.5E+08	4.4E+08	4.6E+09	2.1E+09	1.5E+08	5.5E+08	3.2E+08	9.7E+06	9.6E+07	7.0E+07	1.6E+08	1.9E+08	1.5E+08
2.0E-01	-5.6±7.1	3.0E+08	3.6E+07	1.8E+08	2.0E+09	8.7E+08	1.5E+07	2.1E+08	3.1E+07	2.3E+06	3.3E+07	8.1E+07	1.4E+07	1.8E+08	1.8E+07
1.0E-01	-14±2.6	2.5E+08	2.6E+07	2.9E+08	6.3E+08	3.8E+07	1.1E+07	1.5E+08	4.8E+07	4.1E+06	1.0E+07	9.6E+07	1.1E+07	5.1E+07	1.2E+07
100% MeOH	-23.1±3.8	5.6E+07	2.5E+06	2.9E+07	9.1E+07	1.5E+07	2.4E+06	3.5E+07	9.6E+06	7.9E+04	1.9E+06	2.0E+08	2.0E+06	5.8E+06	1.6E+06
100% EtoAc	-32.1±1.3	6.5E+06	5.1E+05	4.7E+05	6.3E+06	5.9E+05	2.8E+05	1.3E+06	2.1E+07	3.2E+04	1.9E+05	9.3E+07	1.2E+07	5.1E+07	1.1E+07
Correlation with bioactivity		0.9	0.8	0.4	0.4	0.5	0.9	0.7	0.4	0.3	0.9	0.0	0.9	0.5	0.9

Table S4: Bacterial growth inhibition results (n=3) of the fractions at 0.5 mg/mL obtained from the fractionation of 431 mg of active fractions 40% and 30% H₂O-MeOH. Green cells represent most active fractions.

Fractions	Weight (mg)	Activity
F1	22.6	9.0±3.9
F2	109.6	6.2±2.6
F3	80.3	1.1±3.0
F4	23.7	2.0±2.4
F5	12.8	3.1±2.7
F6	19.4	2.7±2.1
F7	22.7	7.6±2.3
F8	22.1	13.6±1.0
F9	23	99±0.0
F10	19.2	93.7±0.3
F11	11.2	-2.1±8.3
F12	3.4	-6.6±0.9
F13	0.8	-2.6±3.0
F14	0.4	-6.8±5.1

Table S5: Table of the manually integrated surface area in the fractions of the second fractionation of the 6 ions most correlated to the activity in the first fractionation and the calculated correlation (Pearson correlation) of these surface areas with the bioactivity of the fractions (second fractionation). *m/z* displayed is the mass of the most intense ions High correlations ($r>0.8$) are in red and bold. Abbreviation: RT= Retention Time

Fractions	Bioactivity	572.502 (RT=8.85 min)	527.2532 (RT=8.11 min)	527.2536 (RT=8.24 min)	492.5941 (RT=7.31 min)	492.5939 (RT=8.8 min)	448.6444 (RT=7.06 min)	336.7544 (RT=8.39 min)	528.5526 (RT=8.72 min)
F1	9.0±3.9	0.0E+00	3.5E+05	9.5E+05	0.0E+00	0.0E+00	0.0E+00	0.0E+00	0.0E+00
F2	6.2±2.6	0.0E+00	1.6E+06	8.4E+05	1.1E+04	2.0E+05	0.0E+00	0.0E+00	0.0E+00
F3	1.1±3.0	0.0E+00	1.0E+05	3.3E+05	0.0E+00	0.0E+00	0.0E+00	0.0E+00	0.0E+00
F4	2.0±2.4	0.0E+00	3.5E+05	4.1E+05	0.0E+00	3.7E+04	0.0E+00	0.0E+00	0.0E+00
F5	3.1±2.7	0.0E+00	1.4E+06	7.9E+06	0.0E+00	2.6E+05	0.0E+00	0.0E+00	0.0E+00
F6	2.7±2.1	0.0E+00	4.0E+06	2.3E+06	0.0E+00	1.0E+04	0.0E+00	0.0E+00	0.0E+00
F7	7.6±2.3	0.0E+00	6.8E+06	1.4E+07	0.0E+00	2.4E+05	0.0E+00	0.0E+00	0.0E+00
F8	13.6±1.0	7.7E+06	5.4E+08	1.1E+09	0.0E+00	4.1E+07	1.7E+06	0.0E+00	1.8E+05
F9	99±0.0	2.5E+08	4.0E+08	3.9E+09	2.6E+08	1.3E+09	4.9E+07	4.9E+06	1.2E+07
F10	93.7±0.3	1.3E+08	2.3E+07	1.6E+08	2.2E+08	1.2E+09	5.1E+07	3.0E+06	3.9E+06
F11	-2.1±8.3	0.0E+00	5.3E+07	3.9E+08	2.0E+05	1.9E+06	7.8E+04	0.0E+00	0.0E+00
F12	-6.6±0.9	4.1E+07	7.4E+07	2.5E+08	0.0E+00	2.8E+07	9.2E+05	6.7E+05	1.1E+06
F13	-2.6±3.0	5.4E+07	1.0E+08	6.9E+08	4.0E+06	3.1E+07	2.1E+06	1.3E+06	2.1E+06
F14	-6.8±5.1	2.4E+08	1.5E+08	6.2E+08	3.0E+07	9.1E+07	8.8E+06	1.3E+07	1.4E+07
Correlation with bioactivity		0.89	0.34	0.63	0.98	0.98	0.97	0.91	0.84

Table S6: Number of reads for each samples after the different filtration steps

Sample	input	filtered	denoisedF	denoisedR	merged	nonchim	no_singleton
GC1	167811	114310	111401	112883	104588	100709	62489
GC2	229782	160123	154281	157495	137154	116141	67264
GC3	150427	103686	99668	101562	88948	79867	45139
GC4	144550	102028	99157	100441	90281	78371	47259
GC5	88462	60578	57063	58822	47794	41626	24710
G1	101266	68906	66653	67681	60534	54083	31513
G2	126408	87280	83788	85650	73552	67203	45666
G3	153079	102335	96723	99368	81022	73375	46696
G4	151628	98927	92893	96188	77117	70188	49155
G5	268857	180346	174037	177258	155842	142030	100805
T1	221733	154444	148897	151351	133999	113725	48854
T2	151741	104651	97942	100988	81817	74311	48605
T3	94794	63536	60041	61486	51858	49609	34068
T4	78937	53506	50068	51364	42925	41469	29462
T5	106281	73904	70896	71834	64249	62220	42236

Table S7: Average relative abundance of the 19 most abundant (>1% in at least one group of samples) and discriminant ASV (according to IndVal index). Yellow cells represent ASV significantly associated with GC, Orange cells ASV significantly associated with G and Green cells ASV significantly associated with T.

ASV	GC	G	T	Indicator Value	p-value	Family	Genus
ASV_4	6.53	4.60	3.15	0.46	0.013	Granulosicoccaceae	Granulosicoccus
ASV_7	3.64	2.21	0.86	0.54	0.02	Sapspiraceae	Rubidimonas
ASV_10	3.46	1.70	0.88	0.57	0.011	Granulosicoccaceae	Granulosicoccus
ASV_12	2.66	1.88	0.74	0.50	0.029	Thiotrichaceae	Leucothrix
ASV_13	1.27	3.15	0.09	0.70	0.004	Cellvibrionaceae	NA
ASV_14	1.51	2.77	0.18	0.62	0.007	Arenicellaceae	NA
ASV_17	2.45	1.57	0.16	0.59	0.018	Granulosicoccaceae	Granulosicoccus
ASV_18	0.00	0.00	5.90	1.00	0.003	Sapspiraceae	Lewinella
ASV_27	0.86	1.58	0.07	0.63	0.011	Cellvibrionaceae	NA
ASV_29	1.32	0.99	0.49	0.47	0.005	Sapspiraceae	NA
ASV_30	0.67	1.85	0.27	0.66	0.008	Rhodobacteraceae	NA
ASV_31	0.11	0.18	2.83	0.91	0.001	Flavobacteriaceae	Winogradskyella
ASV_35	1.15	0.77	0.41	0.49	0.01	Hypomonadaceae	Litorimonas
ASV_37	1.28	0.77	0.00	0.62	0.021	Thiotrichaceae	Thiothrix
ASV_38	0.45	1.32	0.02	0.74	0.002	Cellvibrionaceae	NA
ASV_44	0.23	1.21	0.06	0.81	0.002	Thiotrichaceae	Cocleimonas
ASV_48	0.11	0.17	1.47	0.84	0.001	Flavobacteriaceae	Croceitalea
ASV_65	0.06	0.08	1.19	0.90	0.002	Microtrichaceae	Sva0996
ASV_83	0.00	0.00	1.14	1.00	0.002	Rhodobacteraceae	Roseobacter

Table S8: GO terms associated with the predicted functions of the bacterial communities of the three algal stages. Numbers in bracket represent the number of predicted functions associated with the GO term.

Global and overview maps
01100 Metabolic pathways (2206)
01110 Biosynthesis of secondary metabolites (736)
01120 Microbial metabolism in diverse environments (760)
01200 Carbon metabolism (230)
01210 2-Oxocarboxylic acid metabolism (41)
01212 Fatty acid metabolism (39)
01230 Biosynthesis of amino acids (179)
01232 Nucleotide metabolism (77)
01250 Biosynthesis of nucleotide sugars (109)
01240 Biosynthesis of cofactors (260)
01220 Degradation of aromatic compounds (113)
Carbohydrate metabolism
00010 Glycolysis / Gluconeogenesis (79)
00020 Citrate cycle (TCA cycle) (45)
00030 Pentose phosphate pathway (58)
00040 Pentose and glucuronate interconversions (52)
00051 Fructose and mannose metabolism (78)
00052 Galactose metabolism (46)
00053 Ascorbate and aldarate metabolism (35)
00500 Starch and sucrose metabolism (70)
00520 Amino sugar and nucleotide sugar metabolism (107)
00620 Pyruvate metabolism (96)
00630 Glyoxylate and dicarboxylate metabolism (81)
00640 Propanoate metabolism (71)
00650 Butanoate metabolism (82)
00660 C5-Branched dibasic acid metabolism (23)
00562 Inositol phosphate metabolism (22)
Energy metabolism
00190 Oxidative phosphorylation (90)
00195 Photosynthesis (55)
00196 Photosynthesis - antenna proteins (30)
00710 Carbon fixation in photosynthetic organisms (25)
00720 Carbon fixation pathways in prokaryotes (78)
00680 Methane metabolism (114)
00910 Nitrogen metabolism (43)
00920 Sulfur metabolism (76)
Lipid metabolism
00061 Fatty acid biosynthesis (23)
00062 Fatty acid elongation (1)
00071 Fatty acid degradation (26)
00100 Steroid biosynthesis (1)
00120 Primary bile acid biosynthesis (3)
00121 Secondary bile acid biosynthesis (5)
00140 Steroid hormone biosynthesis (2)
00561 Glycerolipid metabolism (31)
00564 Glycerophospholipid metabolism (42)
00565 Ether lipid metabolism (5)
00600 Sphingolipid metabolism (14)
00590 Arachidonic acid metabolism (5)
00591 Linoleic acid metabolism (2)
00592 alpha-Linolenic acid metabolism (4)
01040 Biosynthesis of unsaturated fatty acids (9)
Nucleotide metabolism
00230 Purine metabolism (112)
00240 Pyrimidine metabolism (72)
Amino acid metabolism
00250 Alanine, aspartate and glutamate metabolism (47)
00260 Glycine, serine and threonine metabolism (84)
00270 Cysteine and methionine metabolism (73)
00280 Valine, leucine and isoleucine degradation (47)
00290 Valine, leucine and isoleucine biosynthesis (15)
00300 Lysine biosynthesis (31)
00310 Lysine degradation (26)
00220 Arginine biosynthesis (35)
00330 Arginine and proline metabolism (64)
00340 Histidine metabolism (32)
00350 Tyrosine metabolism (40)
00360 Phenylalanine metabolism (45)
00380 Tryptophan metabolism (33)
00400 Phenylalanine, tyrosine and tryptophan biosynthesis (44)

4. Annexe Chapitre IV

Supplementary materials for

Asparagopsis spp. as feed supplement for a critically endangered species? Effect on the European eel (*Anguilla anguilla*) and on its pathogens

Christelle Parchemin ^{*,1,2}, Gaël Simon², Edouard Jobet¹, Cristian Chaparro ³, Marie-Christine Carpentier ⁴, Elsa Amilhat², Nathalie Tapissier-Bontemps¹, Pierre Sasal¹, Elisabeth Faliex²

¹Centre de Recherches Insulaires et Observatoire de l'Environnement (CRIOBE), UAR 3278 UPVD-EPHE-CNRS, Université de Perpignan - Via Domitia, 52 Av. Paul Alduy, 66860 Perpignan CEDEX, France

²Centre de Formation et de Recherche sur les Environnements Méditerranéens (CEFREM), UMR 5110 UPVD-CNRS, Université de Perpignan - Via Domitia, 52 Av. Paul Alduy, 66860 Perpignan CEDEX, France

³Interaction Hôtes Pathogènes Environnement (IHPE), UMR 5244, Université de Montpellier-CNRS-Ifremer-UPVD, Université de Perpignan - Via Domitia, 52 Av. Paul Alduy, 66860 Perpignan CEDEX, France

⁴Laboratoire Génome et Développement des Plantes (LGDP), UMR 5096, UPVD-CNRS, Université de Perpignan - Via Domitia, 52 Av. Paul Alduy, 66860 Perpignan CEDEX, France

*Corresponding authors: Christelle Parchemin (christelle.parchemin@univ-perp.fr); Elisabeth Faliex (faliex@univ-perp.fr)

4.1 Supplementary figures

Figure S1: Venn diagram presenting the shared UP regulated genes (A) and shared DOWN regulated genes (B) in the different conditions. A: Algae diet, C: Classic diet, P: Parasitized

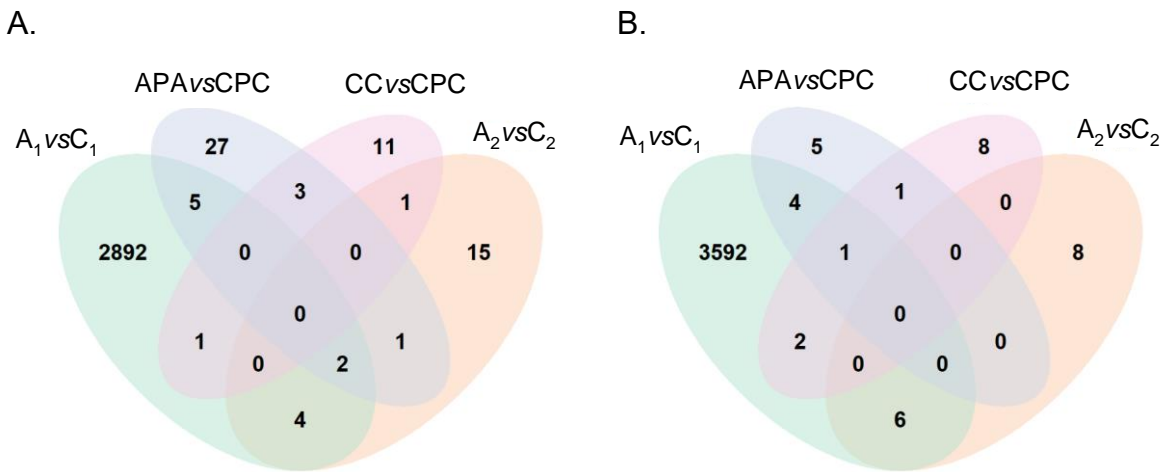
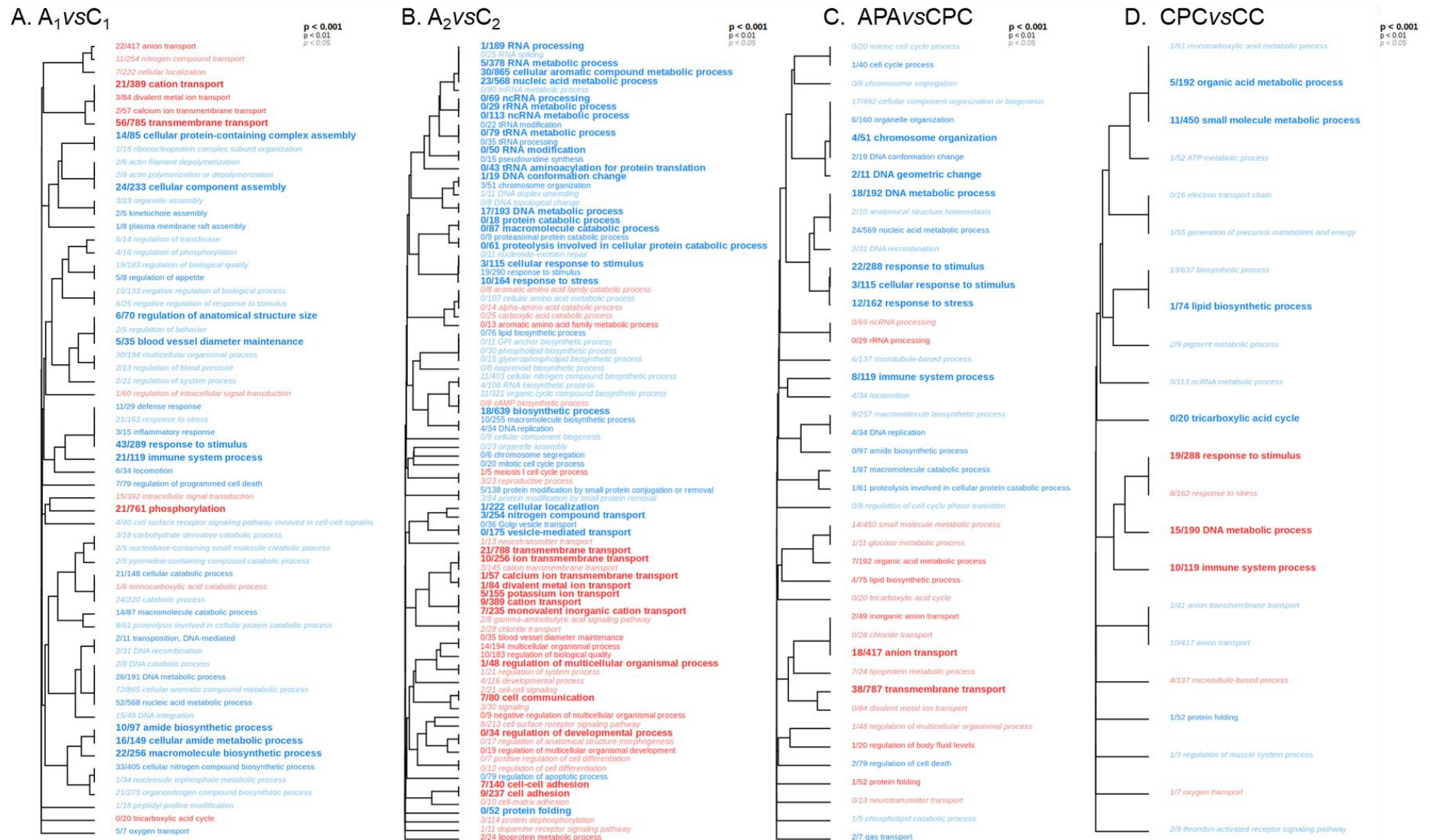


Figure S2: Biological processes (GO terms) significantly enriched (Mann–Whitney U test) between the different conditions: A1 vs C1 (A), A2 vs C2 (B), APAvsCPC (C) and CPCvsCC (D). Over-expressed/represented genes/GO terms are in red and under-expressed/represented genes/GO terms are in blue. *p* values under the 0.05, 0.01, and 0.001 thresholds are indicated in italic, in normal font, and in bold, respectively. x/y reflects the number of genes with a $\log_2\text{FC} \geq \pm 1$ in the GO category/the total number of genes in the GO category. GO terms involved in transport are framed in blue, in stress response and the immune system in yellow, and in biosynthetic processes in green



4.2 Supplementart tables

Table S1: Results of the permutational pairwise permutation test for on the survival curves differentiation of *A. crassus* exposed to different three concentrations of algae extracts of *A. armata* and *A. taxiformis* algae extracts, DMSO, and 8g/L NaCl (P value adjustment method: fdr). Statistically significant results are in bold (p > 0.05).

	Aa0.05	Aa0.5	Aa1	At0.05	At0.5	At1	Control
Aa0.5	2.50E-06						
Aa1	< 2e-16	7.50E-16					
At0.05	0.1977	0.0042	< 2e-16				
At0.5	< 2e-16	1.60E-13	0.099	< 2e-16			
At1	< 2e-16	2.40E-15	0.9436	< 2e-16	0.1258		
Control	0.6954	0.0016	1.10E-15	0.6001	2.70E-13	5.10E-15	
Solvent	0.2758	0.0038	< 2e-16	0.9661	4.10E-14	< 2e-16	0.6121

Table S2: Log2FC, padj and annotation of shared DEG genes between A_C_1 and A_C_2

gene_id	A_C_1		A_C_2		DEG	annotation
	log2FC	padj	log2FC	padj		
LOC118213021	2.76	0	2.65	0.03	UP	up-regulator of cell proliferation-like
LOC118209402	1.17	0	1.55	0	UP	cytochrome P450 2C20-like
zanl	0.93	0	0.83	0.02	UP	zonadhesin, like
rdh1	0.84	0.04	0.71	0.03	UP	retinol dehydrogenase 1, transcript variant X5
LOC118234873	0.77	0	0.58	0.01	UP	vitronectin-like, transcript variant X5
crata	0.36	0.04	0.45	0.02	UP	carnitine O-acetyltransferase a, transcript variant X2
LOC118227321	-2.5	0.02	-2.32	0.03	DOWN	uncharacterized LOC118227321
LOC118225488	-2.28	0.04	-2.3	0	DOWN	E3 ubiquitin/ISG15 ligase TRIM25-like
LOC118225505	-2.89	0.02	-1.94	0.03	DOWN	uncharacterized LOC118225505
LOC118232240	-2.04	0	-1.44	0.01	DOWN	tetratricopeptide repeat protein 39B, transcript variant X1
LOC118221722	-2.91	0.01	-1.25	0.03	DOWN	neovernucotoxin subunit beta-like
LOC118225954	-1.82	0	-0.87	0.03	DOWN	tripartite motif-containing protein 16-like, transcript variant X1

En Europe, l'anguille (*Anguilla anguilla*) est une espèce en danger critique d'extinction. Or en Région Occitanie, environ 160 professionnels vivent de la pêche à l'anguille. Au-delà de son intérêt économique, elle joue un rôle écologique majeur dans les écosystèmes, tant comme source d'alimentation que comme prédateur. L'infection par des pathogènes est considérée comme l'un des facteurs de l'effondrement de la population d'anguilles. Depuis quelques années, des traitements alternatifs aux antibiotiques, préventifs et plus respectueux de l'environnement sont mis au point, tels que les préparations à base de plantes terrestres ou d'algues. Des études ont montré le potentiel des algues du genre *Asparagopsis* comme complément dans l'aquaculture puisque leur inclusion dans l'alimentation de certains poissons a permis d'augmenter la croissance et l'expression de certains gènes liés à l'immunité. En Méditerranée, *A. armata* et *A. taxiformis* sont considérées comme envahissantes et représentent une biomasse peu valorisée dans ce cadre. Ainsi, l'objectif de la thèse est d'étudier le potentiel des deux espèces d'algues du genre *Asparagopsis* afin de prévenir et/ou traiter certaines pathologies (l'infection bactérienne par *Edwardsiella anguillarum* et l'infection parasitaire par le nématode *Anguillicola crassus*), affectant l'anguille européenne. Pour cela, une approche combinant métabolomique, métabarcoding, tests *in vitro* sur parasites et bactéries, tests *in vivo* de nourrissage et d'infection par des pathogènes et transcriptomique a été utilisée. Cette approche transdisciplinaire a permis dans un premier temps, de mieux caractériser les facteurs de variation du métabolome, des activités biologiques et du microbiote des deux espèces du genre *Asparagopsis*, et dans un deuxième temps d'évaluer les effets d'extraits d'algues *in vitro* et de poudre d'algue *in vivo* sur la physiologie de l'anguille européenne et sur ses pathogènes. Ainsi, les deux espèces présentent des différences significatives de composition chimique qui pourraient expliquer les différences d'effets sur la survie du parasite *A. crassus* observées *in vitro* et les différences d'appétences d'anguilles nourries avec les deux algues. Par ailleurs, l'activité antibactérienne des extraits des deux algues ne présente pas de variation saisonnière ce qui permet d'envisager l'utilisation annuelle d'échantillons de ces deux espèces. En revanche, les différents stades du cycle de vie de l'algue présentent des variations d'activité, de composition chimique et de microbiote. Enfin, *in vivo*, les traits phénotypiques comme la diminution de la croissance des anguilles, l'augmentation du taux d'infestation et du nombre de larves du parasite ainsi que la sur-expression de gènes liés à des processus de proliférations cellulaires ou de détoxicifications observée en transcriptomique chez les anguilles nourries avec l'algue *A. taxiformis* suggèrent une toxicité de celle-ci pour l'anguille.

Mots-clés : macroalgues, *Asparagopsis*, *Anguilla anguilla*, pathogènes, bioactivités, multi-omiques

In Europe, the eel (*Anguilla anguilla*) is a critically endangered species. In the Occitanie region, approximately 160 professionals make a living from eel fishing. Beyond its economic interest, it plays a major ecological role in ecosystems, both as a source of food and as a predator. Infection by pathogens is considered to be one of the factors in the collapse of the eel population. In recent years, alternative, preventive and more environmentally friendly treatments to antibiotics have been developed, such as preparations based on terrestrial plants or algae. Studies have shown the potential of algae of the genus *Asparagopsis* as a supplement in aquaculture since their inclusion in the diet of certain fish has increased growth and the expression of certain genes related to immunity. In the Mediterranean, *A. armata* and *A. taxiformis* are considered invasive and represent a biomass that is little used in this context. Thus, the objective of the thesis is to study the potential of two species of algae of the genus *Asparagopsis* to prevent/treat certain pathologies (bacterial infection by *Edwardsiella anguillarum* and parasitic infection by the nematode *Anguillicola crassus*), affecting the European eel. To do this, an approach combining metabolomics, metabarcoding, *in vitro* tests on parasites and bacteria, *in vivo* tests of feeding and infection by pathogens and transcriptomics was used. The transdisciplinary approach made it possible, firstly to better characterise the factors of variation in the metabolome, biological activities and microbiota of the two species of the genus *Asparagopsis*, and secondly, to evaluate the effects of *in vitro* algal extracts and *in vivo* algal powder on the physiology of the European eel and on its pathogens. Thus, the two species show significant differences in chemical composition which could explain the differences in effects on the survival of the parasite *A. crassus* observed *in vitro* and the differences in the palatability of eels fed with the two algae. Furthermore, the antibacterial activity of the extracts of the two algae does not show any seasonal variation, which makes it possible to consider the annual use of samples of these two species. On the other hand, the different stages of the alga's life cycle show variations in activity, chemical composition and microbiota. Finally, *in vivo*, phenotypic traits such as the decrease in eel growth, the increase in the infestation rate and the number of parasite larvae, as well as the over-expression of genes linked to cellular proliferation or detoxification processes observed in transcriptomics in eels fed with the alga *A. taxiformis* suggest that the latter is toxic to eels.

Keywords: algae, *Asparagopsis*, *Anguilla anguilla*, pathogens, bioactivities, multi-omics